HIV/AIDS and Air Pollution as Emerging Cardiovascular Risk Factors in Cape Town Populations: Is Endothelial Function a Marker of Effect?

by

Frans Pieter Everson

Dissertation presented for the degree of Doctor of Philosophy in the Faculty of Medicine and Health Sciences at Stellenbosch University.

This dissertation has also been presented at the Faculty of Sciences at Hasselt University in terms of the partnership agreement governing the joint supervision and awarding of doctorates between Hasselt University (Belgium), Transnationale Universiteit Limburg (The Netherlands) and Stellenbosch University (South Africa).

Supervisor: **Prof. H. Strijdom** (Stellenbosch University)

Co-supervisor: **Prof. P. De Boever** (VITO; University of Hasselt, Belgium)

Co-supervisor: **Prof. T.S. Nawrot** (University of Hasselt, Belgium)

Co-supervisor: **Prof. N. Goswami** (Medical University of Graz, Austria)

March 2020

DECLARATION:

By submitting this dissertation electronically, I declare that the entirety of the work contained therein is my own, original work, that I am the sole author thereof (save to the extent explicitly otherwise stated), that reproduction and publication thereof by Stellenbosch University will not infringe any third party rights and that I have not previously in its entirety or in part submitted it for obtaining any qualification.

This dissertation has also been presented at the Faculty of Sciences at Hasselt University in terms of the partnership agreement governing the joint supervision and awarding of doctorates between Hasselt University and Stellenbosch University.

Signature: …………………………   Date: ……March 2020………

A. Abstract

Background:

HIV and antiretroviral therapy (ART) are associated with cardiovascular disease (CVD). Concomitantly, air pollution is a global health concern and associated with CVD. Although South Africa (SA) has the largest HIV population, ART roll-out programme and also one of the most carbon-intensive economies in world, the effects of these emerging cardiovascular risk factors remain under investigated.

Aim:

The current study aimed to investigate whether endothelial function (an early marker of cardiovascular risk/disease) is a marker of effect of HIV, ART and air pollution in a study cohort residing in the Cape Town region.

Methods:

Volunteering participants were recruited from health-care clinics in Worcester and Cape Town. A health questionnaire was completed (demographic, lifestyle, and socioeconomic information), anthropometric measurements taken (BMI and blood pressure) and fasting blood and urine samples collected from each participant for chemical pathology and biomarker analyses. Sub-study 1 followed a repeated measures design (baseline and 18-month follow-up visit) to investigate the effects of HIV (viral load) and ART (pre- *vs.* post-ART treatment and an 18-month ART treatment period) on markers of endothelial function. Sub-study 2 investigated the effects of personal air pollution exposure (NO_2 and BTEX *via* passive diffusion samplers) in a repeated measures design (baseline and 6-month follow-up visit) on markers of endothelial function. Markers of endothelial function for both sub-studies included: tumor necrosis factor-alpha (TNF-α), high sensitivity C-reactive protein (hsCRP), intercellular adhesion molecule-1 (ICAM-1),vascular cellular adhesion molecule-1 (VCAM-1), e-selectin, p-selectin, vascular endothelial growth factor (VEGF), plasminogen activator inhibitor-1 (PAI-1), retinal microvascular calibres (including central retinal arteriolar/venular equivalent (CRAE; CRVE), CRAE/CRVE ratio (AVR)) and flow-mediated dilation (FMD).

Results:

Sub-study 1: Each interquartile range (IQR) increment increase in viral load (1300 copies mRNA/ml) was associated with CRVE (9.29 μm), AVR (-0.016) and %FMD (-2.13%). Compared to baseline, initiating ART was associated with VCAM-1 (-148 ng/ml), VEGF (40.6%), PAI-1 (14.12 ng/ml) and CRVE (-6.42 μm). An 18-month ART treatment period was associated with TNF-α (-1.22 pg/ml), ICAM-1 (-45%), e-selectin (-5.57 ng/ml) CRVE (–7.00 μm) and % FMD (-9.8%).

Sub-study 2: Each IQR increment increase in NO_2 (7.0 μg/m³) was associated with VEGF (-18.9%), CRVE (-2.93 μm) and baseline brachial artery diameter (-0.29 μm). Benzene (IQR: 3.3 μg/m³) was associated with p-selectin (-5.8 pg/ml), toluene (IQR: 30.0 μg/m³) was associated with PA1-1 (7.2 ng/ml). Ethyl-benzene (IQR: 3.8 μg/m³) was associated with VCAM-1 (-4.9%) and PA1-1 (9.1 ng/ml). *m+p*-Xylene and *o*-Xylene (IQR 3.8 μg/m³

respectively) were associated with VCAM-1 (-1.47% and -4.5%) and PA1 (3.08 ng/ml and 11.7 ng/ml). 3+4MHA (1380 ng/ml) was associated with %FMD (-0.40%).

Discussion and Conclusion:

The study showed that endothelial function is a marker of effect of HIV, ART and air pollutants (NO_2 and BTEX) in the current study population, and that HIV and air pollution contribute to an increased cardiovascular risk profile while ART exhibited varying effects. This study underscores the relevance of these emerging cardiovascular risk factors in South Africa and the greater sub-Saharan Africa region. This study strongly supports the need for further investigation, also in study populations beyond the Western Cape.

B. Opsomming

Inleiding:

MIV en anti-retrovirale terapie (ART) is geassosieer met kardiovaskulêre siekte (KVS). Terselfdertyd is daar wêreldwye kommer oor die gesondheidsimpak van lugbesoedeling met lg. wat ook met KVS geassosieer word. Alhoewel Suid-Afrika (SA) die grootste MIV populasie, die grootste ART voorsieningsprogram en ook een van die mees koolstof-intensiewe ekonomieë ter wêreld het, word daar min navorsing oor die effekte van hierdie ontluikende kardiovaskulêre risikofaktore onderneem.

Doelstelling:

Die huidige studie het ten doel gehad om vas te stel of endoteelfunksie ('n vroeë merker van kardiovaskulêre risiko/siekte) 'n merker van die effekte van MIV, ART en lugbesoedeling is in 'n studie-populasie in die Kaapstad omgewing.

Metodes:

Vrywillige deelnemers was by gesondheidsklinieke in Worcester en Kaapstad gewerf. 'n Gesondheidsvraelys is voltooi (demografiese, leefstyl en sosioekonomiese inligting), antropometriese afmetings (liggaam-massa indeks en bloeddruk) is ingesamel en vastende bloed- en urinemonsters is van elke deelnermer verkry vir chemiese patologie en biomerker analises. Sub-studie 1 het 'n herhaalde-metings-ontwerp gevolg (basislyn en 'n 18-maande opvolg) om die effekte van MIV (virale lading) en ART (pre- *vs.* post-ART behandeling en 'n 18-maande ART behandelingsperiode) op merkers van endoteelfunksie te bepaal. Sub-studie 2 het ook *via* 'n heraalde metings-ontwerp (basislyn en 'n 6-maande opvolg besoek) die effekte van persoonlike lugbesoedeling blootstelling (NO_2 en BTEX m.b.v. passiewe duffusie toestelle) op 'n reeks merkers van endoteelfunksie bepaal. Die volgende merkers van endoteelfunksie is vir beide sub-studies in ag geneem: tumor nekrose faktor-alfa (TNF-α), hoë sensitiwiteits C-reaktiewe proteïen (hsCRP), intersellulêre adhesiemolekule-1 (ICAM-1), vaskulêre adhesie molekule-1 (VCAM-1), e-selectin, p-selectin, vaskulêre endoteel groeifaktor (VEGF), plasminogeen aktiveerder inhibitor-1 (PAI-1), retinale mikrovaskulêre afmetings (insluitende sentrale retinale arteriolêre / venulêre ekwivalent (CRAE; CRVE), CRAE/CRCE verhouding (AVR) en vloei-gemedieerde dilatasie (FMD).

Resultate:

Sub-studie 1: Elke inkrementele interkwartielreikwydte (IKR) verhoging in virale lading (1300 kopieë mRNS/ml) was geassosieer met CRVE (9.29 µm), AVR (-0.016) and % FMD (-2.13%). In vergelyking met basislyn, was die inisiëring van ART geassosieer met VCAM-1 (-148 ng/ml), VEGF (40.6%), PAI-1 (14.12 ng/ml) en CRVE (-6.42 µm). 'n 18-maande ART behandelingsperiode was geassosieer met TNF-α (-1.22 pg/ml), ICAM-1 (-45%), e-selectin (-5.57 ng/ml) CRVE (–7.00 µm) en % FMD (-9.8%).

Sub-studie 2: Elke inkrementele IKR verhoging in NO_2 (7.0 µg/m³) was geassosieer met VEGF (-18.9%), CRVE (-2.93 µm) en basislyn brachiale arterie deursnee (-0.29 µm). Benseen (IKR: 3.3 µg/m³) was geassosieer

met p-selectin (-5.8 pg/ml) en tolueen (IKR: 30.0 µg/m³) met PA1-1 (7.2 ng/ml). Etiel-benseen (IKR: 3.8 µg/m³) was geassosieer met VCAM-1 (-4.9%) en PA1-1 (9.1 ng/ml). *m+p*-Xileen and *o*-Xileene (IKR: 3.8 µg/m³ onderskeidelik) was geassosieer met VCAM-1 (-1.47% en -4.5%) en PAI-1 (3.08 ng/ml en 11.7 ng/ml). 3+4MHA (1380 ng/ml) was gesosieer met % FMD (-0.40%).

Gevolgtrekking:

Die studie het aangetoon dat endoteelfunksie 'n merker van die effekte van MIV, ART en verskeie lugbesoedelingstowwe (NO$_2$ en BTEX) in die huidige studie-populasie is. Die resultate toon dat MIV en lugbesoedeling bydra tot 'n verhoogde kardiovaskulêre risiko profiel terwyl ART wisselende effekte getoon het. Die studie beklemtoon verder die relevansie van hierdie ontluikende kardiovaskulêre risikofaktore in Suid-Afrika en die groter sub-Sahara Afrika streek. Laastens beklemtoon die studie die behoefte aan verdere navorsing, ook in populasies buite die Wes-Kaap.

C. Acknowledgements

D. Table of Contents

E. List of Abbreviations:

2dC	: 2-methylcytosine
3+4MHA	: 3+4-methylhippuric acid
5mdC	: 5-methylcytosine
ABCA1	: Adenosine triphosphate (ATP)-binding cassette transporter-1
ART	: Antiretroviral therapy
ATP	: Adenosine triphosphate
AVR	: CRAE/CRVE ratio
BMA	: N-acetyl-s-(benzyl)-L-cysteine / Benzyl mercapturic acid
BMI	: Body mass index
BTEX	: Benzene, toluene, ethyl-benzene and xylene
CD4	: Differentiation-4$^+$ T-lymphocyte cells
CNS	: Central nervous system
CO_x	: Carbon oxides
CRAE	: Central retinal arteriolar equivalent
CRP	: C-reactive protein
CRVE	: Central retinal venular equivalent
CV	: Coefficient of variation
CVD	: Cardiovascular disease
CYP450	: Cytochrome P450
DAD	: The Data Collection on Adverse Events of Anti-HIV Drugs
DBP	: Diastolic blood pressure
DNA	: Deoxyribonucleic acid
EDTA	: Ethylenediamine tetra-acetic acid
eGFR	: Estimated glomerular filtration rate
eNOS	: Endothelial nitric oxide synthase
ERK	: Extracellular signal-regulated kinase
FMD	: Flow-mediated dilatation
GGT	: γ–Glutamyl transferase
GLUT4	: Glucose transporter type 4
gp120	: Glycoprotein-120
GST	: Glutathione S-transferase;
HAART	: Highly active antiretroviral therapy
Hb	: Haemoglobin
HbA1c	: Glycated haemoglobin

HDL	: High-density lipoprotein
HIV/AIDS	: Human immunodeficiency virus/acquired immunodeficiency syndrome
HIV/noART	: HIV-infected ART-naïve participants
HIV+ART	: HIV-infected participants on ART
HIV-1	: HIV type-1
HIV-free	: HIV-free control participants
HO-1	: Heme-oxygenase-1
HPMA	: N-acetyl-S-(3-hydroxypropyl)-L-cysteine
hsCRP	: High-sensitivity C-reactive protein
ICAM-1	: Intercellular adhesion molecule-1
IL	: Interleukin
IQR	: Interquartile range
JNK	: c-Jun N-terminal kinase
LC/MS	: Liquid chromatography/mass spectrometry
LDL	: Low-density lipoprotein
LOD	: Limit of detection
LTL	: Leukocyte telomere length
MAP	: Mitogen-activated protein
MAPK	: Mitogen activated protein kinase
MHA	: Methyl hippuric acid
MMP	: Matrix metalloproteinases
MPC-1	: Mesenchymal precursor cell-1
mRNA	: Messenger RNA
MS	: Mass spectrometry
mtDNA	: Mitochondrial DNA
MTF	: Mitochondrial forward primer sequence
MT-ND1	: Mitochondrial encoded NADH dehydrogenase 1
MU	: Trans-trans-Muconic acid / Muconic acid
NAD(P)H	: Nicotinamide adenine dinucleotide (phosphate) hydrogen
NCD	: Noncommunicable diseases
NEDD	: Sulphanilamide solution
Nef	: HIV-1 negative factor
NF-κB	: Nuclear factor kappa-light-chain enhancer of activated B cells
NHLS	: National Health Laboratory Service
NNRTI	: Non-nucleoside reverse transcriptase inhibitor
NO	: Nitric oxide

NO_2	: Nitrogen dioxide
NO_2^-	: Nitrogen dioxide ion
NOS	: Nitric oxide synthase
NO_x	: Nitrogen oxides
NRTI	: Nucleoside reverse transcriptase inhibitor
O_2	: Oxygen
O_2^-	: Superoxide ion
$ONOO^-$	: Peroxynitrite ion
oxLDL	: Oxidized LDL
PAH	: Polycyclic aromatic hydrocarbons
PAI-1	: Plasminogen activator inhibitor-1
PI	: Protease inhibitor
PKB/Akt	: Protein kinase B/Akt
PLWH	: People living with HIV/AIDS
PM	: Particulate matter
$PM_{0.1}$	: Ultra-fine PM (≤ 0.1 μm)
PM_{10}	: Coarse PM (2.5-10 μm)
$PM_{2.5}$	: Particulate matter (≤ 2.5 μm)
PMA	: N-acetyl-s-(phenyl)-L-cysteine / Phenyl mercapturic acid
PRF	: Pulse repetition frequency
qPCR	: Quantitative real-time polymerase chain reaction
Rac1	: Reservation against cancellation gene 1
RNA	: Ribonucleic acid
ROS	: Reactive oxygen species
SA	: South Africa
SANAS	: SA National Accreditation System
SBP	: Systolic blood pressure
SD	: Standard deviation
SSA	: Sub-Saharan Africa
SST	: Serum separator tube
T/S ratios	: Telomere repeated copy number / single gene copy number ratios
Tat	: Trans-activator of viral replication
TNF-α	: Tumor necrosis factor alpha
t-PA	: Tissue plasminogen activator
UK	: United Kingdom
UNAIDS	: Joint United Nations Programme on HIV and AIDS

UPLC/MS	: Ultra-pressure liquid chromatography / mass spectrometry
USA	: United States of America
UV	: Ultraviolet
VCAM-1	: Vascular cellular adhesion molecule-1
VEGF	: Vascular endothelial growth factor
VITO	: Flemish Institute for Technological Research
vLDL	: Very LDL
VOCs	: Volatile organic compounds
WHO	: World Health Organization

F. List of Figures

Appendix C: Additional Information

A. List of Tables

Chapter 5: Conclusion

Contains no tables.

Appendix A: Supplementary data for Sub-Study 1

1. Chapter 1: Literature Review.

1.1. Introduction.

Cardiovascular disease (CVD) remains the greatest global health concern and is responsible for more than 18 million deaths annually.[1,2] Although the burden of CVD has substantially decreased in high-income countries over recent years, low- and middle-income countries have experienced the greatest increase and currently represent 80% of CVD mortality worldwide.[2–4] While communicable diseases such as human immunodeficiency virus/acquired immunodeficiency syndrome (HIV/AIDS) remains the greatest contributor to the burden of disease in sub-Saharan Africa (SSA), the noncommunicable diseases (NCD) mortality rate is expected to exceed that of communicable diseases by 2030 in the region.[3] These trends strongly underscore the currently evolving epidemiological transition in the SSA region.[5] Although, the aetiology and epidemiology of traditional cardiovascular risk factors such as hypertension, obesity and diabetes mellitus in the development of CVD are relatively well recognised, an increasing body of evidence - mostly from the developed world - is indicating that lesser known non-traditional cardiovascular risk factors such as infectious diseases including HIV/AIDS[6,7] and environmental risk factors such as air pollution also play a significant role.[3,8,9]

At the height of the global HIV/AIDS-epidemic (early 2000's), more than 1.7 million people died annually (more than 20% annual mortality rate) as a result of HIV/AIDS, but since the introduction of antiretroviral therapy (ART) the prognosis of people living with HIV/AIDS (PLWH) has significantly improved (less than 2% annual mortality rate).[10–13] Despite the success of ART, reports on the numerous HIV/AIDS- and ART-associated comorbidities have emerged and currently set new challenges in HIV/AIDS healthcare.[14–17] CVD in particular has emerged a major health concern in PLWH and appears complex and multifactorial in nature.[7,18,19] Factors such as increased exposure to traditional cardiovascular risk factors as a result of improved ART-associated longevity, HI-virus viral factors, ART drug toxicity and numerous HIV- and ART-associated comorbidities such as lipodystrophy and dyslipidaemia have been implicated.[7,20,21] A 2-fold increase in risk for developing CVD in PLWH compared to the general population has previously been reported.[22] The pathogenesis of HIV- and ART-associated CVD is not well understood, but pro-atherosclerotic processes such as inflammation, oxidative stress and endothelial dysfunction have been identified as candidate mechanisms.[7,23–25]

Environmental health risk factors such as ambient air pollution have also become a global environmental and health concern and are associated with numerous adverse health effects including respiratory diseases and CVDs.[26–28] The World Health Organization (WHO) estimated that about 7 million premature deaths occur globally each year as a result of air pollution, nearly 1 million from Africa, and has furthermore identified gaseous air pollutants as dangerous to public health.[29–31] These harmful gaseous pollutants include nitrogen dioxide (NO_2) and numerous aromatic hydrocarbons (benzene, toluene, ethyl-benzene and xylene (ortho (o)-, meta (m)- and para (p)-xylene) (BTEX)).[32–36] These pollutants are mostly produced through the incomplete combustion of

fossil fuels during industrial, vehicle and household processes and are therefore especially relevant in the urban setting.[34,37] Although several gaseous chemical components present in the heterogeneous mixture of ambient air pollution have been implicated in adverse cardiovascular outcomes, the exact underlying mechanisms involved are not yet fully described, but evidence is pointing to the vascular endothelium and genetic factors as important intersections.[26,38–41]

HIV/AIDS, ART and air pollution are important emerging cardiovascular risk factors in South Africa (SA).[42–45] SA is currently in the midst of epidemiological transition that is characterised by high rates of communicable diseases such as HIV/AIDS while a simultaneous increase in NCDs such as CVD is also observed.[45,46] Furthermore, as a developing country, SA is currently experiencing economic transition that is characterised by an increase in industrialisation and urbanisation while the escalation of environmental health risk factors such as air pollution is observed.[47–50] The current status of HIV/AIDS, its treatment with ART and air pollution as emerging cardiovascular risk factors in SA is not well-documented and requires urgent investigation.[42,51]

Endothelial function is considered to be a reliable early marker of cardiovascular risk.[52,53] Numerous methods have been developed to assess endothelial function as marker of cardiovascular risk/health.[54–57] Currently flow-mediated dilatation (FMD) is regarded as the non-invasive golden standard method for assessing endothelial function in clinical research.[54] In addition, retinal microvascular imaging has gained much research interest in recent years as it offers a unique opportunity to non-invasively observe/assess the microvasculature *in vivo*.[58–60] Numerous microvascular geometric features have been associated with endothelial function and considered markers of cardiovascular risk.[58,61–63] Both FMD and retinal microvascular imaging have previously been found to be useful in assessing the effects of HIV/AIDS, ART and air pollution on cardiovascular health.[64–68] These techniques could also be applied in assessing the status of emerging cardiovascular risk factors in the SA context.[64–68] Therefore the current study set out to investigate whether HIV/AIDS, ART and personal exposure to various gaseous air pollutants as emerging cardiovascular risk factors in SA are associated with endothelial dysfunction in a SA population by making use of FMD and retinal imaging techniques.

1.2. The cardiovascular system and vascular endothelium.

It is well known that the cardiovascular system (also referred to as the circulatory system) comprises of the heart and a network of blood vessels (vascular system) and is mainly responsible for the transportation of blood throughout the whole body.[53,69–71] CVD in turn collectively represents diseases of the heart and blood vessels.[3,72] CVD is mostly degenerative in nature and develops undetected from an early age until it manifests later in life.[3,73] The process of vascular deterioration over time is also known as atherosclerosis and its progression mostly depends on the type, intensity and duration of present risk factors.[74–77] Most cardiovascular

risk factors such as smoking, an unhealthy diet, obesity and diabetes mellitus contribute to the development CVD through major pro-atherosclerotic mechanisms such as reactive oxygen species (ROS) production, inflammation and endothelial dysfunction (**Figure 1.1.**).[25,75,77]
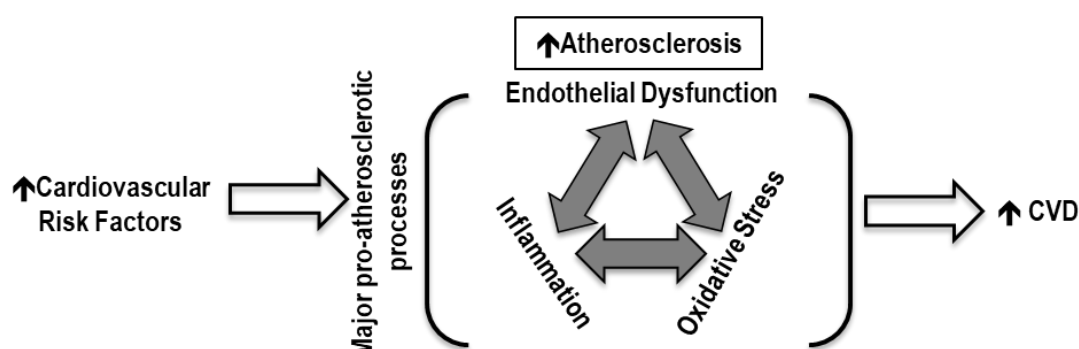
Figure 1.1. Major pro-atherosclerotic process involved in the development of CVD. Figure designed by the author of this dissertation based on content from [52,78–80]. **Abbreviations and Symbols:** CVD: Cardiovascular disease; ↑: Increase.

Over the last thirty years, scientific research has established that the vascular endothelium and dynamic changes in its biology play a central role in the process of atherosclerosis as well as general cardiovascular health and disease development.[81–83] Consequently, the vascular endothelium has increasingly become a focus of intense cardiovascular research and is now considered to be the pivotal intersection where most cardiovascular risk factors converge to exert their harmful effects.[76,77,84]

1.2.1.   The vascular endothelium.

The vascular endothelium, located within the tunica intima, is the inner most lining of the blood vessel and forms the barrier between circulating blood and underlying tissue (**Figure 1.2.**).[52,74,85]
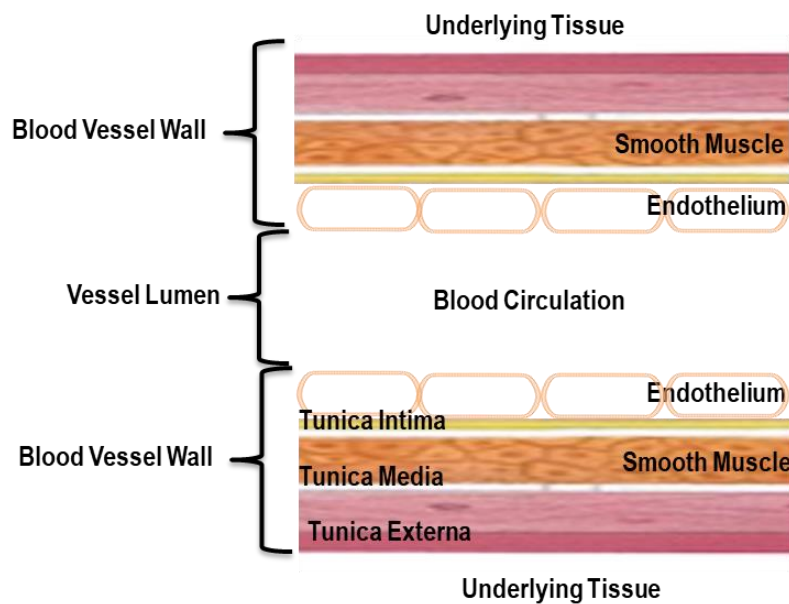
Figure 1.2. Location of the vascular endothelium in the blood vessel wall. Figure designed by the author of this dissertation based on content from [70,86].

The vascular endothelium is metabolically active, highly specialised and mostly responsible for maintaining vascular homeostasis.[52,74,85] As the interface between blood and underlying tissue, the vascular endothelium is to a large extent involved with cellular signal transduction which involves synthesising and releasing many vasoactive substances such as nitric oxide (NO) in response to various endogenous/exogenous chemical (e.g. bradykinin, thrombin and toxins) and mechanical (e.g. shear stress from increased intravascular pressure) stimuli in an ultimate attempt to restore and maintain optimal homeostasis.[53,87,88] The role of the vascular endothelium in regulating vascular tone (contraction and relaxation) is particularly important as it is directly related to vessel diameter, blood pressure, organ perfusion and tissue oxygen (O_2) supply.[70,89] Central to many of the vascular endothelium's functions is its ability to produce optimal levels of NO, and the bioavailability of NO is therefore also considered an important surrogate marker for endothelial function and general vascular health.[52,90,91]

1.2.2. The importance of endothelial-derived NO in vascular function.

NO is a gaseous, lipophilic, free radical, that is involved in vessel dilatation, neuronal transmission, cardiac contraction, immunomodulation, and stem cell differentiation/proliferation.[92–95] NO is highly diffusible, has a half-life of only seconds, and can be found both inter- and intracellular.[92,94] The biosynthesis of NO is catalysed by nitric oxide synthase (NOS) enzymes.[70,84] In the vascular endothelium, NO is mostly produced by the NOS isoform called endothelial NOS (eNOS) located in cellular compartments called caveolae (**Figure 1.3.**).[70,88,96]
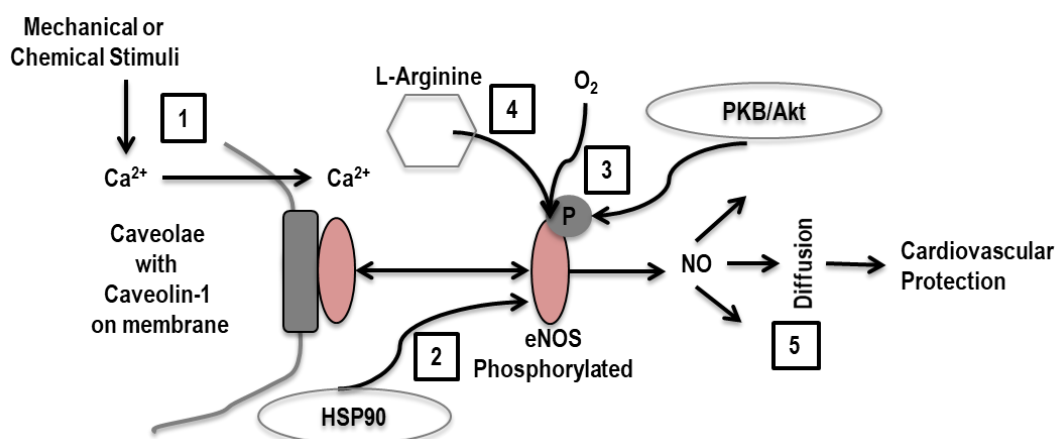
Figure 1.3. NO production by eNOS in endothelial cells. **Description: 1.** Stimuli (e.g. shear stress) triggers Ca^{2+}-influx through caveolae ion channels and eNOS dissociates from caveolin. **2.** eNOS associates with HSP90 for protection from proteasomal degradation and other cofactors (e.g. B_4H). **3.** eNOS activation (phosphorylation by PKB/Akt for example). **4.** NO is produced by eNOS using mainly L-arginine (amino acid) as substrate in the presence of O_2. **5.** NO rapidly diffuses inter- and intracellularly. Figure designed by the author of this dissertation based on content from [70,88,96]. **Abbreviations and Symbols:** eNOS: Endothelial nitric oxide synthase; NO: Nitric oxide; P: Phosphorylated; HSP90: Heat-shock protein 90; PKB/Akt: Protein kinase B/Akt.

NO was first recognised as a potent vasodilator and still remains central to much of vascular research done today.[84,93] NO's function also extends beyond its vasodilation capabilities as it inhibits intimal hyperplasia in immunologically or mechanically injured vessels, inhibits cellular apoptosis, promotes proliferation/migration of endothelial and smooth muscle cells, inhibits cell proliferation/migration during thrombosis, inhibits platelet aggregation/adhesion, monocyte and leucocyte activation/accumulation, and reduces oxidation of low-density lipoprotein cholesterol (LDL) and other scavenging lipid radicals.[92–94,96,97] In the heart, NO plays and important role in the cardiac contraction and relaxation cycle.[93,98] When cardiovascular risk factors interfere with the vascular endothelium's ability to produce optimal levels of NO, vascular homeostasis becomes dysregulated a state of endothelial dysfunction ensues.[89]

1.2.3. Endothelial dysfunction.

Endothelial dysfunction is a complex phenomenon and involves many mechanisms that mostly affect the endothelium's ability to produce NO.[79,89] Endothelial dysfunction can be defined as the partial or complete loss of balance between vasoactive (e.g. pro-vasodilatory and pro-vasoconstrictor), growth promoting and growth inhibiting, pro-atherogenic and anti-atherogenic, and pro-coagulant and anti-coagulant factors.[79,89,99] Major pro-atherosclerotic processes such as oxidative stress and inflammation play an important mechanistic role on the development of endothelial dysfunction.[52,89,100]

1.2.3.1. Reactive oxygen species (ROS) and endothelial dysfunction.

ROS are potentially cytotoxic free oxygen radicals and collectively include numerous oxidative substances that typically have an oxygen and at least one unpaired electron present (e.g. superoxide ion (O_2^-), hydroxyl radical (OH^-) and peroxynitrite ion ($ONOO^-$)) that accounts for their reactive nature.[101–103] ROS can be produced by several intracellular kinases and oxygenases such as members of the mitogen activated protein kinases (MAPK), cyclooxygenase, lipoxygenase, cytochrome P450 (CYP450) enzyme mono-oxygenase, xanthine oxidase and the nicotinamide adenine dinucleotide (phosphate) hydrogen (NAD(P)H) oxidase (major source of O_2^-) enzyme systems in response to harmful stimuli.[101,104–108] Although ROS also play important roles in cellular signalling and homeostasis, excessive levels of ROS can cause oxidative stress and tissue damage.[101,109] ROS, such as $ONOO^-$, can be particularly harmful to the vasculature as they are highly reactive/oxidative and can cause cellular/tissue damage by reacting with vascular proteins, lipids, carbohydrates and deoxyribonucleic acid (DNA).[97,110] $ONOO^-$ can also react with carbon and nitrogen oxides (CO_x and NO_x) to form other radicals such as nitroso-peroxo carbonate.[97,110] In the mitochondria, ROS such as $ONOO^-$ can irreversibly inhibit cellular respiration and cause structural and functional mitochondrial DNA (mtDNA) damage.[97,110] As a more indirect consequence, ROS can promote endothelial dysfunction through disabling cardioprotective antioxidants (e.g. ascorbic acid) and antioxidant enzymes (e.g. glutathione peroxidase).[97]

On the other hand, endothelial dysfunction may contribute to ROS production *via* a process known as eNOS uncoupling which favours redox signalling and involves the upregulation of eNOS expression and activation.[77,97] During the process of eNOS uncoupling, excessive O_2^- is produced that can associate with haem-containing (Fe^{2+}) proteins and/or oxygen radicals to produce other ROS (e.g. nitrogen oxides ions: nitrogen dioxide ion (NO_2^-), nitrate ion (NO_3^-), dinitrogen trioxide ion ($N_2O_3^-$), $ONOO^-$ and hydrogen oxide ions: hydrogen peroxide (**Figure 1.4.**).
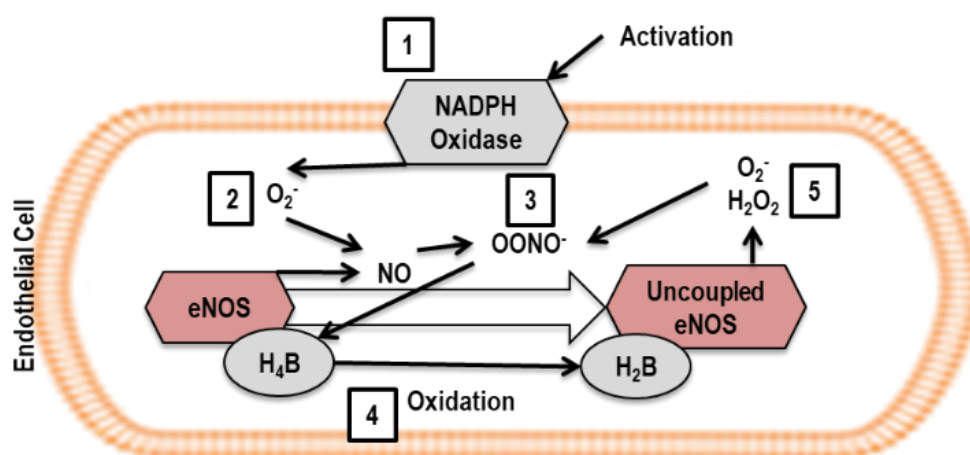
Figure 1.4. ROS production through eNOS uncoupling during endothelial dysfunction. **Description: 1.** Activation of NADPH oxidase (primary source of ROS in the vascular wall). **2.** Production of O_2^-. **3.** O_2^- rapidly reacts with eNOS derived NO and forms H_2O_2 and $ONOO^-$. **4.** $ONOO^-$ (cytotoxic protein oxidant) degradation (oxidation) of H_4B (an essential eNOS cofactor) to H_2B and (eNOS uncoupled: oxygenase dimer is inactive and reductase dimer active). **5.** NO production diverted to ROS production by uncoupled eNOS. Figure designed by the author of this dissertation based on content from [109,113,114]. **Abbreviations:** eNOS: Endothelial nitric oxide synthase; NO: Nitric oxide; NADPH: Nicotinamide adenine dinucleotide phosphate hydrogenase; H_4B: Tetrahydrobiopterin; H_2B: Dihydrobiopterin; O_2^-: Superoxide; H_2O_2: Hydrogen peroxide; $OONO^-$: peroxynitrite ion.

ROS also play a role in upregulating pro-inflammatory pathways by modulating pro-inflammatory enzyme activity (e.g. prostaglandin endoperoxide synthase, CYP450 and 5-lipo-oxygenase) that may further promote endothelial dysfunction and atherosclerosis and lead to CVD.[97,115]

1.2.3.2. Inflammation and endothelial dysfunction.

Vascular inflammation is initiated once the vascular endothelium or underlying tissue of the vascular wall is exposed to harmful stimuli and/or becomes injured.[116–121] During the acute phase of inflammation the endothelium is activated and the release of eNOS-derived NO is upregulated (causes vasorelaxation, increases blood supply and endothelium permeability).[122–124] Chemoattractant molecules are also released and initiate the recruitment and translocation of circulating monocytes across the endothelium to the injured/affected area.[104,119] The translocation of monocytes is achieved through an adhesion cascade between monocytes (e.g. leukocytes (e.g. neutrophils)) and endothelium-derived adhesion molecules (e.g. vascular cell adhesion molecule-1 (VCAM-1) and intercellular adhesion molecule-1 (ICAM-1)).[125,126] Once translocated into the vascular wall, monocytes differentiate into macrophages and further upregulate the inflammatory response by releasing inflammatory cytokines (e.g. interleukin (IL)-1 and tumor necrosis factor-alpha (TNF-α)).[125,126] These inflammatory cytokines in turn upregulate the expression of more adhesion proteins such as p-selectin (increased monocyte translocation across the vascular endothelium).[125,127,128] Cytokines also upregulate the expression

of e-selectin on endothelial cells surface (act similarly to p-selectin).[125] Finally, macrophages initiate the cellular "healing" process by removing pathogens and dead cellular remnants (**Figure 1.5.**).[75]
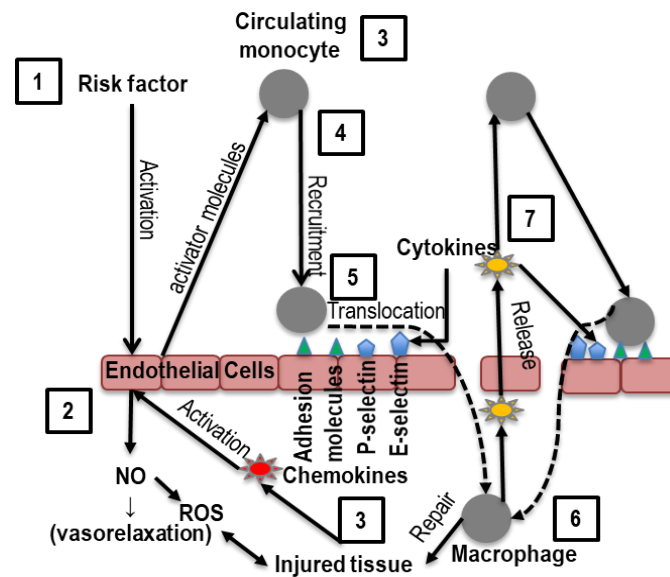
Figure 1.5. The involvement of the vascular endothelium in the inflammatory process. **Description: 1.** Activation of the vascular endothelial cells by risk factor exposure. **2**. Release of endothelium derived NO that results in vasorelaxation. **3**. Activation of the endothelial cells by chemokines released from injured tissue/cells. **4**. Activation and recruitment of circulating monocytes to the vascular endothelium. **5**. Translocation of monocytes across the vascular endothelium by means of adhesion molecules. **6**. Differentiation of monocytes into macrophages and the release of inflammatory cytokines. **7**. Upregulation of the inflammatory response by cytokines. Figure designed by the author of this dissertation based on content from [82,122–124]. **Abbreviations:** NO: Nitric oxide; ROS: Reactive oxygen species.

Endothelial dysfunction is also linked to inflammation through various mechanism that mostly involve reduced NO bioavailability.[53,82] Reduction in NO bioavailability can directly upregulate the expression of monocyte chemoattractant protein-1 (increases monocyte recruitment and translocation) and nuclear factor kappa-light-chain enhancer of activated B cells (NF-κB: upregulates VCAM-1 expression).[82,92,129] Increased ROS and C-reactive protein (CRP) production (associated with endothelial dysfunction) can also upregulate the expression of vascular adhesion molecules and promotes monocyte accumulation in the vascular wall that can ultimately develop into lipid-loaded foam cells and plaque formation (thrombosis) over time.[82,108,121] Endothelial dysfunction can also increase the oxidation and infiltration of LDL cholesterol into the vascular wall (*via* lectin-like oxidized LDL (oxLDL) receptor-1).[82,108,121] oxLDL in turn has been implicated in reduced eNOS expression and increase expression of vascular adhesion molecule.[82,108,121] Reduced NO bioavailability additionally promotes thrombogenicity (NO is a potent inhibitor of platelet aggregation) and cause plaque destabilisation through activation of matrix metalloproteinases (MMPs; increase risk for thromboembolism).[82,92]

Although inflammation is generally considered to be a protective biological response to harmful stimuli (e.g. pathogens, damaged cells and irritants), an excessive or prolonged (chronic) inflammatory response can have detrimental effects on vascular health/function and contribute to the progression of atherosclerosis.[130–133]

1.2.3.3. Atherosclerosis and endothelial dysfunction.

As a result of chronic ROS generation, inflammation and endothelial dysfunction, white blood cells, dead cell remnants, oxLDL and triglycerides continuously accumulate in the vascular wall and a sub-endothelium plaque forms.[75,89] Over time the plaque enlarges and vascular smooth muscle cells located in the arterial media proliferate (partly as a result of the release of endothelium-derived vascular endothelial growth factors (VEGF)) and translocate into the sub-intimal space to form a thrombus (fibrous cap to seal off the plaque).[75,91,134] A large thrombus can reduce blood supply distally to the vessel occlusion and cause ischaemia (ischaemic heart disease when the thrombus is located in the coronary arteries: greatest cause of death worldwide).[135–137] When multiple plaques are formed, vessel elasticity decreases and an increase in pulse pressure is observed.[135–137] The increase in blood pressure and the release of fibrinolytic factors may furthermore result in erosion of the fibrous cap and cause thromboembolism (ruptures into the vessel lumen) resulting in more serious adverse events such as myocardial infarction or a stroke (**Figure 1.6.**)**.**[75,81,132]
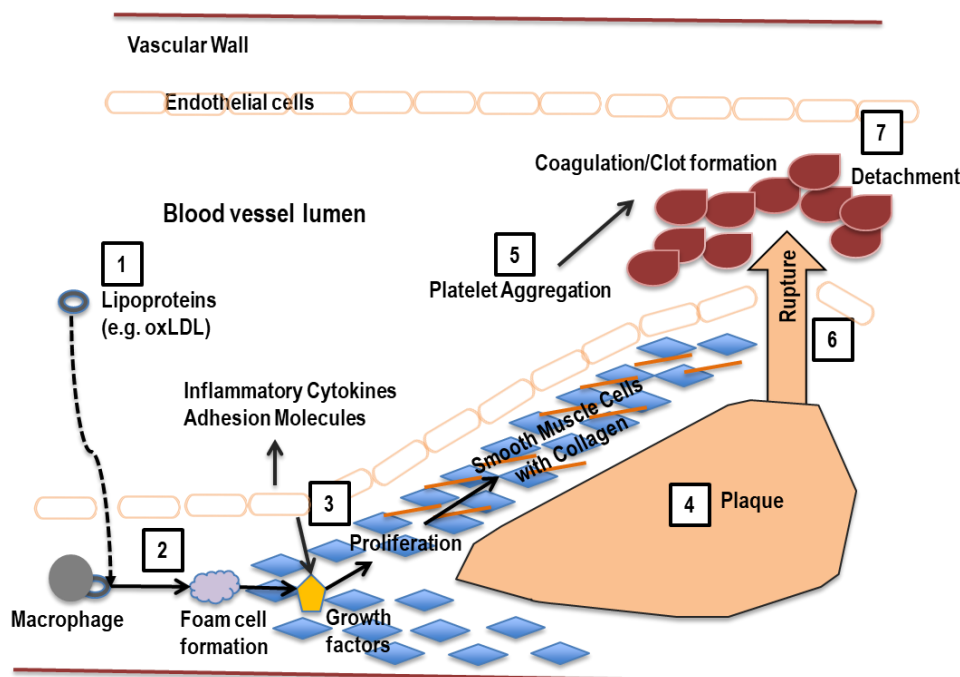
Figure 1.6. Plaque formation in the arterial wall during advanced atherosclerosis. **Description: 1.** Translocation and accumulation of LDL in the vascular wall. **2.** Formation of lipid-loaded foam cells. **3.** Release of vascular growth factors. **4.** Plaque formation in the vascular wall. **5.** Clot formation within the vessel lumen. **6.** Rupture of the plaque. **7.** Detachment of the blood clot. Figure designed by the author of this dissertation based on content from [82,96,109,132]. **Abbreviations:** LDL: Low-density lipoprotein cholesterol; oxLDL: Oxidised LDL.

1.2.4. The vascular endothelium as marker of cardiovascular risk.

Total cardiovascular risk represents the cumulative effect of cardiovascular risk factors on cardiovascular health over time.[138] Therefore, early assessment and detection of cardiovascular risk allow for timely intervention that could prevent or even reverse the pathophysiological processes leading to CVD.[139–141] Determining cardiovascular risk is often difficult as numerous known and unknown cardiovascular risk factors may play a role.[142–144] Also, the intensity and duration of risk factors, as well as the overlapping of physiological pathways seem to have variable effects on cardiovascular health.[142–144] Numerous methods have been developed over the years to quantify cardiovascular risk, including mathematical algorithms, electronic instrumentation and chemical biomarkers.[54,57,140,145–149]

Due to its ideal location and central role in many vascular mechanisms, the vascular endothelium and its function has become an integrative, yet independent, marker of the cumulative effects of cardiovascular risk factors on the vasculature.[77,81,130] Therefore, assessing the degree of endothelial function in the clinical setting has proven valuable in terms of the detection, prevention, prediction, management and treatment of not only CVDs, but also other health risk factors, disease burdens and their outcomes.[77,80,84] The assessment of endothelial function has not only clinical importance in established diseases, but also as early marker at subclinical level where underlying diseases/risk factors have not yet manifested into clearly defined complications.[77,80,150]

1.2.4.1. Non-invasive methods for assessing endothelial function.

Appreciation for the vascular endothelium's role in cardiovascular health and risk assessment has increased over the years.[52,77,80] Currently numerous non-invasive techniques such as FMD, brachial-ankle index pressure, pulse wave analysis, carotid intima-media thickness measurement, retinal microvascular imaging and computed tomography are available to assess endothelial function as marker of cardiovascular risk.[25,76,80,151–153] Also, numerous circulating biomarkers that are mechanistically involved in various aspects of endothelial function such as ICAM-1, VCAM-1 and p-selectin (see section 1.2.3.2. and Figure 1.5) have been identified and proven valuable in endothelial and vascular health assessment.[127,151,154]

1.2.4.1.1. Flow-mediated dilatation (FMD): Principles of the method.

FMD was first described in 1992 and is now considered the non-invasive gold standard technique for evaluating vascular endothelial function in clinical research, because of its sensitivity and non-invasive nature.[77,150,155] FMD currently remains more applicable in clinical research setting with larger study populations rather than individual risk assessment due to lack of a universal standardised protocol.[80]

The principle of FMD is based on the endothelium's ability to produce NO (mainly *via* eNOS' L-arginine pathway) during induced reactive hyperaemia distally and in response to a localised occlusion (usually *via* inflating

a pneumatic blood pressure cuff at 50 mmHg supra-systolic pressure).[77,80,151] During the period of ischaemic occlusion, decreased O_2 supply and pH (due to increased hydrogen ion (H^+)), shear stress (internal and external pressure) and changes in metabolite concentrations (increased carbon dioxide (CO_2), lactate, adenosine and potassium ion (K^+) concentrations) disrupt vascular homeostasis.[77,80,151] Following release of the occlusion (deflation of the blood-pressure cuff), reactive hyperaemia is triggered as a result of the homeostatic imbalance created during ischaemia and massive amounts of eNOS-derived NO is released (results in vasodilation until most metabolic waste is removed) in an ultimate attempt to restore homeostatic balance.[77,151,156] At the end of reactive hyperaemia, NO-bioavailability decreases and vascular tone (diameter) returns to basal levels (**Figure 1.7.**).[77,151,157]
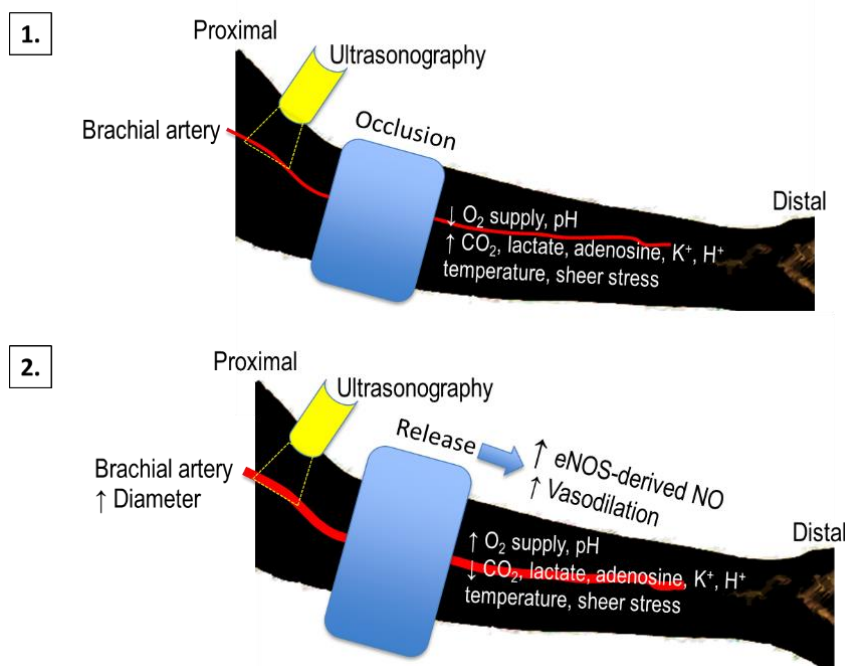
Figure 1.7. Principle of flow-mediated dilatation. **Description: 1.** Inducing transient ischaemia through vascular occlusion of the brachial artery in the forearm. **2.** Release of the occlusion triggers reactive hyperaemia and vasodilation. Figure designed by the author of this dissertation based on content from [77,80,151,157]. **Abbreviations and Symbols:** NO: Nitric Oxide; eNOS: Endothelial nitric oxide synthase. O_2: Oxygen; CO_2: Carbon dioxide; K^+: Potassium ion; H^+: Hydrogen ion; ↑: Increase; ↓: Decrease.

Visualisation and quantification of vascular endothelial function during the process of FMD is achieved by means of ultrasonography techniques coupled with computerized edge detection technology that measures vascular metrics (vessel lumen diameter) at baseline (before occlusion) and during reactive hyperaemia.[77,151] The maximum vessel lumen diameter change during reactive hyperaemia (from the baseline measurement) is directly related to the vascular endothelium's ability to produce NO and expressed as a percentage of baseline brachial lumen diameter (% FMD).[156,158]

1.2.4.1.2.   Retinal imaging: Principles of method.

Retinal microvascular imaging by means of a digital retinal camera is a very useful, non-invasive technique to probe microvasculature physiology *in vivo* (**Figure 1.8.**).[59,159,160]
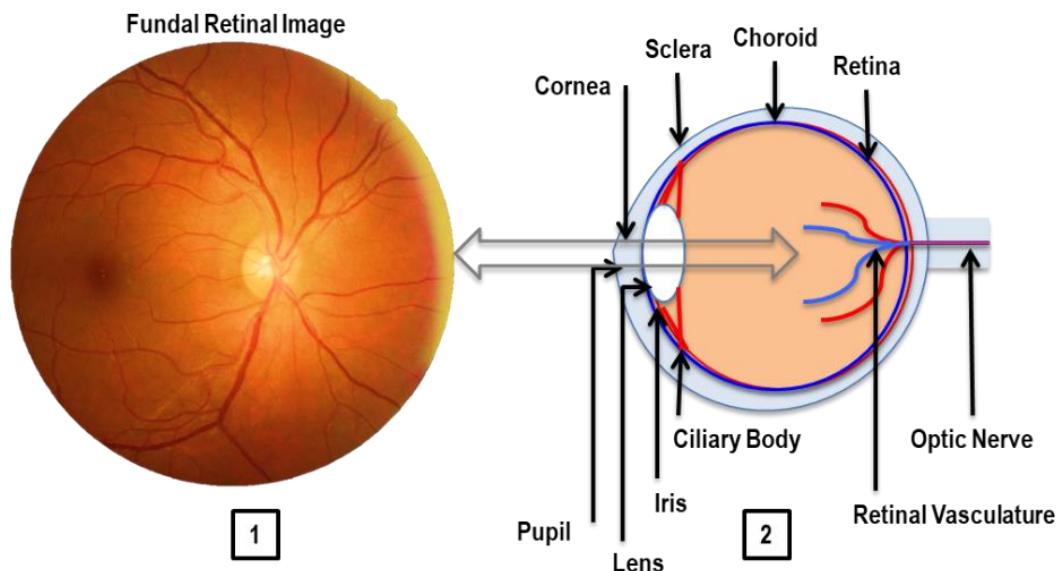
Figure 1.8. A digital fundal retinal image depicting retinal microvasculature is taken through the pupil of the eye. **Description: 1.** Digital fundal image of retinal microvasculature (photographed by the author). **2.** Cross-sectional representation of the eye (designed by the author of this dissertation based on content from [66]).

The pupil of the eye offers a unique point of access to non-invasively assess the internal structures of the eye including the retinal microvasculature (vessel diameter: 50 – 300 µm).[59,161] Currently, high-resolution digital photographs of the retinal microvasculature are used against standardised grading protocols to evaluate microvascular characteristics.[59,160,162] Using retinal imaging for cardiovascular risk assessment focus largely on geometric features, in particular retinal vessel calibers (arteriole and venule diameters and diameter ratios), although vessel network fractals and branching angle features have also found application.[59,163,164]

Numerous metabolic, anthropometric, demographic, behavioural and environmental cardiovascular risk factors have been associated with retinal microvascular geometric features.[58,165–167] Hypertension and cardiometabolic risk factors such as dyslipidaemia and diabetes, for example, have been associated with retinal arteriole narrowing and wider venules.[62,168,169] Wider retinal venules and narrower retinal arterioles have furthermore been linked to pro-atherosclerotic processes such as inflammation, endothelial dysfunction, and increased risk for stroke and myocardial infarction.[58,170–172] In terms of branching and vessel network geometrics, hypertension, cardiometabolic disorders and degenerative age-related disorders have been shown to reduce branching angles, increase tortuosity, and reduce fractal dimensions.[164,173,174]

1.2.4.1.3.   Chemical biomarkers.

Numerous biochemical markers of endothelial function have been identified.[57,77,133] These biomarkers have direct or indirect molecular involvement in physiological pathways related to vascular/endothelial dysfunction and atherosclerosis.[57,82,175,176]

Inflammatory biomarkers include CRP and cytokines such as tumour necrosis factor-alpha (TNF-α) and IL-6.[77,83,132,133] Cytokines are mostly acute phase inflammatory proteins that are involved in regulating the immune response by stimulating the release of other inflammatory-related factors such as CRP and fibrinogen by the liver.[142,177] CRP in particular has been identified as an important marker of inflammation and cardiovascular risk and involved with propagating the inflammatory response through monocyte and adhesion molecule activation during the early stages of atherosclerosis (even at sub-clinical level).[77,142,177]

Adhesion molecules in turn are also reliable markers of endothelial function and atherosclerosis and include VCAM-1, ICAM-1, e-selectin and p-selectin.[71,77] The expression of adhesion molecules is mediated by cytokines (e.g. IL-1) and CRP in regions of inflammation.[76,77,178,179] Adhesion molecules participate in the process of atherosclerosis by promoting monocyte, macrophage and neutrophil recruitment into the arterial intima.[76,77,178,179] Adhesion molecules also play a role in the activation of specific kinases, resulting in transcription factor activation that lead to further cytokine production, increased ROS production and vascular cell proliferation.[77,82,83,125,180]

Cellular growth factors such as VEGF mediate vascular cell proliferation.[181] VEGF plays an important role in endothelial cell migration, proliferation, survival and NO production.[142,181–183] VEGF also functions as a pro-inflammatory cytokine that increases endothelial permeability, induces the expression/activation of adhesion molecules and assists with leukocytes adhesion to endothelial cells.[142,181–183]

Haemostatic factors such as plasminogen activator inhibitor-1 (PAI-1), Von Willebrand factor and fibrinogen are well-established markers of endothelial function and markers of cardiovascular risk.[83,142,176,184] Von Willebrand factor is mostly produced by the endothelium upon endothelial activation and released into blood circulation as a glycoprotein.[77,142,177] Von Willebrand factor, PAI-1 and fibrinogen play a role in promoting endothelial activation, cell adhesion, cell proliferation, vasoconstriction, platelet activation and blood aggregation and coagulation.[77,142,177] These factors have been independently associated with risk for stroke and myocardial infarction.[142,177]

Other biomarkers of cardiovascular risk include numerous ROS and lipid-related factors such as LDL and apolipoproteins (A and B) levels.[142,177] Pro-inflammatory cytokines such as TNF-α and ILs are also known to induce endothelial ROS production.[71,142,177] ROS is a major source of LDL oxidation.[142,177] oxLDL in turn stimulates endothelial monocyte production and promotes macrophage accumulation and foam cell formation in the vascular wall.[142,177] Lipoprotein-A acts similar to LDL as it contains about 40% cholesterol and is thus

considered highly atherogenic and plays a role in endothelial cell activation, macrophages function, cell proliferation and fibrolysis.[142,177]

1.3. Traditional cardiovascular risk factors: Classification and Prevalence.

Traditional cardiovascular risk factors can be classified as controllable/modifiable or uncontrollable/non-modifiable cardiovascular risk factors.[3,7,185] Major controllable cardiovascular risk factors such as hypertension, abnormal lipid levels, smoking, physical inactivity, an unhealthy diet, diabetes, obesity, socioeconomic factors, infection and some pharmaceuticals are relatively well-described in literature.[2,186–188]

Also, uncontrollable cardiovascular risk factors (often related to genetic factors) such as sex/gender and family history of CVD are well-recognised.[189–194] Men, for example, have larger arteries than women while women usually have more apparent stenosis.[192,194] Men in general are more likely to engage in risk behaviors such as smoking and excessive drinking compared to women, while female hormones such as oestrogen predispose women to increased cardiovascular risk as it has been associated with pro-thrombotic effects.[152,194] Ageing alone induces tremendous alterations in cardiovascular physiology and carries major cardiovascular risk in itself.[189,190] Aside from vascular aging, secondary age related factors such as a sedentary lifestyle and dietary alteration/factors also play a role.[195,196]

Despite the complexity of often interlinked pathophysiological pathways of traditional cardiovascular risk factors, ROS production, inflammation and endothelial dysfunction remain the most important junctures where they meet.[109,197,198]

Cardiovascular risk factors are highly prevalent and relevant in the SSA context as the continent has vast socio-, demographic-, ethnic- and economic diversity.[199–203] Income level, education, urban living and psychosocial stress appear to be strong determinants of cardiovascular risk in SSA.[200] Also, a complex relationship between overweight (In some countries up to one third of woman is obese) and underweight exist in SSA with both being highly prevalent.[200]

There are furthermore an estimated 10.8 million people in Africa living with diabetes (8-10% of men and women).[199,200,204] Raised glucose levels are present in an estimated 10% of people while hypertension (systolic blood pressure (SBP) ≥140 mmHg or diastolic blood pressure DBP) ≥90 mmHg) are present in an estimated 35% of men and 28% of women.[199] SSA is also burdened heavily by infectious diseases.[200] Tuberculosis, for example has been shown to contribute to 45% of new pericarditis cases in low- and middle-income countries in the region.[200]

In SA, cardiovascular risk factors are highly prevalent compared to other parts of SSA and comparable to the developed world.[46,198] The South African Heart Foundation reported that an estimated 80% people of over 50 years of age in SA are clinically hypertensive.[205] This rate is the highest in the world.[205] Also, two-thirds of women and one-third of men are overweight or obese (~40% of women and ~11% of men are obese in SA).[205]

An estimated 20% of people in South-Africa are consuming a high-fat diet with 25% of adults present with elevated total cholesterol, a third with elevated LDL-cholesterol and almost one-half low HDL-cholesterol.[205] A furthermore 25% of adults in SA have impaired blood glucose levels with 10% being diagnosed diabetic.[205] Smoking rates are high in both adults and adolescents (20% respectively) (**Figure 1.9.**).[205]

Prevalent Cardiovascular Risk Factors in SA
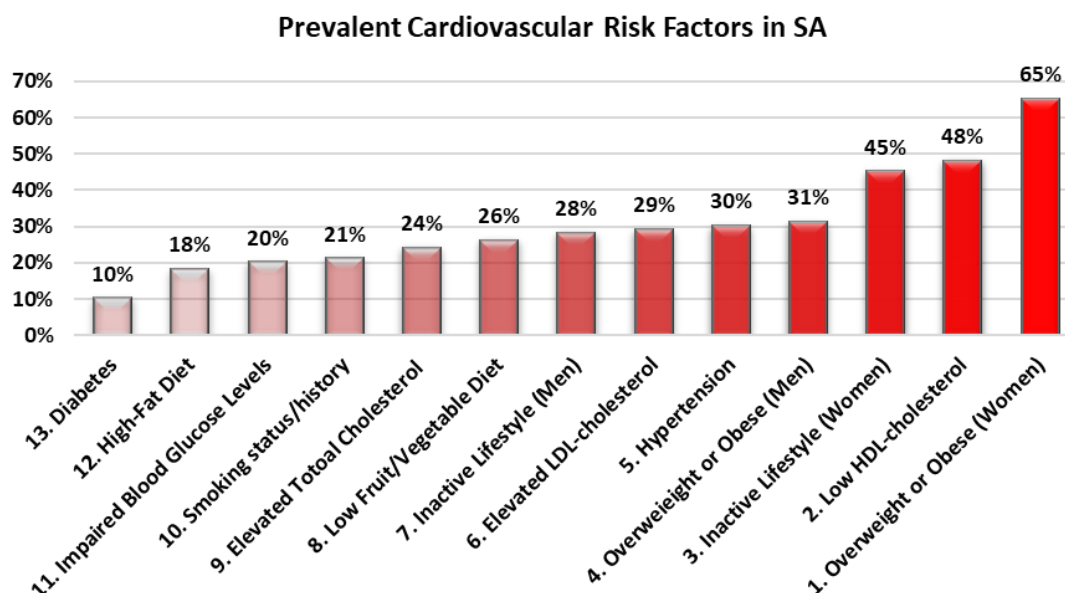
Figure 1.9. Prevalence of prominent cardiovascular risk factors in the SA adult population (more than 15 years of age).[205,206] **Standards: 1 and 4.** BMI (kg/m^2): Normal Weight: 15.5 to 24.9; Overweight: 25 to 29.9; Obese: equal to or more than 30. **2.** Less than 1.2 mmol/L (Less than 1.0 mmol/L in men and less than 1.30 mmol/L in women). **3 and 7.** Based on criteria as described by SANHANES-1. **5.** Systolic blood pressure (SBP) equal to or more than 140 mmHg or diastolic blood pressure DBP) equal to or more than 90 mmHg.[207] **6.** More than 3 mmol/L. **8.** Based on criteria as described by SANHANES-1. **9.** More than 5 mmol/L (Triglycerides: more than 1.7 mmol/L). 10. Currently smoking or history of smoking. 11. Glycated haemoglobin (HbA1c) equal to or more than 6.1% 12. Based on a dietary fat score as described by SANHANES-1.[206] **13.** Random blood glucose level more than 7 mm/L or HbA1c equal to or more than 6.5%. Figure designed by the author of this dissertation based on content from [206,207]. **Abbreviations:** BMI: Body mass index; SBP: Systolic blood pressure; DBP: Diastolic blood pressure; HDL: High-density lipoprotein cholesterol; LDL: Low-density lipoprotein cholesterol.

The Heart of Soweto Study highlighted the prevalence of cardiovascular risk factors in the SA urban setting and described it as "a ticking time bomb".[46] In 1600 subjects (65% women) with a mean age of 46 years about 78% of the subjects had at least 1 major cardiovascular risk factor present.[46] The most prevalent risk factors were obesity (total 43%; men *vs.* women (23% *vs.* 55%), hypertension (33%), elevated glucose (14%) and elevated cholesterol (13%).[46]

In the Bellville area of Western Cape province, a large population-based study (*n* = more than 500) reported highly prevalent cardiovascular risk factors across different age groups.[208] Smoking was highly

prevalent in the younger age group (63%: 20 to 30 years of age) compared to the older age group (44%: 51 to 60 years of age).[208] The obesity (BMI equal to or more than 30 kg/m^2) rate was high in middle-aged subjects (20% in 20-30 years of age, 44-52% in 31-60 years of age) while the incidence of overweight (BMI equal to or more than 25, less than 30 kg/m^2) was similar across all age groups (range 25 to 30%).[208] The mean SBP increased across age groups from 113 mmHg (20 to 30 years of age) to 126 mmHg (51 to 60 years of age).[208] Reports from other parts of SA have made similar findings.[201–203]

1.4.   Cardiovascular disease epidemiology.

At the beginning of the 20th century, CVD was responsible for less than 10% of global mortality.[188,209] In 2008, 39% of NCD deaths (36 million) under the age of 70 were due to CVD, while 2010 witnessed about 17 million deaths (48% of all NCD deaths) due to CVD.[2,3,210] Although CVD has substantially decreased in high-income countries over the last 20 years (due to population wide intervention strategies), it remained the biggest contributor to mortality and morbidity in the world with low- and middle-income countries disproportionately affected (representing 80% of CVD mortality worldwide).[2–4] Ischaemic heart disease specifically remained the most prominent contributor to global mortality in 2010 (13 million deaths due to ischaemic heart disease (13.3% of total global deaths, an increase of about 26%-35% from 1990).[3,211] Recent WHO figures (2016) report 17.9 million deaths occurred globally due to CVD (More than 75% from low- and middle-income countries).[212] Global projections furthermore indicate an increase of 6 million deaths due to CVDs over the next two decades (to about 23.9 million) with ischaemic heart disease expected to remain one of the three biggest contributors to the global burden of disease.[213,214]

SSA is in the earlier stages of epidemiological transition that is characterised by a dual burden of both infectious diseases and NCDs.[215] Almost 80% of global NCD and CVDs occur in low- and middle-income countries (mostly represented by SSA countries) and rates are rising most rapidly in SSA compared to other regions.[46,200,210,215] These trends suggest that CVD is evolving into a major public health issue in Africa.[4,200,216] More specifically, the WHO projected a doubling of ischaemic heart disease in the SSA Region by 2030.[204] In SA, CVD is the second largest cause of death (following HIV/AIDS) with an estimated 1/6 deaths (215 deaths/day) in SA caused by CVD (more than 17% of total deaths) (**Figure 1.10.**).[205]
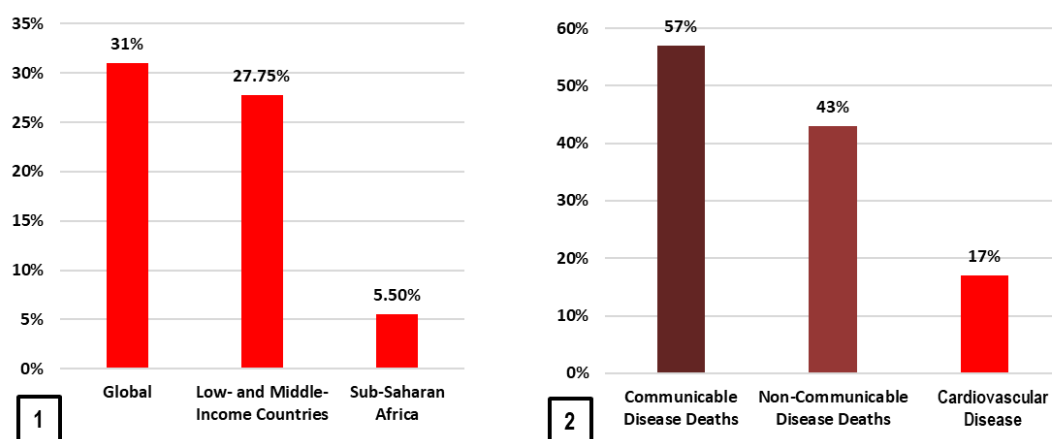
Figure 1.10. The burden of CVD **(1)** globally, regionally and **(2)** in South Africa. Figure designed by the author of this dissertation based on content from [205,217,218]. **Abbreviations:** CVD: Cardiovascular disease.

1.5. Emerging cardiovascular risk factors: HIV-infection and ART.

1.5.1. Background.

HIV/AIDS was first described by the Centres for Disease Control and Prevention (United States of America (USA) in 1981.[219–222] While unexplained immunodeficiency and associated opportunistic infections continued to emerge between 1981 and 1983, the causal factor remained unknown, but sexual behaviour was quickly implicated.[219,221] The human immunodeficiency (HI) virus (HI-virus) was finally isolated and identified by French scientists and confirmed as the cause of AIDS in 1984.[219–221] Since the discovery of HIV, two types of HIV-infections were identified.[219,221] HIV type-1 (HIV-1), a virus that was thought to have crossed the animal-to-human barrier in Western Africa, was identified as the main cause of the HIV/AIDS epidemic.[221] HIV type-2 (HIV-2) was also identified soon after and was thought to have originated in central/Western Africa, but is rarely found outside central Africa.[219,221,223]

The rapid spread of HIV/AIDS in the 1980's across the world resulted in a massive upscaling of international efforts to fight the disease.[219,221] HIV/AIDS singlehandedly reformed the architecture of global health and healthcare systems.[219,221] A significant breakthrough in HIV-treatment came when different classes of ART were developed.[219,220,224] Zidovudine was the first ART approved for human use.[225]The first protease inhibitor (PI; saquinavir) was approved in 1995, but bioavailability was low while high doses needed to be administered that led to low tolerance (metabolized by the cytochrome 3A4 isoenzyme of the CYP450 system).[224] Nevirapine, was the first non-nucleoside reverse transcriptase inhibitor (NNRTI) approved (1996), but drug resistance was highly prevalent when administered as a monotreatment.[219,220,224] Another PI, Indinavir, was approved in 1996 and set a new hallmark in HIV-treatment when it was realised that combination ART (also known as highly active antiretroviral therapy (HAART)) was effective in controlling viral replication and that a triple combination ART drug-treatment regime was most often completely viral-

suppressive.[219,220,224,226] Combination ART quickly revolutionised HIV-care and ultimately changed HIV from a fatal infection into a chronic, but manageable disease that required lifelong treatment.[220,224] More than 30 anti-HIV-1 drugs are currently approved and used in the fight against HIV-infection.[220,224,227] Enormous international efforts are still currently continuing to reach 100% coverage across the globe.[228,229]

Although ART treatment was successful in controlling HIV replication and substantially improve the longevity of PLWH, drug toxicity has remained a concern, and reports on HIV- and ART-associated co-morbidities started to emerge.[230–232] Currently, CVD in PLWH has become a major cause of morbidity and mortality and accounting for about one-third of serious non-AIDS conditions and at least 10 % of deaths.[223] A recent study found that the relative risk for developing CVD was 1.61-fold higher in HIV-infected patients without ART compared to HIV-infected patients on ART-treatment, and 2-fold higher in HIV-infected patients receiving no ART-treatment compared to HIV- and ART-naïve controls.[20]

Although not fully understood, increased exposure to traditional cardiovascular risk factors (as a result of improved longevity and risky lifestyle), the HI-virus itself, ART drug toxicity, as well as HIV- and ART-associated comorbidities (e.g. lipodystrophy and dyslipidaemia) appear to play a role (**Figure 1.11.**).[7,20,21,233]
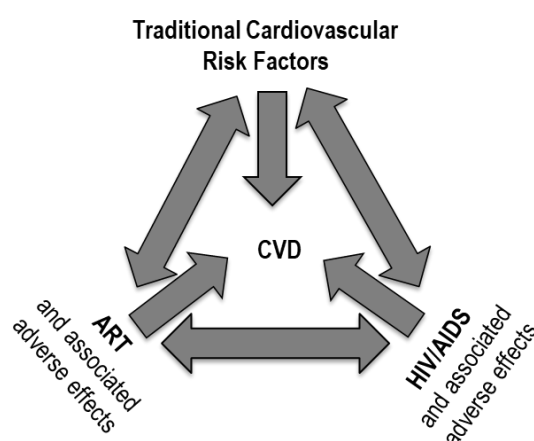
Figure 1.11. Major factors contributing to CVD in PLWH. Figure designed by the author of this dissertation based on content from [7,18,19]. **Abbreviations:** CVD: Cardiovascular disease, ART: Antiretroviral therapy, HIV/AIDS: human immunodeficiency virus/acquired immunodeficiency syndrome.

1.5.2.   The HI-virus: Structure and lifecycle.

HIV-1 is a conical shaped retrovirus with a capsid length of 100-120 nm and width of 50-60 nm that can cross the nuclear membrane and insert its genome into metabolically active, non-dividing cells.[234,235] HIV-1 can cross the nuclear membrane of circulating cluster of differentiation-4$^+$ T-lymphocyte cells (CD4 cells) independently of mitosis (indicating an active process rather than passive).[234,235] The HIV-capsid (essential for

infectivity) contains two single ribonucleic acid (RNA) strands, and viral proteins such as reverse transcriptase and integrase.[234–236] After the HI-virus gains access to the body (through bodily fluid transfer), it starts its lifecycle by binding to a CD4 cell receptor and its lifecycle ensues (**Figure 1.12.**).[227,235–238]
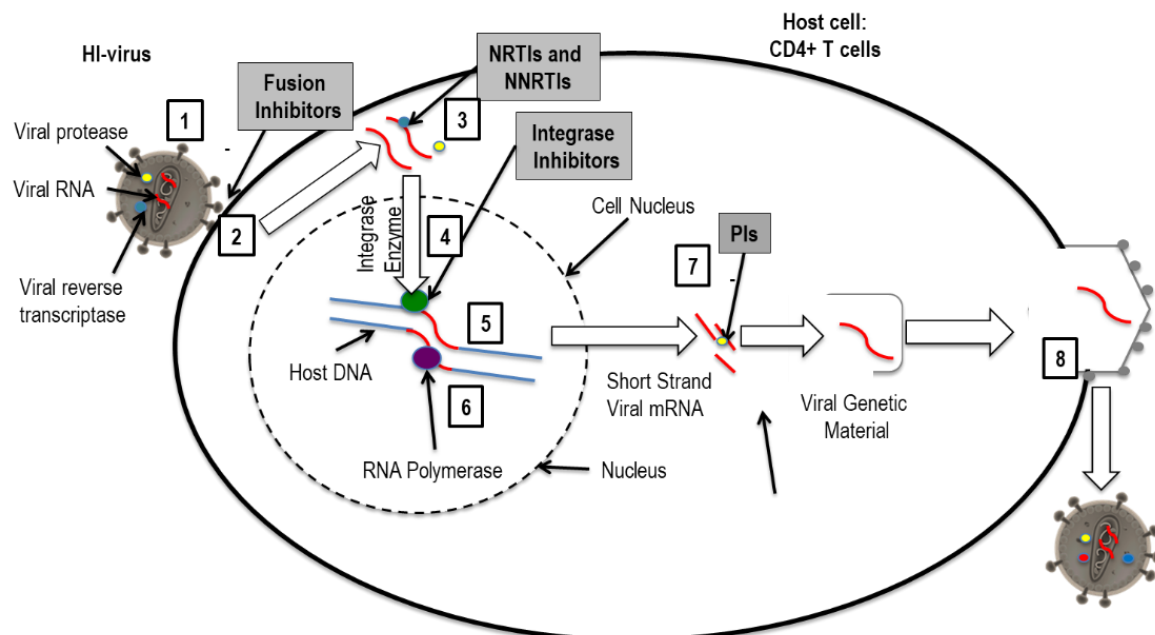
Figure 1.12. Lifecycle of the HI-virus with key steps blocked by ART drug classes. **Description: 1.** Fusion with cellular membrane of host cell mediated by HIV-1 envelope glycoprotein-120 (gp120) subunit (Target for fusion inhibitor ART). **2.** Uncoating: release of viral genetic material (ribonucleic acid) into host cell cytoplasm one hour after fusion. **3.** HIV reverse transcriptase enzyme converts the single-strand virus RNA into double-strand linear HIV DNA 3-4 hours after fusion (Target for reverse transcriptase inhibitor ART). **4.** Integration: Viral pre-integration complex crosses the nuclear membrane, and integrase enzymes catalyse integration of the viral DNA into the host's own DNA 15-20 hours after fusion (Target for integrase inhibitor ART). **5.** Integrated HIV DNA may remain inactive for a period of time (even several years) until the host cell becomes activated (encounters a recall antigen or certain types of cytokines). **6.** Transcription activation: RNA-polymerase replicate the HIV genomic material including messenger RNA (mRNA). **7.** The HIV protease cuts HIV proteins into smaller HIV proteins (Target for protease inhibitor ART). **8.** Budding: Newly formed HIV pushes out from the host cell. Figure designed by the author of this dissertation based on content from [227,235–238]. **Abbreviations and symbols:** HIV: Human Immunodeficiency virus; RNA: Ribonucleic acid; DNA: Deoxyribonucleic acid; PI: Protease inhibitor; NRTI: Nucleoside reverse transcriptase inhibitor; NNRTI: Non-nucleoside reverse transcriptase inhibitor; **-** = Inhibit.

The acute phase of HIV-infection is the initial phase when a burst of viremia is experienced.[223] HIV antibodies remain undetectable during the acute phase with only about 65% of infected individuals experiencing acute retroviral syndrome (fever, lymphadenopathy, pharyngitis, skin rash, myalgias and/or arthralgias).[223] Without treatment, HIV-1 most commonly develops into AIDS in less than 7 years from inital infection occurred while death offen occurs within 3 years once detected.[222]

1.5.3.   Antiretroviral therapy (ART).

1.5.3.1.   ART treatment guidelines.

ART drugs are designed to block key steps during viral replication in an ultimate attempt to suppress viral replication (**Figure 1.12.**).[227,239,240] Although highly successful in controlling viral replication, ART cannot eradicate the virus or its DNA from the host.[220,224,227] A single ART is also not successful in treating HIV/AIDS as HIV-1 shows high genetic variability and is capable of quickly developing resistance against single ART treatment.[223,236] For more potent viral suppression and to prevent the HI-virus from becoming drug-resistant, ART-drugs are administered in a combination of at least three different ARTs from at least two different drug-classes.[227,241,242]

According to WHO guidelines, ART treatment should be initiated when CD4 count is ≤500 cells/mm^3 with a first-line ART combinations containing tenofovir (an NRTI) + lamivudine (an NRTI) or emtricitabine (an NRTI) + efavirenz (an NNRT) and if plasma HIV RNA reaches more than 1000 copies/ml a second-line ART-combination consisting of two NRTIs + a ritonavir-boosted PI for adults.[243] These combination recommendations are also followed by the SA Government for its Government-sponsored ART programme; however, a strategy has recently been implemented to provide ART treatment for all PLWH regardless of CD4 count or viral load.[244] Similar to the WHO guidelines, the South African Government also recommends a first line ART treatment combination containing two NRTIs and one NNRTI (tenofovir + emtricitabine (or lamivudine) + efavirenz (preferred)), and a PI-containing combination (zidovudine + lamivudine + lopinavir booster with ritonavir (lopinavir/r)) for second-line treatment (Patients with anaemia and renal failure switch to abacavir (an NRTI).[245] First-line ART fixed-dose combination preparations containing tenofovir / emtricitabine / efavirenz are widely used in SA and available as Atripla™ or Odimune™ and the second-line PI-containing ART contains lopinavir/r is available as Aluvia™.[240,246–248]

1.5.3.2.   Major ART drugs and drug classes: Mechanism of action and adverse effects.

Major ART drug classes include the NRTIs, NNRTIs, PIs, fusion inhibitors and integrase inhibitors. Generally, the NRTIs, NNRTIs and PIs are most commonly prescribed.[223,245] NRTIs inhibit HIV viral replication by actively inhibiting HIV-1 reverse transcriptase (incorporated into nascent viral DNA that leads to chain termination; **Figure 1.12. number 3**).[240,249,250] NNRTIs block HIV replication by binding adjacent to the active site (hydrophobic pocket) of the HIV reverse transcriptase.[240,250] This conformational change inhibits reverse transcriptase to add nucleosides to the DNA chain, thus preventing viral DNA transcription from being completed.[240,250] HIV protease plays a critical role in the HIV lifecycle and is responsible for HIV virion cleavage.[227,240] PIs inhibit viral replication by binding to the HIV protease enzyme's active site that renders it inactive (**Figure 1.12. number 7**).[240,251]

Efavirenz (Sustiva™) is a NNRTI that is commonly selected as a first-line ART drug for HIV-1 in SA.[252–254] It diffuses into the cells and binds next to the active site of reverse transcriptase.[252–254] Efavirenz is highly plasma protein-bound (predominantly albumin) and the CYP450 enzyme system (mostly isozymes CYP3A4 and CYP2B6) is responsible for its metabolization (hydroxylated metabolites that undergo glucuronidation).[240,252–254] Efavirenz has a long half-life (52-76 hours for oral administration) and has been associated with increased non-fasting total cholesterol (~20%) and HDL (~25%) levels in treated patients.[252–254] Efavirenz is also strongly associated with mitochondrial toxicity and central nervous system (CNS) effects (neuronal toxicity through metabolite 8-hydroxy-efavirenz) and with mood and sleep disorders often reported.[240,255] Possible ART associated neuronal effects involve pathways related to brain creatine kinase depletion, calcium haemostasis alterations, mitochondrial toxicity and inflammation.[255,256]

Various NRTIs are available commercially (abacavir, emtricitabine, didanosine, lamivudine, stavudine, and zidovudine.[240,257] Emtricitabine (Emtriva™) is a synthetic nucleoside (dideoxycytidine) analog (structure and resistance similar to lamivudine.[258–261] Cellular enzymes phosphorylate emtricitabine to emtricitabine-5'-triphosphate which in turn competes with the natural substrate, deoxycytidine 5'-triphosphate.[258–261] Tenofovir (Viread™) is an acyclic nucleoside phosphonate diester analogue of adenosine monophosphate.[262,263] It requires initial diester hydrolysis to convert to tenofovir, then phosphorylated by cellular enzymes and subsequently converted into active tenofovir diphosphate.[258–261] As is the case with emtricitabine, tenofovir diphosphate inhibits HIV-1 reverse transcriptase (competitor for natural substance deoxyadenosine 5'-triphosphate) and leads to DNA chain termination after incorporated into the viral-DNA.[258–261] Tenofovir is associated with increased fat absorption and increased plasma lipid concentrations.[258–261]

Various PIs are also commercially available (saquinavir, lopinavir, darunavir, indinavir, tipranavir, atazanavir, nelfinavir, and RTV).[227,240] The hepatic enzyme CYP3A4 is mostly responsible for metabolizing PIs.[264] PIs are strongly associated with dyslipidaemia (increased hepatic clearance of LDL) and other metabolic diseases such as insulin resistance, type-II-diabetes and lipodystrophy.[265–267] lopinavir/r forms part of the South African Government's recommended second-line ART combination.[245,268] Ritonavir (Norvir™) has low gastrointestinal tolerance and is therefore administered at a lower dose, but with a PI-booster for example lopinavir (increase plasma concentrations and decrease and pill burden and cytochrome enzyme metabolism).[241,269,270] Lopinavir/r is co-formulated as Kaletra™ or Aluvia™.[271,272] Lopinavir and ritonavir are both metabolized by CYP3A4 and associated with hypertriglyceridemia.[240,273]

1.5.4. Markers of HIV/AIDS disease progression/status: Viral load and CD4 cell count.

Viral load represents the quantity of viral RNA copies in a given blood serum volume and is directly related to viral activity/replication.[223,274,275] The HI-virus is also known to target CD4 cells (hence its ability to cause

immune deficiency) and therefore CD4 cell count is often inversely related to viral load.[276,277] Viral load and CD4 cell count have important prognostic value in terms of monitoring the status of HIV/AIDS disease progression and ART post-treatment response.[223] The EuroSIDA collaboration found (after adjustment for age, region, and ART) that non-AIDS health events were 61% (p = 0.001) and 66% (p = 0.004) higher respectively in participants with viral loads 500 to 9999 copies/ml than in individuals with viral loads less than 500 copies/ml.[223] CD4 count on the other hand is a strong indicator of the state of immune function and therefor often directly associated with developing HIV-associated malignancies including cancers (lung, anal, oropharyngeal, liver and skin), intraepithelial neoplasia (papilloma virus-related), Kaposi sarcoma, melanoma and non-Hodgkin lymphoma.[223]

1.5.5.   Epidemiology of HIV/AIDS and coverage of ART treatment.

HIV/AIDS has become a major cause of global mortality in a relatively short period of time and one of most prominent infectious diseases that confronted civilisation in the 21st century.[222] Estimating global mortality due to HIV/AIDS is very difficult, as mortality is often not reported as being linked to HIV/AIDS status.[228,278] Nonetheless, the WHO estimated that at the height of the HIV-epidemic (around 2000) 15 000 people became HIV-infected each day, 8000 people died each day and that 25 million people were HIV-infected in the world.[228,278,279] In 2004 alone, HIV- and tuberculosis-mortality combined amounted to 3.5 million deaths worldwide (5th leading cause of the Global Burden of Disease (GBD)).[228,278] By 2008, the WHO estimated that about 60 million people had become infected with the HI-virus since its discovery.[222] The Joint United Nations Programme on HIV and AIDS (UNAIDS) reported in 2012 that more than 35 million people have already died as a result of AIDS since the pandemic started and that a further 35.3 million were living with the disease.[228,280] Due to the success of ART and up-scaled ART coverage efforts, the number of AIDS deaths declined by 1.6 million in 2012 compared to 2.3 million in 2005.[280] Also in 2012, 9.7 million PLWH in low- and middle-income countries (7.6 million people in SSA) had access to ART (61% of all who were eligible according to the 2010 WHO HIV treatment guidelines).[224,281]

More recent estimated data (2017) from UNAIDS show that 36.9 million were living with HIV/AIDS, 21.7 million PLWH had access to ART, 1.8 million people became newly infected (77.3 million in total have become infected since the discovery of HIV) and 0.94 million peopled died of HIV that year (35.4 million total deaths since the discovery of HIV) across the world (**Figure 1.13.**).[282]
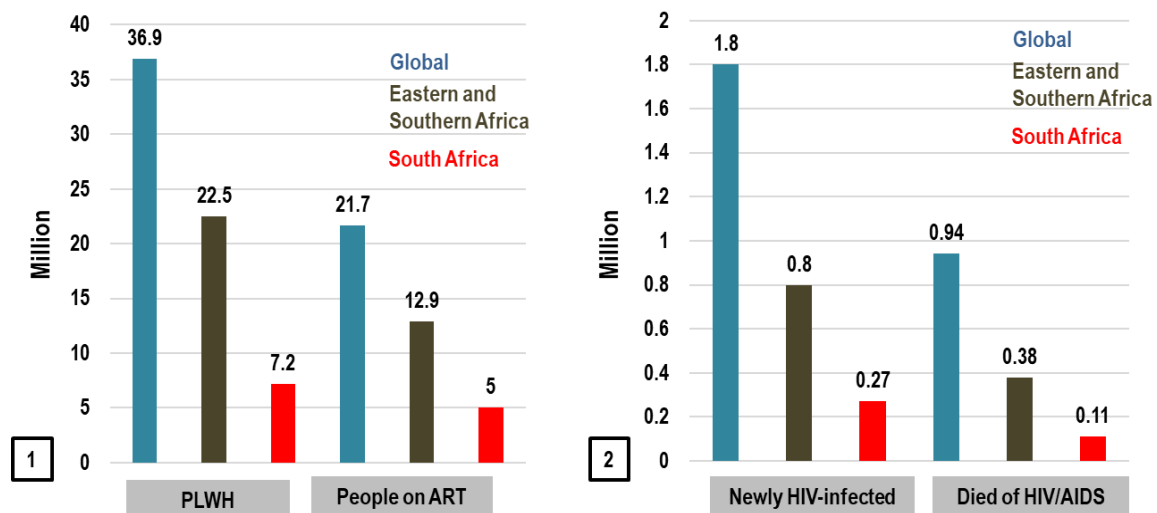
Figure 1.13. Burden of HIV/AIDS according to UNAIDS for 2017 presented on global, regional and local level. **Description: 1.** PLWH and PLWH on ART. **2.** New HIV-infections that occurred and people who died of HIV/AIDS in 2017. Figure designed by the author of this dissertation based on content from [282,283]. **Abbreviation:** HIV/AIDS: HIV/AIDS: human immunodeficiency virus/acquired immunodeficiency syndrome; PLWH: People living with HIV; ART: Antiretroviral therapy.

The vast majority of PLWH reside in developing countries (34 million).[5,222,223,228] The WHO estimated in 2001 that 3.4 million people from SSA were HIV-infected (700 000 children less than 15 years of age), 2.3 million HIV/AIDS-associated deaths occurred, and that the region accounted for more than 75% of the 20 million HIV-related deaths global deaths since the HIV/AIDS epidemic started.[5,222,228] Recent UNAIDS figures (2017) for Eastern and Southern Africa estimated that 19.6 million people lived with HIV, 12.9 million PLWH has access to ART, 0.8 million people became newly infected and 0.38 million people died of HIV/AIDS that year.[282] HIV/AIDS currently remains the leading burden on health in SSA with more than 22.5 million people living with HIV on the continent and a 40% higher burden per capita for women than for men aged 15-59 years of age in the region.[5,222,228]

SA has the largest population of PLWH in world and has the largest Government supported ART treatment programme.[229,283] An estimated 7.1 million people are living with HIV/AIDS in SA and represents about 18% of the South African population ages 15 to 49 years of age.[283,284] Despite ART being freely available in SA and large preventative measures by the SA Government, more than 100 000 HIV/AIDS deaths still occur each year while more than 250 000 people become newly infected.[283,284] It is estimated that only 61% of HIV-infected adults and 58% of HIV-infected children (less than 15 years of age) in SA are on ART treatment.[283,284]

1.5.6. The HI-virus, endothelial dysfunction and CVD.

The effects of the HI-virus on the cardiovascular system were recognised early on in the HIV-epidemic during the pre-ART era.[285,286] Cardiomyopathy and pericarditis in HIV/AIDS patients were reported in the early 1990's during the pre-ART era.[287–289] Studies that reported progressive atherosclerotic lesions in young men (mean age of 31 years) who died of AIDS soon followed.[285] Other early pre-ART post-mortem reports noted an increase in the frequency of dysplasia in coronary arteries in people who died of AIDS compared to controls.[290] Also, direct associations between CVD, uncontrolled HIV viremia (untreated viral load) and immune (dys)function (CD4 cell depletion) have been found.[19,291,292]

The HI-virus is a well-adapted virus that can enter the host undetected, infects numerous types of cells and take advantage of the hosts cellular machinery to replicate.[292] The main target cells for the HI-virus are CD4 cells, monocytes and macrophages.[292] Other target cells include cells that are sensitive to viral infections such as endothelial cells, but do not play an major role in HIV replication.[292] As the vascular endothelium serves as the interface between circulating blood and underlying tissue, it is vulnerable to HIV-associated effects/factors and may play an important role HIV-related CVD.[293–295] Although the exact mechanism involved is not fully understood, viral proteins such as gp120, trans-activator of viral replication (Tat) and HIV-1 negative factor (Nef) proteins have been implicated in pro-atherosclerotic events such as increased levels of inflammatory cytokines and chemokines (e.g. interferon-alpha and -γ, TNF-α, CRP, IL-1, -6, -8, -10, -15 and -18, monocyte chemoattractant protein-1 (MCP-1) and C-C motif ligand-2 (CCL2)), vascular adhesion molecules (e.g. soluble VCAM-1, soluble ICAM-1, e-selectin and p-selectin), hemostatic and fibrinolytic factors (e.g. von Willebrand factor, tissue plasminogen activator (t-PA) and PAI-1)(**Figure 1.14.**).[23,25,103,292,295–314]
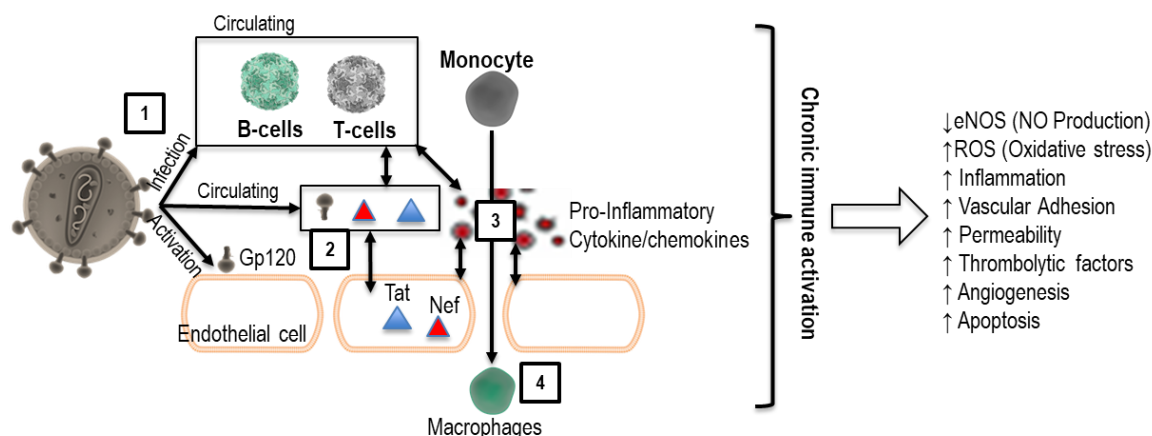
Figure 1.14. HIV-viral factors associated with chronic immune activation and cardiovascular risk. **Description**: **1**. Circulating HIV virus infects immune cells. **2**. Viral factors such as gp120, Tat and Nef activate endothelial and immune cells. **3** Activated endothelial cells and immune cells increase circulating pro-inflammatory cytokines and the expression of vascular adhesion factors are upregulated. **4**. Macrophage recruitment into the vascular wall is increased and vascular inflammation increased. Figure designed by the author of this dissertation based on content from [240,286,292,293,295,304]. **Abbreviations and symbols**: eNOS: Endothelial nitric oxide synthase; ROS: Reactive oxygen species; NO: Nitric oxide; Tat: trans-activator of viral replication. Nef: HIV-1 negative factor; Gp120: HIV-1 envelope glycoprotein-120.

HIV **gp120** is a glycoprotein expressed on the surface of the HI-virus and infected cells.[293–295] Gp120 plays an important role in the fusion process (*via* CD4 receptor C-X-C chemokine receptor type-4 (CXCR4) and C-C chemokine receptor type-5 (CCR5)) between the HI-virus and the host cells.[293–295] Soluble gp120 can also circulate freely in blood.[293–295] Gp120 has been implicated in numerous atherosclerotic process such as inflammatory cytokine production (IL-6 and IL-8), hepatic CRP synthesis (IL-6 mediated), ROS production, endothelium adhesion molecule expression (e-selectin, ICAM-1 and VCAM-1), monocyte/macrophage recruitment (IL-6 and IL-8 mediated) and translocation (*via* adhesion molecules), increased endothelium permeability, increased expression of endothelial damaging matrix MMP-2 and MMP-9 and apoptosis.[293–295]

The cellular signalling pathways involved in gp120-associated endothelial toxicity are not well described, but activation of protein kinase C (PKC), mitogen-activated protein (MAP) kinase signalling and upregulation of the bcl-2-like protein 4 (Bax) gene have been identified.[293] Gp120 has also been shown to indirectly reduce endothelial NO production or through upregulation of endothelin-1 release.[293,315] As a result of the reduction in NO bioavailability, proliferation/migration of smooth muscle cells are initiated, vasoconstriction promoted and platelet adhesion/aggregation enhanced.[293–295]

Tat protein regulates and promotes HIV viral transcription in monocytes/macrophages and T/B-cells and is released *via* these cells even during ART viral suppression.[293,316] Tat has been implicated as a pro-cytokine with endothelial cell modulating properties that include enhanced membrane transduction.[293] Once bound to the

endothelial cell receptors, Tat has been shown to activate cytokine, inflammatory mediators and adhesion molecule production (e.g. IL-1β, MPC-1, VCAM-1 and e-selectin *via* NF-κB), increase ROS production (*via* NADPH oxidase activity) and permeability, and upregulate other pathways related to angiogenesis or apoptosis.[293–295] Tat appears to be a potent pro-angiogenic and proliferative factor trough fibroblast growth factor-2, reservation against cancellation gene 1 (Rac1) activation (*via* P21 activated kinase-1 and c-Jun N-terminal kinase (JNK)), and NADPH oxidase activation pathways.[293–295] Tat may mediate endothelial cell apoptosis (also observed in cardiomyocytes) though increasing TNF-α production.[292,293]

Nef protein is an adapter protein with numerous domains utilised during HIV molecule and host cell molecule interaction signalling.[293–295] Nef is mostly transferred from circulating monocytes and CD4 cells to the endothelial cell and found both intra- and intercellular.[293–295] Nef has been implicated in cellular apoptosis (*via* fas by fas ligand pathways).[293] It has furthermore been demonstrated that Nef can increase endothelial-derived ICAM-1 expression (*via* extracellular signal-regulated kinase (ERK) pathway) and Mesenchymal precursor cell-1 (MPC-1) production (*via* NF-κB signalling pathway).[293–295] Nef has also been shown to activate caveolin-1 in endothelial cells resulting in decreased HDL-mediated cholesterol efflux and increase foam cell production through macrophage activation.[292,293]

Indirect HIV-associated cardiovascular consequences including metabolic disorders such as dysregulated lipid levels (hypercholesterolemia: elevated very LDL (vLDL) and triglycerides with lower levels of protective HDL).[302,306–308] The decrease in HDL cholesterol levels usually appears during the early stages of HIV-infection and evidence suggests that it may, at least in part, be a result of thrombotic activity.[314,317] Increased levels of triglycerides and vLDL cholesterol often appear during a later stage in disease progression in conjunction with signs and symptoms of AIDS and may be the result of increased hepatic lipogenesis and impaired clearance of lipids from the blood.[314,317–321] Viral proteins such as Nef may be involved in HIV-dyslipidaemia through inhibition of cell surface cholesterol transporters (e.g. adenosine triphosphate (ATP)-binding cassette transporter-1 (ABCA1)) that subsequently causes impaired hepatic cholesterol efflux.[322–324] On the other hand, the process of HIV-replication also requires cholesterol and may partially contributed to HIV-associated lipid level dysregulation.[322,323]

Other prevalent HIV-associated adverse effects that may contribute to CVD in PLWH include renal and haematological dysfunction.[325–327] Direct infection of kidney cells and chronic HIV-associated immune/inflammation have been linked to renal impairment in PLWH.[325–327] HIV-associated anaemia is also commonly observed and may be the result of the effects the HI-virus has on haematopoiesis (reduction in erythropoietin concentration and bone marrow suppression by HIV-associated cytokines and immune destruction).[328–330]

1.5.7.   ART, endothelial dysfunction and CVD.

Although ART alleviates some viral-associated effects on cardiovascular health, major ART drug classes such as PIs, NRTI and NNRTIs have been independently associated with increased risk for CVD.[20,321,331] The Data Collection on Adverse Events of Anti-HIV Drugs (DAD) is one of the largest studies (multinational involving 33 000 patients) to examine the relationship between ART and adverse cardiovascular events.[332] One of the major initial findings of the DAD Study was showing an association of ART, especially PIs, with a 16% increased risk for myocardial infarction for each year of ART treatment.[333] The DAD Study also reported that PIs were associated with 1.05, NRTIs with 1.11 and NNRTIs with 1.04 risk ratio for adverse cardiovascular events for each year of ART use.[331] The DAD Study also examined the risk for myocardial infarction in terms of individual ART drugs.[334] PIs such as indinavir was associated with a risk of 1.12 for myocardial infarction, while no significant association was observed with saquinavir and nelfinavir.[334] Recent use (within 6 months) of the NRTIs abacavir and didanosine was associated with a risk ratio of 1.68 and 1.41 for myocardial infarction respectively per year of use, while tenofovir showed no significant association.[334]

Although the undesired side-effects of ART have been directly implicated in adverse cardiovascular health, ART-associated metabolic derangements appear to contribute greatly to CVD in PLWH and that organ systems involved in the ART metabolic pathway such as the kidneys and liver are mostly affected (**Figure 1.15.**).[334–336]
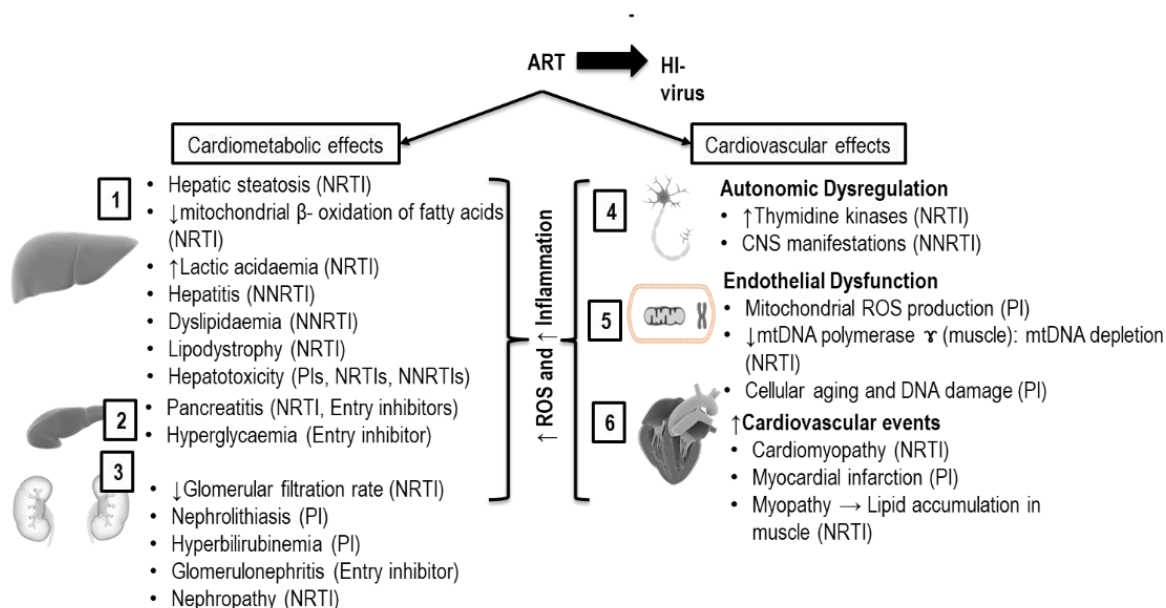
Figure 1.15. Direct cardiovascular effects and cardiometabolic effects of ART. **Description: 1.** Hepatic effects. **2.** Pancreatic effects. **3.** Kidney effects. **4.** Neuronal effects. **5.** Vascular effects. **6.** Cardiac effects. Figure designed by the author of this dissertation based on content from [25,240,300,334–338]. **Abbreviations and symbols:** ART: Antiretroviral therapy; HIV: Human immunodeficiency; CNS: Central nervous system; PI: Protease inhibitor; NRTI: Nucleotide reverse transcriptase inhibitor; NNRTI: Non-nucleoside reverse transcriptase inhibitor. ROS: Reactive oxygen species; DNA: Deoxyribonucleic acid; mtDNA: Mitochondrial DNA; ↑: Increase; ↓Decrease.

Long-term use of all major ART-classes (PIs, NRTIs and NNRTIs) has been associated with liver dysfunction and appear to affect 30-40% of HIV patients.[339–342] ART-associated hepatic morbidities include hepatomegaly, liver fibrosis, liver cirrhosis, non-alcoholic fatty liver disease, hepatic steatosis and elevated liver enzymes such as γ–Glutamyltransferase (GGT), a non-specific marker for liver disease.[340] Due to its central role in lipid metabolism, hepatic dysfunction in PLWH is also often associated with abnormal lipid levels that represent a pro-atherosclerotic profile with increased LDL and decreased HDL concentrations.[231,343–345] Also, secondary effects related to the liver and kidneys such as dysregulated cholesterol, triglyceride and glucose metabolism are often observed in PLWH on ART.[334,346–349] These ART-associated metabolic abnormalities are well-known cardiovascular risk factors.[25,222,350,351]

In the vasculature, available evidence suggests that ART-induced endothelial dysfunction appears to be related to decreased NO production as a result of reduction in NOS expression and/or increased production of ROS such as hydrogen peroxide.[305,352] PIs in particular have been linked to the pathogenesis of endothelial dysfunction, whereas NRTIs and NNRTIs seem to be less detrimental to vascular health.[25,308,337,353] PIs have also shown to inhibit human aspartyl proteases (homology to the catalytic site of HIV-1 protease to which all PIs bind) and LDL receptor-related protein (LRP).[25] On the other hand, NRTIs may contribute to endothelial

dysfunction as a result of mitochondrial toxicity and their associated pro-atherogenic lipid profiles and insulin resistance (*via* inhibition of the enzyme glucose transporter type 4 (GLUT4).[226,314,354]

1.6. Emerging cardiovascular risk factor: Air pollution.
1.6.1. Background.

Air pollution broadly denotes the harmful heterogeneous mixture of solid, liquid and gaseous substances in the Earth's atmosphere.[8,355,356] Air pollution has emerged globally as a major environmental and health concern in both developing and developed countries with an estimated (WHO) 80% of people living in cities (population more than 100 000) breathing polluted air (levels that exceed recommended standards).[28,357]

Inhalable air pollution can be classified according to particle size as particulate matter (PM) or gaseous pollutants.[358,359] The aerodynamic equivalent diameter of coarse PM is between 2.5 and 10 μm (PM_{10}), fine PM ≤2.5 μm ($PM_{2.5}$) and ultra-fine PM ≤0.1 μm ($PM_{0.1}$).[358–360] Gaseous pollutants are the smallest pollutants with aerodynamic equivalent diameter in the nanometer range.[358,359] The smaller the pollutant molecule the more readily it can enter the body and cause adverse effects.[358,359,361] PM_{10} is thus mostly associated with upper respiratory tract effects while small ambient air pollutants can passively enter the blood circulation during respiration and disseminate throughout the body, even at the cellular and nuclear level.[26,362–366]

The WHO has also identified small pollutants such as NO_2, BTEX and $PM_{2.5}$ as air pollutants that are most dangerous to public health.[36,367] These pollutants are mostly produced as a result of the incomplete combustion of fossil fuels during industrial, vehicle and household activities and are therefore also considered to be a good indicator of combustion-related emissions.[34,368]

Air pollution, especially gaseous pollutants, has been associated with various adverse health effects including increased mortality.[369–371] Gaseous pollutants such as NO_2, and aromatic hydrocarbons (e.g. BTEX) appear to be particularly relevant in the development of adverse health outcomes.[36,372] Although these chemical components present in ambient air have also been implicated in adverse cardiovascular outcomes such as autonomic nervous system toxicity (dysregulation of vascular tone and heart rate), and pro-atherosclerotic processes (e.g. oxidative stress, inflammation, and endothelial dysfunction), the specific contributions and underlying mechanisms of individual components are not well understood.[26,38,39,373–376] Gaseous pollutants, such as benzene, are also strongly associated with cancer and furthermore linked to structural and functional genomic alterations such as telomere shortening (marker for pre-mature molecular ageing), mtDNA depletion (marker of mitochondrial damage and insufficient cellular energy production) and states of hypo/hyper-methylation (marker of alteration in gene function).[36,377–381] These structural and functional DNA alterations may also associate with poorer cardiovascular outcomes.[382–384]

1.6.2.   Epidemiology of air pollution.

In 2016, the WHO estimated that about 7 million global deaths (94% from low- and middle income countries; almost 1 million from Africa) were attributable to the combined effects of both ambient indoor and outdoor air pollution.[385] Other reports show that 4.2 million deaths and 3.8 million deaths across the world could be attributable to indoor and outdoor ambient air pollution respectively.[386] In terms of attributable fraction of total mortality, an estimated 17% of acute lower respiratory disease, 43% of chronic obstructive pulmonary disease, 29% of lung cancer, 25% of ischaemic heart disease and 24% of stroke deaths in the world in 2016 could be attributed to air pollution (indoor and outdoor combined).[367,385] These rates were even higher for lower- and middle-income countries in Africa (64% acute lower respiratory disease, 55% chronic obstructive pulmonary disease, 39% lung cancer, 38% ischaemic heart disease and 36% stroke).[385]

What is more, it has previously also been shown that demographic factors (e.g. women, children and elderly are regarded as vulnerable populations), socioeconomic factors (e.g. poverty and low education) and lifestyle choices (e.g. smoking, type of employment and housing location and structural features) are also strong determinants of exposure to air pollution and its health effects.[387–390] Women in particular appear to be vulnerable to the effects of air pollution.[36] Previous studies in women populations have shown associations between air pollutants and risk for CVD and death [391], cognitive decline [392], risk for cardiopulmonary mortality [393], incidence of hypertension and diabetes mellitus [394] and risk for lung cancer [395]. Indoor air pollution due to the use of biofuels for cooking purposes places women in developing regions in particular, including SA, at an increased risk.[44,396,397]

Also, communities with lower socioeconomic status have been shown to be disproportionately affected by air pollution and these communities are also more susceptibility to poor health.[398–400] A global review study by Hajat *et al.* (2015) evaluated air pollution in relation to socioeconomic disparities.[401] In this review most studies were from the developed world (North America: *n* = 22; Europe: *n* = 10) while only one study from the African region (Ghana (2012); first study from Africa to report socioeconomic inequalities in terms of air pollution) was included.[401,402] To address air pollution-related socioeconomic disparities, environmental justice research has received increasing attention over recent years and is especially advocating policy changes that would create equal opportunity for all to reduce/avoid environmental exposure to pollutants.[399,403]

Lifestyle choices, especially smoking, significantly contribute to air pollution associated health effects.[36,404] Monocyclic and polycyclic aromatic hydrocarbon air pollutants are present in cigarette smoke.[36,405] Environmental tobacco smoke (including second hand smoke) is a major source of benzene and a major health threat for both smokers and non-smokers especially in the indoor setting.[36] Active smoking has been estimated to add between 400 to 1800 µg benzene exposure per day.[406] In homes of smokers it has been estimated that cigarette smoke may contribute to about 90% of the total indoor PAH levels.[36,407]

Reports on the health effects of air pollution from the African region appear to be relatively scarce compared to those from the developed world.[42,408] This was highlighted in a recent review by Katoto *et al.* (2019) who only identified 23 air pollution-related studies from SSA in all literature.[42] Fourteen of the studies included by Katoto *et al.* (2019) were from South Africa.[42] The lack of evidence-based research from the African continent was also apparent in the WHO's Review of Evidence on Health Aspects of Air Pollution – REVIHAAP Project.[408] A major finding reported by Katoto *et al.* (2019) was that ambient air pollution levels in the SSA region are 10 to 20 fold higher than WHO standards.[42] Health outcomes associated with ambient air pollution reported by Katoto *et al.* (2019) include mostly respiratory effects (wheezing [409–413], cough [412,414,415], phlegm [415], breathlessness [414], airway-hyperresponsiveness [409], bronchitis [409,412], asthma [412,413], rhinitis [416], emphysema [412] an pneumonia [412]) while two reports reported on cardio-respiratory effects and mortality [417]. All studies from the SSA region were furthermore cross-sectional while the longitudinal effects of air pollution on health outcomes remain to be explored.[42]

Air pollution is also an emerging health concern in SA; however, the burden of disease attibutable to air pollution remains relatively poorly explored.[44,50,418] Reports that are available indicate that indoor smoke from the burning of solid fuels is a major health concern as an estimated one-third of the South African popluation uses solid feuls and an additional 20% uses paraffin (kerosene) for heating and cooking.[418] A report by the The South African Medical Research Council in 2000 estimated that 20% of households were exposed to indoor smoke from solid fuels and accounted for 2489 deaths (0.5% of all deaths) in SA.[418] SA has also been identified as one of the world's most carbon intensive economies with power generation, industrial processes, domestic energy use and vehicle exhaust emission the greatest contributors to air pollution in SA.[419–421] Although the South African Government is continuously monitoring outdoor ambient air quality levels through a network of central air quality monitoring stations located mostly in urban areas, linking these air quality levels to health outcomes remain mostly marginalised.[42,50,419] Nonetheless, previous reports from South Africa have also mostly focused on respiratory effects of air pollution.[44,409,418,422] Also, most studies reported on by Katoto *et al.* (2019) were from Gauteng and Kwazulu-Natal (12 reports) and only two reports were from the Western Cape Province (Cape Town) of South Africa.[42] The reports from the Western Cape Province showed that proximity to a refinery (<4 km; meteorological estimated exposure) was associated with wheezing and asthma [410] and ambient air pollution levels recorded between 2001 and 2006 were associated with mortality rates [422].

Air pollution has also been identified as a driving factor of climate change.[423] Climate change has received much attention across the globe, including South Africa over recent years.[423,424] Climate change not only has major ecological, economical and health implications, but also threatens the existence of plant and animal life, including humans.[423,425,426] Therefore, air quality research and monitoring have become highly relevant as the urgency to address this global threat is escalating.[423–425] Environmental policies and acts have been implemented by Governments and recommendations set forth by international organisations over the years to address the threat of air pollution.[36,427,428] In South Africa, the new National Environment Management Act:

Air Pollution was adopted in 2005 to "provide reasonable measures for the prevention of pollution" and to "provide national norms and standards to regulate air quality".[429] Although ambient air quality standards for ozone (0.12 parts per million 1-hour average), NOx (0.2 parts per million annual average), sulphur oxide (0.019 parts per million annual average), lead (2.5 micrograms per cubic meter monthly average), PM (60 micrograms per cubic meter annual average) have been set in the act, standards for various other air pollutants such as polycyclic aromatic hydrocarbons are lacking.[429] The South African air pollution standards are currently under review.[430] In the Western Cape, the Western Cape Government has put forward an Air Quality Management Plan with a vision to ensure "clean and healthy air for all in the Western Cape" through a mission of "ensuring the effective and consistent implementations of sustainable air quality management practices by all spheres of government, stakeholders and civil society to progressively achieve and efficiently maintain clean and healthy air in the Western Cape".[431]

1.6.3.   Gaseous air pollutants.
1.6.3.1. Nitrogen oxides (NOx).

Although several NOx are present in ambient air, NO and NO_2 are considered to be the most predominant.[36,432] NO and NO_2 are produced during combustion where NO is the main NOx by-product (more than 90%; NO_2 less than 10%), but due to its highly reactive nature, it is quickly oxidised by O_2 and O_3 to form the primary pollutant NO_2 (**Figure 1.16.**).[36,432]
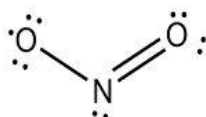
Figure 1.16. Molecular structure of NO_2. Figure based on content from [433].

The most prominent contributors to outdoor NO_2 include traffic-related emission by petrol- and diesel-powered vehicles, while indoor concentrations can be mostly attributed to heating appliances that use wood, kerosene and natural gas as energy sources.[36,432] NO_2 levels can vary greatly across locations (e.g. indoor, outdoor and within a city's microenvironments), regions and seasons.[36,434–436] The EU INDEX report indicated variations between indoor (13 to 62 $\mu g/m^3$), outdoor (24 to 61 $\mu g/m^3$) and personal (25 to 43 $\mu g/m^3$) measurements.[432] The THADE report showed indoor NO_2 concentrations of 10 to 15 $\mu g/m^3$ in Scandinavian countries, while concentrations in Asia appear to be relatively high (43 to 81 $\mu g/m^3$).[437,438] According to the WHO, global annual mean NO_2 concentrations mostly range between 20 and 90 $\mu g/m^3$ across the globe.[36]

In SA, previous studies have reported on NO_2 concentrations ranging between 10.9 to 17.2 $\mu g/m^3$ in Durban (2013: from central air monitoring station) and ~1 to ~7 $\mu g/m^3$ at 37 outdoor sites on the South African

Highveld (2005 to 2007; two annual cycles at 30-day intervals using passive samplers).[409,439] The Johannesburg-Pretoria conurbation was identified as the NO_2 "hot-spot" in SA using satellite-based instruments (Scanning Imaging Absorption Spectrometer).[440] In the Western Cape area, recently reported annual mean NO_2 levels from air quality monitoring stations in the Goodwood and Plattekloof areas were 21 µg/m³ and 10 µg/m³ respectively while a study by Vanker *et al.* (2015) reported a median indoor NO_2 of 7.9 (Interquartile range (IQR): 3.8 – 13.3) µg/m³ from 500 homes.[441,442] NO_2 has also previously been implicated in photochemical (ultra violet) smog formation (brown-haze) in the Cape Town region.[8,443]

NO_2 exposure is associated with various adverse effects that are mostly respiratory- (bronchitis, respiratory infections, decreased respiratory function) neurological- and cardiovascular-related.[444] NO_2 mainly enters the body though inhalation where it acts as a free radical (strong oxidant).[35,36,432] Exposure to NO_2 can increase oxidative stress through depletion of tissue antioxidant defences (ascorbic acid, uric acid, alpha-tocopherol and protein thiol groups), increase lipid peroxidation, dysregulation of O_2^- levels (activation of NADPH oxidase) and inhibition of enhanced glutathione peroxidase expression.[445,446]

NO_2 increases inflammation though increasing cell permeability, upregulating mediators of inflammation (Nytrotyrosine, IL-8, IL-1β, heme-oxygenase-1 (HO-1), and TNF-α), which ultimately results in cell death.[447–450] The genotoxic effects of NO_2 remain less understood, but chromosomal aberrations, sister chromatid exchanges or DNA single strand breaks have previously been reported.[451,452] Current WHO and SA annual ambient mean standards are set at 40 µg/m³.[442,453,454]

1.6.3.2. Volatile organic compounds (VOCs).

VOCs refer to organic chemical compounds with a high volatility (evaporate or sublimate easily) in ambient air (under normal atmospheric temperature and pressure).[32,455,456] Due to their volatility, numerous VOCs are continuously released from organic compound-containing solids (e.g. solid fuels such as wood and coal) and liquids (e.g. various household solvents, detergents and paint) into the atmosphere.[32,457,458] The release of VOCs into the atmosphere is dramatically increased in the presence of heat or during combustion processes and therefore a close relationship exists between temperature/heat and ambient VOC concentrations.[32,459] VOCs can be broadly classified as either cyclic (e.g. benzene) or acyclic (open chain: e.g. ethane and acetic acid).[32] Aromatic compounds form part of cyclic VOCs and often consist of one benzene-like ring structure (monocyclic aromatic hydrocarbons (e.g. BTEX) or multiple cyclic rings (polycyclic aromatic hydrocarbons (PAH): e.g. pyrene, naphthalene, fluorene, and phenanthrene).[32,33]

1.6.3.2.1.   Monocyclic aromatic hydrocarbons.

MAHs include BTEX and consists of an organic hexagon benzene ring (containing elements carbon and hydrogen). [28,34,37,460,461] (**Figure 1.17.**).[32,33]
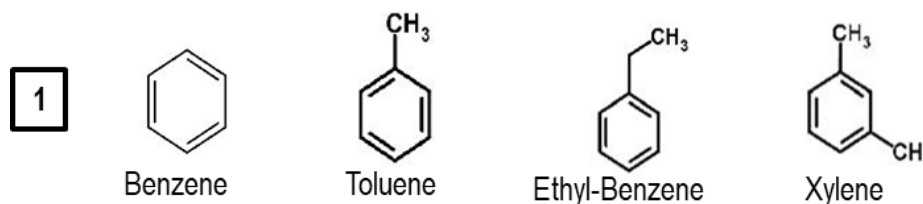
Figure 1.17. Molecular structures of BTEX pollutants present in ambient air. Figure based on content from [433,462,463].

Hydrocarbons are naturally present or added (to improve the octane rating) in gasoline and numerous consumer products (paints, adhesives and cleaning agents) or used in other industrial processes as solvents (e.g. during the production of styrene, nylon, plastics and polyurethanes).[464,465] Aromatic hydrocarbons in ambient air are mostly produced from vehicle fuel and other fossil fuel combustion and considered a marker of industrial (coal, oil, natural gas, chemical plants and steel related industries), vehicle (Diesel and petrol) and household (heating, cooking (kerosene and natural gas stoves) and cigarette smoking) emissions.[33,34,36,37,460,461]

1.6.3.2.2.   Metabolic routes, markers of exposure and exposure standards.

MAHs are mostly metabolised by CYP450 enzymes to optically active phenols which in turn are converted to dihydro-diols by epoxide hydrolase.[466] Diol-epoxides are especially reactive and particularly dangerous to DNA molecules (accounts for their carcinogenic effects).[36,467] CYP450 enzymes can also metabolise aromatic hydrocarbons such as benzene to various carcinogenic quinones.[468] Benzene in particular is a lipophilic carcinogen (WHO group A) and mostly accumulates in fatty tissue such as bone marrow where it is associated with the development of leukaemia.[28,469]

Although the metabolic routes of air pollutants are complex and often overlap, specific metabolites eliminated in urine have been linked to specific exposures and useful in determining exposure concentration.[470–472] Major urinary metabolites for BTEX include N-acetyl-S-(3-hydroxypropyl)-L-cysteine (HPMA; a marker of acrolein exposure[473]), N-acetyl-s-(phenyl)-L-cysteine (PMA; a marker of benzene exposure[468]), N-acetyl-s-(benzyl)-L-cysteine (BMA; a marker of toluene exposure [474]), trans,trans-muconic acid (MU; a marker of benzene exposure[468]), and 3+4-methylhippuric acid (3+4MHA; a marker of *o*-, *m*-, and *p*-xylene exposure[475]) (**Figure 1.18.**).[28,457,476,477]
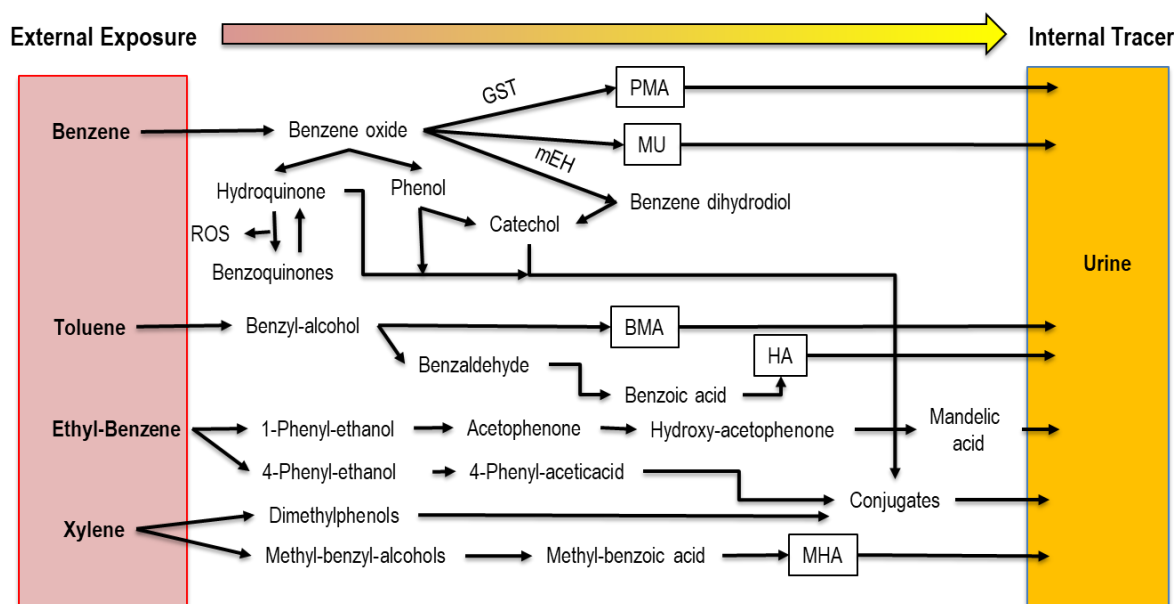
Figure 1.18. Simplified metabolic routes of BTEX. Figure designed by the author of this dissertation based on content from [478–483]. **Abbreviations**: GST: Glutathione S-transferase; mEH: Microsomal epoxide hydrolase; ROS: Reactive oxygen species; PMA: Phenyl mercapturic acid; BMA: Benzyl mercapturic acid; MU: Muconic acid; MHA: Methyl hippuric acid; HA: hippuric acid.

Various organisations and governments have set recommended standards in order to reduce the health, environmental and ecological effects of VOCs.[28,465,484] Currently, the WHO and SA annual mean standard for benzene is set at 5 μg/m^3 although 0 μg/m^3 is recommended for all benzyl-like aromatic hydrocarbons due to their carcinogenic properties (Risk for leukaemia: Benzene: risk for leukaemia 6×10^{-6}/1 μg/m^3 and PAH: 8.7×10^{-5}/1 μg/m^3 Benzo[a]Pyrene (B[a]P; considered the most reliable marker for PAH exposure)).[28,453,485]

1.6.4. Air pollution and cardiovascular disease.

The health effects of air pollution are strongly time-dose dependent and vulnerable populations are usually most at risk (e.g. women, children, the elderly and people living with associated pre-existing conditions e.g. heart and respiratory diseases).[385,486,487] The adverse cardiovascular effects of exposure to air pollution can be traced from initial exposure during inhalation through to effects observed at cellular and nuclear level with the main underlying mechanisms related to CNS toxicity, oxidative stress and inflammation (**Figure 1.19.**).[8,356]

Inhalation

1 Respiratory Effects

Air pollution molecules/particles retained on pulmonary epithelium:
- Sensory receptor activation → Reflex responses →Autonomic dysfunction.
- Pulmonary epithelial and endothelial dysfunction.

↑**Pulmonary ROS and Inflammation**

Spill-over

2 Circulatory Effects

Reactive pollutants react with circulating lipids and proteins:
- Hydroxyl radicals: ↑Lipid oxidation (oxLDL) and protein degradation.

Enter cellular constituents of blood (e.g. leukocytes):
- ↑Cytotoxicity.
- Mitochondrial dysfunction.
- DNA alteration.

↑**Systemic ROS and Inflammation**

Spill-over

3 Organ and Tissue Effects

Cytotoxic effects on organs:
- Liver →impaired glycogen storage, lipid metabolism.
- Pancreas → Impaired glucose metabolism →Insulin resistance/diabetes.
- Kidney → Impaired filtration.
- Bone marrow → Cancer, anaemia.
- Nervous system →CNS dysfunction, autonomic dysregulation.

↑**Tissue and Organ ROS and Inflammation**

Spill-over

4 Cardiovascular Effects

Direct effects
- ↑Cytotoxicity, mitochondrial toxicity, genotoxicity

Indirect effects:
- Autonomic nervous system toxicity →↑Vasoconstriction, blood pressure, arrythmias.
- Cardiometabolic effects →Pro-atherosclerotic profile.
- Endothelial dysfunction: ↓NO production, ↑ROS production, ↑Inflammation
- Vascular remodelling: Cell proliferation, thrombosis

↑**Vascular ROS and Inflammation**

Figure 1.19. Adverse health effects of air pollution on various organ and body systems. **Description: 1**. Toxic effects of air pollution on the respiratory system causes pulmonary ROS production and inflammation. **2.** Circulating reactive pollutants increase systemic oxidative stress and inflammation. **3.** Toxic air pollutants have adverse effects on various organ systems resulting in increased ROS and inflammation. **4.** Air pollutants can lead to CVD though various cytotoxic and pro-atherosclerotic mechanisms. Figure designed by the author of this dissertation based on content from [8,355,356,360,417,488–493]. **Abbreviations**: ROS: Reactive oxygen species; oxLDL: Oxidised low-density lipoprotein cholesterol; DNA: Deoxyribonucleic acid; CNS: Central nervous system; NO: Nitric oxide.

The initial effects of air pollutant exposure can be observed in the respiratory tract where pollutants can cause sensory receptor activation and trigger reflex responses (e.g. coughing and airway constriction especially in people living with asthma).[417,489,490] Air pollutants may also be partially deposited/retained on the pulmonary epithelium for prolonged periods post-exposure and continue to stimulate reflex responses and cause autonomic nervous system dysfunction.[356,360] Depending on the intensity and duration, retained pollutants may furthermore promote pulmonary epithelial and endothelial dysfunction through activation of pulmonary sensory receptors (stimulate the release of neuropeptides e.g. substance P and neurokinin A) and upregulating pulmonary oxidative and inflammatory pathways (upregulate adhesion molecule production and increased pulmonary T- and B-lymphocytes infiltration *via* cytokine release).[8,356,376,490] Chronic pulmonary oxidative stress and inflammation due to air pollution exposure increase the risk for pulmonary hypertension, respiratory infections, chronic obstructive pulmonary disease and lung cancer.[8,494,495] Pulmonary oxidative stress and inflammation

may eventually spill over into the circulatory system and increase systemic oxidative stress and inflammation.[8,356]

Once air pollutants are in the blood circulation, pro-oxidative pollutants alter the oxidative state of circulating blood by forming OH^- through reactions with other radicals such as O_2^-.[8,491,492] OH^- is extremely reactive (reaction rate constant more than 10^8 $M^{-1}.s^{-1}$) and oxidise circulating lipids and proteins.[491–493] The oxidative state of circulating blood is particularly important for vascular health as it is associated with oxidative modification of plasma lipoproteins (e.g. HDL) that ultimately promote atherosclerosis.[490] Air pollution has furthermore been associated with numerous other circulating markers of cardiovascular risk (increased production of TNF-α, IL-6, IL-8, IL1-α, IL1-β, granulocyte-macrophage colony-stimulating factor and macrophage-inflammatory protein-2).[116,490] IL-6 in particular plays a direct role in regulating the synthesis of hepatic CRP and is a marker of systemic inflammation, directly impairs vasoreactivity and promotes monocyte recruitment to the vascular wall.[8] Also increased levels of circulating haemodynamic factors (e.g. fibrinogen and platelet aggregation and coagulation factors) have been associated with air pollution exposure.[355,496] The genotoxic effects of air pollutants on circulating leukocytes appear to be an important link between air pollution and numerous health effects and involve structural and functional DNA alterations.[497–499]

Adverse liver and kidney effects are often associated with air pollution exposure due to the major roles these organs play in pollutant metabolism and elimination.[500–502] Air pollution associated adverse hepatic effects include liver dysfunction related to increased ROS and pro-inflammatory cytokine production, mitochondrial damage, impaired lipid metabolism and lipid peroxidation, hepatic megalocytosis, impaired hepatic glycogen storage, genotoxicity DNA damage and liver cancer.[365,503] Pancreatic-related effects of air pollution include glucose dysregulation, insulin resistance, diabetes and pancreatic cancer.[26,504] In view of their role as the main route of elimination, kidney abnormalities are also associated with air pollution, including impaired kidney function/filtration, decreased low-molecular weight protein excretion, decreased glomeration filtration rate and increased risk for diseases such as nephrocalcinosis.[26,505]

As the interface between circulating blood and underlying tissue, the vascular endothelium is vulnerable to the effects of circulating toxins such as gaseous air pollutants.[41,506,507] Air pollution has been shown to increase vascular oxidative stress through the upregulation of ROS generation (activation p47phox and Rac1 subunits of endothelial NADPH oxidase and increased 3-nitrotyrosine residues), decreased antioxidant gene expression, increased O_2^- production (*via* eNOS uncoupling) and decreased NO production (activation of JNK, p38 mitogen activated protein kinase (MAPK) and ERK1/2 pathways).[490] Air pollution has also been implicated in vascular inflammation (upregulation of NF-kB and TNF-α), increased expression of adhesion molecules (e.g. VCAM, e-selectin and p-selectin) and increased levels of haemodynamic factors (fibrinogen, blood coagulation/viscosity).[8,356,490]

Due to the toxic effects of air pollution on the autonomic nervous system, dysregulation of vascular tone (vasoconstriction) heart rate (including arrythmias) and blood pressure are often observed.[8,355,488] Vasoconstriction and increased blood pressure may ultimately cause cardiac overload, ventricular remodelling (as a result of loss of contractile capacity) and heart failure.[355,488]

1.7. Rationale and problem statement.

SA is currently in the midst of an epidemiological transition that is characterised by a multiple burden of communicable (accounts for 57% of all deaths) and NCD (accounts for 43% of total deaths).[14,46,508] The burden of NCD in SA is already the highest in SSA, comparable to developed countries, and expected to exceed that of communicable diseases within the next two decades.[200,509]

HIV/AIDS remains the greatest contributor to the burden of disease in SA (accounts for more than 100 000 deaths each year – ~24% of total deaths).[510,511] SA also has the largest HIV/AIDS population in the world (7.1 million - 18% of the total SA population and 17% of the global HIV/AIDS population) with 0.25 million new HIV-infections each year.[283,510,511] SA has furthermore the largest Government sponsored ART programme in the world (about 5 million PLWH on ART).[12,45,229] Since September 2016, ART is available to all PLWH in SA regardless of CD4 count or viral loads.[244] Without the dramatic upscale in ART-coverage, more than 500 000 people in SA (about 1% of the SA's total population) would have died each year of HIV/AIDS by 2010.[11,512] What is more, in excess of 10 million people undergo HIV tests each year to assess their status, but only an estimated 85% of PLWH in SA know their status.[510] Taking all in account, it is with relative good certainty that one can expect the HIV/AIDS pandemic to continue to evolve in SA over years to come.[11,219,283]

CVD is currently the second largest cause of death in SA (about 75 000 deaths/year - 17% of all deaths in SA).[205] Industrialisation with subsequent economic development and rapid urbanisation have been associated with the emergence of the more "affluent" causes of CVD in SA.[47,513] Cardiovascular risk factors such as overweight/obesity and hypertension are highly prevalent in the SA population.[205,206] As is the case with most industrialised countries, the rise in environmental health risk factors such as air pollution is of great concern.[50,419] Furthermore, SA has one of the world's most carbon intensive economies and contributes to about 1.4% of global CO_2 emissions.[419,420] The high carbon emission rate in SA is mostly a result of the county's dependence on coal as the most prominent biofuel for power generation while vehicle emissions in the urban settings and the household use of biofuels for cooking and heating in the rural indoor setting (due to high electricity costs and lower accessibility) have been identified as major health concern.[44,49,419,420]

While "The Heart of Soweto Study" has reported on the alarming prevalence of cardiovascular risk factors present in the SA urban population and referred it as "A time bomb in cardiovascular risk factors in SA",[46] a

recent Editorial in Frontiers in Cardiovascular Medicine has pointed out that HIV-related cardiovascular disease in SSA is a "misplaced priority in public health and research agendas" that needs to be recognised and addressed.[51] In terms of air pollution, a recent (2019) systematic review reported on urban ambient air pollution levels of 10 to 20 times higher than recommended WHO standards in some areas of SSA; however, the authors only identified 14 reports from SA and 23 reports in total from the SSA region that described air pollution-associated health outcomes.[42] None of the reports assessed the effects of air pollution exposure on endothelial function or other quantitative measurements of cardiovascular health.[42] These reports strongly underscore the need for more research attention.

1.8.   Aims and objectives.

The overarching aim of the study was to investigate whether an association exists between two emerging, non-traditional cardiovascular risk factors (namely HIV-infection with or without ART and air pollution) and vascular endothelial function in an adult study cohort residing in the Cape Town region. The specific aims of the study were as follows:

Aim 1: To determine whether an association exists between HIV-infection, ART and endothelial dysfunction. This aim was achieved by the following objectives:

- To measure endothelial function in HIV-negative and HIV-infected (with and without ART) study participants visiting health care clinics in the Cape Town region at two time points (baseline and 18-month follow-up) by means of flow-mediated dilatation (FMD) and retinal microvascular morphology imaging techniques.
- To analyse data obtained from comprehensive health questionnaires and anthropometric measurements in order to evaluate the study participants' cardiovascular risk profile.
- To measure and analyse an array of chemical pathology parameters in blood samples of all study participants to determine their cardiovascular risk profile.
- To measure and analyse biomarkers of vascular inflammation and endothelial function.
- To determine, based on analysis of the above data, whether there is an association between HIV-infection ART and endothelial function.

Aim 2: To assess the personal air pollution exposure in a cohort of healthy HIV-negative study participants and determine whether an association exists between personal air pollution exposure and endothelial function. This will be achieved by the following objectives:

- To measure and analyse personal air pollution exposure in participants at two time-points (6-month follow-up) using state-of-the-art passive diffusion air pollution samplers and analyse key urinary biomarkers of air pollution.
- To measure endothelial function in the above participants at the same time-points by means of both FMD and retinal microvascular morphology imaging techniques.
- To analyse data obtained from a comprehensive health questionnaires and anthropometric measurements in order to evaluate the study participants' cardiovascular risk.
- To measure and analyse an array of chemical pathology parameters in blood samples of all study participants to determine their cardiovascular risk profile.
- To measure and analyse biomarkers of vascular inflammation and endothelial function.
- To determine, based on analysis of the above data, whether an association between exposure to air pollution, endothelial function and cardiovascular risk exist.

The current study contributes to various South African Sustainable Development Goals and the National Development Plan:[514]

- **Good health and well-being:** Through investigating the health effects of major health concerns in South Africa (HIV and air pollution).
- **Reduced inequalities:** Through including inequalities such as education level and employment status as confounders in the current research.
- **Sustainable cities and communities:** Through evaluating health and environmental factors that directly impact sustainability.
- **Climate action:** Through evaluating current levels of personal air pollutant exposure.
- **Partnership for the goals:** Through international collaboration in the current project.

1.9. Conclusion.

HIV/AIDS, ART and air pollution have been identified as cardiovascular risk factors; however, their status in this regard remains largely unexplored in SA.[42,418,515–517] These emerging cardiovascular risk factors could potentially already contribute substantially to the increase in cardiovascular morbidity and mortality in SA.[518,519] What is more, these cardiovascular risk factors not only pose a threat to millions of people living in SA, but also threaten the overextension of already strained healthcare resources in SA over the next few years.[42,51,419,518] Despite the looming threat, population-based studies assessing the current status of these emerging cardiovascular risk factors in the SA context are lacking, but urgently needed in order to take early preventative measures that are based on sound scientific knowledge.[42,43,51]

2. Chapter 2: Methods and materials.

2.1. Study background and introduction.

This study was conducted in the context of a joint PhD agreement between Stellenbosch University and the University of Hasselt in Belgium. The study was imbedded in a larger parent study known under the acronym "EndoAfrica".[43] The EndoAfrica research consortium consists of Stellenbosch University (Prof Hans Strijdom – Principal investigator and international project coordinator), the Medical University of Graz (Austria), Hasselt University (Belgium), and the Flemish Institute for Technological Research (VITO, Belgium).

The PhD study consisted of two sub-studies aligned with the two overarching aims as described in Section 1.8 of Chapter 1, with **Sub-study 1** pertaining to Aim 1 (To determine whether an association exists between HIV-infection, ART and endothelial dysfunction) and **Sub-study 2** pertaining to Aim 2 (To assess the personal air pollution exposure in a cohort of healthy study participants and determine whether an association exists between personal air pollution exposure and endothelial function.).

Several aspects of the study design and methods were shared between the two sub-studies. Where relevant, methods that were specific to Sub-study 1 or Sub-study 2 will be described separately in the current chapter (**Figure 2.1.**).
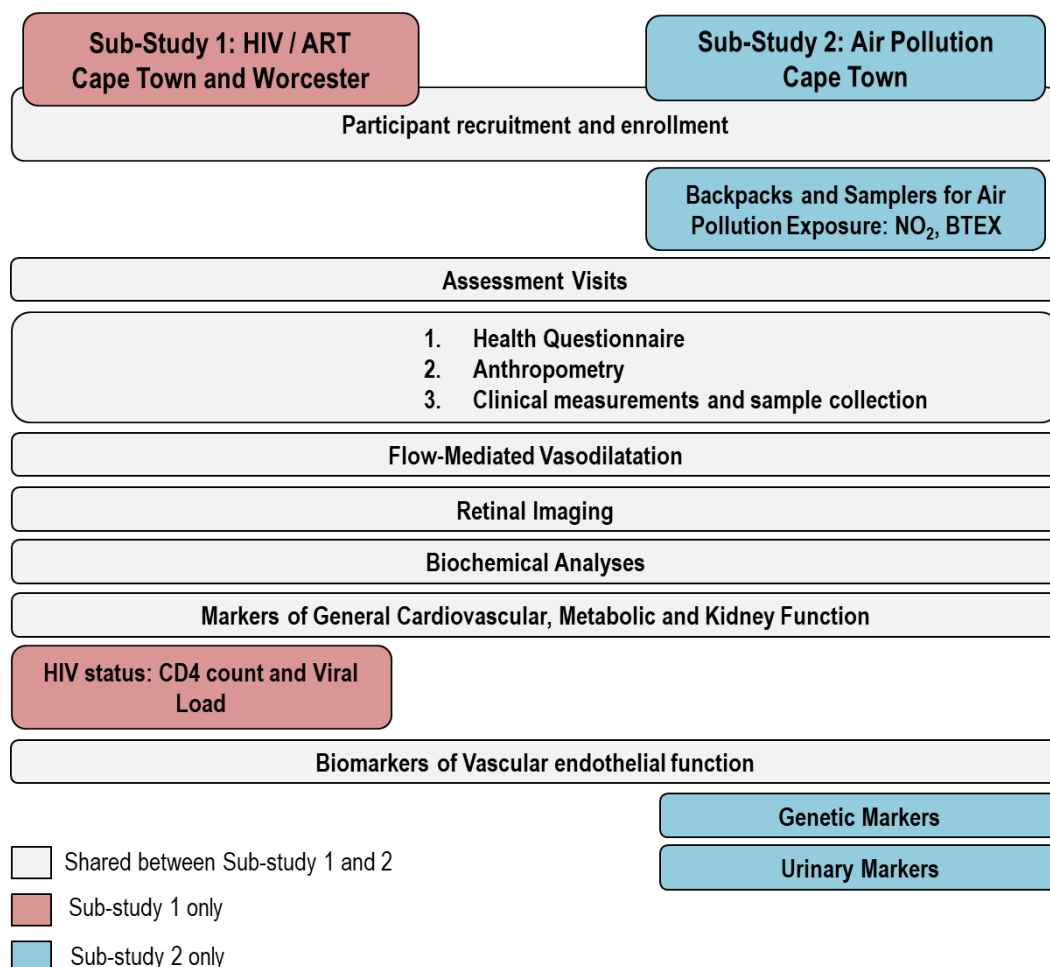
Figure 2.1. General outline of methods applied during the study.

2.2.   Ethics and ethical considerations.

Ethical clearance for the current study was obtained from the Health Research Ethics Committee of Stellenbosch University (Ethics reference number: S16/07/114; in accordance with the Helsinki Declaration) and was renewed annually (July 2017 and August 2018). Participation in the study was strictly voluntary and participants could withdraw from the study at any point if they wished to do so. Informed consent was conducted in the participant's home language or language of choice. No investigations were performed before full informed consent was obtained. Methods for the study were non-invasive (except for blood collection) and without any health risk to participants. Participants additionally provided consent for the storage of their biological samples for future related studies, as well as for transport and analysis of their samples in laboratories elsewhere if necessary. Each participant was given an opportunity to ask questions about uncertain aspects of the study.

Interaction between the research team and participants was managed discretely, and the anonymity of participants in both sub-studies was prioritised throughout. All participants were also assigned a unique participant identification number and used for all future study purposes. Backpacks for sub-study 2 were generic and unmarked and handed out privately to avoid drawing unnecessary attention to the participants. Data obtained from each participant was furthermore stored on a secure database with strictly controlled, password-secured access. Test results, health questionnaires and any other information on paper were filed and locked away in a secure place with strictly controlled access. Participants had access to all their test results upon request. Participants whose assessment indicated health concerns were informed and refereed by the research nurses for further treatment. Participants with an unknown HIV-status received standard pre- and post-test counselling.

2.3.   Study location, study design in inclusion/exclusion criteria.

The PhD study was conducted in the Western Cape Province of SA. Participants for Sub-study 1 (HIV-free and HIV-infected) were randomly recruited at primary health care clinics in Elsies River, Bishop Lavis, Fisantekraal and Ravensmead (Northern suburbs of Cape Town, SA) and Worcester (170 km north of Cape Town). For logistical reasons (collection of backpacks containing air pollution samplers), only participants from the Cape Town area were recruited for Sub-study 2. All participants in the Cape Town area were from the residential areas of Elsies River, Bishop Lavis, Fisantekraal and Ravensmead (**Figure 2.2.**).
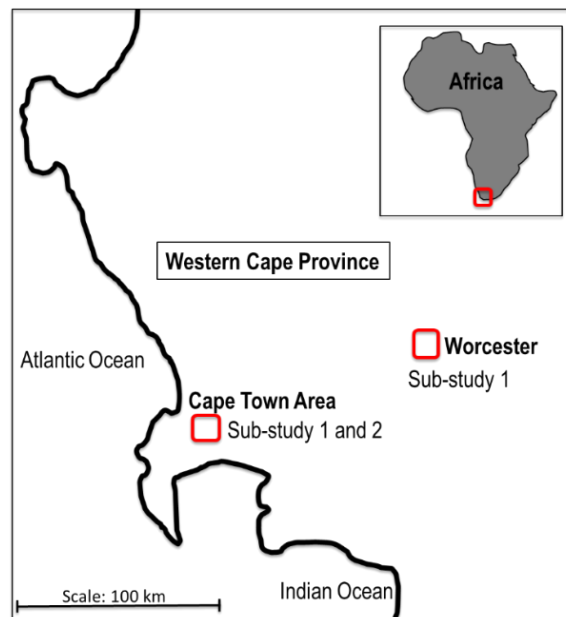
Figure 2.2. Map of the Western Cape Province of SA indicating the study locations of Sub-study 1 and Sub-study 2. Figure designed by the author of this dissertation based on content from [520].

Both sub-studies followed a prospective longitudinal cohort design (non-interventional). The repeated measures for Sub-study 1 were taken at baseline and 18-months follow-up visits and for Sub-study 2 at baseline and 6-month follow-up visits (**Figure 2.3.**).
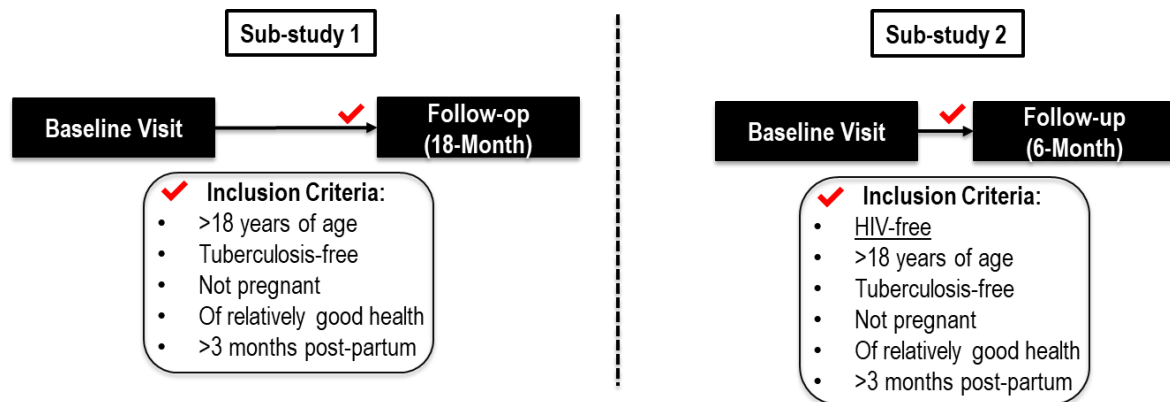
Figure 2.3. Broad outline of study design with inclusion criteria for Sub-study 1 and Sub-study 2.

Participants who were younger than 18 years of age, pregnant (confirmed with pregnancy test), less than 3 months post-partum, of poor health (including current tuberculosis (confirmed from participant clinic file) and/or previous history of heart disease) were excluded. Participants who were HIV-infected were excluded from Sub-study 2. The inclusion/exclusion criteria were applied and checked for each participant before baseline and follow-up visits for Sub-study 1 and Sub-study 2. To evaluate the frequency of baseline assessment visits for study group, please refer to Appendix C, Figure 1 on page 255.

2.4.   Study groups.

Sub-study 1 consisted of three main groups: **1)** HIV-free control participants (HIV-free), **2)** HIV-infected ART-naïve participants (HIV/noART) and **3)** HIV-infected participants on ART (HIV+ART; 90% of participants on fixed-dose, first-line, combination ART containing efavirenz / emtricitabine / tenofovir). Data from participants in the HIV/noART group at baseline who initiated ART treatment before the 18-month follow-up visit (more than 1 month) were additionally evaluated and considered as a sub-group to assess pre- and post-ART effects on variable outcomes.

Participants for Sub-study 2 were assessed at baseline and again after 6-months. The rationale for the 6-month follow-up was to take seasonal variations in ambient air pollutants into account and to evaluate seasonal patterns in ambient NO_2 and BTEX exposure (**Figure 2.4.**).
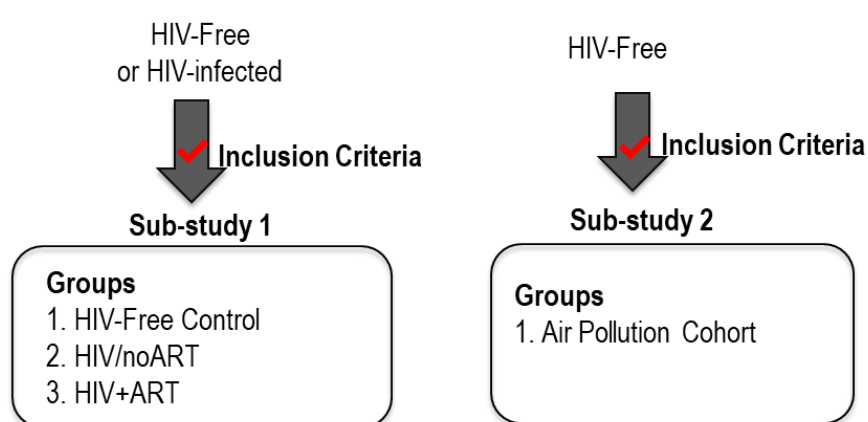
Figure 2.4. Study groups for Sub-study 1 and Sub-study 2. **Abbreviations**: Control: HIV-free control group; HIV/noART: HIV-infected participants that are not on any ART treatment; HIV+ART: HIV-infected participants that are on ART treatment (90% of participants were on first-line combination ART containing efavirenz / emtricitabine / tenofovir).

Sub-study 2 was designed as a smaller sub-study of the larger parent study, EndoAfrica. Due to budget constraints and to limit the number of possible confounding factors, PLWH were excluded from Sub-study 2.

2.5.   Participant recruitment.

Qualified research nurses recruited, screened, and obtained informed consent from all volunteering participants. Participants for Sub-study 2 were recruited from the HIV-free study population of Sub-study 1. After obtaining informed consent participants were officially enrolled in the study (assigned a unique participant number). The HIV-status of each participant was confirmed with a rapid HIV-test (SD Bioline HIV 1/2 3.0

immunochromatographic test kit; Standard Diagnostics, Republic of Korea). All study samples were labelled with bar-codes linked to the participant identification number (**Figure 2.5.**).
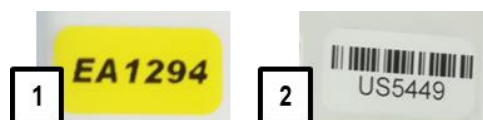
Figure 2.5. Examples of participant identification numbers and sample barcodes used during the study.

Following successful enrolment, appointments were made for a baseline assessment visit with a 6-month follow-up visit for Sub-study 2 and an 18-month follow-up visit for Sub-study 1. Participants who were enrolled in Sub-study 2 were handed a backpack for the purpose of air quality monitoring and an appointment was made for baseline assessment visit 7 days later. The same procedures were followed for the follow-up visits.

2.6.   Air quality monitoring (Sub-study 2).

Each Sub-study 2 participant was equipped with a backpack containing two rapid air monitoring (RAM) devices (Gradko rapid NO_2 passive diffusion sampler (Gradko International Ltd., Winchester, United Kingdom (UK), and a Radiello™ BTEX passive diffusion sampler (Sigma-Aldrich Inc., MO, USA)), as well as an ACR SmartButton® temperature logger (ACR Systems Inc., Surrey, B.C., Canada). The devices were placed in the external mesh pocket of a backpack that allowed unrestricted air flow (**Figure 2.6**).

Figure 2.6. Procedures followed for personal exposure measurements. **Description: 1.** Gradko rapid air NO_2 sampler (product: DIFRAM-100; detection limit: <0.2 µg/m^3 for 1-week exposure). **2.** Activated Gradko rapid air NO_2 sampler. **3.** Radiello™ diffusive cartridge (right) and diffusive body attached to a triangular support plate (left) (products: Rad130, RAD120, and RAD121; detection limit for BTEX: 0.05, 0.01, 0.01, and 0.01 µg/m^3, respectively; calibration: CS_2). **4.** ACR Systems Inc. temperature logger (product: SmartButton® (01-0187); detection limit: −40 °C to 85 °C). **5.** Air monitoring devices in the mesh pocket of a backpack (product: Barron BB0110 Curve and Arch Design backpacks). **6.** Backpack worn by participants with samplers located 50 to 60 cm from the face. Photos taken and figure designed by the author of this dissertation based on information previously described.[521]

The RAM devices are designed for short-term (1 hour to 14 days) air pollution measurement and function on the principle of passive molecular diffusion by collecting air samples at a known rate.[522–524] Pollutants that diffuse into the RAM collect onto an absorbent disk.[522,523] These devices are portable (3.5 cm high, 4.5 cm wide) and are carried on the person.[525] This enabled the investigator to assess both indoor and outdoor personal exposure to air pollutants.

Participants carried the backpack at all times (except during periods of sleep and bathroom use when the backpack was placed next to their beds) for the 7-day period prior to each clinical visit. Temperature was recorded continuously at 30-minute intervals while the NO_2 and BTEX samplers allowed for continuous passive diffusion and accumulation of NO_2 and BTEX. Following continuous 7-day measurements, participants returned for the first assessment visit, during which the backpacks were collected, data extracted from the temperature loggers *via* ACR TrendReader® software (ACR Systems Inc., Surrey, B.C., Canada), and the average temperature (°C) for the 7-day period was recorded. Once collected the NO_2 and BTEX samplers were sealed, stored at 4 °C and sent for quantification according to the manufacturer's protocol.

2.6.1. Quantification of NO_2 exposure concentrations.

NO_2 samplers were analysed according to UKAS method GLM 7 at Gradko International Ltd. Laboratories (United Kingdom Accreditation Services (UKAS) accredited)).[521,525,526] A standard nitrate solution calibration curve was prepared at known concentrations of 0,15,30,60,90 and 120 µg/ml (1 g/L nitrite ion (NO_2^-)). The colour reagent was prepared as previously described and added to each sample (sample:sulphanilamidesolution:N-1(naphthyl-1)ethylene diamine dihydrochloride solution (NEDD) ratio of 1:2:2 (0.003 g NEDD per 1 g sulphanilamide).[525,527] Samples were eluted by a preparation containing 20% triethanolamine (TEA) solution / 80% deionized water and NO_2 concentrations determined *via* chemiluminescence ultraviolet (UV) spectrophotometry (UVS04 Camspec M550; Spectronic Camspec Ltd., Leeds, UK).[525,528] Calibration standards and linearity checks were used to calibrate the spectrophotometer, and mid-range and zero standards were analysed at intervals throughout the sequence for quality assurance.[525] The calibration curve was used to calculate the NO_2^- concentration for each sample. The ambient NO_2 concentration was calculated from NO_2^- concentrations and expressed in $µg/m^3$.[525] NO_2 exposure concentration ($µg/m^3$) represented the mean for the 7-day measuring period. The same procedure was followed for the 6-month follow-up visits.

2.6.2. Quantification of BTEX exposure concentrations.

BTEX samplers were sent to VITO (Mol, Belgium) for quantification as previously described.[521,529,530] BTEX compounds were extracted from samplers by means of elution. Two ml carbon disulphide (CS_2; Sigma-

Aldrich, MO, USA) and 12.5 µL 2-fluorotoluene internal standard (Sigma-Aldrich, MO, USA)) were added into the Radiello™ glass tube containing the cartridge and stirred for 30 minutes (rotational shaker). BTEX quantification was performed by means of gas chromatography (Thermo Trace) / mass spectrometer (Thermo DSQ II with helium as carries gas at constant flow of 1 mL/min)). A cross-bond diphenyl/dimethylpolysiloxane column (RTX 502.2; 0.25 mm by 30 m) with a 1.4 µm-thick film was used for sample separation (temperature program: 35 ∘C for 5 minutes, 14 °C/minute increment until 245 °C). Equipment calibration was performed by injecting a standard solution containing benzene, ethyl-benzene, toluene, m-xylene, p-xylene, and o-xylene in CS_2 (Sigma-Aldrich, MO, USA)) at 0.03 to 30 µg/g before analysis. Sample concentrations were calculated from chromatograms using a standard curve. The limit of detection (LOD) was calculated as 3.3 (standard deviation (SD) of areas/slope). Samples with concentrations less than LOD were not presented in results. Results were expressed as average BTEX exposure concentration ($µg/m^3$) for the 7-day measuring period. The same procedure was followed for the 6-month follow-up visits.

2.7.   Health Questionnaire.

The comprehensive health questionnaire was completed by all participants at baseline and follow-up assessment visits for both sub-studies 1 and 2. Demographic information included age (years), gender (defined as male or female) and ethnicity (self-reported and defined as black or mixed-ancestry). *Note on ethnicity: it is acknowledged that ethnicity (as opposed to "race" as it is still officially defined by the South African Government), should be regarded as an overarching proxy of demographic, socio-economic, cultural and home-language factors for the purposes of this study. It is further acknowledged that socio-economic circumstances, rather than genetic predisposition as a result of ancestry, are more likely to be an important covariate in the context of this study. For this reason, several socioeconomic status indicators were also included (see below).* Lifestyle information included smoking status (defined as current smoker or non-smoker and smoking frequency: more or less than 20 cigarettes/day), alcohol consumption (defined as alcohol consumption in the last 12 months (yes/no), and if so, more or less than 8 days/month), hours or sleep at night (defined as less than 6 hours, 6 to less than 9 hours, and more than 9 hours). Socioeconomic status was defined as unemployed, part-time employed or full-time employed). Additional living environment information pertaining to Sub-study 2 included main source of household energy (defined as electricity or any biofuel), living next to a main road (yes/no; Defined as a road with constant traffic during the day.) and the season during which the assessment visit was conducted (defined as warm season: September to February and cold season: March to August).

2.8.   Anthropometric measurements.

Anthropometric measures for each participant were taken at each clinical visit for both sub-studies.[531] Measurements of body composition included height (cm; measured with a stadiometer), weight (kg; measured on

an electronic scale), waist and hip circumferences (cm; measured with a measuring tape). BMI (expressed as kg body weight/m^2 height) and waist-to-hip ratio ratios were calculated. Body composition was furthermore sub-classified as underweight (BMI less than 18.5 kg/m^2), normal weight (BMI between 18.5 to 24.9 kg/m^2), overweight (BMI 25 to 29.9 kg/m^2) and obese (BMI 30 kg/m^2 or more) according to WHO guidelines.[532] Elevated waist circumference was defined as more than 94 cm men and more than 80 cm for women (increased risk for metabolic complications) according to WHO guidelines.[531] Waist-to-hip ratio was considered elevated at more than 0.90 for men and more than 0.85 for women (substantial increased risk for metabolic complications) according to WHO guidelines.[531]

Blood pressure (SBP, DBP) and **heart rates** (3 measurements at 5-minute intervals) were all measured *via* an Omron M6 automatic digital blood pressure monitor (Omron Healthcare, Kyoto, Japan) on the left arm and expressed in mmHg and beats per minute (bpm) respectively. Hypertension was defined as systolic blood pressure 140 mmHg and above or diastolic blood pressure 90 mmHg or above according to WHO guidelines.[533]

2.9. Biochemical Analysis.

Participants were asked to fast from 22h00 the night before baseline and follow-up visits. Qualified research nurses collected fasting whole blood samples in blood collection tubes (SGVac, The Scientific Group (Pty) Ltd.; Milnerton, Western Cape, SA) and mid-stream urine samples (**Figure 2.7.**).
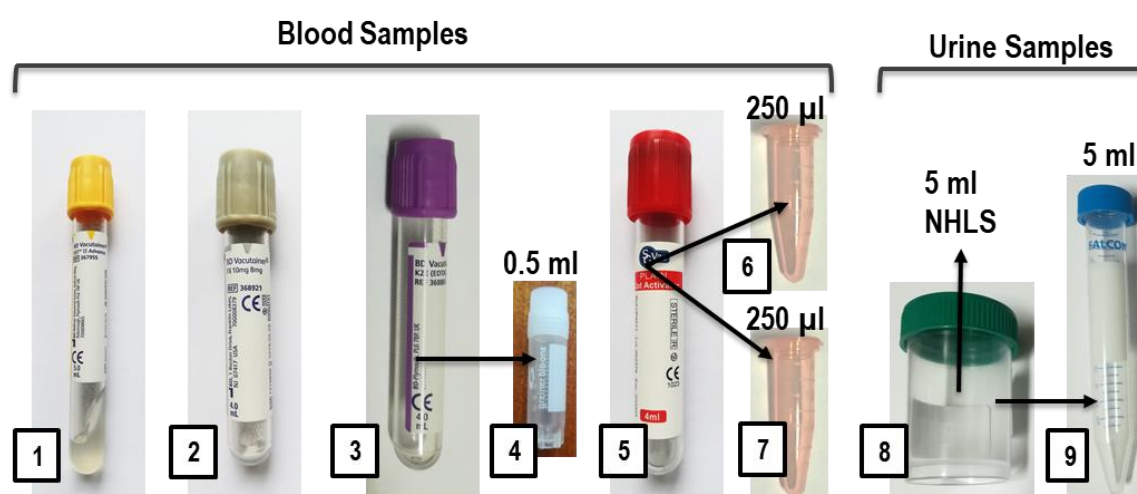
Figure 2.7. Fasting blood and urine samples collected for the study. **Description: 1.** Yellow top (1 x 7 ml): Serum separator tube (SST) containing acid citrate dextrose solution (clot activator) for total cholesterol, HDL, LDL, triglyceride, blood creatinine and GGT analysis. **2.** Grey top (1 x 5 ml): Potassium oxalate (anticoagulant) and sodium fluoride (preservative) tube for fasting glucose analysis. **3.** Purple top (2 x 5 ml): Ethylenediamine tetra-acetic acid (EDTA; strong anticoagulant) tube for haemoglobin (Hb), haemoglobin A1c (HbA1c), HIV viral load and CD4 count determination. **4.** The buffy coat was extracted from the EDTA tube for analysis pertaining to Sub-study 2 (Leukocyte telomere length, mtDNA content and DNA methylation). **5.** Red top (1 x 3 ml): Serum blood collection tube containing a lithium heparin (clot activator). **6.** Serum (250 µl) was allocated into a 1.5 ml microcentrifuge tube

and sent to the NHLS for hsCRP quantification. **7.** Additional serum (250 µl) was allocated into a 1.5 ml microcentrifuge tube and sent to Division of Molecular Biology and Human Genetics, University of Stellenbosch, for determination of biomarkers of vascular endothelial dysfunction.**8.** Mid-stream urine sample (10 ml) was collected. Five ml of the urine was sent to the NHLS for determination of creatinine and microalbuminuria levels. **9.** A 5 ml aliquot urine was sent to VITO (Belgium) for quantification of urinary markers/metabolite of air pollution exposure (only Sub-study 2).

Fasting blood samples were transported (according to SANS 10231 regulations) to the National Health Laboratory Service (NHLS, Tygerberg Hospital: SA National Accreditation System (SANAS) accredited), for determination of fasting glucose and glycated haemoglobin (HbA1c), lipogram (total cholesterol, LDL-cholesterol, HDL-cholesterol and triglycerides), haemoglobin (Hb), blood creatinine, C-reactive protein and GGT. CD4 count and HIV viral load were only determined for HIV-infected participants (Sub-study 1). Urine samples were analysed by the NHLS for urine creatinine, urine microalbuminuria and urine albumin-creatinine ratio.

Fasting serum samples were collected, serum extracted (10 minutes at 2000g or 43 rpm with a DM0412 clinical centrifuge; DLAD Scientific, Beijing, China), stored at -80 °C and sent to the Division of Molecular Biology and Human Genetics, University of Stellenbosch, for determination of markers of vascular endothelial dysfunction (TNF-α, adhesion molecules (VCAM-1 and ICAM-1), PAI-1, e-selectin, and p-selectin). Additionally for Sub-study 2, buffy coat samples (0.5 ml extracted from each participant's EDTA blood collection tube at 10 minutes, 2000g or 43 rpm with a DM0412 clinical centrifuge; DLAD Scientific, Beijing, China) and urine samples (5 ml per participant) was stored at -80 °C and sent to VITO and the University of Hasselt (Belgium) where the buffy coat samples were analysed for the determination of leukocyte DNA methylation, mtDNA content and telomere length, and the urine samples for the quantification of urinary markers/metabolites of air pollution (BTEX) exposure.

2.9.1.   High-sensitivity C-Reactive Protein (hsCRP).

High-sensitivity C-reactive protein (hsCRP) was determined at the NHLS by means of an IMMAGE® Immunochemistry Systems and Calibrator 5 Plus assay kit (LOD: 0.02 mg/dL; Beckman Coulter, Inc., CA, USA).[521] The principle for the specific chemiluminescence analysis was based on the highly sensitive near infrared particle immunoassay rate methodology where anti-CRP antibody-coated particles bind to the CRP in the serum sample resulting in an insoluble aggregate formation. The hsCRP concentration was determined automatically as the rate of aggregate formation (directly proportional).

Circulating hsCRP is a marker of systemic inflammation and a predictor of cardiovascular risk.[131,534] Inflammation as indicated by hsCRP has relevance in PLWH and air pollution exposure.[374,535] For the purposes of this study, increased hsCRP was defined as hsCRP levels of more than 3 mg/L based on previous reports indicating that hsCRP levels above this cut-off value are associated with increased cardiovascular risk.[534]

2.9.2. Lipid Profile: Total cholesterol, HDL, LDL and triglycerides.

Total cholesterol (LOD: 0.1 mmol/L), HDL cholesterol (LOD: 0.08 mmol/L), LDL cholesterol, (LOD: 0.08 mmol/L) and triglyceride levels (LOD: 0.1 mmol/L) were determined by the NHLS *via* chemiluminescence methodology (cobas® 301/501 analyser, Roche/Hitachi cobas® c systems, Basel, Switzerland).[536–539] The principle of the enzymatic, colorimetric method for the determination of total cholesterol and triglyceride levels was based on the cleavage of these esters by cholesterol esterase to produce free cholesterol and fatty acids.[536] Cholesterol oxidase subsequently catalases free cholesterol oxidation to produce chelest-4-en-3-one and hydrogen peroxide.[536] The production of quinone-imine dye is mediated by the reaction of hydrogen peroxide (oxidative coupling of phenol and 4-aminophenazone).[536] A direct relationship between the dye's colour intensity and cholesterol concentration exist.[536]

A homogeneous enzymatic colorimetric test principle was used for the determination of HDL and LDL levels.[537] The test principle for LDL determination is based on the formation of water-soluble complexes of LDL in the presence of magnesium ions and dextran sulphate.[537] The test principal for HDL determination is based on the formation of polyethylene glycol coupled amino groups by cholesterol esterase and cholesterol oxidase reaction. [537] The colour intensities produced during these reactions are determined photometrically and are directly proportional to the respective concentrations.[537]

Dyslipidaemia (High total cholesterol, LDL and triglyceride levels and / or low HDL levels) is an established cardiovascular risk factor.[540–542] HIV/AIDS, ART treatment and exposure to air pollution have been associated with dysregulated lipid levels.[543–545] For the purpose of this study, desirable fasting cholesterol levels were defined as less than 5 mmol/L for total cholesterol (male and female), less than 3 mmol/L for LDL cholesterol (male and female), more than 1.2 mmol/L for female and 1.0 mmol/L for male HDL cholesterol, and less than 1.7 mmol/L for triglyceride levels according to the Heart and Stroke Foundation of SA, NHLS and the US National Institutes of Health (NIH) guidelines.[540,546–548]

2.9.3. Glucose metabolism: Fasting glucose levels and HbA1c.

Fasting glucose (LOD: 0.11 mmol/L) and HbA1c (LOD: 0.186 mmol/L or 4.2%) levels were determined by the NHLS *via* chemiluminescence methodology (Hemolysate application on a cobas® 311/501 analyser; Roche/Hitachi cobas® c systems, Basel, Switzerland).[549] The UV test principal (enzymatic reference method) is based on the formation of glucose-6-phosphate by a hexokinase catalysed phosphorylation reaction of glucose and the subsequent oxidation of glucose-6-phosphate by glucose-6-phosphate dehydrogenase to form gluconate-6-phosphate.[549] The formation of NADPH during this process is directly proportional to the colour intensity (determined photochemically) of the dye and glucose concentration.[549]

The principle of HbA1c determination is based on using haemolysed whole blood (haemolysing reagent: tetradecyltrimethylammonium bromide) in a turbidimetric inhibition immunoassay.[550] Glycohemoglobin reacts with anti-HbA1c antibody to form soluble antigen-antibody complexes that are quantified turbidimetrically.[550] HbA1c is finally expressed as mmol/mol HbA1c or % HbA1c (calculated as a % of HbA1c/Hb ratio).[550]

Fasting glucose is an important marker of cardiometabolic risk and has application in both PLWH and air pollution exposure.[350,551,552] For the purposes of this study, desirable fasting glucose levels were defined as less than 5.6 mmol/L, and elevated as 5.6 mmol/L or more according to The Heart and Stroke Foundation of South Africa.[546] HbA1c levels less than 5.9% were considered normal, elevated when above 5.9% (indication of hyperglycaemia during the preceding 2 to 3 months or longer) and 6.5 % HbA1c or above suitable for the diagnosis of diabetes mellitus according to The South African Heart and Stroke Foundation, NHLS and the American Diabetic Association standards.[546,553–555]

2.9.4. Haemoglobin levels (Hb).

Hb levels (LOD: 2.48 mmol/L (= 4g/dL)) were determined by chemiluminescence methodology (whole blood application on a cobas® 311/501 analyser; Roche/Hitachi cobas® c systems, Basel, Switzerland).[549] The haemolysed sample has a specific absorbance spectrum and determined bichromatically (during pre-incubation phase of HbA1c immunoassay).[550]

Low Hb has been associated with increased cardiovascular risk and has application in HIV/AIDS and air pollution exposure.[556–560] For the purpose of this study, desirable Hb levels were defined as more than 12 and more than 13 g/dL for women and men respectively according to WHO guidelines.[561]

2.9.5. Liver function: γ-Glutamyl transferase (GGT).

GGT levels (LOD: 3 U/L) were determined by chemiluminescence methodology (Enzymatic colorimetric assay [562]) on a cobas® 311/501 analyser (Roche/Hitachi cobas® c systems, Basel, Switzerland).[563] The principal of the test analysis is based on an enzymatic colorimetric assay where γ-glutamyl transferase transfers the γ-glutamyl group of L-γ-glutamyl-3-carboxy-4-nitroanilide to form glycylglycine.[563] The GGT is proportional to 5-amino-2-nitrobenzoate produced during the reaction.[563] GGT levels are determined by photometrically measuring the increase in absorbance.[563]

Increased GGT levels have been associated with increased cardiometabolic and cardiovascular risk.[564] HIV/AIDS, ART treatment and air pollution exposure have been associated with impaired liver function as demonstrated by increased GGT levels.[565,566] Elevated GGT levels have also been shown in people with high

alcohol consumption.[567] GGT levels less than 60 U/L for men and less than 40 U/L for women were considered normal, and elevated when equal to or above these levels according to NHLS standards.[563]

2.9.6. Kidney function: Albuminuria, serum and urine creatinine, urine albumin-to-creatinine ratio and eGFR.

Albuminuria was measured by chemiluminescence methodology (Enzymatic method [562]) on a cobas® 501/502 analyser (Roche/Hitachi cobas® c systems, Basel, Switzerland) (LOD: 3 mg/L (0.05 µmol/L (0.3 mg/dL)).[568] In the immunoturbidimetric assay, antigen in the sample reacts with anti-albumin antibodies and produces (agglutinates) antigen/antibody complexes and quantified turbidimetrically.[568]

Serum and urine creatinine levels were determined by chemiluminescence methodology (Enzymatic method [562]) on a cobas® 311/501 analyser (Roche/Hitachi cobas® c systems, Basel, Switzerland) (LOD: 5 µmol/L (1.1 mg/dL)).[569] The enzymatic method for creatinine determination is based on the production of glycine, formaldehyde and hydrogen peroxide from creatinine in the presence of creatininase, creatinase, and sarcosine oxidase.[569] The colour intensity produced during the formation of quinone imine chromogen (hydrogen peroxide reacts with 4-aminophenazone) is directly proportional to the creatinine concentration in the reaction mixture.[569]

Urine albumin-to-creatinine ratio has application in air pollution and HIV/AIDS.[570,571] Microalbuminuria in particular is associated with cardiovascular risk and considered an independent marker of hypertension and cardiovascular risk.[572–575] albumin-to-creatinine ratio was calculated and expressed as mg/mmol. An albumin-to-creatinine ratio below 30 mg/g has previously been associated with hypertension and increased risk for CVD. A level higher than 3 mg/mmol was considered elevated in for the purpose of the current study according to the South African an UK Renal Association.[576] **Estimated glomerular filtration rates (eGFR)** has been associated with CVD and has application in terms of air pollution and HIV/AIDS.[577–580] eGRF was calculated according the CKD-EPI formula (mL/minute/1.73 m^3) as previously described.[581] eGFR more than 90 mL/minute/1.73 m^3 was considered normal. Decreased (increased risk for diabetes mellitus, hypertension and kidney disease) eGFR was defined as 90 mL/minute/1.73 m^3 and below.[582,583]

2.9.7. Markers of HIV/AIDS progression: CD4 count and viral load.

Flow cytometry (FC 500 MPL) with MXP software (Backman Coulter, Brae, CA, US) were used for the determination of CD4 cell count.[584] The principle of the analysis is based on a cell count after labelling cells with a surface marker.[585] Viral load was determined by a COBAS® AmpliPrep/COBAS® TaqMan® HIV-1 Test, v2.0 (LOD:20 cp/ml or 33 IU/ml).[586] The HIV-1 nucleic acid amplification (PCR) test is based on reverse transcription of the target RNA to generate complementary DNA (cDNA).[587] Viral cDNA is detection by a cleaved dual-labelled oligonucleotide detection probe specific to the target.[587]

For the purpose of this study immunological failure was defined as CD4 count 250 cells/mm^3 and unsuccessful viral suppression at viral load above 1000 copies mRNA/ml according to the WHO guidelines.[588,589]

2.9.8. Biomarkers of vascular endothelial function.

Serum was sent to the Division of Molecular Biology and Human Genetics, University of Stellenbosch, for determination of biomarkers of vascular endothelial dysfunction. A magnetic Luminex® assay with a Luminex® MAGPIX® CCD Imager (xPONENT software; Research & Diagnostics Systems Inc.® a Bio-techne® brand (Catalog number LXSAHM); Minneapolis, NE, USA) was used for the determination of TNF-α, VEGF and adhesion molecules (VCAM-1 and ICAM-1, PAI-1 and e-selectin, and p-selectin).[590] The principle of the chemiluminescence methodology is based on the pre-coating of analyte specific antibodies onto fluorophore embedded microparticles at protein-specific ratios.[590] The specific antibodies bind to the proteins of interest.[590] Excess (unbound) antibodies were washed off and a protein-specific biotinylate antibody was added that binds to the proteins of interest.[590] Excess biotinylate was washed off and streptavidin-phycoerythrin was added. Streptavidin-phycoerythrin binds to the biotinylate antibody and excess (unbound) streptavidin-phycoerythrin is washed off.[590] The coated proteins of interest were resuspended in a buffer solution.[590] The proteins of interest is finally read (CCD camera with differential filters to detect various excitation levels) by the Luminex® MAGPIX® Analyser.[590] This is achieved by magnetic capturing of superparamagnetic proteins in a monolayer which is illuminated by two light emitting diodes.[590] Luminescence generated is directly proportional to protein content and quantified photometrically.[590] Inter-run samples/calibration standards at known concentrations were run between study samples for quality control purposes (Coefficients of variance was achieved between inter-run samples).

2.9.9. Genetic analysis.

For Sub-study 2, buffy coats were extracted (0.5 ml) from EDTA blood collection tubes stored at -80 °C and sent to VITO and the University of Hasselt (Belgium) for analysis (Leukocyte: DNA methylation, mtDNA content and telomere length).

2.9.9.1. DNA extraction from buffy coats.

DNA was extracted from buffy coats by means of a QIAamp® DNA Mini Kit (250) (Catalogue number: 51306; QIAGEN; Hilden, Germany).[591,592] DNA extraction was conducted in the Molecular Epidemiology DNA Laboratory, University of Hasselt.

Sample preparation: Buffy coats (200 µl), RNase A (4 µl), AL buffer (guanidinium chloride) and proteinase K (20 µl) were added to a microcentrifuge tube (1.5 ml) and pulse-vortexed (Avantir ® VWR™ Vortex; Radnor, Pennsylvania, USA) for 15 seconds. Samples were then incubated for 1 hour at 56 °C (1.5 ml microcentrifuge tube *via* ThermoMixer®; Hamburg, Germany) and vortexed (30 seconds short-spin at 14 000 rpm).

DNA purification: Ethanol (200 µl; 96 to 100 % Ethanol) was added to the sample tubes and mixed (15 seconds pulse-vortexing). The samples were transferred to QIAamp Mini spin columns and centrifuged for 1 minute (14 000 rpm). The columns were removed from the collection tube, placed on a new collection tube and 500 µl AW1 buffer added. The samples were centrifuged for 1 minute at 8000 rpm and the flow-through removed. Five-hundred µl AW2 buffer was added to each sample, centrifuged for 3 minutes (14 000 rpm) and the flow-through removed. The column was place in a 1.5 ml microcentrifuge tube, 100 µl AE buffer added, incubated for 1 minute (room temperature) and centrifuged for 1 minute at 8000 rpm. Subsequently another 100 µl AE buffer was added, incubated for 5 minutes (at room temperature) and centrifuged for 1 minute at 14 000 rpm to elute the full sample. The columns were removed, the microcentrifuge tube closed, and placed on ice for DNA concentration determination.

DNA concentration determination: The DNA concentration (ng/ml) in each sample was determined at 260 nm by a NanoDrop™ ND-1000 spectrophotometer (ND-1000, Isogen, Life Science, Belgium). One µl of each sample was placed on the NanoDrop™ pedestal, the arm closed and the concentration recorded. DNA concentration (ng/µl) and purity ratios (A260/280 and A260/230) were determined. Extracted DNA samples were stored (–20°C) and used for the determination of leukocyte DNA methylation, mtDNA content and telomere length.

2.9.9.2. Determination of DNA methylation.

DNA methylation analysis was performed at VITO (Belgium) by means of liquid chromatography/mass spectrometry (LC/MS) coupled with UV detection.

Standard curve preparation: A standard curve was prepared by adding a stock solution 1 (S1) containing internal standards for 2-methylcytosine (2dC: 242 µl at 1002 µg/ml (VITO stock number: MIE-OR-dc-003)) and deaminated 5-methylcytosine (5mdC: 24.0 µl at 1006 µg/ml (VITO stock number: MIE-OR-5mdc-002)) to miliQ (mQ) water (9734 µl). The dilutions for the standard curve was prepared by adding 750 µl mQ water to a vial as a blank and adding S1 to a vial numbered S1 (2dC 24248 µg/L and 5mdC 2414 µg/L). Dilution concentrations for a linear calibrations curve were prepared by adding 750 µl mQ water to vials numbered S2 to S12 and adding 750 µl from S1 to S2 (2dC 12124 µg/L and 5mdC 1207 µg/L), 750 µl S2 to S3 (2dC 6062 µg/L and 5mdC 604 µg/L), 750 µl S3 to S4 (2dC 3031 µg/L and 5mdC 302 µg/L), etc.

Quality control samples: Two pooled DNA samples (P1 and P2 at known concentrations of 500 ng/µl) were prepared for quality control purposes by adding 19.5 µl mQ water, 2 µl Pool DNA, 2.5 µl 10xDNA degradase

reaction buffer (pH 7.5-8) and 1 µl DNA degradase (5 units/µl) in a 1.5 ml microcentrifuge tube (total volume 25 µl).

Sample preparation: The volume of samples needed for 1 µg DNA was calculated by using previously NanoDrop-determined concentrations (µg/µl) (DNA extracted concentration / 1000). Each calculated volume was added to labelled vials. The volume mQ water need for each sample was calculated (21.5 µl minus the calculated amount of sample). If the required parent sample volume exceeded 21.5 µl, no mQ water was added. Samples were incubated (2 hours at 37°C (to activate enzymes)) followed by a 30-minute incubation period at 70°C (to stop enzyme activity) and transferred to GC/MS vials.

Sample analysis: Samples were analysed at the VITO laboratories with Acquity Ultra pressure liquid chromatography / mass spectrometry (UPLC/MS) coupled with UV detection using the following settings: Injection volume 7.5 µl; Injection type PLUNO; Sample temperature: 4°C; Sample loop: 10 µl; Needle loop: 30 µl; Injection needle type: Peek needle. The columns used were Nucleosil SA ion exchange silica columns (150x4.6mm-5µm).

The UPLC system was optimised before and after analysis (column rinsed: 100% acetonitrile (ACN) for 60 minutes and 50/50% ACN/mobile phase for 15 minutes. Equilibration was achieved at 100% mobile phase until no fluctuation of the baseline was observed. Column temperature was set at 30°C. UV detection wavelength for dC was set at 272 nm and for mdC at 279 nm. Running fluid consisted of 50 nM NH4Ac in 15% ACN at pH 4.8 (3854g NH4Ac dissolved in 850ml mQ water + 150ml ACN, pH brought to 4.8 with acetic acid). The washing solvent for the strong needle wash (highly concentrated washing solvent to prevent carryover) consisted of H_2O/IPA/MeOH +0.1% formic acid, for the weak needle wash (to replace the strong wash solvent with a less elutive solvent) consisted of H_2O/ACN (70/30) and for the seal wash (to further elute the weak needle wash): H_2O/ACN (90/10). Sample concentrations were determined (directly proportional) by calculating the area under the curve on chromatograms and substituting the value into the formula for the linear trend line of the calibration curve. Results were expressed as a 5mdC/2dC ratio as previously described.[593]

2.9.9.3. Determination of mtDNA content.

Mitochondrial DNA content was determined on a 7900HT Fast Real-Time PCR System (Applied Biosystems, USA) in a 384-well format. Gene ratios of two mitochondrial gene copy numbers were used to calculate mtDNA content.[594] These gene ratios included MTF3212/R3319 (mitochondrial forward primer sequence from nucleotide 3212 (CACCCAAGAACAGGGTTTGT) and reverse primer sequence from nucleotide 3319 (TGGCCATGGGTATGTTGTTAA)) and MT-ND1 (mitochondrial encoded NADH dehydrogenase 1; Forward: ATGGCCAACCTCCTACTCCT Reverse: CTACAACGTTGGGGCCTTT) to three single-copy nuclear control genes (RPLP0 - acidic ribosomal phosphoprotein P0: forward GGAATGTGGGCTTTGTGTTC and reverse CCCAATTGTCCCCTTACCTT; ACTB - beta actin: forward ACTCTTCCAGCCTTCCTTCC and reverse GGCAGGACTTAGCTTCCACA; and HBB - haemoglobin beta: forward GTGCACCTGACTCCTGAGGAGA and reverse: CCTTGATACCAACCTGCCCAG). All primer sequences were diluted to 300 nM in the master mix.[594]

Extracted DNA samples were diluted with RNase free water to a uniform 5 ng/µl concentration and aliquoted (2.5 µl) into 7.5 µl master mix (Fast SYBR® Green I dye 2× (Applied Biosystems; 5 µL/reaction), forward/reverse primer (0.3./0.3 µL/reaction) in RNase free water (1.9 µL/reaction)) into each well (final volume 10 µL/reaction). For quality control, two control and 6 inter-run calibrators were added to each plate. The thermal cycling specification included 20 sec at 95°C (activation of the AmpliTaq Gold® DNA-polymerase), followed by denaturation (40 1-second cycles at 95°C) and annealing/extension (20 seconds at 60°C). A melting curve analysis (15 seconds at 95°C, 15 seconds at 60°C and 15 sec at 95°C) confirmed amplification specificity and absence of primer dimers at the end of each run. Calculations included C_T (cycle threshold) and normalization of the two mitochondrial genes values relative to the three nuclear reference genes (qBase software (Biogazelle, Zwijnaarde, Belgium)). Data was expressed as mtDNA content relative to nuclear DNA copy number (ratio) as previously described.[595] Inter-run calibration algorithms corrected for run-to-run differences. The coefficient of variation for the mtDNA content in inter-run samples was ~4.0%.[594]

2.9.9.4. Determination of Leukocyte Telomere Length (LTL).

A similar qPCR methodology was applied for LTL determination. Extracted DNA samples were diluted to ensure a uniform DNA input (5 ng) for each quantitative real-time polymerase chain reaction (qPCR) and checked using a Quant-iT PicoGreen dsDNA Assay Kit (LifeTechnologies, Europe).[592] All LTL measurements were performed in triplicate on a 7900HT Fast Real-Time PCR System (Applied Biosystems, USA) in a 384-well format. The telomere-specific qPCR reaction mixture contained 1x QuantiTect SYBR Green PCR master mix (Qiagen, Inc., Venlo, the Netherlands), 2 mM dithiothreitol (DTT), 300 nM telg primer (ACACTAAGGTTTGGGTTTGGGTTTGGGTTTGGGTTAGTGT) and 900 nM telc primer (TGTTAGGTATCCCTATCCCTATCCCTATCCCTATCCCTAACA). Cycling conditions used were: 1 cycle at 95°C for 10 minutes, followed by 2 cycles at 94°C for 15 seconds and 49°C for 2 minutes and 30 cycles at 94°C for 15 seconds, 62°C for 20 seconds, and 74°C for 1 minute and 40 seconds. The single-copy gene qPCR mixture contained 1x QuantiTect SYBR Green PCR master mix, 300 nM 36B4u primer (CAGCAAGTGGGAAGGTGTAATCC) and 500 nM 36B4d primer (CCCATTCTATCATCAACGGGTACAA). After each qPCR a melting curve analysis was performed. On each run, a 6-point serial dilution of pooled buffy coat DNA was run to assess PCR efficiency as well as three inter-run calibrators to account for inter-run variability. We achieved coefficients of variation (CV) within triplicates of the telomere runs, single-copy gene runs, and telomere repeated copy number / single gene copy number ratios (T/S ratios as previously described [596]) of 0.71 %, 0.38 %, and 7.1 %, respectively.[383]

2.9.10.   Urinary markers of BTEX exposure.

Mid-stream urine samples were stored at −80◦C and sent to VITO (Mol, Belgium) for level determination of the following urinary metabolites: N-acetyl-S-(3-hydroxypropyl)-L-cysteine (HPMA; a marker of acrolein exposure [34]), N-acetyl-s-(phenyl)-L-cysteine (PMA; a marker of benzene exposure [35]), N-acetyl-s-(benzyl)-L-cysteine (BMA; a marker of toluene exposure [36]), trans,trans-muconic acid (MU; a marker of benzene exposure [35]), and 3+4-methylhippuric acid (3+4MHA; a marker of o-, m-, and p-xylene exposure [37]).

Calibration curve: A matrix-matched calibration curve was applied for the quantification of HPMA, BMA, and PMA to compensate for the matrix effect. To achieve this, spiked urine samples were used containing 10 µL urine, 25 µL mixed internal standard (MU-d4 and 2,3 and 4 MHA-d7: 2000 ng/ml, 20 µL low and high spiked standards (low spike: HPMA, 37.5 ng/ml; PMA, 0.25 ng/ml; MU 5.0 ng/ml, BMA, 1.25 ng/ml; 3+4MHA, 20.0 ng/ml; and high spike: HPMA, 75.0 ng/ml PMA, 0.5ng/ml; MU, 10.0ng/ml; BMA, 2.5ng/ml; 3+4MHA, 40.0 ng/ml (Toronto Research chemicals Inc., ON, Canada)) and 445 µl 1 acetic acid (HAc; Merck, NJ, USA) in ultra-pure water.

Sample Preparation: Samples were prepared using 10 µL urine, 25 µL mixed internal standard (2000 ng/ml in methanol:water(1:1, v:v)) MU-d4 and MU-d3 (Santa Cruz Biotechnology, TX, USA), and 4 MHA-d7 (Toronto research chemicals Inc., ON, Canada) with 465 µL 1% HAc.

Sample analysis: Twenty microliters of each sample were injected in an ultra-performance liquid chromatography (UPLS; Waters I-class Acquity UPLC system, Milford, MA, USA)/mass spectrometry (MS; Waters Xevo TQ-S tandem in the negative electrospray ionization mode (ESI−)). An Acquity UPLC® high-strength silica T3 column (50 mm×2.1 mm; 1.8 µm; at a constant temperature of 40 °C) with UV detection (Photodiode array (PDA) detector set at 259 nm) was used for the simultaneous quantification of the urinary metabolites [38]. Retained compounds were eluted with 4 mL HAc solution (10%, v:v). Levels of metabolites were calculated based on the corresponding matrix-matched calibration curve.[597,598]

2.10.   Flow-mediated dilatation (FMD).

To create optimal/standardised conditions for the FMD procedure, guidelines from the International Brachial Artery Reactivity Task Force were followed.[156] According to these guidelines, fasting participants were instructed to refrain from smoking, exercise and taking medication the morning (4 to 6 hours) before clinical assessment visits.[156] The FMD procedure was also performed in a temperature-controlled room at constant 22 °C. Time was allowed for participants to feel comfortable and acclimatise before measurements began (more than 10 minutes).[156] To limit inter-operator variability, the number of researchers involved in measuring the FMD was restricted, and each operator was allocated specific tasks in a consistent fashion. All operators were furthermore trained and evaluated by experts in the technique. Random FMD procedures were selected and evaluated by

blinded experts for quality control purposes. Interobserver variability for the FMD procedure was assessed at the end of the study (please refer to Appendix C, Table C2 on page 255).

Fasting participants were positioned comfortably in a supine position with their right arm extended (without hyperextension) at an 80° angle from their body. The blood pressure cuff was positioned around the forearm distal to the elbow. Sonography gel was added onto the transducer (probe) crystal. The probe was fixed in the probe holder and placed in an area 3 to 4 cm proximal to the elbow (cubital fossa) and the brachial artery located by adjusting the probe's angle and position until a clear image was obtained. Correct vessel localisation was verified by visualising the real-time image in the colour-flow mode (doppler mode; arteries will appear red and veins blue). Once the position for a clear digital image was confirmed, the probe holder's arm was fixed to keep the probe in position (**Figure 2.8.**).
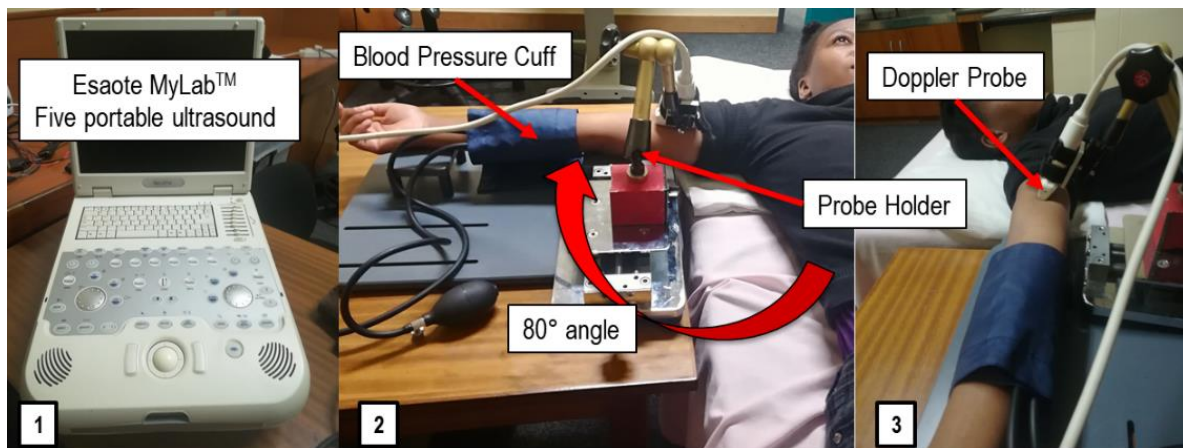
Figure 2.8. Instrumentation and participant position. **Description: 1.** Esaote MyLab™ Five portable ultrasound. **2.** Participant in the supine position with arm extended at an 80° angle in relation to the body. **3.** Doppler probe placed 3–4 cm proximal to the elbow. Photos of the procedure were taken by the author of this dissertation after consent was obtained by the person posing in the photos and the figure was designed by the author of this dissertation.

FMD was determined with a mobile Esaote MyLab™ Five portable ultrasound device (Genoa, Italy) with an Esaote Doppler probe (LA523, 12 MHz) connected to computerized software with edge detection technology (Quipu Cardiovascular Suite™; Pisa, Italy) as previously described.[43,157] The ultrasound was set at a frequency of 6.6 Hz (according to the depth of the artery) and to a depth of 3 cm. The pulse repetition frequency (PRF: determined by the velocity of blood flow rate detected in the blood vessel), also known as scale, was set at 6.7 Hz. To optimise the visualisation of the image the steer was angled so that the top and bottom margins of the steer box were parallel to the vessel walls and set at a 60° angle. The pulse wave setting was adjusted to match the angle of the vessel. Sample volume size was set at 1 (according to vessel size). The basal mode was switched to normal mode (for inverse pulse waves the reverse setting was applied).

Cardiovascular Suite™ UE 2.8.1. (build 120) computerised software was used for edge detection and calculations. The FMS Studio software (part of Cardiovascular Suite™ software) setting was selected (for vascular measurements). The recording times were set (baseline vessel diameter assessment: 60 seconds; period of ischaemia: 300 seconds; period of reactive hyperaemia: 120 seconds). The flow period (seconds) on the Doppler flow profile's x-axis, the flow amount (cm/second) on the y-axis and the doppler flow region was manually selected. The region of interest on the vessel image was selected. Once the edges of the vessel were properly detected the baseline measurements commenced.

The computerized software determined the mean baseline brachial artery lumen diameter (mm) over a 60-second period. Following the baseline measurements, the blood pressure cuff around the forearm was inflated to more than 50 mmHg supra-systolic blood pressure. The ischaemic occlusion was maintained for a 5-minute period according to previously described recommendations. [599,600] Following the 5-minute ischaemic occlusion, deflating the blood pressure cuff triggered reactive hyperaemia and the maximum brachial artery lumen diameter (μm) was recorded during this period. The maximum lumen diameter displacement during reactive hyperaemia from the mean baseline measurements was expressed as the percentage of the mean baseline brachial lumen diameter (% FMD) (**Figure 2.9.**).
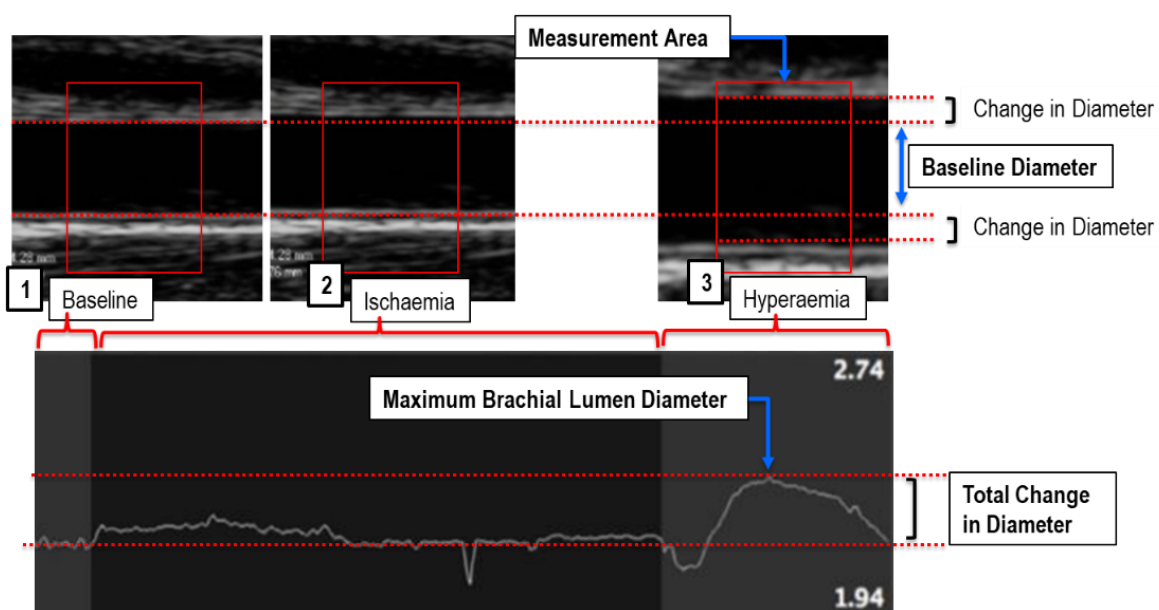
Figure 2.9. Measurement of flow-mediated dilatation with edge detection technology. **Description: 1.** Baseline diameter measurement of the brachial artery. **2.** Period of occlusion/ischaemia. **3.** Brachial artery diameter measurement during reactive hyperaemia. Images were captured and the figure designed by the author of this dissertation.

2.11. Retinal Imaging.

2.11.1. Retinal image capturing.

Retinal images were captured with a Canon CR2 digital camera (Canon Europa NV, The Netherlands) and analysed with semi-automated software (MONA REVA 2.1.1 developed at VITO; https://mona.health) against standardised protocol as previously described (**Figure 2.10.**).[521,601]

Figure 2.10. Procedure for ocular fundus retinal imaging. **Description: 1.** Participant seated in front of the camera in darkened room. **2.** The participant places his/her chin and forehead in the correct position. **3.** The camera is positioned in line with the eye. **4.** An image of the eye is visualised on the digital screen of the camera. **5.** The alignment and focus of the image are adjusted. **6.** The camera's zoom is set on the retina and the focus and alignment adjusted so that the optic disc appears in the centre of image. **7.** The image is captured and appears on the monitor to assess quality. Photos of the procedure were taken after consent was obtained by the person posing in the photos. The figure was designed by the author of this dissertation.

The flash light during image capturing is not harmful to the eye. After fundus images (~15 megapixels) of both eyes were obtained, the best quality image (based on clarity and centrality) was selected for analyses. No significant difference in left and right images were observed (CRAE left *vs.* right eye images (mean ± SD): 157.2 *vs.* 157.7 µm; *p* = 0.865).[163] Image analysis was performed blinded/masked to avoid bias.

2.11.2. Image analysis.

The semi-automated image analysis software is able to determine retinal vessel calibre.[601] The measurements for retinal calibre are standardised (the distance between centre of the optic disc and the fovea and performed in a designated zone against standardised protocol (**Figure 2.11.**).[163]
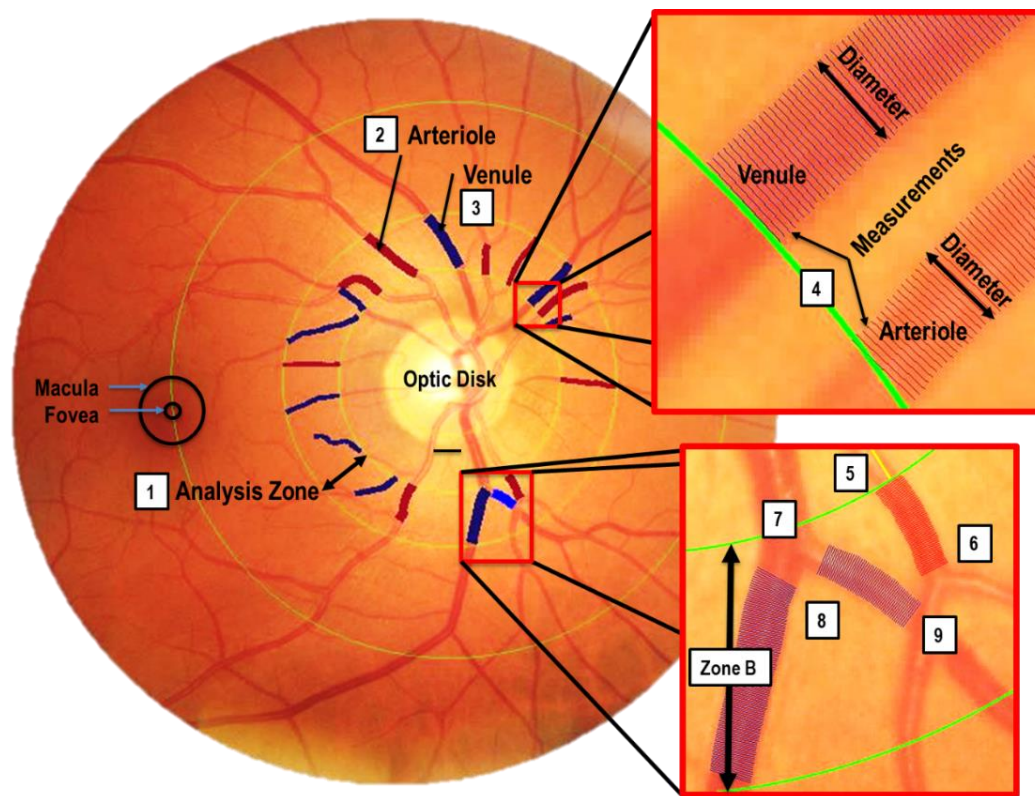
Figure 2.11. Vessel calibre determination.[163,602,603] **Description: 1.** Determination of vessel calibres were performed in the zone 0.5- and 1-disc diameter from the optic disc margin. **2.** Arterioles were presented in red. **3.** Venules were presented in blue. **4.** The vessel diameter was calculated as the mean of multiple cross-sectional measurements (n = >30). **5.** Measurements were performed from the inner border of analysis zone. **6.** Measurements for a vessel were only determined before branches and **6.** the daughter vessels were excluded from further measurements. **7.** When vessel branching was too close to the inner border to allow 30 diameter measurements, **8.** the daughter vessels were used for measurements. **9.** Vessel segments beyond arteriole-venule crossings within the zone for analysis were not included in the measurements.

The semi-automated software detected vessels in the zone 0.5- and 1-disc diameter from the optic disc margin and classified them according to colour (Red: arterioles and blue venules.). The software furthermore automatically measures the diameter of the vessel within the area for analysis and calculated the mean diameter for each vessel (more than 30 individual diameter measurements need to be taken for each vessel). Vessels that were misclassified were corrected and edges that were incorrectly detected were manually adjusted by the grader. Differences in features between arterioles and venules that helped the grader to distinguish vessel from each other included:

- Arterioles appear lighter in colour than venules.
- Arterioles will never cross arterioles and venules will never cross venules in the analysis zone.
- Venules generally appear straighter than arterioles.

- The mean diameters for arterioles are generally smaller than that of venules.

The mean vessel diameter of the six largest arterioles and venules were determined by computerised software according to the revised Knudtson-Pass-Hubbard formula and summarised as central retinal arteriolar equivalent (CRAE) and central retinal venular equivalent (CRVE) values respectively. Finally, an arteriole/venule-ratio was also calculated by the software (**Table 2.1.**). [602]

Table 2.1. Vessel calibre endpoints.[163,602,603]

	Parameter/Feature	Definition
1	Central arteriolar equivalent (CRAE) (µm)	The mean diameter of the 6 largest arterioles 0.5- and 1-disc diameter from the optic disc margin.
2	Central retinal venular equivalent (CRVE) (µm)	The mean diameter of the 6 largest venules 0.5- and 1-disc diameter from the optic disc margin.
3	CRAE/CRVE ratio (AVR)	The ratio of CRAE and CRVE.

CRAE and CRVE measurements are mostly associated with systemic diseases.[160] Venules, for example, may be dilated in response to an inflammatory condition, while the arteriole diameter increases due to underlying hypertension.[160]

2.12. Data capturing.

All participant data obtained for the purpose of this study were captured on Research Electronic Data Capture application (REDCap™). Access to the data was restricted and password-protected, and data were verified only by researchers who had been granted access to the REDCap database management platform. All hard copy documentation such as informed consent documents was filed and stored away in an access-controlled area in the Division of Medical Physiology, Stellenbosch University. Data (no personal information) was extracted from REDCap in the form of excel files for statistical analysis.

2.13. Statistical analysis.

All statistical analyses were performed with IBM® SPSS® software (version 25; New York, NY, USA).

Extensive statistical power analyses have been conducted to justify the proposed sample sizes for this study. A thorough literature search was undertaken with the assistance of the Biostatistics Unit (Faculty of Medicine and Health Sciences, Stellenbosch University), and according to Donald *et al.* (2008),[158] a case sample size of between n=100 - 400 over a 3 month follow-up period is sufficiently powerful to secure endothelial function measurement reproducibility and statistical significance (1-2% effect size; 80% statistical power and 5%

significance). In the EndoAfrica pilot studies performed in 2015, significant correlations (adjusted for age, gender, medication and smoking status) were observed between risk factors such as HbA1C and LDL-cholesterol, and FMD and retinal microvascular diameters in a sample size of n = 65.

A table depicting the distribution of baseline assessment visits for each study group is available in Appendix C (**Figure C1**, page 255). The number of participants lost at follow-up visits and the reasons why were reported in **Table C1**, page 255.). Interobserver variability for the FMD procedure was evaluated and results were reported in Appendix C (**Table C2**, page 255).

The data distribution (parametric or non-parametric) for each variable was determined by a Shapiro-Wilk test and evaluating data histograms and Q-Q-plots. Baseline population characteristics were presented as the mean ± standard deviation (SD) for continuous parametric data and median (range: minimum to maximum) for non-parametric continuous variables. Categorical variable outcomes were presented as the sample size (n, %).

To compare differences between two groups, a paired Student's t-test (parametric data) or a Wilcoxon test (non-parametric data) were used. An independent samples t-test (parametric data) or a Mann-Whitney U test (non-parametric) was used to compare unpaired data between two groups. For comparing 3 groups (Sub-Study 1) a Kruskal Wallis test was used. A Spearman correlation was used in Sub-study 2 to evaluate the relationship between variables.

Linear mixed model regression analysis was applied to determine effects of exposure (Sub-study 1: HIV/AIDS and ART; Sub-study 2: NO_2, BTEX and urinary metabolites of exposure) on variable outcomes. A within group analysis was performed for Sub-study 1 and Sub-Study 2. A between group analysis was not performed in Sub-study 1 due to large differences in groups sizes and large difference in population characteristics. Variables with skewed data distribution (nonparametric) were $\log_{10}$-transformed. For each analysis, participants were nested in each visit and participants at each time point were included as random effects factor variables with random intercept to account for possible inter-individual variation while adjusting for selected covariates. To evaluate effects of exposure on variable outcomes independent of potential confounding effects, *a priori* covariates with a potential link between exposure and dependent variable outcomes were selected. For small groups (e.g. in HIV/no ART) or variables with limited data (biomarkers analysis) models were minimally adjusted. Exposure to other possible residual confounding pollutants were not considered or adjusted for (e.g. through diet and other pollutants beyond the scope of this study). Q-Q plots of the residuals were used to test the assumptions of linearity. Specific linear mixed model adjustments are indicated in the results chapters under each results table. Estimated effects are expressed as a change (parametric data) or a % difference (non-parametric data). The significance threshold for all statistical analysis was set at p < 0.05. All statistical analyses were performed by the PhD candidate, and verified by a professional biostatistician.

3.   Chapter 3 – Results and discussion: HIV and ART (Sub-study 1).

3.1.   Baseline population characteristics.

3.1.1.   Baseline demographic, lifestyle, medical history and socioeconomic characteristics.

A total number of 295 volunteering participants completed baseline and follow-up visits. Participants who did not consent to take part in the follow-up visit or whose follow-up data were not available were excluded from the study. The HIV-free group consisted of n = 107 participants with a mean age of 42.3 years. The HIV-free group was furthermore mostly represented by females (n = 90, 94%), people of mixed ancestry (n = 103, 96%) and participants from the Cape Town area (n = 81, 76%). The HIV+ART group consisted of n = 151 participants with a mean age of 40.4 years. The HIV+ART group was predominantly female (n = 99, 66%), of mixed ancestry (n = 108, 72%) with a more even distribution across recruitment areas (Cape Town area: n = 70, 47%; Worcester: n = 80, 53%) compared to other groups. The HIV/noART group (n =37) represented participants that were not on ART at baseline, but initiated ART before the 18-month follow-up visit. This group consisted mostly of female participants (n = 24, 65%) with a mean age of 35.7 years. Participants in the HIV/noART group were also mostly of mixed ancestry (n = 33, 89%) and from the Worcester recruitment area (n = 23, 62%).

HIV-free represented 36%, HIV+ART 51% and HIV/noART 13% of the total study population. HIV/noART participants were significantly younger than HIV-free (p = 0.005) and HIV+ART (p = 0.012). Group composition in terms of gender significantly differed between HIV-free and HIV+ART (p = 0.001), and HIV-free and HIV/noART (p = 0.013), and in terms of ethnicity between HIV-free and HIV+ART (p < 0.001). Group proportions in terms of recruitment locations also significantly differed between HIV-free and HIV+ART (p < 0.001) and HIV-free and HIV/noART (p < 0.001). No other significant differences were observed (**Table 3.1.**).

Table 3.1. Baseline demographic characteristics.

Variable [a]	HIV-free	HIV+ART	HIV/noART
Age (years)	42.3 ± 11.4	40.4 ± 8.9	35.7 ± 10.1 [b]
Gender, *n* (%)			
Male, *n* (%)	17 (16%)	51 (34%)	13 (35%)
Female, *n* (%)	90 (84%)	99 (66%)	24 (65%)
Ethnicity			
Black, *n* (%)	4 (4%)	42 (28%)	4 (11%)
Mixed, *n* (%)	103 (96%)	108 (72%)	33 (89%)
Location			
Cape Town, *n* (%)	81 (76%)	70 (47%)	14 (39%)
Worcester, *n* (%)	26 (24%)	80 (53%)	23 (62%)

[a] Data presented as mean ± SD or *n* (% of group; HIV-free: *n* = 107; HIV+ART: *n* = 151; HIV/noART: *n* = 37). [b] *vs.* HIV-free, *p* = 0.005 and *vs.* HIV+ART, *p* = 0.012.

The HIV-free group had the highest percentage of smokers (*n* = 69, 65%) while about half of the HIV-free population consumed alcohol in the last 12 months (*n* = 54, 51%) at a frequency of less than 8 days a month (*n* = 48, 89%). About one-third of HIV-free participants were using any other medication other than ART at the baseline visit (*n* = 38, 36%).

About half of HIV+ART participants were current smokers (*n* = 80, 53%) and consumed alcohol within the last 12 months pre-baseline visit (*n* = 78, 52%) at a frequency less than 8 days per month (*n* = 61, 78%). HIV+ART participants mostly reported sleeping between 6 and 9 hours at night (*n* = 70, 47%). Almost three-quarters of HIV+ART participants reported being on some medication aside from ART (*n* = 107, 72%).

The HIV/noART group also consisted mostly of smokers (*n* = 26, 70%). More than half of HIV/noART participants consumed alcohol in the last 12 months pre-baseline visit (*n* = 22, 59%) at frequency less than 8 days per month (*n* = 18, 82%). Participants in the HIV/noART group also mostly reported using some form of medication at the baseline visit (*n* = 26, 70%) (**Table 3.2.**).

Table 3.2. Baseline lifestyle and health characteristics.

Variable [a]	HIV-free	HIV+ART	HIV/noART
Smoking status			
Current smoker, n (%)	69 (65%)	80 (53%)	26 (70%)
Alcohol consumption (Yes), n (%) [b]	54 (51%)	78 (52%)	22 (59%)
< 8 days/month, n (%) [c]	48 (89%)	61 (78%)	18 (82%)
Medication other than ART (Yes), n = (%) [d]	38 (36%)	107 (72%)	26 (70%)

[a] Data presented as n (% of group; HIV-free: n = 107; HIV+ART: n = 151; HIV/noART: n = 37). [b] Within the last 12 months. [c] Data presented as n = (% of population that consumed alcohol in last 12 months within each group). [d] Whether the participant reported currently using any other medication than other ART.

About half of participants in the HIV-free group were unemployed (n = 57, 53%) with education that did not extend beyond primary school level (n = 68, 64%). Similarly, about half of participants in the HIV+ART and HIV/noART groups were unemployed (n = 79, 53% and n = 18, 49%, respectively) with mostly primary school education (n = 90, 60% and n = 22, 60%, respectively) (**Table 3.4.**).

Table 3.4. Socioeconomic characteristics for baseline and follow-up.

Variable [a]	HIV-free	HIV+ART	HIV/noART
Employment			
Unemployed, n (%)	57 (53%)	79 (53%)	18 (49%)
Part-time, n (%)	26 (24%)	26 (17%)	6 (16%)
Full-time, n (%)	24 (22%)	45 (30%)	13 (35%)
Level of education			
None	0 (0%)	16 (11%)	4 (11%)
Primary school	68 (64%)	90 (60%)	22 (60%)
Secondary school	16 (15%)	32 (21%)	9 (24%)
University/collage and/or ABET [b]	23 (21%)	12 (8%)	2 (5%)

[a] Data presented as n (% of group; HIV-free: n = 107; HIV+ART: n = 151; HIV/noART: n = 37). [b] Adult basic education training.

3.1.2. Baseline HIV-related and ART characteristics.

The median viral load in the HIV+ART group (20 copies mRNA/ml) fell within the WHO recommended range (<1000 copies mRNA/ml) for successful viral suppression with only n = 26 (13%) participants exceeding the WHO standard.[588] The median CD4 cell count in the HIV+ART group (503 cells/mm^3) was above the WHO recommended cut-off level of 250 cells/mm^3.[588] Most participants in the HIV+ART group were on first-line ART (n = 135, 90%) with the median ART treatment duration 124 weeks (range: 8 to 780 weeks).

The median viral load for HIV/noART (13123 copies mRNA/ml) was more than 10-fold higher than the maximum WHO recommended level,[588] and most participants presented at their baseline visit with a viral load that exceeded this cut-off level (n = 28, 78%). Despite a relatively high median viral load in the HIV/noART group, the median CD4 cell count (469 cells/mm^3) was within the WHO recommended range with only n = 7 (19%) participants presenting with CD4 cell counts below the WHO recommended cut-off level at the baseline visit.

The median viral load in the HIV/noART group was significantly higher compared to HIV+ART (p < 0.001), but no significant differences were observed in the median CD4 cell count between HIV+ART and HIV/noART (**Table 3.5.**).

Table 3.5. Baseline HIV and ART characteristics.

Variable [a]	HIV+ART	HIV/noART
HIV		
Viral Load (copies mRNA/ml)	20 (10 to 187073)	13123 (10 to 662545) [c]
High, n (%) [b]	20 (13%)	28 (78%)
CD4 count (cells/mm^3)	503 (49 to 1434)	469 (91 to 1236)
Low, n (%) [b]	21 (14%)	7 (19%)
Antiretroviral Therapy		
Duration (Weeks)	124 (8 to 780)	-
First/Second-line ART		
First-line (Yes), n (%) [d]	135 (90%)	-

[a] Data presented as median (range) or n (% of group; HIV+ART: n = 147 to 151; HIV/noART: n = 34 to 37). [b] According to the WHO guidelines.[588] [c] *vs.* HIV+ART, p < 0.001. [d] Fixed-dose, combination ART containing emtricitabine / tenofovir / efavirenz.

3.1.3. Baseline body composition characteristics.

The mean BMI of the HIV-free group (27.8 kg/m^2) was in the overweight range (BMI 25 – 29.9 kg/m^2) although the largest percentage of participants (n = 42, 39%) was defined obese (BMI > 30 kg/m^2) according to

WHO criteria.[531,532] Also, more than half of participants in the HIV-free group presented with an elevated waist-to-hip ratio according to WHO criteria.[531,532] The mean BMI of the HIV+ART was in the normal range (23.7 kg/m³) with almost half of the participants in the HIV+ART group (*n* = 74, 49%) presenting with a normal BMI at baseline according to WHO standards.[531,532] Also, more than two-thirds of participants in the HIV+ART had elevated waist-to-hip ratios (*n* = 98, 65%) according to WHO standards.[531,532] The mean BMI in the HIV/noART group was in the underweight range (22.6 kg/m^2) according to WHO standards.[531,532] About one-third of participants in the HIV/noART was clinically defined as underweight (*n* = 12, 32%). Despite the high frequency of underweight individuals in the HIV/noART group, most participants presented with an elevated waist-to-hip ratio at baseline visit (*n* = 23, 62%) according to WHO standards.[531,532]

Participants in the HIV+ART and HIV/noART groups showed significantly lower mean BMI and body weight values compared to the mean BMI and body weight of the HIV-free group (*p* < 0.001, respectively). Although the waist-to-hip ratio did not significantly differ between groups, the mean waist circumference was significantly lower in HIV/noART compared to HIV-free (*p* = 0.07) while the hip circumferences in HIV+ART and HIV/noART were significantly lower than HIV-free (*p* = 0.001, respectively) (**Table 3.6.**).

Table 3.6. Baseline body composition characteristics.

Variable [a]	HIV-free	HIV+ART	HIV/noART
Body Mass Index (BMI), kg/m^2	27.8 ± 8.3 [c]	23.7 ± 6.0	22.6 ± 7.5
Weight (kg)	70.7 ± 21.4 [d]	62.6 ± 15.8	60.2 ± 17.0
Body composition classification according to BMI[b]			
Underweight (BMI < 18.5 kg/m^2), *n* (%)	12 (11%)	21 (14%)	12 (32%)
Normal weight (BMI 18.5 to < 25 kg/m^2), *n* (%)	34 (32%)	74 (49%)	15 (41%)
Overweight (BMI 25 to < 30 kg/m^2), *n* (%)	19 (18%)	31 (21%)	6 (16%)
Obese (BMI > 30 kg/m^2), *n* (%)	42 (39%)	24 (16%)	4 (11%)
Waist-to-hip ratio	0.89 ± 0.08	0.89 ± 0.07	0.89 ± 0.07
Elevated (>0.95/>0.90 women/men) [b]	60 (56%)	98 (65%)	23 (62%)
Waist circumference (cm)	92.3 ± 17.8 [e]	87.4 ± 12.8	83.9 ± 14.5
Hip circumference (cm)	104 ± 15.7 [f]	97.7 ± 13.1	94.6 ± 14.5

[a] Data presented as mean ± SD or *n* (% of group; HIV-free: *n* = 107; HIV+ART: *n* = 151; HIV/noART: *n* = 37). [b] According to WHO guidelines.[531,532] [c] *vs.* HIV+ART and HIV/noART, *p* < 0.001, respectively. [d] *vs.* HIV+ART, *p* = 0.004 and HIV/noART, *p* = 0.007. [e] *vs.* HIV/noART; *p* = 0.07. [f] *vs.* HIV/+ART and HIV/noART; *p* = 0.001, respectively.

3.1.4. Baseline fasting lipid, glucose and HbA1c measurements.

The mean total cholesterol levels in HIV-free (4.57 mmol/L), HIV+ART (4.61 mmol/L) and HIV/noART (4.05 mmol/L) were in the normal range (≥5 mmol/L) according to the Heart and Stroke Foundation of South Africa criteria.[546] The mean total cholesterol levels of HIV/noART were significantly lower than HIV-free (*p* = 0.003) and HIV+ART (*p* < 0.001). About one-third of participants in the HIV-free (*n* = 31, 29%) and HIV+ART (*n* = 47, 31%) groups presented with elevated total cholesterol levels compared to the HIV/noART group (*n* = 4, 11%).

The mean HDL cholesterol levels in HIV-free (1.42 mmol/L) and HIV+ART (1.51 mmol/L) were above recommended Heart and Stroke Foundation of South Africa cut-off levels (1.2 mmol/L for female and 1.0 mmol/L for male).[546] The mean HDL cholesterol level in HIV/noART (1.12 mmol/L) were between the Heart and Stroke Foundation of South Africa cut-off points for decreased HDL cholesterol levels for men (≤1.0 mmol/L) and women (≤1.2 mmol/L).[546] The mean HDL cholesterol levels in HIV/noART were significantly lower compared to HIV-free and HIV+ART (*p* < 0.001, respectively). Also, significantly (*p* < 0.001, respectively) more participants in the HIV/noART group (*n* = 25, 68%) presented with decreased HDL cholesterol levels compared to HIV-free (*n* = 36, 34%) and HIV+ART (*n* = 36, 24%).

The mean LDL cholesterol levels in HIV-free (2.62 mmol/L), HIV+ART (2.55 mmol/L) and HIV/noART (2.41 mmol/L) were below Heart and Stroke Foundation of South Africa standards (≥3 mmol/L).[546] More than one-quarter of participants in HIV-free (*n* = 38, 36%) and HIV+ART (*n* = 41, 28%) presented with elevated LDL cholesterol levels. In HIV/noART *n* = 6 (16%) presented with elevated LDL cholesterol levels.

The mean triglyceride levels in HIV-free (1.15 mmol/L), HIV+ART (1.27 mmol/L) and HIV/noART (1.14 mmol/L) were below Heart and Stroke Foundation of South Africa standards for elevated triglyceride levels (≥1.7 mmol/L).[546] The frequency of participants in HIV-free (*n* = 10, 9%) and HIV+ART (*n* = 26, 17%) and HIV/noART (*n* = 4, 11%) who presented with elevated triglyceride levels was relatively low. No significant differences in terms of triglyceride measurements were observed between groups.

The mean fasting glucose levels in HIV-free (4.95 mmol/L), HIV+ART (4.87 mmol/L) and HIV/noART (4.98 mmol/L) were below Heart and Stroke Foundation of South Africa standards for elevated fasting glucose levels (≥5.6 mmol/L).[546] Also, the frequency of participants in HIV-free (*n* = 15, 14%) and HIV+ART (*n* = 19, 13%) and HIV/noART (*n* = 3, 8%) who presented with elevated fasting glucose levels was relatively low. No significant differences in terms of fasting glucose levels were observed between groups.

The mean fasting HbA1c levels in HIV-free (5.42%), HIV+ART (5.29%) and HIV/noART (5.46%) were below Heart and Stroke Foundation of South Africa standards for elevated HbA1c levels (≥5.9%).[546] The frequency of participants in HIV-free (*n* = 11, 10%) and HIV+ART (*n* = 11, 7%) and HIV/noART (*n* = 3, 8%) who

presented with elevated HbA1C levels was also relatively low. No significant differences in terms of HbA1c measurements were observed between groups (**Table 3.7.**).

Table 3.7. Baseline fasting lipid, glucose and HbA1c measurements.

Variable [a]	HIV-free	HIV+ART	HIV/noART
Lipid Profile			
Total Cholesterol (mmol/L)	4.57 ± 0.91	4.61 ± 1.02	4.05 ± 0.84 [d]
Elevated (≥5 mmol/L), *n* (%) [b]	31 (29%)	47 (31%)	4 (11%)
High-Density Lipoprotein Cholesterol (HDL) (mmol/L)	1.42 ± 0.47	1.51 ± 0.74	1.12 ± 0.43 [e]
Decreased (≤1.2/1.0 mmol/L women/men), *n* (%) [b]	36 (34%)	36 (24%)	25 (68%)
Low-Density Lipoprotein Cholesterol (LDL) (mmol/L)	2.62 ± 0.84	2.55 ± 0.81	2.41 ± 0.69
Elevated (≥3 mmol/L), *n* (%) [b]	38 (36%)	41 (28%)	6 (16%)
Triglycerides (mmol/L)	1.15 ± 0.61	1.27 ± 0.93 [b]	1.14 ± 0.57
Elevated (≥1.7 mmol/L), *n* (%)	10 (9%)	26 (17%)	4 (11%)
Glucose Homeostasis			
Fasting glucose (mmol/L)	4.95 ± 1.60	4.87 ± 1.04	4.98 ± 1.59
Elevated (≥5.6 mmol/L), *n* (%) [c]	15 (14%)	19 (13%)	3 (8%)
Glycated Haemoglobin (HbA1c) (%)	5.42 ± 0.80	5.29 ± 0.55	5.46 ± 0.99
Elevated (≥5.9%), *n* (%) [c]	11 (10%)	11 (7%)	3 (8%)

[a] Data presented as mean ± SD or *n* (% of group; HIV-free: *n* = 105 to 107; HIV+ART: *n* = 151; HIV/noART: *n* = 36 to 37). [b] According to the Heart and Stroke Foundation of South Africa, NHLS and the US National Institutes of Health (NIH) guidelines.[540,546–548] [c] According to The Heart and Stroke Foundation of South Africa guidelines.[546,553–555] [d] *vs.* HIV-free, *p* = 0.003 and HIV+ART, *p* < 0.001. [e] *vs.* HIV-free and HIV+ART, *p* < 0.001, respectively.

3.1.5. Baseline Hb, GGT and markers of kidney function (serum creatinine, urine albumin, ACR and eGFR levels).

The mean Hb levels in the HIV-free (13.7 g/dL), HIV+ART (13.5 g/dL) and HIV/noART (13.2 g/dL) were within WHO recommended standards (Women: <12.0 g/dL and men: <13.0 g/dL).[561] More than one-third of participants in HIV-free (*n* = 37, 35%), HIV+ART (*n* = 59, 40%) and HIV/noART (*n* = 15, 41%) respectively presented with decreased Hb levels at baseline visit. Hb measurements did not significantly differ between groups.

The median GGT levels in the HIV-free (25.0 U/L), and HIV/noART (24.0 U/L) were within WHO recommended standards, while the median GGT level for HIV+ART (51.0 U/L) were higher than the cut-off value for men (≥60 U/L), but lower than the cut-off value for women (≥40 U/L).[561] The median GGT level in the HIV+ART group was significantly higher compared to HIV-free and HIV/noART ($p < 0.001$, respectively). About one-fifth of participants in the HIV-free group (n = 21, 20%) and HIV/noART group (n = 7, 20%) presented with elevated GGT levels at baseline. Most participants in the HIV+ART group (n = 86, 57%) presented with elevated GGT levels. GGT measurements did not significantly differ between HIV-free and HIV/noART.

The mean serum creatinine and median urine albumin levels did not significantly differ between groups. Also, the median albumin-to-creatinine ratio for HIV-free (0.64 mg/mmol), HIV+ART (1.03 mg/mmol) and HIV/noART (1.14 mg/mmol) were below South African guidelines (>3 mg/mmol).[604]

The median albumin-to-creatinine ratio of HIV+ART (1.03 mg/mmol) was significantly higher (p = 0.011) compared to HIV-free (0.64 mg/mmol). The mean eGRF for HIV-free (106 mL/minute/1.73 m^3), HIV+ART (118 mL/minute/1.73 m^3) and HIV/noART (119 mL/minute/1.73 m^3) were within the recommended range as stipulated for the EPI-CKD formula [581] used for the calculation (< 90 mL/minute/1.73 m^3).[582,583] Compared to HIV-free, the mean eGRF values for both HIV+ART and HIV/noART were significantly higher ($p < 0.001$) with the proportion of participants presenting with decreased eGRF significantly higher in HIV-free (n = 17, 16%) compared to HIV+ART (n = 7, 4%; p = 0.002) and HIV/noART (n = 0, 0%; p = 0.009) (**Table 3.8.**).

Table 3.8. Baseline Hb, GGT, serum creatinine, urine albumin, albumin-to-creatinine ratio and eGFR levels.

Variable [a]	HIV-free	HIV+ART	HIV/noART
Haemoglobin (g/dL)	13.7 ± 1.4	13.5 ± 1.6	13.2 ± 1.4
Decreased (Women: <12.0, men: <13.0 g/dL), *n* (%) [b]	37 (35%)	59 (40%)	15 (41%)
Liver function			
γ-Glutamyl transferase (U/L)	25.0 (7 to 1058)	51.0 (14 to 848) [f]	25.0 (10 to 94)
Elevated (≥40/≥60 U/L women/men), *n* (%) [c]	21 (20%)	86 (57%)	7 (20%)
Kidney Function			
Serum creatinine (µmol/L)	62.9 ± 13.9	59.5 ± 14.5	59.4 ± 12.0
Urine albumin (mg/L)	7.1 (0.12 to 617)	9.0 (0.13 to 578)	13.0 (1.5 to 794)
Albumin-to-creatinine ratio (mg/mmol)	0.64 (0.10 to 29.7)	1.03 (0.01 to 94.8) [g]	1.14 (0.18 to 110)
Increased (>3 mg/mmol), *n* (%) [d]	13 (14%)	27 (21%)	7 (27%)
eGRF (mL/minute/1.73 m³)	106 ± 17.0	118 ± 16.1 [h]	119 ± 12.8 [h]
Decreased (< 90 mL/minute/1.73 m³), *n* (%) [e]	17 (16%)	7 (4%)	0 (0%)

[a] Data presented as mean ± SD or median (range) or *n* (% of group; HIV-free: *n* = 91 to 107; HIV+ART: *n* = 127 to 151; HIV/noART: *n* = 33 to 37). [b] According to WHO guidelines.[561] [c] According to NHLS standards.[563] [d] According to the UK Renal Association.[576] [e] According to information from [582,583]. [f] *vs.* HIV-free and HIV/noART; *p* < 0.001, respectively. [g] *vs.* HIV-free; *p* = 0.011. [h] *vs.* HIV-free, *p* < 0.001.

3.1.6. Baseline blood pressure and heart rate measurements.

The mean SBP values in the HIV-free (126 mmHg), HIV+ART (124 mmHg) and HIV/noART (121 mmHg) groups fell within the clinically normal range (WHO and South African Hypertension Society guidelines) and did not differ significantly between the groups.[533,604] The percentage of participants who presented with elevated SBP in HIV-free (*n* = 22, 21%) was higher than in the HIV+ART (*n* = 21, 14%) and HIV-noART (*n* = 5, 14%) groups respectively at baseline.

Similarly, the mean DBP values in the HIV-free (87 mmHg), HIV+ART (86 mmHg) and HIV/noART (83 mmHg) groups fell within the clinically normal range (WHO and South African Hypertension Society guidelines) and did not differ significantly between the groups.[533,604] More than half of participants in the HIV-free (*n* = 68, 64%), HIV+ART (*n* = 98, 64%) and HIV/noART (*n* =21, 57%) groups respectively presented with elevated DBP at baseline.

The mean heart rate in HIV-free (72 bpm), HIV+ART (71 bpm) and HIV/noART (77 bpm) did not significantly differ between groups (**Table 3.9.**).

Table 3.9. Baseline blood pressure and heart rate measurements.

Variable [a]	HIV-free	HIV+ART	HIV/noART
Systolic Blood Pressure (mmHg)	126 ± 20	124 ± 18	121 ± 17
Elevated (>140 mmHg), *n* (%) [b]	22 (21%)	21 (14%)	5 (14%)
Diastolic Blood pressure (mmHg)	87 ± 13	86 ± 12	83 ± 11
Elevated (>90 mmHg), *n* (%) [b]	68 (64%)	98 (64%)	21 (57%)
Hypertension (SBP >140 mmHg or DBP >90 mmHg), *n* (%) [b]	69 (64%)	98 (64%)	21 (57%)
Heart Rate (bpm)	72 ± 12	71 ± 12	77 ± 18

[a] Data presented as mean ± SD or median (range) or *n* (% of group; HIV-free: *n* = 107; HIV+ART: *n* = 151; HIV/noART: *n* = 37). [b] According to WHO and South African Hypertension Society guidelines.[533,604]

3.1.7. Baseline systemic inflammation and vascular endothelial biomarker measurements.

The median hsCRP levels for HIV-free (5.7 mg/L), HIV+ART (5.3 mg/L) and HIV/noART (8.2 mg/L) were higher than levels previously shown to be associated with increased cardiovascular risk (>3mg/L).[534] Also, more than half of participants in HIV-free (*n* = 64, 60%), HIV+ART (*n* = 95, 60%) and HIV/noART (*n* = 25, 69%) presented with elevated hsCRP levels at baseline.

No significant differences were observed in the mean TNF-α levels between HIV-free (23.3 pg/ml), HIV+ART (22.8 pg/ml) and HIV/noART (23.1 pg/ml). The mean VCAM-1 levels in the HIV/noART group (1157 ng/ml) was significantly higher than HIV-free (829 ng/ml, *p* = 0.005) while the median ICAM-1 levels in the HIV+ART group (225 ng/ml) was significantly lower than HIV-free (351 ng/ml *p* = 0.017). No significant differences in terms of e-selectin, p-selectin and VEGF were observed between groups. The mean PAI1-1 levels in the HIV+ART (82 ng/ml) and HIV/noART (77 ng/ml) groups were significantly lower compared to HIV-free (103 ng/ml) (**Table 3.10.**).

Table 3.10. Baseline levels for circulating biomarkers of systemic inflammation and vascular endothelial function / dysfunction.

Variable [a]	n	HIV-free	n	HIV+ART	n	HIV/noART
hsCRP (mg/L)	103	5.7 (0.2 to 57)	148	5.3 (0.2 to 42)	36	8.2 (0.2 to 200)
Elevated (>3mg/L), n (%) [b]		64 (60%)		95 (60%)		25 (69%)
TNF-α (pg/ml)	50	23.3 ± 4.4	50	22.8 ± 6.8	28	23.1 ± 6.6
VCAM-1 (ng/ml)	50	829 ± 358	50	982 ± 482	29	1157 ± 574 [c]
ICAM-1 (ng/ml)	49	351 (50 to 1343)	49	225 (4 to 1348) [d]	28	376 (155 to 1488)
E-selectin (ng/ml)	49	37.4 ± 13.2	50	38.0 ± 20.0	28	36.5 (12.0 to 75.1)
P-selectin (ng/ml)	50	40.0 ± 15.0	50	34.9 ± 16.4	29	27.9 (3.0 to 61.4)
VEGF (pg/ml)	49	90 (24 to 415)	50	70 (12 to 768)	29	56.2 (1.5 to 317)
PAI-1 (ng/ml)	50	103 ± 35	50	82 ± 39 [e]	29	77 ± 40 [f]

[a] Data presented as mean ± SD or median (range) or n (% of group). [b] According to the cut-off value associated with increased cardiovascular risk.[534] [c] *vs.* HIV-free; p = 0.005. [d] *vs.* HIV-free; p = 0.017. [e] *vs.* HIV-free; p = 0.006. [f] *vs.* HIV-free; p = 0.002.

3.1.8. Baseline retinal microvascular calibers.

The mean CRVE for HIV+ART (229 μm) was significantly lower compared to HIV-free (240 μm) and HIV/noART (243 μm). No significant differences in mean CRAE between HIV-free (156 μm), HIV+ART (153 μm) and HIV/noART (159 μm) were observed. Also, no significantly differences were observed in terms of AVR between the HIV-free (0.65 μm), HIV+ART (0.67 μm) and HIV/noART (0.66 μm) groups respectively (**Table 3.11.**).

Table 3.11. Baseline retinal vessel caliber characteristics.

Variable [a]	HIV-free	HIV+ART	HIV/noART
Central retinal arteriolar equivalent (CRAE) (μm)	156 ± 16	153 ± 15	159 ± 16
Central retinal venular equivalent (CRVE) (μm)	240 ± 21	229 ± 20 [b, c]	243 ± 22
CRAE/CRVE ratio (AVR)	0.65 ± 0.06	0.67 ± 0.06	0.66 ± 0.06

[a] Data presented as mean ± SD (HIV-free: n = 103 to 107; HIV+ART: n = 143; HIV/noART: n = 35. [b] *vs.* HIV-free; p < 0.001. [c] *vs.* HIV/noART; p = 0.002.

3.1.9.   Baseline flow-mediated dilatation measurements.

The mean baseline brachial artery diameter did not significantly differ between the HIV-free (3.37 mm), HIV+ART (3.37 mm) and HIV/noART (3.39 mm) groups. The median % FMD for HIV+ART (7.50 %) was significantly higher than HIV-free (5.66%) and HIV/noART (4.30 %). The median % FMD did not significantly differ between HIV-free and HIV/noART (**Table 3.12)**.

Table 3.12. Baseline FMD variable outcomes.

Variable [a]	HIV-free *n* = 105	HIV+ART *n* = 149	HIV/noART *n* = 37
Baseline brachial artery diameter (mm)	3.37 ± 0.67	3.37 ± 0.67	3.39 ± 0.62
% Flow-mediated dilatation (%)	5.66 (-8.0 to 22.6)	7.50 (-3.10 to 36) [b, c]	4.30 (-1.7 to 16)

[a] Data presented as mean ± SD or median (range) (HIV-free: *n* = 105; HIV+ART: *n* = 49; HIV/noART: *n* = 37). [b] *vs.* HIV-free, *p* = 0.002. [c] *vs.* HIV/noART, *p* = 0.002.

3.2.   Estimated effects of HIV and ART.

Only significant findings are presented in the following sections. For full data tables containing all estimated effects, please refer to Appendix A1 to A9: **A1.** Effects of HIV and ART status on body composition. (Page 216 to 218); **A2.** Effects of HIV and ART on lipid and glucose levels (Page 219 to 221); **A3.** Effects of HIV and ART on Hb levels. (Page 222); **A4.** Effects of HIV and ART on GGT levels (Page 223); **A5.** Effects of HIV and ART on markers of kidney function (Creatinine, microalbumin, ACR and eGFR levels) (Page 224 to 225). **A6.** Effects of HIV and ART on blood pressure and heart rate (Page 226 to 227); **A7.** Effects of HIV and ART on circulating markers of vascular endothelial function (Page 228 to 231); **A8.** Effects of HIV and ART on retinal vessel calibre (Page 232 to 233); **A9.** Effects of HIV and ART on flow-mediated dilation parameters (Page 234).

3.2.1.   HIV disease progression/regression in the HIV+ART and HIV/noART groups between baseline visit and 18-month follow-up visit.

At baseline, the median viral load (20 copies mRNA/ml) and CD4 cell count (503 cells/mm^3) values in the HIV+ART group fell within the normal range as recommended by the WHO (**Table 3.5.**).[588] Viral load and CD4 cell count in the HIV+ART group did not significantly change between baseline and follow-up visit (-10.9%, *p* = 0.639 and 7.1%, *p* = 0.059, respectively). At baseline 20 participants (13%) in HIV+ART did not show viral load suppression according to the WHO guidelines.[72]. Similarly, at 18 months, 20 participants (13%) in HIV+ART did not show viral load suppression. At baseline, 28 participants (78%) in HIV/noART were not viral load suppressed. At 18 months, only 10 participants (29%) in HIV+ART were not viral load suppressed.

What is more, in the HIV/noART group, the median viral load (13123 copies mRNA/ml) and CD4 cell count (469 cells/mm^3) levels were above recommended WHO cut-off levels at baseline (**Table 3.5.**).[588] Compared to baseline (without ART), the median viral load levels in HIV/noART significantly decreased at follow-up visit after initiating ART (-97.7%, p = < 0.001), but the mean CD4 cell count did not significantly differ (12.6%, p = 0.103) (**Table 3.12.**).

Table 3.13. Temporal changes in viral load and CD4 cell count at 18 months post-baseline.

Variable	% Difference [a]	95% CI		p-values
		Lower	Upper	
Baseline *vs.* Follow-up [b]				
HIV+ART				
Viral load (copies mRNA/ml)	-10.9	-45.2	44.8	0.639
CD4 cell count (cells/mm^3)	7.1	-0.3	15.1	0.059
Pre- *vs.* post-ART treatment effects (Initiating ART treatment) [c]				
HIV/noART				
Viral load (copies mRNA/ml)	-97.7	-99.3	-93.0	< 0.001
CD4 cell count (cells/mm^3)	12.6	-2.5	29.9	0.103

[a] Estimates expressed an 18-month % difference. [b] HIV+ART group adjusted for age, gender, ethnicity, recruitment area, smoking, employment, use of medication, alcohol consumption, SBP, BMI and ART duration at baseline visit. [c] HIV/noART group adjusted for age and smoking.

3.2.2. Effects of initiating ART treatment in HIV-infected participants.

To evaluate the effects of pre *vs.* post-ART treatment (i.e. initiating ART during the study period of 18 months) in PLWH, linear mixed model regression analysis was applied to the HIV/noART group. Due to the small population size (n =37), models were only adjusted for age, smoking, viral load and CD4 cell count.

Compared to baseline (HIV-without ART treatment), ART treatment (at 18-month follow-up: HIV with ART treatment), was associated with a significant increase in total cholesterol (0.30 mmol/L), HDL cholesterol (0.39 mmol/L), and GGT levels (37.6%). Initiating ART was associated with a significant decrease in VCAM-1 (-148 ng/ml) and a significant increase in VEGF (40.6%) and PAI-1 (14.12 ng/ml). Initiating ART was also associated with a significant decrease in CRVE (-6.42 µm) (**Table 3.11.**).

Table 3.14. Significant effects of initiating ART in HIV-infected participants.

Variable	Estimate / % Difference [a]	95% CI Lower	95% CI Upper	*p*-values
Lipid metabolism				
Total cholesterol (mmol/L)	0.301	0.072	0.530	0.011
HDL cholesterol levels (mmol/L)	0.393	0.216	0.569	< 0.001
Liver function				
GGT levels (U/L)	37.6%	14.3	65.8	0.001
Cardiovascular effects				
VCAM-1 levels (ng/ml)	-148	-274	-23	0.022
VEGF levels (pg/ml)	40.6%	0.5	96.7	0.047
PAI-1 levels (ng/ml)	14.12	1.16	27.07	0.034
CRVE (µm)	-6.42	-10.99	-1.85	0.007

[a] Adjusted for age, smoking, viral load and CD4 cell count with estimates expressed as change or % difference for baseline *vs.* follow-up visit.

3.2.3. Effects of the 18-month ART treatment period in HIV-infected participants.

To assess the effects if ART over an 18-month treatment period in PLWH, linear mixed model regression analysis was applied in the HIV+ART group. An 18-month ART treatment period was inversely associated with waist circumference (-3.43 cm) and hip circumference (-2.59 cm). The 18-month ART treatment period was positively associated with HDL cholesterol (0.104 mmol/L), and inversely associated with LDL cholesterol levels (-0.138 mmol/L). In terms of renal function, the 18-month ART treatment period was positively associated with serum creatinine (3.71 µmol/L) and inversely associated with eGFR (-2.93 mL/minute/1.73 m^3).

ART was also associated with various vascular outcomes. In terms of circulating endothelial function biomarkers, the 18-month ART treatment period was inversely associated with TNF-α (-1.22 pg/ml), ICAM-1 (-45%) and e-selectin (-5.57 ng/ml). The 18-month ART treatment period was furthermore inversely associated with CRVE (–7.00 µm) and positively associated with AVR (0.019). ART was negatively associated with % FMD (-9.8%) (**Table 3.15.**).

Table 3.15. Estimated effects of the 18-month ART treatment period in HIV-infected participants.

Variable	Estimate / % Difference [a]	95% CI Lower	95% CI Upper	p-values
Body composition				
Waist circumference (cm) [b]	-3.43	-5.02	-1.84	< 0.001
Hip circumference (cm) [b]	-2.59	-4.00	-1.19	< 0.001
Lipid metabolism				
HDL cholesterol levels (mmol/L) [c]	0.104	0.005	0.203	0.040
LDL cholesterol levels (mmol/L) [c]	-0.138	-0.254	-0.022	0.020
Renal effects				
Creatinine levels (µmol/L) [c]	3.71	1.98	5.44	< 0.001
eGFR (mL/minute/1.73 m^3) [c]	-2.93	-4.94	-0.93	0.004
Cardiovascular effects				
TNF-α (pg/ml) [d]	-1.22	-2.29	-0.16	0.025
ICAM-1 (ng/ml) [d]	-45%	-88	-1.3	0.043
E-selectin (ng/ml) [d]	-5.57	-9.52	-1.62	0.006
CRVE (µm) [c]	-7.00	-12.64	-1.36	0.015
AVR [c]	0.019	0.008	0.031	0.001
% FMD [e]	-9.8%	-17.6	-1.2	0.026

[a] Estimates expressed an 18-month change or 18-month % difference. [b] Model A: Adjusted for age, gender, ethnicity, smoking, employment, SBP, recruitment location, use of medication other than ART, alcohol consumption, ART duration at baseline visit, viral load and CD4 cell count. [c] Model A additionally adjusted for BMI. [d] Adjusted for age, smoking, SBP, BMI, viral load and CD4 cell count. [e] Model A additionally adjusted for BMI and baseline brachial artery diameter.

3.2.4. Effects of markers of HIV disease progression/regression.

To evaluate the effects of HIV-disease progression/regression, linear mixed model analysis was applied to the total HIV population (HIV+ART and HIV/noART combined).

Viral load was inversely associated with body composition. Each IQR increment increase in viral load (1300 copies mRNA/ml) was inversely associated with body weight (-0.61 kg), BMI (-0.40 kg/m^3), waist circumference (-1.43 cm) and hip circumference (-0.70 cm). Each IQR increment increase in viral load (1300 copies mRNA/ml) was also inversely associated with total cholesterol (-0.29 mmol/L), HDL cholesterol (-0.20 mmol/L) and LDL cholesterol (-0.11 mmol/L). Furthermore, each IQR increment increase in viral load (1300 copies mRNA/ml) was inversely associated with haemoglobin (-0.31 g/dL) and liver function (GGT: -22.2% U/L).

In terms of vascular variable outcomes, each IQR increment increase in viral load (1300 copies mRNA/ml) was positively associated with CRVE (9.29 µm) and inversely associated with AVR (-0.016) and % FMD (-2.13%) (**Table 3.16.**).

Table 3.16. Significant effects of viral load in HIV-infected participants over an 18-month period.

Variable	Estimate / % Difference [a]	95% CI		p-values
		Lower	Upper	
Body composition				
Body weight (kg) [b]	-0.61	-1.9	0.69	0.043
BMI (kg/m^2) [b]	-0.40	-1.01	0.20	0.026
Waist circumference (cm) [b]	-1.43	-2.84	-0.03	0.046
Hip circumference (cm) [b]	-0.70	-1.99	0.58	0.040
Lipid metabolism				
Total cholesterol (mmol/L) [c]	-0.287	-0.413	-0.162	< 0.001
HDL cholesterol levels (mmol/L) [c]	-0.204	-0.282	-0.125	< 0.001
LDL cholesterol levels (mmol/L) [c]	-0.109	-0.211	-0.007	0.036
Haemoglobin				
Hb levels (g/dL) [c]	-0.31	-0.53	-0.09	0.006
Liver function				
GGT levels (U/L) [c]	-22.2%	-30.1	-13.3	< 0.001
Cardiovascular effects				
CRVE (µm) [c]	9.29	5.28	13.30	< 0.001
AVR [c]	-0.016	-0.025	-0.006	0.001
% FMD [d]	-2.13%	-3.34	-0.92	0.001

[a] Estimates expressed an 18-month change or 18-month % difference. [b] Model A: Adjusted for age, gender, ethnicity, smoking, employment, SBP, recruitment location, use of medication other than ART and alcohol consumption. [c] Model A additionally adjusted for BMI. [d] Model A additionally adjusted for BMI and baseline brachial artery diameter.

Each IQR increment increase in CD4 cell count (320 cells/mm^3) was positively associated with body weight (1.37kg), BMI (0.76 kg/m^2) and waist circumference (1.49 cm). Each IQR increment increase in CD4 cell count (320 cells/mm^3) was positively associated with fasting glucose levels (0.22 mmol/L).

In terms of vascular outcomes, each IQR increment increase in CD4 cell count (320 cells/mm^3) was inversely associated with TNF-α (-2.11 mg/L) and positively associated with % FMD (8.43%) (**Table 3.17.**).

Table 3.17. Significant effects of CD4 cell count in HIV-infected participants over an 18-month period.

Variable	Estimate / % Difference [a]	95% CI Lower	95% CI Upper	p-values
Body composition				
Body weight (kg) [b]	1.37	0.09	2.64	0.036
BMI (kg/m^2) [b]	0.76	0.18	1.35	0.010
Waist circumference (cm) [b]	1.49	0.09	2.89	0.037
Glucose metabolism				
Fasting glucose levels (mmol/L) [c]	0.22	0.036	0.41	0.020
Cardiovascular effects				
TNF-α levels (pg/ml) [d]	-2.11	-3.46	-0.76	0.002
% FMD [e]	8.43%	0.91	15.95	0.028

[a] Estimates expressed an 18-month change or 18-month % difference. [b] Model A: Adjusted for age, gender, ethnicity, smoking, employment, SBP, recruitment location, use of medication other than ART, alcohol consumption, ART duration at baseline visit, viral load and CD4 cell count. [c] Model A additionally adjusted for BMI. [d] Adjusted for age, smoking, SBP, BMI, viral load and CD4 cell count. [e] Model A additionally adjusted for BMI and baseline brachial artery diameter.

3.3. Discussion of Sub-study 1 results.

The main aim of Sub-study 1 was to determine whether endothelial function is a marker of the effect of HIV (disease progression: viral load and disease regression: CD4 cell count) and ART (Initiating ART treatment and an 18-month ART treatment period). The findings of the current study show that HIV and ART are associated with various markers of cardiovascular risk and endothelial function:

- HIV disease progression (using viral load as a marker) in the study population, was inversely associated with various cardiometabolic factors including body composition, lipid metabolism, Hb levels and GGT levels. HIV was furthermore associated with retinal vessel calibres (CRVE and AVR) and with reduced % FMD (**Figure 3.1.**).
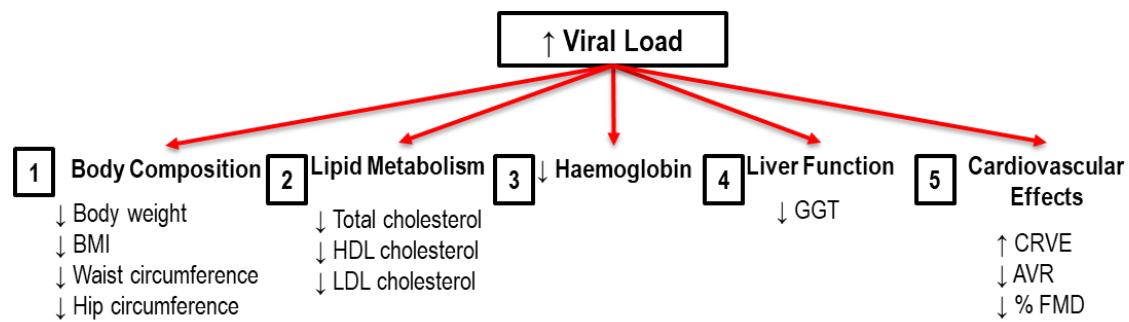
Figure 3.1. Summary of the effect of viral load on markers of cardiovascular risk. **Description: 1.** Inverse association with body composition (body weight, BMI, waist circumference and hip circumference). **2.** Inverse association with serum lipid levels (total cholesterol, HDL cholesterol and LDL cholesterol). **3.** Inverse association with haemoglobin levels. **4.** Inverse association with liver GGT levels. **5.** Positive association with retinal venular diameter (CRVE) and inverse association with AVR. **5.** Inverse association with %FMD. **Abbreviations and symbols**: BMI: Body mass index; HDL: High-density lipoprotein; LDL: Low-density lipoprotein; GGT: γ-Glutamyl transferase; CRVE: Central retinal venular equivalent; FMD: Flow-mediated dilatation; ↑: Increase; ↓: Decrease.

- HIV immune status (using the CD4 cell count as a marker) was positively associated with various cardiometabolic factors including body weight, BMI and waist circumference, fasting glucose levels. CD4 cell count was also associated with markers of vascular endothelial function including reduced TNF-α levels and increased %FMD (**Figure 3.2.**).
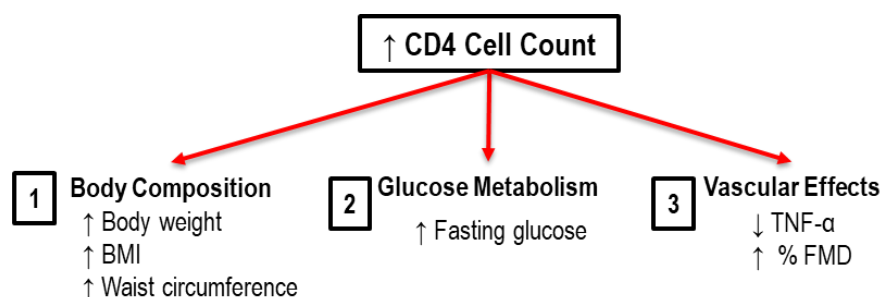
Figure 3.2. Summary of the effect of CD4 cell count on markers of cardiovascular risk. **Description: 1.** Positive association with body composition as indicated by body weight, BMI and waist circumference. **2.** Positive association with fasting glucose levels. **3.** Inverse association with TNF-α and positive association with % FMD. **Abbreviations and symbols**: BMI: Body mass index; TNF-α: Tumour necrosis factor-alpha; FMD: Flow-mediated dilatation; ↑: Increase; ↓: Decrease.

- Initiating ART during the study period (i.e. changing from ART naïve to ART treatment) was associated with various cardiometabolic factors including total and HDL cholesterol levels and GGT levels. Initiating ART was also associated with markers of vascular function including PAI-1, VEGF, VCAM-1 and CRVE. (**Figure 3.1.**).

Initiating ART

1 **Lipid Metabolism**
↑ Total cholesterol
↑ HDL cholesterol

2 **Liver Function**
↑ GGT

3 **Cardiovascular Effects**
↑ PAI-1
↑ VEGF
↓ VCAM-1
↓ CRVE
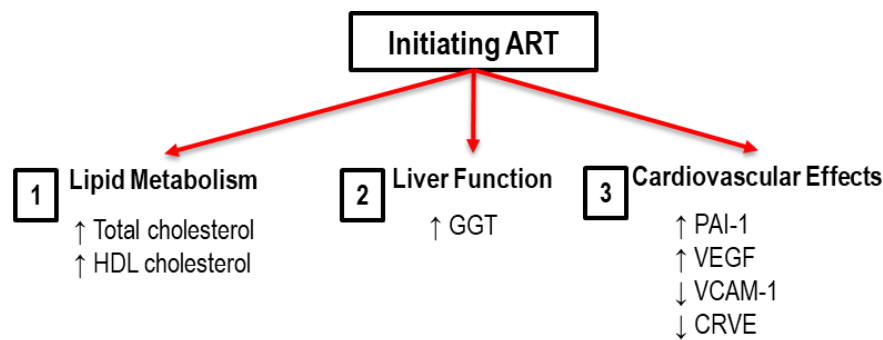
Figure 3.3. Summary of the effect of initiating ART. **Description: 1.** Positive association with total and HDL cholesterol. **2.** Positive association with GGT levels. **3.** Positive association with PAI-1 and VEGF, and a negative association with VCAM and CRVE. **Abbreviations and symbols**: HDL: High-density lipoprotein; GGT: γ-Glutamyl transferase; PAI-1: Plasminogen activator inhibitor-1; VCAM-1: Vascular cell adhesion molecule-1; CRVE: Central retinal venular equivalent; ↑: Increase; ↓: Decrease.

- An 18-month ART treatment period in the current study was associated with various cardiometabolic factors including waist and hip circumference, HDL cholesterol and LDL cholesterol, serum creatinine and eGRF. An 18-month ART treatment period was also associated with markers of vascular function TNF- α, e-selectin, ICAM-1, CRVE, AVR and % FMD (**Figure 3.3.**).

18-month ART Treatment

1 **Body Composition**
↓ Waist circumference
↓ Hip circumference

2 **Lipid Metabolism**
↑ HDL cholesterol
↓ LDL Cholesterol

3 **Kidney Function**
↑ Serum creatinine
↓ eGRF

4 **Cardiovascular Effects**
↓ TNF-α
↓ E-selectin
↓ ICAM-1
↓ CRVE
↑ AVR
↓ % FMD
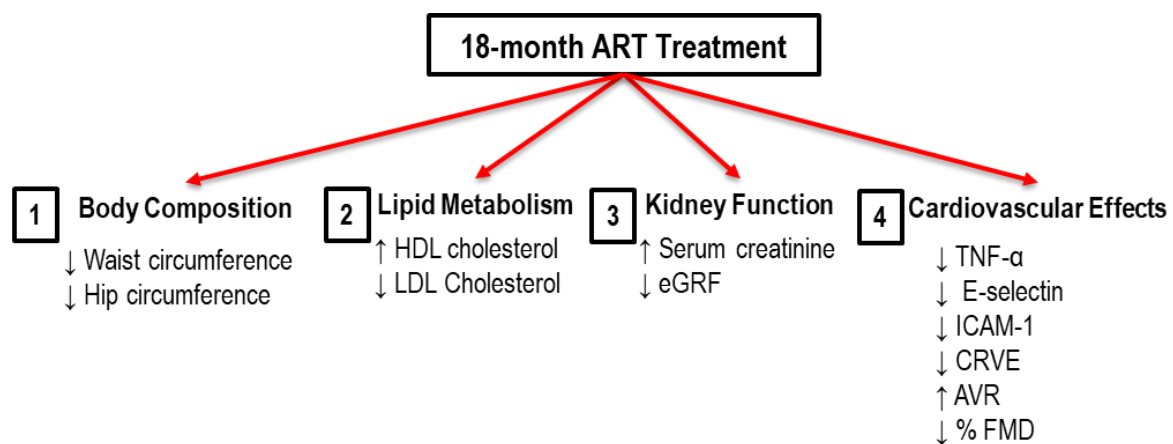
Figure 3.4. Summary of the effect of an 18-months ART treatment period. **Description: 1.** Negative association with waist and hip circumference. **2.** Positive association with HDL cholesterol and negative association with LDL cholesterol. **3.** Positive association with serum creatinine and a negative association with in glomeration filtration rate. **4.** Negative association with TNF-α, e-selectin, ICAM-1, CRVE, % FMD and a positive association AVR and. **Abbreviations and symbols**: HDL: High-density lipoprotein; LDL: Low-density lipoprotein; eGRF: Estimate glomeration filtration rate; TNF-α: Tumour necrosis factor-alpha; ICAM-1: Intercellular adhesion molecule-PAI-1: Plasminogen activator inhibitor-1; VCAM-1: Vascular adhesion molecule-1; CRVE: Central retinal venular equivalent; FMD: Flow-mediated dilatation; ↑: Increase; ↓: Decrease.

3.3.1. The effects of HIV and ART on body composition.

The wasting effects of HIV-infection (especially when progressing to AIDS) on body composition is one of the most well-known consequences of the disease and well documented throughout the pre-highly active antiretroviral therapy (HAART: treatment with multiple types of ART drugs simultaneously) era,[605,606] while the success of ART is characterised by the reversal of HIV-associated weight-loss and improved health.[607]

In unadjusted comparisons between groups at baseline, HIV/noART in the current study presented with a significantly lower body composition parameters (BMI, body weight, waist circumference and hip circumference) compared to HIV-free at baseline (**Table 3.6.**). In addition, 32% of HIV/noART participants were classified underweight [531] at baseline compared to 11% in HIV-free and 14% in HIV+ART respectively (**Table 3.6.**). These results indicate that HIV-associated weight loss is prevalent in the current study population.

After adjusting for confounders, viral load was inversely associated with body weight, BMI, waist circumference and hip circumference (**Table 3.16.**), while CD4 cell count was positively associated with body weight, BMI, waist circumference and hip circumference (**Table 3.17.**). These results show that insufficient viral suppression was associated with decreased body composition parameters. The detrimental effects of HIV-infection on body composition is characterised by the loss of metabolically active tissue such as muscle and especially adipose tissue.[608,609] It has been shown that adipose tissue expresses the receptors (CD4 and CXCR4 and CCR5) necessary to allow the HI-virus to enter adipocytes where they can disrupt cellular metabolism.[610,611] On the other hand, circulatory HIV-proteins such as Tat (mostly produced by infected lymphocytes and macrophages) can also enter adipocytes and inhibit adipogenesis through suppressing peroxisome proliferator-activated receptor-γ (PPAR-γ) activity (involved in preadipocyte cell differentiation).[612]

Neither initiating ART during the study period nor an 18-month ART treatment period was significantly associated with changes in body composition after adjusting for confounding factors (Appendix A, **Table A1.1. to A1.5.**). This finding suggests that ART treatment was not successful in reversing the wasting effects of HIV-infection in the current study-population. Interestingly, an 18-month ART treatment period was inversely associated with waist and hip circumferences while body weight and BMI remained unaffected. At first, these findings appear to indicate ART may be associated with lipodystrophy in the current HIV study-population, but ART-associated lipodystrophy is characterised by the redistribution of adipose tissue from the peripheral area of the body (lipoatrophy) to the central area (lipohypertrophy).[613] It is difficult to explain this finding, but the poor response to ART treatment in terms of body composition suggest that nutritional status or viral factors may still be at play.

Various factors may account for the poor recovery of HIV-associated weight-loss. It has also been shown that a higher BMI at the time of initiating ART treatment is associated with an improved recovery of body composition.[614] The decreased body composition observed in HIV+ART and HIV/noART at the baseline visit

may explain the poor response to ART treatment in terms of reversing the wasting effects of HIV in the current HIV study population. Other ART-associated adverse effects such poor absorption of nutrients and diarrhoea may also have been involved.[615,616] Lifestyle factors such as smoking may also have contributed. More investigation is needed.

Although overweight and obesity are well-known cardiovascular risk factors, a BMI in the underweight range has previously also been shown to be associated with increased cardiovascular risk.[617] These results indicate that the poor recovery of HIV-associated weight loss, may contribute to increased cardiovascular risk in the current HIV study population. These findings also underscore the importance of healthy lifestyle choices and monitoring the nutritional status of PLWH.

3.3.2. Effects of HIV and ART on lipid metabolism.

HIV without ART treatment is often characterised by a rapid decrease in HDL cholesterol levels, which may contribute to increased cardiovascular risk.[618,619] In accordance with previous findings, in our study population, HIV/noART presented with significant lower unadjusted mean total cholesterol and HDL cholesterol levels compared to HIV-free and HIV+ART at the baseline visit (**Table 3.7.**). Also, after adjusting for confounding factors, viral load, a marker of disease progression, was inversely associated with total and HIDL cholesterol levels (**Table 3.16.**).

Findings of the current study support those of Bernel *et al.* (2008), who demonstrated that viral load (even at a concentration less than 50 copies mRNA/ml) is inversely associated with HDL cholesterol levels.[620] In contrast to previous reports,[621] the current study could not demonstrate any significant association between HIV and triglyceride levels (**Table 3.16.**).Reports indicate that HIV-associated hypertriglyceridemia is often a long-term consequence of untreated HIV and becomes more pronounced in advanced HIV and HIV-associated metabolic dysregulation.[231,622–626] Although no significant associations between HIV and ART with triglyceride levels were observed in the current study, previous reports have indicated that the effects of HIV and ART on triglyceride levels may become more pronounced in advanced HIV disease progression or in ART-treated PLWH with metabolic dysregulation.[231,622–626] Continued monitoring is needed.

Reports on the effects of HIV (in PLW HIV without ART) and ART (after adjusting for the effects of HIV) on LDL cholesterol are often conflicting.[627–630] The viral protein Nef may has been shown to impair hepatic cholesterol efflux [631] and may account for the inverse association between viral load and LDL cholesterol observed in the current study, and may also account for the inverse assertion observed between viral load and total, HDL and LDL cholesterol levels, but requires more investigation in the current study population.

Nonetheless, these results show that HIV in the current study may contribute to increased cardiovascular risk through decreasing HDL cholesterol levels. These results also show that HIV-associated dyslipidaemia may be relevant in the current study population and that monitoring lipid dysregulation in the current study population is important.

The effects of ART on lipid metabolism were recognised soon after the introduction of HAART.[543,632,633] ART is generally associated with a pro-atherosclerotic lipid profile in PLWH (increased total cholesterol, LDL cholesterol and triglyceride levels)[20,634] although these effects on lipid metabolism may vary greatly between different ART drug classes and treatment combinations (differential effects of different ART drugs and drug classes fell outside the scope of the current study).[20,619,634]

Initiating ART (**Table 3.14.**) and an 18-month ART treatment period (**Table 3.15.**) were both positively associated with HDL cholesterol levels. These findings support those of Riddler *et al*. (2003), who also found a significant increase in total and HDL cholesterol levels in their HIV study population after initiating ART treatment.[632] These findings also support those of Tadewos *et al.* (2012), who evaluated the effects of ART on the lipid profile in an Ethiopian study population, and found a positive association between ART treatment and total and HDL cholesterol levels.[635] These findings suggest that ART in the current HIV study population may have exerted a measure of HIV-associated cardiovascular risk reduction by increasing cardioprotective HDL cholesterol levels.

Our results showed no association between ART and triglyceride levels (Appendix A2, **Table A2.4.**), which is in contrast to the findings of Tadewos *et al.* (2012) who observed a positive association between ART and triglyceride levels.[635] Tadewos *et al.* (2012) attributed hypertriglyceridemia observed in their study population to a high prevalence in liver steatosis (supported by others [636]).[635] Hypertriglyceridemia often manifests due to ART toxicity (especially PI-containing regimens) and is closely associated with metabolic dysregulation in PLWH.[543,619,637,638] Hypertriglyceridemia is also commonly observed in ART-associated lipodystrophy (redistribution of adiposity from limbs to the central body area).[633,639,640] Liver steatosis and lipodystrophy remained beyond the scope of the current study, but may have accounted with discrepancies between previous studies and the current study.

On the other hand, the negative association between an 18-month ART treatment period was also observed in the HIV-free participants (Appendix A2, **Table A2.3.**). These results suggest that the observed negative association with LDL cholesterol levels may have been unrelated to ART treatment *per se*. One can only speculate that environmental, seasonal or dietary effects may have been involved.[641–643] More investigation is needed.

These results also show that ART is not significantly associated with dyslipidaemia in the current HIV study population, but was associated with putative cardioprotective effects by reversing the effects of HIV on HDL cholesterol levels. ART-associated dyslipidaemia my become more relevant in ART-associated metabolic dysregulation.[633,639,640] Continued monitoring is needed.

3.3.3. Effects of HIV and ART on glucose metabolism.

HIV and ART have previously been associated with increased risk for the development of insulin resistance and type-2 diabetes.[644–647] Possible mechanisms include ART-associated metabolic dysregulation such as lipodystrophy (especially in the presence of hypertriglyceridemia), dyslipidaemia, and ectopic lipid deposition in pancreatic cells (also associated with hypertriglyceridemia), while the direct cytotoxicity of ART has also been implicated.[644–647]

In contrast to these reports, no significant differences were observed in the unadjusted mean values of fasting glucose or HbA1c levels between HIV-free, HIV+ART and HIV/noART at baseline (**Table 3.7.**). In addition, after adjusting for possible confounding factors, no significant associations were observed with either initiating ART or an 18-month ART treatment period (Appendix A2, **Table A2.5 and A2.6.**). These results suggest that HIV and ART in the current study population are not associated with impaired glucose homeostasis.

On the other hand, CD4 cell count was positively associated with fasting glucose levels (**Table 3.17.**). A close relationship between CD4 cells and glucose metabolism in HIV has previously been established.[648] It has been shown that the expression of GLUT1 in HIV-infected CD4 cells is upregulated to compensate for the increased energy demand for viral replication and also associated with CD4 cell apoptosis,[648] These findings may explain the positive association observed between fasting glucose levels and CD4 cell count. The close positive relationship between CD4 cell count, body composition and glucose levels may also explain these findings as increased CD4 cell counts often reflect the successful reversal of HIV-associated wasting.[649]

3.3.4. Effects of HIV and ART on haemoglobin.

The adverse effects of HIV on Hb (a marker of anaemia) is well-recognised, affects 20% to 80% of PLWH, and is associated with disease progression and mortality.[559,650,651] In line with these reports, viral load in the current study was inversely associated with Hb (**Table 3.16.**). Numerous HIV and ART related pathophysiological pathways have been implicated, including bone marrow toxicity/suppression, cytokine mediated haematopoiesis [652], inhibition of erythropoietin [653], secondary infections [654,655], vitamin and iron deficiency [656] and immune destruction of red blood cells.[657] Decreased Hb in PLWH has previously been associated with poorer health outcomes and increased risk for CVD.[558,559,650] Our findings therefore suggest that poor viral suppression may significantly reduce Hb and potentially contribute to increased cardiovascular risk in the study population.

ART is generally associated with reversal of HIV-associated anaemia, although ART-associated cytotoxicity in bone marrow and erythrocytes has been shown to contribute to low Hb levels (a marker of anaemia).[577,658,659] In contrast to these adverse reports, no significant differences in the unadjusted mean Hb

levels between HIV-free, HIV+ART and HIV/noART were observed at baseline, (**Table 3.8.**). Also, after adjusting for possible confounding factors, initiating ART and an 18-month ART treatment period were not significantly associated with Hb levels (Appendix A3, **Table A3.1.**). These findings support those of Takuva *et al*. (2013) who also found that ART was not associated with adverse effects on Hb in a South African HIV-infected population.[660] In contrast, a study by Obirikoran and Yeboah (2009) showed that specific ART drugs such as zidovudine (uncommonly included in the first-line ART treatment in SA) was directly associated with decreased Hb levels.[559] These results suggest that ART does not increase cardiovascular risk through adverse effects on Hb metabolism in the current study population; however, continued monitoring remains important especially in advanced disease progression and in PLWH on ART treatment regimens that may affect red blood cell production or destruction.

3.3.5. Effects of HIV and ART on liver function.

The adverse effects of ART on liver function is well recognised in the literature.[565,661–665] In line with these reports, HIV+ART in the current study presented with a significantly higher unadjusted median GGT level compared to HIV-free and HIV/noART at baseline visit (**Table 3.8.**). Even after adjusting for confounding factors, including alcohol consumption, initiating ART was positively associated with GGT levels (**Table 3.14**.). As elevated GGT levels is associated with liver disease and increased cardiovascular risk,[564] these results suggest that ART in the current HIV study population may increase the risk for developing liver disease and may contribute to increased cardiovascular risk in participants who have initiated ART during the past 18 months.

In contrast, an 18-month ART treatment period was not significantly associated with GGT levels (Appendix A4, **Table A4.1.**). The non-significant association between an 18-month ART treatment period and GGT levels, despite elevated levels compared to HIV-free at baseline, suggest that the continued use of ART in the current HIV+ART study population may not exacerbate the initial effects of initiating ART on GGT levels. As liver function plays an important role in whole-body metabolic regulation (lipid, Hb and glucose), this finding may also explain the non-significant effects observed between an 18-month ART treatment period and other metabolic parameters (such as BMI, triglyceride levels, glucose levels, HbA1C and Hb levels).[663–665]

These results show that the effects of ART-induced liver toxicity in current HIV study population remains relevant. These findings furthermore underscore the need for the further development of less toxic ARTs. Although on-going ART treatment was not significantly associated with GGT levels, the longer-term effects need to be explored.

3.3.6. Effects of HIV and ART on kidney function.

It has been shown that the HI-virus can infect kidney cells (tubular and glomerular epithelium) and cause focal segmental glomerulosclerosis and increase eGFR.[666,667] In line with these reports, eGFR was significantly higher in HIV/noART compared to HIV-free in the current study (**Table 3.8.**). After adjusting for confounding factors,

a borderline significant positive association (p = 0.052) was observed between viral load and eGRF (Appendix A5, **Table A5.4.**). HIV-associated kidney disease has furthermore previously been associated with CVD.[668] These results indicate that uncontrolled HIV is associated with kidney dysfunction in the current study population and contribute to increased cardiovascular risk.

On the other hand, ART has also previously been associated with kidney disease and is characterised by an increase in serum creatinine and a decrease in eGFR levels.[666,667,669,670] ART-associated kidney disease as observed in PLWH on ART is also associated with increased risk for CVD and heart failure.[668,671]

As was observed in the HIV/noART study group, HIV+ART presented with a significant higher unadjusted mean eGFR compared to HIV-free at baseline (**Table 3.8.**). As obesity is often associated with kidney disease as indicated by reduced eGFR,[672,673] the higher unadjusted mean eGRF observed in HIV+ART compared to HIV-free may be explained by the high prevalence of obesity in the HIV-free population (39%, **Table 3.6.**) compared to HIV+ART (16%).

Nonetheless, the unadjusted mean eGRF was well-above the cut-off values for the CKD-EPI formula that indicate chronic kidney disease (<90 mL/minute/1.73 m³ CKD-EPI formula), which indicates that chronic kidney disease may not have been a health concern in the present HIV+ART study population;[581] however, following adjustment for confounders, including BMI, an 18-month ART-treatment period was positively associated with serum creatinine and inversely associated with eGFR (**Table 3.15.**). Although non-significant, the same trend was observed between initiation ART and serum creatinine and eGFR (p = 0.054 and p = 0.073; Appendix A5, **Table A5.1. and A5.4.**). An increase in serum creatine with a simultaneous decrease in eGRF is indicative of impaired kidney function,[674,675] these results suggest that a longer ART treatment period may be associated with renal dysfunction.

These findings indicate that an 18-month ART treatment period may be associated with the reversal of the effects of HIV-infection on eGFR (HIV: increased eGFR), but may also contribute to kidney dysfunction despite a relatively high eGRF compared to HIV-free at baseline. These findings furthermore suggest that kidney dysfunction may become more pronounced in PLWH who are long-term ART. Impaired kidney function may also contribute to an increased cardiovascular risk profile. Therefore, monitoring renal function in the current study population remains pivotal especially in long-term experienced ART-use.[676]

The trends observed for urine albumin and albumin-to-creatinine ratio (used as additional markers of kidney function) did not reflect those observed for serum creatinine and eGFR. The findings suggest that urine albumin may not be associated with ART in the current study population or that urine albumin and urine albumin-to-creatinine ratio may not be reliable markers of kidney function in the current study population. A skewed data distribution, various outliers and a large data range may have contributed to this observation (Appendix A5, **Table A5.2. and A5.3.**). It has been proposed that the CKD-EPI formula (utilised in the current study) may give the most reliable estimation of eGRF and indication of kidney disease in PLWH.[666,667,677,678] As proposed in literature,

the mean of multiple albumin and albumin-to-creatinine ratio determinations over a period of time should be considered in future research for more reliable results.[666,679]

3.3.7. Effects of HIV and ART on markers of cardiovascular risk.
3.3.7.1. Effects of HIV and ART on blood pressure and heart rate.

ART is often associated with hypertension due to direct adverse effects on the vascular endothelium or indirectly through associated metabolic disturbances.[680–682] In contrast to these reports, no significant differences in unadjusted mean SBP, DBP or heart rate were observed between HIV-free and HIV+ART in the current study population (**Table 3.9.**). Also, no significant associations between initiating ART an 18-month ART treatment period and SBP, DBP and heart rate were observed after adjusting for possible confounders (Appendix A6, **Table A6.1 to A6.3.**).

These findings support those of Dimala *et al.* (2018) who reported in a systematic review and meta-analysis that ART status was not significantly associated with hypertension in sub-Saharan African populations.[683] Findings by Dimala *et al.* (2018) were made despite a positive association between ART and other cardiovascular risk factors such as total cholesterol (observed in current study) and hypertriglyceridemia (not observed in the current study).[683] In contrast, a study by Malaza *et al.* (2012) investigated obesity and hypertension in PLWH compared to HIV-free and found that, despite a decreased BMI compared to HIV-negative (also observed in the current study), hypertension was significantly associated with ART status in a rural SA population.[684]

These findings indicate that ART is not associated with blood pressure in the current study's HIV population. It is possible that mostly non-significant effects between ART in terms of cardiometabolic traits observed in the current study population may have contributed to this encouraging result.

Although ART was not significantly associated with blood pressure, the prevalence of hypertension in HIV-free (64%), HIV+ART (64%) and HIV/noART (57%) remained high (**Table 3.9.**). This shows that hypertension may already predispose the current study population for the development of cardiovascular risk and underscore the relevance of hypertension in the combat against CVD in South Africans, regardless of their HIV-status.

Heart rate has also previously been associated with increased cardiovascular risk.[685] Heart rate appears to be closely associated with ART drug classes that exert neurotoxic side-effects (autonomic dysfunction).[686–689] Our findings support those of Askgaard *et al.* (2011) who reported no association between heart rate and ART or ART duration.[687] Askgaard *et al.* (2011) furthermore reported that heart rate was inversely associated with HbA1c and hypertriglyceridemia in their HIV on ART population.[687] ART was not significantly associated with HbA1c or hypertriglyceridemia in the current study. These results show that ART is unlikely to be a contributing factor in the development of increased cardiovascular risk through effects on heart rate in the current study population, but these effects my become more relevant in the presence of ART-associated metabolic

disturbances and neurotoxic properties. Heart rate in PLWH who exhibit metabolic disturbances needs to be monitored.

Although ART and HIV was not significantly associated with blood pressure, the 18-month follow-up period in HIV-free was positively associated with SBP (Appendix A6, **Table A6.1.**). This phenomenon as observed in HIV-free may be explained by the positive association between an 18-month period and waist-to-hip ratio (Appendix A1, **Table A1.5.**) as an increase in body composition (e.g. waist-to-hip ratio) has previously been shown to associate with increased blood pressure.[690,691] These findings indicate that visceral adiposity (as shown by increased waist circumference) was increasing over time in the HIV-free study population and may have contributed to the rise in SBP. On the other hand, these results also suggest that the poor response in HIV+ART to ART in terms of body composition and lack of adverse effects on lipid metabolism may account for the sparing effects of ART exhibited in terms of blood pressure.

3.3.7.2. Effects of HIV and ART on systemic inflammation and circulating markers of vascular function.
3.3.7.2.1. Effects of HIV and ART on hsCRP.

hsCRP is produced by the liver and vascular endothelium during immune activation.[692,693] It has also been shown that hsCRP has a clinical value in PLWH in terms of predicting long-term disease progression, viral activity and risk for developing CVD.[692] At baseline, no significant differences in unadjusted median hsCRP levels were observed between HIV-free, HIV+ART and HIV/noART, although HIV-free, HIV+ART and HIV/noART presented with median hsCRP levels above recommended cut-off values (**Table 3.10.**). Our findings support those of O'Halloran *et al.* (2015), who also reported no significant differences in hsCRP between their HIV treated and untreated study groups. They furthermore found no significant differences at 12 weeks following ART treatment.[694] Nonetheless, a study by De Luca et al, (2013), found that hsCRP levels above 3.3 mg/L in PLWH is associated with increased risk for CVD independent of other metabolic factors.[695] These results show that regardless of HIV or ART, systemic inflammation is prevalent in our study population (possibly due to environmental factors such as chronic microbial exposure and unhealthy lifestyle choices e.g. smoking), which may predispose the participants to develop CVD.

What is more, after adjusting for possible confounders, no significant associations were observed between hsCRP and viral load, CD4 cell count, initiating ART or an 18-month ART treatment period, although relatively large effect sizes between these parameters and hsCRP were noted (Appendix A7, **Table A7.1.**).These findings support other reports that have shown that ART had little to modest effects on hsCRP levels (42 months indinavir treatment,[696] 96 weeks lopinavir/ritonavir treatment [697] and 96 weeks of Efavirenz treatment [303]).

These findings either indicate that HIV and ART are not significantly associated with systemic inflammation as indicated by hsCRP levels in the current study population, or that hsCRP may not be an accurate

predictor of inflammation in the current HIV study population. Nonetheless, based on the disproportionally high median hsCRP levels, systemic inflammation may result in an increased cardiovascular risk in the current study population. Longer term follow-up studies may shed light on this possibility.

3.3.7.2.2. Effects of HIV and ART on TNF-α.

TNF-α is an acute phase inflammatory cytokine produced by immune cells (e.g. macrophages and T-cells) during immune activation and plays a role in cellular apoptosis, proliferation and inflammation regulation.[304] TNF-α has previously been positively associated with endothelial dysfunction and increased cardiovascular risk.[698,699] HIV and viral proteins such as Tat and Nef have been positively associated with TNF-α.[700] It has also been shown that the HI-virus can interact with the TNF-α receptor, activating various related cellular pathways [700] to stimulate pro-survival TNF-α pathways (e.g. NF-κB) to fuel viral replication or apoptotic pathways which lead to cellular death.[701,702]

In contrast to these observations, viral load was not associated with TNF-α in the current study population (Appendix A7, **Table A7.2.**). Our findings do not support those of Keating *et al.* (2012) who reported increased levels of inflammatory cytokines in untreated PLWH and a positive association between TNF-α and viral load.[703] Since TNF-α is an inflammatory cytokine, it is possible that that the effects of HIV on TNF-α may be more pronounced in HIV-associated metabolic dysregulation.[704] Previous studies have indicated a close relationship between TNF-α and HIV-associated metabolic disturbances that resemble the pro-atherosclerotic phenotype such as impaired glucose homeostasis, insulin resistance and dyslipidaemia (especially hypertriglyceridemia) in PLWH as these effects are also closely associated with systemic inflammation.[701,705,706] Viral load in the current study was not significantly associated with triglyceride levels and glucose metabolism. These results suggest that HIV in the current study population is not associated with a pro-inflammatory environment as indicated by TNF-α, or may be more pronounced in terms of other well-established biomarkers of inflammation in HIV such as IL-6 (not measured in the current study).[707–709] These results also indicate that the non-significant effects between viral load and other metabolic parameters such as glucose levels and triglyceride levels may have contribute to this finding.

In PLWH, ART is mostly associated with a reversal of the pro-inflammatory effects of HIV [703,710] although positive associations between ART status and TNF-α have been reported and appears to be mostly related to ART-associated metabolic dysregulation.[710] Similar to the hsCRP results, no significant differences were observed in TNF-α levels between the unadjusted mean HIV-free, HIV+ART or HIV/noART in the current HV study population (**Table 3.10.**). In support of previously reported beneficial effects of ART,[703,710] an 18-month ART treatment period was inversely associated with TNF-α after adjusting for confounders (**Table 3.15.**). These findings indicate that ART treatment in the current study population may exhibit anti-inflammatory properties. Our

findings support those of Keating *et al.* (2012), who also reported an inverse association between ART treatment and TNF-α.[703] Alternatively, a study by Rönsholt *et al.* (2013), positively associated ART with TNF-α in PLWH with 12 years' ART-experienced.[710] These findings show that ART may exhibit (cardioprotective) anti-inflammatory properties when using TNF-α as a marker of effect in the current HIV study population, but that the pro-inflammatory effects, as shown by Rönsholt *et al.* (2013), may become more pronounced in prolonged ART treatment.[710]

3.3.7.2.3. Effects of HIV and ART on VCAM-1 and ICAM-1.

VCAM-1 and ICAM-1 are vascular adhesion molecules upregulated during the inflammatory response and play a role in the adhesion of immune cells to the vasculature.[129,298,711] VCAM-1 and ICAM-1 are also regarded as biomarkers of endothelial dysfunction, including in PLWH.[129,298,711–713]

Reports show that HIV-infection is positively associated with VCAM-1 and ICAM-1 in untreated PLWH.[713–715] In contrast, HIV viral load and CD4 cell count were not significantly associated with ICAM-1 or VCAM-1 levels in the current study (Appendix A7, **Table A7.4.**). As adhesion molecules such as VCAM-1 and ICAM-1 are directly related to an inflammatory response, these results may be explained by the non-significant association between viral load and inflammatory markers (hsCRP and TNF-α) in the current study.

On the other hand, reports on the effects of ART treatment on VCAM-1 and ICAM-1 are conflicting, with studies showing both downregulation [694]) and upregulation.[107,716] Supporting previous reports indicating beneficial effects,[694,713–715] initiating ART was inversely associated with VCAM-1, but not ICAM-1 (**Table 3.14.**) in the current study. As indicated by previous reports,[713–715] these results suggest that initiating ART may reverse the effects of HIV and exhibit anti-inflammatory (and potentially endothelioprotective) properties in the current study population. It has been shown that VCAM-1 plays a major role in the early initiation of atherosclerosis (including preceding endothelial dysfunction), while the role of ICAM-1 becomes more prominent later [178] which may explain the non-significant association between initiating ART and ICAM-1 and a significant association between the longer 18-month treatment period and ICAM-1.

In support of the previous statement, the unadjusted median ICAM-1 level in HIV+ART was significantly lower than HIV-free at baseline (**Table 3.10.**) and an 18-month ART treatment period was inversely associated with ICAM-1 levels after adjustment for confounders (**Table 3.15.**). Findings in the current study support those of O'Halloran *et al.* (2015), who showed a reduction in the levels of ICAM-1 following 12 weeks of ART treatment.[694] The current findings also support Arildson *et al.* (2013) who reported an inverse association between ART and ICAM-1.[354] In contrast, Rönsholt *et al.* (2013), reported a positively associated ART an ICAM-1 in PLWH who were 12 years' ART-experienced.[710] A study by Mosepele *et al.* (2018) also found that ART treatment (> 6 months, PI-containing) was positively associated with ICAM-1 and VCAM-1 levels despite successful viral suppression.[712] Ninety-percent (90%) of the current HIV+ART study population was on PI-free first-line ART

treatment, with a mean of 124 weeks ART experience at baseline (**Table 3.5.**). This may explain the discrepancy between the findings of the current study and those of Rönsholt *et al.* (2013) [710] and Mosepele *et al.* (2018) [712].

These findings indicate that ART in the current study population may exhibit cardioprotective properties through its anti-inflammatory effect. The findings also suggest that the pro-inflammatory effects may become pronounced in long-term ART treatment, as observed by Rönsholt *et al.* (2013),[710] or in PI-containing ART treatment combination, as observed by Mosepele *et al.* (2018).[712]

3.3.7.2.4. Effects of HIV and ART on p-selectin and e-selectin.

P-selectin (produced by endothelial cells and platelets) and e-selectin (mostly produced by endothelial cells) are also vascular adhesion molecules upregulated during immune activation, and hence regarded as biomarkers of endothelial dysfunction.[301,717] As is the case with ICAM-1 and VCAM-1, HIV and ART have previously been associated with p-selectin and e-selectin. The pro-inflammatory effects of HIV-infection are accompanied by the upregulation of p-selectin and e-selectin, while reports on the effects of ART are often conflicting.[296,353,694,718]

In the current study, no significant differences in the unadjusted mean e-selectin or p-selection levels were observed between HIV-free, HIV+ART and HIV/noART at baseline (**Table 3.10.**). After adjusting for confounding factors, no significant associations between viral load, CD4 cell count and initiating ART were observed (Appendix A7, **Table A7.5**. and **Table A7.6.**). As mentioned in the previous section, the non-significant association between circulating markers of inflammation (hsCRP and TNF-α) and viral load, CD4 cell count and initiating ART may account for this result.

On the other hand, an 18-month ART treatment period was inversely associated with e-selectin, although p-selectin remained unaffected after adjusting for confounding factors (**Table 3.15.**). Similar to the current study, O'Halloran *et al.* (2015), reported that ART reduced circulating markers of vascular cell adhesion (including p-selectin) despite no significant ART-associated effects on hsCRP at 12 weeks following ART treatment.[694] Current findings also support those of Kristoffersen *et al.* (2009) who investigated the effects of ART and found that 14 months of ART treatment was inversely associated with e-selectin (but not p-selectin) [300] and Francisci *et al.* (2009) who showed that ART was inversely associated with VCAM-1, while p-selectin also remained unaffected.[353]

In support of the findings reported in the previous section, these results further support the notion that ART exhibits anti-inflammatory (and endothelioprotective) properties in the current study population, but that the detrimental effects of ART may become more pronounced after long-term ART treatment as reported by Mosepele *et al.* (2018) Rönsholt *et al.* (2013.[710,712]

3.3.7.2.5. Effects of HIV and ART on VEGF.

VEGF, also a biomarker of endothelial function, is a well-known mediator of vascular growth (angiogenesis and neovascularisation) and is upregulated during the vascular inflammatory response to initiate vascular repair.[182] During prolonged immune activation (as observed in HIV), VEGF can promote endothelial dysfunction and atherosclerosis by causing thickening of vessel walls that result in arterial stiffness.[182,719–721] HIV and viral proteins such as Tat and Nef have been shown to directly activate endothelial cells and upregulate VEGF.[306,722–724] ART is associated with the reversal of the pro-inflammatory effects of HIV on VEGF [703] while ART-associated metabolic dysregulation (mostly not observed in the current study population) has been shown to promote the pro-atherosclerotic effects of VEGF.[725] In contrast, direct ART-associated cytotoxic effects on the vasculature has also been shown to inhibit vascular growth.[726]

Although not significantly different, trends in the median VEGF levels between HIV-free (90 pg/ml), HIV+ART (70 pg/ml) and HIV/noART (56 pg/ml) indicate that HIV status may lean toward a reduced pro-vascular growth status in the current study population (**Table 3.10.**). A large data range and a skewed data distribution may have contributed to the non-significant differences between the groups. Nonetheless, after adjusting for confounders, the current study could not find an association between viral load or CD4 cell count and VEGF. (Appendix A7, **Table A7.7.**). Findings in the current study do not support those of Sporer *et al.* (2004), who showed that VEGF expression was significantly higher in PLWH without treatment compared to HIV with treatment.[727] Nyagol *et al.* (2008) furthermore showed that HIV proteins Tat can mimic VEGF and was associated with micro-vessel density [724] and associated with HIV-related malignancies.[728,729] These results suggest that HIV is not associated with endothelial dysfunction (when using VEGF as a biomarker) in the current study population. The non-significant association between viral activity and inflammation (hsCRP and TNF-α) in the current study may also account for these results.

In support of the pro-atherosclerotic effects of ART previously reported,[725] initiating ART was positively associated with VEGF after adjusting for confounding factors (**Table 3.14.**) although an 18-month ART treatment period was not significantly associated (**Table 3.15.**). These results suggest that initiating ART may upregulate VEGF, which may potentially suggest a pro-endothelial dysfunction state. On the other hand, based on the non-significant trends observed at baseline between groups, these results may also indicate reversal of the effects of HIV.

3.3.7.2.6. Effects of HIV and ART on PAI-1.

PAI-1 is an inhibitor of t-PA activator and associated with thrombolysis, and regarded as a biomarker of endothelial function.[730,731] Studies indicate that PAI-1 levels are increased in HIV with or without ART and closely associated with HIV and ART-dependent metabolic dysfunction.[517,732]

In contrast to these reports, our findings show that PAI-1 levels were significantly lower in HIV+ART and HIV/noART compared to HIV-free at baseline (**Table 3.10.**), but after adjusting for confounders, initiating ART was positively associated with PAI-1 (**Table 3.14.**). An 18-month ART treatment period was, however, not significantly associated (Appendix A7, **Table A7.8.**). Our findings support those of Jeremiah *et al.* (2012) who reported that initiating ART was associated with a progressive increase in PAI-1 after a 3-month period on ART.[733] Our findings also support Francisci *et al.* (2009), who found that ART did not affect PAI-1 levels over the course of a longer 24-months ART treatment period.[353]

It appears that PAI-1 is also closely associated with HIV and ART associated metabolic dysregulation. This is supported by a study by Masiá *et al.* (2010) who found a strong positive association between PAI-1 and ART-associated lipodystrophy.[734] Also, Yki-Järvinen *et al.* (2003) showed that PLWH on ART with lipodystrophy had high levels of PAI-1 compared to HIV-free control and compared to HIV+ART without lipodystrophy.[735] Wirunsawanya *et al.* (2017) furthermore reported that PAI-1 was a predictor of insulin senility in PLWH.[732]

As ART was not associated with major metabolic abnormalities in the current study population, our results suggest that initiating ART may be associated with cardioprotective effects through lowering of PAI-1 levels.[736] These results furthermore suggest that HIV and ART may contribute to endothelial dysfunction through PAI-1 in PLWH who exhibited HIV- and ART-associated metabolic dysfunction.

3.3.7.3. Effects of HIV and ART on retinal calibre.

At baseline no significant differences were observed in CRAE between HIV-free, HIV+ART and HIV/noART (**Table 3.11.**). Also, no significant associations between CRAE and viral load, CD4 cell count, initiating ART or an 18-month ART treatment period were observed after adjusting for confounding factors (Appendix A8, **Table A8.1.**). These results suggest that HIV and ART in the current study population are not associated with retinal arteriolar morphological changes.

A similar study by Pathia *et al.* (2012) investigated the longitudinal effects of HIV and ART in a study population from the Cape Town region with a similar mean age (40 years) and CD4 cell count (468 cells/µL) to the current study.[65] The mean CRAE in HIV-free control (161.34±17.38 µm) and HIV study group (163.67±17.69 µm) in the study by Pathia *et al.* (2012) appeared to be slightly higher, but comparable to those observed in the current study.[65] In contrast to the current study, HIV and ART duration was associated with a narrower CRAE in the study by Pathia *et al.* (2012).[65] The authors attributed their findings to HIV and ART associated inflammation.[65] Narrowing of CRAE is independently associated with atherosclerosis.[737] It has been shown that ART often presents with pro-atherosclerotic effects in retinal vessels.[738] HIV and ART was not associated with increased inflammation in the current study. On the contrary, ART exhibited anti-inflammatory effects and may account for discrepancies between the findings of the current study and those of previous reports. Nonetheless, these results suggest that HIV and ART are not associated with cardiovascular risk when using CRAE as a marker of effect in the current study population.

On the other hand, atherosclerosis and inflammation are associated with higher CRVE values.[739,740] HIV+ART presented with a significantly lower CRVE compared to HIV-free and HIV/noART (**Table 3.11.**). After adjusting for confounding factors, initiating ART and on-going ART treatment were inversely associated with CRVE (**Table 3.14.** and **Table 3.15.**). The unadjusted mean CRVE in HIV-free (270.81±18.98 μm) and HIV on ART (267.77±18.21 μm) groups in the study by Pathia *et al.* (2012) appeared to be higher than those observed in the current study.[65] Although the mean CRVE in the study by Pathia *et al.* (2012) appeared to be significantly higher, they were also significantly different, as reported in the current study.[65] HIV and ART duration were not significantly associated with CRVE in the study by Pathia *et al.* (2012).[65] Pathia *et al.* (2012) postulated that age-related changes in retinal venular calibre (narrowing) may manifest earlier in PLWH.[65] Narrowing of retinal venules due to age has previously been reported elsewhere.[65,741,742] As initiating ART and an 18 month ART treatment period were both inversely associated with CRVE, these results suggest that ART may exhibit an aging effect on retinal venules. Decreased levels of adhesion molecules, as observed in the current study, are conventionally interpreted as an anti-atherosclerotic and cardioprotective, the effect of upregulation of PAI-1 and reduced vascular adhesion molecules is also strongly associated with apoptosis *via* caspase 3 signaling [743] and deep-vein thrombosis [744,745]. This may explain the significant ART-associated effects on retinal venules, while no effects on arterioles were observed. Alternatively, a more plausible explanation for the inverse association between ART and CRAE may involve the anti-inflammatory properties observed with ART in the current study population.

At baseline, AVR did not significantly differ between HIV-free, HIV+ART and HIV/noART (Appendix A8, **Table A8.1.**). Following regression analysis viral load was inversely associated with AVR and an 18-month ART treatment period was positively associated with AVR (**Table 3.15. and Table 3.16.**). Gangaputra *et al.* (2012) reported that a decrease of 0.1 in AVR was associated with a 12% increase in risk for mortality in their ART treated HIV population.[746] These results show that HIV in current study population may increase the mortality risk, while ART reduces the risk. The results underscore the protective effects ART exhibited in the current study population.

3.3.7.4. Effects of HIV and ART on flow-mediated dilatation.

The adverse effects of HIV on endothelial function is well described in literature [654,747,748] while reports on the effects of ART on endothelial function are often conflicting.[748–751] Variability in the reports may be related to differences in ART combinations, treatment durations and cardiometabolic profiles.[308,748,752]

HIV and ART in the current study did not affect baseline brachial artery diameter. No significant differences in baseline brachial artery diameter were observed between HIV-free, HIV+ART or HIV/noART (**Table 3.12**.). Also, no significant associations were observed between baseline brachial artery diameter and viral load,

CD4 cell count, initiating ART or on-going ART treatment period (Appendix A9, **Table A9.1.**). HIV and ART have previously been implicated in autonomic dysregulation, which may manifest as vasoconstriction (reduced baseline artery diameter), increased blood pressure and heart rate variability, but neither HIV, nor ART, was associated with any of these effects.[753–755] Our baseline brachial artery diameter findings reflect similar trends to those observed with CRAE and suggest that HIV and ART did not affect basal arterial function.

At baseline the unadjusted median % FMD did not significantly differ between HIV-free and HIV/noART (**Table 3.12.**), but after adjusting for confounding factors, viral load was inversely associated with % FMD and CD4 cell count was positively associated with % FMD (**Table 3.17.**). In line with previous reports showing that HIV may exert detrimental effects on endothelial function,[654,747,748] this finding shows that HIV in the current study population is associated with endothelial dysfunction and contributes to increased cardiovascular risk.

On the other hand, ART exhibited cardioprotective effects at baseline as indicated by % FMD. HIV+ART presented with a significant higher unadjusted median % FMD compared to HIV-free and HIV/noART at baseline (**Table 3.12.**), but, surprisingly, an 18-month ART treatment period was negatively associated with % FMD after adjusting for confounding factors, (**Table 3.15.**) while initiating ART was not significantly associated with % FMD (Appendix A9, **Table A9.2.**). These results show that ART is associated with endothelial dysfunction when using FMD as a marker of effect in the current study population.

Our findings support those of various other reports. In a meta-analysis (57 articles) by Sun *et al*. (2015), it was reported that HIV and ART were associated with decreased % FMD.[748] Oliviero *et al.* (2009), who showed that HIV without treatment was associated with endothelial dysfunction compared to healthy controls and that viral load was inversely associated with endothelial dysfunction.[747] Similarly, Hsue *et al*. (2009) showed that ART was associated with endothelial dysfunction as indicated by % FMD.[756] Other studies reported the same effect.[654,757]

A study by Da Silva *et al.* (2011) described a possible mechanism that may underlie HIV-associated endothelial dysfunction. They showed that HIV infection is inversely associated with % FMD through inhibition of endothelial progenitor cells and upregulation of microparticles (released from apoptotic cells) independent of other cardiovascular risk factors such as inflammation.[752] These findings by Da Silva *et al.* (2011) suggest that HIV can inhibit endothelial cell turn-over and inhibit vascular responses to immune activation.[752] These findings may also explain the general lack of response in terms circulating serum biomarkers to increasing viral load (viral load was not significantly associated with any circulating markers of endothelial dysfunction) in the current study. These findings also indicate that HIV may contribute to endothelial cell senescence as previously reported by various other studies.[758–760]

The detrimental effects of ART on endothelial function (as measured with the FMD procedure), despite mostly beneficial effects, suggest that ART may have direct mechanistic involvement in eNOS activity and/or the

release of NO from endothelial cells during a stress response. A review by Wang *et al.* (2009) evaluated the effects of ART on endothelial function [761] and described possible mechanisms, including oxidative stress, activation of MAP-kinases and down-regulation of eNOS expression.[761,762] A study by Kappert *et al.* (2006) showed that ART can also inhibit the endothelial cell healing process.[763] In terms of vascular reactivity (rat aortic ring model), Jiang *et al.* (2006) showed that ART increases mitochondrial ROS production resulting in cellular dysfunction.[764] ART has also been shown to induce the release of microparticles PLWH.[765] Microparticles are released from cells in response to cytokines, thrombin, endotoxins and hypoxia, and is furthermore associated with apoptosis.[750,751] These findings suggest that ART may have contributed to poor recovery following a stress response such as reactive hyperaemia, despite exhibiting anti-inflammatory properties and that these effects may be due to ART-associated oxidative stress.

Almost all participants (90%) that enrolled in the HIV+ART study group in the current study were on a PI-free first-line ART treatment combination (**Table 3.5.**). The detrimental effects of PIs in endothelial function and cardiovascular health are well-recognised in literature.[267,634,726,766] Compared to PIs, NRTIs and NNRTIs are usually associated with an improved cardiovascular risk profile, but have also been implicated in increased cardiovascular risk compared to HIV-free as shown by the large D:A:D study.[767,768] A commonly prescribed first-line ART fixed-dose combination drug in SA contains two NRTIs (emtricitabine and tenofovir) and an NNRTI (efavirenz). A study by Faltz *et al*. (2017) linked efavirenz, but not emtricitabine and tenofovir, directly to endothelial dysfunction through an impaired response to acetylcholine (impaired relaxation), promoting oxidative stress, dysregulating PARP-activity, decreased cell viability and increasing apoptosis and necrosis.[769] A study by Gupta *et al*. (2012) also showed that a 12-month ART treatment period was associated with endothelial dysfunction as indicated by % FMD and that efavirenz-containing treatment combinations exhibited worse effects compared to PI-containing regimens on endothelial function despite a good response to ART in terms of CD4 cell count, viral load, HDL cholesterol and VCAM-1.[338] These results suggest that emtricitabine may have directly promoted endothelial dysfunction in the current study population. The differential effects of individual ART drugs need more investigation to develop safer ART combination.

3.4. Summary of main findings.

The aim of Sub-study 1 was to investigate if endothelial function is a marker of effects of HIV and ART in a study population residing in the Cape Town area. Markers of vascular and endothelial function in the current study included circulating serum biomarkers (markers of inflammation, vascular adhesion and thrombosis), blood pressure (SBP and DBP), retinal vessel diameters (CRAE and CRVE) and flow, mediated dilatation (baseline brachial artery diameter and % FMD). Results in the current study show that HIV (as indicated by viral load), and ART (as indicated by initiation ART and an 18-month ART treatment period) were significantly associated with various markers of endothelial function and cardiometabolic effects (**Table 3.18.**).

Table 3.18. Summary of main findings of Sub-study 1.

Variables [a]		Viral Load	CD4 cell count	Initiating ART	18 months ART
Vascular Endothelial and Cardiovascular	**Biomarkers**				
	Inflammation		↑		↓
	Vascular adhesion			↓	↓
	Vascular growth			↑	
	Thrombolysis			↑	
	Blood pressure				
	Heart rate				
	Retinal vessel diameter				
	CRAE				
	CRVE	↑		↓	↓
	AVR	↓			↑
	FMD				
	Baseline brachial diameter				
	% FMD	↓	↑		↓
Cardiometabolic	**Body composition**	↓	↑		↓
	Lipid metabolism				
	Total cholesterol	↓		↑	↑
	HDL cholesterol	↓		↑	↑
	LDL cholesterol	↓			↓
	Triglycerides				
	Glucose metabolism		↑		
	Haemoglobin	↓			
	Liver function (GGT)	↓		↑	
	Kidney function				↓

[a] **Symbols:** ↑: Positive association; ↓: Negative association. Empty cells indicate no significant association.

3.5. Strengths and limitations specific to Sub-study 1.

There are a number strengths and limitations in Sub-study 1. The overall power of the statistical analyses performed on the HIV-free and HIV+ART data was relatively strong given the reasonable population sizes, which

allowed for the adjustment of various confounding factors. The ability to adopt a repeated measures design for these study groups may also have contributed to statistical power. Sub-study 1 included a wide range of cardiometabolic and cardiovascular endpoints, which contributed to a better understanding in terms of the effects of HIV and ART. The current study was also able to recruit HIV participants that were ART-naïve at their baseline visit before ART commenced. This allowed to evaluate the pre- *vs.* post ART ("initiating ART") effects. Results from the HIV-free groups also provided insight into the cardiovascular risk profile of a relatively comparable sample of the general population in the recruitment area.

The current study cohort was relatively young. The results indicate that HIV and ART, to some extent, may promote the development of premature CVD, since several markers of cardiovascular risk in general, and vascular endothelial impairment in particular, were already observed in our study population. The effects of HIV and ART may become more prominent as the study population ages, and effects not observed during the time of data collection in the current study (e.g. the effects viral load on circulating biomarkers) may become more pronounced over time. The findings of the current study therefore underscore the importance of early screening, detection and management of early warning signs that may later contribute to CVD in PLWH.

Unfortunately, the relative proportions of gender and ethnicity varied between groups, which did pose a statistical challenge. Only 16% (n = 17) of HIV-free participants were male, compared to 34% (n = 51) males in HIV+ART. Almost all participants (98%) in HIV-free consisted of participants of mixed ancestry compared to 72% in HIV+ART. Therefore, results for HIV-free mostly pertain to a population of mixed ancestry as ethnicity was not included as a confounder in this group. Due to large differences and uneven distribution in population characteristics it was decided to rather perform within-group statistical analysis and compare trends between groups as opposed to between-group analysis where controlling for possible confounders such as ethnicity and gender would not have been included in the model.

The total HIV population (HIV+ART and HIV/noART combined) was used to explore the effects of viral replication as indicated by viral load and immune restoration as indicated by CD4 cell count. The rationale for including all HIV-infected participants in this analysis was to have a larger range and thus a better contrast (high/low) in viral load. Unfortunately, this also meant that the results do not exclusively represent the effects of viral load (without the presence of ART). Concomitantly, the exclusive effects of ART (without the presence of viral replication) could not be presented. A larger HIV/noART study population would have allowed for more reliable adjustment of these confounders. This needs to be considered for future research and publications.

Analysis for circulating biomarkers of vascular function were not performed for all participants (due to cost implications and budget constraints), which limited the scope of adjustment possible in the regression analyses. Also, a small population size in HIV/noART restricted statistical power while very limited adjustment could be performed for this group. Adjusting for smoking status based on whether a participant smokes or not may also not have been ideal. For future studies, the inclusion of a biomarker such as cotinine as a marker of tobacco exposure is recommended. This will also allow to account for second-hand smoke exposure. Sub-study 1 also did not include

markers of oxidative stress. This should be considered in future studies as it would provide a clearer picture in terms of role that oxidative stress played in disease mechanisms.

Adherence to ART in the HIV+ART population over the 18-months period could not be verified independently and was therefore not accounted for in the results. Also, the exact duration of HIV-infection remained unknown to a large extent in the current study population and could not be accounted for in regression analysis. Almost all participants (90%) were on first-line ART and therefore adjustment for first-line and second-line ART treatment was not performed in regression analysis. However, the results reported in the current study mostly reflected the effects of SA's recommended first-line ART treatment combination at the time of undertaking the study. These results thus provide a better understanding of the effects of a first-line treatment combination in a SA population. It has furthermore been shown that the health effects of different ART drugs, drug classes and treatment combinations can vary greatly. Results for the Sub-study 1 were discussed in terms of general ART effects as reported in the literature. Drug-specific effects needs to be considered in future research. Despite this, the ART findings presented in this study are novel insofar as it concerns the specific use of a once daily, fixed-dose combination ART drug, for which limited data are available in the literature.

Despite some limitations, results in the current study show that endothelial function is a marker of the effects of HIV and ART in our study population. HIV exhibited detrimental effects on cardiometabolic and vascular function. On the other hand, ART results were mixed showing beneficial and detrimental effects. Overall, this study provides a novel contribution to existing knowledge on the cardiovascular, metabolic and vascular endothelial effects of HIV-infection and first line ART in the context of a South African population. We are not aware of any previous studies that have investigated such a wide range of cardiovascular-related endpoints in a South African study population using a longitudinal study design. The findings of the present study underscore the relevance of cardiovascular disease in PLWH, and that more research in terms of the effects of HIV and ART on cardiovascular health is urgently needed.

4. Chapter 4: Results and discussion: Air pollution (Sub-study 2).

4.1. Baseline population characteristics.

4.1.1. Baseline demographic, lifestyle, socioeconomic and living environment characteristics.

A total number of 77 female and 14 male participants, all of whom were also recruited as HIV-free control participants for Sub-study 1, were enrolled into Sub-study 2. Of these, 16 female participants who completed their baseline visits did not consent to continue with the 6-month follow-up visit and were excluded from the study. Furthermore, only 6 male participants consented for follow-up visits. Due to their low enrollment rate, males were subsequently excluded from Sub-study 2. Therefore, this chapter will present the data collected from a total number of 61 female participants who successfully completed both baseline and follow-up assessment visits.

The study population had a mean age of 42.5 years (mean ± SD: 42.5 ± 13.4 years) at baseline, and most participants were smokers (n = 42, 69%) with a smoking frequency less than 20 cigarettes per day. Twenty-eight (34%) participants indicated that they had consumed alcohol in the preceding 12 months at a frequency of less than 8 days per month. Most participants slept 6 to 9 hours at night (n = 37 (61%)). About half of the participants were unemployed (n = 30 (49%)). All participants used electricity as their main source of energy at home and only 3 participants (5%) indicated that they lived next to a main road (**Table 4.1.**).

Table 4.1. Baseline demographic, lifestyle, socioeconomic and living environment characteristics.

Variable	Baseline [a]
Age (years)	42.5 ± 13.4
Lifestyle	
Smoking status	
Non-smoker, *n* (%)	19 (31%)
Current smoker, *n* (%)	42 (69%)
Smoking frequency (<20 cigarettes/day)	42 (69%)
Alcohol consumption (Last 12 months: Yes, *n* (%))	28 (34%)
<8 days/month, *n* (%)	28 (34%)
Hours of sleep per night	
≤6 hours, *n* (%)	8 (13%)
6 to ≤9 hours, *n* (%)	37 (61%)
>9 hours. *n* (%)	16 (25%)
Socioeconomic	
Employment	
Unemployed, *n* (%)	30 (49%)
Part-time, *n* (%)	25 (41%)
Full-time, *n* (%)	6 (10%)
Living Environment	
Main source of energy	
Electricity, *n* (%)	61 (100%)
Living next to a main road	
Yes, *n* (%)	2 (3%)
No, *n* (%)	59 (97%)

[a] Data presented as mean ± SD or *n* (%) for *n* = 61 women.

4.1.2. Baseline body composition characteristics.

Most participants presented with elevated body mass measurements (overweight *n* = 11 (18%) and obese *n* = 22 (36%)) while the mean ± SD BMI was in the overweight range (27.7 ± 8.4 kg/m^2) according to WHO criteria.[532] Most participants also had an elevated waist circumference (*n* = 36 (59%), but elevated waist-to-hip ratios were less frequently observed (*n* = 24 (39%)) (**Table 4.2.**).

Table 4.2. Baseline body composition population characteristics.

Variable	Baseline [a]
Body Mass Index (BMI), kg/m^2	27.7 ± 8.4
Weight (kg)	68.7 ± 22.7
Height (cm)	157.0 ± 6.9
Body composition classification according to BMI [b]	
Underweight (BMI < 18.5 kg/m^2), *n* (%)	6 (10%)
Normal weight (BMI 18.5 to < 25 kg/m^2), *n* (%)	22 (36%)
Overweight (BMI 25 to < 30 kg/m^2), *n* (%)	11 (18%)
Obese (BMI > 30 kg/m^2), *n* (%)	22 (36%)
Waist-to-hip ratio	0.85 ± 0.08
Waist circumference (cm)	88.0 ± 17.1
Elevated (>80 cm), *n* (%) [b]	36 (59%)

[a] Data presented as mean ± SD or *n* (%) for *n* = 61 women. [b] According to WHO guidelines.[531,532]

4.1.3.   Baseline fasting lipid, glucose and HbA1c measurements.

The mean fasting total-, HDL-, and LDL-cholesterol and triglyceride levels fell within the normal range although 30% (*n* = 18) of the participants presented with elevated LDL cholesterol (**Table 4.3.**).

Table 4.3. Baseline fasting lipid, glucose and HbA1c measurements.

Variable	Baseline [a]
Lipid Profile	
Total Cholesterol (mmol/L)	4.43 ± 0.84
Elevated (≥5 mmol/L), *n* (%) [b]	14 (23%)
High-Density Lipoprotein Cholesterol (HDL) (mmol/L)	1.38 ± 0.37
Decreased (≤1.2 mmol/L), *n* (%) [b]	10 (16%)
Low-Density Lipoprotein Cholesterol (LDL) (mmol/L)	2.54 ± 0.84
Elevated (≥3 mmol/L), *n* (%) [b]	18 (30%)
Triglycerides (mmol/L) [b]	1.11 ± 0.65
Elevated (≥1.7 mmol/L), *n* (%)	6 (10%)
Glucose Homeostasis	
Fasting glucose (mmol/L)	5.11 ± 1.93
Elevated (≥5.6 mmol/L), *n* (%) [c]	4 (7%)
Glycated Haemoglobin (HbA1c) (%)	5.43 ± 0.99
Elevated (≥5.9%), *n* (%) [c]	10 (16%)

[a] Data presented as mean ± SD or *n* (%) for *n* = 61 women. [b] According to the Heart and Stroke Foundation of South Africa, NHLS and the US National Institutes of Health (NIH) guidelines.[540,546–548] [c] According to The Heart and Stroke Foundation of South Africa guidelines.[546,553–555]

4.1.4. Baseline Hb, GGT and eGRF measurements.

The mean baseline values for Hb, GGT and eGFR fell within the normal range. Twenty-five percent (*n* = 15 (25%)) of the study participants had elevated GGT levels (**Table 4.4.**). All linear mixed model regression analysis for the urine metabolite 3+4MHA were adjusted for urine creatinine.

Table 4.4. Baseline Hb, GGT, urine creatinine and eGFR measurements.

Variable	Baseline [a]
Haemoglobin (Hb)	
Haemoglobin (g/dL)	13.42 ± 1.22
Decreased (<12.0 g/dL), *n* (%) [b]	7 (11%)
Liver Function	
γ-Glutamyl transferase (U/L)	41.42 ± 22.44
Elevated (≥40 U/L), *n* (%) [c]	15 (25%)
Kidney Function	
Estimated glomeration filtration rate (mL/minute/1.73 m^3)	103.43 ± 19.14
Decreased (< 90 mL/minute/1.73 m^3), *n* (%) [d]	13 (21%)

[a] Data presented as mean ± SD or *n* (%) for *n* = 61 women. [b] According to WHO guidelines.[561] [c] According to NHLS standards.[563] [d] According to information from [582,583].

4.1.5. Baseline LTL, mtDNA content and % DNA methylation measurements.

Baseline population characteristics for LTL, mtDNA and % DNA methylation are reported in **Table 4.5.**

Table 4.5. Baseline genetic markers.

Variable	Baseline [a]
Leukocyte telomere length (T/S ratio [d]) [b]	0.98 (0.58 to 1.55)
Mitochondrial DNA content [b, e]	1.05 (0.29 to 2.39)
% DNA methylation (%) [c, f]	4.36 (3.31 to 4.95)

[a] Data presented as median (range) for [b] *n* = 57 and [c] *n* = 47 women. [d] Telomere repeated copy number / single gene copy number ratio (T/S ratio) according to methodology previously described [596] [e] mtDNA content relative to nuclear DNA copy number according to methodology previously described.[595] [f] Expressed as a 5mdC/2dC ratio according to methodology previously described.[593]

Baseline age was inversely correlated with LTL (*r* = -0.30; *p* = 0.025; **Figure 4.1a.**) and a positive correlation between baseline and follow-up LTL was achieved (*r* = 0.70; *p* < 0.001; **Figure 4.1b.**).
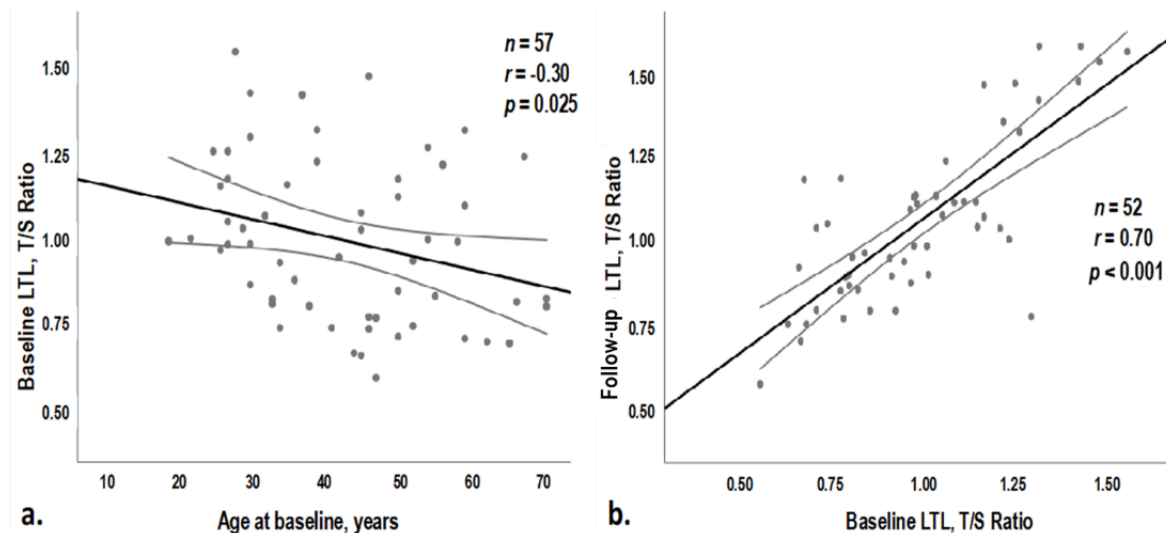
Figure. 4.1a and 4.1b. a. Spearman's Rho correlation between age (years) and LTL (T/S Ratio) at baseline. A trend line with 95% CI was indicated. Four DNA samples at baseline did not yield sufficient DNA content for LTL determination. **b.** Spearman's Rho correlation between LTL (T/S Ratio) at baseline and follow-up. A trend line with 95% CI was indicated. Three samples at baseline and 6 at follow-up did not yield sufficient DNA for LTL quantification. Fifty-two samples had both baseline and follow-up measurements available.

4.1.6. Baseline blood pressure and heart rate measurements.

The mean SBP and DBP values fell within the normal clinical range, although 25% of participants (n = 15) were hypertensive according to WHO and South African Hypertension Society guidelines (SBP >140 mmHg or DBP of >90 mmHg) (**Table 4.6.**).[604]

Table 4.6. Baseline blood pressure and heart rate measurements.

Variable	Baseline [a]
Systolic Blood Pressure (mmHg)	122.5 ± 19.9
Elevated (>140 mmHg), n (%) [b]	11 (18%)
Diastolic Blood pressure (mmHg)	84.1±12.0
Elevated (>90 mmHg), n (%) [b]	16 (26%)
Hypertension (SBP >140 mmHg or DBP >90 mmHg) [b]	
Yes, n (%)	15 (25%)
No, n (%)	46 (75%)
Heart Rate (bpm)	71.6 ± 10.3

[a] Data presented as mean ± SD or n (%) for n = 61 women. [b] According to WHO and South African Hypertension Society guidelines guidelines.[533,604]

4.1.7. Baseline vascular endothelial biomarker measurements.

More than half of participants presented with increased levels of systemic inflammation as indicated by hsCRP (n = 35 (57%)) (**Table 4.7.**).

Table 4.7. Baseline levels for circulating biomarkers of vascular endothelial function / dysfunction.

Variable	Baseline [a]
Markers of inflammation	
High-Sensitivity C-Reactive Protein (mg/L) [b]	6.3 (0.2 to 37.1)
Elevated (>3mg/L), n (%) [d]	35 (57%)
Tumour necrosis factor-alpha (TNF-α) (pg/ml) [c]	23.8 ± 3.9
Markers of vascular adhesion	
Vascular cell adhesion molecule 1 (VCAM-1) (ng/ml) [c]	728 (429 to 2036)
Intercellular adhesion molecule (ICAM-1) (ng/ml) [c]	363 (50 to 1344)
Endothelial-leukocyte adhesion molecule (E-selectin) (ng/ml) [c]	37.1 ± 13.4
Endothelial-Platelet adhesion molecule (P-selectin) (ng/ml) [c]	38.5 ±13.4
Marker of vascular growth	
Vascular endothelial growth factor-A (VEGF) (pg/ml) [c]	97.5 (23.7 to 414.5)
Marker of thrombolysis	
Plasminogen activator inhibitor-1 (PAI-1) (ng/ml) [c]	103 ± 37.1

[a] Data presented as mean ± SD, median (range) or n (%) for [b] n = 57 and [c] n = 36 women. [d] According to the cut-off value associated with increased cardiovascular risk.[534].

4.1.8. Baseline retinal microvascular calibres.

Fifty-eight good quality images were obtained for vessel calibre determination at baseline. The baseline mean ± SD for vessel calibre parameters are reported in **Table 4.8.**

Table 4.8. Baseline retinal vessel caliber characteristics.

Vessel calibre	Baseline [a]
Central retinal arteriolar equivalent (CRAE) (μm)	157.9 ± 16.4
Central retinal venular equivalent (CRVE) (μm)	238.4 ± 20.1
CRAE/CRVE ratio (AVR)	0.66 ± 0.06

[a] Data presented as mean ± SD for n = 58 women.

4.1.9. Baseline flow-mediated dilatation measurements.

Baseline FMD measurements were successfully completed for 58 women. Baseline FMD characteristics are reported in **Table 4.9**.

Table 4.9. Baseline FMD variable outcomes.

FMD parameters	Baseline [a]
Baseline (pre-ischaemia) brachial artery diameter (mm)	3.22 ± 0.69
% Flow-mediated dilatation (%)	6.17 ± 4.45

[a] Data presented as mean ± SD for n = 58 women.

4.2. Air Pollution Exposure.

4.2.1. NO_2 and BTEX exposure measurements at baseline and follow-up.

The mean NO_2 (p = 0.003) and median benzene (p = 0.045), ethyl-benzene (p = 0.042), $m+p$-xylene (p = 0.019) and o-xylene (p =0.014) concentrations were significantly higher at the baseline assessment visit compared to the 6-month follow-up visit. No significant differences were observed in toluene (p = 0.199) concentration and temperature (p = 0.598) (**Table 4.10.**).

Table 4.10. Personal NO_2, BTEX and temperature exposure measurements at baseline and follow-up assessment visits.

Variable	Baseline [a]	Follow-up [a]	Combined [b]		
	Mean ± SD / Median (Range)	Mean ± SD / Median (Range)	Mean / Median	Range	IQR
NO_2 (µg/m³) [c]	13.6 ± 4.8	10.6 ± 4.7**	12.1	4.0 to 25.4	7.0
Benzene (µg/m³) [d]	3.9 (0.7 to 14.2)	2.2 (0.5 to 9.3)*	2.7	0.5 to 14.2	3.3
Toluene (µg/m³) [d]	22.1 (5.6 to 189)	18.0 (3.7 to 284)	19.8	3.7 to 284	30.0
Ethyl-benzene (µg/m³) [d]	2.8 (1.1 to 34.4)	2.3 (0.7 to 21.4)*	2.7	0.6 to 34.4	3.8
$m+p$-xylene [c] (µg/m³) [d]	9.2 (3.4 to 117.4)	7.5 (2.0 to 74.8)*	8.4	2.0 to 43.8	3.8
o-xylene [c] (µg/m³) [d]	3.2 (1.2 to 43.8)	2.7 (0.7 to 24.7)*	3.0	0.7 to 43.8	3.8
Temperature (°C) [e]	21.6 ± 3.2	21.9 ± 2.7	21.7	15 to 27.9	4.4

[a] Data presented as mean ± SD or median (range). Values represent the mean or median for the 7-day period prior to the assessment visit. [b] Baseline and follow-up data combined. [c] Lower limit of detection (LOD): 0.2 µg/m³, n = 60 and 61. [d] LOD for BTEX: 0.05, 0.01, 0.01, and 0.01 µg/m³, respectively, n = 56 and 57. [e] Represents the average 7-day recorded temperatures for all 30-minute interval temperature recordings for each participant for the

7 days prior to the assessment visit (n = 60 and 61 for baseline and follow-up). * p < 0.05 *vs.* Baseline. ** p < 0.01 *vs.* Baseline.

All BTEX concentrations were positively correlated and inversely correlated with temperature (**Table 4.11.**).

Table 4.11. Spearman's rho correlation coefficients (r) between temperature and BTEX exposure concentrations.

Variable [a]	Benzene	Toluene	Ethyl-benzene	*m+p-*Xylene	*o*-Xylene
Temperature (°C)	-0.329***	-0.344***	-0.258**	-0.281**	-0.263**
Benzene (µg/m³) [c]		0.461**	0.585**	0.595**	0.589**
Toluene (µg/m³) [c]			0.652**	0.658**	0.667**
Ethyl-benzene (µg/m³) [c]				0.983**	0.972**
m+p-Xylene (µg/m³) [c]					0.989*

[a] Baseline and follow-up visits combined, n = 111 to 112. **Significance**: * p < 0.05. ** p < 0.01. *** p < 0.001.

Seasonal participant recruitment (cold season *vs.* warm season) was unevenly distributed between baseline and follow-up visits (Chi-square test: (n = 37 *vs.* 24) *vs.* (n = 24 *vs.* 37); p = 0.029). Stratifying all personal NO_2 and BTEX exposure concentrations according to a warmer (September to February) and a colder season (March to August), significantly higher (p < 0.001) exposure concentrations were observed during the colder season *vs.* warmer season (**Figure 4.2.**).
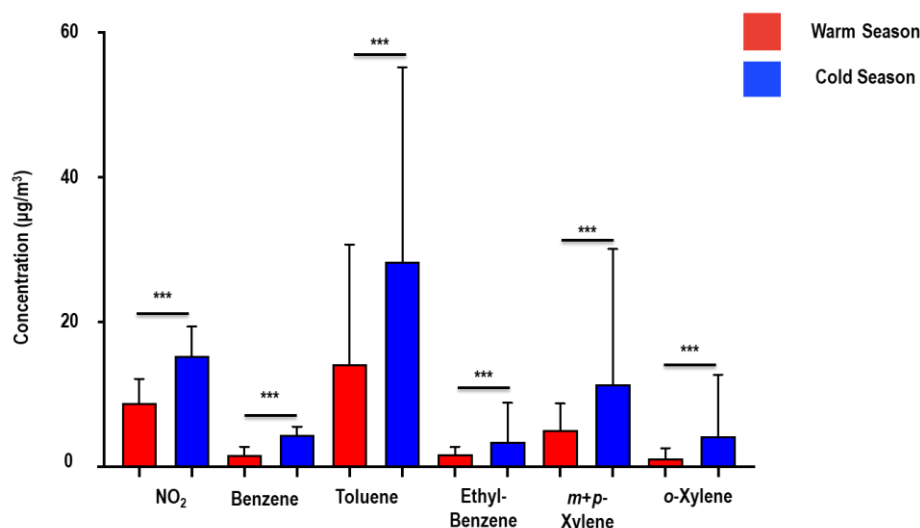
Figure 4.2. NO$_2$ and BTEX exposure concentrations stratified according to warm season and cold season. **NO$_2$** (Independent Student t-test; n = 60 and 61): Mean ± SD 8.7±3.4 *vs.* 15.4 ± 4.0 µg/m³. **BTEX** (Mann-Whitney U-test; n = 58 and 55) median (25-75% IQR): **Benzene** 1.6 (1.0 to 2.8) *vs.* 4.4 (2.7 to 5.5) µg/m; **Toluene** 14.2.1 (6.8 to 30.7) *vs.* 28.3 (15.3 to 55.24) µg/m³; **Ethyl-benzene** 1.7 (1.2 to 2.7) *vs.* 3.5 (2.7 to 8.8) µg/m³; ***m+p*-Xylene** 5.1 (3.8 to 8.7) *vs.* 11.47 (8.3 to 30.1) µg/m³; ***o*-Xylene** 1.28 (0.4 to 2.5) *vs.* 4.2 (3.0 to 12.7) µg/m³. ***p < 0.001.

4.2.2. Urinary markers of BTEX exposure at baseline and follow-up assessment visits.

Urinary markers for BTEX exposure did not differ significantly between baseline and follow-up visits (Wilcoxon signed rank test: p > 0.05). Less than half of PMA (baseline and follow-up n = 10 and 6) and MU (baseline and follow-up n = 14 and 20) sample concentrations were above the lower limit of detection (LOD) and were excluded from further analysis (**Table 4.12.**).

Table 4.12. Urinary concentrations of BTEX exposure markers at baseline and follow-up visits.

Variable	Baseline [a, b]	Follow-up [a, b]	Combined		
	Mean ± SD / Median (Range)	Mean ± SD / Median (Range)	Median	Range	IQR
Urinary metabolites of BTEX					
HPMA (µg/ml) [c]	1.69 (92 to 12.8)	1.8 (0.12 to 12.6)	1.7	92 to 12.8	3.2
PMA (ng/ml) [d]	0.05 (0.05 to 0.34)	0.05 (0.05 to 2.50)	0.05	0.05 to 2.5	0.01
MU (ng/ml) [e]	62.5 (62.5 to 498)	62.5 (62.5 to 595)	62.5	62.5 to 595	97.3
BMA (ng/ml) [f]	14.7 (2.5 to 588.0)	14.3 (2.5 to 699.0)	14.3	2.5 to 699	34.3
3+4MHA (µg/ml) [g]	1.06 (0.03 to 9.5)	0.85 (0.05 to 32)	0.925	0.03 to 32	1.38

[a] Data presented as median (range). [b] Values of samples that were below the lower limit of detection (LOD) were replaced by LOD/2. [c] Samples with concentrations above LOD (>80 ng/ml): Baseline/follow-up n = 61/61. [d] Samples with concentrations above LOD (>0.09 ng/ml): Baseline/follow-up n = 10/6. [e] Samples with concentrations above LOD (>125 ng/mL): Baseline/follow-up n = 14/20. [f] Samples with concentrations above LOD (>5 ng/ml): Baseline/follow-up n = 46/45. [g] Samples with concentrations above LOD (>100 ng/ml): Baseline/follow-up n = 60/58.

The urinary marker 3+4MHA was positively correlated with all BTEX exposure concentrations and inversely correlated with temperature and was therefore considered the most prominent urinary marker for BTEX exposure (**Table 4.13**).

Table 4.13. Spearman's Rho correlations coefficients (r) for NO_2, BTEX, temperature and urinary markers of BTEX exposure.

Urinary markers [a]	Temp.	Benzene	Toluene	Ethyl-benzene	*m+p*-Xylene	*o*-Xylene
HPMA (ng/ml)	-0.113	0.186*	-0.020	-0.002	0.023	0.017
BMA (ng/ml)	0.100	-0.070	0.120	-0.023	-0.018	-0.005
3+4MHA (ng/ml)	-0.200*	0.341***	0.219*	0.192*	0.215*	0.210*

[a] Baseline and follow-up data combined, n = 111 to 121. **Significance:** * $p < 0.005$. ** $p < 0.01$. *** $p < 0.001$.

4.2.3. Relationship between exposure and smoking, employment and hours of sleep at night.

Baseline ambient NO_2 and BTEX exposure concentrations did not differ across smoking status, but the urinary marker 3+4MHA (p = 0.010) was significantly higher in smokers than non-smokers (**Table 4.14.**).

Table 4.14. NO_2, BTEX and 3+4MHA according to smoking status.

Variable [a]	Current smoker	Non-smoker
NO_2 (µg/m³)	13.6 ± 5.1	13.4 ± 5.1
Benzene (µg/m³)	4.1 (0.7 to 12.6)	2.8 (0.9 to 14.2)
Toluene (µg/m³)	24.6 (5.6 to 173.1)	25.5 (8.3 to 189.1)
Ethyl-Benzene (µg/m³)	2.8 (1.1 to 34.4)	2.8 (1.5 to 19.4)
m+p-Xylene (µg/m³)	9.3 (3.4 to 117.3)	8.8 (4.5 to 75.2)
o-Xylene (µg/m³)	3.3 (1.2 to 43.8)	3.2 (1.6 to 20.5)
Urinary metabolite		
3+4MHA (ng/mL)	1268 (31.8 to 9512)	405 (50 to 4192) [b]

[a] Data presented as mean ± SD or median (range). Smoking *vs.* non-smoking: [b] Mann-Whitney U-test (3+4MHA: *n* = 42 and 19): *p* = 0.010.

Baseline ambient NO_2 exposure concentrations were significantly higher in the part-time employed participant group (*p* = 0.000) and full-time employed (*p* = 0.042) compared to the unemployed study population while toluene exposure was significantly higher in the group that was full-time employed compared to the unemployed group (*p* = 0.033) (**Table 4.15.**).

Table 4.15. NO_2, BTEX and 3+4MHA according to employment status.

Variable [a]	Unemployed	Part-time Employed	Full-time Employed
NO_2 (µg/m³)	11.4 ± 4.8	16.6 ± 3.3 [b]	11.8 ± 4.8 [b]
Benzene (µg/m³)	2.7 (0.7 to 7.8)	4.4 (1.6 to 8.3)	2.6 (0.9 to 14.1)
Toluene (µg/m³)	16.0 (5.6 to 189.1)	30.1 (7.7 to 162.4)	58.5 (20.3 to 173.1) [c]
Ethyl-Benzene (µg/m³)	2.4 (1.4 to 34.4)	5.0 (1.4 to 26.2)	6.2 (1.5 to 28.2)
m+p-Xylene (µg/m³)	7.3 (3.7 to 117.3)	16.6 (3.7 to 82.0)	19.5 (5.1 to 91.5)
o-Xylene (µg/m³)	2.8 (1.2 to 43.8)	5.8 (1.2 to 29.2)	6.9 (1.7 to 34.8)
Urinary metabolite			
3+4MHA (ng/mL)	1384 (50 to 9512)	1170 (32 to 5436)	984 (335 to 2548)

[a] Data presented as mean ± SD or median (range). One-way ANOVA with Bonferroni post hoc across employment status: [b] (*n* = 30) *vs.* unemployed (*n* = 25; *p* = 0.000) and *vs.* full-time employed (*n* = 6; *p* 0.042); [c] (*n* = 6) *vs.* unemployed (*n* = 22; *p* = 0.033).

Baseline ambient NO_2, BTEX or 3+4MHA concentrations were not significantly associated (Kruskal-Wallis test for between groups) with self-reported hours of sleep at night (**Table 4.16.**).

Table 4.16. NO_2, BTEX and urinary 3+4MHA according to hours of sleep at night.

Variable [a]	Hours of sleep		
	≤6 hours	6 to ≤9 hours	>9 hours
NO_2 (µg/m³)	10.4 ± 6.14	14.2 ± 4.7	13.7 ± 4.1
Benzene (µg/m³)	4.0 (0.8 to 5.5)	3.5 (0.7 to 14.1)	2.3 (1.0 to 8.0)
Toluene (µg/m³)	37.1 (5.6 to 141.9)	28.3 (7.2 to 173.2)	14.7 (6.0 to 189.1)
Ethyl-Benzene (µg/m³)	2.4 (1.1 to 18.3)	3.5 (1.1 to 34.4)	2.6 (1.2 to 19.4)
m+p-Xylene (µg/m³)	7.2 (3.6 to 58.8)	11.2 (3.7 to 117.3)	8.3 (3.4 to 75.2)
o-Xylene (µg/m³)	2.9 (1.2 to 27.6)	3.9 (1.2 to 43.8)	2.9 (1.4 to 20.5)
Urinary metabolite			
3+4MHA (ng/mL)	1172 (31.8 to 4065)	1170 (50 to 5914)	818 (169 to 9512)

[a] Data presented as mean ± SD or median (range).

4.3. Estimated effects of NO_2, BTEX and 3+4MHA.

Only significant findings are presented in the following sections. For full data tables containing all effect sizes, please refer to Appendix B1 to B9: **B1.** Effects of exposure on body composition (Page 235); **B2.** Effects of exposure on lipid and glucose levels (Page 236 to 238); **B3.** Effects of exposure on Hb. (Page 239); **B4.** Effects of exposure on GGT (Page 240); **B5.** Effects of exposure variable outcomes on eGRF (Page 241). **B6.** Effects of exposure on LTL, mtDNA content and % DNA methylation (Page 242 to 244); **B7.** Effects of exposure on blood pressure and heart rate (Page 245 and 246); **B8.** Effects of exposure on circulating markers of vascular endothelial function (Page 247 and 250); **B9.** Effects of exposure on retinal vessel calibre (Page 251 and 252); **B10.** Effects of exposure on flow-mediated vasodilation parameters (Page 253).

4.3.1. Estimated effects of NO_2.

Each IQR increment increase in NO_2 (7.0 µg/m³) was significantly associated with molecular aging (LTL (-12.9%), raised blood pressure (SBP (3.41 mmHg) and DBP (2.48 mmHg)), decreased vascular endothelial growth factor (VEGF (-18.9%), decreased CRVE (-2.93 µm), and decreased baseline brachial artery diameter (-0.29 µm) (**Table 4.17.**).

Table 4.17. Estimated effects of NO$_2$ (µg/m³).

Exposure	(%) Difference/ Difference [a]	95% CI Lower	95% CI Upper	*p*-values
Genetic markers				
Leukocyte telomere length (LTL) [b]	-12.9%	-20.8	-4.1	0.001
Blood pressure [c]				
Systolic Blood Pressure (SBP) (mmHg)	3.41	0.04	6.77	0.047
Diastolic Blood Pressure (DBP) (mmHg)	2.48	-0.01	4.97	0.050
Biomarkers [d]				
Vascular endothelial growth factor (VEGF) (pg/ml)	-18.9%	-30.7	-5.2	0.010
Retinal vessel calibre [e]				
Central retinal venular equivalent (CRVE) (µm)	-2.93	-5.83	-0.03	0.048
Flow-mediated vasodilation [e]				
Baseline brachial diameter (mm)	-0.29	-0.50	-0.079	0.005

[a] Estimates expressed as a difference or % difference for each IQR (7.0 µg/m³) increment change in NO$_2$. [b] Model adjusted for age, BMI, smoking and employment status. [c] Model adjusted for age, BMI, temperature, date of clinical visit, smoking, hours of sleep at night and employment status. [d] Model adjusted for age, BMI, SBP, temperature and smoking status. [e] Model adjusted for age, BMI, SBP, date of clinical visit, temperature, smoking status and employment status.

4.3.2. Estimated effects of BTEX.

4.3.2.1. Effects of benzene.

Each IQR increment increase in benzene (3.3 µg/m³) was significantly associated with elevated fasting glucose levels (0.34 mmol/L) molecular aging (LTL (-8.5%)) and decreased p-selectin (-5.8 pg/ml) (**Table 4.18.**).

Table 4.18. Estimated effects of benzene (µg/m³).

Exposure	(%) Difference/ Difference [a]	95% CI Lower	95% CI Upper	*p*-values
Glucose levels [b]				
Fasting glucose (mmol/L)	0.34	0.02	0.65	0.037
Genetic markers				
Leukocyte telomere length (LTL) [c]	-8.5%	-15.7	-0.75	0.005
Biomarkers [d]				
P-selectin (pg/ml)	-5.8	-9.33	-2.26	0.002

[a] Estimates expressed as a difference or % difference for each IQR (3.3 µg/m³) increment change in benzene. [b] Model adjusted for age, BMI, SBP, temperature, date of clinical visit, smoking and employment status. [c] Model adjusted for age, BMI, smoking and employment status. [d] Model adjusted for adjusted for age, BMI, SBP, temperature and smoking status.

4.3.2.2.   Estimated effects of toluene.

Each IQR increment increase (30.0 µg/m³) in toluene was significantly associated with raised cholesterol (Total cholesterol (0.10 mmol/L), HDL cholesterol (3.8 mmol/L) and LDL cholesterol (11.1 mmol/L)), decreased eGRF (-7.82 ml/minute/1.73 m³), increased mtDNA content (7.6%) and increased PA1 (7.2 ng/ml) (**Table 4.19.**).

Table 4.19. Estimated effects of toluene (µg/m³).

Exposure	% Difference/ Difference [a]	95% CI		p-values
		Lower	Upper	
Lipid levels [b]				
Total cholesterol (mmol/L)	0.10	0.04	0.17	0.003
High-density lipoprotein cholesterol (HDL) (mmol/L)	3.8	0.2	7.4	0.040
Low-density lipoprotein cholesterol (LDL) (mmol/L)	11.1	1.9	20.2	0.018
Kidney function				
Estimated glomeration filtration rate (eGRF) (ml/minute/1.73 m³)	-7.82	-15.32	-0.439	0.038
Genetic markers [c]				
Mitochondrial DNA content (mtDNA)	7.6%	0.2	15.5	0.044
Biomarkers [d]				
Plasminogen activator inhibitor (PA1-1) (ng/ml)	7.2	2.3	12.1	0.005

[a] Estimates expressed as a difference or % difference for each IQR (30.0 µg/m³) increment change in toluene. [b] Model adjusted for age, BMI, SBP, temperature, date of clinical visit, smoking and employment status. [c] Model adjusted for age, BMI, smoking and employment status. [d] Model adjusted for age, BMI, SBP, temperature and smoking status.

4.3.2.3. Estimated effects of ethyl-benzene.

Each IQR increment increase in ethyl-benzene (3.8 µg/m³) was significantly associated with decreased VCAM-1 (-4.9%) and increased PA1 (9.1 ng/ml) (**Table 4.20.**)

Table 4.20. Estimated effects of ethyl-benzene (µg/m³).

Exposure	(%) Difference/ Difference [a]	95% CI		p-values
		Lower	Upper	
Biomarkers [c]				
Vascular cell adhesion molecule 1 (VCAM-1) (ng/ml)	-4.9%	-8.6	-0.9	0.018
Plasminogen activator inhibitor-1 (PA1-1) (ng/ml)	9.1	2.4	15.7	0.008

[a] Estimates expressed as a difference or % difference for each IQR (3.8 µg/m³) increment change in ethyl-benzene.
[b] Model adjusted for age, BMI, SBP, DBP, smoking and employment status.

4.3.2.4. Estimated effects of *m+p*-xylene.

Each IQR increment increase in *m+p*-xylene (3.8 µg/m³) was significantly associated increased VCAM-1 (-1.47%) and increased PA1 (3.08 ng/ml) (**Table 4.21.**).

Table 4.21. Estimated effects of *m+p*-xylene (µg/m³).

Exposure	(%) Difference/ Difference [a]	95% CI Lower	Upper	*p*-values
Biomarkers [b]				
Vascular cell adhesion molecule 1 (VCAM-1) (ng/ml)	-1.47%	-2.68	-0.25	0.020
Plasminogen activator inhibitor-1 (PA1-1) (ng/ml)	3.08	1.09	5.08	0.003

[a] Estimates expressed as a difference or % difference for each IQR (3.8 µg/m³) increment change in *m+p*-xylene.
[b] Model adjusted for age, BMI, SBP, temperature and smoking status.

4.3.2.5. Estimated effects of *o*-xylene.

Each IQR increment increase in *o*-xylene (3.8 µg/m³) was significantly associated with DBP (0.82 mmHg), increased VCAM-1 (-4.5%) and increased PA1 (11.7 ng/ml) (**Table 4.22.**)

Table 4.22. Estimated effects of *o*-xylene (µg/m³).

Exposure	(%) Difference/ Difference [a]	95% CI Lower	Upper	*p*-values
Blood pressure [b]				
Diastolic Blood Pressure (DBP) (mmHg)	0.82	0.01	1.63	0.029
Biomarkers [c]				
Vascular cell adhesion molecule 1 (VCAM-1) (ng/ml)	-4.5 %	-8.4	-0.4	0.033
Plasminogen activator inhibitor-1 (PA1-1) (ng/ml)	11.7	5.2	18.1	0.001

[a] Estimates expressed as a difference or % difference for each IQR (3.8 µg/m³) increment change in *o*-xylene. [b] Model adjusted for age, BMI, temperature, date of clinical visit, smoking, hours of sleep at night and employment status. [c] Model adjusted for age, BMI, SBP, temperature and smoking status.

4.3.3. Estimated effects of 3+4MHA.

Each IQR increment increase in 3+4MHA (1380 ng/ml) was significantly associated with increased LDL cholesterol (37.461), PA1 (12.9 ng/ml), and decreased % FMD (-0.40%) (**Table 4.23.**).

Table 4.23. Estimated effects of 3+4MHA (ng/ml).

Exposure	Difference [a]	95% CI		p-values
		Lower	Upper	
Lipid levels [b]				
Low-density lipoprotein cholesterol (LDL) (mmol/L)	37.461	2.642	72.280	0.035
Biomarkers [c]				
Plasminogen activator inhibitor-1 (PA1-1) (ng/ml)	12.9	3.2	22.5	0.010
Flow-mediated vasodilation [d]				
% Flow-mediated dilatation (% FMD)	-0.40	-1.28	0.48	0.003

[a] Estimates expressed as a difference for each IQR (1380 ng/ml) increment change in 3+4MHA. [b] Model adjusted for age, BMI, SBP, temperature, date of clinical visit, smoking and employment status. [c] Model adjusted for adjusted for age, BMI, SBP, temperature, urine creatinine and smoking status. [d] Model adjusted for age, BMI, SBP, date of clinical visit, temperature, urine creatinine, brachial diameter, smoking status and employment status.

4.4. Discussion of Sub-study 2 results.

The main aim of Sub-study 2 was to measure personal NO_2 and BTEX air pollution exposure levels in the study population and determine whether endothelial function was a marker of effect. The current study found that air pollution was associated with various markers of endothelial function.

Summary of main personal exposure findings:

- Observation of relatively low personal NO_2 and BTEX exposure concentration in the current study (**Table 4.10.**),
- Observation of significant higher exposure concentrations during the colder season than the warmer season (**Figure 4.2.**), and
- Observation of significantly higher NO_2 and toluene exposure concentrations in employed participants (**Table 4.15.**).

Despite the relatively low exposure concentrations, various significantly associations between NO_2 (**Table 4.17.**), BTEX (including urinary 3+4MHA) (**Table 4.18 to 4.23.**) and markers of cardiovascular risk were observed:

- Cardiometabolic dysregulation: Increased fasting glucose levels (benzene) and increased cholesterol levels (toluene: total cholesterol, HDL and LDL; 3+4MHA: LDL).
- Decreased kidney filtration: eGFR (Toluene).
- Molecular aging and oxidative stress: Decreased LTL (NO_2 and benzene) and increased mtDNA content (toluene).

Associations with markers of endothelial function:

- Decreased vascular growth and adhesion, and increased blood coagulation/clot formation: Decreased VEGF (NO_2), p-selectin (benzene) and VCAM-1 (ethyl-benzene-, *m+p*-xylene- and *o*-xylene) and increased PAI-1 (Toluene, ethyl-benzene-, *m+p*-xylene, *o*-xylene and 3+4MHA).

- Reduced vascular calibres and increased blood pressure: Decreased baseline brachial artery diameter and CRVE (NO_2) and increased SBP (NO_2) and DBP (NO_2 and *o*-xylene).

- Impaired brachial artery endothelial function: Reduced % FMD (3+4MHA).

4.4.1. Personal exposure levels in perspective.

4.4.1.1. NO_2 exposure concentrations compared to other reported levels.

The mean personal NO_2 exposure concentration observed in the current study was significantly lower than the recommended WHO cut-off value for annual mean exposure (NO_2: <40 µg/m³ [36]), while none of the individual NO_2 exposure values in the participants (Range: 4.0 to 25.4 µg/m³) exceeded that of the WHO recommended cut-off level for NO_2 exposure (**Figure 4.3.**).
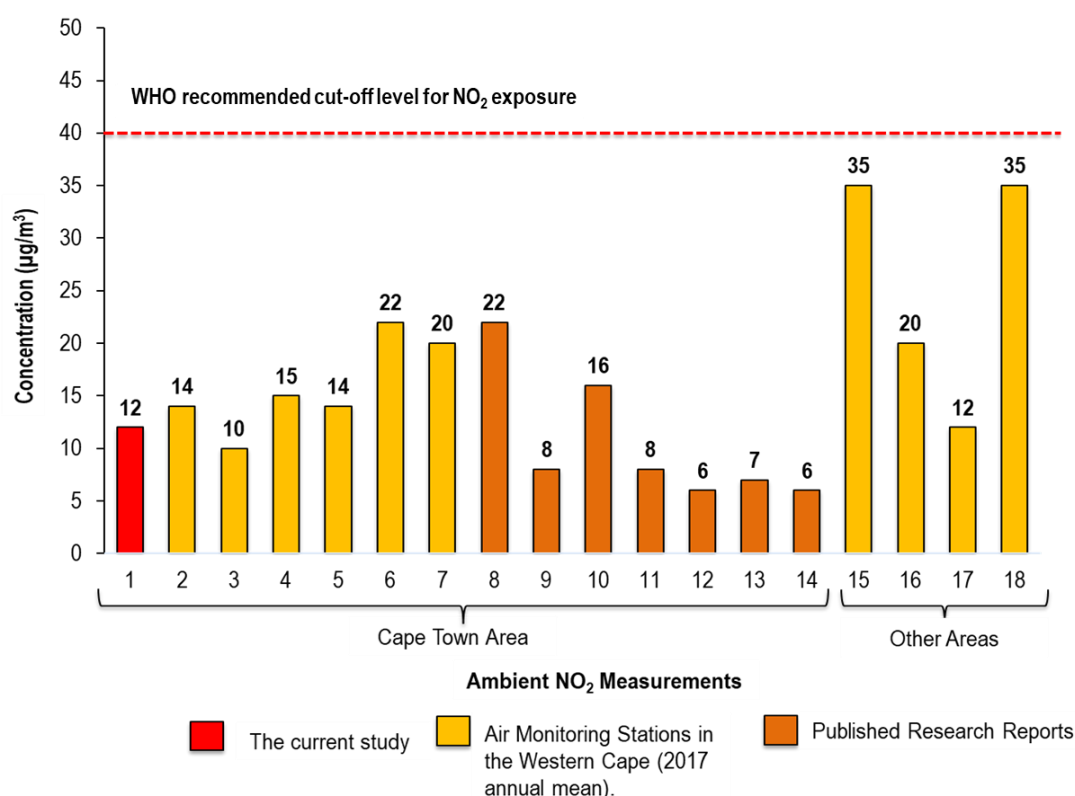
Figure 4.3. Personal NO$_2$ exposure concentrations observed in the current study population compared to previously reported ambient NO$_2$ concentrations in the Cape Town area and other parts of the Western Cape Province, South Africa. **Description: 1.** Mean personal NO$_2$ exposure of the current study: Baseline and follow-up combined. **2.** Cape Town City Hall (Annual outdoor mean; ~24 km from Bellville).[770] **3.** Table View (Annual outdoor mean; ~18 km from Belville).[770] **4.** Plattekloof (Annual outdoor mean; ~9 km from Bellville).[770] **5.** Bothasig (Annual outdoor mean; ~12 km from Bellville).[770] **6.** Goodwood (Annual outdoor mean; ~10 km from Belville).[770] **7.** Khayelitsha (Annual outdoor mean; ~25 km from Bellville).[770] **8. to 10.** Khayelitsha, Marconi-Beam (~14 km from Bellville) and Masiphumulele (~54 km from Bellville) combined outdoor annual mean (8) and mean for the warm season (9) and cold season (10) (1-week measurements (*n* = 106) in each season with passive diffusion samplers placed inside residence).[771] **11. and 13.** Mbekweni (11: indoor 2-week measurements for *n* = 747 women. 13: Indoor 24-hour measurements (*n* > 1000); ~41 km from Bellville).[441,772] **12. and 14.** Newman (11: indoor 2-week measurements for *n* = 747 women. 13: Indoor 24-hour measurements (*n* > 1000); ~42 km from Bellville).[441,772] **15.** Stellenbosch (32 km from Bellville).[770] **16.** Malmesbury (~60 km from Bellville).[770] **17.** George (~414 km from Bellville).[770] **18.** Hermanus (~118 km from Bellville).[770] Bellville is a suburb of Cape Town, and used as the closest geographic reference point from where the majority of the present study participants were recruited. Figure designed by the author of this dissertation based on information from [441,770,772].

Compared to other reported ambient NO$_2$ concentrations in the Cape Town area (**Figure 4.3.**), the mean NO$_2$ exposure concentration in the current study was comparable with the reported annual outdoor mean (Centralised air quality monitoring station) of Cape Town City Centre (City Hall: ~14 µg/m³), within the lower range

of other Cape Town areas (Minimum: Table View: ~10 µg/m³; Maximum: Goodwood: ~22 µg/m³) and lower than other cities/town in the Western Cape Province (Stellenbosch and Hermanus: 35 µg/m³) for the year 2017.[770]

The personal NO_2 exposure concentrations measured in the current study are comparable to previously reported annual outdoor mean values (Plattekloof: ~9 km from Bellville and Bothasig ~12 km from Bellville).[770] Bellville is a suburb of Cape Town, and used as the closest geographic reference point from where the majority of the present study participants were recruited.

Compared to published reported indoor exposure concentrations from the Western Cape Province, our personal NO_2 exposure concentration appeared to be slightly higher (Maximum: Mbekweni ~8 µg/m³)[441,772] ; however, it needs to be considered that the measurements in the present study were reflective of both indoor and outdoor exposure.

Personal mean NO_2 exposure concentrations in the current study were comparable with outdoor concentrations from Tshwane (~12 µg/m³ [773]), but lower than concentrations reported from outdoor monitoring sites in Durban (Minimum: ~21 µg/m³; Maximum ~42 µg/m³ [774,775]) (**Figure 4.4.**).
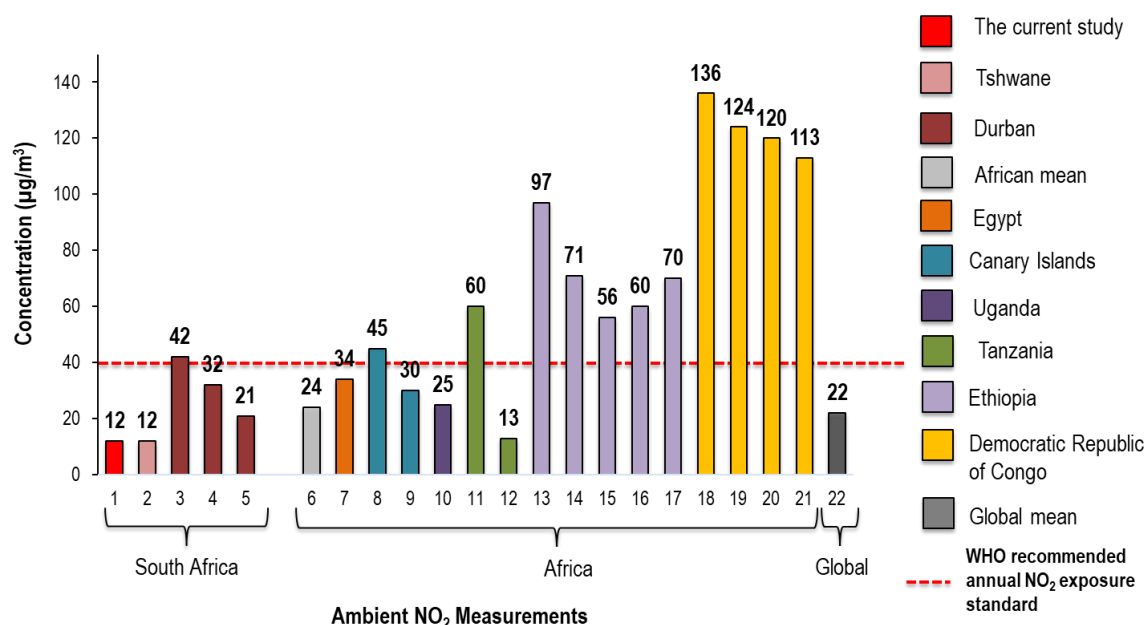
Figure 4.4. Personal NO$_2$ exposure concentrations in the current study compared to reported ambient NO$_2$ concentrations from other parts of South African, Africa and a global estimated mean. **Description: 1.** Mean personal NO$_2$ exposure of the current study: Baseline and follow-up combined. **2.** Outdoor annual mean according to air quality systems data.[773] **3.** Seven outdoor monitoring sites (n = 129 measurements).[774] **4.** Durban North outdoor monitoring sites near schools (24-hour measurements).[775] **5.** Durban South outdoor monitoring sites near schools (24-hour measurements).[775] **6.** Estimated annual mean for the African region using land-use regression analysis of n = 5220 unique monitors globally.[778] **7.** Outdoor monitoring station (n = 15) over 4 years.[779] **8.** Las Palmas de Gran Canaria (outdoor traffic related 24-hour measurements).[780] **9.** Santa Cruz de Tenerife (outdoor traffic related 24-hour measurements).[780] **10.** Kampala and Ninja (2-week outdoor measurements in commercial and residential land use areas).[435] **11. and 12.** Bagamoyo homes (n = 100 24-hour sampling measurements) (11: indoor kitchen and 12: outdoor control).[434] **13. to 17.** Rural residences levels according to fuel sources and seasons (n = 17215 indoor and outdoor measurements) (13: Wood, 14: Cow dung, 15: Crop residues, 16: Dry season, 17: Wet Season).[436] **18. to 21.** Kinshasa at 4 road intersections (n = 425 outdoor measurements).[781] **22.** Estimated annual global mean using land-use regression analysis and n = 5220 unique monitors globally.[778]. Figure designed by the author of this dissertation based on information from [434,435,773–775,778–781].

NO$_2$ exposure concentrations of the current study were also lower than the reported African (~24 µg/m³) and global (~22 µg/m³) estimated means [778] and various other reported indoor and outdoor NO$_2$ exposure concentrations from the African region (Minimum: Bagamoyo (Tanzania) outdoor residential concentration ~13 µg/m³; Maximum: Democratic Republic of Congo outdoor roadside concentrations [434,781]).

These findings indicate that personal NO_2 exposure concentrations observed in the current study are comparable to the annual reported outdoor mean concentrations from the Cape Town area rather than indoor and outdoor NO_2 exposure concentrations reported from other areas in the Western-Cape Province.[441,770,772] The findings of the present study also suggest that the personal NO_2 exposure and associated cardiovascular effects were observed at relatively low NO_2 exposure concentrations compared to WHO air quality guideline levels and other parts of the Western Cape Province and African regions.[36]

According to National Environmental Management Act: Air Quality Act of 2005, air pollution levels need to be monitored,[776] but evaluating the data from the Western Cape State of Air Quality Management Report (State of Air Quality Management 2017) and reports from other parts of SA,[777] large gaps in continuous data recording/monitoring were observed and may influence the accuracy of the data presented in reports, public access to air quality information and the evaluation of aherence to levels sepcified in the National Environmental Management Act: Air Quality Act of 2005.[429,770]

4.4.1.2. BTEX exposure concentrations compared to other reported levels.

Median personal benzene (2.7 µg/m³; range: 0.5 to 14.2 µg/m³) and toluene (19.8 µg/m³; Range: 3.7 to 284 µg/m³) exposure concentrations in the current study (baseline and follow-up combined) were lower than WHO recommended standards (Benzene: 5 µg/m³ annual mean; Toluene (260 µg/m³) weekly mean.).[36,782] Compared to the annual outdoor mean benzene exposure concentrations reported by the Western Cape Government for 2017, the median benzene exposure concentration in the current study was higher than the Southern Cape town of Mossel Bay (~1.2 µg/m³), but lower than other Cape Town areas such as Potsdam (~5.2 µg/m³) and the Foreshore area of Cape Town CBD (~5.1 µg/m), the latter which exceeded WHO recommended standards for benzene.[770] Annual outdoor benzene, ethylbenzene and xylene exposure concentrations were not reported by the Western Cape Government (**Figure 4.5.**).[770]
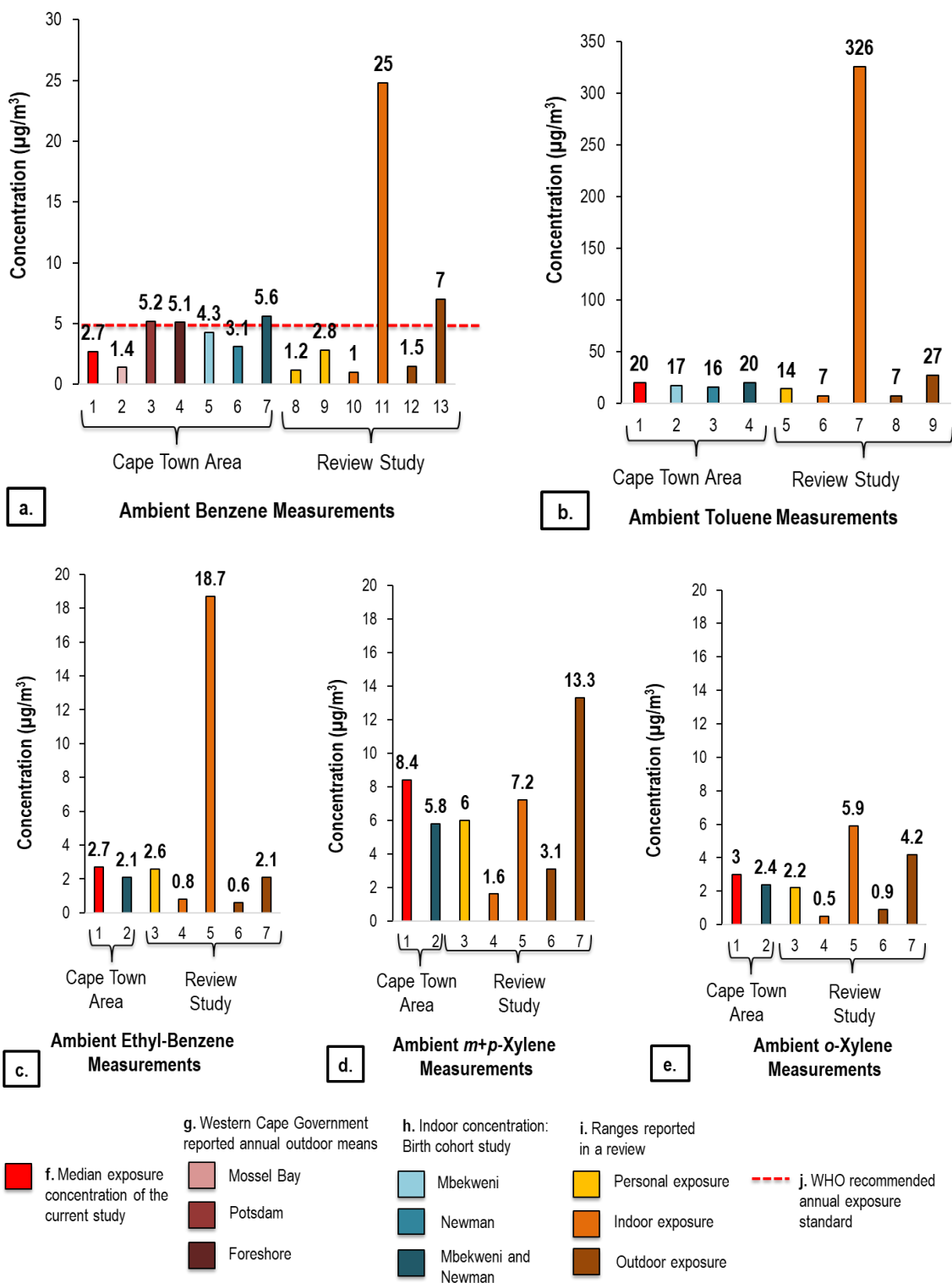
Figure 4.5a. to 4.5e. Personal BTEX exposure concentrations in the current study compared to reported ambient concentrations from other parts of the Western Cape Province [770] and the ranges reported in a review [34] on the health effects of BTEX. **Description: a.** Exposure concentrations for benzene. **b.** Exposure concentrations for toluene. **c.** Exposure concentrations for ethyl-benzene. **d.** Exposure concentrations for *m+p*-xylene. **e.** Exposure concentrations for *o*-xylene. **f.** Median exposure concentrations observed during the current study. **g.** Western Cape Government reported ambient exposure concentrations from centralised air quality monitoring stations in the

Western Cape Province (Mossel Bay: ~370 km from Belville; Potsdam: ~18 km from Belville; Foreshore: ~21 km from Bellville).[770] **h.** Indoor/home exposure concentrations reported in a birth cohort study (Paarl District: Mbekweni: ~41 km from Bellville; Newman ~42 km from Bellville.).[441,772] **i.** BTEX exposure concentration ranges (High and low exposure concentrations) of reports featured in a review by Bolden *et al.* (2015) on the health effects of BTEX exposure (stratified according to personal, indoor and outdoor exposure concentrations).[770] **j.** WHO recommended annual benzene exposure standard.[34] **k.** WHO recommended weekly toluene exposure standard.[782] Bellville is a suburb of Cape Town, and used as the closest geographic reference point from where the majority of the present study participants were recruited. Figure designed by the author of this dissertation based on information from [34,441,770,772].

All median BTEX exposure concentrations measured in the present study were higher than reported indoor mean BTEX exposure concentrations for Mbekweni and Newman (combined mean).[441,772] A review by Bolden *et al.* (2015) on the health effects of BTEX exposure stratified previously published BTEX exposure concentrations according to personal, indoor and outdoor exposure concentrations.[770] All median BTEX exposure concentrations of the current study fell within these personal, indoor and outdoor exposure ranges (minimum and maximum).[770]

The above findings indicate that although relatively low personal BTEX exposure concentrations were observed in the current study, other areas close to the city of Cape Town already exceed annual WHO recommended standards for benzene. It can be speculated that the BTEX-associated effects observed in the current study may be even more pronounced in these highly polluted areas. Also, BTEX exposure concentrations appear to be infrequently measured in SA and the African region. South Africa is also the only country in Africa that has both a national air quality act and also air quality standards.[421,776] More research in terms of BTEX exposure concentrations and their health effects in the African region/context is urgently needed.

4.4.1.3. Seasonal and occupational trends of NO_2 and BTEX exposure concentrations.

Our NO_2 and BEX exposure concentrations were significantly higher during the cold season compared to the warm season (**Figure 4.2.**). Seasonal variation in ambient NO_2 and BTEX exposure concentrations have previously been reported to be higher in the colder season.[770,771] The 2017 State of Air Pollution Reports from the Western Cape Government also indicated increased air pollution concentrations during the colder season compared to warmer season.[770] Our findings in terms of seasonal NO_2 exposure concentrations furthermore support findings by Saucy *et al.* (2018) who reported significantly higher exposure concentrations in the Khayelitsha, Marconi-Beam and Masiphumulele area during the colder season (~18 µg/m³) compared to the warmer season (~8 µg/m³).[771] Similar season trends for BTEX exposure concentrations observed in the current

study have previously been reported and is in part related to an increased in energy demand for heating purposes.[37,770,783–785]

It has previously been shown that higher air pollution levels during the colder season are associated with increased cardiovascular risk.[786–788] These seasonal trends indicate that the NO_2- and BTEX-associated health risk may be greater in the colder season than the warmer season in the Cape Town area. Determining the exact seasonal effects of exposure concentrations remain beyond the scope of the current study, but should be included in future studies.

NO_2 and toluene exposure concentrations in the current study were associated with employment (**Table 4.15.**). The exact occupations of participants in the current study were not evaluated; however, it could be speculated that higher occupational exposure concentration may have played a role, as previously reported and most probably related to combustion process, chemical solvent/mixtures and poor air ventilation.[388,789–791] These results indicate that occupational exposure to NO_2 and toluene may be regarded as a potential health risk factor for the employed participants in the study population. Occupational exposure to air pollution is poorly reported in SA.[418,791] More investigations related to occupation exposure to air pollution in the Cape Town area are needed.

4.4.2. The effects of exposure concentrations on various markers of cardiovascular risk.

The health effects of ambient air pollution are mostly attributable to small chemically reactive pollutant with pro-oxidative potentials [363,371,507,792]. Once translocated into the blood circulation, these air-pollutants mostly act as ROS and ultimately cause oxidative cellular/tissue damage and result in upregulation of the pro-atherosclerotic inflammatory cascade in the vasculature.[793–795] Exposure concentrations in the current study were not significantly associated with markers of inflammation (hsCRP and TNF-α, Appendix **Table B8.1. and Table B8.2.**). On the contrary (albeit not significant), rather large estimated effects in the negative direction between all the measured exposure concentrations and hsCRP suggest exposure-associated suppression of systemic inflammation rather than immune activation may have been more pronounced.[796–798] It could also be speculated that exposure-associated oxidative stress or other possible routes of inflammation (not evaluated in the current study) may have played a role in findings observed.[375,797,799] More investigations with a more integrative panel of markers for oxidative stress and inflammation should be considered in future research.

4.4.2.1. Exposure-associated cardio-metabolic dysregulation.

Personal benzene exposure was positively associated with raised fasting glucose levels (**Table 4.18.**). These findings support those of Brook *et al.* (2008) and Coogan *et al.* (2013) who demonstrated that exposure to traffic/combustion related air pollutants (Canada and USA) was associated with increased risk for developing

diabetes mellitus in women (Brook: 17% increase in odds ratio for developing diabetes mellitus; Coogan: incident rate ratio 1.25 (95% CI 1.07-1.46)) at exposure concentrations relatively lower and higher compared to the current study (~7.5 µg/m³ and ~23 µg/m³, respectively).[394,800] Brook *et al.* (2008) could not demonstrate the same significant effects in their male study population, and postulated that women, as represented by the current study population, are possibly more susceptible to the effects of air pollution on glucose metabolism compared to men.[800]

The findings of the present study are in contrast those of others (Brook *et al.* (2008) and Coogan *et al.* (2013)), who showed an association between NOx exposure and increased risk for developing diabetes in women.[394,800] The current study could not demonstrate a significant association between NO_2 exposure concentrations and fasting glucose levels. Furthermore, no significant associations were observed between exposure concentrations and HbA1c levels, a marker of long-term impaired glucose homeostasis (Appendix **Table B2.6.**). It is possible that the effects of chronic high-level NOx exposure, as observed in the study by Coogan *et al.* (10 years at ~23 µg/m³), may account for more pronounced effects compared to the current study (two 1-week measurements at ~12 µg/m³).[394]

The mechanistic pathway through which benzene exposure may lead to increased fasting glucose levels (glucose intolerance) is not fully described, but the pro-inflammatory and pro-oxidative effects on pancreatic function and insulin receptors/signalling have both been implicated.[504,801–803] Bahadar *et al.* (2015), who investigated the effects of benzene and a benzene metabolite, hydroquinone, on the islets of Langerhans, showed that benzene exposed rats presented with increased higher fasting glucose levels compared to unexposed control.[804] Bahadar *et al.* (2015), furthermore showed that this effect was mediated, in part at least, through glucose 6-phospatase upregulation (phosphorylate glucose 6-phosphate resulting in phosphate and free glucose).[804] The metabolite, hydroquinone, was associated with decreased anti-oxidant capacity/defence and an increase in proteases associated with cellular death (caspase 3).[804] It has furthermore been shown by others that increased circulating reactive oxidants, such as air pollutants, activate c-Jun n-terminal and NF-κB (serine/threonine kinase cascade), and may result in phosphorylation of insulin receptor and the insulin receptor substrate proteins (associated with degradation of insulin reseptor-1).[805]

Toluene was positively associated with total cholesterol, HDL and LDL cholesterol levels (**Table 4.19.**) and the urinary metabolite 3+4MHA (also considered a marker of toluene exposure [469]) was positively associated with increased LDL cholesterol in the current study (**Table 4.23.**). Toluene is a well-known lipophilic monocyclic aromatic hydrocarbon that is widely used as a solvent and thinner in household products and industrial process, ink, coatings and paint [481,806]). Increased exposure to BTEX, including toluene, is often linked to occupational risk factors [472,807,808] and may account, at least in part, for the association that was observed between toluene exposure and employment status (part-time) in the current study.

The effects of air pollution on serum lipid levels have previously been investigated and it has been shown that exposure to air pollution is generally associated with a dyslipideamic profile (raised total cholesterol and LDL with decreased HDL levels).[809–811] Metabolic dysregulation and the toxic effects of air pollution on major organ systems such as the liver, pancreas and kidney seem to mimic those observed in smokers as cigarette smoke contains numerous VOCs.[552,812] Findings in terms of HDL cholesterol appear to be more inconsistent with reports showing positive, negative and no associations with air pollution exposure.[810,811,813–816] Our results support findings by McGuinn *at al.* (2019) who investigated the effects of ultra-fine PM on serum lipid levels and found positive association between ultra-fine PM exposure and total cholesterol, total LDL cholesterol particle count (all subfractions combined) and total HDL cholesterol particle count (All sub-fractions combined), but additionally noted variable effects across HLD sub-fractions.[811]

Our results do not support findings by Bell *et all.* (2017) who reported an inverse association between PM and total HDL cholesterol particle count, but also noted variable effects across HDL sub-fractions.[810] Kim *et al.* (2015) also found an inverse association between toluene exposure and HDL cholesterol.[806] Kim *et al.* (2015) furthermore highlighted differential metabolic effects of toluene across gender and various nationalities of foreign workers in their study population that may in part explain discrepancies between various reports.[806]

Also, compared to men, pre-menopausal women, typically present with higher HDL cholesterol levels due to increased oestrogen production.[817] With limited evidence, it has been postulated that air pollutants may also act as a xenoestrogen and have HDL raising effects in pre-menopausal women.[818,819] These effects may have played a role in the current study, but more investigation is needed.

Despite the positive association between toluene and HDL cholesterol levels, increased HDL may not necessarily offer increased cardiovascular protection. It has also been shown that combustion related air pollutants may disrupt HDL's cholesterol efflux capacity, and cause dysfunctional pro-oxidative and pro-inflammatory HDL molecules through oxidative modifications of either HDL's protein and/or lipid sub-components.[490,814,820] As pointed out by Bell *et al.* (2017), the effects of air pollution on HDL have not been well documented in literature and needs further investigation.[810]

4.4.2.2. Toluene associated adverse effect on kidney filtration.

Toluene was inversely associated with kidney function as indicated by eGFR in the current study (**Table 4.19.**). Combustion related air pollution, including toluene, has previously been associated with adverse effects on kidney function and eGFR.[821–826] Findings in the current study support those of Lue *et al*. (2013) who showed that higher exposure concentrations (living near a major roadway (50 m) *vs.* 1 km away from the roadway) was inversely associated with eGFR (-3.9 ml/min/1.73 m^2 (95% CI 1.0 to 6.7 ml/min/1.73 m^2); *p* = 0.007) in Boston, USA (*n* = 1103).[821]

Toluene-specific nephrotoxicity has previously been investigated although mostly in animal models.[823] Meydan *et al*. (2016) injected male Wistar rats with a once-off 500 g/kg toluene dose.[823] After 14 days superoxide

dismutase and catalase (anti-oxidant enzymes that catalyse the degradation of hydrogen peroxide to oxygen and water) were significantly lower in toluene treated rats compared to untreated control.[823] Histological/morphological analysis furthermore showed glomerular and tubular tissue damage.[823] Similar effects have also been reported in other animal studies evaluating the effects of toluene (gas exposure) on other organ tissues (decreased SOD in frontal cortex of rats [827]; decreased SOD and catalase in liver tissue) with toluene-associated lipid peroxidation as mediating factor in in observed oxidative tissue damage.[827,828] Other adverse effects associated with toluene-related nephrotoxicity reported elsewhere include metabolic acidosis, distal tubular renal acidosis, formation of renal stones, hypokalaemia, haematuria, proteinuria, and pyuria.[824–826]

4.4.2.3. Molecular aging.

NO_2 and benzene exposure concentrations were inversely associated with LTL (**Table 4.17.** and **Table 4.18.**) while toluene was positively associated with mtDNA content (**Table 4.19.**). Findings in the current study are in line with the conclusions of a systematic review by Zhao *et al.* (2018), in which it was reported that the majority of papers reviewed had shown inverse associations between LTL and various air pollutants (*n* = 15 out of 19 reports pertaining to LTL).[829] Findings of the current study furthermore support previous studies that investigated the acute and chronic effects at low exposure concentrations on telomere length.[383,830–834] These studies include students exposed to PAH,[832] traffic-related air pollution (proximity to main roads) in twins,[833] and $PM_{2.5}$ exposure in elderly participants (annual $PM_{2.5}$) and (prenatal $PM_{2.5}$ exposure) new-borns.[383,834] The BTEX-specific findings of the current study are similar to those reported by Hoxha *et al.* (2009) who showed a negative association between short-term benzene (-6.4%) and toluene (-6.2%) exposure on LTL in office workers (referents) and traffic officers.[380] The current study could not confirm a significant association between toluene exposure and LTL, which may be explained by the lower toluene exposure levels in our study compared to those measured in the study by Hoxha *et al.* (2009).

On the other hand, other studies reported positive associations between air pollution exposure and LTL (mostly high-level occupational-related exposure).[497,835,836] These studies include metal-rich PM exposure in steel workers,[497] high-level PM exposure in truck drivers [835] and PAH in asphalt pavers [836]. NO_2-specific effects on LTL observed in the current study also do not support findings by Ward-Gaviness *et al.* (2016) who showed no significant association between NO_2 and NOx exposure and LTL (land-use regression model) at NOx exposure concentrations lower (8.39 $\mu g/m^3$; Augsburg, Germany) than the current study.[831] Higher NO_2 exposure concentrations observed in the current study compared to NOx levels observed by Ward-Gaviness *et al.* (2016) may account for these differences.[831]

LTL findings presented in the current study were more representative of low-level exposure rather than high-level exposure. It has been postulated with limited evidence that chronic oxidative stress/damage most often

inversely associate with TLT at low exposure concentrations than high exposure concentrations[837–839], while acute inflammatory processes in highly exposed (short-term) individuals (as observed by Dioni *et al.* and Hou *et al.*) have been shown to upregulate leucocyte cell proliferation (clonal capacity) that may contribute to an acute increase in LTL.[829,840–842] It is thus possible that the pro-oxidative effects of low NO_2 and benzene exposure concentrations observed in the current study contributed to advanced molecular aging on the level of LTL in our study population consisting of female participants. The study by Ward-Gaviness *et al*. (2016) highlights sex-specific differences and differences between traffic (combustion related pollutants) and non-traffic pollutants (PM) on epigenetic aging.[831] These differences need to be explored in the SA context.

Toluene was positively associated with mtDNA content in the current study (**Table 5.19.**). mtDNA content is an established marker of oxidative stress as the mitochondria are one of the main sources and preferred targets of intracellular ROS.[843,844] As air pollutants are generally strong oxidants and pro-oxidative stimuli, positive associations between exposure to air pollution and mtDNA content are often reported in literature.[373,844,845] Reports also show that upregulation of mtDNA copy numbers in cells under oxidative stress is a response to cope with cellular respiratory demands in an attempt to maintain homeostasis and repair oxidative damage.[846–848] As is the case with LTL, studies also show that high- (inflammatory-associated) and low (oxidative stress-related) exposure concentrations or acute and chronic exposure periods may affect mtDNA content in opposite directions with low-level exposure upregulating cellular respiration while high-level exposure can block cellular respiration irreversibly.[849–852]

Low-level toluene exposure, as observed in the current study, and its metabolites (epoxides) have previously been associated with genotoxicity.[853–855] An *in vitro* study by Revilla *et al*. (2007), investigated possible mechanisms by which toluene and xylene exposure contribute to mitochondrial toxicity.[856] This study showed that toluene (at 0.5 to 2.5 mM exposure) and xylene (at 0.25 to 1 mM exposure) dissipate mitochondrial membrane potentials and Ca^{2+} release (mitochondrial uncoupling) with stimulation of state 4 respiration, but that 2.5 to 5 mM exposure concentrations, toluene and xylene induces state 3 respiration inhibition.[856] At 0.1 to 1 mM xylene exposure concentration resulted in a significant increase in ROS production and mitochondrial swelling, while 1 mM toluene and xylene exposure concentrations caused Ca^{2+}-associated mitochondrial ATP depletion (66.3% and 40.3%, respectively).[856]

Toluene-associated dyslipidaemia (associated with increased lipid peroxidation), also observed in the current study, has previously been implicated in genotoxicity (mitochondrial stress/damage).[857] The positive association between toluene and cholesterol levels in the current study suggest that that toluene associated metabolic dysregulation may also have been a mediating factor in toluene-associated mitochondrial toxicity in the current study. Positive, but borderline non-significant associations with relatively large estimated effects between mtDNA content and ethyl-benzene (p = 0.055), *m+p*-xylene (p = 0.053) and *o*-xylene (p = 0.063) exposure

concentrations were also observed in the current study and suggest possible underlying involvement (Appendix **Table B6.4.**) that may become more pronounced at higher exposure concentrations.

Our findings are in contrast to those of other studies that demonstrated significant negative associations between benzene exposure and mtDNA content, with hyperglycaemia (associated with benzene in the current study) as a possible mediating factor.[850,851,858,859] Positive associations between higher benzene exposure concentrations and mtDNA content (as observed by Carugno *et al.* (2012)) compared to the current study may have played a role in discrepancies between reports (69.9 µg/m^3, 34.4 µg/m^3 and 20 µg/m^3).[850]

4.4.2.4. Exposure-associated effects on biomarkers of vascular endothelial function.

Personal NO_2 exposure in the current study was inversely associated with VEGF levels (**Table 4.17.**). VEGF is a well know vascular signal transduction molecule that promotes the formation of blood vessels (vasculogenesis and angiogenesis) and promotes cell proliferation in the vascular wall.[182,183] It has also been shown than VEGF activates eNOS and thus stimulates the production of NO, while NO has been shown to induce VEGF synthase.[860–863] Expression of VEGF is also upregulated during the inflammatory cascade to help repair damaged vasculature/tissue.[864,865] As NO_2 was not significantly associated with markers of inflammation (hsCRP or TNF-α (**Table B7.1 and B7.2.**)), NO_2-associated oxidative effects on VEGF, may have been more prominent in the current study, but needs further investigation. Also, the significant inverse association between NO_2 exposure concentrations and LTL, an indicator if molecular aging, suggests that reduced immune function may have been involved as previously described.[830,866–871]

The reduction-oxidation (REDOX) reaction in which NO_2 takes part and its relationship with NO indeed provides an attractive underlying candidate mechanistic pathway that could explain various findings observed in the current study. Once translocated into blood circulation, NO_2 also acts as a ROS that can react with NO (Fenton reaction) to form various reactive nitrogen species such as peroxynitrite (ONOO$^-$) and nitrous acid (HONO) resulting in nitrosative and oxidative stress and a reduction in bioavailability of NO.[793,795,872] Nitrosative stress, on the other hand, has also been implicated in immune suppression (through upregulation of anti-inflammatory cytokines such as TGFβ, IL-10 and IL-3/IL-13).[872] The NO_2-associated reduction in NO bioavailability during these reactions/mechanisms may result in decreased expression of VEGF, decreased vasorelaxation and subsequently an increase in vascular tone/vasoconstriction.[793,795,872,873] These pathways may thus also account for the NO_2-associated reduction in vessel diameters discussed later in the current chapter.[85,874]

Benzene was inversely associated with p-selectin (**Table 4.18.**). P-selectin, mostly produced by platelets and endothelial cells, plays a significant role in platelet-endothelial and leukocyte-endothelial cell adhesion during pro-inflammatory immune activation, and is hence regarded as a biomarker of endothelial

function/dysfunction.[126,128,875] Relatively low-level benzene exposure was not significantly associated with immune activation in the current study population (hsCRP and TNF-α, Appendix **Table B7.1. and B7.2.**), which suggests that other possible mechanisms such as immune dysregulation and oxidative stress may have been involved.

Benzene exposure has previously been associated with immune dysfunction in human and animal studies.[876–879] These effects appear to be more prevalent at lower exposure concentrations than at high-exposure concentrations.[876–879] For example, asymptomatic mild benzene-exposed workers from China exhibited reduced gene expression for CD4 and $CD4^+$:$CD8^+$ ratios.[876] Also, chronic low-level benzene exposed residence in Croatia living near a railroad exhibited increase in regulatory T cells (reduces immune response).[877] Benzene exposed mice furthermore showed suppressed splenocyte proliferation and total circulating neutrophils while suppressions of B- and T-cell mitogenesis was observed.[878,879]. Also, benzene metabolites such as hydroquinone have shown strong scavenging properties (react with NO) resulting in reduce NO bioavailability/production (*via* eNOS inhibition), which also may contribute to immune dysregulation.[880–882] A study by Lahiri *et al*. (2010), showed mixed immune effects in women in India exposed to indoor smoke from biofuels (reduction in absolute number of $CD4^+$ T-helper cells (17%) and reduced $CD19^+$ B-lymphocytes (14%) and an increase in $CD16^+$ $CD56^+$ natural killer cells (31%) and $CD8^+$ T-lymphocytes (12%)).[883]

Our findings also do not support those by Schmitt-Sody *et al.* (2007) additionally showed that p-selectin is significantly involved in leukocyte-endothelial cell interaction in mice during immune activation and inflammation (p-selectin wildtype *vs.* p-selectin knockout mice).[717] The negative association between benzene and LTL in the current study (Appendix **Table B6.1.**) suggests that immune function may indeed have played a role in the current study, but in the opposite direction than Schmitt-Sody *et al.* (2007). Similarly Ray *et al.* (2007) also showed a positive association between occupation-related high-level (n = 50) benzene exposure concentrations (55.2 μg/m^3); $p < 0.0001$) and circulating p-selectin (6090/μl in control (n = 35 office workers) *vs*. 13 640/μl in exposed subjects) in Kolkata, India.[884] Ray *et al.* (2007) furthermore attributed their effects (decreased $CD4^+$, $CD8^+$ and $CD19^+$ cells, but increased $CD16^+$ $CD56^+$) to immune activation in their highly exposed study population.[884]

Ray *et al.* (2007) additionally reported increased levels of red blood cells and white blood cells and speculated that these results may be due to benzene-associated pro-inflammatory immune activation and hypoxia that translated into upregulation of the expression of these cells.[884] Reduced red blood cell concentrations were also reported elsewhere and ascribed to possible benzene-associated bone marrow suppression.[885–887] These parameters were not included in the current study and needs to be considered in future studies. Nonetheless, the non-significant associated effects on Hb observed in the current study (Appendix **Table B3.1.**) suggests that hypoxia and bone marrow-suppression may not have been involved in current study.

Ethyl-benzene-, *m+p*-xylene- and *o*-xylene were inversely associated with another biomarker of vascular endothelial function, VCAM-1 (**Table 4.20. to 4.23.**). VCAM-1 plays a mediation role in the adhesion of

lymphocytes, monocytes, eosinophils and basophils to the vascular endothelium during immune activation.[127,129] VCAM-1 is also involved in leukocyte-endothelial adhesion/signal transduction and its expression mostly upregulated by TNF-α (primarily produced by immune cells, including macrophages, T lymphocytes, and natural killer cells) during the inflammatory cascade.[888–890]

Our findings do not support those of Bind *et al*. (2012) who showed positive associations between traffic-related pollutants and CRP, ICAM-1, and VCAM-1 in elderly participants.[506] The author associated these effects with changes in DNA methylation status (hypomethylation), but only at higher exposure concentrations.[506] The current study could not demonstrate any significant association between exposure concentrations and DNA methylation (Appendix **Table B6.5.**). What is more, Bind *et al*. (2014) also showed increased air pollution-related inflammation (CRP) can regulate ICAM-1 expression in a positive direction, with greater effects at higher CRP levels.[891] As no significant associations between ethyl-benzene-, *m+p*-xylene- and *o*-xylene and hsCRP (Appendix **Table B8.1. and B8.2.**) or TNF-α (Appendix **Table B8.2.**) were observed, other possible mechanism may have been involved and needs to be further investigated.

Toluene, ethyl-benzene-, *m+p*-xylene, *o*-xylene and the urinary metabolite 3+4MHA were positively associated with PAI1-1 (Appendix **Table B8.8.**). PAI-1, a serine PI, is the main and potent inhibitor of t-PA (activates plasminogen and fibrinolysis).[126,731,892–894] PAI-1 is primarily produced by the endothelium, but can also be secreted by hepatocytes and adipose tissue (including visceral fat).[894] PAI-1 is often associated with obesity and metabolic dysregulation.[731,895–897] The thrombotic effects of PAI-1 due to oxidative stress, independent of inflammation (not observed in the current study), have also previously been reported.[730,898–901], thus making it useful biomarker of endothelial function/dysfunction.

Our findings support those of various other studies.[902–904] The studies include PM exposure in healthy young students (PAI-1 was positively associated with 1- to 3-day averages for PM_{10}, $PM_{2.5}$, sulfate, and O_3 and 2- to 3-day averages for nitrate)[902] and in highly exposed underground workers in Stockholm (higher plasma concentrations of PAI-1 positively associated with higher exposure concentration).[903] A study by Green *et al*. (2017) investigated the effects of long-term ozone and $PM_{2.5}$ (1999 to 2004) exposure on haemostatic markers in women and showed a 35% (95% CI: 19 to 53%) increase in PAI-1 for every10 μg/m^3 increase in $PM_{2.5}$ exposure.[904]

PAI-1 is also closely associated with metabolic dysregulation including lipid and glucose dysregulation.[905–907] Hepatic, adipose and endothelial derived PAI-1 has been associated with increased insulin and LDL-cholesterol levels.[905–907] The positive associations between benzene and fasting glucose levels (associated with increased insulin), and toluene and cholesterol levels in the current study suggest that exposure-associated metabolic dysregulation may have played a possible mediating role. LDL cholesterol in particular (associated with toluene and 3+4MHA), has been shown to increase PAI-1 transcription in endothelial cells.[908,909] On the other hand, PAI-1 expressed in adipose tissue has been implicated in exacerbating adipose tissue dysfunction, which may contributed to increased LDL levels as observed in the current study.[910,911] PAI-

1 has furthermore been associated with decreased insulin sensitivity by disruption of insulin signaling.[912] This disruption in insulin metabolism may decrease PKB activation, decreased VEGF expression and cell migration.[912]

The exposure-associated effects on PAI-1 may furthermore explain various results observed in the current study. The toluene-, ethylbenzene- and xylene-associated inverse relationship with vascular adhesion molecules may have been mediated by PAI-1 as PAI-1 have been shown to control in part the vascular adhesion/migration (or cause molecular detachment form cells).[913,914] This is accomplished by binding to vitronectin (high affinity) and inhibiting urokinase plasminogen activator (u-PA induces chemotaxis)[913,914] or by direct or indirect association/deactivation of integrins (conformational changes of integrins or associated proteins [915]). Although decreased levels of adhesion molecules are traditionally interpreted as an anti-atherosclerotic and improved vascular profile, the effects of PAI-1 on vascular adhesion is also strongly associated with caspase 3 mediated apoptosis [743] and deep-vein thrombosis [744,745].

4.4.2.5. Exposure associated reduced baseline vessel diameters and increased blood pressure.

NO_2 exposure was inversely associated with both the macro and micro vessel baseline diameters measured in this study (CRVE and baseline brachial artery diameter), whilst NO_2 (SBP and DBP) and *o*-xylene (DBP) were positively associated with blood pressure (**Table 4.17. and 4.22.**). Reports from literature often indicate that air pollution exposure may result in raised blood pressure through various possible mechanistic pathways.[34,916–919] As the determination of CRVE includes the vascular wall in vessel width measurements, inhibition of VEGF may have contributed to decreased micro-venular vessel diameters.[920–922] On the other hand, the measurement of the baseline brachial artery diameter excludes the vessel wall. Possible autonomic nervous system dysregulation with subsequent basal vasoconstriction may have played a role [923,924] while VEGF reduction may have been a more indirect consequence (through decreased NO production).[719–721]

VEGF-associated decreases in vessel growth/diameter is well documented and implemented as a therapeutic target in anti-angiogenic cancer treatment.[920–922] Suppression of VEGF is also closely associated with increased blood pressure due to its relation with pro-NO producing pathways in the vascular endothelium (activation of PKB/Akt, eNOS and MAP kinase pathways).[719–721] In the eye, increased VEGF has been shown to induce retinal vessel dilation while over-expression may contribute to retinal edema.[925]

The effects of blood pressure on retinal vessels have also previously been reported with variable results. A study by Wong *et al.* (2003) associated a 10 mmHg increase in mean arterial blood pressure with a 4.4 μm decrease (95% CI, 3.8–5.0) in CRAE in their study cohort, but failed to find an association between blood pressure and CRVE.[926] A study by Leung et al, (2003) showed inverse associations between blood pressure and CRAE, CRVE and AVR (10 mmHg increase in mean arterial blood pressure was associated with 0.012 μm decrease in

AVR, a 3.5 µm decrease in CRAE and a 0.96 µm decrease in CRVE).[927] Kawasaki *et al*. (2009), on the other hand demonstrated that narrower CRAE and wider CRVE are significantly associated with the development of hypertension (OR per SD decrease in CRAE 1.20 (95%CI 1.02 to 1.42) and CRVE 1.18 (95%CI 1.02 to 1.37)).[928]

The effects of air pollution on the CNS is relatively well documented and include neuronal mitochondria toxicity, oxidative damage to neurons, alterations in neuron membrane potentials that disrupt signal transduction and autoimmune dysregulation.[502,794,929] Also, the vasoconstrictive effects of both long- and short-term at low- and high-exposure concentrations have previously been described. [923,924]

Both NO_2 and xylene exposure have previously been implicated.[36,475,808,930] Our findings support those of Chan *et al.* (2015) who examined the effects of NO_2 and fine PM (≤2.5 µm; $MP_{2.5}$) in a female population and showed that a 10 ppb (~20 µg/m^3) increase in NO_2 was associated with a higher pulse pressure (0.4 mmHg).[931] In the same study, $PM_{2.5}$ was also associated with higher SBP (1.4 mmHg), pulse pressure (1.0 mmHg) and mean arterial pressure (0.8 mmHg).[931] The authors furthermore speculated that exposure-associated autonomic dysregulation of vascular tone may explain their findings.[931,932] In the study by Brook *et al.* (2002), an inverse relationship with brachial artery diameter (ultrasonography) was demonstrated in healthy adults (exposed *vs.* control (filtered clean air): −0.09 ± 0.15 mm *vs*. +0.01 ± 0.18 mm, p = 0.03), albeit at significantly higher exposure concentrations (150 µg/m^3 fine-MP, 120 ppb 0_3) and a shorter exposure period (2-hour) than the current study.[923] Previous studies suggest possible mechanisms such as stimulation of the pulmonary vagal afferent neurons and the subsequent increase in sympathetic nervous system reflex activity or an upregulation (directly or *via* oxidative stress pathways) of vascular endothelin 1 and 3 (vasoconstrictors) may be involved in air pollution exposure-associated vasoconstriction.[923,933] However, more studies are required to fully elucidate the underlying mechanisms involved for individual pollutants.

4.4.2.6.   Exposure associated effects on flow-mediated dilatation.

The urinary metabolite 3+4MHA was significantly associated with PAI-1 and LDL cholesterol, and inversely associated with % FMD (**Table 4.23.**). These findings suggest that increased PAI-1 and LDL cholesterol may, at least in part, explain the pro-endothelial dysfunction effects associated with 3+4MHA.

Findings in the current study support those by Dales *et al.* (2017) who showed that $PM_{2.5}$ at 30 µg/m^3 was inversely associated with % FMD of the brachial artery (0.48% reduction in FMD (p = 0.05)) in a cohort of males and females who were asked to sit for 2 hours at a two different subway stations in the city of Ottawa.[934] A report from the large Multi-Ethnic Study of Atherosclerosis and Air Pollution (MESA) by Krishnan *et al.* (2012) also showed each 3 µg/m^3 change in long-term $PM_{2.5}$ exposure (1 year), but not short-term, was associated with a 0.3% (95% CI: -0.6 to -0.03 %; p = 0.03) change in FMD (n = 3040 in 6 cities using central air quality monitoring station reported exposure concentrations).[935] Also similar to current study, Dales *et al.* (2017) could not find any significant

associations between % FMD and NO_2 in their study population (male and female), suggesting that NO_2 exposure may not be a major role-player in the development of clinically detectable endothelial dysfunction.[934]

Brook *et al.* (2002) failed to demonstrate exposure-associated effects on % FMD following 2-hours exposure to concentrated ambient fine particles at 150 µg/m^3 and 120 ppb ozone *vs.* control (filtered air) although exposure was significantly associated with heart rate variability.[923] These results suggest that different pollutants, different exposure concentrations and different periods of exposure may have variable effects on endothelial function and needs more investigation.

As previously described PAI-1 may have deleterious effects on vascular function though metabolic dysregulation associated with vascular adhesion/migration [913,914] and activation of apoptosis independent of inflammation (**Section 4.4.2.4.**).[743,905–907]. Exposure to gaseous pollutants that are associated with hypertension (e.g. NO_2 and BTEX) may also have also played a role as shown by Brook *et al.*, (2009) who found an inverse association between exposure associated with hypertension and % FMD (-2.0% and -2.9% respectively)).[936] Brook *et al.*, (2009) furthermore postulated that acute autonomic nervous system imbalance through blunting of parasympathetic vascular tone (favouring sympathetic activity) or α-adrenergic stimulation were the most likely mechanisms involved in their findings.[936–938] Although heart rate is associated with air pollution exposure through autonomic nervous system dysregulation,[939], this was not observed in the current study (Appendix **Table B7.3.**) or by Brook *et al.*, (2009).[936] It is possible that increased heart rate may be more pronounced in vulnerable populations such as the elderly,[940] at higher air pollution exposure concentrations [941] or through pro-inflammatory pathways.[942]

Exposure to air pollution may also interfere with vasoactive factors such bradykinin and acetylcholine. Diesel exhaust pollutants has been shown to inhibit acetylcholine-mediated vasorelaxation.[943] Mills *et al.*, (2005) examined the effects of diesel exhaust exposure (300 µg/m^3) 2 to 6 hours after exposure and showed that bradykinin, although a vasodilator, significantly upregulated PAI-1 (dose dependent manner), but these effects were suppressed 6 hours post-exposure.[944] The author speculated that vascular responses to air pollution exposure observed in their study was mediated through smooth muscle and/or endothelial dysfunction and that oxidative stress may have been a prominent mediating factor (diesel exhaust pollutants increases superoxide, reacts with NO to form peroxynitrite, and subsequently reduce NO bioavailability [945]).[944] These findings suggest that the pro-oxidative effects of air pollution exposure may have contributed to endothelial dysfunction through inhibition of acetylcholine-mediated vasodilation in the current study population, but needs further investigation.

4.4.3. Summary of results.

Our results show that relatively low personal NO_2 exposure was associated increased cardiovascular risk in women in the Cape Town area through various possible mechanistic pathways that may include oxidative stress (not measured in the current study), molecular/immunological aging, vascular growth factor inhibition and autonomic nervous system dysregulation (not measured in the current study) (**Figure 4.6.**).
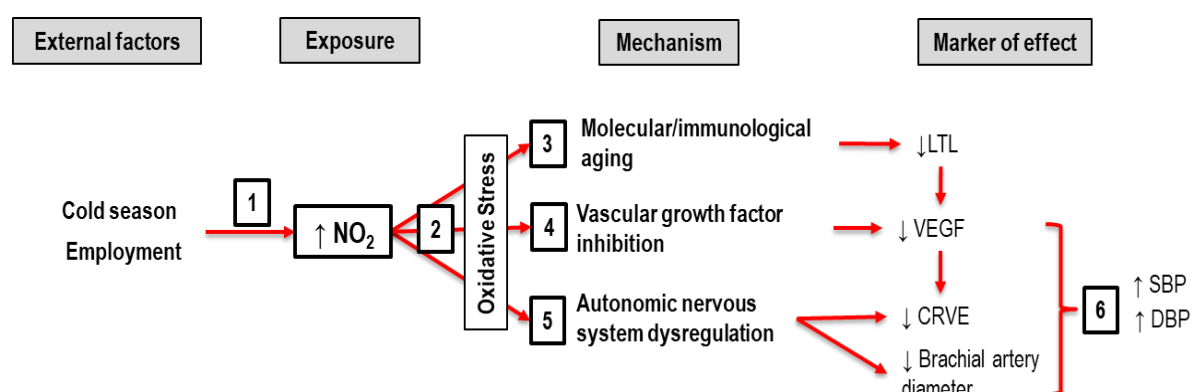
Figure 4.6. Summary of results and a proposed mechanistic pathway through which personal NO_2 exposure concentrations may be associated with increased cardiovascular risk in the current study population. **Description: 1.** Personal NO_2 exposure concentrations were increased in the cold season and associated with employment. **2.** NO_2-associated oxidative stress. **3.** NO_2-associated molecular aging as indicated by shorter LTL. **4.** NO_2-associated vascular growth factor inhibition. **5.** NO_2-associated autonomic nervous system activation as indicated by CRVE and baseline brachial artery diameter. **6.** NO_2-associated increase in blood pressure. The figure was designed by the author of this dissertation based on cited information from **Section 4.4.2**. **Abbreviations and symbols:** NO_2: Nitrogen dioxide; LTL: Leukocyte telomere length; VEGF: Vascular endothelial growth factor; CRVE: Central retinal venular equivalent; SBP: Systolic blood pressure; DBP: Diastolic blood pressure; ↑: Increase; ↓: Decrease.

Relatively low personal BTEX exposure was also associated with numerous cardiovascular risk factors in the study population through mechanisms that include metabolic dysregulation, molecular/immunological aging and dysregulation of vascular function and endothelial dysfunction (**Figure 4.7.**).
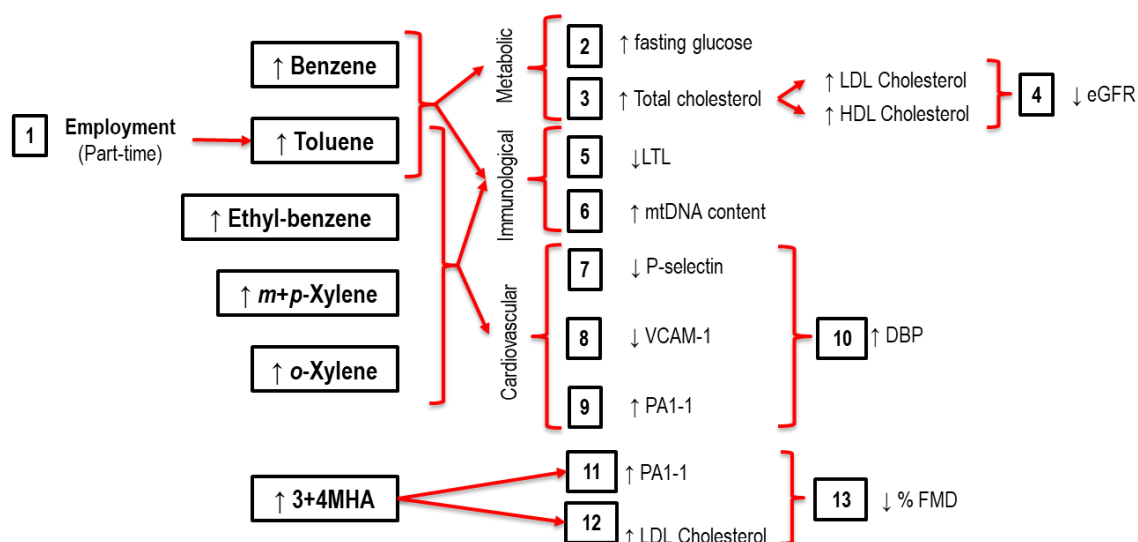
Figure 4.7. Summary of results and a proposed mechanistic pathway through which personal BTEX exposure concentrations are associated with increased cardiovascular risk in the study population. **Description: 1.** Personal exposure to BEX was associated with the cold season and toluene with employment. **2.** BTEX associated oxidative stress may be the mediating factor in BTEX associated cardiovascular risk. **3.** Benzene (glucose intolerance) and toluene (dyslipidaemia) were associated with metabolic dysregulation. **4.** Benzene was associated with molecular/immunological aging (LTL shortening) and toluene with mitochondrial oxidative stress (mtDNA content). **5.** Toluene was associated with a pro-clotting effects as shown by an association with increased PAI-1; Ethyl-benzene and xylenes were associated vascular adhesion dysregulation. **6.** Toluene associated metabolic dysregulation may have mediated decreased kidney function. **7.** o-Xylene was associated with increased DBP with vascular adhesion dysregulation as a possible mediating factor. **8.** The urinary metabolite 3+4MHA, predominantly a xylene and toluene metabolite, exhibited pro-thrombotic properties (as shown by an association with increased PAI-1) and was associated with increased LDL, **9.** which was associated with endothelial dysfunction (as indicated by reduced % FMD). The figure was designed by the author of this dissertation based on cited information from **Section 4.4.2**. **Abbreviations and symbols:** 3+4MHA: 3+4-Methylhippuric acid; eGRF: estimated glomeration filtration rate; LTL: Leukocyte telomere length; mtDNA: Mitochondrial DNA; VCAM-1: Vascular adhesion molecule-1; PAI-1: Plasminogen activator inhibitor-1;LDL: Low-density lipoprotein; DBP: Diastolic blood pressure; FMD: Flow-mediated dilatation; ↑: Increase; ↓: Decrease.

4.4.4. Limitations specific to Sub-study 2 and future direction.

Results from the current study are presented with some strengths and limitations. Measurement of personal exposure levels compared to centralised air quality monitoring stations and spatial distribution/land-use regression models are considered more accurate in terms investing exposure-associated health effects.[946] The study furthermore evaluated numerous markers of cardiovascular risk to elucidate possible mechanistic pathways involved in exposure-associated cardiovascular risk. The study followed a repeated measures design, which may

have contributed to greater statistical power despite a relatively small population size. With repeated measures taken once in the cold season and once in the warm season for each participant provided a clearer understanding in terms of the seasonal trends of pollutants investigated in the current study. The inclusion of various urinary metabolite measurements provided additional support to findings observed in the current study although only 3+4MHA appeared to be a reliable urinary marker of exposure in the current study.

Limitations of the study include a relatively small population size representing only women, of whom the majority was smokers. Male participant enrolment rate was low and attributed in part to employment obligations that prevented participation in the current study. The high prevalence of smokers in the current study population may be ascribed to the high smoking rates that have previously been reported in the region.[208,947,948] The recruitment of only non-smokers in the current study may have eliminated possible effects of smoking not accounted for in the current study. Also, the correction for the effects of smoking on various outcomes based only on smoking status, may not have been optimal. Using biomarkers for smoking exposure such as cotinine would have been a more accurate adjustment for smoking effects and would have also included the effects of possible second-hand smoke exposure. As previously shown, the effects of air pollution vary across sex, ethnicity and health status.[390,831,949–952] Our results represent only the effects of exposure in an apparently healthy, female population of mixed ancestry and care should be taken to not extrapolate our findings to the general population.

The study also did not account for possible background exposure or other possible sources of exposure (e.g. dietary exposure).[953] Although blank samplers were included for analysis, the inclusion of blank field samples should be considered in future studies. Future studies should include blood cell counts and markers of oxidative stress such as urinary isoprostanes [954] that could give a clearer picture in terms of metabolic pathways and the role oxidative stress in exposure-associated effects.

Finally, air pollution consists of a heterogeneous mixture of numerous reactive chemicals that can take part in various chemical reactions.[36,955,956] The heterogeneous nature and complex dynamics of air pollution remains a challenge to elucidate the individual contribution and exact underlying mechanisms involved in the health effects of specific air pollutants. Air pollution is also influenced by geographical and meteorological factors such as humidity, UV-radiation and temperature.[957,958] The health effects of air pollutants may furthermore vary across demographic factors such age, gender and ethnicity.[36,389,461] Many of these factors remained beyond the scope of the study, and were hence unaccounted for.

Results presented in the current chapter show that endothelial function is a marker of effect of personal NO_2 and BTEX exposure. These results furthermore show that personal NO_2 and BTEX exposure increases cardiovascular risk in women in the Cape Town area despite relative low exposure concentrations. The current study also indicates various possible mechanistic pathways that may have been involved such as molecular aging, vascular growth factor inhibition and autonomic nervous system dysregulation.

5. **Chapter 5: Conclusion.**

5.1. **Final conclusion.**

Populations in the developing world, including SSA, are confronted with major socioeconomic and environmental challenges on a daily basis. These challenges translate into an increased burden of disease and poorer health outcomes. The current study set out to investigate two major contributors to the burden of disease in SA that confront millions of people each day. The one a well-known contributor to the burden of disease in SA, the other greatly underestimated: HIV (including treatment with ART) and air pollution. Although unrelated on most levels, these health risk factors share commonality as major cardiovascular risk factors. This is especially relevant and of great concern in the SA context as this country hosts the largest population living with HIV in the world, has the largest Government-sponsored ART roll-out programme in the world, and is one of the most carbon-intensive economies in the world.[12,283,419] The current study postulated that the vascular endothelium is an important intersection where these cardiovascular risk factors converge in the development of CVD. Following the successful completion of all aims and objectives of the current study, it can be concluded that endothelial function is a marker of effect of HIV, ART and air pollution (**Figure 5.1.**).
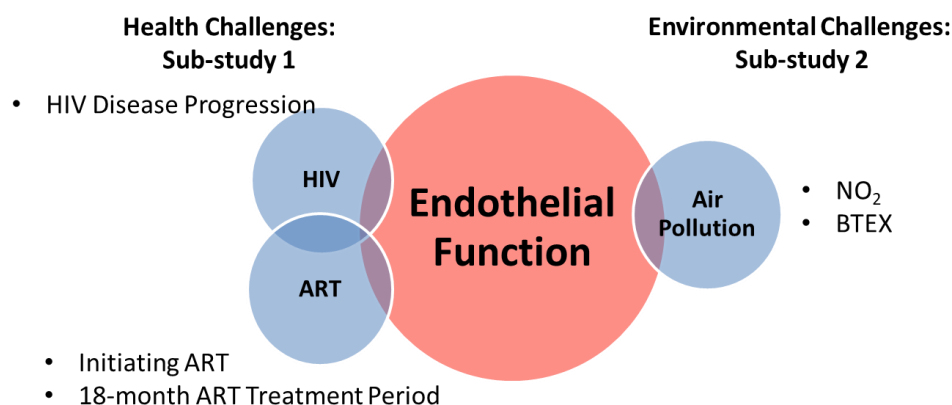
Figure 5.1. Endothelial function as the interface of major health challenges in SA. **Abbreviations:** HIV: Human immunodeficiency syndrome; ART: Antiretroviral therapy, NO_2: Nitrogen dioxide; BTEX: Benzene, toluene, ethyl-benzene and xylene (ortho (*o*)-, meta (*m*)- and para (*p*)-xylene.

CVD is a leading cause of death globally and affects lower-income regions, such as SSA disproportionately compared to the rest of world.[959] Although CVD is a major contributor to the burden of disease in SSA, including SA, its impact has historically been overshadowed by the high prevalence of communicable diseases such as HIV/AIDS in the region. The current study showed that the convergence of communicable

diseases such as HIV and NCDs such as CVD is a major health concern and could potentially overextend already strained healthcare resources in the region. The findings of the study emphasize the need to prioritise CVD in PLWH in the healthcare setting.

Interpreting the results of the current study also shed more light on the *temporal* effects of HIV and ART in terms of endothelial function (and cardiovascular risk). Results indicate that HIV disease progression decreases endothelial function, while initiating ART mostly reverses these effects and contribute to an improved cardiovascular risk profile. On the other hand, results also indicate that although pro-longed ART-use may exhibit mostly beneficial effects, it may also have deleterious effects over time (**Figure 5.2.**).
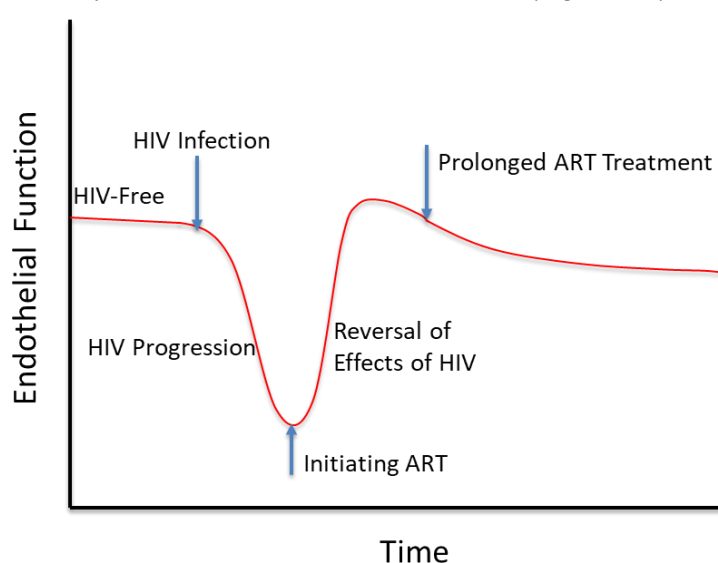
Figure 5.2. Temporal effects of HIV and ART. **Abbreviations:** HIV: Human immunodeficiency virus. ART: Antiretroviral therapy.

More specifically in terms of the effects of HIV disease progression (using viral load as the indicator): Many of the vascular endpoints showed adverse trends (endothelial dysfunction, increased CRVE and reduced AVR). On the other hand, ART was also associated with various markers of endothelial function. Initiating ART appeared to be mainly vasculo-and endothelioprotective (reduced vascular adhesion molecule levels, reduced thrombosis and reduced CRVE). Interestingly, the 18-month ART treatment period demonstrated both beneficial and adverse effects (anti-inflammatory and reduced vascular adhesion profile on the one hand, and impaired endothelial function on the other). This is a key finding of the current study with potentially future relevance. It demonstrates that although the first line fixed-dose combination ART drug used by the participants in this study was mostly associated with beneficial effects on the vasculature, it was also shown that vascular reactivity may be compromised by longer exposure to ART. Following these participants for longer periods may shed further light.

The status of air pollution on the African continent has not received sufficient research attention, but reports indicate that it already contributes substantially to the burden of disease.[42] The current study shows that

air pollution is an evolving public health issue in SA and contributes to an increased cardiovascular risk profile in the Cape Town region even at relatively low exposure concentrations. Results of the current study underscore the need for more investigation in terms of the status of air pollution and its health effects, not only in SA but also the greater SSA region.

More specifically, personal air pollution was associated with vascular and endothelial effects. NO_2 exposure was associated with reduced vascular growth, increased SBP and DBP, reduced CRVE and reduced baseline brachial artery diameter, whereas personal BTEX exposure was associated with reduced vascular adhesion biomarkers and a pro-clotting profile. In a novel finding in the context of the sub-Saharan African and South African research setting, the study showed that air pollution (NO_2 and benzene) was associated with molecular ageing as indicated by decreased LTL. This finding was particularly relevant as LTL is a marker for numerous degenerative diseases including CVD and various malignancies.[382,960,961]

This study furthermore indicates that, non-invasive, relatively quick and inexpensive techniques such as retinal microvascular imaging have the potential to be utilised as screening tests of cardiovascular risk, especially in a limited resource setting such as the African region. Results also show that FMD has application as a marker of effect of HIV and ART and could, together with retinal imaging, be further explored as measures of cardiovascular risk, but standardisation is currently lacking. The study furthermore showed that circulating biomarkers such as adhesion molecules have application in cardiovascular risk assessment in PLWH in SA and provide better insight in the mechanistic pathways that underlie die development of CVD in PLWH. Understanding the mechanistic pathways involved in disease development remains pivotal in prevention and treatment.

In conclusion, the present study, despite its limitations that were discussed in previous chapters, generated several novel findings. Our results show that endothelial function, and many other markers of vascular function in general, may be regarded as a candidate marker of effect in people exposed to HIV, ART and air pollution. This study also showed that HIV and air pollution are possibly associated with increased cardiovascular risk through endothelial dysfunction. This study underscores the need for further research in terms of the effects of HIV, ART and air pollution on cardiovascular health in SA.

5.2. Future directions.

The current study evaluated the effects of HIV and ART, and the effects of air pollution in two separate sub-studies. As HIV, ART and air pollution were implicated in the cardiovascular continuum in the current study population, a possible intersection between these cardiovascular risk factors may exist. Previous studies have shown that air pollution contributes to the disease burden in PLWH and that PLWH are more susceptible to the effects of air pollution.[962–964] Reports already indicate that NCD and HIV/AIDS are on a collision course and that the convergence of these diseases may overextend already strained heath resources.[14] More investigation

is needed to elucidate the combined effects of HIV (with and without ART) and air pollution in SA. A larger study population would have been required to account for additional confounding factors. Due to financial constraints the intersection between HIV, ART and air pollution was not explored in the current study. Due to the large number of variables assessed in the current study, false positive/negative findings are likely. As an observational study, findings in the current study were furthermore discussed in relation to findings from other reports. For possible future publication purposes, the relationship between all variable outcomes assessed in the current study needs to be further explored to elucidate true causality. Also, testing the robustness of models used in regression analysis should be assessed by means of sensitivity analysis.

Telomere length has been shown to be a relevant marker of the effects of HIV/AIDS and ART in terms of immune function and other associated degenerative disease.[965–968] Future studies may consider including telomere length as an endpoint.

Other air pollutants such as SO_2 and 0_3 are also relevant in CVD and the SA context. The Western Cape Government reported on these levels in their annual air quality report, but the health effect of these pollutants are not investigated and needs further investigation.[969,970] What is more, occupational exposure to air pollution is poorly reported in SA although health and safety regulations are in place.[429,971] Our results indicate that this needs to be further investigated.

The relationship between demographic, socioeconomic and lifestyle factors and HIV, ART and air pollution were beyond the scope of the current study although reports indicate that these factors play a role in health outcomes.[199,972] Future studies should include more defined questions pertaining to smoking (e.g. pack/day) and alcohol consumption (e.g. alcoholic drinks per session) frequencies. Also, the long-term effects of HIV, ART and air pollution need further investigation. Literature shows that the long- *vs.* short-term exposure may vary.[353,973,974] These factors need to be investigated.

Retinal microvascular image analysis is a non-invasive, operator-friendly and relatively inexpensive technique for the assessment of cardiovascular risk/health.[160] Retinal imaging as a marker of cardiovascular risk has gained research attention in HIV/AIDS recently as numerous retinal microvascular markers of cardiovascular risk have been associated with HIV/ART-associated adverse health effects including systemic, cardiovascular, cardiometabolic, renal, liver and cognitive diseases.[64,65,160] More validation of the use of retinal imaging techniques in the current study population is still needed. Also, the potential value of non-invasive, retinal microvascular imaging as a marker of cardiovascular risk/health in HIV/AIDS, particularly in a resource-constrained setting such as SA, warrants further investigation.

5.3. Role and activities of the Ph.D. candidate pertaining to the study.

- Active member of the EndoAfrica research team; participated in field-work and gathering and capturing of data for both sub-studies.

- Assisted in general laboratory work for both sub-studies: Collecting blood and urine samples from research nurses, processing these samples for storage and delivering samples to the NHLS for further analyses.
- Sub-study 2: Co-ordinated most research activities pertaining to Sub-study 2. Setting up, handing out and gathering backpacks. Storage and shipment of samples and samplers for analysis. Extracting and capturing data from temperature loggers. Capturing data of laboratory results after analysis.
- Laboratory work in Belgium pertaining to Sub-study 2: Preparation of samples for quantification of BTEX and urinary metabolite concentrations. DNA extraction and sample preparation for determination of DNA methylation, mtDNA content and telomere length. Responsible for all retinal imaging activities, capturing retinal images, analysing all images for both sub-studies, capturing and analyzing data.
- Performed all statistical analysis for Sub-study 1 and 2. Biostatisticians and other experts in the field of epidemiology were consulted when and if necessary to ensure validity of statistical models.
- Responsible for two original research manuscripts, one published, and the other currently under revision.

5.4.   Research outputs pertaining to the current study produced.

First-author peer reviewed journal publications:

- **Everson, F**.; De Boever, P.; Nawrot, T.S.; Goswami, N.; Mthethwa, M.; Webster, I.; Martens, D.S.; Mashele, N.; Charania, S.; Kamau, F.; Strijdom, H. Personal NO_2 and Volatile Organic Compounds Exposure Levels are Associated with Markers of Cardiovascular Risk in Women in the Cape Town Region of South Africa. *Int. J. Environ. Res. Public Health* 2019, *16*, 2–18.[521]
- **Everson, F**.; Martens, D.S.; Nawrot, T.S.; Goswami, N.; Mthethwa, M.; Webster, I.; Mashele, N.; Charania, S.; Kamau, F.; De Boever, P.; et al. Personal exposure to NO2 and benzene in the Cape Town region of South Africa is associated with shorter leukocyte telomere length in women. *Environ. Res.* 2020, *182*, 108993.[975]

Co-author peer reviewed journal publication

- Strijdom, H., De Boever, P., Walzl, G., Essop, F., Nawrot, T.S., Webster, I.,Westcott, C., Mashele, N., **Everson, F.**, Malherbe, S.T., Stanley, K, Kessler, H.H.,Stelzl, H., Goswami, N. Cardiovascular risk and endothelial function in people living with HIV/AIDS: Design of the multi-site, longitudinal EndoAfrica study in the Western Cape Province of South Africa. *BMC Infect. Dis.* 2017, *17*, 1–9.[43]

First-author peer reviewed conference proceedings:

- **2018:** 12th International Symposium on Molecular Diagnostics. 12th International Symposium on Molecular Diagnostics.

The effect of HIV/AIDS and combination ART on retinal microvascular in a South African HIV-infected (with and without ART) study population. **Frans Everson**, Patrick De Boever, Nandu Goswami, Tim S. Nawrot, M. Faadiel Essop, Mashudu Mthethwa, Nyiko Mashele, Sana Charania, Yolandi Espach, Ingrid Webster, Hans Strijdom. Graz, Austria.[976]

- **2018:** Conference of Biomedical and Natural Sciences and Therapeutics (Physiology Society of Southern Africa Annual Conference).

Repeated measurements study to investigate exposure to ambient air pollution and possible association with cardiovascular physiology indicators in the Cape Town region.

Frans Everson, Nandu Goswami, Patrick De Boever, Tim S. Nawrot, M. Faadiel Essop, Mashudu Mthethwa, Nyiko Mashele, Sana Charania, Yolandi Espach, Ingrid Webster, Hans Strijdom. South Africa.[977]

- **2018:** 19th Annual SA Heart Congress. The effect of a fixed-dose combination ART regimen on retinal microvascular calibres in a South African HIV-infected study population. **Frans Everson**, Nandu Goswami, Patrick De Boever, Tim S. Nawrot, M. Faadiel Essop, Mashudu Mthethwa, Nyiko Mashele, Sana Charania, Yolandi Espach, Ingrid Webster, Hans Strijdom. Sun City, South Africa.[978]

<u>Other related research outputs:</u>

- **2018:** Stellenbosch University: Annual Academic Day.

Poster presentation: *HIV/AIDS (ART-naive) and cardiovascular risk: Are retinal microvascular geometric features markers of effects?* **Frans Everson**, Nandu Goswami, Patrick De Boever, Tim S. Nawrot, M. Faadiel Essop, Mashudu Mthethwa, Nyiko Mashele, Sana Charania, Yolandi Espach, Ingrid Webster, Hans Strijdom.

- **2019:** Stellenbosch University Annual Academic Day.

Oral presentation: *Personal air pollution is associated with markers of cardiovascular risk: Findings from the EndoAfrica Study.* **Everson, F**., De Boever, P., Nawrot, T.S., Goswami, N., Mthethwa, M., Webster, I., Martens, D.S., Mashele, N., Charania, S., Kamau, F., Strijdom, H.

S., Kamau, F., Strijdom, H.

- **2019**: Stellenbosch University Biomedical Research Day.

Poster Presentation: *Personal exposure to NO_2 and benzene is associated with molecular ageing in women in the Cape Town region.* **Frans Everson**, Dries S. Martens, Tim S. Nawrot, Nandu Goswami, Mashudu Mthethwa, Ingrid Webster, Nyiko Mashele, Sana Charania, Festus Kamau, Patrick De Boever, and Hans Strijdom.

6.   References

1.   World Health Organization (WHO). Technical package for cardiovascular disease management in primary health care. Available online: https://www.who.int/cardiovascular_diseases/publications/en/.

2.   World Health Organization. Global status report on noncommunicable diseases 2010. Available online: www.who.int/nmh/publications/ncd_report2010/en/ (accessed on Jan 17, 2017).

3.   Mendis, S.; Puska, P.; Norrving, B. Global atlas on cardiovascular disease prevention and control. Available online: https://www.who.int/cardiovascular_diseases/publications/atlas_cvd/en/ (accessed on Sep 19, 2018).

4.   Anand, S.S.; Yusuf, S. Stemming the global tsunami of cardiovascular disease. *Lancet* 2011, *377*, 529–532.

5.   Lozano, R.; Naghavi, M.; Foreman, K.; Lim, S.; Shibuya, K.; Aboyans, V.; Abraham, J.; Adair, T.; Aggarwal, R.; Ahn, S.Y.; et al. Global and regional mortality from 235 causes of death for 20 age groups in 1990 and 2010 : a systematic analysis for the Global Burden of Disease Study 2010. *Lancet* 2010, *380*, 2095–2128.

6.   Escárcega, R.O.; Franco, J.J.; Chokkalingam, B.; Vyas, A.; Tedaldi, E.M.; Bove, A.A. Cardiovascular disease in patients with chronic human immunodeficiency virus infection. *Int. J. Cardiol.* 2014, *175*, 1–7.

7.   Fedele, F.; Bruno, N.; Mancone, M. Cardiovascular Risk Factors and HIV Disease. *Aids Rev* 2011, *13*, 119–129.

8.   Brook, R.D.; Franklin, B.; Cascio, W.; Hong, Y.; Howard, G.; Lipsett, M.; Luepker, R.; Mittleman, M.; Samet, J.; Smith, S.C.; et al. Air pollution and cardiovascular disease: A statement for healthcare professionals from the expert panel on population and prevention science of the American Heart Association. *Circulation* 2004, *109*, 2655–2671.

9.   Committee on the Medical Effects of Air Pollution (COMEAP). Cardiovascular Disease and Air Pollution. Available   online: https://www.gov.uk/government/uploads/system/uploads/attachment_data/file/304668/COMEAP_cardiovascular_disease_and_air_pollution.pdf (accessed on Sep 5, 2019).

10.   Fairall, L.R.; Bachman, M.O.; Louwagie, G.M.C.; Van Vuuren, C.; Chikobvu, P.; Seebragts, C.J.; Boulle, A.; Nhiwatiwa, R.; Bateman, E.D.; Zwarenstein, M.F.; et al. Effectiveness of Antiretroviral Treatment in a South African Program. *Arch Intern Med.* 2008, *168*, 86–93.

11.   Statistics South Africa. Mortality and causes of death in South Africa, 2011: Findings from death notification. Available online: http://www.statssa.gov.za/publications/P03093/P030932016.pdf (accessed on Jun 22, 2019).

12.   Shisana, O.; Rehle, T.; Simbayi, L.; Zuma, K.; Jooste, S.; Pillay-van-Wyk, V.; Mbelle, N.; Van Zyl, J.; Parker, W.; Zungu, N.; et al. South African national HIV prevalence, incidence, behaviour and communication survey, 2008: A turning tide among teenagers? Available online: http://www.hsrc.ac.za/en/research-outputs/view/4505 (accessed on Jan 24, 2019).

13. May, M.T.; Sterne, J.A.C.; Costagliola, D.; Sabin, C.A.; Phillips, A.N.; Justice, A.C.; Dabis, F.; Gill, J.; Lundgren, J.; Hogg, R.S.; et al. HIV treatment response and prognosis in Europe and North America in the first decade of highly active antiretroviral therapy: a collaborative analysis. *Lancet (London, England)* 2006, *368*, 451–8.

14. Levitt, N.S.; Steyn, K.; Dave, J.; Bradshaw, D. Chronic noncommunicable diseases and HIV-AIDS on a collision course: Relevance for health care delivery, particularly in low-resource settings - Insights from South Africa. *Am. J. Clin. Nutr.* 2011, *94*, 1690–1696.

15. Herbst, A.J.; Cooke, G.S.; Bärnighausen, T.; KanyKany, A.; Tanser, F.; Newell, M.L. Adult mortality and antiretroviral treatment roll-out in rural KwaZulu-Natal, South Africa. *Bull. World Health Organ.* 2009, *87*, 754–762.

16. Sanne, I.M.; Westreich, D.; Macphail, A.P.; Rubel, D.; Majuba, P.; Van Rie, A. Long term outcomes of antiretroviral therapy in a large HIV/AIDS care clinic in urban South Africa: a prospective cohort study. *J. Int. AIDS Soc.* 2009, *12*, 38–49.

17. Ford, N.; Vitoria, M.; Penazzato, M.; Doherty, M.; Shubber, Z.; Meintjes, G.; Grinsztejn, B.; Eholie, S.; Mills, E.J.; Ford, N.; et al. Causes of hospital admission among people living with HIV worldwide: A systematic review and meta-analysis. *Lancet HIV* 2015, *2*, e438-44.

18. Boccara, F. Cardiovascular health in an aging HIV population. *AIDS* 2017, *31*, S157–S163.

19. Palella, F.J.; Phair, J.P. Cardiovascular disease in HIV infection. *Curr Opin HIV AIDS* 2011, *6*, 266–71.

20. The Data Collection on Adverse Events of Anti-HIV Drugs (DAD) Study Combination antiretroviral therapy and the risk of myocardial infarction. *N Engl J Med* 2003, *349*, 1993–2004.

21. Das, S. Risk of cardiovascular disease in HIV-infected patients. *J. Antimicrob. Chemother.* 2010, *65*, 386–389.

22. Shah, A.S.V.; Stelzle, D.; Lee, K.K.; Beck, E.J.; Alam, S.; Clifford, S.; Longenecker, C.T.; Strachan, F.; Bagchi, S.; Whiteley, W.; et al. Global burden of atherosclerotic cardiovascular disease in people living with HIV. *Circulation* 2018, *138*, 1100–1112.

23. Baker, J. V.; Lundgren, J.D. Cardiovascular implications from untreated human immunodeficiency virus infection. *Eur. Heart J.* 2011, *32*, 945–951.

24. Ngondi, J.L.; Oben, J.; Forkah, D.M.; Etame, L.H.; Mbanya, D. The effect of different combination therapies on oxidative stress markers in HIV infected patients in Cameroon. *AIDS Res. Ther.* 2006, *3*, 1–7.

25. Andrade, A.C.O.; Cotter, B.R. Endothelial function and cardiovascular diseases in HIV infected patient. *Braz. J. Infect. Dis.* 2006, *10*, 139–145.

26. Kampa, M.; Castanas, E. Human health effects of air pollution. *Environ. Pollut.* 2008, *151*, 362–367.

27. Zhang, J.; Smith, K.R. Indoor air pollution: A global health concern. *Br. Med. Bull.* 2003, *68*, 209–225.

28. Soldatova, L.N.; Rocca-Serra, P.; Dumontier, M.; Shah, N.H. Selected papers from the 16th annual Bio-Ontologies Special Interest Group Meeting. *J. Biomed. Semantics* 2014, *5*, 484–490.

29. Łatka, P.; Nowakowska, D.; Nowomiejska, K.; Rejdak, R. How air pollution affects the eyes — a review.

Ophthalmol. J. 2018, *3*, 58–62.

30. World Health Organization. World Health Statistics - Minitoring Health for the Sustainable Development Goals. Available online: https://www.who.int/gho/publications/world_health_statistics/2019/en/ (accessed on May 8, 2019).

31. World Health Organization. World Health Organization releases new global air pollution data. Available online: http://ccacoalition.org/en/news/world-health-organization-releases-new-global-air-pollution-data (accessed on Mar 8, 2019).

32. Carlos, J.O. Air pollutants: Volatile Organic Compounds. Available online: https://www.airgo2.com/air-pollution/pollutants/volatile-organic-compounds/ (accessed on Jun 23, 2019).

33. Atkinson, R.; Aschmann, S.M.; Arey, J.; Carter, W.P.L. Formation of ring-retaining products from the OH radical-initiated reactions of benzene and toluene. *Int. J. Chem. Kinet.* 1989, *21*, 801–827.

34. Bolden, A.L.; Kwiatkowski, C.F.; Colborn, T. New look at BTEX: Are ambient levels a problem. *Environ. Sci. Technol.* 2015, *49*, 5261–5276.

35. Katsouyanni, K. Ambient air pollution and health. *Br. Med. Bull.* 2003, *68*, 143–156.

36. World Health Organization: Regional Office for Europe. WHO guidelines for indoor air quality: selected pollutants. Available online: https://afro.who.int/publications/selected-pollutants-who-guideline-indoor-air-quality (accessed on Jun 22, 2019).

37. Miri, M.; Rostami Aghdam Shendi, M.; Ghaffari, H.R.; Ebrahimi Aval, H.; Ahmadi, E.; Taban, E.; Gholizadeh, A.; Yazdani Aval, M.; Mohammadi, A.; Azari, A. Investigation of outdoor BTEX: Concentration, variations, sources, spatial distribution, and risk assessment. *Chemosphere* 2016, *163*, 601–609.

38. Bernstein, J.A.; Alexis, N.; Barnes, C.; Bernstein, I.L.; Bernstein, J.A.; Nel, A.; Peden, D.; Diaz-Sanchez, D.; Tarlo, S.M.; Williams, P.B. Health effects of air pollution. *J. Allergy Clin. Immunol.* 2004, *114*, 1116–1123.

39. Mannucci, P.M.; Harari, S.; Martinelli, I.; Franchini, M. Effects on health of air pollution: a narrative review. *Intern. Emerg. Med.* 2015, *10*, 657–662.

40. Künzli, N.; Jerrett, M.; Garcia-Esteban, R.; Basagaña, X.; Beckermann, B.; Gilliland, F.; Medina, M.; Peters, J.; Hodis, H.N.; Mack, W.J. Ambient air pollution and the progression of atherosclerosis in adults. *PLoS One* 2010, *5*, e9096.

41. Gori, T.; Daiber, A.; Al-Kindi, S.; Lelieveld, J.; Deanfield, J.; Rajagopalan, S.; Münzel, T.; Gori, T.; Al-Kindi, S.; Deanfield, J.; et al. Effects of gaseous and solid constituents of air pollution on endothelial function. *Eur. Heart J.* 2018, *39*, 3543–3550.

42. Katoto, P.D.M.C.; Byamungu, L.; Brand, A.S.; Mokaya, J.; Strijdom, H.; Goswami, N.; De Boever, P.; Nawrot, T.S.; Nemery, B. Ambient air pollution and health in Sub-Saharan Africa: Current evidence, perspectives and a call to action. *Environ. Res.* 2019, *173*, 174–188.

43. Strijdom, H.; De Boever, P.; Walzl, G.; Essop, M.F.; Nawrot, T.S.; Webster, I.; Westcott, C.; Mashele, N.; Everson, F.; Malherbe, S.T.; et al. Cardiovascular risk and endothelial function in people living with

HIV/AIDS: Design of the multi-site, longitudinal EndoAfrica study in the Western Cape Province of South Africa. *BMC Infect. Dis.* 2017, *17*, 1–9.

44. The South African Institute of Race Relations. Indoor pollution is SA's most serious air quality problem. Available online: https://irr.org.za/reports/occasional-reports/files/irr-air-quality.pdf (accessed on Jun 22, 2019).

45. Pillay-van Wyk V; Msemburi W; Laubscher R; Dorrington RE; Groenewald P; Matzopoulos R; Prinsloo M; Nojilana B; Nannan N; Gwebushe N; et al. Second National Burden of Disease Study South Africa: national and subnational mortality trends, 1997–2009. *Lancet* 2013, *381*, S113.

46. Tibazarwa, K.; Ntyintyane, L.; Sliwa, K.; Gerntholtz, T.; Carrington, M.; Wilkinson, D.; Stewart, S. A time bomb of cardiovascular risk factors in South Africa: Results from the Heart of Soweto Study "Heart Awareness Days." *Int. J. Cardiol.* 2009, *132*, 233–239.

47. Cameron, N. Physical growth in a transitional economy: The aftermath of South African apartheid. *Econ. Hum. Biol.* 2003, *1*, 29–42.

48. Ezzati, M. Indoor Air Pollution And Health In Developing Countries. *Lancet* 2005, *366*, 104–106.

49. Spalding-Fecher, R.; Matibe, D.K. Electricity and externalities in South Africa. *Energy Policy* 2003, *31*, 721–734.

50. Naidoo, M.; Zunckel, M.; John, J.; Taviv, I. Overview of ambient air quality monitoring in South Africa. Available online: https://researchspace.csir.co.za/dspace/handle/10204/1710 (accessed on Mar 19, 2019).

51. Bain, L.E.; Gwain, G.C. Cardiovascular Disease and HIV Infection in Sub-Saharan Africa: Misplaced Priorities in the Public Health and Research Agendas? *Front. Cardiovasc. Med.* 2019, *6*, 10–12.

52. Strijdom, H.; Lochner, A. Cardiac endothelium : More than just a barrier. *SAHeart* 2009, *6*, 174–185.

53. Behrendt, D.; Ganz, P. Endothelial function: From vascular biology to clinical applications. *Am. J. Cardiol.* 2002, *90*, L40–L48.

54. Van Wijk, J.P.H.; De Koning, E.J.P.; Cabezas, M.C.; Joven, J.; Op't Roodt, J.; Rabelink, T.J.; Hoepelman, A.M. Functional and structural markers of atherosclerosis in human immunodeficiency virus-infected patients. *J. Am. Coll. Cardiol.* 2006, *47*, 1117–1123.

55. van den Oord, S.C.H.; Sijbrands, E.J.G.; ten Kate, G.L.; van Klaveren, D.; van Domburg, R.T.; van der Steen, A.F.W.; Schinkel, A.F.L. Carotid intima-media thickness for cardiovascular risk assessment: Systematic review and meta-analysis. *Atherosclerosis* 2013, *228*, 1–11.

56. Mulè, G.; Vadalà, M.; Geraci, G.; Cottone, S. Retinal vascular imaging in cardiovascular medicine: New tools for an old examination. *Atherosclerosis* 2018, *268*, 188–190.

57. Badimon, L.; Romero, J.C.; Cubedo, J.; Borrell-Pagès, M. Circulating Biomarkers. *Thromb. Res.* 2012, *130*, S12–S15.

58. Bernardes, R.; Serranho, P.; Lobo, C. Digital ocular fundus imaging: A review. *Ophthalmologica* 2011, *226*, 161–181.

59. Abràmoff, M.; Garvin, M.K.M.K.M.K.; Sonka, M.; Abràmoff, M.D.; Garvin, M.K.M.K.M.K.; Sonka, M. Retinal Imaging and Image Analysis. *Eng. IEEE Rev.* 2010, *1*, 169–208.

60. Stosic, T.; Stosic, B.D. Multifractal analysis of human retinal vessels. *IEEE Trans. Med. Imaging* 2006, *25*, 1101–1107.

61. Mimoun, L.; Massin, P.; Steg, G. Retinal microvascularisation abnormalities and cardiovascular risk. *Arch. Cardiovasc. Dis.* 2009, *102*, 449–456.

62. Bhargavaa, M.; Ikrama, M.K.; Wonga, T.Y. Ocular Manifestations of Hypertension. *Hipertens Riesgo Vasc.* 2014, *54*, 105–110.

63. Ataer-Cansizoglu, E. Retinal image analytics: A complete framework from segmentation to diagnosis. Available online: https://www.lib.uwo.ca/cgi-bin/ezpauthn.cgi.

64. Tan, P.B.; Hee, O.K.; Cheung, C.; Yeo, T.K.; Agrawal, R.; Ng, J.; Lim, T.H.; Wong, T.Y.; Teoh, S.C. Retinal vascular parameter variations in patients with human immunodeficiency virus. *Investig. Ophthalmol. Vis. Sci.* 2013, *54*, 7962–7967.

65. Pathai, S.; Weiss, H. a.; Lawn, S.D.; Peto, T.; D'Costa, L.M.; Cook, C.; Wong, T.Y.; Gilbert, C.E. Retinal Arterioles Narrow with Increasing Duration of Anti-Retroviral Therapy in HIV Infection: A Novel Estimator of Vascular Risk in HIV? *PLoS One* 2012, *7*, 1–8.

66. De Boever, P.; Louwies, T.; Provost, E.; Int Panis, L.; Nawrot, T.S. Fundus photography as a convenient tool to study microvascular responses to cardiovascular disease risk factors in epidemiological studies. *J. Vis. Exp.* 2014, e51904.

67. Dysangco, A.; Liu, Z.; Stein, J.H.; Dubé, M.P.; Gupta, S.K. HIV infection, antiretroviral therapy, and measures of endothelial function, inflammation, metabolism, and oxidative stress. *PLoS One* 2017, *12*, 1–15.

68. Williams, R.; Brook, R.; Bard, R.; Conner, T.; Shin, H.; Burnett, R. Impact of personal and ambient-level exposures to nitrogen dioxide and particulate matter on cardiovascular function. *Int. J. Environ. Health Res.* 2012, *22*, 71–91.

69. Libby, P. Vascular biology of atherosclerosis: overview and state of the art. *Am J Cardiol* 2003, *91*, 3A-6A.

70. Quillon, A.; Fromy, B.; Debret, R. Endothelium microenvironment sensing leading to nitric oxide mediated vasodilation: A review of nervous and biomechanical signals. *Nitric Oxide - Biol. Chem.* 2015, *45*, 20–26.

71. Alexander, W.R. Hypertension and the Pathogenesis of Atherosclerosis Oxidative Stress and the Mediation of Arterial Inflammatory Response: A New Perspective. *AHA J.* 1995, *25*, 1–19.

72. World Health Organization. Types of cardiovascular disease. Available online: https://www.who.int/cardiovascular_diseases/en/cvd_atlas_01_types.pdf (accessed on Jun 25, 2019).

73. Go, A.S.; Mozaffarian, D.; Roger, V.L.; Benjamin, E.J.; Berry, J.D.; Borden, W.B.; Bravata, D.M.; Dai, S.; Ford, E.S.; Fox, C.S.; et al. Executive summary: Heart disease and stroke statistics-2013 update: A Report from the American Heart Association. *Circulation* 2013, *127*, 143–152.

74. Chhabra, N. Endothelial dysfunction – A predictor of atherosclerosis. *Internet J Med Updat.* 2009, *4*, 33–

41.

75. Lo, J.; Plutzky, J. The biology of atherosclerosis: General paradigms and distinct pathogenic mechanisms among HIV-infected patients. *J. Infect. Dis.* 2012, *205*, S368–74.

76. Widlansky, M.E.; Gokce, N.; Keaney, J.F.; Vita, J. a. The clinical implications of endothelial dysfunction. *J. Am. Coll. Cardiol.* 2003, *42*, 1149–1160.

77. Deanfield, J.E.; Halcox, J.P.; Rabelink, T.J. Endothelial function and dysfunction: Testing and clinical relevance. *Circulation* 2007, *115*, 1285–1295.

78. Strijdom, H. Endothelial dysfunction: are we ready to heed the vasculature's early-warning signal? *Cardiovasc. J. Afr.* 2012, *23*, 210–211.

79. Strijdom, H.; Chamane, N.; Lochner, A. Nitric oxide in the cardiovascular system: a simple molecule with complex actions. *Cardiovasc. J. Afr.* 2009, *20*, 303–10.

80. Arrebola-Moreno, A.L.; Laclaustra, M.; Kaski, J.C. Noninvasive assessment of endothelial function in clinical practice. *Rev. Esp. Cardiol. (Engl. Ed).* 2012, *65*, 80–90.

81. Poredos, P. Endothelial dysfunction in the pathogenesis of atherosclerosis. *Clin Appl Thromb Hemost* 2001, *7*, 276–280.

82. Endemann, D.H.; Schiffrin, E. Endothelial Dysfunction. *J Am Soc Nephrol* 2004, *15*, 1983–1992.

83. Hirata, Y.; Nagata, D.; Suzuki, E.; Nishimatsu, H.; Suzuki, J.-I.; Nagai, R. Diagnosis and treatment of endothelial dysfunction in cardiovascular disease. *Int. Heart J.* 2010, *51*, 1–6.

84. Yetik-Anacak, G.; Catravas, J.D. Nitric oxide and the endothelium: History and impact on cardiovascular disease. *Vascul. Pharmacol.* 2006, *45*, 268–276.

85. Vita, J. a.; Keaney, J.F. Endothelial function: A barometer for cardiovascular risk? *Circulation* 2002, *106*, 640–642.

86. Stenmark, K.R.; Yeager, M.E.; El Kasmi, K.C.; Nozik-Grayck, E.; Gerasimovskaya, E. V.; Li, M.; Riddle, S.R.; Frid, M.G. The Adventitia: Essential Regulator of Vascular Wall Structure and Function. *Annu. Rev. Physiol.* 2013, *75*, 23–47.

87. Balligand, J.; Feron, O.; Dessy, C. eNOS Activation by Physical Forces : From Short-Term Regulation of Contraction to Chronic Remodeling of Cardiovascular Tissues. *Physiol Rev* 2009, *89*, 481–534.

88. Dudzinski, D.M.; Michel, T. Life history of eNOS: Partners and pathways. *Cardiovasc. Res.* 2007, *75*, 247–260.

89. Mudau, M.; Genis, A.; Lochner, A.; Strijdom, H. Endothelial dysfunction: the early predictor of atherosclerosis. *Cardiovasc. J. Afr.* 2012, *23*, 222–231.

90. Rajendran, P.; Rengarajan, T.; Thangavel, J.; Nishigaki, Y.; Sakthisekaran, D.; Sethi, G.; Nishigaki, I. The vascular endothelium and human diseases. *Int. J. Biol. Sci.* 2013, *9*, 1057–1069.

91. Poredo, P. Markers of preclinical atherosclerosis and their clinical relevance. *Open Ateroscler. Thromb. J.* 2015, *44*, 247–256.

92. Lei, J.; Vodovotz, Y.; Tzeng, E.; Billiar, T.R. Nitric oxide, a protective molecule in the cardiovascular system.

Nitric Oxide - Biol. Chem. 2013, *35*, 175–185.

93. Naseem, K.M. The role of nitric oxide in cardiovascular diseases. *Mol. Aspects Med.* 2005, *26*, 33–65.

94. Liu, V.W.T.; Huang, P.L. Cardiovascular roles of nitric oxide: A review of insights from nitric oxide synthase gene disrupted mice. *Cardiovasc. Res.* 2008, *77*, 19–29.

95. Napoli, C.; Paolisso, G.; Casamassimi, A.; Al-Omran, M.; Barbieri, M.; Sommese, L.; Infante, T.; Ignarro, L.J. Effects of nitric oxide on cell proliferation: Novel insights. *J. Am. Coll. Cardiol.* 2013, *62*, 89–95.

96. Dias, R.G.; Negrão, C.E.; Krieger, M.H. Nitric oxide and the cardiovascular system: cell activation, vascular reactivity and genetic variant. *Arq. Bras. Cardiol.* 2011, *96*, 68–75.

97. Aktan, F. iNOS-mediated nitric oxide production and its regulation. *Life Sci.* 2004, *75*, 639–653.

98. Massion, P.B.; Balligand, J.-L. Modulation of cardiac contraction, relaxation and rate by the endothelial nitric oxide synthase (eNOS): lessons from genetically modified mice. *J. Physiol.* 2003, *546*, 63–75.

99. Steyers, C.M.; Miller, F.J. Endothelial dysfunction in chronic inflammatory diseases. *Int. J. Mol. Sci.* 2014, *15*, 11324–11349.

100. Papaharalambus, C. a; Griendling, K.K. Basic Mechanisms of Oxidative Stress and Reactive Oxygen Species in Cardiovascular Injury Atherosclerotic lesion Normal carotid. *Trends Cardiovasc Med* 2007, *17*, 48–54.

101. Abe, J.; Berk, B.C. Reactive oxygen species as mediators of signal transduction in cardiovascular disease. *Trends Cardiovasc. Med.* 1998, *8*, 59-64.

102. Ho, E.; Karimi Galougahi, K.; Liu, C.-C.; Bhindi, R.; Figtree, G.A. Biological markers of oxidative stress: Applications to cardiovascular research and practice. *Redox Biol.* 2013, *1*, 483–91.

103. El Assar, M.; Angulo, J.; Rodr??guez-Ma??as, L. Oxidative stress and vascular inflammation in aging. *Free Radic. Biol. Med.* 2013, *65*, 380–401.

104. Ray, R.; Shah, A.M. NADPH oxidase and endothelial cell function. *Clin. Sci. (Lond).* 2005, *109*, 217–226.

105. Hausenloy, D.J.; Yellon, D.M. New directions for protecting the heart against ischaemia-reperfusion injury: Targeting the Reperfusion Injury Salvage Kinase (RISK)-pathway. *Cardiovasc. Res.* 2004, *61*, 448–460.

106. Peluffo, G.; Radi, R. Biochemistry of protein tyrosine nitration in cardiovascular pathology. *Cardiovasc. Res.* 2007, *75*, 291–302.

107. Mondal, D.; Pradhan, L.; Ali, M.; Agrawal, K.C. HAART drugs induce oxidative stress in human endothelial cells and increase endothelial recruitment of mononuclear cells: exacerbation by inflammatory cytokines and amelioration by antioxidants. *Cardiovasc. Toxicol.* 2004, *4*, 287–302.

108. Madamanchi, N.R.; Runge, M.S. Redox signaling in cardiovascular health and disease. *Free Radic. Biol. Med.* 2013, *61*, 473–501.

109. Li, H.; Horke, S.; Förstermann, U. Vascular oxidative stress, nitric oxide and atherosclerosis. *Atherosclerosis* 2014, *237*, 208–219.

110. Pacher, P.; Beckman, J.S.; Liaudet, L. Nitric oxide and peroxynitrite in health and disease. *Physiol. Rev.* 2007, *87*, 315–424.

111. Miller, F.J.; Gutterman, D.D.; Rios, C.D.; Heistad, D.D.; Davidson, B.L. Superoxide production in vascular smooth muscle contributes to oxidative stress and impaired relaxation in atherosclerosis. *Circ. Res.* 1998, *82*, 1298–1305.

112. Ferdinandy, P.; Schulz, R. Nitric oxide, superoxide, and peroxynitrite in myocardial ischaemia-reperfusion injury and preconditioning. *Br. J. Pharmacol.* 2003, *138*, 532–43.

113. Landmesser, U.; Dikalov, S.; Price, S.R.; McCann, L.; Fukai, T.; Holland, S.M.; Mitch, W.E.; Harrison, D.G. Oxidation of tetrahydrobiopterin leads to uncoupling of endothelial cell nitric oxide synthase in hypertension. *J. Clin. Invest.* 2003, *111*, 1201–1209.

114. Cai, H. NAD(P)H oxidase-dependent self-propagation of hydrogen peroxide and vascular disease. *Circ. Res.* 2005, *96*, 818–822.

115. Morrow, J.D. Quantification of isoprostanes as indices of oxidant stress and the risk of atherosclerosis in humans. *Arterioscler. Thromb. Vasc. Biol.* 2005, *25*, 279–286.

116. Delfino, R.J.; Staimer, N.; Tjoa, T.; Polidori, A.; Arhami, M.; Gillen, D.L.; Kleinman, M.T.M.T.; Vaziri, N.D.; Longhurst, J.; Zaldivar, F.; et al. Circulating biomarkers of inflammation, antioxidant activity, and platelet activation are associated with primary combustion aerosols in subjects with coronary artery disease. *Environ. Health Perspect.* 2008, *116*, 898–906.

117. Flammer, A.J.; Lüscher, T.F. Human endothelial dysfunction: EDRFs. *Pflugers Arch. Eur. J. Physiol.* 2010, *459*, 1005–1013.

118. Spadaro, F.; Cecchetti, S.; Fantuzzi, L. Macrophages and phospholipases at the intersection between inflammation and the pathogenesis of HIV-1 infection. *Int. J. Mol. Sci.* 2017, *18*, 1–22.

119. Esmon, C.T. Crosstalk between inflammation and thrombosis. *Maturitas* 2004, *47*, 305–314.

120. Ramji, D.P.; Davies, T.S. Cytokines in atherosclerosis: Key players in all stages of disease and promising therapeutic targets. *Cytokine Growth Factor Rev.* 2015, *26*, 673–685.

121. McLaren, J.E.; Michael, D.R.; Ashlin, T.G.; Ramji, D.P. Cytokines, macrophage lipid metabolism and foam cells: Implications for cardiovascular disease therapy. *Prog. Lipid Res.* 2011, *50*, 331–347.

122. Clapp, B.R.; Hirschfield, G.M.; Storry, C.; Gallimore, J.R.; Stidwill, R.P.; Singer, M.; Deanfield, J.E.; MacAllister, R.J.; Pepys, M.B.; Vallance, P.; et al. Inflammation and endothelial function: Direct vascular effects of human C-reactive protein on nitric oxide bioavailability. *Circulation* 2005, *111*, 1530–1536.

123. Li, H.; Han, M.; Guo, L.; Li, G.; Sang, N. Oxidative stress, endothelial dysfunction and inflammatory response in rat heart to NO2 inhalation exposure. *Chemosphere* 2011, *82*, 1589–1596.

124. Klein, R.; Myers, C.E.; Cruickshanks, K.J.; Gangnon, R.E.; Danforth, L.G.; Sivakumaran, T.A.; Iyengar, S.K.; Tsai, M.Y.; Klein, B.E.K. Markers of inflammation, oxidative stress, and endothelial dysfunction and the 20-year cumulative incidence of early age-related macular degeneration: the Beaver Dam Eye Study. *JAMA Ophthalmol.* 2014, *132*, 446–55.

125. Albelda, S.M.; Smith, C.W.; Ward, P.A. Adhesion molecules and inflammatory injury. *FASEB J.* 1994, *8*, 504–512.

126. Wiseman, S.; Marlborough, F.; Doubal, F.; Webb, D.J.; Wardlaw, J. Blood markers of coagulation, fibrinolysis, endothelial dysfunction and inflammation in lacunar stroke versus non-lacunar stroke and non-stroke: Systematic review and meta-analysis. *Cerebrovasc. Dis.* 2014, *37*, 64–75.

127. Constans, J.; Conri, C. Circulating markers of endothelial function in cardiovascular disease. *Clin. Chim. Acta* 2006, *368*, 33–47.

128. Trzeciak, S.; Schuetz, P.; Aird, W.C.; Shapiro, N.I. Biomarkers of endothelial cell activation in early sepsis. *Shock* 2014, *39*, 427–432.

129. Ley, K.; Huo, Y. VCAM-1 is critical in atherosclerosis. *J. Clin. Invest.* 2001, *107*, 1209–1210.

130. Gonzalez, M.A.; Selwyn, A.P. Endothelial function, inflammation, and prognosis in cardiovascular disease. *Am. J. Med.* 2003, *115*, 99–106.

131. Willerson, J.T.; Ridker, P.M. Inflammation as a cardiovascular risk factor. *Circulation* 2004, *109*, II2-II10.

132. Libby, P.; Ridker, P.M.; Maseri, A. Inflammation and atherosclerosis. *Circulation* 2002, *105*, 1135–1143.

133. Ammirati, E.; Moroni, F.; Norata, G.D.; Magnoni, M.; Camici, P.G. Markers of inflammation associated with plaque progression and instability in patients with carotid atherosclerosis. *Mediators Inflamm.* 2015, *2015*, 1–15.

134. Zhang, C. The role of inflammatory cytokines in endothelial dysfunction. *Basic Res. Cardiol.* 2008, *103*, 398–406.

135. He, Q.; Johnston, J.; Zeitlinger, J.; City, K.; City, K. Markers of Endothelial Dysfunction, Coagulation and Tissue Fibrosis Independently Predict Venous Thromboembolism in HIV. *AIDS* 2015, *33*, 395–401.

136. Naghavi, M.; Libby, P.; Falk, E.; Casscells, S.W.; Litovsky, S.; Rumberger, J.; Badimon, J.J.; Stefanadis, C.; Moreno, P.; Pasterkamp, G.; et al. From Vulnerable Plaque to Vulnerable Patient: A Call for New Definitions and Risk Assessment Strategies: Part II. *Circulation* 2003, *108*, 1772–1778.

137. Tabas, I.; García-Cardeña, G.; Owens, G.K. Recent insights into the cellular biology of atherosclerosis. *J. Cell Biol.* 2015, *209*, 13–22.

138. Dzau, V.J.; Antman, E.M.; Black, H.R.; Hayes, D.L.; Manson, J.E.; Plutzky, J.; Popma, J.J.; Stevenson, W. The cardiovascular disease continuum validated: Clinical evidence of improved patient outcomes: Part I: Pathophysiology and clinical trial evidence (risk factors through stable coronary artery disease). *Circulation* 2006, *114*, 2850–2870.

139. Murray, C.J.L.; Lopez, A.D. Global mortality , disability , and the contribution of risk factors : Global Burden of Disease Study. *Lancet* 1997, *349*, 1436–1442.

140. D'Agostino, R.B.; Vasan, R.S.; Pencina, M.J.; Wolf, P.A.; Cobain, M.; Massaro, J.M.; Kannel, W.B.; D'Agostino, R.B.; Vasan, R.S.; Pencina, M.J.; et al. General cardiovascular risk profile for use in primary care: The Framingham heart study. *Circulation* 2008, *117*, 743–753.

141. Greenland, P.; Smith, S.C.; Grundy, S.M. Improving coronary heart disease risk assessment in asymptomatic people: role of traditional risk factors and noninvasive cardiovascular tests. *Circulation* 2001, *104*, 1863–1867.

142.   Anand, S.S.H.D.G. Emerging Risk Factors for Atherosclerotic Vascular Disease: A Critical Review of the Evidence. *JAMA J. Am. Med. Assoc.* 2003, *290*, 932–940.

143.   Kannel, W.B.; McGee, D.; Gordon, T. A general cardiovascular risk profile: The Framingham study. *Am. J. Cardiol.* 1976, *38*, 46–51.

144.   Deaton, C.; Froelicher, E.S.; Wu, L.H.; Ho, C.; Shishani, K.; Jaarsma, T. The global burden of cardiovascular disease. *Eur. J. Cardiovasc. Nurs.* 2011, *10*, S5–S13.

145.   Brindle, P.; Beswick, A.; Fahey, T.; Ebrahim, S. Accuracy and impact of risk assessment in the primary prevention of cardiovascular disease: a systematic review. *Heart* 2006, *92*, 1752–9.

146.   Cooney, M.T.; Dudina, A.L.; Graham, I.M. Value and Limitations of Existing Scores for the Assessment of Cardiovascular Risk. A Review for Clinicians. *J. Am. Coll. Cardiol.* 2009, *54*, 1209–1227.

147.   Hadi, H.A.; Carr, C.S.; Al Suwaidi, J. Endothelial dysfunction: cardiovascular risk factors, therapy, and outcome. *Vasc Heal. Risk Manag* 2005, *1*, 183–198.

148.   MBoistat, K.M.; Liew, G.; Macashill, P.; Irwig, L.; Klein, R.; K., K.B.E.; Wang, J.J.; Mitvhell, P.; Vingerling, J.R.; DeJong, P.T.V.M.; et al. Retinal Vessel Caliber and Risk for Coronary Heart Disease: A Systematic Review and Meta-Analysis. *Ann Intern Med.* 2007, *151*, 404–413.

149.   Wang, T.J. Assessing the role of circulating, genetic, and imaging biomarkers in cardiovascular risk prediction. *Circulation* 2011, *123*, 551–565.

150.   Flammer, A.J.; Anderson, T.; Celermajer, D.S.; Creager, M.A.; Deanfield, J.; Ganz, P.; Hamburg, N.M.; Lüscher, T.F.; Shechter, M.; Taddei, S.; et al. The assessment of endothelial function: From research into clinical practice. *Circulation* 2012, *126*, 753–767.

151.   Lekakis, J.; Abraham, P.; Balbarini, A.; Blann, A.; Boulanger, C.M.; Cockcroft, J.; Cosentino, F.; Deanfield, J.; Gallino, A.; Ikonomidis, I.; et al. Methods for evaluating endothelial function: a position statement from the European Society of Cardiology Working Group on Peripheral Circulation. *Eur. J. Cardiovasc. Prev. Rehabil.* 2011, *18*, 775–89.

152.   Bailey, A.L.; Smyth, S.S. Invasive coronary vasoreactivity testing to diagnose microvascular dysfunction in women. *JACC Cardiovasc. Interv.* 2012, *5*, 654–655.

153.   Wang, J.J.; Liew, G.; Klein, R.; Rochtchina, E.; Knudtson, M.D.; Klein, B.E.K.; Wong, T.Y.; Burlutsky, G.; Mitchell, P. Retinal vessel diameter and cardiovascular mortality: Pooled data analysis from two older populations. *Eur. Heart J.* 2007, *28*, 1984–1992.

154.   Grover-Páez, F.; Zavalza-Gómez, A.B. Endothelial dysfunction and cardiovascular risk factors. *Diabetes Res. Clin. Pract.* 2009, *84*, 1–10.

155.   Corretti, M.C.; Anderson, T.J.; Benjamin, E.J.; Celermajer, D.; Charbonneau, F.; Creager, M. a; Deanfield, J.; Drexler, H.; Gerhard-Herman, M.; Herrington, D.; et al. Guidelines for the ultrasound assessment of endothelial-dependent flow- mediated vasodilation of the brachial artery: a report of the International Brachial Artery Reactivity Task Force. *J Am Coll Cardiol* 2002, *39*, 257–65.

156.   Corretti, M.C.; Anderson, T.J.; Benjamin, E.J.; Celermajer, D.; Charbonneau, F.; Creager, M.A.; Deanfield,

J.; Drexler, H.; Gerhard-Herman, M.; Herrington, D.; et al. Guidelines for the ultrasound assessment of endothelial-dependent flow-mediated vasodilation of the brachial artery. *J. Am. Coll. Cardiol.* 2002, *39*, 257–265.

157. Charakida, M.; Masi, S.; Luscher, T.F.; Kastelein, J.J.P.; Deanfield, J.E. Assessment of atherosclerosis: the role of flow-mediated dilatation. *Eur. Heart J.* 2010, *31*, 2854–2861.

158. Donald, A.E.; Halcox, J.P.; Charakida, M.; Storry, C.; Wallace, S.M.L.; Cole, T.J.; Friberg, P.; Deanfield, J.E. Methodological Approaches to Optimize Reproducibility and Power in Clinical Studies of Flow-Mediated Dilation. *J. Am. Coll. Cardiol.* 2008, *51*, 1959–1964.

159. Liew, G.; Wang, J.J.; Mitchell, P.; Wong, T.Y. Retinal vascular imaging: a new tool in microvascular disease research. *Circ. Cardiovasc. Imaging* 2008, *1*, 156–161.

160. Patton, N.; Aslam, T.M.; MacGillivray, T.; Deary, I.J.; Dhillon, B.; Eikelboom, R.H.; Yogesan, K.; Constable, I.J. Retinal image analysis: Concepts, applications and potential. *Prog. Retin. Eye Res.* 2006, *25*, 99–127.

161. Liew, G.; Wang, J.J. Retinal Vascular Signs: A Window to the Heart? *Rev. Española Cardiol. (English Ed.* 2011, *64*, 515–521.

162. Patton, N.; Aslam, T.; MacGillivray, T.; Pattie, A.; Deary, I.J.; Dhillon, B. Retinal vascular image analysis as a potential screening tool for cerebrovascular disease: A rationale based on homology between cerebral and retinal microvasculatures. *J. Anat.* 2005, *206*, 319–348.

163. Wang, S.B.; Mitchell, P.; Liew, G.; Wong, T.Y.; Phan, K.; Thiagalingam, A.; Joachim, N.; Burlutsky, G.; Gopinath, B. A spectrum of retinal vasculature measures and coronary artery disease. *Atherosclerosis* 2017, *268*, 215–224.

164. Luo, T.; Gast, T.J.; Vermeer, T.J.; Burns, S.A. Retinal vascular branching in healthy and diabetic subjects. *Investig. Ophthalmol. Vis. Sci.* 2017, *58*, 2685–2694.

165. Yin, Y.; Adel, M.; Bourennane, S. Automatic Segmentation and Measurement of Vasculature in Retinal Fundus Images Using Probabilistic Formulation. *Comput. Math. Methods Med.* 2013, *2013*, 1–16.

166. Frost, S.; Kanagasingam, Y.; Sohrabi, H.; Vignarajan, J.; Bourgeat, P.; Salvado, O.; Villemagne, V.; Rowe, C.C.; Lance MacAulay, S.; Szoeke, C.; et al. Retinal vascular biomarkers for early detection and monitoring of Alzheimer's disease. *Transl. Psychiatry* 2013, *3*, e233-8.

167. Trucco, E.; Ruggeri, A.; Karnowski, T.; Giancardo, L.; Chaum, E.; Hubschman, J.P.; al-Diri, B.; Cheung, C.Y.; Wong, D.; Abramoff, M.; et al. Validating Retinal Fundus Image Analysis Algorithms: Issues and a ProposalValidating Retinal Fundus Image Analysis Algorithms. *Invest. Ophthalmol. Vis. Sci.* 2013, *54*, 3546–3559.

168. Leung, H.; Wang, J.J.; Rochtchina, E.; Wong, T.Y.; Klein, R.; Mitchell, P. Dyslipidaemia and microvascular disease in the retina. *Eye (Lond).* 2005, *19*, 861–868.

169. Li, L.-J.; Ikram, M.K.; Wong, T.Y. Retinal vascular imaging in early life: insights into processes and risk of cardiovascular disease. *J. Physiol.* 2016, *594*, 2175–2203.

170. Chapman, N.; Dell'omo, G.; Sartini, M.S.; Witt, N.; Hughes, a; Thom, S.; Pedrinelli, R. Peripheral vascular

disease is associated with abnormal arteriolar diameter relationships at bifurcations in the human retina. *Clin. Sci. (Lond).* 2002, *103*, 111–6.

171. Kalitzeos, A. Retinal Vessel Analysis : Flicker Reproducibility, Methodological Standardisations and Practical Limitations. 2013, 1–116.

172. Sun, C.; Liew, G.; Wang, J.J.; Mitchell, P.; Saw, S.M.; Aung, T.; Tai, E.S.; Wong, T.Y. Retinal vascular caliber, blood pressure, and cardiovascular risk factors in an asian population: The Singapore malay eye study. *Investig. Ophthalmol. Vis. Sci.* 2008, *49*, 1784–1790.

173. Hart, W.E.; Goldbaum, M.; Côté, B.; Kube, P.; Nelson, M.R. Measurement and classification of retinal vascular tortuosity. *Int. J. Med. Inform.* 1999, *53*, 239–252.

174. Joshi, V.S. Analysis of retinal vessel networks using quantitative descriptors of vascular morphology. Available online: http://ir.uiowa.edu/etd/3321/ (accessed on Jun 11, 2019).

175. Burger, D.; Touyz, R.M. Cellular biomarkers of endothelial health: Microparticles, endothelial progenitor cells, and circulating endothelial cells. *J. Am. Soc. Hypertens.* 2012, *6*, 85–99.

176. Lip, G.Y.; Blann, a von Willebrand factor: a marker of endothelial dysfunction in vascular disorders? *Cardiovasc. Res.* 1997, *34*, 255–65.

177. Aiello, A.E.; Kaplan, G.A. Socioeconomic position and inflammatory and immune biomarkers of cardiovascular disease: applications to the Panel Study of Income Dynamics. *Biodemography Soc. Biol.* 2009, *55*, 178–205.

178. Cybulsky, M.I.; Iiyama, K.; Li, H.; Zhu, S.; Chen, M.; Iiyama, M.; Davis, V.; Gutierrez-Ramos, J.C.; Connelly, P.W.; Milstone, D.S. A major role for VCAM-1, but not ICAM-1, in early atherosclerosis. *J. Clin. Invest.* 2001, *107*, 1255–1262.

179. Lawson, C.; Wolf, S. ICAM-1 signaling in endothelial cells. *Pharmacol. Reports* 2009, *61*, 22–32.

180. Hubbard, A.; Rothlein, R. Intercellular adhesion molecule-1 (ICAM-1) expression and cell signaling cascades. *Free Radic. Biol. Med.* 2000, *28*, 1379–1386.

181. Kim, I.; Moon, S.O.; Kim, S.H.; Kim, H.J.; Koh, Y.S.; Koh, G.Y. Vascular endothelial growth factor expression of intercellular adhesion molecule 1 (ICAM-1), vascular cell adhesion molecule 1 (VCAM-1), and E-selectin through nuclear factor-kappa B activation in endothelial cells. *J. Biol. Chem.* 2001, *276*, 7614–20.

182. Ferrara, N.; Gerber, H.P.; LeCouter, J. The biology of VEGF and its receptors. *Nat. Med.* 2003, *9*, 669–676.

183. Coultas, L.; Chawengsaksophak, K.; Rossant, J. Endothelial cells and VEGF in vascular development. *Nature* 2005, *438*, 937–945.

184. Boos, C.J.; Lip, G.Y.H.; Blann, A.D. Circulating Endothelial Cells in Cardiovascular Disease. *J. Am. Coll. Cardiol.* 2006, *48*, 1538–1547.

185. Yusuf, S.; Hawken, S.; Ôunpuu, S.; Dans, T.; Avezum, A.; Lanas, F.; McQueen, M.; Budaj, A.; Pais, P.; Varigos, J.; et al. Effect of potentially modifiable risk factors associated with myocardial infarction in 52

countries in a case-control study based on the INTERHEART study. *Lancet* 2004, *364*, 937–952.

186. Anderson, K.M.; Odell, P.M.; Wilson, P.W.F.; Kannel, W.B. Cardiovascular disease risk profiles. *Am. Heart J.* 1991, *121*, 293–298.

187. Lim, S.S.; Vos, T.; Flaxman, A.D.; Danaei, G.; Shibuya, K.; Adair-Rohani, H.; Amann, M.; Anderson, H.R.; Andrews, K.G.; Aryee, M.; et al. A comparative risk assessment of burden of disease and injury attributable to 67 risk factors and risk factor clusters in 21 regions, 1990-2010: A systematic analysis for the Global Burden of Disease Study 2010. *Lancet* 2012, *380*, 2224–2260.

188. World Health Organization. The global burden of disease - 2004 Update. Available online: www.who.int/healthinfo/global_burden_disease/2004_report_update/en/ (accessed on Nov 18, 2018).

189. Lakatta, E.G.; Levy, D. Arterial and Cardiac Aging : Major Shareholders in Cardiovascular Disease Enterprises Part II : The Aging Heart in Health : Links to Heart Disease. *Circulation* 2003, *107*, 139–146.

190. Lakatta, E.G. Age-associated cardiovascular changes in health: impact on cardiovascular disease in older persons. *Hear. Fail.* 2002, *7*, 29–49.

191. Wood, D. Established and emerging cardiovascular risk factors. *Am. Heart J.* 2001, *141*, S49-57.

192. Winham, S.J.; de Andrade, M.; Miller, V.M. Genetics of cardiovascular disease: Importance of sex and ethnicity. *Atherosclerosis* 2014, *241*, 219–228.

193. Cooper, R.S. Social inequality, ethnicity and cardiovascular disease. *Int. J. Epidemiol.* 2001, *30 Suppl 1*, S48-52.

194. Spence, J.D.; Pilote, L. Importance of sex and gender in atherosclerosis and cardiovascular disease. *Atherosclerosis* 2015, *241*, 208–210.

195. Csiszar, A.; Wang, M.; Lakatta, E.G.; Ungvari, Z. Inflammation and endothelial dysfunction during aging: role of NF-kappaB. *J. Appl. Physiol.* 2008, *105*, 1333–1341.

196. North, B.J.; Sinclair, D.A. The intersection between aging and cardiovascular disease. *Circ. Res.* 2012, *110*, 1097–1108.

197. Ross, R. Inflammation or Atherogenesis. *N. Engl. J. Med.* 1999, *340*, 115–126.

198. World Health Organization Global Health Risks: Mortality and burden of disease attributable to selected major risks. *Bull. World Health Organ.* 2009, *87*, 646–646.

199. Sliwa, K.; Acquah, L.; Gersh, B.J.; Mocumbi, A.O. Impact of Socioeconomic Status, Ethnicity, and Urbanization on Risk Factor Profiles of Cardiovascular Disease in Africa. *Circulation* 2016, *133*, 1199–1208.

200. Dalal, S.; Beunza, J.J.; Volmink, J.; Adebamowo, C.; Bajunirwe, F.; Njelekela, M.; Mozaffarian, D.; Fawzi, W.; Willett, W.; Adami, H.O.; et al. Non-communicable diseases in sub-Saharan Africa: What we know now. *Int. J. Epidemiol.* 2011, *40*, 885–901.

201. Alberts, M.; Urdal, P.; Steyn, K.; Stensvold, I.; Tverdal, A.; Nel, J.H.; Steyn, N.P. Prevalence of cardiovascular diseases and associated risk factors in a rural black population of South Africa. *Eur. J. Prev. Cardiol.* 2005, *12*, 347–354.

202. Kruger, H.S.; Venter, C.S.; Vorster, H.H.; THUSA Study Physical inactivity as a risk factor for cardiovascular disease in communities undergoing rural to urban transition: the THUSA study. *Cardiovasc. J. South Africa.* 2003, *14*, 16–23.

203. Oosthuizen, W.; Vorster, H.H.; Kruger, A.; Venter, C.S.; Kruger, H.S.; Ridder, J.H. de Impact of urbanisation on Serum lipid profiles -the thusa survey. *South African Med. J. 92*, 723–728.

204. Adeboye, B.; Bermano, G.; Rolland, C. Obesity and its health impact in Africa: a systematic review. *Cardiovasc. J. Afr.* 2012, *23*, 512–21.

205. Heart and Stroke Foundation South Africa. Cardiovascular Disease Statistics Reference Document. Available online: http://www.heartfoundation.co.za/wp-content/uploads/2017/10/CVD-Stats-Reference-Document-2016-FOR-MEDIA-1.pdf (accessed on Jul 2, 2019).

206. Department of Health:; Human Sciences Research Council. The South African National Health and Nutrition Examination Survey, SANHANES-1. Available online: http://www.hsrc.ac.za/uploads/pageNews/72/SANHANES-launch edition (online version).pdf (accessed on May 13, 2019).

207. South African Department of Health. Standard Treatment Guidelines and Essnetial Medicine List for South Africa Primary Health Care. Available online: http://www.health.gov.za/index.php/standard-treatment-guidelines-and-essential-medicines-list/category/285-phc (accessed on Apr 14, 2019).

208. Matsha, T.E.; Hassan, M.S.; Kidd, M.; Erasmus, R.T. The 30-year cardiovascular risk profile of South Africans with diagnosed diabetes, undiagnosed diabetes, pre-diabetes or normoglycaemia: the Bellville, South Africa pilot study. *Cardiovasc. J. Afr.* 2012, *23*, 5–11.

209. Mathers, C.D.; Boerma, T.; Ma Fat, D. Global and regional causes of death. *Br. Med. Bull.* 2009, *92*, 7–32.

210. Mendis, S.; Alwan, A. A Prioritized Research Agenda for the Prevention and Control of Noncimmunicable Diseases. Available online: www.who.int/cardiovascular_disease/publications/ncd_agenda2011/en. (accessed on Apr 17, 2018).

211. Moran, A.E.; Forouzanfar, M.H.; Roth, G. a.; Mensah, G. a.; Ezzati, M.; Flaxman, A.; Murray, C.J.L.; Naghavi, M. The global burden of ischemic heart disease in 1990 and 2010: The global burden of disease 2010 study. *Circulation* 2014, *129*, 1493–1501.

212. World Health Organisation Cardiovascular diseases (CVDs): WHO key facts. Available online: https://www.who.int/news-room/fact-sheets/detail/cardiovascular-diseases-(cvds) (accessed on Jul 2, 2019).

213. Mathers, C.D.; Loncar, D. Projections of global mortality and burden of disease from 2002 to 2030. *PLoS Med.* 2006, *3*, 2011–2030.

214. Mathers, C.D.; Loncar, D. Updated projections of global mortalityand burden of disease, 2002-2030:data sources, methods and results. Available online: https://www.who.int/healthinfo/statistics/bod_projections2030_paper.pdf (accessed on Jul 22, 2018).

215. Yusuf S, Reddy S, O.S.A. Global Burden of Cardiovascular Diseases. *Circulation* 2001, *104*, 2746–53.

216. Dahlöf, B. Cardiovascular Disease Risk Factors: Epidemiology and Risk Assessment. *Am. J. Cardiol.* 2010, *105*, 3A-9A.

217. World Heart Federation. Cardiovascular diseases in South Africa. Available online: https://www.world-heart-federation.org/wp-content/uploads/2017/05/Cardiovascular_diseases_in_South_Africa.pdf (accessed on Aug 27, 2019).

218. World Health Organization WHO: Cardiovascular diseases (CVDs) Available online: https://www.who.int/news-room/fact-sheets/detail/cardiovascular-diseases-(cvds) (accessed on Jul 3, 2019).

219. Cock, K.M. De; Jaffe, H.W.; Curran, J.W. The evolving epidemiology of HIV / AIDS. *AIDS* 2012, *26*, 1205–1213.

220. Cock, K.M. De; Jaffe, H.W.; Curran, J.W. Reflections on 30 Years of AIDS. *AIDS* 2011, 1–11.

221. Sharp, P.M.; Hahn, B.H. Origins of HIV and the AIDS Pandemic. *Cold Spring Harb Perspect Med* 2011, *1*, 1–22.

222. Anuurrad, E.; Bremer, A.; Beglund, L.; Anuurad, E.; Bremer, A.; Berglund, L. HIV Protease Inhibitors and Obesity. *Curr Opin Endocrinol Diabetes Obes* 2012, *29*, 997–1003.

223. AIDS Research Advisory Council. Guidelines for the Use of Antiretroviral Agents in HIV-1-Infected Adults and Adolescents. Available online: https://aidsinfo.nih.gov/contentfiles/lvguidelines/adultandadolescentgl.pdf (accessed on Nov 15, 2018).

224. Vella, S.; Schwartländer, B.; Sow, S.P.; Eholie, S.P.; Murphy, R.L. The history of antiretroviral therapy and of its implementation in resource-limited areas of the world. *AIDS* 2012, *26*, 1231–41.

225. Broder, S. The development of antiretroviral therapy and its impact on the HIV-1/AIDS pandemic. *Antiviral Res.* 2010, *85*, 1–18.

226. Aboud, M.; Elgalib, A.; Kulasegaram, R.; Peters, B. Insulin resistance and HIV infection: a review. *Int. J. Clin. Pract.* 2007, *61*, 463–472.

227. Arts, E.J.; Hazuda, D.J. HIV-1 antiretroviral drug therapy. *Cold Spring Harb. Perspect. Med.* 2012, *2*, a007161.

228. World Health Organization. Towards universal access: Scaling up priority HIV/AIDS interventions in the health sector. Available online: https://www.who.int/hiv/pub/2010progressreport/en/ (accessed on Oct 18, 2018).

229. Hontelez, J.A.C.; Lurie, M.N.; Bärnighausen, T.; Bakker, R.; Baltussen, R.; Tanser, F.; Hallett, T.B.; Newell, M.L.; de Vlas, S.J. Elimination of HIV in South Africa through Expanded Access to Antiretroviral Therapy: A Model Comparison Study. *PLoS Med.* 2013, *10*, e1001534.

230. Chu, C.; Umanski, G.; Blank, A.; Meissner, P.; Grossberg, R.; Selwyn, P.A. Comorbidity-related treatment outcomes among HIV-Infected adults in the Bronx, NY. *J. Urban Heal.* 2011, *88*, 507–516.

231. Calvo, M.; Martinez, E. Update on metabolic issues in HIV patients. *Curr. Opin. HIV AIDS* 2014, *9*, 332–9.

232. Althoff, K.N.; Smit, M.; Reiss, P.; Justice, A.C. HIV and ageing: Improving quantity and quality of life. *Curr. Opin. HIV AIDS* 2016, *11*, 527–536.

233. Salmen, S.; Colmenares, M.; Peterson, D.L.; Reyes, E.; Rosales, J.D.; Berrueta, L. HIV-1 Nef associates with p22-phox, a component of the NADPH oxidase protein complex. *Cell. Immunol.* 2010, *263*, 166–171.

234. Arhel, N. Revisiting HIV-1 uncoating. *Retrovirology* 2010, *7*, 96–106.

235. AIDSinfo: A Service of the U.S. Department of Health and Human Services. The HIV Life Cycle. Available online: http://aidsinfo.nih.gov (accessed on Jul 25, 2017).

236. Arhel, N.; Kirchhoff, F. Host proteins involved in HIV infection: new therapeutic targets. *Biochim. Biophys. Acta* 2010, *1802*, 313–321.

237. Ruelas, D.S.; Greene, W.C. An integrated overview of HIV-1 latency. *Cell* 2013, *155*, 519–529.

238. AIDSinfonet. HIV life cycle - Fact Sheet. Available online: http://aids.gov/hiv-aids-basics/just-diagnosed-with-hiv-aids/hiv-in-your-body/hiv-lifecycle/ (accessed on Nov 20, 2018).

239. de Bethune, M.-P. Non-nucleoside reverse transcriptase inhibitors (NNRTIs), their discovery, development, and use in the treatment of HIV-1 infection: A review of the last 20 years (1989-2009). *Antiviral Res.* 2010, *85*, 75–90.

240. Margolis, A.M.; Heverling, H.; Pham, P.A.; Stolbach, A. A Review of the Toxicity of HIV Medications. *J.Med. Toxicol* 2014, *10*, 26–39.

241. De Clercq, E. Antiviral drugs in current clinical use. *J. Clin. Virol.* 2004, *30*, 115–133.

242. Jochmans, D. Novel HIV-1 reverse transcriptase inhibitors. *Virus Res.* 2008, *134*, 171–185.

243. World Health Organization. WHO: Summery of new ART recommendations. Available online: http://www.who.int/hiv/pub/guidelines/arv2013/intro/summarynewrecommendations.pdf?ua=1 (accessed on May 21, 2018).

244. Joint United Nations Programme on HIV/AIDS. South Africa takes bold step to provide HIV treatment for all. Available online: https://www.unaids.org/en/resources/presscentre/pressreleaseandstatementarchive/2016/may/20160513_UTT (accessed on Dec 12, 2018).

245. South African Department of Health. The South African Antiretroviral Treatment Guidelines 2013. Available online: http://www.kznhealth.gov.za/medicine/2013_art_guidelines.pdf.

246. Cipla. ODIMUNE. Available online: https://www.cipla.co.za (accessed on Feb 13, 2017).

247. Deeks, E.D.; Perry, C.M. Efavirenz / Emtricitabine / Tenofovir Disoproxil Fumarate Single-Tablet Regimen (Atripla). *Aids Drug Eval.* 2010, *70*, 2315–2338.

248. Feng, J.Y.; Ly, J.K.; Myrick, F.; Goodman, D.; White, K.L.; Svarovskaia, E.S.; Borroto-esoda, K.; Miller, M.D. The triple combination of tenofovir , emtricitabine and efavirenz shows synergistic anti-HIV-1 activity in vitro : a mechanism of action study. *Retrovirology* 2009, *6*, 44.

249. Kakuda, T.N. Pharmacology of nucleoside and nucleotide reverse transcriptase inhibitor-induced mitochondrial toxicity. *Clin. Ther.* 2000, *22*, 685–708.

250. Waters, L.; John, L.; Nelson, M. Non-nucleoside reverse transcriptase inhibitors: a review. *Int. J. Clin. Pract.* 2007, *61*, 105–118.

251. Sierra-Aragón, S.; Walter, H. Targets for inhibition of HIV replication: Entry, enzyme action, release and maturation. *Intervirology* 2012, *55*, 84–97.

252. University of Liverpool. Efavirenz. Available online: www.hiv-druginteractions.org (accessed on Jan 29, 2017).

253. Maggiolo, F. Efavirenz: A decade of clinical experience in the treatment of HIV. *J. Antimicrob. Chemother.* 2009, *64*, 1–19.

254. Vrouenraets, S.M.E.; Wit, F.W.N.M.; Tongeren, J. van; Lange, J.M.A. Efavirenz: a review. *Expert Opin. Pharmacother.* 2007, *8*, 851–871.

255. Decloedt, E.H.; Maartens, G. Neuronal toxicity of efavirenz: a systematic review. *Expert Opin. Drug Saf.* 2013, *12*, 841–846.

256. Walker, U.A.; Setzer, B.; Venhoff, N. Increased long-term mitochondrial toxicity in combinations of nucleoside analogue reverse-transcriptase inhibitors. *Aids* 2002, *16*, 2165–2173.

257. De Clercq, E. Anti-HIV drugs: 25 compounds approved within 25 years after the discovery of HIV. *Int. J. Antimicrob. Agents* 2009, *33*, 307–320.

258. Frampton, J.E.; Perry, C.M. Emtricitabine: A review of its use in the management of HIV infection. *Drugs* 2005, *65*, 1427–1448.

259. Richman, D.D. Antiretroviral activity of emtricitabine, a potent nucleoside reverse transcriptase inhibitor. *Antivir. Ther.* 2001, *6*, 83–88.

260. Nelson, M.; Schiavone, M. Emtricitabine (FTC) for the treatment of HIV infection. *Int. J. Clin. Pract.* 2004, *58*, 504–510.

261. University of Liverpool. Emtricitabine. Available online: www.hiv-druginteractions.org (accessed on Feb 12, 2017).

262. University of Liverpool. Tenofovir. Available online: www.hiv-druginteractions.org (accessed on Feb 15, 2017).

263. Cooper, R.D.; Wiebe, N.; Smith, N.; Keiser, P.; Naicker, S.; Tonelli, M. Systematic review and meta-analysis: renal safety of tenofovir disoproxil fumarate in HIV-infected patients. *Clin Infect Dis* 2010, *51*, 496–505.

264. Mallon, P.W.G. Pathogenesis of Lipodystrophy and Lipid Abnormalities in Patients Takng Antiretroviral Therapy. *AIDS Rev.* 2007, *9*, 3–15.

265. Yarasheski, K.; Kotler, D.P.; Parker, R. a The Role of Protease Inhibitors in the Pathogenesis of HIV-Associated Lipodystrophy: Cellular Mechanisms and Clinical Implications. *Toxicol Pathol* 2011, *37*, 65–77.

266. Mavroudis, C.A.; Majumder, B.; Loizides, S.; Christophides, T.; Johnson, M.; Rakhit, R.D. The role of protease inhibitors in the pathogenesis of HIV-associated lipodystrophy: cellular mechanisms and clinical implications. *Int. J. Cardiol.* 2013, *167*, 1147–1153.

267.   Pao, V.; Lee, G.A.; Grunfeld, C. HIV therapy, metabolic syndrome, and cardiovascular risk. *Curr. Atheroscler. Rep.* 2008, *10*, 61–70.

268.   South African National Department of Health National Consolidated Guidelines for the Prevention of Mother-To-Child Transmission of HIV (PMTCT) and the Managment of HIV in Children, Adolescents and Adults. *Dep. Heal. Repub. South Africa* 2015, 1–128.

269.   Reyskens, K.M.S.E.; Fisher, T.-L.; Schisler, J.J.C.; O'Connor, W.G.; Rogers, A.B.; Willis, M.S.; Planesse, C.; Rondeau, P.; Bourdon, E.; Essop, M.F. The Maladaptive Effects of HIV Protease Inhibitors (Lopinavir/Ritonavir) on the Rat Heart. *PLoS One* 2013, *8*, e73347.

270.   Cavenaghi, F.M.; Bataglion, C.A.N.; Paula, P.C.; Motta, A.C.F.; Komesu, M.C. Protease inhibitor and metabolic alteration | Inhibidor de la proteasa y alteraciones metabólicas. *Int. J. Morphol.* 2012, *30*, 439–444.

271.   Orrell, C. Antiretroviral adverse drug reactions and their management. *CME* 2011, *29*, 234–237.

272.   Blair, W.; Perros, M. 5th Antiviral Drug Discovery and Development Summit. *Expert Opin. Investig. Drugs.* 2004, *13*, 1065–9.

273.   Jeric ´O, C.; Knobel, H.; Montero, M.; Ordo˜Nez-Llanos, J.; Guelar, A.; Gimeno, J.L.; Saballs, P.; L´Opez-Colom´Es, J.L.; Pedro-Botet, J. Metabolic Syndrome Among HIV-Infected. *Diabetes Care* 2005, *28*, 144–149.

274.   Hsue, P.; Hunt, P.W.; Schnell, A.; Kalapus, S.C.; Hoh, R.; Ganz, P.; Martin, J.N.; Deeks, S.G. Role of Viral Replication, Antiretroviral Therapy, and Immunodeficiency in HIV- Associated Atherosclerosis. *AIDS (London, …* 2009, *23*, 1059–1067.

275.   Lapadula, G.; Chatenoud, L.; Gori, A.; Castelli, F.; Di Giambenedetto, S.; Fabbiani, M.; Maggiolo, F.; Focà, E.; Ladisa, N.; Sighinolfi, L.; et al. Risk of severe non AIDS events is increased among patients unable to increase their CD4 + T-cell counts more than 200+/micro-L despite effective HAART. *PLoS One* 2015, *10*, e0124741.

276.   Lewthwaite, P.; Wilkins, E. Natural history of HIV/AIDS. *Medicine (Baltimore).* 2009, *37*, 333–337.

277.   Yoshimura, K. Current status of HIV/AIDS in the ART era. *J. Infect. Chemother.* 2017, *23*, 12–16.

278.   World Health Organization. World Health Statistics 2011. Available online: https://www.who.int/whosis/whostat/2011/en/ (accessed on Apr 11, 2017).

279.   Anabwani, G.; Navario, P. Nutrition and HIV/AIDS in sub-Saharan Africa: An overview. *Nutrition* 2005, *21*, 96–99.

280.   Joint United Nations Programme on HIV/AIDS. Global Rport: UNAIDS report on the global AIDS epidemic 2013. Available online: www.unaids.org/.../unaids/.../2013/gr2013/UNAIDS_Global_Report_2013 (accessed on May 25, 2018).

281.   Abrahams, Z.; Dave, J.A.; Maartens, G.; Levitt, N.S. Changes in blood pressure, glucose levels, insulin secretion and anthropometry after long term exposure to antiretroviral therapy in South African women. *AIDS Res. Ther.* 2015, *12*, 24.

282. UNAIDS. Global HIV and AIDS statistics — 2018. Available online: http://www.unaids.org/sites/default/files/media_asset/UNAIDS_FactSheet_en.pdf (accessed on May 28, 2019).

283. AIDS Virus Education Research Trust. HIV and AIDS in South Africa. Available online: https://www.avert.org/printpdf/node/404 (accessed on Jul 3, 2019).

284. Joint United Nations Programme on HIV/AIDS (UNAIDS). Global AIDS Monitoring 2019. Available online: http://www.unaids.org/en/dataanalysis/knowyourresponse/globalaidsprogressreporting (accessed on Apr 6, 2019).

285. Paton, P.; Tabib, A.; Loire, R.; Tete, R. Coronary artery lesions and human immunodeficiency virus infection. *Res. Virol.* 1993, *144*, 225–231.

286. Monsuez, J.-J.; Charniot, J.-C.; Escaut, L.; Teicher, E.; Wyplosz, B.; Couzigou, C.; Vignat, N.; Vittecoq, D. HIV-associated vascular diseases: structural and functional changes, clinical implications. *Int. J. Cardiol.* 2009, *133*, 293–306.

287. De Palo, V.A.; Millstein, B.H.; Mayo, P.H.; Salzman, S.H.; Rosen, M.J. Outcome of Intensive Care in Patients With HIV Infection. *Chest* 1995, *107*, 506–510.

288. Saville, M.W.; Lietzau, J.; Pluda, J.M.; Wilson, W.H.; Humphrey, R.W.; Feigel, E.; Steinberg, S.M.; Broder, S.; Yarchoan, R.; Odom, J.; et al. Treatment of HIV-associated Kaposi's sarcoma with paclitaxel. *Lancet* 1995, *346*, 26–28.

289. Miller, R.F.; Gilson, R.; Hage, C.; Scaravilli, F.; Michaels, L. HIV-associated dilated cardiomyopathy. *Genitourin. Med.* 1991, *67*, 453–9.

290. Best, P.J.M.; Edwards, W.D.; Holmes, D.R.; Lemmer, A. Journal of the American College of Cardiology. *J. Am. Coll. Cardiol.* 1988, *31*, 272A.

291. Phillips, A.N.; Carr, A.; Neuhaus, J.; Visnegarwala, F.; Prineas, R.; Burman, W.J.; Williams, I.; Drummond, F.; Duprez, D.; Belloso, W.H.; et al. Interruption of antiretroviral therapy and risk of cardiovascular disease in persons with HIV-1 infection: Exploratory analyses from the SMART trial. *Antivir. Ther.* 2008, *13*, 177–187.

292. Mazzuca, P.; Caruso, A.; Caccuri, F. HIV-1 infection, microenvironment and endothelial cell dysfunction. *New Microbiol.* 2016, *39*, 1121–7138.

293. Anand, A.R.; Rachel, G.; Parthasarathy, D. HIV Proteins and Endothelial Dysfunction: Implications in Cardiovascular Disease. *Front. Cardiovasc. Med.* 2018, *5*, 185–195.

294. Kalakech, H.; Hibert, P.; Prunier-Mirebeau, D.; Tamareille, S.; Letournel, F.; Macchi, L.; Pinet, F.; Furber, A.; Prunier, F. Risk and safe signaling pathway involvement in apolipoprotein a-i-induced cardioprotection. *PLoS One* 2014, *9*, 1–7.

295. Marincowitz, C.; Genis, A.; Goswami, N.; De Boever, P.; Nawrot, T.S.; Strijdom, H. Vascular endothelial dysfunction in the wake of HIV and ART. *FEBS J.* 2019, *286*, 1256–1270.

296. Calmy, a; Gayet-Ageron, a; Montecucco, F.; Nguyen, a; Mach, F.; Burger, F.; Ubolyam, S.; Carr, a;

Ruxungtham, K.; Hirschel, B.; et al. HIV increases markers of cardiovascular risk: results from a randomized, treatment interruption trial. *Aids* 2009, *23*, 929–939.

297. Gillard, B.K.; Raya, J.L.; Ruiz-Esponda, R.; Iyer, D.; Coraza, I.; Balasubramanyam, A.; Pownall, H.J. Impaired lipoprotein processing in hiv patients on antiretroviral therapy aberrant high-density lipoprotein lipids, stability, and function. *Arterioscler. Thromb. Vasc. Biol.* 2013, *33*, 1714–1721.

298. Melendez, M.M.; McNurlan, M. a; Mynarcik, D.C.; Khan, S.; Gelato, M.C. Endothelial adhesion molecules are associated with inflammation in subjects with HIV disease. *Clin Infect Dis* 2008, *46*, 775–80.

299. Zietz, C.; Hotz, B.; Stürzl, M.; Rauch, E.; Penning, R.; Löhrs, U. Aortic endothelium in HIV-1 infection: chronic injury, activation, and increased leukocyte adherence. *Am. J. Pathol.* 1996, *149*, 1887–98.

300. Kristoffersen, U.S.; Kofoed, K.; Kronborg, G.; Giger, a K.; Kjaer, a; Lebech, a M. Reduction in circulating markers of endothelial dysfunction in HIV-infected patients during antiretroviral therapy. *HIV Med* 2009, *10*, 79–87.

301. Rasmussen, T.A.; Tolstrup, M.; Melchjorsen, J.; Frederiksen, C.A.; Nielsen, U.S.; Langdahl, B.L.; Østergaard, L.; Laursen, A.L. Evaluation of cardiovascular biomarkers In HIV-infected patients switching to abacavir or tenofovir based therapy. *BMC Infect. Dis.* 2011, *11*, 267–277.

302. Mangili, A.; Polak, J.F.; Quach, L.A.; Gerrior, J.; Wanke, C.A. Markers of atherosclerosis and inflammation and mortality in patients with HIV infection. *Atherosclerosis* 2011, *214*, 468–473.

303. Regimens, A.; Individuals, H.; Shikuma, C.M.; Ribaudo, H.J.; Zheng, Y.; Gulick, R.M.; Iii, W.A.M.; Tashima, K.T.; Bastow, B.; Kuritzkes, D.R.; et al. Change in High-Sensitivity C-Reactive Protein Levels Following Initiation of Efavirenz-Based. *AIDS Res. Hum. Retroviruses* 2011, *27*, 461–468.

304. Jiang, J.; Fu, W.; Wang, X.; Lin, P.H.; Yao, Q.; Chen, C. HIV gp120 induces endothelial dysfunction in tumour necrosis factor-alpha-activated porcine and human endothelial cells. *Cardiovasc. Res.* 2010, *87*, 366–374.

305. Dubé, M.P.; Lipshultz, S.E.; Fichtenbaum, C.J.; Greenberg, R.; Schecter, A.D.; Fisher, S.D. Effects of HIV Infection and Antiretroviral Therapy on the Heart and Vasculature. *Circulation* 2008, *118*, 36–41.

306. Wang, T.; Green, L.A.; Gupta, S.K.; Kim, C.; Wang, L.; Almodovar, S.; Flores, S.C.; Prudovsky, I.A.; Jolicoeur, P.; Liu, Z.; et al. Transfer of intracellular HIV Nef to endothelium causes endothelial dysfunction. *PLoS One* 2014, *9*, e91063.

307. Toborek, M.; Lee, Y.W.; Pu, H.; Malecki, A.; Flora, G.; Garrido, R.; Hennig, B.; Bauer, H.C.; Nath, A. HIV-Tat protein induces oxidative and inflammatory pathways in brain endothelium. *J. Neurochem.* 2003, *84*, 169–179.

308. Torriani, F.J.; Komarow, L.; Parker, R.A.; Cotter, B.R.; Currier, J.S.; Dubé, M.P.; Fichtenbaum, C.J.; Gerschenson, M.; Mitchell, C.K.C.C.; Murphy, R.L.; et al. Endothelial function in human immunodeficiency virus-infected antiretroviral-naive subjects before and after starting potent antiretroviral therapy. *J. Am. Coll. Cardiol.* 2008, *52*, 569–576.

309. Lo, J.; Abbara, S.; Shturman, L.; Soni, A.; Wei, J.; Rocha-Filho, J.; Nasir, K.; Grinspoon, S.K. Increased

prevalence of subclinical coronary atherosclerosis detected by coronary computed tomography agiography in HIV-infected men. *Aids* 2010, *24*, 243–253.

310. Ross, A.C.; Armentrout, R.; O'Riordan, M.A.; Storer, N.; Rizk, N.; Harrill, D.; El Bejjani, D.; McComsey, G.A. Endothelial activation markers are linked to HIV status and are independent of antiretroviral therapy and lipoatrophy. *J. Acquir. Immune Defic. Syndr.* 2008, *49*, 499–506.

311. De Larrañaga, G.F.; Bocassi, A.R.; Puga, L.M.; Alonso, B.S.; Benetucci, J.A. Endothelial markers and HIV infection in the era of highly active antiretroviral treatment. *Thromb. Res.* 2003, *110*, 93–98.

312. Koethe, J.R.; Dee, K.; Bian, A.; Shintani, A.; Turner, M.; Bebawy, S.; Sterling, T.R.; Hulgan, T. Circulating Interleukin-6, Soluble CD14, and Other Inflammation Biomarker Levels Differ Between Obese and Nonobese HIV-Infected Adults on Antiretroviral Therapy. *AIDS Res. Hum. Retroviruses* 2013, *29*, 1019–1025.

313. Wohl, D.A.; Arnoczy, G.; Fichtenbaum, C.J.; Campbelle, T.; Taiwo, B.; Hicks, C.; McComsey, C.A.; Koletar, S.; Sax, P.; Tebas, P.; et al. Comparison of cardiovascular disease risk markers in HIV- infected patients receiving abacavir and tenofovir: the nucleoside inflammation, coagulation and endothelial function (NICE) study. *Antiviral Res.* 2014, *19*, 141–147.

314. Aberg, J.A. Cardiovascular Complications in HIV Management: Past, Present, and Future Judith. *J Acquir Immune Defic Syndr* 2010, *50*, 1–5.

315. Dorr, P.; Westby, M.; Dobbs, S.; Griffin, P.; Irvine, B.; Macartney, M.; Mori, J.; Rickett, G.; Smith-Burchnell, C.; Napier, C.; et al. Maraviroc (UK-427,857), a potent, orally bioavailable, and selective small-molecule inhibitor of chemokine receptor CCR5 with broad-spectrum anti-human immunodeficiency virus type 1 activity. *Antimicrob. Agents Chemother.* 2005, *49*, 4721–32.

316. Duffy, P.; Wang, X.; Lin, P.H.; Yao, Q.; Chen, C. HIV Nef Protein Causes Endothelial Dysfunction in Porcine Pulmonary Arteries and Human Pulmonary Artery Endothelial Cells1. *J. Surg. Res.* 2009, *156*, 257–264.

317. Fessel, W.J.; Follansbee, S.E.; Rego, J. High-density lipoprotein cholesterol is low in HIV-infected patients with lipodystrophic fat expansions: implications for pathogenesis of fat redistribution. *AIDS* 2002, *16*, 1785–1789.

318. Floris-Moore, M.; Howard, A.A.; Lo, Y.; Arnsten, J.H.; Santoro, N.; Schoenbaum, E.E. Increased serum lipids are associated with higher CD4 lymphocyte count in HIV-infected women. *HIV Med.* 2006, 7, 421–430.

319. Magkos, F.; Mantzoros, C. Body fat redistribution and metabolic abnormalities in HIV-infected patients on HAART: novel insights into pathophysiology and emerging opportunities for treatment. *Metabolism.* 2011, *60*, 749–753.

320. Lake, J.E.; Currier, J.S. Metabolic disease in HIV infection. *Lancet Infect. Dis.* 2013, *13*, 964–975.

321. Albuquerque, V.M.G.; Zírpoli, J.C.; de Barros Miranda-Filho, D.; Albuquerque, M.D.F.P.M.; Montarroyos, U.R.; de Alencar Ximenes, R.A.; Lacerda, H.R. Risk factors for subclinical atherosclerosis in HIV-infected

patients under and over 40 years: a case-control study. *BMC Infect. Dis.* 2013, *13*, 274–287.

322. Parikh, N.I.; Gerschenson, M.; Bennett, K.; Gangcuangco, L.M.M.; Lopez, M.S.; Mehta, N.N.; Playford, M.P.; Nakamoto, B.K.; Seto, T.B.; Chow, D.C.; et al. Lipoprotein concentration, particle number, size and cholesterol efflux capacity are associated with mitochondrial oxidative stress and function in an HIV positive cohort. *Atherosclerosis* 2015, *239*, 50–4.

323. Deeks, S.G.; Overbaugh, J.; Phillips, A.; Buchbinder, S. HIV infection. *Nat. Rev. Dis. Prim.* 2015, *1*, 15035.

324. Manfredi, R.; Chiodo, F. Disorders of lipid metabolism in patients with HIV disease treated with antiretroviral agents: Frequency, relationship with administered drugs, and role of hypolipidaemic therapy with bezafibrate. *J. Infect.* 2001, *42*, 181–188.

325. Wong, T.Y.; Coresh, J.; Klein, R.; Muntner, P.; Couper, D.J.; Sharrett, a R.; Klein, B.E.K.; Heiss, G.; Hubbard, L.D.; Duncan, B.B. Retinal microvascular abnormalities and renal dysfunction: the atherosclerosis risk in communities study. *J. Am. Soc. Nephrol.* 2004, *15*, 2469–2476.

326. Barber, T.J.; Moyle, G.; Hill, A.; Jagjit Singh, G.; Scourfield, A.; Yapa, H.M.; Waters, L.; Asboe, D.; Boffito, M.; Nelson, M. A cross-sectional study to evaluate the association of hyperbilirubinaemia on markers of cardiovascular disease, neurocognitive function, bone mineral density and renal markers in HIV-1 infected subjects on protease inhibitors. *HIV Clin. Trials* 2016, *17*, 123–30.

327. Grunfeld, C.; Kotler, D.P.; Arnett, D.K.; Falutz, J.M.; Haffner, S.M.; Hruz, P.; Masur, H.; Meigs, J.B.; Mulligan, K.; Reiss, P.; et al. Contribution of metabolic and anthropometric abnormalities to cardiovascular disease risk factors. *Circulation* 2008, *118*, 20–29.

328. Boyvin, L.; Edjème-Aké, A.; M'Boh, G.; Achi, A.; Djaman, J. Macrocytosis anemia, Dyslipidemia and Hyperamylasemia in patients living with HIV in Cote d'Ivoire. *Der Pharm. Lett.* 2016, *8*, 174–180.

329. Vreeman, R.C.; Scanlon, M.L.; McHenry, M.S.; Nyandiko, W.M. The physical and psychological effects of HIV infection and its treatment on perinatally HIV-infected children. *J. Int. AIDS Soc.* 2015, *18*, 20258.

330. Denue, B.A.; Gashau, W.; Ekong, E.; Ngoshe, R.M. Prevalence of non HIV related co-morbidity in HIV patients on Highly Active Anti Retroviral Therapy (HAART): A retrospective study. *Ann. Biol. Res.* 2012, *3*, 3333–3339.

331. Islam, F.M.; Wu, J.; Jansson, J.; Wilson, D.P. Relative risk of cardiovascular disease among people living with HIV: A systematic review and meta-analysis. *HIV Med.* 2012, *13*, 453–468.

332. Wilcox, R.D. D:A:D study shows that HIV therapy affects incidence rate of cardiac diseases. *HIV Clin.* 2008, *20*, 1–3.

333. Friis-møller, N.; Thiébaut, R.; Reiss, P.; Weber, R.; D'Arminio Monforte, A.; De Wit, S.; El-Sadr, W.; Fontas, E.; Worm, S.; Kirk, O.; et al. Predicting the risk of cardiovascular disease in HIV-infected patients: the Data collection on Adverse Effects of Anti-HIV Drugs Study. *Eur. J. Cardiovasc. Prev. Rehabil.* 2010, *17*, 491–501.

334. Hawkins, T. Understanding and managing the adverse effects of antiretroviral therapy. *Antiviral Res.* 2010, *85*, 201–209.

335.   Bretagnol, A.; Barbier, F. Renal failure in HIV-infected patient | Défaillance rénale chez le patient infecté par le VIH. *Reanimation* 2015, *24*, 636–647.

336.   Ingiliz, P.; Valantin, M.A.; Duvivier, C.; Medja, F.; Dominguez, S.; Charlotte, F.; Tubiana, R.; Poynard, T.; Katlama, C.; Lomb??s, A.; et al. Liver damage underlying unexplained transaminase elevation in human immunodeficiency virus-1 mono-infected patients on antiretroviral therapy. *Hepatology* 2009, *49*, 436–442.

337.   Dubé, M.P.; Shen, C.; Mather, K.J.; Waltz, J.; Greenwald, M.; Gupta, S.K. Relationship of body composition, metabolic status, antiretroviral use, and HIV disease factors to endothelial dysfunction in HIV-infected subjects. *AIDS Res. Hum. Retroviruses* 2010, *26*, 847–54.

338.   Gupta, S.K.; Shen, C.; Moe, S.M.; Kamendulis, L.M.; Goldman, M.; Dubé, M.P. Worsening endothelial function with efavirenz compared to protease inhibitors: A 12-month prospective study. *PLoS One* 2012, *7*, e45716.

339.   Guaraldi, G.; Squillace, N.; Stentarelli, C.; Orlando, G.; D'Amico, R.; Ligabue, G.; Fiocchi, F.; Zona, S.; Loria, P.; Esposito, R.; et al. Nonalcoholic fatty liver disease in HIV-infected patients referred to a metabolic clinic: prevalence, characteristics, and predictors. *Clin. Infect. Dis.* 2008, *47*, 250–257.

340.   Ramana, K. V. Effect of Highly Active Antiretroviral Therapy (HAART) on Human Immunodeficiency Virus Disease Pathogenesis and Progression. *Am. J. Public Heal. Res.* 2014, *2*, 68–74.

341.   Dieterich, D.T.; Robinson, P. a; Love, J.; Stern, J.O. Drug-induced liver injury associated with the use of nonnucleoside reverse-transcriptase inhibitors. *Clin. Infect. Dis.* 2004, *38 Suppl 2*, S80–S89.

342.   Preiss, D.; Sattar, N. Non-alcoholic fatty liver disease : an overview of prevalence , diagnosis , pathogenesis and treatment considerations. *Clin. Sci.* 2008, *115*, 141–150.

343.   Vu, C.N.; Ruiz-Esponda, R.; Yang, E.; Chang, E.; Gillard, B.; Pownall, H.J.; Hoogeveen, R.C.; Coraza, I.; Balasubramanyam, A. Altered relationship of plasma triglycerides to HDL cholesterol in patients with HIV/HAART-associated dyslipidemia: Further evidence for a unique form of Metabolic Syndrome in HIV patients. *Metabolism.* 2013, *62*, 1014–1020.

344.   Uysal, S.; Başoğlu, M.T.; Boydak, B.; Gökengin, D. Dyslipidemia and cardiovascular risk assessment in HIV-positive patients | HIV pozitif hastalarda dislipidemi ve kardiyovasküler risk değerlendirilmesi. *Turk Kardiyol. Dern. Ars.* 2017, *45*, 145–152.

345.   Fontas, E.; van Leth, F.; Sabin, C.; Friis-Moller, N.; Rickenbach, M.; Monforte, A.; Kirk, O.; Dupon, M.; Morfeldt, L.; Mateu, S.; et al. Lipid profiles in HIV-infected patients receiving combination antiretroviral therapy: Are different antiretroviral drugs associated with different lipid profiles? *J. Infect. Dis.* 2004, *189*, 1056–1074.

346.   Cowell, A.; Shenoi, S.V.; Kyriakides, T.C.; Friedland, G.; Barakat, L.A. Trends in hospital deaths among human immunodeficiency virus-infected patients during the antiretroviral therapy era, 1995 to 2011. *J. Hosp. Med.* 2015, *10*, 608–14.

347.   Milburn, J.; Jones, R.; Levy, J.B. Renal effects of novel antiretroviral drugs. *Nephrol. Dial. Transplant.* 2017, *32*, 434–439.

348. Estrada, V.; Portilla, J. Dyslipidemia related to antiretroviral therapy. *AIDS Rev.* 2011, *13*, 49–56.

349. Dillon, D.G.; Gurdasani, D.; Riha, J.; Ekoru, K.; Asiki, G.; Mayanja, B.N.; Levitt, N.S.; Crowther, N.J.; Nyirenda, M.; Njelekela, M.; et al. Association of HIV and ART with cardiometabolic traits in sub-Saharan Africa: A systematic review and meta-analysis. *Int. J. Epidemiol.* 2013, *42*, 1754–1771.

350. Willig, A.L.A.L.; Overton, E.T.E.T. Metabolic Complications and Glucose Metabolism in HIV Infection: A Review of the Evidence. *Curr. HIV/AIDS Rep.* 2016, *13*, 289–96.

351. Jain, R.G.; Furfine, E.S.; Pedneault, L.; White, a J.; Lenhard, J.M. Metabolic complications associated with antiretroviral therapy. *Antiviral Res.* 2001, *51*, 151–177.

352. Baker, J. V; Henry, W.K.; Neaton, J.D. The Consequences of HIV Infection and Antiretroviral Therapy Use For Cardiovascular Disease Risk: Shifting Paradigms. *Curr Opin HIV AIDS* 2010, *4*, 176–182.

353. Francisci, D.; Giannini, S.; Baldelli, F.; Leone, M.; Belfiori, B.; Guglielmini, G.; Malincarne, L.; Gresele, P. HIV type 1 infection, and not short-term HAART, induces endothelial dysfunction. *AIDS* 2009, *23*, 589–596.

354. Arildsen, H.; Sørensen, K.E.K.; Ingerslev, J.M.J.; Østergaard, L.J.L.; Laursen, A.L. AL Endothelial dysfunction, increased inflammation, and activated coagulation in HIV-infected patients improve after initiation of highly active antiretroviral therapy. *HIV Med.* 2013, *14*, 1–9.

355. Newby, D.E.; Mannucci, P.M.; Tell, G.S.; Baccarelli, A.A.; Brook, R.D.; Donaldson, K.; Forastiere, F.; Franchini, M.; Franco, O.H.; Graham, I.; et al. Expert position paper on air pollution and cardiovascular disease. *Eur. Heart J.* 2015, *36*, 83–93.

356. Knol, A.B.; de Hartog, J.J.; Boogaard, H.; Slottje, P.; van der Sluijs, J.P.; Lebret, E.; Cassee, F.R.; Wardekker, J.A.; Ayres, J.G.; Borm, P.J.; et al. Expert elicitation on ultrafine particles: likelihood of health effects and causal pathways. *Part. Fibre Toxicol.* 2009, *6*, 1–16.

357. World Health Organization (WHO) WHO | WHO Global Ambient Air Quality Database (update 2018) Available online: https://www.who.int/airpollution/data/cities/en/ (accessed on Jun 20, 2019).

358. US Environmental Protection Agency Air Quality Criteria for Particulate Matter. Available online: file:///C:/Users/Lassa/Downloads/VOL_II_FINAL_PM_AQCD_OCT2004.PDF (accessed on Feb 27, 2019).

359. World Health Organization (WHO). Particulate matter. Available online: http://www.euro.who.int/__data/assets/pdf_file/0019/123085/AQG2ndEd_7_3Particulate-matter.pdf?ua=1 (accessed on Jun 22, 2019).

360. Anderson, J.O.; Thundiyil, J.G.; Stolbach, A. Clearing the Air: A Review of the Effects of Particulate Matter Air Pollution on Human Health. *J. Med. Toxicol.* 2012, *8*, 166–175.

361. Polichetti, G.; Cocco, S.; Spinali, A.; Trimarco, V.; Nunziata, A. Effects of particulate matter (PM10, PM2.5 and PM1) on the cardiovascular system. *Toxicology* 2009, *261*, 1–8.

362. Autrup, H. Ambient air pollution and adverse health effects. *Procedia - Soc. Behav. Sci.* 2010, *2*, 7333–7338.

363. Mills, N.L.; Miller, M.R.; Lucking, A.J.; Beveridge, J.; Flint, L.; Boere, A.J.F.; Fokkens, P.H.; Boon, N.A.; Sandstrom, T.; Blomberg, A.; et al. Combustion-derived nanoparticulate induces the adverse vascular effects of diesel exhaust inhalation. *Eur. Heart J.* 2011, *32*, 2660–71.

364. Nel, A. Air Pollution – Related Illness : Effects of Particles. *Science (80-.).* 2005, *308*, 804–806.

365. Lee, B.-J.J.; Kim, B.; Lee, K. Air pollution exposure and cardiovascular disease. *Toxicol. Res.* 2014, *30*, 71–75.

366. Zanobetti, A.; Schwartz, J. The effect of fine and coarse particulate air pollution on mortality: A national analysis. *Environ. Health Perspect.* 2009, *117*, 898–903.

367. World Health Organization. WHO | Ambient air pollution: Health impacts Available online: https://www.who.int/airpollution/ambient/health-impacts/en/ (accessed on Jun 22, 2019).

368. Cohen, A.J.; Anderson, H.R.; Ostro, B.; Pandey, K.D.; Krzyzanowski, M.; Kunzli, N.; Gutschmidt, K.; Pope, A.; Romieu, I.; Samet, J.M.; et al. The global burden of disease due to outdoor air pollution. *J. Toxicol. Environ. Heal. Part A Curr. Issues* 2005, *68*, 1301–1307.

369. Kaufman, J.D.; Spalt, E.W.; Curl, C.L.; Hajat, A.; Jones, M.R.; Kim, S.-Y.; Vedal, S.; Szpiro, A.A.; Gassett, A.; Sheppard, L.; et al. Advances in Understanding Air Pollution and CVD. *Glob. Heart* 2016, *11*, 343–352.

370. Tong, Y.; Luo, K.; Li, R.; Pei, L.; Li, A.; Yang, M.; Xu, Q. Association between multi-pollutant mixtures pollution and daily cardiovascular mortality: An exploration of exposure-response relationship. *Atmos. Environ.* 2018, *186*, 136–143.

371. Meng, Q.; Richmond-Bryant, J.; Lu, S.E.; Buckley, B.; Welsh, W.J.; Whitsel, E.A.; Hanna, A.; Yeatts, K.B.; Warren, J.; Herring, A.H.; et al. Cardiovascular outcomes and the physical and chemical properties of metal ions found in particulate matter air pollution: A QICAR study. *Environ. Health Perspect.* 2013, *121*, 558–564.

372. Ran, J.; Qiu, H.; Sun, S.; Tian, L. Short-term effects of ambient benzene and TEX (toluene, ethylbenzene, and xylene combined) on cardiorespiratory mortality in Hong Kong. *Environ. Int.* 2018, *117*, 91–98.

373. Brook, R.D.; Rajagopalan, S.; Pope, C.A.; Brook, J.R.; Bhatnagar, A.; Diez-Roux, A. V.; Holguin, F.; Hong, Y.; Luepker, R. V.; Mittleman, M.A.; et al. Particulate matter air pollution and cardiovascular disease: An update to the scientific statement from the american heart association. *Circulation* 2010, *121*, 2331–2378.

374. Nelin, T.D.; Joseph, A.M.; Gorr, M.W.; Wold, L.E. Direct and indirect effects of particulate matter on the cardiovascular system. *Toxicol. Lett.* 2012, *208*, 293–299.

375. Kelly, F.J.; Fussell, J.C. Role of oxidative stress in cardiovascular disease outcomes following exposure to ambient air pollution. *Free Radic. Biol. Med.* 2017, *110*, 345–367.

376. Künzli, N.; Tager, I.B. Air pollution: From lung to heart. *Swiss Med. Wkly.* 2005, *135*, 697–702.

377. Han, M.; Guo, Z.; Li, G.; Sang, N. Nitrogen dioxide inhalation induces genotoxicity in rats. *Chemosphere* 2013, *90*, 2737–2742.

378. Desai, G.; Chu, L.; Guo, Y.; Myneni, A.A.; Mu, L. Biomarkers used in studying air pollution exposure during pregnancy and perinatal outcomes: a review. *Biomarkers Med.* 2017, *22*, 489–501.

379. Clemente, D.B.P.P.; Casas, M.; Vilahur, N.; Begiristain, H.; Bustamante, M.; Carsin, A.-E.E.; Fernández, M.F.; Fierens, F.; Gyselaers, W.; Iñiguez, C.; et al. Prenatal ambient air pollution, placental mitochondrial DNA content, and birth weight in the INMA (Spain) and ENVIRONAGE (Belgium) birth Cohorts. *Environ. Health Perspect.* 2016, *124*, 659–665.

380. Hoxha, M.; Dioni, L.; Bonzini, M.; Pesatori, A.C.; Fustinoni, S.; Cavallo, D.; Carugno, M.; Albetti, B.; Marinelli, B.; Schwartz, J.; et al. Association between leukocyte telomere shortening and exposure to traffic pollution: a cross-sectional study on traffic officers and indoor office workers. *Environ. Heal.* 2009, *8*, 41.

381. Bollati, V.; Baccarelli, A.; Hou, L.; Bonzini, M.; Fustinoni, S.; Cavallo, D.; Byun, H.M.; Jiang, J.; Marinelli, B.; Pesatori, A.C.; et al. Changes in DNA methylation patterns in subjects exposed to low-dose benzene. *Cancer Res.* 2007, *67*, 876–880.

382. Fitzpatrick, A.L.; Kronmal, R.A.; Gardner, J.P.; Psaty, B.M.; Jenny, N.S.; Tracy, R.P.; Walston, J.; Kimura, M.; Aviv, A. Leukocyte telomere length and cardiovascular disease in the cardiovascular health study. *Am. J. Epidemiol.* 2007, *165*, 14–21.

383. Pieters, N.; Janssen, B.G.; Dewitte, H.; Cox, B.; Cuypers, A.; Lefebvre, W.; Smeets, K.; Vanpoucke, C.; Plusquin, M.; Nawrot, T.S. Biomolecular markers within the core axis of aging and particulate air pollution exposure in the elderly: A cross-sectional study. *Environ. Health Perspect.* 2016, *124*, 943–950.

384. Baccarelli, A.A.; Ghosh, S. Enviromental exposure, epigenetics and cardiovascular disease. *Curr Opin Clin Nutr Metab Care* 2012, *4*, 323–329.

385. World Health Organization (WHO). Burden of disease from the joint effects of household and ambient Air pollution for 2016 Summary of results. Available online: http://apps.who.int/gho/data/node.sdg. (accessed on Jun 22, 2019).

386. World Health Organization. Air pollution. Available online: https://www.who.int/airpollution/en/ (accessed on Jun 22, 2019).

387. D'Souza, J.C.; Jia, C.; Mukherjee, B.; Batterman, S. Ethnicity, housing and personal factors as determinants of VOC exposures. *Atmos. Environ.* 2009, *43*, 2884–2892.

388. Temam, S.; Burte, E.; Adam, M.; Antó, J.M.; Basagaña, X.; Bousquet, J.; Carsin, A.-E.; Galobardes, B.; Keidel, D.; Künzli, N.; et al. Socioeconomic position and outdoor nitrogen dioxide (NO2) exposure in Western Europe: A multi-city analysis. *Environ. Int.* 2017, *101*, 117–124.

389. Cole, M.A.; Neumayer, E. Examining the Impact of Demographic Factors on Air Pollution. *Popul. Environ.* 2004, *26*, 5–21.

390. O'Neill, M.S.; Breton, C. V.; Devlin, R.B.; Utell, M.J. Air pollution and health: Emerging information on susceptible populations. *Air Qual. Atmos. Heal.* 2012, *5*, 189–201.

391. Miller, K.A.; Siscovick, D.S.; Sheppard, L.; Shepherd, K.; Sullivan, J.H.; Anderson, G.L.; Kaufman, J.D. Long-Term Exposure to Air Pollution and Incidence of Cardiovascular Events in Women. *N. Engl. J. Med.* 2007, *356*, 447–458.

392. Weuve, J.; Puett, R.C.; Schwartz, J.; Yanosky, J.D.; Laden, F.; Grodstein, F. Exposure to Particulate Air

Pollution and Cognitive Decline in Older Women. *Arch. Intern. Med.* 2012, *172*, 219.

393. Dockery, D.W.; Pope, C.A.I.I.I.; Xu, X.; Spengler, J.D.; Ware, J.H.; Fay, M.E.; Ferris, B.G.; Speizer, F.E. An association between air pollution and mortality in six U.S. cities. *N. Engl. J. Med.* 1993, *329*, 1753–1759.

394. Coogan, P.F.; White, L.F.; Jerrett, M.; Brook, R.D.; Su, J.G.; Seto, E.; Burnett, R.; Palmer, J.R.; Rosenberg, L. Air pollution and incidence of hypertension and diabetes mellitus in black women living in Los Angeles. *Circulation* 2012, *125*, 767–72.

395. Behera, D.; Balamugesh, T. Indoor Air Pollution as a Risk Factor for Lung Cancer in Women Available online: https://www.researchgate.net/profile/Thangakunam_Balamugesh/publication/7814641_Indoor_air_polluti on_as_a_risk_factor_fo_lung_cancer_in_women/links/00b49524edeb1a9e89000000/Indoor-air-pollution-as-a-risk-factor-fo-lung-cancer-in-women.pdf (accessed on Dec 11, 2019).

396. Bruce, N.; Perez-padilla, R.; Albalak, R. Indoor air pollution in developing countries : a major environmental and public health challenge. *Bull. World Health Organ.* 2000, *78*, 1078–1092.

397. Baumgartner, J.; Schauer, J.J.; Ezzati, M.; Lu, L.; Cheng, C.; Patz, J.A.; Bautista, L.E. Indoor Air Pollution and Blood Pressure in Adult Women Living in Rural China. *Environ. Health Perspect.* 2011, *119*, 1390–1395.

398. Morello-Frosch, R.; Shenassa, E.D. The environmental "riskscape" and social inequality: implications for explaining maternal and child health disparities. *Environ. Health Perspect.* 2006, *114*, 1150–3.

399. O'Neill, M.S.; Jerrett, M.; Kawachi, I.; Levy, J.I.; Cohen, A.J.; Gouveia, N.; Wilkinson, P.; Fletcher, T.; Cifuentes, L.; Schwartz, J.; et al. Health, wealth, and air pollution: advancing theory and methods. *Environ. Health Perspect.* 2003, *111*, 1861–70.

400. World Health Organization Environmental Health Inequalities in Europe.

401. Hajat, A.; Hsia, C.; O'Neill, M.S. Socioeconomic Disparities and Air Pollution Exposure: a Global Review. *Curr. Environ. Heal. Reports* 2015, *2*, 440–450.

402. Rooney, M.S.; Arku, R.E.; Dionisio, K.L.; Paciorek, C.; Friedman, A.B.; Carmichael, H.; Zhou, Z.; Hughes, A.F.; Vallarino, J.; Agyei-Mensah, S.; et al. Spatial and temporal patterns of particulate matter sources and pollution in four communities in Accra, Ghana. *Sci. Total Environ.* 2012, *435–436*, 107–114.

403. Harper, S.; Ruder, E.; Roman, H.; Geggel, A.; Nweke, O.; Payne-Sturges, D.; Levy, J. Using Inequality Measures to Incorporate Environmental Justice into Regulatory Analyses. *Int. J. Environ. Res. Public Health* 2013, *10*, 4039–4059.

404. Gilmour, M.I.; Jaakkola, M.S.; London, S.J.; Nel, A.E.; Rogers, C.A. How Exposure to Environmental Tobacco Smoke, Outdoor Air Pollutants, and Increased Pollen Burdens Influences the Incidence of Asthma. *Environ. Health Perspect.* 2006, *114*, 627–633.

405. McAuley, T.R.; Hopke, P.K.; Zhao, J.; Babaian, S. Comparison of the effects of e-cigarette vapor and cigarette smoke on indoor air quality. *Inhal. Toxicol.* 2012, *24*, 850–857.

406. Duarte-Davidson, R.; Courage, C.; Rushton, L.; Levy, L. Benzene in the environment: an assessment of the potential risks to the health of the population. *Occup. Environ. Med.* 2001, *58*, 2–13.

407. Mitra, S.; Ray, B. Patterns and sources of polycyclic aromatic hydrocarbons and their derivatives in indoor air. *Atmos. Environ.* 1995, *29*, 3345–3356.

408. World Health Organization (Regional Office for Europe Review of evidence on health aspects of air pollution – REVIHAAP Project: Technical Report Available online: http://www.euro.who.int/__data/assets/pdf_file/0004/193108/REVIHAAP-Final-technical-report-final-version.pdf?ua=1 (accessed on Dec 10, 2019).

409. Naidoo, R.N.; Robins, T.G.; Batterman, S.; Mentz, G.; Jack, C. Ambient pollution and respiratory outcomes among schoolchildren in Durban, South Africa. *SAJCH South African J. Child Heal.* 2013, *7*, 127–134.

410. White, N.; teWaterNaude, J.; van der Walt, A.; Ravenscroft, G.; Roberts, W.; Ehrlich, R. Meteorologically estimated exposure but not distance predicts asthma symptoms in schoolchildren in the environs of a petrochemical refinery: a cross-sectional study. *Environ. Heal.* 2009, *8*, 45.

411. Venn, A.; Yemaneberhan, H.; Lewis, S.; Parry, E.; Britton, J. Proximity of the home to roads and the risk of wheeze in an Ethiopian population. *Occup. Environ. Med.* 2005, *62*, 376–80.

412. Nkosi, V.; Wichmann, J.; Voyi, K. Mine dumps, wheeze, asthma, and rhinoconjunctivitis among adolescents in South Africa: any association? *Int. J. Environ. Health Res.* 2015, *25*, 583–600.

413. Wichmann, J.; Voyi, K. Ambient Air Pollution Exposure and Respiratory, Cardiovascular and Cerebrovascular Mortality in Cape Town, South Africa: 2001–2006. *Int. J. Environ. Res. Public Health* 2012, *9*, 3978–4016.

414. Naidoo, R.N.; Robins, T.G.; Batterman, S.; Mentz, G.; Jack, C. Ambient pollution and respiratory outcomes among schoolchildren in Durban, South Africa. *SAJCH* 2013, *7*, 127–134.

415. Lawin, H.; Agodokpessi, G.; Ayelo, P.; Kagima, J.; Sonoukon, R.; Mbatchou Ngahane, B.H.; Awopeju, O.; Vollmer, W.M.; Nemery, B.; Burney, P.; et al. A cross-sectional study with an improved methodology to assess occupational air pollution exposure and respiratory health in motorcycle taxi driving. *Sci. Total Environ.* 2016, *550*, 1–5.

416. Shirinde, J.; Wichmann, J.; Voyi, K. Allergic rhinitis, rhinoconjunctivitis and hayfever symptoms among children are associated with frequency of truck traffic near residences: a cross sectional study. *Environ. Health* 2015, *14*, 84.

417. Wichmann, J.; Voyi, K.; Wichmann, J.; Voyi, K. Ambient air pollution exposure and respiratory, cardiovascular and cerebrovascular mortality in Cape Town, South Africa: 2001-2006. *Int. J. Environ. Res. Public Health* 2012, *9*, 3978–4016.

418. Norman, R.; Bradshaw, D. Estimating the burden of disease attributable to indoor air pollution from household use of solid fuels in South Africa in 2000. *SAMJ* 2007, *97*, 1–8.

419. Klausbruckner, C.; Annegarn, H.; Henneman, L.R.F.; Rafaj, P. A policy review of synergies and trade-offs in South African climate change mitigation and air pollution control strategies. *Environ. Sci. Policy* 2016,

57, 70–78.

420. South African Department of Environmental Affairs. Long Term Mitigation Scenarios Strategic Options for South Africa. Available online: https://open.uct.ac.za/bitstream/handle/11427/16804/Scenario_Building_Team_Long_Term_Mitigation_2 007.pdf?sequence=1&isAllowed=y (accessed on Mar 8, 2019).

421. South African Goverment. Air quality standards and objectives: At a glance. Available online: https://www.environment.gov.za/sites/default/files/docs/stateofair_executive_iaiquality_standardsonjectiv es.pdf (accessed on Jun 22, 2019).

422. Wichmann, J.; Voyi, K. Ambient air pollution exposure and respiratory, cardiovascular and cerebrovascular mortality in Cape Town, South Africa: 2001-2006. *Int. J. Environ. Res. Public Health* 2012, *9*, 3978–4016.

423. World Health Organization. Air Pollution, Climate and Health. Available online: https://www.who.int/sustainable-development/AirPollution_Climate_Health_Factsheet.pdf (accessed on Dec 10, 2019).

424. Sweijd, N.A.; Wright, C.Y.; Westwood, A.; Rouault, M.; Landman, W.A.; MacKenzie, M.L.; Nuttall, J.J.C.; Mahomed, H.; Cousins, T.; Winter, K.; et al. Climate change is catchy – But when will it really hurt? *South African Med. J.* 2015, *105*, 1018–1023.

425. Kinney, P.L. Climate Change, Air Quality, and Human Health. *Am. J. Prev. Med.* 2008, *35*, 459–467.

426. McMichael, A.J. Globalization, Climate Change, and Human Health. *N. Engl. J. Med.* 2013, *368*, 1335–1343.

427. WHO WHO Indoor Air Quality Guidelines. *WHO Indoor Air Qual. Guidel. Househ. Fuel Combust.* 2014, 3–4.

428. World Health Organization. World Health Organization guidelines for indoor air quality: Household fuel combustion. Available online: http://www.who.int/indoorair/guidelines/hhfc/HHFC_guidelines.pdf.

429. South African Government Republic of South Africa, Government Gazette, National Environment Management: Air Quality Act, 2004. Available online: https://www.golegal.co.za/wp-content/uploads/2018/02/National-Environmental-Management-Air-Quality-Act-39-of-2004.pdf (accessed on Oct 10, 2019).

430. South African Government NATIONAL FRAMEWORK: FOR AIR QUALITY MANAGEMENT IN THE REPUBLIC OF SOUTH AFRICA Available online: https://cer.org.za/wp-content/uploads/2018/10/National-Environmental-Managerment-Air-Quality-Act-39-2004-the-2017-National-20181026-GGN-41996-01144.pdf (accessed on Dec 18, 2019).

431. Western Cape Government Air Quality Management Plan Available online: https://www.westerncape.gov.za/eadp/files/atoms/files/Western Cape Air Quality Management Plan.pdf (accessed on Dec 17, 2019).

432. EU Report; Kotzias, D.; Koistinen, K.; Kephalopoulos, S.; Schlitt, C.; Carrer, P.; Maroni, M.; Jantunen, M.; Cochet, C.; Kirchner, S.; et al. The INDEX project Critical Appraisal of the Setting and Implementation of

Indoor Exposure Limits in the EU. Available online: http://publications.jrc.ec.europa.eu/repository/bitstream/JRC31622/1622 - INDEX EUR 21590 EN report%5B1%5D.pdf (accessed on Jul 17, 2019).

433. U.S. National Library of Medicine;; National Center for Biotechnology Information PubChem Available online: https://pubchem.ncbi.nlm.nih.gov/ (accessed on Aug 14, 2019).

434. Kilabuko, J.H.; Matsuki, H.; Nakai, S. Air quality and acute respiratory illness in biomass fuel using homes in Bagamoyo, Tanzania. *Int. J. Environ. Res. Public Health* 2007, *4*, 39–44.

435. Kirenga, B.; Meng, Q.; van Gemert, F.; Aanyu-Tukamuhebwa, H.; Chavannes, N.; Katamba, A.; Obai, G.; Molen, T.; Schwander, S.; Mohsenin, V.; et al. The State of Ambient Air Quality in Two Ugandan Cities: A Pilot Cross-Sectional Spatial Assessment. *Int. J. Environ. Res. Public Health* 2015, *12*, 8075–8091.

436. Kumie, A.; Emmelin, A.; Wahlberg, S.; Berhane, Y.; Ali, A.; Mekonen, E.; Worku, A.; Brandstrom, D. Sources of variation for indoor nitrogen dioxide in rural residences of Ethiopia. *Environ. Heal.* 2009, *8*, 51.

437. Van Bronswijk, J.E.M.H.; Doevendans, C.H.; Smeets, J.J.A.M.; Verbeke, J. USO-Built Report Series 1. Available online: www.uso.tue.nl (accessed on Jun 16, 2019).

438. Leung, R.; Lam, C.W.; Chan, A.; Lee, M.; Chan, I.H.; Pang, S.W.; Lai, C.K. Indoor environment of residential homes in Hong Kong--relevance to asthma and allergic disease. *Clin. Exp. Allergy* 1998, *28*, 585–90.

439. Josipovic, M.; Annegarn, H.J.; Kneen, M.A.; Pienaar, J.J.; Piketh, S.J. Concentrations, distributions and critical level exceedance assessment of SO2, NO2 and O3 in South Africa. *Environ. Monit. Assess.* 2010, *171*, 181–196.

440. Lourens, A.S.M.; Butler, T.M.; Beukes, J.P.; van Zyl, P.G.; Beirle, S.; Wagner, T.K.; Heue, K.-P.; Pienaar, J.J.; Fourie, G.D.; Lawrence, M.G. Re-evaluating the NO2 hotspot over the South African Highveld. *S. Afr. J. Sci.* 2012, *108*, 83–91.

441. Vanker, A.; Barnett, W.; Nduru, P.M.; Gie, R.P.; Sly, P.D.; Zar, H.J. Home environment and indoor air pollution exposure in an African birth cohort study. *Sci. Total Environ.* 2015, *536*, 362–367.

442. South African Western Cape Government. Western Cape state of air quality management report : 2013. Available online: https://www.westerncape.gov.za/eadp/files/atoms/files/SoAR 2014.pdf (accessed on Jul 1, 2019).

443. Wicking-Baird, M.C.; De Villiers, M.G.; Dutkiewicz, R.K. Cape Town Brown Haze Study Available online: https://open.uct.ac.za/bitstream/handle/11427/.../Wicking-Baird_ERC_1997.pdf (accessed on Aug 12, 2019).

444. World Health Organization. Ambient air pollution: Pollutants. Available online: https://www.who.int/airpollution/ambient/pollutants/en/ (accessed on Jun 22, 2019).

445. Ölker, C.; Siese, A.; Stumpf, S.; Müller, B.; Gemsa, D.; Garn, H. Impaired superoxide radical production by bronchoalveolar lavage cells from NO2-exposed rats. *Free Radic. Biol. Med.* 2004, *37*, 977–987.

446. Kelly, F.J.; Tetley, T.D. Nitrogen dioxide depletes uric acid and ascorbic acid but not glutathione from lung

lining fluid. *Biochem. J.* 1997, *325*, 95.

447. Devalia, J.L.; Sapsford, R.J.; Cundell, D.R.; Rusznak, C.; Campbellt, A.M.; Davies, R.J. Human bronchial epithelial cell dysfunction following in vitro exposure to nitrogen dioxide. *Eur Respir J .•* 1993, *6*, 1308–1316.

448. Schierhorn, K.; Zhang, M.; Matthias, C.; Kunkel, G. Influence of Ozone and Nitrogen Dioxide on Histamine and Interleukin Formation in a Human Nasal Mucosa Culture System. *Am. J. Respir. Cell Mol. Biol.* 1999, *20*, 1013–1019.

449. Ayyagari, V.N.; Januszkiewicz, A.; Nath, J. Effects of Nitrogen Dioxide on the Expression of Intercellular Adhesion Molecule-1, Neutrophil Adhesion, and Cytotoxicity: Studies in Human Bronchial Epithelial Cells. *Inhal. Toxicol.* 2007, *19*, 181–194.

450. Ayyagari, V.N.; Januszkiewicz, A.; Nath, J. Pro-inflammatory responses of human bronchial epithelial cells to acute nitrogen dioxide exposure. *Toxicology* 2004, *197*, 148–163.

451. Witschi, H. Ozone, nitrogen dioxide and lung cancer: A review of some recent issues and problems. *Toxicology* 1988, *48*, 1–20.

452. Takamichi, I.; Keiji, F.; Masaru, S. Experimental studies on tumor promotion by nitrogen dioxide. *Toxicology* 1991, *67*, 211–225.

453. World Health Organization. Household Fuel Combustion: WHO Gguidelines For Indoor Air Quality. Available online: https://apps.who.int/iris/bitstream/handle/10665/141496/9789241548885_eng.pdf?sequence=1 (accessed on Jun 22, 2019).

454. Brauer, M.; Amann, M.; Burnett, R.T.; Cohen, A.; Dentener, F.; Ezzati, M.; Henderson, S.B.; Krzyzanowski, M.; Martin, R. V; Dingenen, R. Van; et al. Exposure Assessment for Estimation of the Global Burden of Disease Attributable to Outdoor Air Pollution. *Environ. Sci. Technol.* 2012, *46*, 652–660.

455. Ji, Y.; Zhao, J.; Terazono, H.; Misawa, K.; Levitt, N.P.; Li, Y.; Lin, Y.; Peng, J.; Wang, Y.; Duan, L.; et al. Reassessing the atmospheric oxidation mechanism of toluene. *Proc. Natl. Acad. Sci. U. S. A.* 2017, *114*, 8169–8174.

456. Na, K.; Kim, Y.P.; Moon, K.C. Diurnal characteristics of volatile organic compounds in the Seoul atmosphere. *Atmos. Environ.* 2003, *37*, 733–742.

457. Maliszewska-Kordybach, B. Sources, Concentrations, Fate and Effects of Polycyclic Aromatic Hydrocarbons (PAHs) in the Environment. Part A: PAHs in Air Available online: https://www.researchgate.net/profile/Barbara_Maliszewska-Kordybach/publication/267736764_Sources_Concentrations_Fate_and_Effects_of_Polycyclic_Aromatic_Hydrocarbons_PAHs_in_the_Environment_Part_A_PAHs_in_Air/links/5458b6ee0cf26d5090ac63c2/Sources-Concentr (accessed on Jun 16, 2019).

458. Class, T.; Ballschmiter, K. Chemistry of organic traces in air. *J. Atmos. Chem.* 1988, *6*, 35–46.

459. Argacha, J.F.; Bourdrel, T.; van de Borne, P. Ecology of the cardiovascular system: A focus on air-related

environmental factors. *Trends Cardiovasc. Med.* 2018, *28*, 112–126.

460. Collart, P.; Dubourg, D.; Levêque, A.; Sierra, N.B.; Coppieters, Y. Short-term effects of nitrogen dioxide on hospital admissions for cardiovascular disease in Wallonia, Belgium. *Int. J. Cardiol.* 2018, *255*, 231–236.

461. World Health Organization. Ambient Air Pollution: A global assessment of exposure and burden of disease. Available online: https://www.who.int/phe/publications/air-pollution-global-assessment/en/ (accessed on Feb 26, 2019).

462. Corn, M. *Handbook of Hazardous Materials.*; Elsevier Science, 1993; ISBN 0323139558.

463. Kansal, A. Sources and reactivity of NMHCs and VOCs in the atmosphere: A review. *J. Hazard. Mater.* 2009, *166*, 17–26.

464. EPA's Integrated Risk Information Systems. Toluene Available online: https://www.epa.gov/iris (accessed on May 25, 2019).

465. U.S. Department of Health and Human Services. Toxicological Profile For Ethylbenzene. Available online: https://www.atsdr.cdc.gov/toxprofiles/tp110.pdf (accessed on Jun 23, 2019).

466. Kotin, P.; Falk, H.L.; Busser, R. Distribution, Retention, and Elimination of C14-3,4-Benzpyrene After Administration to Mice and Rats. *JNCI J. Natl. Cancer Institute.* 1986, *23*, 541–555.

467. Wolff, R.K.; Bond, J.A.; Sun, J.D.; Henderson, R.F.; Harkema, J.R.; Griffith, W.C.; Mauderly, J.L.; McClellan, R.O. Effects of adsorption of benzo[a]pyrene onto carbon black particles on levels of DNA adducts in lungs of rats exposed by inhalation. *Toxicol. Appl. Pharmacol.* 1989, *97*, 289–299.

468. Qu, Q.; Shore, R.; Li, G.; Su, L.; Jin, X.; Melikian, A.A.; Roy, N.; Chen, L.C.; Wirgin, I.; Cohen, B.; et al. Biomarkers of benzene: Urinary metabolites in relation to individual genotype and personal exposure. *Chem. Biol. Interact.* 2005, *153–154*, 85–95.

469. Wilbur, S.; Bosch, S.; Services, H. Interaction profile for Benzene, Toluene, Ethylbenzene, and Xylenes (BTEX). Available online: https://www.atsdr.cdc.gov/interactionprofiles/ip05.html (accessed on Jun 17, 2019).

470. Bergamaschi, E.; Brustolin, A.; De Palma, G.; Manini, P.; Mozzoni, P.; Andreoli, R.; Cavazzini, S.; Mutti, A. Biomarkers of dose and susceptibility in cyclists exposed to monoaromatic hydrocarbons. *Toxicol. Lett.* 1999, *108*, 241–247.

471. Rappaport, S.M.; Kim, S.; Lan, Q.; Vermeulen, R.; Waidyanatha, S.; Zhang, L.; Li, G.; Yin, S.; Hayes, R.B.; Rothman, N.; et al. Evidence that humans metabolize benzene via two pathways. *Environ. Health Perspect.* 2009, *117*, 946–952.

472. Hormozi, M.; Mirzaei, R.; Nakhaee, A.; Payandeh, A.; Izadi, S.; Dehghan Haghighi, J.; Rahimpoor, R. Quantification of urinary metabolites of toluene and xylene isomers as biological indices of occupational exposure in printing industry workers. *Heal. Scope* 2019, e82962.

473. Stevens, J.F.; Maier, C.S. Acrolein: Sources, metabolism, and biomolecular interactions relevant to human health and disease. *Mol. Nutr. Food Res.* 2008, *52*, 7–25.

474. Angerer, J.; Schildbach, M.; Krämer, A. S- p -Toluylmercapturic acid in the urine of workers exposed to

toluene: a new biomarker for toluene exposure. *Arch. Toxicol.* 1997, 72, 119–123.

475. Jacobson, G.A.; McLean, S. Biological Monitoring of Low Level Occupational Xylene Exposure and the Role of Recent Exposure. *Ann. Occup. Hyg.* 2003, *47*, 331–336.

476. Fustinoni, S.; Rossella, F.; Campo, L.; Mercadante, R.; Bertazzi, P.A. Urinary BTEX, MTBE and naphthalene as biomarkers to gain environmental exposure profiles of the general population. *Sci. Total Environ.* 2010, *408*, 2840–2849.

477. Ranzi, A.; Fustinoni, S.; Erspamer, L.; Campo, L.; Gatti, M.G.; Bechtold, P.; Bonassi, S.; Trenti, T.; Goldoni, C.A.; Bertazzi, P.A.; et al. Biomonitoring of the general population living near a modern solid waste incinerator: A pilot study in Modena, Italy. *Environ. Int.* 2013, *61*, 88–97.

478. McConnell, E.E.; United Nations Environment Programme.; International Labour Organisation.; World Health Organization. Benzene Available online: http://www.inchem.org/documents/ehc/ehc/ehc150.htm (accessed on Jun 22, 2019).

479. Kuranchie, F.A.; Angnunavuri, P.N.; Attiogbe, F.; Nerquaye-Tetteh, E.N. Occupational exposure of benzene, toluene, ethylbenzene and xylene (BTEX) to pump attendants in Ghana: Implications for policy guidance. *Cogent Environ. Sci.* 2019, *5*, 1–18.

480. United Nations Environmental Program.; International Labour Organisation.; World Health Organization.; International Program on Chemical Safety. Toluene. Available online: http://www.inchem.org/documents/ehc/ehc/ehc52.htm (accessed on Jun 22, 2019).

481. U.S. Environmental Protection Agency *Toxicological Review of Toluene*; 2005;

482. World Health Organization. Ethylbenzene. Available online: http://www.inchem.org/documents/ehc/ehc/ehc186.htm (accessed on Jun 22, 2019).

483. United Nations Environment Programme. Xylenes. Available online: http://www.inchem.org/documents/ehc/ehc/ehc190.htm (accessed on Jun 22, 2019).

484. U.S. Department of Health and Human Services: Food and Drug Administration. Guidance for Industry: Estimating the Maximum Safe Starting Dose in Initial Clinical Trials for Therapeutics in Adult Healthy Volunteers. *Pharmacol. Toxicol.* 2005, 1–27.

485. South African Goverment. Air quality. Available online: https://www.environment.gov.za/sites/default/files/reports/environmentoutlook_chapter10.pdf (accessed on Jun 22, 2019).

486. Schwartz, J.; Coull, B.; Laden, F.; Ryan, L. The effect of dose and timing of dose on the association between airborne particles and survival. *Environ. Health Perspect.* 2008, *116*, 64–69.

487. Puett, R.C.; Schwartz, J.; Hart, J.E.; Yanosky, J.D.; Speizer, F.E.; Suh, H.; Paciorek, C.J.; Neas, L.M.; Laden, F. Chronic particulate exposure, mortality, and coronary heart disease in the Nurses' Health Study. *Am. J. Epidemiol.* 2008, *168*, 1161–1168.

488. Auchincloss, A.H.; Diez Roux, A. V.; Dvonch, J.T.; Brown, P.L.; Barr, R.G.; Daviglus, M.L.; Goff, D.C.; Kaufman, J.D.; O'Neill, M.S.; O'Neill, M.S. Associations between recent exposure to ambient fine

particulate matter and blood pressure in the multi-ethnic study of atherosclerosis (MESA). *Environ. Health Perspect.* 2008, *116*, 486–491.

489. Wing, S.E.; Bandoli, G.; Telesca, D.; Su, J.G.; Ritz, B. Chronic exposure to inhaled, traffic-related nitrogen dioxide and a blunted cortisol response in adolescents. *Environ. Res.* 2018, *163*, 201–207.

490. Araujo, J.A. Particulate air pollution, systemic oxidative stress, inflammation, and atherosclerosis. *Air Qual. Atmos. Heal.* 2011, *4*, 79–93.

491. Dellinger, B.; Pryor, W.A.; Cueto, R.; Squadrito, G.L.; Hegde, V.; Deutsch, W.A. Role of Free Radicals in the Toxicity of Airborne Fine Particulate Matter. *Chem. Res. Toxicol.* 2001, *14*, 1371–1377.

492. Donaldson, K.; Stone, V.; Borm, P.J.A.; Jimenez, L.A.; Gilmour, P.S.; Schins, R.P.F.; Knaapen, A.M.; Rahman, I.; Faux, S.P.; Brown, D.M.; et al. Oxidative stress and calcium signaling in the adverse effects of environmental particles (PM10). *Free Radic. Biol. Med.* 2003, *34*, 1369–1382.

493. Sørensen, M.; Daneshvar, B.; Hansen, M.; Dragsted, L.O.; Hertel, O.; Knudsen, L.; Loft, S. Personal PM2.5 exposure and markers of oxidative stress in blood. *Environ. Health Perspect.* 2003, *111*, 161–165.

494. Pope, C.A.; Burnett, R.T.; Thun, M.J.; Calle, E.E.; Krewski, D.; Ito, K.; Thurston, G.D. Lung cancer, cardiopulmonary mortality, and long-term exposure to fine particulate air pollution. *JAMA* 2002, *287*, 1132–41.

495. Brook, R.D.; Brook, J.R.; Rajagopalan, S. Air pollution: the "Heart" of the problem. *Curr. Hypertens. Rep.* 2003, *5*, 32–39.

496. Schwartz, J. Air pollution and blood markers of cardiovascular risk. *Environ. Health Perspect.* 2001, *109*, 405–409.

497. Dioni, L.; Hoxha, M.; Nordio, F.; Bonzini, M.; Tarantini, L.; Albetti, B.; Savarese, A.; Schwartz, J.; Bertazzi, P.A.; Apostoli, P.; et al. Effects of short-term exposure to inhalable particulate matter on telomere length, telomerase expression, and telomerase methylation in steel workers. *Environ. Health Perspect.* 2011, *119*, 622–627.

498. Mirabello, L.; Huang, W.-Y.; Wong, J.Y.Y.; Chatterjee, N.; Reding, D.; David Crawford, E.; De Vivo, I.; Hayes, R.B.; Savage, S.A. The association between leukocyte telomere length and cigarette smoking, dietary and physical variables, and risk of prostate cancer. *Aging Cell* 2009, *8*, 405–413.

499. Demarini, D.M. Genotoxicity biomarkers associated with exposure to traffic and near-road atmospheres: A review. *Mutagenesis* 2013, *28*, 485–505.

500. Snyder, R.; Hedli, C.C. An overview of benzene metabolism. *Environ. Health Perspect.* 1996, *104*, 1165–1171.

501. Brunekreef, B.; Holgate, S.T. Air pollution and health. *Lancet* 2002, *360*, 1233–1242.

502. Genc, S.; Zadeoglulari, Z.; Fuss, S.H.; Genc, K. The adverse effects of air pollution on the nervous system. *J. Toxicol.* 2012, *2012*, 1–23.

503. Kim, J.W.; Park, S.; Lim, C.W.; Lee, K.; Kim, B. The role of air pollutants in initiating liver disease. *Toxicol. Res.* 2014, *30*, 65–70.

504. Chen, Z.; Salam, M.T.; Toledo-Corral, C.; Watanabe, R.M.; Xiang, A.H.; Buchanan, T.A.; Habre, R.; Bastain, T.M.; Lurmann, F.; Wilson, J.P.; et al. Ambient Air Pollutants Have Adverse Effects on Insulin and Glucose Homeostasis in Mexican Americans. *Diabetes Care* 2016, *39*, 547–54.

505. Afsar, B.; Elsurer Afsar, R.; Kanbay, A.; Covic, A.; Ortiz, A.; Kanbay, M. Air pollution and kidney disease: review of current evidence. *Clin. Kidney J.* 2019, *12*, 19–32.

506. Bind, Marie-Abele; Baccareli, Andrea; Zanobetti, Antonella; Tarantini, Letizia; Suh, Helen; Vokonas, Pantel; Schwartz, J.; Bind, M.-A.; Baccarelli, A.; Zanobetti, A.; Tarantini, L.; Suh, H.; Vokonas, P.; Schwartz, J. Air pollution and markers of coagulation, inflammation and endothelial function: Associations and epigene-environment interactions in an elderly cohort. *Epidemiology* 2013, *23*, 332–340.

507. Bourdrel, T.; Bind, M.-A.; Béjot, Y.; Morel, O.; Argacha, J.-F. Cardiovascular effects of air pollution. *Arch. Cardiovasc. Dis.* 2017, *110*, 634–642.

508. Norman, R.; Bradshaw, D.; Schneider, M.; Pieterse, D.; Groenewald, P. *Revised Burden of Disease Estimates for the Comparative Risk Factor Assessment , South Africa 2000*; 2006;

509. Mayosi, B.M.; Flisher, A.J.; Lalloo, U.G.; Sitas, F.; Tollman, S.M.; Bradshaw, D. The burden of non-communicable diseases in South Africa. *Lancet* 2009, *374*, 934–947.

510. SANAC *LET OUR ACTIONS COUNT: Reflections on NSP 2012-2016 and moving forward to NSP 2017-2022*; Pretoria, 2016;

511. Joint United Nations Programme on HIV/AIDS (UNAIDS) HIV estimates from 1990 to 2017 2018.

512. Kassebaum, N.J.; Bertozzi-Villa, A.; Coggeshall, M.S.; Shackelford, K. a.; Steiner, C.; Heuton, K.R.; Gonzalez-Medina, D.; Barber, R.; Huynh, C.; Dicker, D.; et al. Global, regional, and national levels and causes of maternal mortality during 1990-2013: a systematic analysis for the Global Burden of Disease Study 2013. *Lancet* 2014, *6736*, 1–25.

513. Cappuccio, F.P.; Miller, M.A. Cardiovascular disease and hypertension in sub-Saharan Africa: burden, risk and interventions. *Intern. Emerg. Med.* 2016, *11*, 299–305.

514. UNDP Sustainable Development Goals | UNDP in South Africa Available online: https://www.za.undp.org/content/south_africa/en/home/sustainable-development-goals.html (accessed on Dec 17, 2019).

515. Glesby, M.J. Cardiovascular complications of HIV infection. *Top. Antivir. Med.* 2016, *24*.

516. Hemkens, L.G.; Bucher, H.C. HIV infection and cardiovascular disease. *Eur. Heart J.* 2014, *35*, 1373–1381.

517. Kamin, D.S.; Grinspoon, S.K. Cardiovascular disease in HIV-positive patients. *Aids* 2005, *19*, 641–652.

518. Rabkin, M.; Mutiti, A.; Chung, C.; Zhang, Y.; Wei, Y.; El-Sadr, W.M. Missed opportunities to address cardiovascular disease risk factors amongst adults attending an urban HIV clinic in South Africa. *PLoS ONE.* 2015, *10*, e0140298.

519. Mashinya, F.; Alberts, M.; Van geertruyden, J.-P.; Colebunders, R. Assessment of cardiovascular risk factors in people with HIV infection treated with ART in rural South Africa: A cross sectional study. *AIDS*

Res. Ther. 2015, *12*, 42–52.

520. Western Cape Government Western Cape Government: Overview | Western Cape Government Available online: https://www.westerncape.gov.za/your_gov/70 (accessed on Jul 27, 2019).

521. Everson, F.; De Boever, P.; Nawrot, T.S.; Goswami, N.; Mthethwa, M.; Webster, I.; Martens, D.S.; Mashele, N.; Charania, S.; Kamau, F.; et al. Personal NO2 and Volatile Organic Compounds Exposure Levels are Associated with Markers of Cardiovascular Risk in Women in the Cape Town Region of South Africa. *Int. J. Environ. Res. Public Health* 2019, *16*, 2–18.

522. Cocheo, V.; Boaretto, C.; Sacco, P.; Baoretto, C.; Sacco, P. High uptake rate radial diffusive sampler suitable for both solvent and thermal desorption. *Am. Ind. Hyg. Assoc. J.* 1996, *57*, 897–904.

523. Kot-Wasik, A.; Zabiegała, B.; Urbanowicz, M.; Dominiak, E.; Wasik, A.; Namieśnik, J. Advances in passive sampling in environmental studies. *Anal. Chim. Acta* 2007, *602*, 141–163.

524. Ockenden, W.A.; Jaward, F.M.; Jones, K.C. Atmospheric sampling of persistent organic pollutants: needs, applications and advances in passive air sampling techniques. *ScientificWorldJournal.* 2001, *1*, 557–75.

525. AEA Energy & Environment. *Diffusion Tubes for Ambient NO 2 Monitoring: Practical Guidance for Laboratories and Users Report to Defra and the Devolved Administrations ED48673043 Issue 1a.*; 2008;

526. Targa, J.; Loader, A. Diffusion tubes for ambient NO2 monitoring: Practical guidance for laboratories and Users. Available online: https://uk-air.defra.gov.uk/assets/documents/reports/cat05/0802141004_NO2_WG_PracticalGuidance_Issue1a.pdf (accessed on Mar 11, 2019).

527. Palmes, E.D.; Gunnison, A.F.; DiMattio, J.; Tomczyk, C. Personal sampler for nitrogen dioxide. *Am. Ind. Hyg. Assoc. J.* 1976, *37*, 570–577.

528. ScienceDirect Chemiluminescence - an overview | ScienceDirect Topics Available online: https://www.sciencedirect.com/topics/materials-science/chemiluminescence (accessed on Jul 24, 2019).

529. McAlary, T.; Groenevelt, H.; Disher, S.; Arnold, J.; Seethapathy, S.; Sacco, P.; Crump, D.; Schumacher, B.; Hayes, H.; Johnson, P.; et al. Passive sampling for volatile organic compounds in indoor air-controlled laboratory comparison of four sampler types. *Environ. Sci. Process. Impacts* 2015, *17*, 896–905.

530. Pegas, P.N.; Alves, C.A.; Evtyugina, M.G.; Nunes, T.; Cerqueira, M.; Franchi, M.; Pio, C.A.; Almeida, S.M.; Freitas, M.C. Indoor air quality in elementary schools of Lisbon in spring. *Environ. Geochem. Health* 2011, *33*, 455–468.

531. Geneva *Waist Circumference and Waist-Hip Ratio: Report of a WHO Expert Consultation*; ISBN 9789241501491.

532. World Health Organization Expert Committee on Physical Status Physical Status: The use and interpretation of anthropometry. Available online: http://www.who.int/childgrowth/publications/physical_status/en/ (accessed on Apr 9, 2019).

533. World Health Organization Hypertension Available online: https://www.who.int/news-room/fact-sheets/detail/hypertension (accessed on Aug 21, 2019).

534. Ridker PM; Hennekens CH; Buring JE; Rifai, N. C-reactive protein and other markers of inflammation in the prediction of cardiovascular disease in women. *N Engl J Med* 2000, *342*, 836–843.

535. Beltrán, L.M.; Rubio-Navarro, A.; Amaro-Villalobos, J.M.; Egido, J.; García-Puig, J.; Moreno, J.A. Influence of immune activation and inflammatory response on cardiovascular risk associated with the human immunodeficiency virus. *Vasc. Health Risk Manag.* 2015, *11*, 35–48.

536. Roche. Total Cholesterol. Available online: http://labogids.sintmaria.be/sites/default/files/files/chol2_2016-12_v12.pdf (accessed on Jul 19, 2019).

537. Roche. HDL Cholesterol. Available online: http://labogids.sintmaria.be/sites/default/files/files/hdlc4_2017-07_v2.pdf (accessed on Jul 19, 2019).

538. Roche. LDL Cholesterol. Available online: http://labogids.sintmaria.be/sites/default/files/files/ldlc3_2017-06_v3.pdf (accessed on Jul 19, 2019).

539. Roche. Triglycerides. Available online: http://labogids.sintmaria.be/sites/default/files/files/trigl_2017-11_v12.pdf (accessed on Jul 19, 2019).

540. National Institues of Health. High Blood Cholesterol Evaluation Treatment Detection: Expert Panel on Detection, Evaluation, and Treatment of High Blood Cholesterol in Adults. Available online: https://www.nhlbi.nih.gov/files/docs/resources/heart/atp-3-cholesterol-full-report.pdf (accessed on Jul 19, 2019).

541. Nordestgaard, B.G.; Varbo, A. Triglycerides and cardiovascular disease. *Lancet* 2014, *384*, 626–635.

542. Rader, D.J.; Hovingh, G.K. HDL and cardiovascular disease. *Lancet* 2014, *384*, 618–625.

543. Duro, M.; Sarmento-Castro, R.; Almeida, C.; Medeiros, R.; Rebelo, I. Lipid profile changes by high activity anti-retroviral therapy. *Clin. Biochem.* 2013, *46*, 740–744.

544. Jones, R.; Sawleshwarkar, S.; Michailids, C.; Jackson, A.; Mandalia, S.; Stebbing, J.; Bower, M.; Nelson, M.; Gazzard, B.G.; Moyle, G.J. Impact of antiretroviral choice on hypercholesterolaemia events: The role of the nucleoside reverse transcriptase inhibitor backbone. *HIV Med.* 2005, *6*, 396–402.

545. Gong, K.W.; Zhao, W.; Li, N.; Barajas, B.; Kleinman, M.; Sioutas, C.; Horvath, S.; Lusis, A.J.; Nel, A.; Araujo, J.A. Air-pollutant chemicals and oxidized lipids exhibit genome-wide synergistic effects on endothelial cells. *Genome Biol.* 2007, *8*, R149.

546. Heart & Stroke Foundation South Africa Cholesterol | Heart & Stroke Foundation South Africa Available online: http://www.heartfoundation.co.za/cholesterol/ (accessed on Jul 27, 2019).

547. Assmann, G. At what levels of total low- or high-density lipoprotein cholesterol should diet/drug therapy be initiated? European guidelines. *Am. J. Cardiol.* 1990, *65*, 11–15.

548. Strategies for the prevention of coronary heart disease: A policy statement of the European Atherosclerosis Society. *Eur. Heart J.* 1987, *8*, 77–88.

549. Roche. Fasting Glucose. Available online: http://labogids.sintmaria.be/sites/default/files/files/gluc3_hk_2019-02_v14.pdf (accessed on Jul 19, 2019).

550. Roche. HbA1c. Available online: http://labogids.sintmaria.be/sites/default/files/files/.

551. Youn, J.-Y.; Siu, K.L.; Lob, H.E.; Itani, H.; Harrison, D.G.; Cai, H. Role of vascular oxidative stress in obesity and metabolic syndrome. *Diabetes* 2014, *63*, 2344–55.

552. Hutcheson, R.; Rocic, P. The Metabolic Syndrome , Oxidative Stress , Environment , and Cardiovascular Disease : The Great Exploration. *Exp. Diabetes Res.* 2012, *2012*.

553. Consensus Committee Consensus statement on the worldwide standardization of the hemoglobin A1C measurement: the American Diabetes Association, European Association for the Study of Diabetes, International Federation of Clinical Chemistry and Laboratory Medicine, and the International Diabetes Federation. *Diabetes Care* 2007, *30*, 2399–400.

554. American Diabetes Association, A.D. Diagnosis and classification of diabetes mellitus. *Diabetes Care* 2010, *33 Suppl 1*, S62-9.

555. Lothar, T. Diagnose Indikation und Bewertung von Laborbefunden für die medizinische Diagnostik 8. Auflage TH-Books Labor und Available online: https://www.flick-werk.de/images/Auszug Labor und Diagnose - 8te Auflage.pdf (accessed on Jul 19, 2019).

556. Seaton, A.; Soutar, A.; Crawford, V.; Elton, R.; McNerlan, S.; Cherrie, J.; Watt, M.; Agius, R.; Stout, R. Particulate air pollution and the blood. *Thorax* 1999, *54*, 1027–32.

557. Kim, M.-Y.; Jee, S.H.; Yun, J.E.; Baek, S.J.; Lee, D.-C. Hemoglobin concentration and risk of cardiovascular disease in Korean men and women - the Korean heart study. *J. Korean Med. Sci.* 2013, *28*, 1316–22.

558. Chonchol, M.; Nielson, C. Hemoglobin levels and coronary artery disease. *Am. Heart J.* 2008, *155*, 494–498.

559. Obirikorang, C.; Yeboah, F.A. Blood haemoglobin measurement as a predictive indicator for the progression of HIV/AIDS in resource-limited setting. *J. Biomed. Sci.* 2009, *16*, 1–7.

560. United States Environmental Protection Agency Biologica Markers of Exposure to Benzene: Research Project Database. Available online: https://cfpub.epa.gov/ncer_abstracts/index.cfm/fuseaction/display.abstractDetail/abstract/886 (accessed on Aug 21, 2019).

561. World Health Organization (WHO) Haemoglobin concentrations for the diagnosis of anaemia and assessment of severity Available online: https://www.who.int/vmnis/indicators/haemoglobin.pdf (accessed on Jul 27, 2019).

562. Szasz, G. New substrates for measuring gamma-glutamyl transpeptidase activity. *Z. Klin. Chem. Klin. Biochem.* 1974, *12*, 228.

563. Roche. γ-Glutamyltransferase. Available online: http://labogids.sintmaria.be/sites/default/files/files/ggt-2_2017-01_v10.pdf (accessed on Jul 20, 2019).

564. Ndrepepa, G.; Kastrati, A. Gamma-glutamyl transferase and cardiovascular disease. *Ann. Transl. Med.* 2016, *4*, 481.

565. Osakunor, D.N.M.; Obirikorang, C.; Fianu, V.; Asare, I.; Dakorah, M. Hepatic Enzyme Alterations in HIV

Patients on Antiretroviral Therapy: A Case-Control Study in a Hospital Setting in Ghana. *PLoS One* 2015, *10*, e0134449.

566. Zhang, Z.; Guo, C.; Chang, L.-Y.; Bo, Y.; Lin, C.; Tam, T.; Hoek, G.; Wong, M.C.; Chan, T.-C.; Lau, A.K.; et al. Long-term exposure to ambient fine particulate matter and liver enzymes in adults: a cross-sectional study in Taiwan. *Occup. Environ. Med.* 2019, *76*, 488–494.

567. van Beek, J.H.D.A.; de Moor, M.H.M.; Geels, L.M.; Sinke, M.R.T.; de Geus, E.J.C.; Lubke, G.H.; Kluft, C.; Neuteboom, J.; Vink, J.M.; Willemsen, G.; et al. The association of alcohol intake with γ-glutamyl transferase (GGT) levels: evidence for correlated genetic effects. *Drug Alcohol Depend.* 2014, *134*, 99–105.

568. Roche. Albumin. Available online: http://labogids.sintmaria.be/sites/default/files/files/albt2_tq_urine-csf_2014-01_v11.pdf (accessed on Jul 20, 2019).

569. Roche. Creatinine. Available online: http://labogids.sintmaria.be/sites/default/files/files/ (accessed on Jul 20, 2019).

570. Kim, N.H.; Hyun, Y.Y.; Lee, K.-B.; Chang, Y.; Rhu, S.; Oh, K.-H.; Ahn, C. Environmental Heavy Metal Exposure and Chronic Kidney Disease in the General Population. *J. Korean Med. Sci.* 2015, *30*, 272.

571. Phair, J.; Palella, F. Renal disease in HIV-infected individuals. *Curr. Opin. HIV AIDS* 2011, *6*, 285–9.

572. Agewall, S.; Wikstrand, J.; Ljungman, S.; Fagerberg, B. Usefulness of microalbuminuria in predicting cardiovascular mortality in treated hypertensive men with and without diabetes mellitus. Risk Factor Intervention Study Group. *Am. J. Cardiol.* 1997, *80*, 164–9.

573. Mann, J.F.E.; Yi, Q.-L.; Gerstein, H.C. Albuminuria as a predictor of cardiovascular and renal outcomes in people with known atherosclerotic cardiovascular disease. *Kidney Int.* 2004, *66*, S59–S62.

574. Rifkin, D.E.; Katz, R.; Chonchol, M.; Fried, L.F.; Cao, J.; de Boer, I.H.; Siscovick, D.S.; Shlipak, M.G.; Sarnak, M.J. Albuminuria, impaired kidney function and cardiovascular outcomes or mortality in the elderly. *Nephrol. Dial. Transplant.* 2010, *25*, 1560–1567.

575. Sung, K.; Ryu, S.; Lee, J.; Lee, S.H.; Cheong, E.; Hyun, Y.; Lee, K.; Kim, H.; Byrne, C.D. Urine Albumin/Creatinine Ratio Below 30 mg/g is a Predictor of Incident Hypertension and Cardiovascular Mortality. *J. Am. Heart Assoc.* 2016, *5*.

576. UK Renal Association Proteinuria - The Renal Association Available online: https://renal.org/information-resources/the-uk-eckd-guide/proteinuria/ (accessed on Sep 5, 2019).

577. Matsushita, K.; Mahmoodi, B.K.; Woodward, M.; Emberson, J.R.; Jafar, T.H.; Jee, S.H.; Polkinghorne, K.R.; Shankar, A.; Smith, D.H.; Tonelli, M.; et al. Comparison of Risk Prediction Using the CKD-EPI Equation and the MDRD Study Equation for Estimated Glomerular Filtration Rate. *JAMA* 2012, *307*, 1941–1951.

578. Pugliese, G.; Solini, A.; Bonora, E.; Orsi, E.; Zerbini, G.; Giorgino, F.; Cavalot, F.; Pontiroli, A.E.; Baroni, M.G.; Morano, S.; et al. The Chronic Kidney Disease Epidemiology Collaboration (CKD-EPI) equation provides a better definition of cardiovascular burden associated with CKD than the Modification of Diet in

Renal Disease (MDRD) Study formula in subjects with type 2 diabetes. *Atherosclerosis* 2011, *218*, 194–199.

579.   Chen, S.-Y.; Chu, D.-C.; Lee, J.-H.; Yang, Y.-R.; Chan, C.-C. Traffic-related air pollution associated with chronic kidney disease among elderly residents in Taipei City. *Environ. Pollut.* 2018, *234*, 838–845.

580.   Ibrahim, F.; Hamzah, L.; Jones, R.; Nitsch, D.; Sabin, C.; Post, F.A. Comparison of CKD-EPI and MDRD to estimate baseline renal function in HIV-positive patients. *Nephrol. Dial. Transplant.* 2012, *27*, 2291–2297.

581.   Levey, A.S.; Stevens, L.A.; Schmid, C.H.; Zhang, Y.L.; Iii, A.F.C.; Feldman, H.I.; Kusek, J.W.; Eggers, P.; Lente, F. Van; Greene, T. A New Equation to Estimate Glomerular Filtration Rate. *Ann. Intern. Med.* 2009, *150*, 604–612.

582.   South African Goverment. Nephrological and Urological Disorders. Available online: http://www.globalrph.com/index_renal.htm (accessed on Jul 28, 2019).

583.   Du Plessis, M. Chronic kidney disease: Updated recommendations on definition and classification. Available online: https://www.ampath.co.za/pdfs/ampathchats/pathchat-18-chronic-kidney-disease-updated-recommendations-on-definition-and-classification.pdf (accessed on Jul 28, 2019).

584.   BeckmanCoulter. CYTOMICS FC 500 MPL. Available online: https://www.analis.be/site/objects/media/0/0/6/1/7/0061774_media/media1.pdf (accessed on Jul 21, 2019).

585.   Who *Laboratory Guidelines for enumerating CD4 T Lymphocytes in the context of HIV/AIDS*; 2007; ISBN 9789290222989.

586.   World Health Organization. WHO: Prequalification of Diagnostics Programme. Available online: https://www.who.int/diagnostics_laboratory/evaluations/pq-list/hiv-vrl/160530_0147_046_00_public_report_v1_final.pdf (accessed on Jul 21, 2019).

587.   Roche COBAS ® AmpliPrep/COBAS ® TaqMan ® HIV-1 Test, version 2.0.

588.   World Health Organization. HIV Treatment and Care: WHO Treatment initiation. Available online: www.who.int/hiv (accessed on Jul 28, 2019).

589.   WHO | What's new in treatment monitoring: viral load and CD4 testing. *WHO* 2017.

590.   R & D Systems. Human Premixed Multi-Analyte Kit Magnetic Luminex ® Assay. Available online: www.RnDSystems.com (accessed on Jul 22, 2019).

591.   QIAGEN Blood Mini Handbook QIAGEN Sample and Assay Technologies cat 51304 Available online: https://www.qiagen.com/us/products/discovery-translational-research/dna-rna-purification/dna/qiaamp-dna-mini-kit/#orderinginformation.

592.   Martens, D.S.; Plusquin, M.; Gyselaers, W.; De Vivo, I.; Nawrot, T.S. Maternal pre-pregnancy body mass index and newborn telomere length. *BMC Med.* 2016, *14*, 148.

593.   Liu, Z.; Wu, J.; Xie, Z.; Liu, S.; Fan-Havard, P.; Huang, T.H.-M.; Plass, C.; Marcucci, G.; Chan, K.K. Quantification of Regional DNA Methylation by Liquid Chromatography/Tandem Mass Spectrometry. *Anal.*

Biochem. 2009, *391*, 106–113.

594. Janssen, B.G.; Munters, E.; Pieters, N.; Smeets, K.; Cox, B.; Cuypers, A.; Fierens, F.; Penders, J.; Vangronsveld, J.; Gyselaers, W.; et al. Placental mitochondrial DNA content and particulate air pollution during in utero life. *Environ. Health Perspect.* 2012, *120*, 1–9.

595. Gonzalez-Hunt, C.P.; Rooney, J.P.; Ryde, I.T.; Anbalagan, C.; Joglekar, R.; Meyer, J.N. PCR-Based Analysis of Mitochondrial DNA Copy Number, Mitochondrial DNA Damage, and Nuclear DNA Damage. *Curr. Protoc. Toxicol.* 2016, *67*, 11–25.

596. Montpetit, A.J.; Alhareeri, A.A.; Montpetit, M.; Starkweather, A.R.; Elmore, L.W.; Filler, K.; Mohanraj, L.; Burton, C.W.; Menzies, V.S.; Lyon, D.E.; et al. Telomere length: a review of methods for measurement. *Nurs. Res.* 2014, *63*, 289–99.

597. Ducos, P.; Gaudin, R.; Robert, A.; Francin, J.M.; Maire, C. Improvement in HPLC analysis of urinary trans, trans-muconic acid, a promising substitute for phenol in the assessment of benzene exposure. *Int. Arch. Occup. Environ. Health* 1990, *62*, 529–534.

598. Tharnpoophasiam, Prapin Kongtip, P.; Wongwit, W.; Fungladda, W.; Kitayaporn, D. Simultaneous determination of trans,trans muconic acid and s-phynylmercapturic acid by HPLC and its application. *Southeast Asian J Trop Med Public Heal.* 2004, *35*, 717–723.

599. Thijssen, D.H.J.; Black, M.A.; Pyke, K.E.; Padilla, J.; Atkinson, G.; Harris, R.A.; Parker, B.; Widlansky, M.E.; Tschakovsky, M.E.; Green, D.J. Assessment of flow-mediated dilation in humans: a methodological and physiological guideline. *Am. J. Physiol. Heart Circ. Physiol.* 2011, *300*, H2-12.

600. Harris, R.A.; Nishiyama, S.K.; Wray, D.W.; Richardson, R.S. Ultrasound Assessment of Flow-Mediated Dilation. *Hypertension* 2010, *55*, 1075–1085.

601. Prabhakar, P.; Zhang, H.; Chen, D.; Faber, J.E. Genetic variation in retinal vascular patterning predicts variation in pial collateral extent and stroke severity. *Angiogenesis* 2015, *18*, 97–114.

602. Knudtson, M.D.; Lee, K.E.; Hubbard, L.D.; Wong, T.Y.; Klein, R.; Klein, B.E.K. Revised formulas for summarizing retinal vessel diameters. *Curr. Eye Res.* 2003, *27*, 143–149.

603. Ong, Y.T.; De Silva, D.A.; Cheung, C.Y.; Chang, H.M.; Chen, C.P.; Wong, M.C.; Wong, T.Y.; Ikram, M.K. Microvascular structure and network in the retina of patients with ischemic stroke. *Stroke* 2013, *44*, 2121–2127.

604. Seedat, Y.K.; Rayner, B.L. The abridged South African hypertension guideline 2011. *South African Fam. Pract.* 2013, *55*, 111–116.

605. Rivera, S.; Briggs, W.; Qian, D.; Sattler, F.R. Levels of HIV RNA are quantitatively related to prior weight loss in HIV-associated wasting. *J. Acquir. Immune Defic. Syndr. Hum. Retrovirol.* 1998, *17*, 411–8.

606. Coodley, G.O.; Loveless, M.O.; Merrill, T.M. The HIV wasting syndrome: a review. *J. Acquir. Immune Defic. Syndr.* 1994, *7*, 681–94.

607. Koethe, J.R.; Jenkins, C.A.; Lau, B.; Shepherd, B.E.; Justice, A.C.; Tate, J.P.; Buchacz, K.; Napravnik, S.; Mayor, A.M.; Horberg, M.A.; et al. Rising Obesity Prevalence and Weight Gain Among Adults Starting

Antiretroviral Therapy in the United States and Canada. *AIDS Res. Hum. Retroviruses* 2016, *32*, 50–58.

608. Grinspoon, S.; Mulligan, K. Weight Loss and Wasting in Patients Infected with Human Immunodeficiency Virus. *Clin. Infect. Dis.* 2003, *36*, S69–S78.

609. Wheeler, D.A.; Gibert, C.L.; Launer, C.A.; Muurahainen, N.; Elion, R.A.; Abrams, D.I.; Bartsch, G.E. Weight loss as a predictor of survival and disease progression in HIV infection. Terry Beirn Community Programs for Clinical Research on AIDS. *J. Acquir. Immune Defic. Syndr. Hum. Retrovirol.* 1998, *18*, 80–5.

610. Hazan, U.; Romero, I.; Canello O, R.; Valente, S.; Perrin, V.; Mariot, V.; Dumonceaux, J.; Gerhardt, C.C.; Strosberg, A.D.; Couraud, P.-O.; et al. Human adipose cells express CD4, CXCR4, CCR5 and receptors: a new target cell type for the immunodeficiency virus-1? *FASEB J.* 2002, *16*, 1254–1256.

611. Giralt, M.; Domingo, P.; Villarroya, F. Adipose tissue biology and HIV-infection. *Best Pract. Res. Clin. Endocrinol. Metab.* 2011, *25*, 487–499.

612. Koethe, J.R.; Hulgan, T.; Niswender, K. Adipose tissue and immune function: A review of evidence relevant to HIV infection. *J. Infect. Dis.* 2013, *208*, 1194–1201.

613. McDermott, A.Y.; Shevitz, A.; Knox, T.; Roubenoff, R.; Kehayias, J.; Gorbach, S. Effect of highly active antiretroviral therapy on fat, lean, and bone mass in HIV-seropositive men and women. *Am. J. Clin. Nutr.* 2001, *74*, 679–686.

614. Koethe, J.R.; Jenkins, C.A.; Lau, B.; Shepherd, B.E.; Wester, W.; Rebeiro, P.F.; Silverberg, M.J.; Thorne, J.E.; Gill, J.; Mayor, A.M.; et al. Higher Time-Updated Body Mass Index: Association With Improved CD4+ Cell Recovery on HIV Treatment. *J. Acquir. Immune Defic. Syndr.* 2016, *73*, 197–204.

615. Sharpstone, D.; Gazzard, B. Gastrointestinal manifestations of HIV infection. *Lancet* 1996, *348*, 379–383.

616. Feasey, N.A.; Healey, P.; Gordon, M.A. Review article: the aetiology, investigation and management of diarrhoea in the HIV-positive patient. *Aliment. Pharmacol. Ther.* 2011, *34*, 587–603.

617. Park, D.; Lee, J.-H.; Han, S. Underweight: another risk factor for cardiovascular disease?: A cross-sectional 2013 Behavioral Risk Factor Surveillance System (BRFSS) study of 491,773 individuals in the USA. *Medicine (Baltimore).* 2017, *96*, e8769.

618. Lee, F.J.; Carr, A. Dyslipidemia in HIV-Infected Patients. In; Humana Press, Totowa, NJ, 2015; pp. 155–176.

619. Feeney, E.R.; Mallon, P.W.G. HIV and HAART-Associated Dyslipidemia. *Open Cardiovasc. Med. J.* 2011, *5*, 49–63.

620. Bernal, E.; Masiá, M.; Padilla, S.; Gutiérrez, F. High-Density Lipoprotein Cholesterol in HIV-Infected Patients: Evidence for an Association with HIV-1 Viral Load, Antiretroviral Therapy Status, and Regimen Composition. *AIDS Patient Care STDS* 2008, *22*, 569–575.

621. Grunfeld, C.; Kotler, D.P.; Hamadeh, R.; Tierney, A.; Wang, J.; Pierson, R.N. Hypertriglyceridemia in the acquired immunodeficiency syndrome. *Am. J. Med.* 1989, *86*, 27–31.

622. Scott R. Penzak, Susan K. Chuck, S.K.C. Hyperlipidemia Associated with HIV Protease Inhibitor Use: Pathophysiology, Prevalence, Risk Factors and Treatment. *Scand. J. Infect. Dis.* 2000, *32*, 111–123.

623. Lee, G.A.; Rao, M.N.; Grunfeld, C. The effects of HIV protease inhibitors on carbohydrate and lipid metabolism. *Curr. HIV/AIDS Rep.* 2005, *2*, 39–50.

624. Green, M.L. Evaluation and management of dyslipidemia in patients with HIV infection. *J. Gen. Intern. Med.* 2002, *17*, 797–810.

625. Crane, H.M.; Grunfeld, C.; Willig, J.H.; Mugavero, M.J.; Van Rompaey, S.; Moore, R.; Rodriguez, B.; Feldman, B.J.; Lederman, M.M.; Saag, M.S.; et al. Impact of NRTIs on lipid levels among a large HIV-infected cohort initiating antiretroviral therapy in clinical care. *AIDS* 2011, *25*, 185–95.

626. Armstrong, C.; Liu, E.; Okuma, J.; Spiegelman, D.; Guerino, C.; Njelekela, M.; Grinspoon, S.; Fawzi, W.; Hawkins, C. Dyslipidemia in an HIV-positive antiretroviral treatment-naive population in Dar es Salaam, Tanzania. *J. Acquir. Immune Defic. Syndr.* 2011, *57*, 141–5.

627. Rasheed, S.; Yan, J.S.; Lau, A.; Chan, A.S. HIV Replication Enhances Production of Free Fatty Acids, Low Density Lipoproteins and Many Key Proteins Involved in Lipid Metabolism: A Proteomics Study. *PLoS One* 2008, *3*, e3003.

628. Sandler, N.G.; Zhang, X.; Bosch, R.J.; Funderburg, N.T.; Choi, A.I.; Robinson, J.K.; Fine, D.M.; Coombs, R.W.; Jacobson, J.M.; Landay, A.L.; et al. Sevelamer Does Not Decrease Lipopolysaccharide or Soluble CD14 Levels But Decreases Soluble Tissue Factor, Low-Density Lipoprotein (LDL) Cholesterol, and Oxidized LDL Cholesterol Levels in Individuals With Untreated HIV Infection. *J. Infect. Dis.* 2014, *210*, 1549–1554.

629. Funderburg, N.T.; Mehta, N.N. Lipid Abnormalities and Inflammation in HIV Inflection. *Curr. HIV/AIDS Rep.* 2016, *13*, 218–225.

630. Rose, H.; Hoy, J.; Woolley, I.; Tchoua, U.; Bukrinsky, M.; Dart, A.; Sviridov, D. HIV infection and high density lipoprotein metabolism. *Atherosclerosis* 2008, *199*, 79–86.

631. Asztalos, B.F.; Mujawar, Z.; Morrow, M.P.; Grant, A.; Pushkarsky, T.; Wanke, C.; Shannon, R.; Geyer, M.; Kirchhoff, F.; Sviridov, D.; et al. Circulating Nef Induces Dyslipidemia in Simian Immunodeficiency Virus–Infected Macaques by Suppressing Cholesterol Efflux. *J. Infect. Dis.* 2010, *202*, 614–623.

632. Riddler, S.A.; Smit, E.; Cole, S.R.; Li, R.; Chmiel, J.S.; Dobs, A.; Palella, F.; Visscher, B.; Evans, R.; Kingsley, L.A. Impact of HIV Infection and HAART on Serum Lipids in Men. *JAMA* 2003, *289*, 2978.

633. Villarroya, F.; Domingo, P.; Giralt, M. Drug-induced lipotoxicity: Lipodystrophy associated with HIV-1 infection and antiretroviral treatment. *Biochim. Biophys. Acta - Mol. Cell Biol. Lipids* 2010, *1801*, 392–399.

634. Reiss, P.; Sabin, C.A.; Weber, R.; El-sadr, W.; Wit, S. De; Universi-, C.H.; Kirk, O.; Fontas, E.; Hos-, C.; Law, M.G.; et al. Class of Antiretroviral Drugs and the Risk of Myocardial Infarction. *new Engl. J. o f Med.* 2007, *356*, 1723–1735.

635. Tadewos, A.; Addis, Z.; Ambachew, H.; Banerjee, S. Prevalence of dyslipidemia among HIV-infected patients using first-line highly active antiretroviral therapy in Southern Ethiopia: a cross-sectional comparative group study. *AIDS Res. Ther.* 2012, *9*, 31–39.

636. Xiao, J.; Han, N.; Yang, D.; Zhao, H. Liver steatosis in Chinese HIV-infected patients with

hypertriglyceridemia: characteristics and independent risk factors. *Virol. J.* 2013, *10*, 261–269.

637.   Oh, J.; Hegele, R. a. HIV-associated dyslipidaemia: pathogenesis and treatment. *Lancet Infect. Dis.* 2007, *7*, 787–796.

638.   Acosta, E.P. Pharmacokinetic Enhancement of Protease Inhibitors. *JAIDS J. Acquir. Immune Defic. Syndr.* 2002, *29*, S11–S18.

639.   Signorini, D.J.H.P.; Monteiro, M.C.M.; Andrade, M.D.F.C. De; Signorini, D.J.H.P.; Eyer-Silva, W. de A.; Pontes Signorini, D.J.H.; Miranda Monteiro, M.C.; de Andrade, M. de F.C.; Signorini, D.J.H.P.; Eyer-Silva, W. de A. What should we know about metabolic syndrome and lipodystrophy in AIDS? *Rev. Assoc. Med. Bras.* 2012, *58*, 70–75.

640.   Meininger, G.; Hadigan, C.; Laposata, M.; Brown, J.; Rabe, J.; Louca, J.; Aliabadi, N.; Grinspoon, S. Elevated concentrations of free fatty acids are associated with increased insulin response to standard glucose challenge in human immunodeficiency virus-infected subjects with fat redistribution. *Metabolism.* 2002, *51*, 260–6.

641.   Lans, A.A.J.J. van der; Hoeks, J.; Brans, B.; Vijgen, G.H.E.J.; Visser, M.G.W.; Vosselman, M.J.; Hansen, J.; Jörgensen, J.A.; Wu, J.; Mottaghy, F.M.; et al. Cold acclimation recruits human brown fat and increases nonshivering thermogenesis. *J. Clin. Invest.* 2013, *123*, 3395–3403.

642.   Thayer, Z.M.; Kuzawa, C.W. Biological memories of past environments: Epigenetic pathways to health disparities. *Epigenetics* 2011, *6*, 798–803.

643.   Brouwer, I.A.; Wanders, A.J.; Katan, M.B. Effect of Animal and Industrial Trans Fatty Acids on HDL and LDL Cholesterol Levels in Humans – A Quantitative Review. *PLoS One* 2010, *5*, e9434.

644.   Van Wijk, J.P.H.; Cabezas, M.C. Hypertriglyceridemia, metabolic syndrome, and cardiovascular disease in HIV-infected patients: Effects of antiretroviral therapy and adipose tissue distribution. *Int. J. Vasc. Med.* 2012, *2012*, 1–14.

645.   Dubé, M.P. Disorders of glucose metabolism in patients infected with human immunodeficiency virus. *Clin. Infect. Dis.* 2000, *31*, 1467–1475.

646.   Lesi, O.A.; Soyebi, K.S.; Eboh, C.N. Fatty liver and hyperlipidemia in a cohort of HIV-positive Africans on highly active antiretroviral therapy. *J. Natl. Med. Assoc.* 2009, *101*, 151–155.

647.   van der Valk, M.; Bisschop, P.H.; Romijn, J. a; Ackermans, M.T.; Lange, J.M.; Endert, E.; Reiss, P.; Sauerwein, H.P. Lipodystrophy in HIV-1-positive patients is associated with insulin resistance in multiple metabolic pathways. *AIDS* 2001, *15*, 2093–2100.

648.   Palmer, C.S.C.S.; Cherry, C.L.C.L.; Sada-Ovalle, I.; Singh, A.; Crowe, S.M.S.M. Glucose Metabolism in T Cells and Monocytes: New Perspectives in HIV Pathogenesis. *EBioMedicine* 2016, *6*, 31–41.

649.   Martinez, S.S.; Campa, A.; Bussmann, H.; Moyo, S.; Makhema, J.; Huffman, F.G.; Williams, O.D.; Essex, M.; Marlink, R.; Baum, M.K. Effect of BMI and fat mass on HIV disease progression in HIV-infected, antiretroviral treatment-naïve adults in Botswana. *Br. J. Nutr.* 2016, *115*, 1–8.

650.   Belperio, P.S.; Rhew, D.C. Prevalence and outcomes of anemia in individuals with human

immunodeficiency virus: a systematic review of the literature. *Am. J. Med.* 2004, *116*, 27–43.

651. Redig, A.J.; Berliner, N. Pathogenesis and clinical implications of HIV-related anemia in 2013. *Hematol. Am. Soc. Hematol. Educ. Progr.* 2013, *2013*, 377–81.

652. Zauli, G.; Re, M.C.; Visani, G.; Furlini, G.; Mazza, P.; Vignoli, M.; La Placa, M. Evidence for a Human Immunodeficiency Virus Type 1-Mediated Suppression ofUninfected Hematopoietic (CD34+) Cells in AIDS Patients. *J. Infect. Dis.* 1992, *166*, 710–716.

653. Spivak, J.L.; Barnes, D.C.; Fuchs, E.; Quinn, T.C. Serum immunoreactive erythropoietin in HIV-infected patients. *JAMA* 1989, *261*, 3104–7.

654. Solages, A.; Vita, J.A.; Thornton, D.J.; Murray, J.; Heeren, T.; Craven, D.E.; Horsburgh, C.R. Endothelial Function in HIV-Infected Persons. *HIV/AIDS* 2006, *02118*, 1325–1332.

655. Mlisana, K.; Auld, S.C.; Grobler, A.; van Loggerenberg, F.; Williamson, C.; Iriogbe, I.; Sobieszczyk, M.E.; Abdool Karim, S.S.; Team, for the C.A.I.S. Anaemia in Acute HIV-1 Subtype C Infection. *PLoS One* 2008, *3*, e1626.

656. Remacha, A.F.; Rierasp, A.; Cadafalch, J.; Gimferrer, E. Vitamin B-12 abnormalities in HIV-infected patients. *Eur. J. Haematol.* 2009, *47*, 60–64.

657. Ciaffoni, S.; Luzzati, R.; Roata, C.; Turrini, A.; Antonello, O.; Aprili, G. Presence and significance of cold agglutinins in patients with HIV infection. *Haematologica* 77, 233–6.

658. Parrish, D.D.; Blevins, M.; Megazzini, K.M.; Shepherd, B.E.; Mohammed, M.Y.; Wester, C.W.; Vermund, S.H.; Aliyu, M.H. Haemoglobin recovery among HIV-1 infected patients on zidovudine-based antiretroviral therapy and other regimens in north-central Nigeria. *Int. J. STD AIDS* 2014, *25*, 355–9.

659. Gedefaw, L.; Yemane, T.; Sahlemariam, Z.; Yilma, D. Anemia and risk factors in HAART naïve and HAART experienced HIV positive persons in south west Ethiopia: a comparative study. *PLoS One* 2013, *8*, e72202.

660. Takuva, S.; Maskew, M.; Brennan, A.T.; Sanne, I.; Macphail, A.P.; Fox, M.P. Anemia among HIV-Infected Patients Initiating Antiretroviral Therapy in South Africa: Improvement in Hemoglobin regardless of Degree of Immunosuppression and the Initiating ART Regimen. *J. Trop. Med.* 2013, *2013*, 162950.

661. Soriano, V.; Barreiro, P.; Sherman, K.E. The changing epidemiology of liver disease in HIV patients. *AIDS Rev.* 2013, *15*, 25–31.

662. Barve, S.; Kapoor, R.; Moghe, A.; Ramirez, J.A.; Eaton, J.W.; Gobejishvili, L.; Joshi-Barve, S.; McClain, C.J. Focus on the liver: alcohol use, highly active antiretroviral therapy, and liver disease in HIV-infected patients. *Alcohol Res. Health* 2010, *33*, 229–36.

663. Vallet-Pichard, A.; Mallet, V.; Pol, S. Nonalcoholic Fatty Liver Disease and HIV Infection. *Semin. Liver Dis.* 2012, *32*, 158–166.

664. Mayanja, B.N.; Kasamba, I.; Levin, J.; Namakoola, I.; Kazooba, P.; Were, J.; Kaleebu, P.; Munderi, P.; Nalwadda, J.; Nakibuuka, G.; et al. COHORT PROFILE: The Complications of Long-Term Antiretroviral Therapy study in Uganda (CoLTART), a prospective clinical cohort. *AIDS Res. Ther.* 2017, *14*.

665. Azu, O.O.; Jegede, A.I.; Ugochukwu, O.; Onanuga, I.O.; Kharwa, S.; Naidu, E.C. Hepatic

histomorphological and biochemical changes following highly active antiretroviral therapy in an experimental animal model: Does Hypoxis hemerocallidea exacerbate hepatic injury? *Toxicol. Reports* 2016, *3*, 114–122.

666. Lucas, G.M.; Ross, M.J.; Stock, P.G.; Shlipak, M.G.; Wyatt, C.M.; Gupta, S.K.; Atta, M.G.; Wools-Kaloustian, K.K.; Pham, P.A.; Bruggeman, L.A.; et al. Clinical Practice Guideline for the Management of Chronic Kidney Disease in Patients Infected With HIV: 2014 Update by the HIV Medicine Association of the Infectious Diseases Society of America. *Clin. Infect. Dis.* 2014, *59*, e96–e138.

667. Cristelli, M.P.; Cofán, F.; Rico, N.; Trullàs, J.C.; Manzardo, C.; Agüero, F.; Bedini, J.L.; Moreno, A.; Oppenheimer, F.; Miro, J.M.; et al. Estimation of renal function by CKD-EPI versus MDRD in a cohort of HIV-infected patients: a cross-sectional analysis. *BMC Nephrol.* 2017, *18*, 58–65.

668. George, E.; Lucas, G.M.; Nadkarni, G.N.; Fine, D.M.; Moore, R.; Atta, M.G. Kidney function and the risk of cardiovascular events in HIV-1-infected patients. *AIDS* 2010, *24*, 387–94.

669. Menezes, A.M.; Torelly, J.; Real, L.; Bay, M.; Poeta, J.; Sprinz, E. Prevalence and Risk Factors Associated to Chronic Kidney Disease in HIV-Infected Patients on HAART and Undetectable Viral Load in Brazil. *PLoS One* 2011, *6*, e26042.

670. Kalyesubula, R.; Perazella, M.A. Nephrotoxicity of HAART. *AIDS Res. Treat.* 2011, *2011*, 562790.

671. Choi, A.I.; Li, Y.; Deeks, S.G.; Grunfeld, C.; Volberding, P.A.; Shlipak, M.G. Association between kidney function and albuminuria with cardiovascular events in HIV-infected persons. *Circulation* 2010, *121*, 651–8.

672. Lo, J.C.; Go, A.S.; Chandra, M.; Fan, D.; Kaysen, G.A. GFR, Body Mass Index, and Low High-Density Lipoprotein Concentration in Adults With and Without CKD. *Am. J. Kidney Dis.* 2007, *50*, 552–558.

673. Panwar, B.; Hanks, L.J.; Tanner, R.M.; Muntner, P.; Kramer, H.; McClellan, W.M.; Warnock, D.G.; Judd, S.E.; Gutiérrez, O.M. Obesity, metabolic health, and the risk of end-stage renal disease. *Kidney Int.* 2015, *87*, 1216–1222.

674. Jafar, T.H.; Schmid, C.H.; Levey, A.S. Serum creatinine as marker of kidney function in South Asians: a study of reduced GFR in adults in Pakistan. *J. Am. Soc. Nephrol.* 2005, *16*, 1413–9.

675. Irie, F.; Iso, H.; Sairenchi, T.; Fukasawa, N.; Yamagishi, K.; Ikehara, S.; Kanashiki, M.; Saito, Y.; Ota, H.; Nose, T. The relationships of proteinuria, serum creatinine, glomerular filtration rate with cardiovascular disease mortality in Japanese general population. *Kidney Int.* 2006, *69*, 1264–1271.

676. Miro, J.M.; Cofan, F.; Trullas, J.C.; Manzardo, C.; Cervera, C.; Tuset, M.; Oppenheimer, F.; Brunet, M.; Moreno, A.; Campistol, J.M.; et al. Renal Dysfunction in the Setting of HIV/AIDS. *Curr. HIV/AIDS Rep.* 2012, *9*, 187–199.

677. Wyatt, C.M. Kidney Disease and HIV Infection. *Top. Antivir. Med.* 2017, *25*, 13–16.

678. Sociedad Española de Nefrología. Nefrología. Available online: https://www.revistanefrologia.com/en-estadisticas-X2013251414054695 (accessed on Oct 2, 2019).

679. Eknoyan, G.; Hostetter, T.; Bakris, G.L.; Hebert, L.; Levey, A.S.; Parving, H.-H.; Steffes, M.W.; Toto, R.

Proteinuria and other markers of chronic kidney disease: a position statement of the national kidney foundation (NKF) and the national institute of diabetes and digestive and kidney diseases (NIDDK). *Am. J. Kidney Dis.* 2003, *42*, 617–22.

680. Nduka, C.U.; Stranges, S.; Sarki, A.M.; Kimani, P.K.; Uthman, O.A. Evidence of increased blood pressure and hypertension risk among people living with HIV on antiretroviral therapy: a systematic review with meta-analysis. *J. Hum. Hypertens.* 2016, *30*, 355–362.

681. Antonello, V.S.; Carlos Ferreira Antonello, I.; Grossmann, T.K.; Tovo, C.V.; Brasil Dal Pupo, B.; De Quadros Winckler, L. Hypertension - An emerging cardiovascular risk factor in HIV infection. *J. Am. Soc. Hypertens.* 2015, *9*, 403–407.

682. Dimala, C.A.; Atashili, J.; Mbuagbaw, J.C.; Wilfred, A.; Monekosso, G.L. Prevalence of hypertension in HIV/AIDS patients on highly active antiretroviral therapy (HAART) compared with HAART-naïve patients at the Limbe Regional Hospital, Cameroon. *PLoS One* 2016, *11*, e0148100.

683. Dimala, C.A.; Blencowe, H.; Choukem, S.P. The association between antiretroviral therapy and selected cardiovascular disease risk factors in sub-Saharan Africa: A systematic review and meta-analysis. *PLoS One* 2018, *13*, e0201404.

684. Malaza, A.; Mossong, J.; Bärnighausen, T.; Newell, M.-L. Hypertension and obesity in adults living in a high HIV prevalence rural area in South Africa. *PLoS One* 2012, *7*, e47761.

685. Fox, K.; Borer, J.S.; Camm, A.J.; Danchin, N.; Ferrari, R.; Lopez Sendon, J.L.; Steg, P.G.; Tardif, J.-C.; Tavazzi, L.; Tendera, M.; et al. Resting Heart Rate in Cardiovascular Disease. *J. Am. Coll. Cardiol.* 2007, *50*, 823–830.

686. Benseñor, I.M.; Eira, M.; Dorea, E.L.; Dantas, E.M.; Mill, J.G.; Lotufo, P.A. Heart Rate Variability in HIV Patients, Diabetics, and Controls: The AGATAA Study. *ISRN Vasc. Med.* 2011, *2011*, 1–8.

687. Askgaard, G.; Kristoffersen, U.S.; Mehlsen, J.; Kronborg, G.; Kjaer, A.; Lebech, A.-M. Decreased Heart Rate Variability in HIV Positive Patients Receiving Antiretroviral Therapy: Importance of Blood Glucose and Cholesterol. *PLoS One* 2011, *6*, e20196.

688. Lebech, A.-M.; Kristoffersen, U.S.; Mehlsen, J.; Wiinberg, N.; Petersen, C.L.; Hesse, B.; Gerstoft, J.; Kjaer, A. Autonomic dysfunction in HIV patients on antiretroviral therapy: studies of heart rate variability. *Clin. Physiol. Funct. Imaging* 2007, *27*, 363–367.

689. Chow, D.C.; Wood, R.; Choi, J.; Grandinetti, A.; Gerschenson, M.; Sriratanaviriyakul, N.; Nakamoto, B.; Shikuma, C.; Low, P. Cardiovagal Autonomic Function in HIV-Infected Patients with Unsuppressed HIV Viremia. *HIV Clin. Trials* 2011, *12*, 141–150.

690. Huxley, R.; Mendis, S.; Zheleznyakov, E.; Reddy, S.; Chan, J. Body mass index, waist circumference and waist:hip ratio as predictors of cardiovascular risk—a review of the literature. *Eur. J. Clin. Nutr.* 2009, *64*, 16–22.

691. Fuchs, F.D.; Gus, M.; Moreira, L.B.; Moraes, R.S.; Wiehe, M.; Pereira, G.M.; Fuchs, S.C. Anthropometric Indices and the Incidence of Hypertension: A Comparative Analysis. *Obes. Res.* 2005, *13*, 1515–1517.

692. Vishwanath, A.; Quaiser, S.; Khan, R. Role of high-sensitivity C-reactive protein measurements in HIV patients. *Indian J. Sex. Transm. Dis. AIDS* 2016, *37*, 123–128.

693. Pepys, M.B.; Hirschfield, G.M. C-reactive protein: a critical update. *J. Clin. Invest.* 2003, *111*, 1805–1812.

694. O'Halloran, J.A.; Dunne, E.; Gurwith, M.M.P.M.; Lambert, J.J.J.S.J.; Sheehan, G.G.J.; Feeney, E.E.R.; Pozniak, A.; Reiss, P.; Kenny, D.; Mallon, P.P.W.G.; et al. The effect of initiation of antiretroviral therapy on monocyte, endothelial and platelet function in HIV-1 infection. *HIV Med.* 2015, *16*, 608–619.

695. De Luca, A.; de Gaetano Donati, K.; Colafigli, M.; Cozzi-Lepri, A.; De Curtis, A.; Gori, A.; Sighinolfi, L.; Giacometti, A.; Capobianchi, M.R.; D'Avino, A.; et al. The association of high-sensitivity c-reactive protein and other biomarkers with cardiovascular disease in patients treated for HIV: a nested case–control study. *BMC Infect. Dis.* 2013, *13*, 414–426.

696. Henry, K.; Kitch, D.; Dube, M.; Zackin, R.; Parker, R.A.; Sprecher, D.; Hammer, S.; Currier, J.; Adult AIDS Clinical Trials Group C-Reactive protein levels over time and cardiovascular risk in HIV-infected individuals suppressed on an indinavir-based regimen: AIDS Clinical Trials Group 5056s. *AIDS* 2004, *18*, 2434–7.

697. McComsey, G.A.; Kitch, D.; Daar, E.S.; Tierney, C.; Jahed, N.C.; Melbourne, K.; Ha, B.; Brown, T.T.; Bloom, A.; Fedarko, N.; et al. Inflammation markers after randomization to abacavir/lamivudine or tenofovir/emtricitabine with efavirenz or atazanavir/ritonavir. *AIDS* 2012, *26*, 1371–85.

698. Popa, C.; Netea, M.G.; van Riel, P.L.C.M.; van der Meer, J.W.M.; Stalenhoef, A.F.H. The role of TNF-alpha in chronic inflammatory conditions, intermediary metabolism, and cardiovascular risk. *J. Lipid Res.* 2007, *48*, 751–62.

699. Zhang, H.; Park, Y.; Wu, J.; Chen, X. ping; Lee, S.; Yang, J.; Dellsperger, K.C.; Zhang, C. Role of TNF-alpha in vascular dysfunction. *Clin. Sci. (Lond).* 2009, *116*, 219–30.

700. Pasquereau, S.; Kumar, A.; Herbein, G. Targeting TNF and TNF Receptor Pathway in HIV-1 Infection: from Immune Activation to Viral Reservoirs. *Viruses* 2017, *9*, 1–17.

701. Duh, E.J.; Maury, W.J.; Folks, T.M.; Fauci, A.S.; Rabson, A.B. Tumor necrosis factor alpha activates human immunodeficiency virus type 1 through induction of nuclear factor binding to the NF-kappa B sites in the long terminal repeat. *Proc. Natl. Acad. Sci.* 1989, *86*, 5974–5978.

702. Vaidya, S.A.; Korner, C.; Sirignano, M.N.; Amero, M.; Bazner, S.; Rychert, J.; Allen, T.M.; Rosenberg, E.S.; Bosch, R.J.; Altfeld, M. Tumor necrosis factor α is associated with viral control and early disease progression in patients with HIV type 1 infection. *J. Infect. Dis.* 2014, *210*, 1042–6.

703. Keating, S.M.; Golub, E.T.; Nowicki, M.; Young, M.; Anastos, K.; Crystal, H.; Cohen, M.H.; Zhang, J.; Greenblatt, R.M.; Desai, S.; et al. The effect of HIV infection and HAART on inflammatory biomarkers in a population-based cohort of women. *AIDS* 2011, *25*, 1823–32.

704. Swami, A. Metabolic Syndrome and HIV Infection. *J. HIV Retro Virus* 2016, *02*, 1–5.

705. Gutierrez, A.D.; Balasubramanyam, A. Dysregulation of glucose metabolism in HIV patients: epidemiology, mechanisms, and management. *Endocrine* 2012, *41*, 1–10.

706. Domingo, P.; Vidal, F.; Domingo, J.C.; Veloso, S.; Sambeat, M.A.; Torres, F.; Sirvent, J.J.; Vendrell, J.;

Matias-Guiu, X.; Richart, C. Tumour necrosis factor alpha in fat redistribution syndromes associated with combination antiretroviral therapy in HIV-1-infected patients: Potential role in subcutaneous adipocyte apoptosis. *Eur. J. Clin. Invest.* 2005, *35*, 771–80.

707. Tanaka, T.; Narazaki, M.; Kishimoto, T. IL-6 in inflammation, immunity, and disease. *Cold Spring Harb. Perspect. Biol.* 2014, *6*, a016295.

708. Borges, Á.H.; O'Connor, J.L.; Phillips, A.N.; Rönsholt, F.F.; Pett, S.; Vjecha, M.J.; French, M.A.; Lundgren, J.D.; INSIGHT SMART and ESPRIT Study Groups and the SILCAAT Scientific Committee Factors Associated With Plasma IL-6 Levels During HIV Infection. *J. Infect. Dis.* 2015, *212*, 585–95.

709. Hearps, A.C.; Martin, G.E.; Rajasuriar, R.; Crowe, S.M. Inflammatory Co-morbidities in HIV+ Individuals: Learning Lessons from Healthy Ageing. *Curr. HIV/AIDS Rep.* 2014, *11*, 20–34.

710. Rönsholt, F.F.; Ullum, H.; Katzenstein, T.L.; Gerstoft, J.; Ostrowski, S.R. Persistent Inflammation and Endothelial Activation in HIV-1 Infected Patients after 12 Years of Antiretroviral Therapy. *PLoS One* 2013, *8*, e65182.

711. Blankenberg, S.; Barbaux, S.; Tiret, L. Adhesion molecules and atherosclerosis. *Atherosclerosis* 2003, *170*, 191–203.

712. Mosepele, M.; Mohammed, T.; Mupfumi, L.; Moyo, S.; Bennett, K.; Lockman, S.; Hemphill, L.C.; Triant, V.A.; Shahin, L.; Linda, C.H.; et al. HIV disease is associated with increased biomarkers of endothelial dysfunction despite viral suppression on long-term antiretroviral therapy in Botswana. *Cardiovasc. J. Afr.* 2018, *29*, 155–161.

713. Graham, S.; Rajwans, N.; Jaoko, W.; Estambale, B.; McClelland, R.; Overbaugh, J.; Liles, W. Endothelial Activation Biomarkers Increase after HIV-1 Acquisition: Plasma VCAM-1 Predicts Disease Progression. *AIDS* 2013, *27*, 1803–1813.

714. Gibellini, D.; Borderi, M.; Clò, A.; Morini, S.; Miserocchi, A.; Bon, I.; Ponti, C.; Re, M.C. HIV-related mechanisms in atherosclerosis and cardiovascular diseases. *J. Cardiovasc. Med.* 2013, *14*, 780–790.

715. Fourie, C.; van Rooyen, J.; Pieters, M.; Conradie, K.; Hoekstra, T.; Schutte, a Is HIV-1 infection associated with endothelial dysfunction in a population of African ancestry in South Africa? *Cardiovasc. J. Afr.* 2011, *22*, 134–140.

716. Hileman, C.O.; Funderburg, N.T. Inflammation, Immune Activation, and Antiretroviral Therapy in HIV. *Curr. HIV/AIDS Rep.* 2017, *14*, 93–100.

717. Schmitt-Sody, M.; Metz, P.; Gottschalk, O.; Birkenmaier, C.; Zysk, S.; Veihelmann, A.; Jansson, V. Platelet P-selectin is significantly involved in leukocyte-endothelial cell interaction in murine antigen-induced arthritis. *Platelets* 2007, *18*, 365–372.

718. De Gaetano Donati, K.; Rabagliati, R.; Iacoviello, L.; Cauda, R. HIV infection, HAART, and endothelial adhesion molecules: Current perspectives. *Lancet Infect. Dis.* 2004, *4*, 213–222.

719. Brinda, B.J.; Viganego, F.; Vo, T.; Dolan, D.; Fradley, M.G. Anti-VEGF-Induced Hypertension: a Review of Pathophysiology and Treatment Options. *Curr. Treat. Options Cardiovasc. Med.* 2016, *18*, 33.

720. Lankhorst, S.; Baelde, H.J.; Clahsen-van Groningen, M.C.; Smedts, F.M.M.; Danser, A.H.J.; van den Meiracker, A.H. Effect of high salt diet on blood pressure and renal damage during vascular endothelial growth factor inhibition with sunitinib. *Nephrol. Dial. Transplant.* 2016, *31*, 914–921.

721. Lal, B.K.; Varma, S.; Pappas, P.J.; Hobson, R.W.; Durán, W.N. VEGF Increases Permeability of the Endothelial Cell Monolayer by Activation of PKB/akt, Endothelial Nitric-Oxide Synthase, and MAP Kinase Pathways. *Microvasc. Res.* 2001, *62*, 252–262.

722. Rusnati, M.; Presta, M. HIV-1 Tat protein and endothelium: From protein/cell interaction to AIDS-associated pathologies. *Angiogenesis* 2002, *5*, 141–151.

723. Gupta, S.K.; Liu, Z.; Sims, E.C.; Repass, M.J.; Haneline, L.S.; Yoder, M.C. Endothelial Colony-Forming Cell Function Is Reduced During HIV Infection. *J. Infect. Dis.* 2019, *219*, 1076–1083.

724. Nyagol, J.; De Falco, G.; Lazzi, S.; Luzzi, A.; Cerino, G.; Shaheen, S.; Palummo, N.; Bellan, C.; Spina, D.; Leoncini, L. HIV-1 Tat mimetic of VEGF correlates with increased microvessels density in AIDS-related diffuse large B-cell and Burkitt lymphomas. *J. Hematop.* 2008, *1*, 3–10.

725. Paula, A.A.; Falcão, M.C.; Pacheco, A.G. Metabolic syndrome in HIV-infected individuals: underlying mechanisms and epidemiological aspects. *AIDS Res. Ther.* 2013, *10*, 32–40.

726. Baliga, R.S.; Liu, C.; Hoyt, D.G.G.D.G.D.G.G.; Chaves, A.A.A.A.; Bauer, J.A.A.J.A. Vascular endothelial toxicity induced by HIV protease inhibitor: Evidence of oxidant-related dysfunction and apoptosis. *Cardiovasc. Toxicol.* 2004, *4*, 199–206.

727. Sporer, B.; Koedel, U.; Paul, R.; Eberle, J.; Arendt, G.; Pfister, H.-W. Vascular endothelial growth factor (VEGF) is increased in serum, but not in cerebrospinal fluid in HIV associated CNS diseases. *J. Neurol. Neurosurg. Psychiatry* 2004, *75*, 298–300.

728. Dai, L.; Bratoeva, M.; Toole, B.P.; Qin, Z.; Parsons, C. KSHV activation of VEGF secretion and invasion for endothelial cells is mediated through viral upregulation of emmprin-induced signal transduction. *Int. J. Cancer* 2012, *131*, 834–843.

729. Aoki, Y.; Tosato, G. Targeted inhibition of angiogenic factors in AIDS-related disorders. *Curr. Drug Targets. Infect. Disord.* 2003, *3*, 115–28.

730. Zhu, Y.; Carmeliet, P.; Fay, W.P. Plasminogen activator inhibitor-1 is a major determinant of arterial thrombolysis resistance. *Circulation* 1999, *99*, 3050–5.

731. Emeis, J.J. The control of tPA and PAI-1 secretion from the vessel wall. *Vasc. Rev.* 1995, *6*, 153–166.

732. Wirunsawanya, K.; Belyea, L.; Shikuma, C.; Watanabe, R.M.; Kohorn, L.; Shiramizu, B.; Mitchell, B.I.; Souza, S.A.; Keating, S.M.; Norris, P.J.; et al. Plasminogen Activator Inhibitor-1 Predicts Negative Alterations in Whole-Body Insulin Sensitivity in Chronic HIV Infection. *AIDS Res. Hum. Retroviruses* 2017, *33*, 723–727.

733. Jeremiah, Z.A.; Obazee, Y.; Okogun, G.R.; Adias, T.C.; Mgbere, O.; Essien, E.J. Impact of short-term antiretroviral therapy (START) on some fibrinolytic markers in HIV-infected Nigerian adults: preliminary findings from the START study. *HIV. AIDS. (Auckl).* 2012, *4*, 87–94.

734. Masiá, M.; Padilla, S.; García, N.; Jarrin, I.; Bernal, E.; López, N.; Hernández, I.; Gutiérrez, F. Endothelial function is impaired in HIV-infected patients with lipodystrophy. *Antivir. Ther.* 2010, *15*, 101–110.

735. Yki-Järvinen, H.; Sutinen, J.; Silveira, A.; Korsheninnikova, E.; Fisher, R.M.; Kannisto, K.; Ehrenborg, E.; Eriksson, P.; Hamsten, A. Regulation of Plasma PAI-1 Concentrations in HAART-Associated Lipodystrophy During Rosiglitazone Therapy. *Arterioscler. Thromb. Vasc. Biol.* 2003, *23*, 688–694.

736. Tofler, G.H.; Massaro, J.; O'Donnell, C.J.; Wilson, P.W.F.; Vasan, R.S.; Sutherland, P.A.; Meigs, J.B.; Levy, D.; D'Agostino, R.B.; Sr. Plasminogen activator inhibitor and the risk of cardiovascular disease: The Framingham Heart Study. *Thromb. Res.* 2016, *140*, 30–35.

737. Ikram, M.K.; de Jong, F.J.; Vingerling, J.R.; Witteman, J.C.M.; Hofman, A.; Breteler, M.M.B.; de Jong, P.T.V.M. Are Retinal Arteriolar or Venular Diameters Associated with Markers for Cardiovascular Disorders? The Rotterdam Study. *Investig. Opthalmology Vis. Sci.* 2004, *45*, 2129–2135.

738. Currier, J.S.; Lundgren, J.D.; Carr, A.; Klein, D.; Sabin, C.A.; Sax, P.E.; Schouten, J.T.; Smieja, M.; Working Group 2; Group, W.; et al. Epidemiological Evidence for Cardiovascular Disease in HIV-Infected Patients and Relationship to Highly Active Antiretroviral Therapy. *Circulation* 2008, *118*, e29–e35.

739. Klein, R.; Klein, B.E.K.; Knudtson, M.D.; Wong, T.Y.; Tsai, M.Y. Are Inflammatory Factors Related to Retinal Vessel Caliber? *Arch. Ophthalmol.* 2006, *124*, 87–95.

740. Wong, T.Y.; Islam, F.M.A.; Klein, R.; Klein, B.E.K.; Cotch, M.F.; Castro, C.; Sharrett, A.R.; Shahar, E. Retinal Vascular Caliber, Cardiovascular Risk Factors, and Inflammation: The Multi-Ethnic Study of Atherosclerosis (MESA). *Investig. Opthalmology Vis. Sci.* 2006, *47*, 2341–51.

741. Wong, T.Y.T.; Klein, R.; Sharrett, A.R.A.; Duncan, B.B.; Couper, D.J.; Tielsch, J.M.; Klein, B.E.K.; Hubbard, L.D. Retinal arteriolar narrowing and risk of coronary heart disease in men and women. *JAMA J. …* 2002, *287*, 1153–1159.

742. McGeechan, K.; Liew, G.; Macaskill, P.; Irwig, L.; Klein, R.; Klein, B.E.K.; Wang, J.J.; Mitchell, P.; Vingerling, J.R.; Dejong, P.T.V.M.; et al. Meta-analysis: retinal vessel caliber and risk for coronary heart disease. *Ann. Intern. Med.* 2009, *151*, 404–13.

743. Al-Fakhri, N.; Chavakis, T.; Schmidt-Wöll, T.; Huang, B.; Cherian, S.M.; Bobryshev, Y.V.; Lord, R.S.A.; Katz, N.; Preissner, K.T. Induction of Apoptosis in Vascular Cells by Plasminogen Activator Inhibitor-1 and High Molecular Weight Kininogen Correlates with Their Anti-Adhesive Properties. *Biol. Chem.* 2003, *384*, 423–35.

744. Tabernero, M.D.; Estellés, A.; Vicente, V.; Alberca, I.; Aznar, J. Incidence of increased plasminogen activator inhibitor in patients with deep venous thrombosis and/or pulmonary embolism. *Thromb. Res.* 1989, *56*, 565–70.

745. Ridker, P.M.; Vaughan, D.E.; Stampfer, M.J.; Manson, J.E.; Shen, C.; Newcomer, L.M.; Goldhaber, S.Z.; Hennekens, C.H. Baseline fibrinolytic state and the risk of future venous thrombosis. A prospective study of endogenous tissue-type plasminogen activator and plasminogen activator inhibitor. *Circulation* 1992, *85*, 1822–7.

746.   Gangaputra, S.; Kalyani, P.S.; Fawzi, A.A.; Van Natta, M.L.; Hubbard, L.D.; Danis, R.P.; Thorne, J.E.; Holland, G.N.; Studies of the Ocular Complications of AIDS Research Group Retinal Vessel Caliber Among People With Acquired Immunodeficiency Syndrome: Relationships With Disease-Associated Factors and Mortality. *Am. J. Ophthalmol.* 2012, *153*, 434-444.e1.

747.   Oliviero, U.; Bonadies, G.; Apuzzi, V.; Foggia, M.; Bosso, G.; Nappa, S.; Valvano, A.; Leonardi, E.; Borgia, G.; Castello, G.; et al. Human immunodeficiency virus per se exerts atherogenic effects. *Atherosclerosis* 2009, *204*, 586–589.

748.   Sun, D.; Wu, Y.; Yuan, Y.; Wang, Y.; Liu, W.; Yang, J. Is the atherosclerotic process accentuated under conditions of HIV infection, antiretroviral therapy, and protease inhibitor exposure? Meta-analysis of the markers of arterial structure and function. *Atherosclerosis* 2015, *242*, 109–116.

749.   Blanco, J.J.R.; García, I.S.; Cerezo, J.G.; de Rivera, J.M.P.S.; Anaya, P.M.; Raya, P.G.; García, J.G.; López, J.R.A.; Hernández, F.J.B.; Rodríguez, J.J.V. Endothelial function in HIV-infected patients with low or mild cardiovascular risk. *J. Antimicrob. Chemother.* 2006, *58*, 133–9.

750.   Tuttolomondo, A.; Di Raimondo, D.; Pecoraro, R.; Arnao, V.; Pinto, A.; Licata, G. Atherosclerosis as an Inflammatory Disease. *Curr. Pharm. Des.* 2012, *18*, 4266–4288.

751.   Martínez, M.C.; Tesse, A.; Zobairi, F.; Andriantsitohaina, R. Shed membrane microparticles from circulating and vascular cells in regulating vascular function. *Am. J. Physiol. Circ. Physiol.* 2005, *288*, H1004–H1009.

752.   da Silva, E.F.R.; Fonseca, F.A.H.; França, C.N.; Ferreira, P.R.A.; Izar, M.C.O.; Salomão, R.; Camargo, L.M.; Tenore, S.B.; Lewi, D.S. Imbalance between endothelial progenitors cells and microparticles in HIV-infected patients naive for antiretroviral therapy. *AIDS* 2011, *25*, 1595–1601.

753.   Robinson-Papp, J.; Simpson, D.M. Neuromuscular diseases associated with HIV-1 infection. *Muscle Nerve* 2009, *40*, 1043–1053.

754.   Correia, D.; Rodrigues de Resende, L.; Molina, R.; Colombari, F.; Barbosa, C.; Da Silva, V. Power Spectral Analysis of Heart Rate Variability in HIV-Infected and AIDS Patients. *Pacing Clin. Electrophysiol.* 2006, *29*, 53–58.

755.   Chow, D.; Kocher, M.; Shikuma, C.; Parikh, N.; Grandinetti, A.; Nakamoto, B.; Seto, T.; Low, P. Effects of antiretroviral therapy on autonomic function in early HIV infection: a preliminary report. *Int. J. Med. Sci.* 2012, *9*, 397–405.

756.   Hsue, P.Y.; Hunt, P.W.; Wu, Y.; Schnell, A.; Ho, J.E.; Hatano, H.; Xie, Y.; Martin, J.N.; Ganz, P.; Deeks, S.G. Association of abacavir and impaired endothelial function in treated and suppressed HIV-infected patients. *AIDS* 2009, *23*, 2021–7.

757.   Stein, J.H.; Klein, M.A.; Bellehumeur, J.L.; McBride, P.E.; Wiebe, D.A.; Otvos, J.D.; Sosman, J.M. Use of human immunodeficiency virus-1 protease inhibitors is associated with atherogenic lipoprotein changes and endothelial dysfunction. *Circulation* 2001, *104*, 257–262.

758.   Pathai, S.; Lawn, S.D.; Shiels, P.G.; Weiss, H.A.; Cook, C.; Wood, R.; Gilbert, C.E. Corneal Endothelial

Cells Provide Evidence of Accelerated Cellular Senescence Associated with HIV Infection: A Case-Control Study. *PLoS One* 2013, *8*, e57422.

759. Hijmans, J.G.; Stockleman, K.; Reiakvam, W.; Levy, M. V.; Brewster, L.M.; Bammert, T.D.; Greiner, J.J.; Connick, E.; DeSouza, C.A. Effects of HIV-1 gp120 and tat on endothelial cell sensescence and senescence-associated microRNAs. *Physiol. Rep.* 2018, *6*, e13647.

760. Lefèvre, C.; Auclair, M.; Boccara, F.; Bastard, J.-P.P.; Capeau, J.; Vigouroux, C.; Caron-Debarle, M. Premature senescence of vascular cells is induced by HIV protease inhibitors: Implication of prelamin a and reversion by statin. *J. Am. Heart Assoc.* 2010, *30*, 2611–2620.

761. Wang, X.; Chai, H.; Lin, P.H.; Yao, Q.; Chen, C. Roles and mechanisms of human immunodeficiency virus protease inhibitor ritonavir and other anti-human immunodeficiency virus drugs in endothelial dysfunction of porcine pulmonary arteries and human pulmonary artery endothelial cells. *Am. J. Pathol.* 2009, *174*, 771–781.

762. Fu, W.; Chai, H.; Yao, Q.; Chen, C. Effects of HIV protease inhibitor ritonavir on vasomotor function and endothelial nitric oxide synthase expression. *J. Acquir. Immune Defic. Syndr.* 2005, *39*, 152–158.

763. Kappert, K.; Lepp??nen, O.; Paulsson, J.; Furuhashi, M.; Carlsson, M.-A.; Heldin, C.-H.; F??tkenheuer, G.; Rosenkranz, S.; ??stman, A.; Leppänen, O.; et al. Highly active antiretroviral therapy attenuates re-endothelialization and alters neointima formation in the rat carotid artery after balloon injury. *J. Acquir. Immune Defic. Syndr.* 2006, *43*, 383–92.

764. Jiang, B.; Hebert, V.Y.; Li, Y.; MATHIS, J.M.; Alexander, J.S.; DUGAS, T.R. HIV antiretroviral drug combination induces endothelial mitochondrial dysfunction and reactive oxygen species production, but not apoptosis. *Toxicol. Appl. Pharmacol.* 2007, *224*, 60–71.

765. Corrales-Medina, V.F.; Simkins, J.; Chirinos, J.A.; Serpa, J.A.; Horstman, L.L.; Jy, W.; Ahn, Y.-S. Increased Levels of Platelet Microparticles in HIV-Infected Patients With Good Response to Highly Active Antiretroviral Therapy. *JAIDS J. Acquir. Immune Defic. Syndr.* 2010, *54*, 217–218.

766. Riddler, S.A.; Li, X.; Otvos, J.; Post, W.; Palella, F.; Kingsley, L.; Visscher, B.; Jacobson, L.P.; Sharrett, A.R. Antiretroviral therapy is associated with an atherogenic lipoprotein phenotype among HIV-1-infected men in the Multicenter AIDS Cohort Study. *J. Acquir. Immune Defic. Syndr.* 2008, *48*, 281–8.

767. Ryom, L.; Lundgren, J.D.; El-Sadr, W.; Reiss, P.; Kirk, O.; Law, M.; Phillips, A.; Weber, R.; Fontas, E.; d'Arminio Monforte, A.; et al. Cardiovascular disease and use of contemporary protease inhibitors: the D:A:D international prospective multicohort study. *Lancet HIV* 2018, *5*, e291–e300.

768. Smith, C.J.; Ryom, L.; Weber, R.; Morlat, P.; Pradier, C.; Reiss, P.; Kowalska, J.D.; de Wit, S.; Law, M.; el Sadr, W.; et al. Trends in underlying causes of death in people with HIV from 1999 to 2011 (D:A:D): a multicohort collaboration. *Lancet* 2014, *384*, 241–248.

769. Faltz, M.; Bergin, H.; Pilavachi, E.; Grimwade, G.; Mabley, J.G. Effect of the antiretroviral drugs Efavirenz, Tenofovir and Emtricitabine on endothelial cell function: Role of PARP. *Cardiovasc. Toxicol.* 2017, *17*, 393–404.

770.   Benson, M.S.; Parker, B. Western Cape State of Air Quality Management Report State of Air Quality Management 2017 Available online: https://www.westerncape.gov.za/eadp/files/atoms/files/SoAR_2017_1.pdf (accessed on May 17, 2019).

771.   Saucy, A.; Röösli, M.; Künzli, N.; Tsai, M.-Y.; Sieber, C.; Olaniyan, T.; Baatjies, R.; Jeebhay, M.; Davey, M.; Flückiger, B.; et al. Land Use Regression Modelling of Outdoor NO2 and PM2.5 Concentrations in Three Low Income Areas in the Western Cape Province, South Africa. *Int. J. Environ. Res. Public Health* 2018, *15*, 1452.

772.   Vanker, A.; Barnett, W.; Workman, L.; Nduru, P.M.; Sly, P.D.; Gie, R.P.; Zar, H.J. Early-life exposure to indoor air pollution or tobacco smoke and lower respiratory tract illness and wheezing in African infants: a longitudinal birth cohort study. *Lancet Planet. Heal.* 2017, *1*, e328–e336.

773.   Morakinyo, O.M.; Adebowale, A.S.; Mokgobu, M.I.; Mukhola, M.S. Health risk of inhalation exposure to sub-10 μm particulate matter and gaseous pollutants in an urban-industrial area in South Africa: An ecological study. *BMJ Open* 2017, *7*, 1–9.

774.   Makamure, M.T.; Reddy, P.; Chuturgoon, A.; Naidoo, R.N.; Mentz, G.; Batterman, S.; Robins, T.G. Allergy and Immunology Tumour necrosis factor α polymorphism (TNF-308α G/A) in association with asthma related phenotypes and air pollutants among children in KwaZulu-Natal. *Asian Pacific J. Allergy Immunol.* 2016, *34*, 217–222.

775.   Mentz, G.; Robins, T.G.; Batterman, S.; Naidoo, R.N. Acute respiratory symptoms associated with short term fluctuations in ambient pollutants among schoolchildren in Durban, South Africa. *Environ. Pollut.* 2018, *233*, 529–539.

776.   South African Government NATIONAL ENVIRONMENTAL MANAGEMENT: AIR QUALITY ACT, 2004 (ACT NO. 39 OF 2004) Available online: https://www.environment.gov.za/sites/default/files/gazetted_notices/nemaqa_listofactivities_g33064gon248_0.pdf (accessed on Dec 19, 2019).

777.   Department of Environmental Affairs, S.A.G. 2017 STATE OF AIR REPORT AND NATIONAL AIR QUALITY INDICATOR Available online: http://www.airqualitylekgotla.co.za/assets/2017_1.3-state-of-air-report-and-naqi.pdf (accessed on Dec 19, 2019).

778.   Larkin, A.; Geddes, J.A.; Martin, R. V.; Xiao, Q.; Liu, Y.; Marshall, J.D.; Brauer, M.; Hystad, P. Global Land Use Regression Model for Nitrogen Dioxide Air Pollution. *Environ. Sci. Technol.* 2017, *51*, 6957–6964.

779.   Wheida, A.; Nasser, A.; El Nazer, M.; Borbon, A.; Abo El Ata, G.A.; Abdel Wahab, M.; Alfaro, S.C. Tackling the mortality from long-term exposure to outdoor air pollution in megacities: Lessons from the Greater Cairo case study. *Environ. Res.* 2018, *160*, 223–231.

780.   López-Villarrubia, E.; Ballester, F.; Iñiguez, C.; Peral, N. Air pollution and mortality in the Canary Islands: a time-series analysis. *Environ. Heal.* 2010, *9*, 8–19.

781.   Papy Mbelambela, E.; Hirota, R.; Eitoku, M.; Marie Joelle Muchanga, S.; Kiyosawa, H.; Yasumitsu-Lovell, K.; Leader Lawanga, O.; Suganuma, N. Occupation exposed to road-traffic emissions and respiratory

health among Congolese transit workers, particularly bus conductors, in Kinshasa: a cross-sectional study. *Environ. Health Prev. Med.* 2017, *22*, 11–20.

782. World Health Organization (WHO) WHO - Toluene: Air quality guidelines. *Air Qual. Guidel.* 2000, *2*, 1–20.

783. Majumdar, D.; Mukherjeea, A.K.; Sen, S. BTEX in Ambient Air of a Metropolitan City. *J. Environ. Prot. (Irvine,. Calif).* 2011, 11–20.

784. Kasim, O.F.; Abshare, M.W.; Agbola, S.B. Analysis of air quality in Dire Dawa, Ethiopia. *J. Air Waste Manag. Assoc.* 2018, *68*, 801–811.

785. Vignati, E.; Beukes, J.P.; Virkkula, A.; van Zyl, P.G.; Wiedensohler, A.; Gilardoni, S.; Lihavainen, H.; Josipovic, M.; Kerminen, V.-M.; Piketh, S.; et al. South African EUCAARI measurements: seasonal variation of trace gases and aerosol optical properties. *Atmos. Chem. Phys.* 2012, *12*, 1847–1864.

786. Näyhä, S. Cold and the risk of cardiovascular diseases. *Int. J. Circumpolar Health* 2002, *61*, 373–380.

787. Dėdelė, A.; Miškinytė, A. Seasonal variation of indoor and outdoor air quality of nitrogen dioxide in homes with gas and electric stoves. *Environ. Sci. Pollut. Res.* 2016, *23*, 17784–17792.

788. Carter, E.; Archer-Nicholls, S.; Ni, K.; Lai, A.M.; Niu, H.; Secrest, M.H.; Sauer, S.M.; Schauer, J.J.; Ezzati, M.; Wiedinmyer, C.; et al. Seasonal and Diurnal Air Pollution from Residential Cooking and Space Heating in the Eastern Tibetan Plateau. *Environ. Sci. Technol.* 2016, *50*, 8353–8361.

789. Bassig, B.A.; Zhang, L.; Cawthon, R.M.; Smith, M.T.; Yin, S.; Li, G.; Hu, W.; Shen, M.; Rappaport, S.; Barone-Adesi, F.; et al. Alterations in leukocyte telomere length in workers occupationally exposed to benzene. *Environ. Mol. Mutagen.* 2014, *55*, 673–678.

790. Rutowski, J.; Moszczyński, P.; Dobrowolski, J.W.; Bem, S.; Krochmal, D. [The effects of occupational exposure to nitrogen dioxide (NO2) on the immunological parameters in workers]. *Med. Pr.* 1998, *49*, 341–51.

791. Moolla, R.; Curtis, C.J.; Knight, J.; Moolla, R.; Curtis, C.J.; Knight, J. Occupational Exposure of Diesel Station Workers to BTEX Compounds at a Bus Depot. *Int. J. Environ. Res. Public Health* 2015, *12*, 4101–4115.

792. Mills, N.L.; Donaldson, K.; Hadoke, P.W.; Boon, N.A.; MacNee, W.; Cassee, F.R.; Sandstrom, T.; Blomberg, A.; Newby, D.E. Adverse cardiovascular effects of air pollution. *Nat. Clin. Pract. Cardiovasc. Med.* 2009, *6*, 36–44.

793. O'Donnell, V.B.; Eiserich, J.P.; Bloodsworth, A.; Chumley, P.H.; Kirk, M.; Barnes, S.; Darley-Usmar, V.M.; Freeman, B.A. [47] Nitration of unsaturated fatty acids by nitric oxide-derived reactive species. *Methods Enzymol.* 1999, *301*, 454–470.

794. Brook, R.D. Cardiovascular effects of air pollution. *Clin. Sci. (Lond).* 2008, *115*, 175–87.

795. Bedada, G.B.; Smith, C.J.; Tyrrell, P.J.; Hirst, A.A.; Agius, R. Short-term effects of ambient particulates and gaseous pollutants on the incidence of transient ischaemic attack and minor stroke : a case-crossover study. *Environ. Heal.* 2012, *11*, 77–79.

796. Bedard, K.; Krause, K.-H. The NOX family of ROS-generating NADPH oxidases: physiology and

pathophysiology. *Physiol. Rev.* 2007, *87*, 245–313.

797. Lodovici, M.; Bigagli, E. Oxidative stress and air pollution exposure. *J. Toxicol.* 2011, *2011*, 487074.

798. Szczeklik, A.; Szczeklik, J.; Galuszka, Z.; Musial, J.; Kolarzyk, E.; Targosz, D. Humoral immunosuppression in men exposed to polycyclic aromatic hydrocarbons and related carcinogens in polluted environments. *Environ. Health Perspect.* 1994, *102*, 302–304.

799. De Oliveira, B.F.A.; Chacra, A.P.M.; Frauches, T.S.; Vallochi, A.; Hacon, S. A curated review of recent literature of biomarkers used for assessing air pollution exposures and effects in humans. *J. Toxicol. Environ. Heal. - Part B Crit. Rev.* 2014, *17*, 369–410.

800. Brook, R.D.; Jerrett, M.; Brook, J.R.; Bard, R.L.; Finkelstein, M.M. The Relationship Between Diabetes Mellitus and Traffic-Related Air Pollution. *J. Occup. Environ. Med.* 2008, *50*, 32–38.

801. Bahadar, H.; Maqbool, F.; Mostafalou, S.; Baeeri, M.; Rahimifard, M.; Navaei-Nigjeh, M.; Abdollahi, M. Assessment of benzene induced oxidative impairment in rat isolated pancreatic islets and effect on insulin secretion. *Environ. Toxicol. Pharmacol.* 2015, *39*, 1161–1169.

802. Barbaro, G.; Iacobellis, G. Metabolic syndrome associated with HIV and highly active antiretroviral therapy. *Curr. Diab. Rep.* 2009, *9*, 37–42.

803. Choi, Y.-H.; Kim, J.H.; Lee, B.-E.; Hong, Y.-C. Urinary benzene metabolite and insulin resistance in elderly adults. *Sci. Total Environ.* 2014, *482–483*, 260–268.

804. Bahadar, H.; Maqbool, F.; Mostafalou, S.; Baeeri, M.; Gholami, M.; Ghafour-Boroujerdi, E.; Abdollahi, M. The molecular mechanisms of liver and islets of Langerhans toxicity by benzene and its metabolite hydroquinone *in vivo* and *in vitro*. *Toxicol. Mech. Methods* 2015, *25*, 628–636.

805. Ismail, W.I.W.; King, J. a; Pillay, T.S. Insulin resistance induced by antiretroviral drugs: Current understanding of molecular mechanisms. *J. Endocrinol. Metab. Diabetes South Africa* 2009, *14*, 129–132.

806. Kim, K.-W.; Won, Y.L.; Ko, K.S. Ethnic Differences in the Metabolism of Toluene: Comparisons between Korean and Foreign Workers Exposed to Toluene. *Toxicol. Res.* 2015, *31*, 25–32.

807. Edokpolo, B.; Yu, Q.J.; Connell, D.; Edokpolo, B.; Yu, Q.J.; Connell, D. Health Risk Assessment of Ambient Air Concentrations of Benzene, Toluene and Xylene (BTX) in Service Station Environments. *Int. J. Environ. Res. Public Health* 2014, *11*, 6354–6374.

808. Niaz, K.; Bahadar, H.; Maqbool, F.; Abdollahi, M. A review of environmental and occupational exposure to xylene and its health concerns. *EXCLI J.* 2015, *14*, 1167–86.

809. Sørensen, M.; Hjortebjerg, D.; Eriksen, K.T.; Ketzel, M.; Tjønneland, A.; Overvad, K.; Raaschou-Nielsen, O. Exposure to long-term air pollution and road traffic noise in relation to cholesterol: A cross-sectional study. *Environ. Int.* 2015, *85*, 238–243.

810. Bell, G.; Mora, S.; Greenland, P.; Tsai, M.; Gill, E.; Kaufman, J.D. Association of Air Pollution Exposures With High-Density Lipoprotein Cholesterol and Particle Number: The Multi-Ethnic Study of Atherosclerosis. *Arterioscler. Thromb. Vasc. Biol.* 2017, *37*, 976–982.

811. McGuinn, L.A.; Schneider, A.; McGarrah, R.W.; Ward-Caviness, C.; Neas, L.M.; Di, Q.; Schwartz, J.;

Hauser, E.R.; Kraus, W.E.; Cascio, W.E.; et al. Association of long-term PM2.5 exposure with traditional and novel lipid measures related to cardiovascular disease risk. *Environ. Int.* 2019, *122*, 193–200.

812. Lim, S.; Cho, Y.M.; Park, K.S.; Lee, H.K.; Lee, H.K. Persistent organic pollutants, mitochondrial dysfunction, and metabolic syndrome. *Ann. N.Y. Acad. Sci* 2010, *1201*, 166–176.

813. Yin, F.; Ramanathan, G.; Zhang, M.; Araujo, J.A. Prooxidative Effects of Ambient Pollutant Chemicals Are Inhibited by HDL. *J. Biochem. Mol. Toxicol.* 2013, *27*, 172–183.

814. Yin, F.; Lawal, A.; Ricks, J.; Fox, J.R.; Larson, T.; Navab, M.; Fogelman, A.M.; Rosenfeld, M.E.; Araujo, J.A. Diesel exhaust induces systemic lipid peroxidation and development of dysfunctional pro-oxidant and pro-inflammatory high-density lipoprotein. *Arterioscler. Thromb. Vasc. Biol.* 2013, *33*, 1153–61.

815. Li, R.; Navab, M.; Pakbin, P.; Ning, Z.; Navab, K.; Hough, G.; Morgan, T.E.; Finch, C.E.; Araujo, J.A.; Fogelman, A.M.; et al. Ambient ultrafine particles alter lipid metabolism and HDL anti-oxidant capacity in LDLR-null mice. *J. Lipid Res.* 2013, *54*, 1608–15.

816. Maiseyeu, A.; Yang, H.-Y.; Ramanathan, G.; Yin, F.; Bard, R.L.; Morishita, M.; Dvonch, J.T.; Wang, L.; Spino, C.; Mukherjee, B.; et al. No effect of acute exposure to coarse particulate matter air pollution in a rural location on high-density lipoprotein function. *Inhal. Toxicol.* 2014, *26*, 23–9.

817. Miller, V.T. Lipids, lipoproteins, women and cardiovascular disease. *Atherosclerosis* 1994, *108*, S73–S82.

818. Huo, Q.; Zhang, N.; Wang, X.; Jiang, L.; Ma, T.; Yang, Q. Effects of Ambient Particulate Matter on Human Breast Cancer: Is Xenogenesis Responsible? *PLoS One* 2013, *8*, e76609.

819. Chen, S.-T.; Lin, C.-C.; Liu, Y.-S.; Lin, C.; Hung, P.-T.; Jao, C.-W.; Lin, P.-H. Airborne particulate collected from central Taiwan induces DNA strand breaks, Poly(ADP-ribose) polymerase-1 activation, and estrogen-disrupting activity in human breast carcinoma cell lines. *J. Environ. Sci. Heal. Part A* 2013, *48*, 173–181.

820. Li, J.; Zhou, C.; Xu, H.; Brook, R.D.; Liu, S.; Yi, T.; Wang, Y.; Feng, B.; Zhao, M.; Wang, X.; et al. Ambient Air Pollution Is Associated With HDL (High-Density Lipoprotein) Dysfunction in Healthy Adults. *Arterioscler. Thromb. Vasc. Biol.* 2019, *39*, 513–522.

821. Lue, S.-H.; Wellenius, G.A.; Wilker, E.H.; Mostofsky, E.; Mittleman, M.A. Residential proximity to major roadways and renal function. *J. Epidemiol. Community Health* 2013, *67*, 629–34.

822. Soderland, P.; Lovekar, S.; Weiner, D.E.; Brooks, D.R.; Kaufman, J.S. Chronic Kidney Disease Associated With Environmental Toxins and Exposures. *Adv. Chronic Kidney Dis.* 2010, *17*, 254–264.

823. Meydan, S.; Nacar, A.; Oztürk, H.O.; Tas, U.; Köse, E.; Zararsiz, I.; Yılmaz, N.; Kus, I. The protective effects of caffeic acid phenethyl ester against toluene-induced nephrotoxicity in rats. *Toxicol. Ind. Health* 2016, *32*, 15–21.

824. Gehle, K.; Pharagood-Wade, F.; Johnson, D.; Rosales-Guevara, L.; Dennis-Flagler, D.; Drehobl, P.; Cdc, B.; Jr, C.; Hoffman, H.; McLellan, R.K.; et al. *ATSDR - CSEM - Toluene Toxicity: Environmental Medicine Case Study*;

825. Streicher, H.Z.; Gabow, P.A.; Moss, A.H.; Kono, D.; Kaehny, W.D. Syndromes of Toluene Sniffing in Adults. *Ann. Intern. Med.* 1981, *94*, 758–62.

826. Kroeger, R.M.; Moore, R.J.; Lehman, T.H.; Giesy, J.D.; Skeeters, C.E. Recurrent urinary calculi associated with toluene sniffing. *J. Urol.* 1980, *123*, 89–91.

827. Kanter, M. Protective effects of quercetine on the neuronal injury in frontal cortex after chronic toluene exposure. *Toxicol. Ind. Health* 2013, *29*, 643–651.

828. Otitoloju, A.; Olagoke, O. Lipid peroxidation and antioxidant defense enzymes in Clarias gariepinus as useful biomarkers for monitoring exposure to polycyclic aromatic hydrocarbons. *Environ. Monit. Assess.* 2011, *182*, 205–213.

829. Zhao, B.; Vo, H.Q.; Johnston, F.H.; Negishi, K. Air pollution and telomere length: a systematic review of 12,058 subjects. *Cardiovasc. Diagn. Ther.* 2018, *8*, 480–492.

830. Martens, D.S.; Nawrot, T.S. Ageing at the level of telomeres in association to residential landscape and air pollution at home and work: a review of the current evidence. *Toxicol. Lett.* 2018, *298*, 42–52.

831. Ward-Caviness, C.K.; Nwanaji-Enwerem, J.C.; Wolf, K.; Wahl, S.; Colicino, E.; Trevisi, L.; Kloog, I.; Just, A.C.; Vokonas, P.; Cyrys, J.; et al. Long-term exposure to air pollution is associated with biological aging. *Oncotarget* 2016, *7*, 74510–74525.

832. Ling, X.; Zhang, G.; Chen, Q.; Yang, H.; Sun, L.; Zhou, N.; Wang, Z.; Zou, P.; Wang, X.; Cui, Z.; et al. Shorter sperm telomere length in association with exposure to polycyclic aromatic hydrocarbons: Results from the MARHCS cohort study in Chongqing, China and in vivo animal experiments. *Environ. Int.* 2016, *95*, 79–85.

833. Bijnens, E.; Zeegers, M.P.; Gielen, M.; Kicinski, M.; Hageman, G.J.; Pachen, D.; Derom, C.; Vlietinck, R.; Nawrot, T.S. Lower placental telomere length may be attributed to maternal residential traffic exposure; a twin study. *Environ. Int.* 2015, *79*, 1–7.

834. Martens, D.S.; Cox, B.; Janssen, B.G.; Clemente, D.B.P.; Gasparrini, A.; Vanpoucke, C.; Lefebvre, W.; Roels, H.A.; Plusquin, M.; Nawrot, T.S. Prenatal Air Pollution and Newborns' Predisposition to Accelerated Biological Aging. *JAMA Pediatr.* 2017, *171*, 1160–1167.

835. Hou, L.; Wang, S.; Dou, C.; Zhang, X.; Yu, Y.; Zheng, Y.; Avula, U.; Hoxha, M.; Díaz, A.; McCracken, J.; et al. Air pollution exposure and telomere length in highly exposed subjects in Beijing, China: A repeated-measure study. *Environ. Int.* 2012, *48*, 71–77.

836. Xu, Y.; Lindh, C.H.; Jönsson, B.A.G.; Broberg, K.; Albin, M. Occupational exposure to asphalt mixture during road paving is related to increased mitochondria DNA copy number: a cross-sectional study. *Environ. Heal.* 2018, *17*, 29–39.

837. Weng, N. Regulation of telomerase expression in human lymphocytes. *Springer Semin. Immunopathol.* 2002, *24*, 23–33.

838. Grahame, T.J.; Schlesinger, R.B. Oxidative stress-induced telomeric erosion as a mechanism underlying airborne particulate matter-related cardiovascular disease. *Part. Fibre Toxicol.* 2012, *9*, 21–40.

839. Heath Effects Institute: Panel on the Health Effects of Traffic-Related Air Pollution. Traffic-related air pollution: a critical review of the literature on emissions, exposure, and health effects. Available online:

https://www.healtheffects.org/system/files/SR17Traffic Review.pdf (accessed on Jul 15, 2019).

840.   Weng, N.P.; Granger, L.; Hodes, R.J. Telomere lengthening and telomerase activation during human B cell differentiation. *Proc. Natl. Acad. Sci. U. S. A.* 1997, *94*, 10827–32.

841.   Hodes, R.J.; Hathcock, K.S.; Weng, N. Telomeres in T and B cells. *Nat. Rev. Immunol.* 2002, *2*, 699–706.

842.   O'Sullivan, R.J.; Karlseder, J. Telomeres: protecting chromosomes against genome instability. *Nat. Rev. Mol. Cell Biol.* 2010, *11*, 171–181.

843.   Iodice, S.; Hoxha, M.; Ferrari, L.; Carbone, I.F.; Anceschi, C.; Miragoli, M.; Pesatori, A.C.; Persico, N.; Bollati, V. Particulate Air Pollution, Blood Mitochondrial DNA Copy Number, and Telomere Length in Mothers in the First Trimester of Pregnancy: Effects on Fetal Growth. *Oxid. Med. Cell. Longev.* 2018, *2018*, 5162905.

844.   Shadel, G.S. Expression and maintenance of mitochondrial DNA: new insights into human disease pathology. *Am. J. Pathol.* 2008, *172*, 1445–56.

845.   Stark, R.; Roden, M. Mitochondrial function and endocrine diseases. *Eur. J. Clin. Invest.* 2007, *37*, 236–248.

846.   Miranda, S.; Foncea, R.; Guerrero, J.; Leighton, F. Oxidative Stress and Upregulation of Mitochondrial Biogenesis Genes in Mitochondrial DNA-Depleted HeLa Cells. *Biochem. Biophys. Res. Commun.* 1999, *258*, 44–49.

847.   Pohjoismäki, J.L.O.; Boettger, T.; Liu, Z.; Goffart, S.; Szibor, M.; Braun, T. Oxidative stress during mitochondrial biogenesis compromises mtDNA integrity in growing hearts and induces a global DNA repair response. *Nucleic Acids Res.* 2012, *40*, 6595–607.

848.   Yoboue, E.D.; Devin, A. Reactive Oxygen Species-Mediated Control of Mitochondrial Biogenesis. *Int. J. Cell Biol.* 2012, *2012*, 1–8.

849.   Bouhours-Nouet, N.; May-Panloup, P.; Coutant, R.; de Casson, F.B.; Descamps, P.; Douay, O.; Reynier, P.; Ritz, P.; Malthièry, Y.; Simard, G. Maternal smoking is associated with mitochondrial DNA depletion and respiratory chain complex III deficiency in placenta. *Am. J. Physiol. Metab.* 2005, *288*, E171–E177.

850.   Carugno, M.; Pesatori, A.C.; Dioni, L.; Hoxha, M.; Bollati, V.; Albetti, B.; Byun, H.-M.; Bonzini, M.; Fustinoni, S.; Cocco, P.; et al. Increased mitochondrial DNA copy number in occupations associated with low-dose benzene exposure. *Environ. Health Perspect.* 2012, *120*, S1–S4.

851.   Shen, M.; Zhang, L.; Bonner, M.R.; Liu, C.; Li, G.; Vermeulen, R.; Dosemeci, M.; Yin, S.; Lan, Q. Association between mitochondrial DNA copy number, blood cell counts, and occupational benzene exposure. *Environ. Mol. Mutagen.* 2008, *49*, 453–457.

852.   Hou, L.; Zhang, X.; Dioni, L.; Barretta, F.; Dou, C.; Zheng, Y.; Hoxha, M.; Bertazzi, P.A.; Schwartz, J.; Wu, S.; et al. Inhalable particulate matter and mitochondrial DNA copy number in highly exposed individuals in Beijing, China: a repeated-measure study. *Part. Fibre Toxicol.* 2013, *10*, 17–26.

853.   Moro, A.M.; Brucker, N.; Charão, M.; Bulcão, R.; Freitas, F.; Baierle, M.; Nascimento, S.; Valentini, J.; Cassini, C.; Salvador, M.; et al. Evaluation of genotoxicity and oxidative damage in painters exposed to

low levels of toluene. *Mutat. Res. Toxicol. Environ. Mutagen.* 2012, *746*, 42–48.

854. Oxidative DNA Damage by Minor Metabolites of Toluene May Lead to Carcinogenesis and Reproductive Dysfunction. *Biochem. Biophys. Res. Commun.* 1999, *261*, 478–483.

855. Kodavanti, P.R.S.; Royland, J.E.; Moore-Smith, D.A.; Besas, J.; Richards, J.E.; Beasley, T.E.; Evansky, P.; Bushnell, P.J. Acute and subchronic toxicity of inhaled toluene in male Long–Evans rats: Oxidative stress markers in brain. *Neurotoxicology* 2015, *51*, 10–19.

856. Revilla, A.S.; Pestana, C.R.; Pardo-Andreu, G.L.; Santos, A.C.; Uyemura, S.A.; Gonzales, M.E.; Curti, C. Potential toxicity of toluene and xylene evoked by mitochondrial uncoupling. *Toxicol. Vitr.* 2007, *21*, 782–788.

857. Moro, A.M.; Charão, M.; Brucker, N.; Bulcão, R.; Freitas, F.; Guerreiro, G.; Baierle, M.; Nascimento, S.; Waechter, F.; Hirakata, V.; et al. Effects of low-level exposure to xenobiotics present in paints on oxidative stress in workers. *Sci. Total Environ.* 2010, *408*, 4461–4467.

858. Malik, A.N.; Czajka, A. Is mitochondrial DNA content a potential biomarker of mitochondrial dysfunction? *Mitochondrion* 2013, *13*, 481–492.

859. Eom, H.-Y.; Kim, H.-R.; Kim, H.-Y.; Han, D.-K.; Baek, H.-J.; Lee, J.-H.; Moon, J.D.; Shin, J.-H.; Suh, S.-P.; Ryang, D.-W.; et al. Mitochondrial DNA copy number and hnRNP A2/B1 protein: Biomarkers for direct exposure of benzene. *Environ. Toxicol. Chem.* 2011, *30*, 2762–2770.

860. Dulak, J.; Józkowicz, A. Nitric oxide and angiogenic activity of endothelial cells: direct or VEGF-dependent effect? *Cardiovasc. Res.* 2002, *56*, 487–488.

861. Dulak, J.; Józkowicz, A.; Dembinska-Kiec, A.; Guevara, I.; Zdzienicka, A.; Zmudzinska-Grochot, D.; Florek, I.; Wójtowicz, A.; Szuba, A.; Cooke, J.P. Nitric oxide induces the synthesis of vascular endothelial growth factor by rat vascular smooth muscle cells. *Arterioscler. Thromb. Vasc. Biol.* 2000, *20*, 659–66.

862. Jozkowicz, A.; Cooke, J.P.; Guevara, I.; Huk, I.; Funovics, P.; Pachinger, O.; Weidinger, F.; Dulak, J. Genetic augmentation of nitric oxide synthase increases the vascular generation of VEGF. *Cardiovasc. Res.* 2001, *51*, 773–83.

863. Dulak, J.; Józkowicz, A.; Dichtl, W.; Alber, H.; Schwarzacher, S.P.; Pachinger, O.; Weidinger, F.; Dulakk, J. Vascular endothelial growth factor synthesis in vascular smooth muscle cells is enhanced by 7-ketocholesterol and lysophosphatidylcholine independently of their effect on nitric oxide generation. *Atherosclerosis* 2001, *159*, 325–32.

864. Kim, I.; Moon, S.-O.; Park, S.K.; Chae, S.W.; Koh, G.Y. Angiopoietin-1 Reduces VEGF-Stimulated Leukocyte Adhesion to Endothelial Cells by Reducing ICAM-1, VCAM-1, and E-Selectin Expression Injune. *Circ. Res.* 2014, *1555*, 1–22.

865. Palmefors, H.; DuttaRoy, S.; Rundqvist, B.; Börjesson, M. The effect of physical activity or exercise on key biomarkers in atherosclerosis - A systematic review. *Atherosclerosis* 2014, *235*, 150–161.

866. Caren, L.D. Environmental Pollutants: Effects on the Immune System and Resistance to Infectious Disease. *Bioscience* 1981, *31*, 582–586.

867. Frampton, M.W.; Smeglin, A.M.; Roberts, N.J.; Finkelstein, J.N.; Morrow, P.E.; Utell, M.J. Nitrogen dioxide exposure in vivo and human alveolar macrophage inactivation of influenza virus in vitro. *Environ. Res.* 1989, *48*, 179–92.

868. Sandström, T.; Ledin, M.C.; Thomasson, L.; Helleday, R.; Stjernberg, N. Reductions in lymphocyte subpopulations after repeated exposure to 1.5 ppm nitrogen dioxide. *Br. J. Ind. Med.* 1992, *49*, 850–4.

869. Sandstrom, T.; Helleday, R.; Bjermer, L.; Stjernberg, N. *Effects of repeated exposure to 4 ppm nitrogen dioxide on bronchoalveolar lymphocyte subsets and macrophages in healthy men*; 1992; Vol. 5;.

870. Folinsbee, L.J. Human health effects of air pollution. *Environ. Health Perspect.* 1993, *100*, 45–56.

871. Sanders, J.L.; Newman, A.B. Telomere length in epidemiology: A biomarker of aging, age-related disease, both, or neither? *Epidemiol. Rev.* 2013, *35*, 112–131.

872. Wink, D.A.; Hines, H.B.; Cheng, R.Y.S.; Switzer, C.H.; Flores-Santana, W.; Vitek, M.P.; Ridnour, L.A.; Colton, C.A. Nitric oxide and redox mechanisms in the immune response. *J. Leukoc. Biol.* 2011, *89*, 873–891.

873. Langrish, J.P.; Lundbäck, M.; Barath, S.; Söderberg, S.; Mills, N.L.; Newby, D.E.; Sandström, T.; Blomberg, A. Exposure to nitrogen dioxide is not associated with vascular dysfunction in man. *Inhal. Toxicol.* 2010, *22*, 192–198.

874. Cherng, T.W.; Paffett, M.L.; Jackson-Weaver, O.; Campen, M.J.; Walker, B.R.; Kanagy, N.L. Mechanisms of diesel-induced endothelial nitric oxide synthase dysfunction in coronary arterioles. *Environ. Health Perspect.* 2011, *119*, 98–103.

875. Robinson, S.D.; Frenette, P.S.; Rayburn, H.; Cummiskey, M.; Ullman-Culleré, M.; Wagner, D.D.; Hynes, R.O. Multiple, targeted deficiencies in selectins reveal a predominant role for P-selectin in leukocyte recruitment. *Proc. Natl. Acad. Sci. U. S. A.* 1999, *96*, 11452–7.

876. Li, B.; Niu, Y.; Liu, S.; Yu, W.; Chen, J.; Wu, L.; Liu, W.; Chen, S.; Yang, L.; Li, Y. A change in CD3 γ, CD3 δ, CD3 ϵ, and CD3 ζ gene expression in T-lymphocytes from benzene-exposed and benzene-poisoned workers. *J. Immunotoxicol.* 2012, *9*, 160–167.

877. Mićović, V.; Vojniković, B.; Bulog, A.; Coklo, M.; Malatestinić, D.; Mrakovcić-Sutić, I. Regulatory T cells (Tregs) monitoring in environmental diseases. *Coll. Antropol.* 2009, *33*, 743–6.

878. McMurry, S.T.; Lochmiller, R.L.; Vestey, M.R.; Qualls, C.W. Cellular immune responses of nutritionally stressed juvenile cotton rats (Sigmodon hispidus) during acute benzene exposure. *Arch. Environ. Contam. Toxicol.* 1994, *27*, 14–19.

879. Hsieh, G.C.; Parker, R.D.R.; Sharma, R.P.; Hughes, B.J. Subclinical effects of groundwater contaminants. *Arch. Toxicol.* 1990, *64*, 320–328.

880. Kim, A.R.; Cho, J.Y.; Lee, J.Y.; Choi, J.S.; Chung, H.Y. Hydroquinone modulates reactivity of peroxynitrite and nitric oxide production. *J. Pharm. Pharmacol.* 2005, *57*, 475–481.

881. Clancy, R.M.; Amin, A.R.; Abramson, S.B. The role of nitric oxide in inflammation and immunity. *Arthritis Rheum.* 1998, *41*, 1141–1151.

882. Bogdan, C. Nitric oxide and the immune response. *Nat. Immunol.* 2001, *2*, 907–916.

883. Lahiri, T.; Ray, M.R.; Ray, M.R. Effects of Indoor Air Pollution from Biomass Fuel Use on Women's Health in India Available online: https://www.taylorfrancis.com/books/e/9780429075599/chapters/10.1201/EBK1439809624-12 (accessed on Sep 1, 2019).

884. Ray, M.R.; Roychoudhury, S.; Mukherjee, S.; Lahiri, T. Occupational benzene exposure from vehicular sources in India and its effect on hematology, lymphocyte subsets and platelet P-selectin expression Available online: http://www.ncbi.nlm.nih.gov/pubmed/18220159 (accessed on Aug 31, 2019).

885. Abdalla AgabEldour, A.; Osman Khalafallah, T.; Mohammed Ahmed AbdAllah, A.; Mohammed Ahmed Abd Allah, A. Hematological changes among Sudanese petroleum workers with a broad range of benzene exposure. Available online: www.saspublisher.com (accessed on Aug 31, 2019).

886. Avogbe, P.; Ayi-Fanou, L.; Cachon, B.; Chabi, N.; Debende, A.; Dewaele, D.; Aissi, F.; Cazier, F.; Sanni, A. Hematological changes among Beninese motor-bike taxi drivers exposed to benzene by urban air pollution. Available online: https://www.ajol.info/index.php/ajest/article/view/72031 (accessed on Aug 31, 2019).

887. Dede, E.B.; Kagbo, H.D. A Study On The Acute Toxicological Effects Of Commercial Diesel Fuel In Nigeria In Rats (Ratus ratus.) Using Hematological Parameters. *J. Appl. Sci. Environ. Manag.* 2002, *6*, 84–86.

888. Silber, A.; Newman, W.; Reimann, K.A.; Hendricks, E.; Walsh, D.; Ringler, D.J. Kinetic expression of endothelial adhesion molecules and relationship to leukocyte recruitment in two cutaneous models of inflammation. *Lab. Invest.* 1994, *70*, 163–75.

889. Lukacs, N.; Strieter, R.; Elner, V.; Evanoff, H.; Burdick, M.; Kunkel, S. Intercellular adhesion molecule-1 mediates the expression of monocyte- derived MIP-1 alpha during monocyte-endothelial cell interactions. *Blood* 1994, *83*, 1174–8.

890. Kong, D.-H.; Kim, Y.K.; Kim, M.R.; Jang, J.H.; Lee, S. Emerging Roles of Vascular Cell Adhesion Molecule-1 (VCAM-1) in Immunological Disorders and Cancer. *Int. J. Mol. Sci.* 2018, *19*, 1057–1073.

891. Bind, M.-A.; Coull, B.; Suh, H.; Wright, R.; Baccarelli, A.; Vokonas, P.; Schwartz, J. A Novel Genetic Score Approach Using Instruments to Investigate Interactions between Pathways and Environment: Application to Air Pollution. *PLoS One* 2014, *9*, e96000.

892. Kannel, W.B. Overview of hemostatic factors involved in atherosclerotic cardiovascular disease. *Lipids* 2005, *40*, 1215–1220.

893. Ichimura, A.; Matsumoto, S.; Suzuki, S.; Dan, T.; Yamaki, S.; Sato, Y.; Kiyomoto, H.; Ishii, N.; Okada, K.; Matsuo, O.; et al. A small molecule inhibitor to plasminogen activator inhibitor 1 inhibits macrophage migration. *Arterioscler. Thromb. Vasc. Biol.* 2013, *33*, 935–942.

894. Shimomura, I.; Funahasm, T.; Takahashi, M.; Maeda, K.; Kotani, K.; Nakamura, T.; Yamashita, S.; Miura, M.; Fukuda, Y.; Takemura, K.; et al. Enhanced expression of PAI–1 in visceral fat: Possible contributor to vascular disease in obeisty. *Nat. Med.* 1996, *2*, 800–803.

895.   Zhen, L.W.; Ling, M.C.; Wickham, N. Endothelial Cell PAI-1 Production — Modulation by Malignant Cells in vitro. In *Vascular Endothelium*; Springer US: Boston, MA, 1998; pp. 287–290.

896.   Alessi, M.-C.; Poggi, M.; Juhan-Vague, I. Plasminogen activator inhibitor-1, adipose tissue and insulin resistance. *Curr. Opin. Lipidol.* 2007, *18*, 240–245.

897.   Engelson, E.S.; Agin, D.; Kenya, S.; Werber-Zion, G.; Luty, B.; Albu, J.B.; Kotler, D.P. Body composition and metabolic effects of a diet and exercise weight loss regimen on obese, HIV-infected women. *Metabolism.* 2006, *55*, 1327–1336.

898.   Krishnamurti, C.; Barr, C.F.; Hassett, M.A.; Young, G.D.; Alving, B.M. Plasminogen activator inhibitor: a regulator of ancrod-induced fibrin deposition in rabbits. *Blood* 1987, *69*, 798–803.

899.   Levi, M.; Biemond, B.J.; van Zonneveld, A.J.; ten Cate, J.W.; Pannekoek, H. Inhibition of plasminogen activator inhibitor-1 activity results in promotion of endogenous thrombolysis and inhibition of thrombus extension in models of experimental thrombosis. *Circulation* 1992, *85*, 305–12.

900.   Erickson, L.A.; Fici, G.J.; Lund, J.E.; Boyle, T.P.; Polites, H.G.; Marotti, K.R. Development of venous occlusions in mice transgenic for the plasminogen activator inhibitor-1 gene. *Nature* 1990, *346*, 74–76.

901.   Carmeliet, P.; Stassen, J.M.; Schoonjans, L.; Ream, B.; van den Oord, J.J.; De Mol, M.; Mulligan, R.C.; Collen, D. Plasminogen activator inhibitor-1 gene-deficient mice. II. Effects on hemostasis, thrombosis, and thrombolysis. *J. Clin. Invest.* 1993, *92*, 2756–2760.

902.   Chuang, K.-J.J.; Chan, C.-C.C.; Su, T.-C.C.; Lee, C.-T. Te; Tang, C.-S.S. The effect of urban air pollution on inflammation, oxidative stress, coagulation, and autonomic dysfunction in young adults. *Am. J. Respir. Crit. Care Med.* 2007, *176*, 370–376.

903.   Bigert, C.; Alderling, M.; Svartengren, M.; Plato, N.; de Faire, U.; Gustavsson, P. Blood markers of inflammation and coagulation and exposure to airborne particles in employees in the Stockholm underground. *Occup. Environ. Med.* 2008, *65*, 655–8.

904.   Green, R.; Broadwin, R.; Malig, B.; Basu, R.; Gold, E.B.; Qi, L.; Sternfeld, B.; Bromberger, J.T.; Greendale, G.A.; Kravitz, H.M.; et al. Long- and short-term exposure to air pollution and inflammatory/hemostatic markers in midlife women. *Epidemiology* 2016, *27*, 211–20.

905.   Alessi, M.-C.; Juhan-Vague, I. PAI-1 and the Metabolic Syndrome. *Arterioscler. Thromb. Vasc. Biol.* 2006, *26*, 2200–2207.

906.   Kodaman, N.; Aldrich, M.C.; Sobota, R.; Asselbergs, F.W.; Brown, N.J.; Moore, J.H.; Williams, S.M. Plasminogen Activator Inhibitor-1 and Diagnosis of the Metabolic Syndrome in a West African Population. *J. Am. Heart Assoc.* 2016, *5*, S1–S8.

907.   Yarmolinsky, J.; Bordin Barbieri, N.; Weinmann, T.; Ziegelmann, P.K.; Duncan, B.B.; Schmidt, M.I. Plasminogen activator inhibitor-1 and type 2 diabetes: a systematic review and meta-analysis of observational studies. *Sci. Rep.* 2016, *6*, 17714–27.

908.   Eriksson, P.; Nilsson, L.; Karpe, F.; Hamsten, A. Very-low-density lipoprotein response element in the promoter region of the human plasminogen activator inhibitor-1 gene implicated in the impaired fibrinolysis

of hypertriglyceridemia. *Arterioscler. Thromb. Vasc. Biol.* 1998, *18*, 20–6.

909. Somodi, S.; Seres, I.; Lőrincz, H.; Harangi, M.; Fülöp, P.; Paragh, G. Plasminogen Activator Inhibitor-1 Level Correlates with Lipoprotein Subfractions in Obese Nondiabetic Subjects. *Int. J. Endocrinol.* 2018, *2018*, 1–9.

910. Kaji, H. Adipose Tissue-Derived Plasminogen Activator Inhibitor-1 Function and Regulation. In *Comprehensive Physiology*; John Wiley & Sons, Inc.: Hoboken, NJ, USA, 2016; Vol. 6, pp. 1873–1896.

911. Wang, L.; Chen, L.; Liu, Z.; Liu, Y.; Luo, M.; Chen, N.; Deng, X.; Luo, Y.; He, J.; Zhang, L.; et al. PAI-1 Exacerbates White Adipose Tissue Dysfunction and Metabolic Dysregulation in High Fat Diet-Induced Obesity. *Front. Pharmacol.* 2018, *9*, 1087–1095.

912. López-Alemany, R.; Redondo, J.M.; Nagamine, Y.; Muñoz-Cánoves, P. Plasminogen activator inhibitor type-1 inhibits insulin signaling by competing with αvβ3 integrin for vitronectin binding. *Eur. J. Biochem.* 2003, *270*, 814–821.

913. Degryse, B.; Sier, C.F.; Resnati, M.; Conese, M.; Blasi, F. PAI-1 inhibits urokinase-induced chemotaxis by internalizing the urokinase receptor. *FEBS Lett.* 2001, *505*, 249–54.

914. Deng, G.; Curriden, S.A.; Wang, S.; Rosenberg, S.; Loskutoff, D.J. Is plasminogen activator inhibitor-1 the molecular switch that governs urokinase receptor-mediated cell adhesion and release? *J. Cell Biol.* 1996, *134*, 1563–1571.

915. Czekay, R.-P.; Aertgeerts, K.; Curriden, S.A.; Loskutoff, D.J. Plasminogen activator inhibitor-1 detaches cells from extracellular matrices by inactivating integrins. *J. Cell Biol.* 2003, *160*, 781–791.

916. Franchini, M.; Mannucci, P.M. Air pollution and cardiovascular disease. *Thromb. Res.* 2012, *129*, 230–234.

917. Hoffmann, B.; Luttmann-Gibson, H.; Cohen, A.; Zanobetti, A.; de Souza, C.; Foley, C.; Suh, H.H.; Coull, B.A.; Schwartz, J.; Mittleman, M.; et al. Opposing effects of particle pollution, ozone, and ambient temperature on arterial blood pressure. *Environ. Health Perspect.* 2012, *120*, 241–246.

918. Weichenthal, S.; Hatzopoulou, M.; Goldberg, M.S. Exposure to traffic-related air pollution during physical activity and acute changes in blood pressure, autonomic and micro-vascular function in women: a cross-over study. *Part. Fibre Toxicol.* 2014, *11*, 70–86.

919. Yang, B.; Qian, Z.; Howard, S.W.; Vaughn, M.G.; Fan, S.; Liu, K.; Dong, G. Global association between ambient air pollution and blood pressure: A systematic review and meta-analysis. *Environ. Pollut.* 2018, *235*, 576–588.

920. Chen, W.-H.; Yang Sung, S.; Fadeev, M.; Cecconello, A.; Nechushtai, R.; Willner, I. Targeted VEGF-triggered release of an anti-cancer drug from aptamer-functionalized metal–organic framework nanoparticles. *Nanoscale* 2018, *10*, 4650–4657.

921. Carter, J.G.; Gammons, M.V.R.; Damodaran, G.; Churchill, A.J.; Harper, S.J.; Bates, D.O. The carboxyl terminus of VEGF-A is a potential target for anti-angiogenic therapy. *Angiogenesis* 2015, *18*, 23–30.

922. Kim, M.G.; Jo, S.D.; Yhee, J.Y.; Lee, B.S.; Lee, S.J.; Park, S.G.; Kang, S.-W.; Kim, S.H.; Jeong, J.H.

Synergistic anti-tumor effects of bevacizumab and tumor targeted polymerized VEGF siRNA nanoparticles. *Biochem. Biophys. Res. Commun.* 2017, *489*, 35–41.

923. Brook, R.D.; Brook, J.R.; Urch, B.; Vincent, R.; Rajagopalan, S.; Silverman, F. Inhalation of fine particulate air pollution and ozone causes acute arterial vasoconstriction in healthy adults. *Circulation* 2002, *105*, 1534–1536.

924. Adar, S.D.; Klein, R.; Klein, B.E.K.; Szpiro, A.A.; Cotch, M.F.; Wong, T.Y.; O'Neill, M.S.; Shrager, S.; Barr, R.G.; Siscovick, D.S.; et al. Air pollution and the microvasculature: a cross-sectional assessment of in vivo retinal images in the population-based multi-ethnic study of atherosclerosis (MESA). *PLoS Med.* 2010, *7*, e1000372.

925. Edelman, J.L.; Lutz, D.; Castro, M.R. Corticosteroids inhibit VEGF-induced vascular leakage in a rabbit model of blood–retinal and blood–aqueous barrier breakdown. *Exp. Eye Res.* 2005, *80*, 249–258.

926. Wong, T.Y.; Klein, R.; Klein, B.E.K.; Meuer, S.M.; Hubbard, L.D. Retinal Vessel Diameters and Their Associations with Age and Blood Pressure. *Investig. Opthalmology Vis. Sci.* 2003, *44*, 4644–51.

927. Leung, H.; Wang, J.J.; Rochtchina, E.; Tan, A.G.; Wong, T.Y.; Klein, R.; Hubbard, L.D.; Mitchell, P. Relationships between Age, Blood Pressure, and Retinal Vessel Diameters in an Older Population. *Investig. Opthalmology Vis. Sci.* 2003, *44*, 2900–2905.

928. Kawasaki, R.; Cheung, N.; Wang, J.J.; Klein, R.; Klein, B.E.; Cotch, M.F.; Sharrett, A.R.; Shea, S.; Islam, F.A.; Wong, T.Y. Retinal vessel diameters and risk of hypertension: the Multiethnic Study of Atherosclerosis. *J. Hypertens.* 2009, *27*, 2386–93.

929. Block, M.L.; Calderón-Garcidueñas, L. Air pollution: mechanisms of neuroinflammation and CNS disease. *Trends Neurosci.* 2009, *32*, 506–516.

930. Langman, J.M. Xylene: its toxicity, measurement of exposure levels, absorption, metabolism and clearance. *Pathology* 1994, *26*, 301–309.

931. Chan, S.H.; Van Hee, V.C.; Bergen, S.; Szpiro, A.A.; DeRoo, L.A.; London, S.J.; Marshall, J.D.; Kaufman, J.D.; Sandler, D.P.; Kaufman, J.D.; et al. Long-term air pollution exposure and blood pressure in the sister study. *Environ. Health Perspect.* 2015, *123*, 951–958.

932. Chen, J.-C.; Wang, X.; Wellenius, G.A.; Serre, M.L.; Driscoll, I.; Casanova, R.; McArdle, J.J.; Manson, J.E.; Chui, H.C.; Espeland, M.A. Ambient air pollution and neurotoxicity on brain structure: Evidence from women's health initiative memory study. *Ann. Neurol.* 2015, *78*, 466–476.

933. Langrish, J.P.; Lundbäck, M.; Mills, N.L.; Johnston, N.R.; Webb, D.J.; Sandström, T.; Blomberg, A.; Newby, D.E.; Sandström, T.; Lundbäck, M.; et al. Contribution of endothelin 1 to the vascular effects of diesel exhaust inhalation in humans. *Hypertension* 2009, *54*, 910–915.

934. Dales, R.; Liu, L.; Szyszkowicz, M.; Dalipaj, M.; Willey, J.; Kulka, R.; Ruddy, T.D. Particulate air pollution and vascular reactivity: the bus stop study. *Int. Arch. Occup. Environ. Health* 2007, *81*, 159–164.

935. Krishnan, R.M.; Adar, S.D.; Szpiro, A.A.; Jorgensen, N.W.; Van Hee, V.C.; Barr, R.G.; O'Neill, M.S.; Herrington, D.M.; Polak, J.F.; Kaufman, J.D. Vascular Responses to Long- and Short-Term Exposure to

Fine Particulate Matter. *J. Am. Coll. Cardiol.* 2012, *60*, 2158–2166.

936. Brook, R.D.; Urch, B.; Dvonch, J.T.; Bard, R.L.; Speck, M.; Keeler, G.; Morishita, M.; Marsik, F.J.; Kamal, A.S.; Kaciroti, N.; et al. Insights into the mechanisms and mediators of the effects of air pollution exposure on blood pressure and vascular function in healthy humans. *Hypertension* 2009, *54*, 659–667.

937. Widdicombe, J.; Lee, L.Y. Airway reflexes, autonomic function, and cardiovascular responses. *Environ. Health Perspect.* 2001, *109 Suppl 4*, 579–84.

938. Bartoli, C.R.; Wellenius, G.A.; Diaz, E.A.; Lawrence, J.; Coull, B.A.; Akiyama, I.; Lee, L.M.; Okabe, K.; Verrier, R.L.; Godleski, J.J. Mechanisms of Inhaled Fine Particulate Air Pollution–Induced Arterial Blood Pressure Changes. *Environ. Health Perspect.* 2009, *117*, 361–366.

939. Pope Iii, C.A.; Verrier, R.L.; Lovett, E.G.; Larson, A.C.; Raizenne, M.E.; Kanner, R.E.; Schwartz, J.; Villegas, G.M.M.; Gold, D.R.; Dockery, D.W.; et al. Heart rate variability associated with particulate air pollution. *Am. Heart J.* 1999, *138*, 890–899.

940. Mordukhovich, I.; Coull, B.; Kloog, I.; Koutrakis, P.; Vokonas, P.; Schwartz, J. Exposure to sub-chronic and long-term particulate air pollution and heart rate variability in an elderly cohort: the Normative Aging Study. *Environ. Heal.* 2015, *14*, 87–97.

941. Cole-Hunter, T.; Weichenthal, S.; Kubesch, N.; Foraster, M.; Carrasco-Turigas, G.; Bouso, L.; Martínez, D.; Westerdahl, D.; de Nazelle, A.; Nieuwenhuijsen, M. Impact of traffic-related air pollution on acute changes in cardiac autonomic modulation during rest and physical activity: a cross-over study. *J. Expo. Sci. Environ. Epidemiol.* 2016, *26*, 133–140.

942. Mirowsky, J.E.; Peltier, R.E.; Lippmann, M.; Thurston, G.; Chen, L.-C.; Neas, L.; Diaz-Sanchez, D.; Laumbach, R.; Carter, J.D.; Gordon, T. Repeated measures of inflammation, blood pressure, and heart rate variability associated with traffic exposures in healthy adults. *Environ. Heal.* 2015, *14*, 66–78.

943. Watarai, K. Impairment of Endothelium-Dependent Particles in Rat Relaxation Thoracic by Diesel Exhaust Aorta. *J. Pharmacol.* 1994, *68*, 183–189.

944. Mills, N.L.; Törnqvist, H.; Robinson, S.D.; Gonzalez, M.; Darnley, K.; MacNee, W.; Boon, N.A.; Donaldson, K.; Blomberg, A.; Sandstrom, T.; et al. Diesel exhaust inhalation causes vascular dysfunction and impaired endogenous fibrinolysis. *Circulation* 2005, *112*, 3930–6.

945. Miller, M.R.; Borthwick, S.J.; Shaw, C.A.; McLean, S.G.; McClure, D.; Mills, N.L.; Duffin, R.; Donaldson, K.; Megson, I.L.; Hadoke, P.W.F.; et al. Direct impairment of vascular function by diesel exhaust particulate through reduced bioavailability of endothelium-derived nitric oxide induced by superoxide free radicals. *Environ. Health Perspect.* 2009, *117*, 611–6.

946. Koehler, K.A.; Peters, T.M. New Methods for Personal Exposure Monitoring for Airborne Particles. *Curr. Environ. Heal. Reports* 2015, *2*, 399–411.

947. Croxford, J.; Viljoen, D. Alcohol consuption by pregnant women in the Western Cape. *SAMJ* 1999, *89*, 962–965.

948. Reddy, P.; Zuma, K.; Shisana, O.; Kim, J.; Sewpaul, R.; Jonas, K.; Sewpaul, R. Prevalence of tobacco use

among adults in South Africa: Results from the first South African national health and Nutrition Examination Survey. *South African Med. J.* 2015, *105*, 648–655.

949. Oliveira, A.R.; Campos Neto, A.A.; de Andrade, M.J.O.; de Medeiros, P.C.B.; dos Santos, N.A. Organic solvent exposure and contrast sensitivity: Comparing men and women. *Brazilian J. Med. Biol. Res.* 2018, *51*, e6568.

950. Walton, R.T.; Mudway, I.S.; Dundas, I.; Grigg, J.; Marlin, N.; Koh, L.C.; Aitlhadj, L.; Vulliamy, T.; Jamaludin, J.B.; Wood, H.E.; et al. Air pollution, ethnicity and telomere length in east London schoolchildren: An observational study. *Environ. Int.* 2016, *96*, 41–47.

951. Gardner, M.; Bann, D.; Wiley, L.; Cooper, R.; Hardy, R.; Nitsch, D.; Martin-Ruiz, C.; Shiels, P.; Sayer, A.A.; Barbieri, M.; et al. Gender and telomere length: Systematic review and meta-analysis. *Exp. Gerontol.* 2014, *51*, 15–27.

952. Clougherty, J.E. A growing role for gender analysis in air pollution epidemiology. *Environ. Health Perspect.* 2010, *118*, 167–176.

953. World Health Organization. Petroleum Products in Drinking-water: Background document for development of WHO Guidelines for Drinking-water Quality. Available online: https://www.who.int/water_sanitation_health/dwq/chemicals/petroleumproducts_2add_june2008.pdf (accessed on Sep 4, 2019).

954. Montuschi, P.; Barnes, P.J.; ROBERTS, L.J.; Robersts, L.J. Isoprostanes: markers and mediators of oxidative stress. *FASEB J.* 2004, *18*, 1791–1800.

955. Peng, R.D.; Bell, M.L.; Geyh, A.S.; McDermott, A.; Zeger, S.L.; Samet, J.M.; Dominici, F. Emergency Admissions for Cardiovascular and Respiratory Diseases and the Chemical Composition of Fine Particle Air Pollution. *Environ. Health Perspect.* 2009, *117*, 957–963.

956. Alves, C.A.; Vicente, A.M.; Custódio, D.; Cerqueira, M.; Nunes, T.; Pio, C.; Lucarelli, F.; Calzolai, G.; Nava, S.; Diapouli, E.; et al. Polycyclic aromatic hydrocarbons and their derivatives (nitro-PAHs, oxygenated PAHs, and azaarenes) in PM2.5 from Southern European cities. *Sci. Total Environ.* 2017, *595*, 494–504.

957. Solecki, W.D.; Rosenzweig, C.; Parshall, L.; Pope, G.; Clark, M.; Cox, J.; Wiencke, M. Mitigation of the heat island effect in urban New Jersey. *Environ. Hazards* 2005, *6*, 39–49.

958. Seinfeld, J.H.; Pandis, S.N. *Atmospheric chemistry and physics : from air pollution to climate change*; ISBN 9781118947401.

959. World Health Organization Findings from the Global Burden of Disease Study 2017 Available online: http://www.healthdata.org/sites/default/files/files/policy_report/2019/GBD_2017_Booklet.pdf (accessed on Oct 9, 2019).

960. Oeseburg, H.; De Boer, R.A.; Van Gilst, W.H.; Van Der Harst, P. Telomere biology in healthy aging and disease. *Pflugers Arch. Eur. J. Physiol.* 2010, *459*, 259–268.

961. Wentzensen, I.M.; Mirabello, L.; Pfeiffer, R.M.; Savage, S.A. The Association of Telomere Length and Cancer: a Meta-analysis. *Cancer Epidemiol. Biomarkers Prev.* 2011, *20*, 1238–1250.

962.   Suter, M.; Karr, C.; John-Stewart, G.; Gómez, L.; Moraa, H.; Nyatika, D.; Wamalwa, D.; Paulsen, M.; Simpson, C.; Ghodsian, N.; et al. Implications of Combined Exposure to Household Air Pollution and HIV on Neurocognition in Children. *Int. J. Environ. Res. Public Heal.* 2018, *15*, 163–170.

963.   Medical Association of South Africa., A.; Cowan, M.N. *SAMJ : South African medical journal = SAMT : Suid-Afrikaanse mediese tydskrif.*; Medical Association of South Africa, 2014; Vol. 104;.

964.   Matooane, M.; John, J.; Oosthuizen, R.; Binedell, M. *Vulnerability of South African Communities to Air Pollution.*; 2004; ISBN 0-9584663-7-8.

965.   Van Epps, P.; Kalayjian, R.C. Human Immunodeficiency Virus and Aging in the Era of Effective Antiretroviral Therapy. *Infect. Dis. Clin. North Am.* 2017, *31*, 791–810.

966.   Blanco, J.-R.; Jarrin, I.; Martinez, A.; Siles, E.; Larrayoz, I.M.; Cañuelo, A.; Gutierrez, F.; Gonzalez-Garcia, J.; Vidal, F.; Moreno, S. Shorter Telomere Length Predicts Poorer Immunological Recovery in Virologically Suppressed HIV-1–Infected Patients Treated With Combined Antiretroviral Therapy. *JAIDS J. Acquir. Immune Defic. Syndr.* 2015, *68*, 21–29.

967.   Kaushal, S.; Landay, A.L.; Lederman, M.M.; Connick, E.; Spritzler, J.; Kuritzkes, D.R.; Kessler, H.; Levine, B.L.; St. Louis, D.C.; June, C.H. Increases in T Cell Telomere Length in HIV Infection after Antiretroviral Combination Therapy for HIV-1 Infection Implicate Distinct Population Dynamics in CD4+ and CD8+ T Cells. *Clin. Immunol.* 1999, *92*, 14–24.

968.   Gonzalez-Serna, A.; Ajaykumar, A.; Gadawski, I.; Muñoz-Fernández, M.A.; Hayashi, K.; Harrigan, P.R.; Côté, H.C.F. Rapid Decrease in Peripheral Blood Mononucleated Cell Telomere Length After HIV Seroconversion, but Not HCV Seroconversion. *J. Acquir. Immune Defic. Syndr.* 2017, *76*, e29–e32.

969.   Shippey, K.; Mukanya, R.; van Staden, F.; Dalgliesh, C.; Jones, S.; du Toit, J.; Fubesi, M.; Allan, K. State of Environment Outlook Report For The Western Cape Province Executive Summary 2018. Available online: https://www.westerncape.gov.za/eadp/files/atoms/files/00_Executive Summary.pdf (accessed on Jun 20, 2019).

970.   Davidson, A.; Naidoo, D. State of environment outlook report for the Western Cape Province - Air quality. Available online: http://eadp.westerncape.gov.za/sites/default/files/your-resource-library/WCSoEOR_07_ClimateChange.pdf (accessed on May 17, 2019).

971.   South African Government South African Occupational Health and Safety Act. Available online: https://www.golegal.co.za/wp-content/uploads/2018/02/Occupational-Health-and-Safety-Act-85-of-1993.pdf (accessed on Oct 10, 2019).

972.   Jerrett, M.; Burnett, R.T.; Brook, J.; Kanaroglou, P.; Giovis, C.; Finkelstein, N.; Hutchison, B. Do socioeconomic characteristics modify the short term association between air pollution and mortality? Evidence from a zonal time series in Hamilton, Canada. *J. Epidemiol. Community Health* 2004, *58*, 31–40.

973.   Elliott, P.; Shaddick, G.; Wakefield, J.C.; de Hoogh, C.; Briggs, D.J. Long-term associations of outdoor air pollution with mortality in Great Britain. *Thorax* 2007, *62*, 1088–94.

974.   Adar, S.D.; Chen, Y.-H.; D'Souza, J.C.; O'Neill, M.S.; Szpiro, A.A.; Auchincloss, A.H.; Park, S.K.; Daviglus,

M.L.; Diez Roux, A. V.; Kaufman, J.D. Longitudinal Analysis of Long-Term Air Pollution Levels and Blood Pressure: A Cautionary Tale from the Multi-Ethnic Study of Atherosclerosis. *Environ. Health Perspect.* 2018, *126*, e107003.

975. Everson, F.; Martens, D.S.; Nawrot, T.S.; Goswami, N.; Mthethwa, M.; Webster, I.; Mashele, N.; Charania, S.; Kamau, F.; De Boever, P.; et al. Personal exposure to NO2 and benzene in the Cape Town region of South Africa is associated with shorter leukocyte telomere length in women. *Environ. Res. 182*, 108993.

976. Medical University of Graz; Austrian Society for Laboratory Medicine and Clinical Chemistry ISMD2018: Twelfth International Symposium on Molecular Diagnostics Available online: https://www.degruyter.com/downloadpdf/j/cclm.2018.56.issue-6/cclm-2018-0281/cclm-2018-0281.pdf (accessed on Oct 10, 2019).

977. CoBNeST 2018 SANS symposium within CoBNeST, 7-10 October 2018. Available online: https://saneurosoc.co.za/2017/11/save-the-date-2018-sans-symposium-within-cobnest/ (accessed on Oct 10, 2019).

978. SA Heart Association SA Heart Congress South Africa 2018 – SA Heart Congress South Africa 2018, 4 - 7 October. Available online: http://saheartcongress.org/2018/ (accessed on Oct 10, 2019).

7. Appendix A: Supplementary data for Sub-study 1.

7.1. Appendix A1 – Effects of HIV and ART on body composition.

Table A1.1. Estimated effects of HIV and ART status on body weight (kg).

	Estimate	95% CI Lower	95% CI Upper	p-values
Temporal effects (18-months) [a]				
HIV-free [b]	0.13	-1.02	1.28	0.818
HIV+ART [c]	-0.05	-1.57	1.47	0.948
Initiating ART treatment [a]				
HIV/noART [d]	0.29	-1.64	2.22	0.764
Effects of markers of HIV progression/regression [e]				
Viral load (copies mRNA/ml) [f]	-0.61	-1.90	0.69	0.043
CD4 cell count (cells/mm^3) [f]	1.37	0.09	2.64	0.036

[a] Estimates expressed as an 18-month change. [b] Model A: adjusted for age, gender, recruitment location, smoking, employment, use of medication, alcohol consumption and SBP. [c] Model A additionally adjusted for ethnicity, ART duration at baseline visit, viral load and CD4-cell count. [d] Adjusted for age, smoking viral load and CD4-cell count. [e] HIV+ART and HIV/noART combined with estimate expressed as change for each IQR increment in CD4 count (320 cells/mm^3) and viral load (1300 copies mRNA/ml). [f] Model A additionally adjusted for ethnicity.

Table A1.2. Estimated effects of HIV and ART status on BMI (kg/m^2).

	Estimate	95% CI Lower	95% CI Upper	p-values
Temporal effects (18-months) [a]				
HIV-free [b]	0.03	-0.46	0.51	0.904
HIV+ART [c]	0.41	-0.24	1.07	0.214
Initiating ART treatment [a]				
HIV/noART [d]	0.64	-0.24	1.52	0.147
Effects of markers of HIV progression/regression [e]				
Viral Load (copies mRNA/ml) [f]	-0.40	-1.01	0.20	0.026
CD4 cell count (cells/mm^3) [f]	0.76	0.18	1.35	0.010

[a] Estimates expressed an 18-month change. [b] Model A: adjusted for age, gender, recruitment location, smoking, employment, use of medication, alcohol consumption and SBP. [c] Model A additionally adjusted for ethnicity, ART duration at baseline visit, viral load and CD4-cell count. [d] Adjusted for age, smoking viral load and CD4-cell count.

[e] HIV+ART HIV/noART combined with estimate expressed as change for each IQR increment in CD4 count (320 cells/mm^3) and viral load (1300 copies mRNA/ml). [f] Model A additionally adjusted for ethnicity.

Table A1.3. Estimated effects of HIV and ART status on waist circumference (cm).

	Estimate	95% CI Lower	95% CI Upper	p-values
Temporal effects (18-months) [a]				
HIV-free [b]	0.18	-1.20	1.56	0.795
HIV+ART [c]	-3.43	-5.02	-1.84	< 0.001
Initiating ART treatment [a]				
HIV/noART [d]	0.51	-2.03	3.05	0.686
Effects of markers of HIV progression/regression [e]				
Viral Load (copies mRNA/ml) [f]	-1.43	-2.84	-0.03	0.046
CD4 cell count (cells/mm^3) [f]	1.49	0.09	2.89	0.037

[a] Estimates expressed an 18-month change. [b] Model A: adjusted for age, gender, recruitment location, smoking, employment, use of medication, alcohol consumption and SBP. [c] Model A additionally adjusted for ethnicity, ART duration at baseline visit, viral load and CD4-cell count. [d] Adjusted for age, smoking viral load and CD4-cell count. [e] HIV+ART and HIV/noART combined with estimate expressed as change for each IQR increment in CD4 count (320 cells/mm^3) and viral load (1300 copies mRNA/ml). [f] Model A additionally adjusted for ethnicity.

Table A1.4. Estimated effects of HIV and ART status on hip circumference (cm).

	Estimate	95% CI Lower	95% CI Upper	p-values
Temporal effects (18-months) [a]				
HIV-free [b]	-1.22	-2.54	0.10	0.069
HIV+ART [c]	-2.59	-4.00	-1.19	< 0.001
Initiating ART treatment [a]				
HIV/noART [d]	-2.16	-4.35	0.02	0.052
Effects of markers of HIV progression/regression [e]				
Viral Load (copies mRNA/ml) [f]	-0.70	-1.99	0.58	0.040
CD4 cell count (cells/mm^3) [f]	1.12	-0.11	2.34	0.074

[a] Estimates expressed an 18-month change. [b] Model A: adjusted for age, gender, recruitment location, smoking, employment, use of medication, alcohol consumption and SBP. [c] Model A additionally adjusted for ethnicity, ART duration at baseline visit, viral load and CD4-cell count. [d] Adjusted for age, smoking viral load and CD4-cell count. [e] HIV+ART and HIV/noART combined with estimate expressed as change for each IQR increment in CD4 count (320 cells/mm^3) and viral load (1300 copies mRNA/ml). [f] Model A additionally adjusted for ethnicity.

Table A1.5. Estimated effects of HIV and ART status on waist-to-hip ratio.

	Estimate	95% CI		p-values
		Lower	Upper	
Temporal (18-months) [a]				
HIV-free [b]	0.012	0.000	0.024	0.047
HIV+ART [c]	-0.010	-0.021	0.002	0.100
Initiating ART treatment [a]				
HIV/noART [d]	-0.011	-0.035	0.013	0.358
Effects of markers of HIV progression/regression [e]				
Viral Load (copies mRNA/ml) [f]	-0.002	-0.015	0.012	0.810
CD4 cell count (cells/mm^3) [f]	-0.005	-0.015	0.005	0.347

[a] Estimates expressed an 18-month change. [b] Model A: adjusted for age, gender, recruitment location, smoking, employment, use of medication, alcohol consumption and SBP. [c] Model A additionally adjusted for ethnicity, ART duration at baseline visit, viral load and CD4-cell count. [d] Adjusted for age, smoking viral load and CD4-cell count. [e] HIV+ART and HIV/noART combined with estimate expressed as change for each IQR increment in CD4 count (320 cells/mm^3) and viral load (1300 copies mRNA/ml). [f] Model A additionally adjusted for ethnicity.

7.2. Appendix A2 – Effects of HIV and ART status on lipid and glucose levels.

Table A2.1. Estimated effects of HIV and ART status on total cholesterol (mmol/L).

	Estimate	95% CI		p-values
		Lower	Upper	
Temporal effects (18-months) [a]				
HIV-free [b]	-0.091	-0.209	0.027	0.131
HIV+ART [c]	-0.016	-0.156	0.124	0.826
Initiating ART treatment [a]				
HIV/noART [d]	0.301	0.072	0.530	0.011
Effects of markers of HIV progression/regression [e]				
Viral Load (copies mRNA/ml) [f]	-0.287	-0.413	-0.162	< 0.001
CD4 cell count (cells/mm^3) [f]	0.052	-0.066	0.171	0.384

[a] Estimates expressed an 18-month change. [b] Model A: adjusted for age, gender, recruitment area, smoking, employment, use of medication, alcohol consumption, SBP and BMI. [c] Model A additionally adjusted for ethnicity, ART duration at baseline visit, viral load and CD4-cell count. [d] Adjusted for age, smoking, viral load and CD4-cell count. [e] HIV+ART and HIV/noART combined with estimate expressed as change for each IQR increment in CD4 count (320 cells/mm^3) and viral load (1300 copies mRNA/ml). [f] Model A additionally adjusted for ethnicity.

Table A2.2. Estimated effects of HIV and ART status on HDL cholesterol levels (mmol/L).

	Estimate	95% CI		p-values
		Lower	Upper	
Temporal effects (18-months) [a]				
HIV-free [b]	0.014	-0.055	0.084	0.681
HIV+ART [c]	0.104	0.005	0.203	0.040
Initiating ART treatment [a]				
HIV/noART [d]	0.393	0.216	0.569	< 0.001
Effects of markers of HIV progression/regression [e]				
Viral Load (copies mRNA/ml) [f]	-0.204	-0.282	-0.125	< 0.001
CD4 cell count (cells/mm^3) [f]	0.070	-0.016	0.156	0.111

[a] Estimates expressed an 18-month change. [b] Model A: adjusted for age, gender, recruitment area, smoking, employment, use of medication, alcohol consumption, SBP and BMI. [c] Model A additionally adjusted for ethnicity, ART duration at baseline visit, viral load and CD4-cell count. [d] Adjusted for age, smoking, viral load and CD4-cell count. [e] HIV+ART and HIV/noART combined with estimate expressed as change for each IQR increment in CD4 count (320 cells/mm^3) and viral load (1300 copies mRNA/ml). [f] Model A additionally adjusted for ethnicity.

Table A2.3. Estimated effects of HIV and ART status on LDL cholesterol levels (mmol/L).

	Estimate	95% CI Lower	95% CI Upper	p-values
Temporal effects (18-months) [a]				
HIV-free [b]	-0.108	-0.210	-0.006	0.038
HIV+ART [c]	-0.138	-0.254	-0.022	0.020
Initiating ART treatment [a]				
HIV/noART [d]	-0.031	-0.233	0.171	0.755
Effects of markers of HIV progression/regression [e]				
Viral Load (copies mRNA/ml) [f]	-0.109	-0.211	-0.007	0.036
CD4 cell count (cells/mm^3) [f]	-0.028	-0.122	0.066	0.553

[a] Estimates expressed an 18-month change. [b] Model A: adjusted for age, gender, recruitment area, smoking, employment, use of medication, alcohol consumption, SBP and BMI. [c] Model A additionally adjusted for ethnicity, ART duration at baseline visit, viral load and CD4-cell count. [d] Adjusted for age, smoking, viral load and CD4-cell count. [e] HIV+ART and HIV/noART combined with estimate expressed as change for each IQR increment in CD4 count (320 cells/mm^3) and viral load (1300 copies mRNA/ml). [f] Model A additionally adjusted for ethnicity.

Table A2.4. Estimated effects of HIV and ART status on triglyceride levels (mmol/L).

	Estimate	95% CI Lower	95% CI Upper	p-values
Temporal effects (18-months) [a]				
HIV-free [b]	0.023	-0.053	0.099	0.549
HIV+ART [c]	0.037	-0.095	0.168	0.584
Initiating ART treatment [a]				
HIV/noART [d]	-0.114	-0.298	0.070	0.218
Effects of markers of HIV progression/regression [e]				
Viral Load (copies mRNA/ml) [f]	0.044	-0.068	0.155	0.443
CD4 cell count (cells/mm^3) [f]	-0.019	-0.118	0.080	0.707

[a] Estimates expressed an 18-month change. [b] Model A: adjusted for age, gender, recruitment area, smoking, employment, use of medication, alcohol consumption, SBP and BMI. [c] Model A additionally adjusted for ethnicity, ART duration at baseline visit, viral load and CD4-cell count. [d] Adjusted for age, smoking, viral load and CD4-cell count. [e] HIV+ART and HIV/noART combined with estimate expressed as change for each IQR increment in CD4 count (320 cells/mm^3) and viral load (1300 copies mRNA/ml). [f] Model A additionally adjusted for ethnicity.

Table A2.5. Estimated effects of HIV and ART status on fasting glucose levels (mmol/L).

	Estimate	95% CI		p-values
		Lower	Upper	
Temporal effects (18-months) [a]				
HIV-free [b]	-0.086	-0.289	0.117	0.402
HIV+ART [c]	0.091	-0.257	0.439	0.605
Initiating ART treatment [a]				
HIV/noART [d]	0.015	-0.485	0.515	0.952
Effects of markers of HIV progression/regression [e]				
Viral Load (copies mRNA/ml) [f]	-0.116	-0.322	0.090	0.270
CD4 cell count (cells/mm^3) [f]	0.221	0.036	0.407	0.020

[a] Estimates expressed an 18-month change. [b] Model A: adjusted for age, gender, recruitment area, smoking, employment, use of medication, alcohol consumption, SBP and BMI. [c] Model A additionally adjusted for ethnicity, ART duration at baseline visit, viral load and CD4-cell count. [d] Adjusted for age, smoking, viral load and CD4-cell count. [e] HIV+ART and HIV/noART combined with estimate expressed as change for each IQR increment in CD4 count (320 cells/mm^3) and viral load (1300 copies mRNA/ml). [f] Model A additionally adjusted for ethnicity.

Table A2.6. Estimated effects of HIV and ART status on % HbA1c.

	Estimate	95% CI		p-values
		Lower	Upper	
Temporal effects (18-months) [a]				
HIV-free [b]	0.061	-0.047	0.169	0.264
HIV+ART [c]	-0.035	-0.186	0.117	0.654
Initiating ART treatment [a]				
HIV/noART [d]	-0.121	-0.359	0.117	0.309
Effects of markers of HIV progression/regression [e]				
Viral Load (copies mRNA/ml) [f]	0.055	-0.057	0.166	0.334
CD4 cell count (cells/mm^3) [f]	0.088	-0.014	0.191	0.092

[a] Estimates expressed an 18-month change. [b] Model A: adjusted for age, gender, recruitment area, smoking, employment, use of medication, alcohol consumption, SBP and BMI. [c] Model A additionally adjusted for ethnicity, ART duration at baseline visit, viral load and CD4-cell count. [d] Adjusted for age, smoking, viral load and CD4-cell count. [e] HIV+ART and HIV/noART combined with estimate expressed as change for each IQR increment in CD4 count (320 cells/mm^3) and viral load (1300 copies mRNA/ml). [f] Model A additionally adjusted for ethnicity.

7.3. Appendix A3 – Effects of HIV and ART status on Hb levels.

Table A3.1. Estimated effects of HIV and ART status on Hb levels (g/dL).

	Estimate	95% CI		p-values
		Lower	Upper	
Temporal effects (18-months) [a]				
HIV-free [b]	-0.206	-0.419	0.006	0.056
HIV+ART [c]	-0.078	-0.309	0.153	0.506
Initiating ART treatment [a]				
HIV/noART [d]	0.143	-0.316	0.602	0.532
Effects of markers of HIV progression/regression [e]				
Viral Load (copies mRNA/ml) [f]	-0.31	-0.53	-0.09	0.006
CD4 cell count (cells/mm^3) [f]	0.16	-0.04	0.35	0.121

[a] Estimates expressed an 18-month change. [b] Model A: adjusted for age, gender, recruitment area, smoking, employment, use of medication, alcohol consumption, SBP and BMI. [c] Model A additionally adjusted for ethnicity, ART duration at baseline visit, viral load and CD4-cell count. [d] Adjusted for age, smoking, viral load and CD4-cell count. [e] HIV+ART and HIV/noART combined with estimate expressed as change for each IQR increment in CD4 count (320 cells/mm^3) and viral load (1300 copies mRNA/ml). [f] Model A additionally adjusted for ethnicity.

7.4.   Appendix A4 – Effects of HIV and ART status on GGT levels.

Table A4.1. Estimated effects of HIV and ART status on GGT levels (U/L).

	% Difference	95% CI		p-values
		Lower	Upper	
Temporal effects (18-months) [a]				
HIV-free [b]	9.0	0.3	18.5	0.042
HIV+ART [c]	-9.3	-19.4	2.0	0.101
Initiating ART treatment [a]				
HIV/noART [d]	37.6	14.3	65.8	0.001
Effects of markers of HIV progression/regression [e]				
Viral Load (copies mRNA/ml) [f]	-22.2	-30.1	-13.3	< 0.001
CD4 cell count (cells/mm^3) [f]	-5.0	-14.8	5.8	0.347

[a] Estimates expressed an 18-month % difference. [b] Model A: adjusted for age, gender, recruitment area, smoking, employment, use of medication, alcohol consumption, SBP and BMI. [c] Model A additionally adjusted for ethnicity, ART duration at baseline visit, viral load and CD4-cell count. [d] Adjusted for age, smoking, viral load and CD4-cell count. [e] HIV+ART and HIV/noART combined with estimate expressed as % difference for each IQR increment in CD4 count (320 cells/mm^3) and viral load (1300 copies mRNA/ml). [f] Model A additionally adjusted for ethnicity.

7.5. **Appendix A5 – Effects of HIV and ART status on markers of kidney function (Creatinine, microalbumin, ACR and eGFR levels).**

Table A5.1. Estimated effects of HIV and ART status on creatinine levels (μmol/L).

	Estimate	95% CI Lower	95% CI Upper	p-values
Temporal effects (18-months) [a]				
HIV-free [b]	-0.92	-2.68	0.85	0.305
HIV+ART [c]	3.71	1.98	5.44	< 0.001
Initiating ART treatment [a]				
HIV/noART [d]	3.03	-0.05	6.11	0.054
Effects of markers of HIV progression/regression [e]				
Viral Load (copies mRNA/ml) [f]	-0.29	-1.91	1.32	0.720
CD4 cell count (cells/mm^3) [f]	-0.93	-3.02	1.16	0.383

[a] Estimates expressed an 18-month change. [b] Model A: adjusted for age, gender, recruitment area, smoking, employment, use of medication, alcohol consumption, SBP and BMI. [c] Model A additionally adjusted for ethnicity, ART duration at baseline visit, viral load and CD4-cell count. [d] Adjusted for age, smoking, viral load and CD4-cell count. [e] HIV+ART and HIV/noART combined with estimate expressed as change for each IQR increment in CD4 count (320 cells/mm^3) and viral load (1300 copies mRNA/ml). [f] Model A additionally adjusted for ethnicity.

Table A5.2. Estimated effects of HIV and ART status on urine albumin levels (mg/L).

	% Difference	95% CI Lower	95% CI Upper	p-values
Temporal effects (18-months) [a]				
HIV-free [b]	11.5	-22.4	60.2	0.553
HIV+ART [c]	22.8	-11.1	69.7	0.211
Initiating ART treatment [a]				
HIV/noART [d]	-20.1	-50.9	30.0	0.352
Effects of markers of HIV progression/regression [e]				
Viral Load (copies mRNA/ml) [f]	20.0	-5.3	52.1	0.131
CD4 cell count (cells/mm^3) [f]	-7.9	-25.9	14.4	0.459

[a] Estimates expressed an 18-month %difference. [b] Model A: adjusted for age, gender, recruitment area, smoking, employment, use of medication, alcohol consumption, SBP and BMI. [c] Model A additionally adjusted for ethnicity, ART duration at baseline visit, viral load and CD4-cell count. [d] Adjusted for age, smoking, viral load and CD4-cell count. [e] HIV+ART and HIV/noART combined with estimate expressed as % difference for each IQR increment in CD4 count (320 cells/mm^3) and viral load (1300 copies mRNA/ml). [f] Model A additionally adjusted for ethnicity.

Table A5.3. Estimated effects of HIV and ART status on albumin-to-creatinine ratio (mg/g).

	% Difference	95% CI		p-values
		Lower	Upper	
Temporal effects (18-months) [a]				
HIV-free [b]	17.3	-13.6	59.4	0.303
HIV+ART [c]	-8.3	-32.9	25.2	0.582
Initiating ART treatment [a]				
HIV/noART [d]	-30.0	-56.7	13.1	0.137
Effects of markers of HIV progression/regression [e]				
Viral Load (copies mRNA/ml) [f]	-0.05	-0.18	0.08	0.476
CD4 cell count (cells/mm³) [f]	-7.03	-23.97	13.68	0.476

[a] Estimates expressed an 18-month %difference. [b] Model A: adjusted for age, gender, recruitment area, smoking, employment, use of medication, alcohol consumption, SBP and BMI. [c] Model A additionally adjusted for ethnicity, ART duration at baseline visit, viral load and CD4-cell count. [d] Adjusted for age, smoking, viral load and CD4-cell count. [e] HIV+ART and HIV/noART combined with estimate expressed as % difference for each IQR increment in CD4 count (320 cells/mm³) and viral load (1300 copies mRNA/ml). [f] Model A additionally adjusted for ethnicity.

Table A5.4. Estimated effects of HIV and ART status on eGFR (mL/minute/1.73 m³).

	Estimate	95% CI		p-values
		Lower	Upper	
Temporal effects (18-months) [a]				
HIV-free [b]	1.01	-0.90	2.91	0.298
HIV+ART [c]	-2.93	-4.94	-0.93	0.004
Initiating ART treatment [a]				
HIV/noART [d]	-3.41	-7.16	0.33	0.073
Effects of markers of HIV progression/regression [e]				
Viral Load (copies mRNA/ml) [f]	2.18	-0.02	4.38	0.052
CD4 cell count (cells/mm³) [f]	0.67	-1.38	2.71	0.522

[a] Estimates expressed an 18-month change. [b] Model A: adjusted for age, gender, recruitment area, smoking, employment, use of medication, alcohol consumption, SBP and BMI. [c] Model A additionally adjusted for ethnicity, ART duration at baseline visit, viral load and CD4-cell count. [d] Adjusted for age, smoking, viral load and CD4-cell count. [e] HIV+ART and HIV/noART combined with estimate expressed as change for each IQR increment in CD4 count (320 cells/mm³) and viral load (1300 copies mRNA/ml). [f] Model A additionally adjusted for ethnicity.

7.6. Appendix A6 – Effects of HIV and ART status on blood pressure and heart rate.

Table A6.1. Estimated effects of HIV and ART status on SBP (mmHg).

	Estimate	95% CI		p-values
		Lower	Upper	
Temporal effects (18-months) [a]				
HIV-free [b]	3.46	0.20	6.72	0.038
HIV+ART [c]	-0.88	-3.95	2.18	0.570
Initiating ART treatment [a]				
HIV/noART [d]	-3.47	-9.07	2.13	0.217
Effects of markers of HIV progression/regression [e]				
Viral Load (copies mRNA/ml) [f]	-1.73	-5.62	2.17	0.384
CD4 cell count (cells/mm^3) [f]	1.49	-1.02	4.01	0.244

[a] Estimates expressed an 18-month change. [b] Model A: adjusted for age, gender, recruitment area, smoking, employment, use of medication, alcohol consumption and BMI. [c] Model A additionally adjusted for ethnicity, ART duration at baseline visit, viral load and CD4-cell count. [d] Adjusted for age, smoking, viral load and CD4-cell count. [e] HIV+ART and HIV/noART combined with estimate expressed as change for each IQR increment in CD4 count (320 cells/mm^3) and viral load (1300 copies mRNA/ml). [f] Model A additionally adjusted for ethnicity.

Table A6.2. Estimated effects of HIV and ART status on DBP (mmHg).

	Estimate	95% CI		p-values
		Lower	Upper	
Temporal effects (18-months) [a]				
HIV-free [b]	1.80	-0.41	4.01	0.108
HIV+ART [c]	-1.25	-3.24	0.75	0.219
Initiating ART treatment [a]				
HIV/noART [d]	-1.47	-5.73	2.78	0.487
Effects of markers of HIV progression/regression [e]				
Viral Load (copies mRNA/ml) [f]	-0.33	-6.03	5.37	0.826
CD4 cell count (cells/mm^3) [f]	0.57	-1.13	2.27	0.511

[a] Estimates expressed an 18-month change. [b] Model A: adjusted for age, gender, recruitment area, smoking, employment, use of medication, alcohol consumption and BMI. [c] Model A additionally adjusted for ethnicity, ART duration at baseline visit, viral load and CD4-cell count. [d] Adjusted for age, smoking, viral load and CD4-cell count. [e] HIV+ART and HIV/noART combined with estimate expressed as change for each IQR increment in CD4 count (320 cells/mm^3) and viral load (1300 copies mRNA/ml). [f] Model A additionally adjusted for ethnicity.

Table A6.3. Estimated effects of HIV and ART status on heart rate (bpm).

	Estimate	95% CI		p-values
		Lower	Upper	
Temporal effects (18-months) [a]				
HIV-free [b]	-1.28	-3.33	0.78	0.221
HIV+ART [c]	0.26	-1.64	2.17	0.787
Initiating ART treatment [a]				
HIV/noART [d]	0.72	-3.48	4.93	0.729
Effects of markers of HIV progression/regression [e]				
Viral Load (copies mRNA/ml) [f]	0.66	-2.75	4.07	0.705
CD4 cell count (cells/mm^3) [f]	-1.30	-3.07	0.48	0.151

[a] Estimates expressed an 18-month change. [b] Model A: adjusted for age, gender, recruitment area, smoking, employment, use of medication, alcohol consumption, SBP and BMI. [c] Model A additionally adjusted for ethnicity, ART duration at baseline visit, viral load and CD4-cell count. [d] Adjusted for age, smoking, viral load and CD4-cell count. [e] HIV+ART and HIV/noART combined with estimate expressed as change for each IQR increment in CD4 count (320 cells/mm^3) and viral load (1300 copies mRNA/ml). [f] Model A additionally adjusted for ethnicity.

7.7. **Appendix A7 – Effects of HIV and ART status on circulating biomarkers of systemic inflammation and vascular endothelial function.**

Table A7.1. Estimated effects of HIV and ART status on hsCRP levels (mg/L).

	% Difference	95% CI Lower	95% CI Upper	*p*-values
Temporal effects (18-months) [a]				
HIV-free [b]	0.8	-22.0	30.3	0.950
HIV+ART [c]	10.8	-12.6	40.3	0.395
Initiating ART treatment [a]				
HIV/noART [d]	-24.8	-57.4	32.9	0.318
Effects of markers of HIV progression/regression [e]				
Viral Load (copies mRNA/ml) [f]	12.5	-42.4	37.2	0.594
CD4 cell count (cells/mm³) [f]	-38.2	-96.2	45.5	0.734

[a] Estimates expressed an 18-month change. [b] Model A: adjusted for age, gender, recruitment area, smoking, employment, use of medication, alcohol consumption, SBP and BMI. [c] Model A additionally adjusted for ethnicity, ART duration at baseline visit, viral load and CD4-cell count. [d] Adjusted for age, smoking, viral load and CD4-cell count. [e] HIV+ART and HIV/noART combined with estimate expressed as change for each IQR increment in CD4 count (320 cells/mm³) and viral load (1300 copies mRNA/ml). [f] Model A additionally adjusted for ethnicity.

Table A7.2. Estimated effects of HIV and ART status on TNF-α levels (pg/ml).

	Estimate	95% CI Lower	95% CI Upper	*p*-values
Temporal effects (18-months) [a]				
HIV-free [b]	0.11	-1.56	1.79	0.893
HIV+ART [c]	-1.22	-2.29	-0.16	0.025
Initiating ART treatment [a]				
HIV/noART [d]	0.30	-3.40	4.00	0.870
Effects of markers of HIV progression/regression [e]				
Viral Load (copies mRNA/ml) [b]	0.26	-1.58	2.10	0.783
CD4 cell count (cells/mm³) [b]	-2.11	-3.46	-0.76	0.002

[a] Estimates expressed an 18-month change. [b] Model A: adjusted for age, smoking, SBP and BMI. [c] Model A additionally adjusted for ART duration at baseline visit, viral load and CD4-cell count. [d] Adjusted for age, smoking, viral load and CD4-cell count. [e] HIV+ART and HIV/noART combined with estimate expressed as change for each IQR increment in CD4 count (320 cells/mm³) and viral load (1300 copies mRNA/ml).

Table A7.3. Estimated effects of HIV and ART status on VCAM-1 levels (ng/ml).

	Estimate	95% CI		p-values
		Lower	Upper	
Temporal effects (18-months) [a]				
HIV-free [b]	21.1	-50.7	92.9	0.559
HIV+ART [c]	-128	-270	14	0.076
Initiating ART treatment [a]				
HIV/noART [d]	-148	-274	-23	0.022
Effects of markers of HIV progression/regression [e]				
Viral Load (copies mRNA/ml) [b]	13.6	-4.0	34.3	0.136
CD4 cell count (cells/mm^3) [b]	-2.8	-12.4	8.0	0.598

[a] Estimates expressed an 18-month change. [b] Model A: adjusted for age, smoking, SBP and BMI. [c] Model A additionally adjusted for ART duration at baseline visit, viral load and CD4-cell count. [d] Adjusted for age, smoking, viral load and CD4-cell count. [e] HIV+ART and HIV/noART combined with estimate expressed as change for each IQR increment in CD4 count (320 cells/mm^3) and viral load (1300 copies mRNA/ml).

Table A7.4. Estimated effects of HIV and ART status on ICAM-1 levels (ng/ml).

	% Difference	95% CI		p-values
		Lower	Upper	
Temporal effects (18-months) [a]				
HIV-free [b]	2.4	-3.2	8.4	0.394
HIV+ART [c]	-45	-88	-1.3	0.043
Initiating ART treatment [a]				
HIV/noART [d]	15	-37	68	0.555
Effects of markers of HIV progression/regression [e]				
Viral Load (copies mRNA/ml) [b]	3.7	-9.8	19.2	0.610
CD4 cell count (cells/mm^3) [b]	-3.5	-13.7	8.0	0.535

[a] Estimates expressed an 18-month % difference. [b] Model A: adjusted for age, smoking, SBP and BMI. [c] Model A additionally adjusted for ART duration at baseline visit, viral load and CD4-cell count. [d] Adjusted for age, smoking, viral load and CD4-cell count. [e] HIV+ART and HIV/noART combined with estimate expressed as % difference for each IQR increment in CD4 count (320 cells/mm^3) and viral load (1300 copies mRNA/ml).

Table A7.5. Estimated effects of HIV and ART status on e-selectin levels (ng/ml).

	Estimate	95% CI		p-values
		Lower	Upper	
Temporal effects (18-months) [a]				
HIV-free [b]	1.83	-0.73	4.39	0.157
HIV+ART [c]	-5.57	-9.52	-1.62	0.006
Initiating ART treatment [a]				
HIV/noART [d]	-0.22	-5.39	4.96	0.933
Effects of markers of HIV progression/regression [e]				
Viral Load (copies mRNA/ml) [b]	-2.99	-7.06	1.07	0.147
CD4 cell count (cells/mm^3) [b]	0.42	-2.79	3.63	0.796

[a] Estimates expressed an 18-month change. [b] Model A: adjusted for age, smoking, SBP and BMI. [c] Model A additionally adjusted for ART duration at baseline visit, viral load and CD4-cell count. [d] Adjusted for age, smoking, viral load and CD4-cell count. [e] HIV+ART and HIV/noART combined with estimate expressed as change for each IQR increment in CD4 count (320 cells/mm^3) and viral load (1300 copies mRNA/ml).

Table A7.6. Estimated effects of HIV and ART status on p-selectin levels (ng/ml).

	Estimate	95% CI		p-values
		Lower	Upper	
Temporal effects (18-months) [a]				
HIV-free [b]	-2.39	-6.05	1.27	0.195
HIV+ART [c]	-2.09	-5.63	1.45	0.243
Initiating ART treatment [a]				
HIV/noART [d]	3.25	-1.42	7.92	0.165
Effects of markers of HIV progression/regression [e]				
Viral Load (copies mRNA/ml) [b]	1.87	-1.08	4.83	0.212
CD4 cell count (cells/mm^3) [b]	-2.80	-6.52	0.92	0.139

[a] Estimates expressed an 18-month change. [b] Model A: adjusted for age, smoking, SBP and BMI. [c] Model A additionally adjusted for ART duration at baseline visit, viral load and CD4-cell count. [d] Adjusted for age, smoking, viral load and CD4-cell count. [e] HIV+ART and HIV/noART combined with estimate expressed as change for each IQR increment in CD4 count (320 cells/mm^3) and viral load (1300 copies mRNA/ml).

Table A7.7. Estimated effects of HIV and ART status on VEGF levels (pg/ml).

	% Difference	95% CI Lower	95% CI Upper	p-values
Temporal effects (18-months) [a]				
HIV-free [b]	-0.5	-12.8	13.6	0.941
HIV+ART [c]	4.6	-9.7	21.2	0.545
Initiating ART treatment [a]				
HIV/noART [d]	40.6	0.5	96.7	0.047
Effects of markers of HIV progression/regression [e]				
Viral Load (copies mRNA/ml) [b]	-13.2	-29.2	6.5	0.173
CD4 cell count (cells/mm^3) [b]	2.2	-13.2	20.4	0.793

[a] Estimates expressed an 18-month % difference. [b] Model A: adjusted for age, smoking, SBP and BMI. [c] Model A additionally adjusted for ART duration at baseline visit, viral load and CD4-cell count. [d] Adjusted for age, smoking, viral load and CD4-cell count. [e] HIV+ART and HIV/noART combined with estimate expressed as % difference for each IQR increment in CD4 count (320 cells/mm^3) and viral load (1300 copies mRNA/ml).

Table A7.8. Estimated effects of HIV and ART status on PAI-1 levels (ng/ml).

	Estimate	95% CI Lower	95% CI Upper	p-values
Temporal effects (18-months) [a]				
HIV-free [b]	-7.09	-19.34	5.16	0.251
HIV+ART [c]	-3.97	-16.20	8.26	0.518
Initiating ART treatment [a]				
HIV/noART [d]	14.12	1.16	27.07	0.034
Effects of markers of HIV progression/regression [e]				
Viral Load (copies mRNA/ml) [a]	7.49	-4.07	19.06	0.202
CD4 cell count (cells/mm^3) [a]	-4.27	-11.46	2.93	0.243

[a] Estimates expressed an 18-month change. [b] Model A: adjusted for age, smoking, SBP and BMI. [c] Model A additionally adjusted for ART duration at baseline visit, viral load and CD4-cell count. [d] Adjusted for age, smoking, viral load and CD4-cell count. [e] HIV+ART and HIV/noART combined with estimate expressed as change for each IQR increment in CD4 count (320 cells/mm^3) and viral load (1300 copies mRNA/ml).

7.8. Appendix A8 – Effects of HIV and ART status on retinal vessel calibre.

Table A8.1. Estimated effects of HIV and ART status on CRAE (µm).

	Estimate	95% CI		p-values
		Lower	Upper	
Temporal effects (18-months) [a]				
HIV-free [b]	1.01	-0.47	2.50	0.180
HIV+ART [c]	0.94	-0.96	2.83	0.332
Initiating ART treatment [a]				
HIV/noART [d]	-0.038	-3.01	2.93	0.980
Effects of markers of HIV progression/regression [e]				
Viral Load (copies mRNA/ml) [f]	1.97	-0.73	4.67	0.152
CD4 cell count (cells/mm³) [f]	0.18	-1.67	2.02	0.849

[a] Estimates expressed an 18-month change. [b] Model A: adjusted for age, gender, recruitment area, smoking, employment, use of medication, alcohol consumption, SBP and BMI. [c] Model A additionally adjusted for ethnicity, ART duration at baseline visit, viral load and CD4-cell count. [d] Adjusted for age, smoking, viral load and CD4-cell count. [e] HIV+ART and HIV/noART combined with estimate expressed as change for each IQR increment in CD4 count (320 cells/mm³) and viral load (1300 copies mRNA/ml). [f] Model A additionally adjusted for ethnicity.

Table A8.2. Estimated effects of HIV and ART status on CRVE (µm).

	Estimate	95% CI		p-values
		Lower	Upper	
Temporal effects (18-months) [a]				
HIV-free [b]	-0.64	-2.84	1.56	0.565
HIV+ART [c]	-7.00	-12.64	-1.36	0.015
Initiating ART treatment [a]				
HIV/noART [d]	-6.42	-10.99	-1.85	0.007
Effects of markers of HIV progression/regression [e]				
Viral Load (copies mRNA/ml) [f]	9.29	5.28	13.30	< 0.000
CD4 cell count (cells/mm³) [f]	-2.66	-5.39	0.07	0.056

[a] Estimates expressed an 18-month change. [b] Model A: adjusted for age, gender, recruitment area, smoking, employment, use of medication, alcohol consumption, SBP and BMI. [c] Model A additionally adjusted for ethnicity, ART duration at baseline visit, viral load and CD4-cell count. [d] Adjusted for age, smoking, viral load and CD4-cell count. [e] HIV+ART and HIV/noART combined with estimate expressed as change for each IQR increment in CD4 count (320 cells/mm³) and viral load (1300 copies mRNA/ml). [f] Model A additionally adjusted for ethnicity.

Table A8.3. Estimated effects of HIV and ART status on AVR.

	Estimate	95% CI Lower	95% CI Upper	p-values
Temporal effects (18-months) [a]				
HIV-free [b]	0.007	-0.001	0.014	0.068
HIV+ART [c]	0.019	0.008	0.031	0.001
Initiating ART treatment [a]				
HIV/noART [d]	0.014	0.000	0.028	0.051
Effects of markers of HIV progression/regression [e]				
Viral Load (copies mRNA/ml) [f]	-0.016	-0.025	-0.006	0.001
CD4 cell count (cells/mm^3) [f]	0.007	-0.001	0.015	0.067

[a] Estimates expressed an 18-month change. [b] Model A: adjusted for age, gender, recruitment area, smoking, employment, use of medication, alcohol consumption, SBP and BMI. [c] Model A additionally adjusted for ethnicity, ART duration at baseline visit, viral load and CD4-cell count. [d] Adjusted for age, smoking, viral load and CD4-cell count. [e] HIV+ART and HIV/noART combined with estimate expressed as change for each IQR increment in CD4 count (320 cells/mm^3) and viral load (1300 copies mRNA/ml). [f] Model A additionally adjusted for ethnicity.

7.9. Appendix A9 – Effects of HIV and ART status on flow-mediated dilation parameters.

Table A9.1. Estimated effects of HIV and ART status on baseline brachial artery diameter (mm).

	Estimate	95% CI		p-values
		Lower	Upper	
Temporal effects (18-months) [a]				
HIV-free [b]	-0.062	-0.148	0.025	0.161
HIV+ART [c]	0.023	-0.052	0.098	0.548
Initiating ART treatment [a]				
HIV/noART [d]	-0.018	-0.169	0.133	0.810
Effects of markers of HIV progression/regression [e]				
Viral Load (copies mRNA/ml) [f]	0.046	-0.060	0.152	0.398
CD4 cell count (cells/mm^3) [f]	-0.006	-0.076	0.065	0.875

[a] Estimates expressed an 18-month change. [b] Model A: adjusted for age, gender, recruitment area, smoking, employment, use of medication, alcohol consumption, SBP and BMI. [c] Model A additionally adjusted for ethnicity, ART duration at baseline visit, viral load and CD4-cell count. [d] Adjusted for age, smoking, viral load and CD4-cell count. [e] HIV+ART and HIV/noART combined with estimate expressed as change for each IQR increment in CD4 count (320 cells/mm^3) and viral load (1300 copies mRNA/ml). [f] Model A additionally adjusted for ethnicity.

Table A9.2. Estimated effects of HIV and ART status on % FMD.

	% Difference	95% CI		p-values
		Lower	Upper	
Temporal effects (18-months) [a]				
HIV-free [b]	1.9	-7.2	11.8	0.692
HIV+ART [c]	-9.8	-17.6	-1.2	0.026
Initiating ART treatment [a]				
HIV/noART [d]	11.1	-6.9	32.6	0.234
Effects of markers of HIV progression/regression [e]				
Viral Load (copies mRNA/ml) [f]	-2.127	-3.337	-0.918	0.001
CD4 cell count (cells/mm^3) [f]	8.43	0.91	15.95	0.028

[a] Estimates expressed an 18-month % difference. [b] Model A: adjusted for age, gender, recruitment area, smoking, employment, use of medication, alcohol consumption, SBP, BMI and baseline brachial artery diameter. [c] Model A additionally adjusted for ethnicity, ART duration at baseline visit, viral load and CD4-cell count. [d] Adjusted for age, smoking, baseline brachial artery diameter and viral load and CD4-cell count. [e] HIV+ART and HIV/noART combined with estimate expressed as % difference for each IQR increment in CD4 count (320 cells/mm^3) and viral load (1300 copies mRNA/ml). [f] Model A additionally adjusted for ethnicity.

8. Appendix B: Supplementary data for Sub-study 2.

8.1. Appendix B1 – Effects of exposure variable outcomes on body composition.

Table B1.1. Estimated effects of exposure variable outcomes on BMI (kg/m^2).

Exposure [a]	Estimate [b]	95% CI		p-values
		Lower	Upper	
NO_2 (µg/m³)	0.064	-0.285	0.413	0.716
Benzene (µg/m³)	-0.071	-0.535	0.392	0.759
Toluene (µg/m³)	0.053	-0.141	0.247	0.589
Ethyl-Benzene (µg/m³)	0.003	-0.158	0.163	0.975
m+p-Xylene (µg/m³)	0.001	-0.048	0.048	0.996
o-Xylene (µg/m³)	0.007	-0.131	0.144	0.924
Urinary metabolite [c]				
3+4MHA (ng/ml)	0.059	-0.033	0.152	0.201

[a] Model adjusted for age, temperature, date of clinical visit, smoking and employment status. [b] Estimates expressed as a difference in BMI (kg/m^2) for each IQR increment in exposure [c] Additionally adjusted for urine creatinine. **IQR:** NO_2 7.0 µg/m³; BTEX 3.3, 30.0, 3.8, 3.8, 3.8 µg/m³; 3+4MHA 1380 ng/ml.

Table B1.2. Estimated effects of exposure variable outcomes on waist-to-hip ratio.

Exposure [a]	Estimate [b]	95%CI		p-values
		Lower	Upper	
NO_2 (µg/m³)	0.003	-0.013	0.019	0.682
Benzene (µg/m³)	0.003	-0.014	0.021	0.702
Toluene (µg/m³)	0.001	-0.007	0.009	0.780
Ethyl-Benzene (µg/m³)	0.003	-0.004	0.010	0.336
m+p-Xylene (µg/m³)	0.001	-0.001	0.003	0.293
o-Xylene (µg/m³)	0.003	-0.003	0.009	0.333
Urinary metabolite [c]				
3+4MHA (ng/ml)	-0.0003	-0.0055	0.0041	0.901

[a] Model adjusted for age, temperature, date of clinical visit, smoking and employment status. [b] Estimates expressed as a difference in waist-to-hip ratio for each IQR increment in exposure [c] Additionally adjusted for urine creatinine. **IQR:** NO_2 7.0 µg/m³; BTEX 3.3, 30.0, 3.8, 3.8, 3.8 µg/m³; 3+4MHA 1380 ng/ml.

8.2.   Appendix B2 – Effects of exposure variable outcomes on lipid and glucose variable outcomes.

Table B2.1. Estimated effects of exposure variable outcomes on total cholesterol levels (mmol/L).

Exposure [a]	Estimate [b]	95%CI		p-values
		Lower	Upper	
NO$_2$ (µg/m³)	0.021	-0.144	0.187	0.798
Benzene (µg/m³)	0.153	-0.013	0.319	0.070
Toluene (µg/m³)	0.104	0.036	0.173	0.003
Ethyl-Benzene (µg/m³)	0.065	-0.004	0.134	0.064
m+p-Xylene (µg/m³)	0.020	-0.001	0.041	0.061
o-Xylene (µg/m³)	0.044	-0.014	0.103	0.137
Urinary metabolite [c]				
3+4MHA (ng/ml)	0.036	-0.006	0.077	0.084

[a] Model adjusted for age, BMI, SBP, temperature, date of clinical visit, smoking and employment status. [b] Estimates expressed as a difference in total cholesterol levels (mmol/L) for each IQR increment in exposure [c] Additionally adjusted for urine creatinine. **IQR:** NO$_2$ 7.0 µg/m³; BTEX 3.3, 30.0, 3.8, 3.8, 3.8 µg/m³; 3+4MHA 1380 ng/ml.

Table B2.2. Estimated effects of exposure variable outcomes on HDL cholesterol levels (mmol/L).

Exposure [a]	Estimate [b]	95%CI		p-values
		Lower	Upper	
NO$_2$ (µg/m³)	-0.010	-0.069	0.050	0.749
Benzene (µg/m³)	0.274	-0.232	0.781	0.283
Toluene (µg/m³)	3.805	0.173	7.436	0.040
Ethyl-Benzene (µg/m³)	0.244	-0.181	0.669	0.254
m+p-Xylene (µg/m³)	0.213	-0.214	0.640	0.321
o-Xylene (µg/m³)	0.179	-0.262	0.620	0.420
Urinary metabolite [c]				
3+4MHA (ng/ml)	10.239	-1.713	22.191	0.092

[a] Model adjusted for age, BMI, SBP, temperature, date of clinical visit, smoking and employment status. [b] Estimates expressed as a difference in total HDL cholesterol for each IQR increment in exposure [c] Additionally adjusted for urine creatinine. **IQR:** NO$_2$ 7.0 µg/m³; BTEX 3.3, 30.0, 3.8, 3.8, 3.8 µg/m³; 3+4MHA 1380 ng/ml.

Table B2.3. Estimated effects of exposure variable outcomes on LDL cholesterol levels (mmol/L).

Exposure [a]	Estimate [b]	95%CI		p-values
		Lower	Upper	
NO$_2$ (µg/m³)	-0.043	-0.221	0.134	0.629
Benzene (µg/m³)	0.486	-0.846	1.818	0.471
Toluene (µg/m³)	11.050	1.900	20.199	0.018
Ethyl-Benzene (µg/m³)	0.763	-0.455	1.981	0.216
m+*p*-Xylene (µg/m³)	0.830	-0.390	2.050	0.180
o-Xylene (µg/m³)	0.475	-0.776	1.726	0.453
Urinary metabolite [c]				
3+4MHA (ng/ml)	37.461	2.642	72.280	0.035

[a] Model adjusted for age, BMI, SBP, temperature, date of clinical visit, smoking and employment status. [b] Estimates expressed as a difference in LDL cholesterol for each IQR increment in exposure [c] Additionally adjusted for urine creatinine. **IQR:** NO$_2$ 7.0 µg/m³; BTEX 3.3, 30.0, 3.8, 3.8, 3.8 µg/m³; 3+4MHA 1380 ng/ml.

Table B2.4. Estimated effects of exposure variable outcomes on triglyceride levels (mmol/L).

Exposure [a]	Estimate [b]	95%CI		p-values
		Lower	Upper	
NO$_2$ (µg/m³)	0.016	-0.075	0.107	0.727
Benzene (µg/m³)	0.089	-0.011	0.189	0.080
Toluene (µg/m³)	-0.012	-0.059	0.035	0.610
Ethyl-Benzene (µg/m³)	-0.002	-0.037	0.034	0.920
m+*p*-Xylene (µg/m³)	0.000	-0.011	0.010	0.926
o-Xylene (µg/m³)	-0.009	-0.040	0.021	0.545
Urinary metabolite [c]				
3+4MHA (ng/ml)	0.014	-0.017	0.044	0.362

[a] adjusted for age, BMI, SBP, temperature, date of clinical visit, smoking and employment status. [b] Estimates expressed as a difference in triglyceride levels (mmol/L) for each IQR increment in exposure [c] Additionally adjusted for urine creatinine. **IQR:** NO$_2$ 7.0 µg/m³; BTEX 3.3, 30.0, 3.8, 3.8, 3.8 µg/m³; 3+4MHA 1380 ng/ml.

Table B2.5. Estimated effects of exposure variable outcomes on fasting glucose levels (mmol/L).

Exposure [a]	Estimate [b]	95%CI		p-values
		Lower	Upper	
NO_2 (µg/m³)	0.183	-0.110	0.476	0.216
Benzene (µg/m³)	0.335	0.021	0.649	0.037
Toluene (µg/m³)	-0.052	-0.200	0.096	0.482
Ethyl-Benzene (µg/m³)	-0.001	-0.119	0.117	0.988
m+*p*-Xylene (µg/m³)	0.002	-0.033	0.038	0.899
o-Xylene (µg/m³)	0.013	-0.089	0.115	0.800
Urinary metabolite [c]				
3+4MHA (ng/ml)	-0.004	-0.094	0.087	0.939

[a] Model adjusted for age, BMI, SBP, temperature, date of clinical visit, smoking and employment status. [b] Estimates expressed as a difference in fasting glucose levels (mmol/L) for each IQR increment in exposure [c] Additionally adjusted for urine creatinine. **IQR:** NO_2 7.0 µg/m³; BTEX 3.3, 30.0, 3.8, 3.8, 3.8 µg/m³; 3+4MHA 1380 ng/ml.

Table B2.6. Estimated effects of exposure variable outcomes on % HbA1c levels.

Exposure [a]	Estimate [b]	95%CI		p-values
		Lower	Upper	
NO_2 (µg/m³)	-0.034	-0.134	0.066	0.500
Benzene (µg/m³)	-0.057	-0.183	0.069	0.367
Toluene (µg/m³)	-0.018	-0.072	0.036	0.510
Ethyl-Benzene (µg/m³)	-0.016	-0.059	0.027	0.457
m+*p*-Xylene (µg/m³)	-0.005	-0.018	0.008	0.422
o-Xylene (µg/m³)	-0.010	-0.047	0.027	0.573
Urinary metabolite [c]				
3+4MHA (ng/ml)	0.012	-0.015	0.041	0.374

[a] Model adjusted for age, BMI, SBP, temperature, date of clinical visit, smoking and employment status. [b] Estimates expressed as a difference in %HbA1c levels for each IQR increment in exposure [c] Additionally adjusted for urine creatinine. **IQR:** NO_2 7.0 µg/m³; BTEX 3.3, 30.0, 3.8, 3.8, 3.8 µg/m³; 3+4MHA 1380 ng/ml.

8.3. Appendix B3 – Effects of exposure variable outcomes on Hb levels.

Table B3.1. Estimated effects of exposure variable outcomes on Hb levels (g/dL).

Exposure [a]	Estimate [b]	95%CI		p-values
		Lower	Upper	
NO$_2$ (µg/m³)	0.070	-0.171	0.311	0.564
Benzene (µg/m³)	0.070	-0.199	0.338	0.607
Toluene (µg/m³)	0.067	-0.039	0.173	0.215
Ethyl-Benzene (µg/m³)	0.029	-0.078	0.136	0.590
m+*p*-Xylene (µg/m³)	0.014	-0.018	0.046	0.395
o-Xylene (µg/m³)	0.032	-0.059	0.123	0.485
Urinary metabolite [c]				
3+4MHA (ng/ml)	0.003	-0.058	0.062	0.940

[a] Model adjusted for adjusted for age, BMI, SBP, temperature, date of clinical visit, smoking and employment status. [b] Estimates expressed as a difference in Hb levels (g/dL) for each IQR increment in exposure [c] Additionally adjusted for urine creatinine. **IQR:** NO$_2$ 7.0 µg/m³; BTEX 3.3, 30.0, 3.8, 3.8, 3.8 µg/m³; 3+4MHA 1380 ng/ml.

8.4.   Appendix B4 – Effects of exposure variable outcomes on GGT.

Table B4.1. Estimated effects of exposure variable outcomes on GGT levels (U/L).

Exposure [a]	Estimate [b]	95%CI		p-values
		Lower	Upper	
NO$_2$ (µg/m³)	-0.74	-4.95	3.47	0.726
Benzene (µg/m³)	-0.75	-5.76	4.27	0.768
Toluene (µg/m³)	-0.14	-2.23	1.96	0.896
Ethyl-Benzene (µg/m³)	-0.12	-1.94	1.71	0.897
m+*p*-Xylene (µg/m³)	-0.01	-0.55	0.55	0.991
o-Xylene (µg/m³)	9.9	-22.6	42.5	0.546
Urinary metabolite [c]				
3+4MHA (ng/ml)	-0.20	-2.40	2.90	0.853

[a] Model adjusted for age, BMI, SBP, temperature, date of clinical visit, smoking and employment status. [b] Estimates expressed as a difference in GGT levels (U/L) for each IQR increment in exposure [c] Additionally adjusted for urine creatinine. **IQR:** NO$_2$ 7.0 µg/m³; BTEX 3.3, 30.0, 3.8, 3.8, 3.8 µg/m³; 3+4MHA 1380 ng/ml.

8.5.   **Appendix B5 – Effects of exposure variable outcomes on eGRF.**

Table B5.1. Estimated effects of exposure variable outcomes on eGRF levels (ml/minute/1.73 m³).

Exposure [a]	Estimate [b]	95%CI		p-values
		Lower	Upper	
NO$_2$ (µg/m³)	0.35	-1.08	1.79	0.629
Benzene (µg/m³)	0.19	1.76	1.99	0.900
Toluene (µg/m³)	-7.82	-15.32	-0.439	0.038
Ethyl-Benzene (µg/m³)	0.25	-1.27	1.72	0.745
m+p-Xylene (µg/m³)	0.17	-1.35	1.69	0.826
o-Xylene (µg/m³)	0.028	-1.11	1.17	0.962
Urinary metabolite [c]				
3+4MHA (ng/ml)	-1.385	-3.38	0.614	0.172

[a] Model adjusted for age, BMI, SBP, temperature, date of clinical visit, smoking and employment status. [b] Estimates expressed as a difference in eGRF levels (ml/minute/1.73 m³) for each IQR increment in exposure [c] Additionally adjusted for urine creatinine. **IQR:** NO$_2$ 7.0 µg/m³; BTEX 3.3, 30.0, 3.8, 3.8, 3.8 µg/m³; 3+4MHA 1380 ng/ml.

8.6. **Appendix B6 – Effects of exposure variable outcomes on LTL, mtDNA content and % DNA methylation.**

Table B6.1. Estimated effects of exposure variable outcomes on LTL (Main LMM).

Exposure [a]	% Difference [b]	95%CI		p-values
		Lower	Upper	
NO_2 (µg/m³)	-12.9	-20.8	-4.1	0.001
Benzene (µg/m³)	-8.5	-15.7	-0.8	0.005
Toluene (µg/m³)	1.53	-1.26	4.41	0.480
Ethyl-Benzene (µg/m³)	1.27	-4.27	7.13	0.110
m+p-Xylene (µg/m³)	0.46	-1.20	2.15	0.120
o-Xylene (µg/m³)	0.73	-3.87	5.54	0.160
Urinary metabolite [c]				
3+4MHA (ng/ml)	-0.95	-2.82	0.96	0.130

[a] Main model adjusted for age, BMI, smoking and employment status. [b] Estimates expressed as a % difference in LTL for each IQR increment in exposure [c] Additionally adjusted for urine creatinine. **IQR:** NO_2 7.0 µg/m³; BTEX 3.3, 30.0, 3.8, 3.8, 3.8 µg/m³; 3+4MHA 1380 ng/ml.

Table B6.2. Estimated effects of exposure variable outcomes on LTL (Main model additionally adjusted for temperature).

Exposure [a]	% Difference [b]	95%CI		p-values
		Lower	Upper	
NO_2 (µg/m³)	-12.7	-21.3	-3.2	0.005
Benzene (µg/m³)	-8.1	-15.5	-0.1	0.030
Toluene (µg/m³)	1.69	-1.66	5.17	0.830
Ethyl-Benzene (µg/m³)	1.12	-4.66	7.25	0.200
m+p-Xylene (µg/m³)	0.42	-1.29	2.17	0.220
o-Xylene (µg/m³)	0.71	-3.89	5.53	0.290
Urinary metabolite [c]				
3+4MHA (µg/mL)	-1.26	-2.82	0.96	0.150

[a] Model adjusted for adjusted for age, BMI, temperature, smoking and employment status. [b] Estimates expressed as a % difference in LTL (*n* = 61 at baseline and *n* = 61 at follow-up) for each SD increment in exposure [c] Additionally adjusted for urine creatinine. **IQR:** NO_2 7.0 µg/m³; BTEX 3.3, 30.0, 3.8, 3.8, 3.8 µg/m³; 3+4MHA 1380 ng/ml.

Table B6.3. Estimated effects of exposure variable outcomes on LTL (Main model additionally adjusted for SBP and DBP).

Exposure [a]	% Difference [b]	95%CI		p-values
		Lower	Upper	
NO$_2$ (µg/m³)	-10.9	-20.52	-0.32	0.001
Benzene (µg/m³)	-8.1	-16.18	0.83	0.004
Toluene (µg/m³)	1.23	-2.20	4.79	0.310
Ethyl-Benzene (µg/m³)	0.63	-5.01	6.60	0.09
m+*p*-Xylene (µg/m³)	0.277	-1.494	2.08	0.045
o-Xylene (µg/m³)	0.60	-4.63	4.97	0.060
Urinary metabolite [c]				
3+4MHA (µg/mL)	-1.58	-3.74	0.64	0.180

[a] Model adjusted for adjusted for age, BMI, SBP, DBP, smoking and employment status. [b] Estimates expressed as a % difference in LTL for each SD increment in exposure [c] Additionally adjusted for urine creatinine. **IQR:** NO$_2$ 7.0 µg/m³; BTEX 3.3, 30.0, 3.8, 3.8, 3.8 µg/m³; 3+4MHA 1380 ng/ml.

Table B6.4. Estimated effects of exposure variable outcomes on mtDNA content.

Exposure [a]	% Difference [b]	95%CI		p-values
		Lower	Upper	
NO$_2$ (µg/m³)	-1.36	-9.73	7.78	0.760
Benzene (µg/m³)	-3.56	-10.73	4.17	0.352
Toluene (µg/m³)	7.57	0.21	15.45	0.044
Ethyl-Benzene (µg/m³)	8.62	-0.19	18.21	0.055
m+*p*-Xylene (µg/m³)	8.63	-0.09	18.12	0.053
o-Xylene (µg/m³)	8.12	-0.44	17.43	0.063
Urinary metabolite [c]				
3+4MHA (ng/ml)	-1.43	-7.60	4.40	0.604

[a] Model adjusted for adjusted for age, BMI, smoking and employment status. [b] Estimates expressed as a % difference in mtDNA content (*n* = 61 at baseline and *n* = 61 at follow-up) for each IQR increment in exposure. [c] Additionally adjusted for urine creatinine. **IQR:** NO$_2$ 7.0 µg/m³; BTEX 3.3, 30.0, 3.8, 3.8, 3.8 µg/m³; 3+4MHA 1380 ng/ml.

Table B6.5. Estimated effects of exposure variable outcomes on % DNA methylation.

Exposure [a]	% Difference [b]	95%CI		p-values
		Lower	Upper	
NO$_2$ (µg/m³)	-1.54	-4.61	1.637	0.332
Benzene (µg/m³)	-2.28	-4.94	0.45	0.099
Toluene (µg/m³)	-0.35	-1.75	1.07	0.624
Ethyl-Benzene (µg/m³)	-0.53	-1.61	0.56	0.328
m+p-Xylene (µg/m³)	-0.17	-0.50	0.15	0.288
o-Xylene (µg/m³)	-0.57	-1.46	0.34	0.214
Urinary metabolite [c]				
3+4MHA (ng/ml)	-0.95	-2.82	0.96	0.259

[a] Model adjusted for age, BMI, smoking and employment status. [b] Estimates expressed as a % difference in % DNA methylation for each IQR increment in exposure. [c] Additionally adjusted for urine creatinine. **IQR:** NO$_2$ 7.0 µg/m³; BTEX 3.3, 30.0, 3.8, 3.8, 3.8 µg/m³; 3+4MHA 1380 ng/ml.

8.7.   Appendix B7 – Effects of exposure variable outcomes on blood pressure and heart rate.

Table B7.1. Estimated effects of exposure variable outcomes on SBP (mmHg).

Exposure [a]	Estimate [b]	95%CI		p-values
		Lower	Upper	
NO$_2$ (µg/m³)	3.41	0.04	6.77	0.047
Benzene (µg/m³)	2.80	-0.87	6.48	0.070
Toluene (µg/m³)	0.01	-1.56	1.58	0.539
Ethyl-Benzene (µg/m³)	0.18	-1.27	1.63	0.272
m+*p*-Xylene (µg/m³)	0.07	-0.37	0.50	0.224
o-Xylene (µg/m³)	2.12	-0.50	4.74	0.112
Urinary metabolite [c]				
3+4MHA (ng/ml)	0.71	-0.25	1.67	0.687

[a] Model adjusted for age, BMI, temperature, date of clinical visit, smoking, hours of sleep at night and employment status. [b] Estimates expressed as a difference in SBP (mmHg) for each IQR increment in exposure. [c] Additionally adjusted for urine creatinine. **IQR:** NO$_2$ 7.0 µg/m³; BTEX 3.3, 30.0, 3.8, 3.8, 3.8 µg/m³; 3+4MHA 1380 ng/ml.

Table B7.2. Estimated effects of exposure variable outcomes on DBP (mmHg).

Exposure [a]	Estimate [b]	95%CI		p-values
		Lower	Upper	
NO$_2$ (µg/m³)	2.48	-0.01	4.97	0.050
Benzene (µg/m³)	1.44	-1.15	4.03	0.220
Toluene (µg/m³)	0.93	-0.15	2.01	0.860
Ethyl-Benzene (µg/m³)	0.71	-0.29	1.70	0.080
m+*p*-Xylene (µg/m³)	0.22	-0.08	0.52	0.062
o-Xylene (µg/m³)	0.82	0.01	1.63	0.029
Urinary metabolite [c]				
3+4MHA (ng/ml)	0.60	-0.09	1.29	0.673

[a] Model adjusted for adjusted for age, BMI, temperature, date of clinical visit, smoking, hours of sleep at night and employment status. [b] Estimates expressed as a difference in DBP (mmHg) for each IQR increment in exposure. [c] Additionally adjusted for urine creatinine. **IQR:** NO$_2$ 7.0 µg/m³; BTEX 3.3, 30.0, 3.8, 3.8, 3.8 µg/m³; 3+4MHA 1380 ng/ml.

Table B7.3. Estimated effects of exposure variable outcomes on heart rate (bpm).

Exposure [a]	Estimate [b]	95%CI Lower	95%CI Upper	p-values
NO$_2$ (µg/m³)	-1.30	-3.51	0.91	0.244
Benzene (µg/m³)	-1.00	-3.28	1.29	0.388
Toluene (µg/m³)	0.54	-0.45	1.53	0.280
Ethyl-Benzene (µg/m³)	-0.33	-1.21	0.55	0.456
m+p-Xylene (µg/m³)	-0.07	-0.33	0.20	0.612
o-Xylene (µg/m³)	-0.09	-0.85	0.67	0.808
Urinary metabolite [c]				
3+4MHA (ng/ml)	0.04	-0.58	0.67	0.892

[a] Model adjusted for adjusted for age, BMI, SBP, temperature, date of clinical visit, smoking and employment status. [b] Estimates expressed as a difference in heart rate (bpm) for each IQR increment in exposure. [c] Additionally adjusted for urine creatinine. **IQR:** NO$_2$ 7.0 µg/m³; BTEX 3.3, 30.0, 3.8, 3.8, 3.8 µg/m³; 3+4MHA 1380 ng/ml.

8.8. Appendix B8 – Effects of exposure on circulating markers of vascular endothelial function.

Table B8.1. Estimated effects of exposure variable outcomes on hsCRP levels (mg/L).

Exposure [a]	% Difference [b]	95%CI		p-values
		Lower	Upper	
NO$_2$ (µg/m³)	-12.8	-34.0	15.1	0.328
Benzene (µg/m³)	-7.7	-30.2	22.2	0.574
Toluene (µg/m³)	-2.9	-14.3	10.0	0.643
Ethyl-Benzene (µg/m³)	-9.5	-18.7	0.8	0.069
m+p-Xylene (µg/m³)	-3.0	-6.1	0.2	0.068
o-Xylene (µg/m³)	-7.4	-15.6	1.5	0.100
Urinary metabolite [c]				
3+4MHA (ng/ml)	0.96	-7.05	10.00	0.806

[a] Model adjusted for adjusted for age, BMI, SBP, temperature, date of clinical visit, smoking status and employment. [b] Estimates expressed as a % difference in hsCRP levels (mg/L) for each IQR increment in exposure. [c] Additionally adjusted for urine creatinine. **IQR:** NO$_2$ 7.0 µg/m³; BTEX 3.3, 30.0, 3.8, 3.8, 3.8 µg/m³; 3+4MHA 1380 ng/ml.

Table B8.2. Estimated effects of exposure variable outcomes on TNF-α levels (pg/ml).

Exposure [a]	Estimate [b]	95%CI		p-values
		Lower	Upper	
NO$_2$ (µg/m³)	-0.70	-1.93	0.54	0.260
Benzene (µg/m³)	-0.20	-1.38	0.98	0.736
Toluene (µg/m³)	0.01	-0.58	0.59	0.977
Ethyl-Benzene (µg/m³)	-0.04	-0.68	0.60	0.896
m+p-Xylene (µg/m³)	-0.02	-0.21	0.18	0.873
o-Xylene (µg/m³)	-0.05	-0.68	0.58	0.260
Urinary metabolite [c]				
3+4MHA (ng/ml)	0.87	-0.09	1.83	0.877

[a] Model adjusted for adjusted for age, BMI, SBP, temperature and smoking status. [b] Estimates expressed as a difference TNF-α levels (pg/ml) for each IQR increment in exposure. [c] Additionally adjusted for urine creatinine. **IQR:** NO$_2$ 7.0 µg/m³; BTEX 3.3, 30.0, 3.8, 3.8, 3.8 µg/m³; 3+4MHA 1380 ng/ml.

Table B8.3. Estimated effects of exposure variable outcomes on VCAM-1 levels (ng/ml).

Exposure [a]	% Difference [b]	95%CI		p-values
		Lower	Upper	
NO$_2$ (µg/m³)	1.70	-6.39	10.49	0.683
Benzene (µg/m³)	-3.21	-10.94	5.18	0.433
Toluene (µg/m³)	-0.52	-4.36	3.48	0.792
Ethyl-Benzene (µg/m³)	-4.85	-8.64	-0.91	0.018
m+p-Xylene (µg/m³)	-1.47	-2.68	-0.25	0.020
o-Xylene (µg/m³)	-4.47	-8.39	-0.39	0.033
Urinary metabolite [c]				
3+4MHA (ng/ml)	-0.95	-6.75	5.55	0.777

[a] Model adjusted for adjusted for age, BMI, SBP, temperature and smoking status. [b] Estimates expressed as a % difference in VCAM-1 levels (ng/ml) for each IQR increment in exposure. [c] Additionally adjusted for urine creatinine. **IQR:** NO$_2$ 7.0 µg/m³; BTEX 3.3, 30.0, 3.8, 3.8, 3.8 µg/m³; 3+4MHA 1380 ng/ml.

Table B8.4. Estimated effects of exposure variable outcomes on ICAM-1 levels (ng/ml).

Exposure [a]	% Difference [b]	95%CI		p-values
		Lower	Upper	
NO$_2$ (µg/m³)	-3.25	-9.45	3.37	0.317
Benzene (µg/m³)	-1.93	-9.47	6.24	0.625
Toluene (µg/m³)	-0.01	-3.60	3.72	0.995
Ethyl-Benzene (µg/m³)	-0.65	-4.67	3.55	0.752
m+p-Xylene (µg/m³)	-0.19	-1.44	1.08	0.767
o-Xylene (µg/m³)	-0.66	-4.97	3.84	0.762
Urinary metabolite [c]				
3+4MHA (ng/ml)	-1.26	-5.86	3.23	0.540

[a] Model adjusted for adjusted for age, BMI, SBP, temperature and smoking status. [b] Estimates expressed as a % difference in ICAM-1 for each IQR increment in exposure. [c] Additionally adjusted for urine creatinine. **IQR:** NO$_2$ 7.0 µg/m³; BTEX 3.3, 30.0, 3.8, 3.8, 3.8 µg/m³; 3+4MHA 1380 ng/ml.

Table B8.5. Estimated effects of exposure variable outcomes on e-selectin levels (ng/ml).

Exposure [a]	Estimate [b]	95%CI Lower	95%CI Upper	p-values
NO_2 (µg/m³)	0.11	-2.24	2.45	0.927
Benzene (µg/m³)	-1.00	-3.27	1.27	0.378
Toluene (µg/m³)	-0.50	-1.68	0.68	0.395
Ethyl-Benzene (µg/m³)	-0.44	-1.64	0.76	0.458
m+p-Xylene (µg/m³)	-0.11	-0.47	0.25	0.541
o-Xylene (µg/m³)	-0.20	-1.40	1.00	0.739
Urinary metabolite [c]				
3+4MHA (ng/ml)	-0.91	-2.67	0.85	0.303

[a] Model adjusted for adjusted for age, BMI, SBP, temperature and smoking status. [b] Estimates expressed as a difference in e-selectin levels (ng/ml) for each IQR increment in exposure. [c] Additionally adjusted for urine creatinine. **IQR:** NO_2 7.0 µg/m³; BTEX 3.3, 30.0, 3.8, 3.8, 3.8 µg/m³; 3+4MHA 1380 ng/ml.

Table B8.6. Estimated effects of exposure variable outcomes on p-selectin levels (ng/ml).

Exposure [a]	Estimate [b]	95%CI Lower	95%CI Upper	p-values
NO_2 (µg/m³)	-1.05	-5.47	3.37	0.635
Benzene (µg/m³)	-5.79	-9.33	-2.26	0.002
Toluene (µg/m³)	-0.45	-2.07	1.17	0.581
Ethyl-Benzene (µg/m³)	0.20	-2.05	2.45	0.859
m+p-Xylene (µg/m³)	-0.04	-0.72	0.64	0.906
o-Xylene (µg/m³)	-0.26	-2.48	1.97	0.813
Urinary metabolite [c]				
3+4MHA (ng/ml)	-0.44	-3.65	2.77	0.786

[a] Model adjusted for adjusted for age, BMI, SBP, temperature and smoking status. [b] Estimates expressed as a difference in p-selectin levels (ng/ml) for each IQR increment in exposure. [c] Additionally adjusted for urine creatinine. **IQR:** NO_2 7.0 µg/m³; BTEX 3.3, 30.0, 3.8, 3.8, 3.8 µg/m³; 3+4MHA 1380 ng/ml.

Table B8.7. Estimated effects of exposure variable outcomes on VEGF levels (pg/ml).

Exposure [a]	% Difference [b]	95%CI		p-values
		Lower	Upper	
NO$_2$ (µg/m³)	-18.9	-30.7	-5.2	0.010
Benzene (µg/m³)	-4.0	-19.2	13.9	0.632
Toluene (µg/m³)	0.1	-7.8	8.5	0.990
Ethyl-Benzene (µg/m³)	-5.5	-13.8	3.5	0.216
m+*p*-Xylene (µg/m³)	-1.7	-4.4	1.0	0.209
o-Xylene (µg/m³)	-3.2	-11.8	6.3	0.491
Urinary metabolite [c]				
3+4MHA (ng/ml)	4.2	-9.1	19.5	0.545

[a] Model adjusted for adjusted for age, BMI, SBP, temperature and smoking status. [b] Estimates expressed as a % difference in VEGF (pg/ml) for each IQR increment in exposure [c] Additionally adjusted for urine creatinine. **IQR:** NO$_2$ 7.0 µg/m³; BTEX 3.3, 30.0, 3.8, 3.8, 3.8 µg/m³; 3+4MHA 1380 ng/ml.

Table B8.8. Estimated effects of exposure variable outcomes on PAI-1 levels (ng/ml).

Exposure [a]	Estimate [b]	95%CI		p-values
		Lower	Upper	
NO$_2$ (µg/m³)	-3.4	-16.7	9.9	0.612
Benzene (µg/m³)	1.4	-10.4	13.2	0.811
Toluene (µg/m³)	7.2	2.3	12.1	0.005
Ethyl-Benzene (µg/m³)	9.1	2.4	15.7	0.008
m+*p*-Xylene (µg/m³)	3.08	1.09	5.1	0.003
o-Xylene (µg/m³)	11.7	5.2	18.1	0.001
Urinary metabolite [c]				
3+4MHA (ng/ml)	12.9	3.8	22.6	0.010

[a] Model adjusted for adjusted for age, BMI, SBP, temperature and smoking status. [b] Estimates expressed as a difference in PAI-1 levels (ng/ml) for each IQR increment in exposure [c] Additionally adjusted for urine creatinine. **IQR:** NO$_2$ 7.0 µg/m³; BTEX 3.3, 30.0, 3.8, 3.8, 3.8 µg/m³; 3+4MHA 1380 ng/ml.

8.9. Appendix B9 – Effects of exposure variable outcomes on retinal vessel calibre.

Table B9.1. Estimated effects of exposure variable outcomes on CRAE (µm).

Exposure [a]	Estimate [b]	95%CI		*p*-values
		Lower	Upper	
NO_2 (µg/m³)	-0.66	-3.17	1.84	0.599
Benzene (µg/m³)	-0.69	-3.49	2.10	0.582
Toluene (µg/m³)	-0.04	-1.16	1.09	0.500
Ethyl-Benzene (µg/m³)	-0.46	-1.44	0.52	0.579
m+*p*-Xylene (µg/m³)	-0.16	-0.45	0.14	0.511
o-Xylene (µg/m³)	-0.43	-1.27	0.41	0.461
Urinary metabolite [c]				
3+4MHA (ng/ml)	-0.02	-2.48	2.45	0.517

[a] Model adjusted for adjusted for age, BMI, SBP, date of clinical visit, temperature, smoking status and employment status. [b] Estimates expressed as a difference in CRAE (µm) for each IQR increment in exposure [c] Additionally adjusted for urine creatinine. **IQR:** NO_2 7.0 µg/m³; BTEX 3.3, 30.0, 3.8, 3.8, 3.8 µg/m³; 3+4MHA 1380 ng/ml.

Table B9.2. Estimated effects of exposure variable outcomes on CRVE (µm).

Exposure [a]	Estimate [b]	95%CI		*p*-values
		Lower	Upper	
NO_2 (µg/m³)	-2.93	-5.83	-0.03	0.048
Benzene (µg/m³)	-0.38	-3.81	3.04	0.588
Toluene (µg/m³)	0.51	-0.89	1.91	0.768
Ethyl-Benzene (µg/m³)	-0.36	-1.50	0.79	0.616
m+*p*-Xylene (µg/m³)	-0.10	-0.45	0.25	0.638
o-Xylene (µg/m³)	-0.34	-1.32	0.65	0.587
Urinary metabolite [c]				
3+4MHA (ng/ml)	-0.32	-1.05	0.42	0.890

[a] Model adjusted for age, BMI, SBP, date of clinical visit, temperature, smoking status and employment status. [b] Estimates expressed as a difference in CRVE (µm) for each IQR increment in exposure [c] Additionally adjusted for urine creatinine. **IQR:** NO_2 7.0 µg/m³; BTEX 3.3, 30.0, 3.8, 3.8, 3.8 µg/m³; 3+4MHA 1380 ng/ml.

Table B9.3. Estimated effects of exposure variable outcomes on AVR.

Exposure [a]	Estimate [b]	95%CI		p-values
		Lower	Upper	
NO$_2$ (µg/m³)	0.0073	-0.0034	0.0179	0.179
Benzene (µg/m³)	-0.0006	-0.0124	0.0113	0.924
Toluene (µg/m³)	-0.0008	-0.0057	0.0040	0.721
Ethyl-Benzene (µg/m³)	-0.0004	-0.0049	0.0041	0.842
m+p-Xylene (µg/m³)	-0.0002	-0.0015	0.0012	0.729
o-Xylene (µg/m³)	-0.0003	-0.0037	0.0031	0.869
Urinary metabolite [c]				
3+4MHA (ng/ml)	0.0005	-0.0028	0.0028	0.735

[a] Model adjusted for adjusted for age, BMI, SBP, date of clinical visit, temperature, smoking status and employment status. [b] Estimates expressed as a difference in AVR for each IQR increment in exposure [c] Additionally adjusted for urine creatinine. **IQR:** NO$_2$ 7.0 µg/m³; BTEX 3.3, 30.0, 3.8, 3.8, 3.8 µg/m³; 3+4MHA 1380 ng/ml.

8.10. **Appendix B10 – Effects of exposure variable outcomes on flow-mediated vasodilation parameters.**

Table B10.1. Estimated effects of exposure variable outcomes on baseline brachial artery diameter (mm).

Exposure [a]	Estimate [b]	95%CI		p-values
		Lower	Upper	
NO$_2$ (µg/m³)	-0.11	-0.19	-0.03	0.005
Benzene (µg/m³)	-1.01	-0.10	0.08	0.760
Toluene (µg/m³)	-0.09	-0.17	0.01	0.065
Ethyl-Benzene (µg/m³)	-0.08	-0.17	0.00	0.057
m+*p*-Xylene (µg/m³)	-0.06	-0.15	0.02	0.144
o-Xylene (µg/m³)	-0.06	-0.15	0.03	0.189
Urinary metabolites [c]				
3+4MHA (ng/ml)	0.02	-0.07	0.11	0.647

[a] Model adjusted for age, BMI, SBP, date of clinical visit, temperature, smoking status and employment status. [b] Estimates expressed as a difference in baseline brachial artery diameter (mm) for each IQR increment in exposure [c] Additionally adjusted for urine creatinine. **IQR:** NO$_2$ 7.0 µg/m³; BTEX 3.3, 30.0, 3.8, 3.8, 3.8 µg/m³; 3+4MHA 1380 ng/ml.

Table B10.2. Estimated effects of exposure variable outcomes on % FMD.

Exposure [a]	Estimate [b]	95%CI		p-values
		Lower	Upper	
NO$_2$ (µg/m³)	-0.11	-1.00	0.77	0.801
Benzene (µg/m³)	-0.01	-0.87	0.85	0.982
Toluene (µg/m³)	0.36	-0.50	1.22	0.403
Ethyl-Benzene (µg/m³)	0.35	-0.76	0.90	0.870
m+*p*-Xylene (µg/m³)	0.07	-0.77	0.92	0.862
o-Xylene (µg/m³)	0.16	-0.68	1.00	0.705
Urinary metabolites [c]				
3+4MHA (ng/ml)	-1.45	-2.38	-0.51	0.003

[a] Model adjusted for adjusted for age, BMI, SBP, date of clinical visit, temperature, brachial diameter, smoking status and employment status. [b] Estimates expressed as a difference in % FMD for each IQR increment in exposure [c] Additionally adjusted for urine creatinine. **IQR:** NO$_2$ 7.0 µg/m³; BTEX 3.3, 30.0, 3.8, 3.8, 3.8 µg/m³; 3+4MHA 1380 ng/ml.

9. Appendix C: Additional Information.
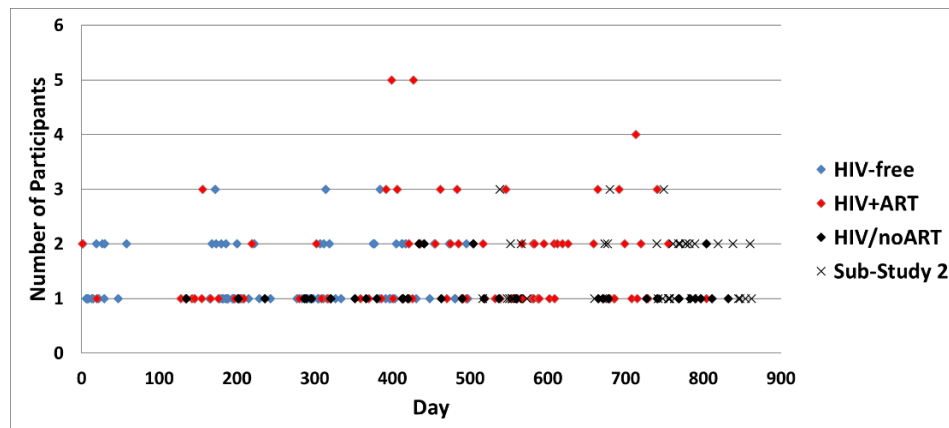
Figure C1. A figure depicting the distribution of baseline assessment visits for each study group.

Table C1. Reasons for loss of participants at follow-up visit for Sub-study 1 and 2 combined.

Number of Participants	Reason
n = 48	Moved away from recruitment area or could not be located.
n = 32	Did not wish to continue with the study.
n = 17	Did not show up for appointments.
n = 16	Could not attend follow-up visit due to employment obligations.
n = 13	Diseased before follow-up visit.
n = 7	Enrolled in study, but baseline visit was incomplete.
n = 5	Participant became pregnant.
n = 4	Contracted tuberculosis.
n = 142	**Total**

Table C2. Assessment of interobserver variability for the FMD procedure.

Probe Operator	Baseline Brachial Lumen Diameter [a, b]	% FMD [a, c]
1	3.2 (0.84) mm	6.2 (7.2) %
2	3.2 (0.72) mm	6.2 (7.8) %
3	3.3 (0.81) mm	6.2 (6.0) %
4	3.3 (0.64) mm	6.6 (6.2) %

[a] Data presented as the median (IQR). Kruskal Wallis test: Between-subjects effects [b] $p = 0.401$ and [c] $p = 0.396$.

10. Appendix D: First-Author Publications.

Personal exposure to NO_2 and benzene in the Cape Town region of South Africa is associated with shorter leukocyte telomere length in women

Frans Everson[a], Dries S. Martens[b], Tim S. Nawrot[b,*], Nandu Goswami[c], Mashudu Mthethwa[a], Ingrid Webster[a], Nyiko Mashele[a], Sana Charania[a], Festus Kamau[a], Patrick De Boever[b,d], Hans Strijdom[a]

[a] Centre for Cardio-metabolic Research in Africa, Division of Medical Physiology, Faculty of Medicine and Health Sciences, Stellenbosch University, Cape Town, 8000, South Africa
[b] Centre for Environmental Sciences, Hasselt University, 3590, Diepenbeek, Belgium
[c] Division of Physiology, Otto Loewi Research Center of Vascular Biology, Immunity and Inflammation, Medical University of Graz, 8036, Graz, Austria
[d] Health Unit, Flemish Institute for Technological Research (VITO), 2400, Mol, Belgium

ARTICLE INFO

ABSTRACT

Air pollution exposure is a major global health concern and has been associated with molecular aging. Unfortunately, the situation has not received much attention in the African region. The aim of this study was to investigate whether current personal ambient NO_2 and benzene, toluene, ethyl-benzene and xylenes (ortho (o)-, meta (m)- and para (p)-xylene (BTEX) exposure is associated with leukocyte telomere length (LTL), a marker of molecular ageing, in apparently healthy women (mean ± SD age: 42.5 ± 13.4 years) residing in the Cape Town region of South Africa. The repeated measures study collected data from 61 women. Seven-day median (interquartile range (IQR)) personal NO_2 and BTEX exposure levels were determined via compact passive diffusion samplers carried on the person prior to baseline (NO_2: 14.2 (9.4–17.2) μg/m³; Benzene: 3.1 (2.1–5.3) μg/m³) and 6-month follow-up (NO_2: 10.6 (6.6–13.6) μg/m³; Benzene: 2.2 (1.3–4.9) μg/m³) visits. LTL was measured at baseline and follow-up using a real-time PCR method. Multiple linear mixed model analyses (adjusting for age, body mass index, smoking, employment status, level of education and assessment visit) showed that each IQR increment increase in NO_2 (7.0 μg/m³) and benzene (3.3 μg/m³) was associated with −7.30% (95% CI: −10.98 to −3.46%; p < 0.001) and −6.78% (95% CI: −11.88 to −1.39%; p = 0.015) difference in LTL, respectively. The magnitude of these effects of NO_2 and benzene corresponds to the effect of an increase of 10.3- and 6.0-year in chronological age on LTL. Our study shows that personal exposures to NO_2 and benzene are associated with molecular ageing as indicated by LTL in healthy women residing in the Cape Town region.

1. Introduction

The World Health Organization (WHO) estimates that 7 million premature deaths occur globally each year due to air pollution, including almost 1 million in Africa (Kuehn, 2014). Pollutants such as NO_2, benzene, toluene, ethyl-benzene and xylenes (ortho (o)-, meta (m)- and para (p)-xylene (BTEX) and small ambient particulate matter (< 2.5 μm diameter ($PM_{2.5}$) have been identified as culprits (Bolden et al., 2015; Łatka et al., 2018; World Health Organization, 2018, 2016). They are mostly produced through the incomplete combustion of fossil fuels during industrial, vehicle and household processes and therefore relevant in the indoor and outdoor setting in both urban and rural spaces (Bolden et al., 2015; Miri et al., 2016).

Telomeres, protein complexes located at the end of chromosomes, play an important role in maintaining chromosomal structural and functional integrity by protecting the chromosome against degradation and loss of genetic information (O'Sullivan and Karlseder, 2010). Telomeres shorten over time due to DNA replication and the adverse effects of oxidative stress and inflammation (O'Sullivan and Karlseder, 2010). Leukocyte telomere length (LTL) is therefor considered a marker of cellular ageing and is associated with degenerative diseases/disorders such as atherosclerosis, cancer and all-cause mortality (Haycock et al., 2014; Martens and Nawrot, 2016; Miri et al., 2019; Wang et al., 2018).

Evidence has shown that telomeres may also be an important intermediate marker of health outcomes following air pollution exposure

(Desai et al., 2017; Hoxha et al., 2009; Miri et al., 2019; Zglinicki et al., 2005; Zhao et al., 2018). Although the exact underlying mechanisms involved remain incompletely described (De Prins et al., 2013; Desai et al., 2017; Zglinicki et al., 2005; Zhao et al., 2018), acute high-level exposure to air pollution is often associated with increased telomere length (TL) that could be attributed to an acute inflammatory response (Dioni et al., 2011; Hou et al., 2012; Xu et al., 2018), while negative associations between LTL and air pollution exposure are often reported in studies investigating chronic high- and low-level exposure with oxidative damage as a possible major mechanism (Bijnens et al., 2015; Ling et al., 2016; Pieters et al., 2016).

Reports on the effects of air pollution on TL in South African and sub-Saharan African populations are currently lacking, as mentioned in a recent systematic review and meta-analysis on the effects of air pollution on LTL (Miri et al., 2019), which showed that none of the 19 eligible publications were from the African region (Miri et al., 2019). In fact there seems to be a general shortage of studies on the health effects of air pollution in the Sub-Saharan Africa region. A recent review by Katoto et al. (2019) highlighted this general paucity by identifying only 23 reports from the sub-Saharan Africa region that assessed associations between air pollution and health outcomes (Katoto et al., 2019). Reports have furthermore shown that combustion processes used for coal-based power generation, industries, domestic heating and cooking and transport are mostly contributing to air pollution in South Africa, but air pollution levels are seldom linked to health outcomes (Klausbruckner et al., 2016; South African Department of Environmental Affairs, 2007). In light of the general paucity of available data, especially on intermediate health markers such as LTL, the aim of the current repeated measures study was to investigate whether LTL is a marker of the effect of personal ambient NO_2 and BTEX exposure in apparently healthy women (with no medical history or signs of overt disease) residing in the Cape Town region of South Africa.

2. Materials and methods

2.1. Study ethics, design and population

The study formed part of a larger parent study called EndoAfrica (Strijdom et al., 2017). Ethics clearance for the current study was obtained from The Health Research Ethics Committee, Stellenbosch University, South Africa (in accordance with the Helsinki Declaration; Reference number: S16/07/114). The methodologies used for participant recruitment, air quality and temperature monitoring, and the quantification of biochemical analysis have previously been reported (Everson et al., 2019).

The study followed a repeated measures design with a baseline visit and one 6-month follow-up visit. Qualified research nurses recruited and obtained informed consent from apparently healthy volunteering women with no recorded history or signs of overt disease (confirmed from participant file at local clinics). A total number of 77 women successfully completed the first clinical visit (Baseline visit). Sixteen participants did not give consent to be included for the 6-month follow-up assessment and were subsequently excluded. All volunteering participants were from neighbouring residential areas in the northern suburbs of Cape Town area. Healthy participants who were > 18 years of age, HIV-negative (confirmed with a rapid HIV-test; SD Bioline HIV 1/2 3.0 immunochromatographic test kit; Standard Diagnostics, Republic of Korea), free of genetic, chronic and acute diseases such as diabetes- and tuberculosis (confirmed from participant file at local clinics), not pregnant (confirmed with pregnancy test) and > 3 months post-partum were included. Baseline assessments were conducted from September 2016 to August 2017 and 6-month follow-up visits were completed by February 2018. All backpacks containing samplers were handed out and collected between 8h00 and 11h00 in the morning.

2.2. Air quality and temperature monitoring

A NO_2 passive diffusion sampler (Gradko International Ltd., UK), Radiello™ BTEX passive diffusion sampler (Sigma-Aldrich Inc., USA) and ACR SmartButton® temperature logger (ACR Systems, Surrey, B.C. Canada) were placed inside the external mesh pocket of a backpack for each participant. All participants carried the backpacks for a 7-day period prior to each assessment visit. The passive diffusion samplers allowed continuous air diffusion and the temperature logger recorded temperature (°C) at 30-min intervals in a 50–60 cm radius from the face for the 7-day period prior to each assessment visit. Backpacks were placed next to the participant's bed during periods of sleep and bathroom use.

Following 7 days of continuous measurements, participants returned for assessment visits. Data were extracted from the temperature loggers *via* ACR TrendReader® software (ACR Systems, Surrey, B.C. Canada). NO_2 and BTEX samplers were sealed, stored at 4 °C and sent for quantification as previously described (Everson et al., 2019). NO_2 samplers (a total of $n = 121$; one sampler lost by a participant) were sent to Gradko International (Ltd.) Laboratories (United Kingdom) for quantification by means of United Kingdom Accreditation Services (UKAS: GLM 7) accredited chemiluminescence ultra-violet (UV) spectrophotometry methodology (UVS04 Camspec M550; Spectronic Camspec Ltd., Leeds, UK) as previously described (Everson et al., 2019; Targa and Loader, 2008). A calibration curve consisted of a blank (deionised water only) and standard nitrate solutions (nitrite ion (NO_2^-) at 15, 30, 60, 90 μg/mL). Samples were eluted by means of a 20% triethanolamine solution/80% deionised water. The colour reagent was prepared according to previously described specification (0.003 g naphthyl-1 ethylene diamine dihydrochloride per 1 g sulphanilamide) (Palmes et al., 1976). For quality assurance, calibration standards and linearity checks were performed and mid-range and zero standards were analysed at intervals throughout the sequence. The NO_2^- concentration of each sample was determined against the calibration curve and expressed as μg/m³. All NO_2 exposure concentration levels were within the detectable range (LOD - NO_2: > 0.2 μg/m³).

BTEX samplers were analysed at the Flemish Institute for Technological Research (VITO; Mol, Belgium) by accredited Thermo Trace gas chromatography/mass spectrometry methodology (Thermo DSQ II with helium as carries gas (at a constant flow of 1 ml/min) as previously described (Everson et al., 2019; McAlary et al., 2015; Pegas et al., 2011). Samples were eluted (30 min on a rotational shaker) by means of 2 ml carbon disulphide (Sigma-Aldrich, MO, USA) containing 12.5 μl 2-fluorotoluene internal standard (Sigma-Aldrich, MO, USA). For sample separation, an RTX 502.2, 0.25 mm by 30 m crossbond diphenyl/dimethylpolysiloxane column with a 1.4 μm-thick film was used. The temperature program was set at 35 °C for 5 min with subsequent 14 °C/min increment increases until 245 °C. A 0.03–30 μg/g calibration curve that comprised of a standard solution containing benzene, ethyl-benzene, toluene, *m*-xylene, *p*-xylene, and *o*-xylene in carbon disulphide (Sigma-Aldrich, MO, USA) was injected before analysis to calibrate the equipment. Results were expressed as mean BTEX exposure concentrations respective (μg/m³) for the 7-day measuring period.

Results from a total number of $n = 114$ BTEX samplers were successfully obtained. One BTEX sampler was lost by a participant. Three samplers were returned damaged and were excluded for analysis. Results from two samplers were flagged by the laboratory as questionable and were subsequently excluded. Also, two BTEX samplers yielded exposure concentrations below the detectable range (Benzene: 0.05 μg/m³, toluene: 0.01 μg/m³, ethyl-benzene: 0.01 μg/m³ and xylene: 0.01 μg/m³) and were excluded from further analysis. Excluding results form the two samples that yielded below detectable range from further analysis as opposed to using LOD/2 values did not significantly affect any results presented in the current study.

Stellenbosch University https://scholar.sun.ac.za

F. Everson, et al.   Environmental Research 182 (2020) 108993

2.3. Study endpoints

2.3.1. Health questionnaire and anthropometric measurements

Age, lifestyle and socioeconomic information were collected from each participant at each visit. Lifestyle information included smoking status (defined as smoking or non-smoking) and alcohol constitution (defined as yes/no and if yes, more or less than 8 days a month). Socioeconomic information included employment status (defined as either unemployed, part-time employed or full-time employed) and highest level of education obtained (defined as either primary school, secondary school or a tertiary education). Anthropometric measurements included body-mass index (BMI) expressed as kg body weight/m^2 height (measured on an electronic scale and stadiometer), and resting systolic and diastolic blood pressure (SBP and DBP) expressed as the average mmHg of three measurements taken at 5-min intervals on the left arm (Omron M6 automatic digital blood pressure monitor: Omron Healthcare, Kyoto, Japan) as previously described (Everson et al., 2019).

2.3.2. Biochemical and telomere measurements

Fasting blood samples were collected in serum blood collection tubes (SGVac, The Scientific Group (Pty) Ltd.; Milnerton, Western Cape, SA) at each clinical visit and transported to South African National Health Laboratory Service (Tygerberg Hospital, South Africa) for determination of high-sensitivity C-reactive protein (hsCRP) levels (Everson et al., 2019). HsCRP levels > 0.3 mg/L were considered to be elevated (Ridker, 2016).

The buffy coats of fasted peripheral blood samples (EDTA blood collection tubes (SGVac, The Scientific Group (Pty) Ltd.; Milnerton, Western Cape, SA)) were extracted, stored at −80 °C and sent to the University of Hasselt (Belgium) for DNA extraction (QIAamp® DNA Mini Kit QIAGEN, Hilden, Germany) and quantification as previously described (Martens et al., 2016). After DNA extraction, the DNA content in each sample was quantified by a Nanodrop 1000 spectrophotometer (Isogen, Life Science, Belgium) and the DNA quality evaluated using agarose gelelectrophoresis. Extracted DNA samples were diluted to ensure a uniform DNA input (5 ng) for each quantitative real-time polymerase chain reaction (qPCR) and checked using a Quant-iT Pico-Green dsDNA Assay Kit (LifeTechnologies, Europe).

All LTL measurements were performed in triplicate on a 7900HT Fast Real-Time PCR System (Applied Biosystems, USA) in a 384-well format. The telomere-specific qPCR reaction mixture contained 1x QuantiTect SYBR Green PCR master mix (Qiagen, Inc., Venlo, the Netherlands), 2 mM dithiothreitol (DTT), 300 nM telg primer (ACACT AAGGTTTGGGTTTGGGTTTGGGTTTGGGTTAGTGT) and 900 nM telc primer (TGTTAGGTATCCCTATCCCTATCCCTATCCCTAACA). Cycling conditions used were: 1 cycle at 95 °C for 10 min, followed by 2 cycles at 94 °C for 15 s and 49 °C for 2 min and 30 cycles at 94 °C for 15 s, 62 °C for 20 s, and 74 °C for 1 min and 40 s. The single-copy gene qPCR mixture contained 1x QuantiTect SYBR Green PCR master mix, 300 nM 36B4u primer (CAGCAAGTGGGAAGGTGTAATCC) and 500 nM 36B4d primer (CCCATTCTATCATCAACGGGTACAA).

After each qPCR a melting curve analysis was performed. On each run, a 6-point serial dilution of pooled buffy coat DNA was run to assess PCR efficiency as well as three inter-run calibrators to account for inter-run variability. We achieved coefficients of variation (CV) within triplicates of the telomere runs, single-copy gene runs, and T/S ratios of 0.71%, 0.38%, and 7.1%, respectively.

2.4. Statistical analysis

All statistical analyses were performed with IBM SPSS software (version 25; New York, USA). Paired sample Student's t-tests (parametric) or Wilcoxon signed ranks tests (non-parametric) were performed to identify significant differences between baseline and follow-up visits. Spearman rank correlations were used for all correlation

analysis. Multiple linear mixed model analysis (LMM) was applied to evaluate the associations of NO$_2$ and BTEX compounds with LTL. Variables with skewed data distribution were log$_{10}$-transformed. All LMMs included participants nested in each visit as a random effects factor variable with random intercept (to account for possible inter-individual variation). Covariates that are known determinants of LTL and variables with a potential link between personal air pollution exposure and LTL were selected (Cherkas et al., 2006; Fitzpatrick et al., 2007; Sanders and Newman, 2013; Valdes et al., 2005). Model A was only adjusted for age while the fully adjusted Model B was adjusted for age and BMI, as continuous fixed effects, smoking status, employment status level of education and assessment visit (baseline and follow-up) as fixed categorical variables. Sensitivity analyses were performed by means of additionally adjusting Model B for average temperature (Model B1), SBP and DBP (Model B2), and alcohol consumption (Model B3) respectively. To further evaluate the robustness of the fully adjusted model, a non-linear term age*age was included in the model. Estimates were presented as a % difference in LTL for an IQR increment in exposure. Q-Q plots and distribution (Shapiro-Wilk test) of residuals were used to test the assumptions of linearity and normality. The significant threshold was set at $p < 0.05$ for all statistical analysis.

3. Results

3.1. Baseline population characteristics

Sixty-one healthy women with a mean ± SD age of 42.5 ± 13.4 years (range: 19–70 years) completed the study (Table 1). The majority of study participants were unemployed (49%) and current smokers (69%) with a smoking frequency < 20 cigarettes/day. Less than half of the participants reported that they consumed alcohol (46%; at a frequency of less than 8 days a month for all). Seventy-two percent of participants reporting primary school education as their highest level of education obtained.

The mean SBP and DBP were furthermore clinically normal according to South African Hypertension Society guidelines (SBP < 140 mmHg or DBP of < 90 mmHg) (Seedat and Rayner, 2013). The mean ± SD BMI of the study population (27.7 ± 8.4 kg/m^2) fell within the overweight range (BMI 25 to < 30 kg/m^2 (World Health Organization Expert Committee on Physical Status, 1995). Most participants (61%) presented with elevated hsCRP levels (Table 2).

Baseline age was negatively correlated with LTL ($r = −0.30$; $p = 0.025$; Supplementary Figs. 1a) and a positive correlation between baseline and follow-up LTL was observed ($r = 0.70$; $p < 0.001$; Supplementary Fig. 1b). NO$_2$ ($r = 0.321$; $p = 0.018$) and benzene

Table 1
Baseline demographic, lifestyle and socioeconomic characteristics for 61 women living in the Cape Town region.

Variable	Baseline
Age, years	42.5 ± 13.4
Smoking Status	
Yes, n (%)	42 (69%)
No, n (%)	19 (31%)
Alcohol consumption	
No, n (%)	33 (54%)
Yes, n (%)	28 (46%)
Frequency (< 8 days a month)	28 (46%)
Employment	
Unemployed, n (%)	30 (49%)
Part-time, n (%)	25 (41%)
Full-time, n (%)	6 (10%)
Education Level	
Primary school, n (%)	44 (72%)
Secondary school, n (%)	12 (20%)
Tertiary education, n (%)	5 (8%)

Data presented as mean ± standard deviation (SD) or n (%).

Table 2

Baseline anthropometric and biochemical characteristics for 61 women living in the Cape Town region.

Variable	Baseline
Blood Pressure	
SBP, mmHg	122.5 ± 19.9
DBP, mmHg	84.1 ± 12.0
Hypertension (SBP > 140 mmHg or DBP > 90 mmHg)	
Yes, n (%)	15 (25%)
No, n (%)	46 (75%)
BMI, kg/m^2	27.7 ± 8.4
Underweight (BMI < 18.5 kg/m^2), n (%)	6 (10%)
Normal weight (BMI 18.5 to < 25 kg/m^2), n (%)	22 (36%)
Overweight (BMI 25 to < 30 kg/m^2), n (%)	11 (18%)
Obese (BMI > 30 kg/m^2), n (%)	22 (36%)
hsCRP, mg/L [a]	6.3 (0.2–37.1)
Elevated hsCRP (> 3 mg/L)	
Yes, n (%)	35 (61%)
No, n (%)	22 (39%)
Leukocyte Telomere Length (LTL) [b]	0.98 (0.58–1.55)

Data presented as mean $\pm$ standard deviation (SD) or median (range) or n (%).
[a] Sample size: $n = 58$. [b] $n = 57$, four samples had insufficient DNA content.

($r = 0.322$; $p = 0.020$) was inversely correlated with LTL and a higher level of education was positively correlated with LTL ($r = 0.332$; $p = 0.012$) (Supplementary Table 1). Employment status was positively correlated with NO$_2$ ($r = 0.369$; $p = 0.003$), benzene, ($r = 0.285$; $p = 0.028$), toluene ($r = 0.382$; $p = 0.003$), ethyl-benzene ($r = 0.340$; $p = 0.008$), $m + p$-xylene ($r = 0.358$; $p = 0.005$) and o-xylene ($r = 0.337$; $p = 0.009$) exposure concentrations. Inflammation was evaluated as a potential mediator between exposure effects and LTL; however, no significant associations between exposure, hsCRP and LTL were observed (Supplementary Table 1).

3.2. Personal ambient exposure

NO$_2$, benzene, ethyl-benzene and xylene levels were significantly higher ($p < 0.05$) at baseline than follow-up visit (Fig. 1). The median (IQR) temperature for baseline (21.9 (19.4–24.3) °C) and follow-up

Table 3

Estimated effects of personal NO$_2$ and BTEX on LTL in $n = 61$ women from the Cape Town region.

	Exposure	% Difference (95%CI) [a]	p-values
Model A	NO$_2$	-11.4 (-19.9; -2.08)	0.019
	BTEX		
	Benzene	-10.0 (-19.2; 0.28)	0.056
	Toluene	-1.37 (-21.3; 23.7)	0.90
	Ethyl-benzene	-4.17 (-13.5; 6.17)	0.41
	$m + p$-Xylene	-7.72 (-24.8; 13.2)	0.44
	o-Xylene	-4.22 (-14.45; 7.24)	0.45
Model B	NO$_2$	-7.30 (-10.9; -3.46)	< 0.001
	BTEX		
	Benzene	-6.78 (-11.9; -1.39)	0.015
	Toluene	-1.56 (-13.6; 12.1)	0.81
	Ethyl-benzene	-2.13 (-6.61; 2.57)	0.36
	$m + p$-Xylene	-3.75 (-12.4; 5.72)	0.42
	o-Xylene	-1.62 (-6.74; 3.78)	0.54

All models include participants ($n = 61$) nested in each visit with random intercept (Random factor: participant). **Model A**: adjusted for age. **Model B** (fully adjusted model; Residual distribution (Shapiro-Wilk test): $p = \geq 0.05$ for all analyses): Adjusted for age, BMI, smoking, employment status, level of education and assessment visit (baseline and follow-up visit). [a] Estimates presented as the % difference in LTL for a IQR increment in exposure (NO$_2$: 7.0 μg/m^3; Benzene: 3.3 μg/m^3; Toluene 30 μg/m^3: Ethyl-benzene: 3.3 μg/m^3; $m + p$-Xylene: 11.4 μg/m^3; o-xylene 3.8 μg/m^3). LTL: $n = 57$ at baseline and $n = 55$ at follow-up.

(22.0 (20.4–23.9) °C) did not significantly differ ($p > 0.05$). NO$_2$ and BTEX exposure concentrations were positively correlated and inversely associated with temperature (Supplemental Table 2).

3.3. Air pollution exposure and leukocyte telomere length

At baseline, determinants of LTL included age, level of education, NO$_2$ and benzene exposure while employment and temperature were determinants of NO$_2$ and BTEX exposure (Supplementary Table 1). After controlling for age only, each IQR increment in NO$_2$ (7.0 μg/m^3) and benzene (3.3 μg/m^3) exposure was associated with a -11.4% and
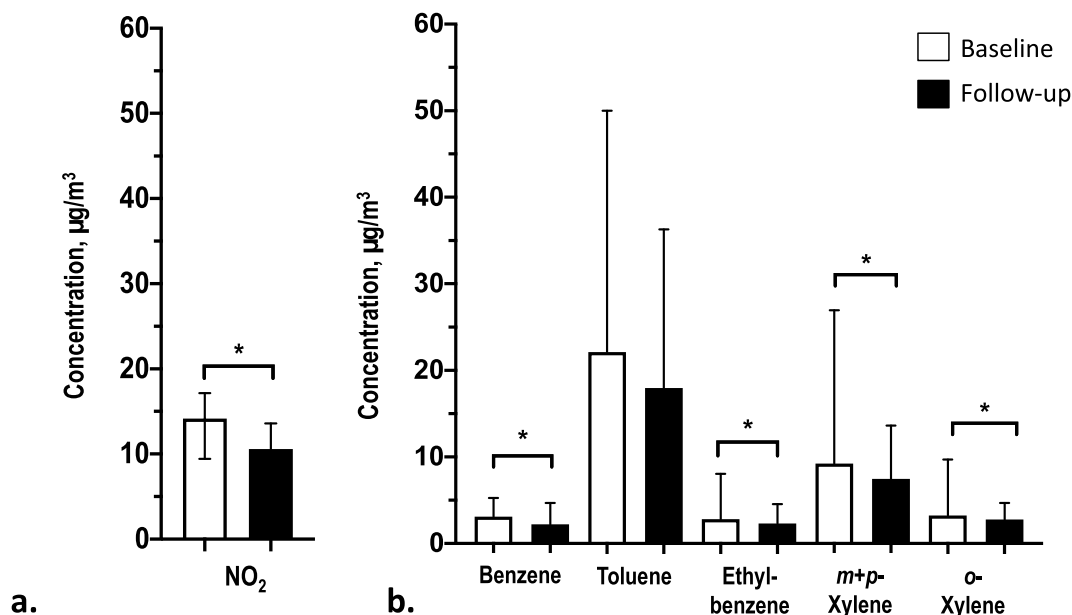
Fig. 1. a and b. Personal **(a.)** NO$_2$ and **(b.)** BTEX exposure concentrations (Median (IQR)) at baseline *vs.* 6-month follow-up for 61 women living in the Cape Town region. **a.)** **NO$_2$**: 14.2 (9.4–17.4) *vs.* 10.6 (6.6–13.6) μg/m^3, $p = 0.003$. **b.)** BTEX: **Benzene** 3.1 (2.1–5.3) *vs.* 2.2 (1.3–4.9) μg/m^3, $p = 0.045$; **Toluene** 22.1 (12.7–50.7) *vs.* 18.0 (10.3–36.7) μg/m^3, $p = 0.199$; **Ethyl-benzene** 2.8 (2.0–8.9) *vs.* 2.3 (1.5–4.6) μg/m^3, $p = 042$; *m* +*p*-Xylene 9.2 (6.3–29.6) *vs.* 7.5 (4.6–14.2) μg/m^3, $p = 0.019$; *o*-Xylene 3.2 (2.3–10.7) *vs.* 2.8 (1.7–4.7) μg/m^3, $p = 0.014$. *$p < 0.05$ for Baseline *vs.* Follow-up.

−10.0% difference in LTL (Table 3). After controlling for age, BMI, smoking, employment, level of education and assessment visit (baseline and follow-up visit) in the fully adjusted model, the effects of NO_2 and benzene on LTL significantly decreased. In the fully adjusted model each IQR increment in personal NO_2 and benzene exposure was associated with a −7.30% and −6.78% difference in LTL, respectively. In the fully adjusted models associating NO_2 and benzene with LTL, a 1-year increase in chronological age was associated with a −0.67% (95%CI -1.11 to −0.20; $p = 0.007$) and a −0.55% (95%CI -1.02 to −0.01; $p = 0.045$) difference in LTL, respectively. The magnitudes of 1 IQR increment increase in NO_2 and benzene concentrations therefore correspond to a 10.4-year and a 6.0-year increase in chronological age on the level of LTL. We did not observe significant associations between other BTEX exposure and LTL (Table 3).

In sensitivity analysis, the fully adjusted model (model B) was additionally adjusted for average temperature (Supplementary Table 3), for SBP and DBP (Supplementary Table 4), and alcohol consumption (Supplementary Table 5) respectively. Compared to the fully adjusted model, additional adjustment for temperature slightly increased the effect size of NO_2 on LTL from −7.30% to −8.17% while additional adjustment for alcohol consumption slightly increased the effect size of benzene on LTL from −6.78% to −7.73%. Also, additional adjustment of model B for a non-linear variable (age*age) appeared to have little effect compared to the fully adjusted model (Supplementary Table 6).

4. Discussion

In this study we evaluated NO_2 and BTEX exposure and LTL in a continuous way, and we expressed our effects of air pollutants on LTL for an IQR increment of exposure. Our findings show that personal exposure to NO_2 and benzene was negatively associated with LTL, a proxy for molecular ageing phenotype, in healthy women residing in the Cape Town region of South Africa. To our knowledge, the current study is the first from sub-Sahara Africa to investigate the effects of personal air pollution exposure on LTL (Miri et al., 2019). The findings contribute in a meaningful way to the general paucity of data on the health effects of air pollution in the sub-Saharan region (Katoto et al., 2019).

Our results may gain some further strength if exposure effects on LTL could be performed using a high vs. low or non-exposed population. However, because we have a rather low sample size to contrast our population in a high vs. low exposed group, we were not able to evaluated exposure effects in this way. Our findings, however support those of a study by Hoxha et al. (2009) who examined the effects of benzene and toluene exposure on LTL in a low exposed group of office workers (mean benzene: 13.0 µg/m³ and toluene: 43.4 µg/m³) and a high exposed group of traffic officers (mean benzene: 31.8 µg/m³ and toluene: 128.7 µg/m³). They showed a negative association between short-term personal traffic-related benzene exposure (−6.4%) and LTL. Hoxha et al. (2009) furthermore showed a negative association between toluene (−6.2%) exposure and LTL at higher (128.7 µg/m³) exposure concentrations compared to our observed concentrations (Fig. 1) (Hoxha et al., 2009). As observed in the current study, the effect of toluene on LTL was not observed in their low-exposure referents (Hoxha et al., 2009). These findings suggest that although toluene was not associated with LTL in the current study population, the effect may become more pronounced at higher toluene exposure concentrations. Our findings in terms of the effect of ageing on the level of LTL (−0.55% for each year increase in chronological age) are also in line with those observed by Hoxha et al. (2009) in their low-exposure referent population (0.5% for each year increase in chronological age) (Hoxha et al., 2009). The aging effect of benzene in LTL observed by Hoxha et al. (2009) translated into a > 12-year ageing effect on LTL in their highly-exposed study population for each IQR increment change in benzene (Hoxha et al., 2009), compared to 6 years in the current study.

The significant negative association between exposure concentrations and LTL in the present study are also consistent with previous studies that investigated the acute and chronic effects at lower exposure concentrations on TL (Martens and Nawrot, 2018). These studies include annual $PM_{2.5}$ concentrations in elderly participants (Pieters et al., 2016), proximity to traffic-related air pollution in twins (Bijnens et al., 2015), prenatal $PM_{2.5}$ exposure in newborns (Martens et al., 2017) and PAH exposure in students (Ling et al., 2016).

In contrast to our findings, several studies that investigated the effects of acute high-level exposure on TL (mostly occupational-related) reported positive associations. These studies include metal-rich PM exposure in steel workers (Dioni et al., 2011), high-level PM exposure in truck driver (Hou et al., 2012) and PAH in asphalt pavers (Xu et al., 2018). The negative associations reported in our study appear to be representative of observations made for chronic long-term exposure rather than acute high-level exposure. Although not fully understood, it has been proposed that at chronic lower exposure concentrations, the cumulative effects of chronic oxidative stress/damage may be more pronounced in a negative direction (Grahame and Schlesinger, 2012; Heath Effects Institute: Panel on the Health Effects of Traffic-Related Air Pollution., 2010; Weng, 2002). On the other hand, upregulation of leukocyte cell proliferation (clonal capacity) during acute inflammatory processes in highly short-term exposed cells/populations (as observed Dioni et al. and Hou et al.) may contribute to an increase in TL (Hodes et al., 2002; Weng et al., 1997). Since, we could not confirm associations between our exposure concentrations and inflammation (hsCRP) and LTL, these findings suggest exposure-associated oxidative damage or other routes of inflammation may have played a role in our findings. Investigation with a more integrative panel of markers for oxidative stress and inflammation should be performed in subsequent research. Other factors such as type of exposure, age, gender and socioeconomic differences between studies may also account for discrepancies between reports (Gardner et al., 2014; O'Neill et al., 2012; Oeseburg et al., 2010; World Health Organization: Regional Office for Europe., 2010).

The present study also has clinical and public health relevance as TL is regarded to be a surrogate marker of cellular aging (Müezzinler et al., 2013). TL is also considered a biosignature of the cumulative effects of oxidative stress and inflammation, and considered to be an intermediate marker of risk for various degenerative adverse health outcomes such as atherosclerosis and cancer (Haycock et al., 2014; Sanders and Newman, 2013; Wentzensen et al., 2011). The estimate effects of 1 IQR increment increase in NO_2 and benzene exposure equated to a chronological aging equivalent of more than 10 years and 6 years respectively on LTL in our study population. Our findings were observed at median NO_2 and median benzene exposure concentrations below WHO and South African recommended standards (annual mean: 40 µg/m³ and 5 µg/m³ respectively) (South African Western Cape Government., 2014; World Health Organization: Regional Office for Europe., 2010). These findings underscore the relevance of ambient NO_2 and benzene exposure as public health concerns despite the relative low exposure concentration observed in our study (World Health Organization: Regional Office for Europe., 2010).

Findings in our study are presented with some strengths and limitations. Personal exposure measurements are considered more accurate in linking ambient exposure and health outcomes (Koehler and Peters, 2015) and in combination with repeated measures taken in the same population may have contributed to significant findings despite a relative small study population. We did not account for possible background exposure. The inclusion of blank field samples should be considered in future studies. We furthermore did not conduct full blood count analyses; therefore the effects of air pollution exposure on leukocyte and platelet counts are not available. Previous studies have shown the importance of taking these parameters into account (Gutmajster et al., 2013; Mazidi et al., 2017) and should be included in future studies. The majority of our study population were current smokers. The high prevalence of smokers in similar South African study

populations has previously been shown by others (Matsha et al., 2012; Sitas et al., 2013). Using a biomarker for exposure to tobacco smoke, such as cotinine, would have been more accurate in correcting for the effects of active and passive smoking. Also, the inclusion of markers of oxidative stress such as urinary isoprostanes (Montuschi et al., 2004) could have provided a clearer understanding in terms of the role of oxidative stress in findings observed in the current study. In our study, the effects were observed in healthy women. Gender and socioeconomic differences in terms of LTL and air pollution-related health outcomes have previously been described in other populations (Clougherty, 2010; Gardner et al., 2014; Ward-Caviness et al., 2016). It therefore is important to note that the findings shown in the current study population may not be universally representative of all South African populations.

5. Conclusion

These findings show that current personal NO$_2$ and benzene exposure concentrations are associated with molecular aging as indicated by LTL in a cohort of apparently healthy women in the Cape Town region of South Africa and may contribute to future adverse health effects.

Funding information

Conflicts of interest

The authors declare no conflict of interest.

Acknowledgements

Appendix A. Supplementary data

Supplementary data to this article can be found online at https://doi.org/10.1016/j.envres.2019.108993.

Author contributions

Conceptualization, H.S., P.D.B., T.S.N. and N.G.; Methodology, H.S., P.D.B., T.S.N. and N.G; Validation, H.S., P.D.B., T.S.N., N.G, D.S.M., and F.E.; Formal analysis, F.E. D.S.M., H.S., P.D.B., T.S.N.; Investigation, F.E., M.M., I.W., N.M., S.C. and F.K.; Resources, H.S., P.D.B., T.S.N. and N.G.; Data curation, F.E., M.M., I.W., N.M., S.C. and F.K.; Writing—original draft preparation, F.E.; Writing—review and editing, F.E., H.S., P.D.B., T.S.N., N.G., D.S.M., M.M., I.W., N.M., S.C. and F.K.; Visualization, F.E.; Supervision, H.S., P.D.B., T.S.N. and N.G.; Project administration, H.S., P.D.B., T.S.N. and N.G.; Funding acquisition, H.S., P.D.B., T.S.N. and N.G.

References

Bijnens, E., Zeegers, M.P., Gielen, M., Kicinski, M., Hageman, G.J., Pachen, D., Derom, C., Vlietinck, R., Nawrot, T.S., 2015. Lower placental telomere length may be attributed to maternal residential traffic exposure; a twin study. Environ. Int. 79, 1–7. https://doi.org/10.1016/J.ENVINT.2015.02.008.

Bolden, A.L., Kwiatkowski, C.F., Colborn, T., 2015. New look at BTEX: are ambient levels a problem. Environ. Sci. Technol. 49, 5261–5276. https://doi.org/10.1021/es505316f.

Cherkas, L.F., Aviv, A., Valdes, A.M., Hunkin, J.L., Gardner, J.P., Surdulescu, G.L., Kimura, M., Spector, T.D., 2006. The effects of social status on biological aging as measured by white-blood-cell telomere length. Aging Cell 5, 361–365. https://doi.org/10.1111/j.1474-9726.2006.00222.x.

Clougherty, J.E., 2010. A growing role for gender analysis in air pollution epidemiology. Environ. Health Perspect. 118, 167–176. https://doi.org/10.1289/ehp.0900994.

De Prins, S., Koppen, G., Jacobs, G., Dons, E., Van de Mieroop, E., Nelen, V., Fierens, F., Int Panis, L., De Boever, P., Cox, B., Nawrot, T.S., Schoeters, G., 2013. Influence of ambient air pollution on global DNA methylation in healthy adults: a seasonal follow-up. Environ. Int. 59, 418–424. https://doi.org/10.1016/J.ENVINT.2013.07.007.

Desai, G., Chu, L., Guo, Y., Myneni, A.A., Mu, L., 2017. Biomarkers used in studying air pollution exposure during pregnancy and perinatal outcomes: a review. Biomark. Med. 22, 489–501. https://doi.org/10.1080/1354750X.2017.1339294.

Dioni, L., Hoxha, M., Nordio, F., Bonzini, M., Tarantini, L., Albetti, B., Savarese, A., Schwartz, J., Bertazzi, P.A., Apostoli, P., Hou, L., Baccarelli, A., 2011. Effects of short-term exposure to inhalable particulate matter on telomere length, telomerase expression, and telomerase methylation in steel workers. Environ. Health Perspect. 119, 622–627. https://doi.org/10.1289/ehp.1002486.

Everson, F., De Boever, P., Nawrot, T.S., Goswami, N., Mthethwa, M., Webster, I., Martens, D.S., Mashele, N., Charania, S., Kamau, F., Strijdom, H., 2019. Personal NO2 and volatile organic compounds exposure levels are associated with markers of cardiovascular risk in women in the Cape Town region of South Africa. Int. J. Environ. Res. Public Health 16, 2–18. https://doi.org/10.3390/ijerph16132284.

Fitzpatrick, A.L., Kronmal, R.A., Gardner, J.P., Psaty, B.M., Jenny, N.S., Tracy, R.P., Walston, J., Kimura, M., Aviv, A., 2007. Leukocyte telomere length and cardiovascular disease in the cardiovascular health study. Am. J. Epidemiol. 165, 14–21. https://doi.org/10.1093/aje/kwj346.

Gardner, M., Bann, D., Wiley, L., Cooper, R., Hardy, R., Nitsch, D., Martin-Ruiz, C., Shiels, P., Sayer, A.A., Barbieri, M., Bekaert, S., Bischoff, C., Brooks-Wilson, A., Chen, W., Cooper, C., Christensen, K., De Meyer, T., Deary, I., Der, G., Roux, A.D., Fitzpatrick, A., Hajat, A., Halaschek-Wiener, J., Harris, S., Hunt, S.C., Jagger, C., Jeon, H.-S., Kaplan, R., Kimura, M., Lansdorp, P., Li, C., Maeda, T., Mangino, M., Nawrot, T.S., Nilsson, P., Nordfjall, K., Paolisso, G., Ren, F., Riabowol, K., Robertson, T., Roos, G., Staessen, J.A., Spector, T., Tang, N., Unryn, B., van der Harst, P., Woo, J., Xing, C., Yadegarfar, M.E., Park, J.Y., Young, N., Kuh, D., von Zglinicki, T., Ben-Shlomo, Y., 2014. Gender and telomere length: systematic review and meta-analysis. Exp. Gerontol. 51, 15–27. https://doi.org/10.1016/j.exger.2013.12.004.

Grahame, T.J., Schlesinger, R.B., 2012. Oxidative stress-induced telomeric erosion as a mechanism underlying airborne particulate matter-related cardiovascular disease. Part. Fibre Toxicol. 9, 21–40. https://doi.org/10.1186/1743-8977-9-21.

Gutmajster, E., Witecka, J., Wyskida, M., Koscinska-Marczewska, J., Szwed, M., Owczarz, M., Mossakowska, M., Milewicz, A., Puzianowska-Kuznicka, M., Zejda, J., Wiecek, A., Chudek, J., Sieron, A.L., 2013. Telomere length in elderly caucasians weakly correlates with blood cell counts. Sci. World J. 2013, 1–8. https://doi.org/10.1155/2013/153608.

Haycock, P.C., Heydon, E.E., Kaptoge, S., Butterworth, A.S., Thompson, A., Willeit, P., 2014. Leucocyte telomere length and risk of cardiovascular disease: systematic review and meta-analysis. Bmj 349 https://doi.org/10.1136/bmj.g4227. g4227–g4227.

Hodes, R.J., Hathcock, K.S., Weng, N., 2002. Telomeres in T and B cells. Nat. Rev. Immunol. 2, 699–706. https://doi.org/10.1038/nri890.

Hou, L., Wang, S., Dou, C., Zhang, X., Yu, Y., Zheng, Y., Avula, U., Hoxha, M., Díaz, A., McCracken, J., Barretta, F., Marinelli, B., Bertazzi, P.A., Schwartz, J., Baccarelli, A.A., 2012. Air pollution exposure and telomere length in highly exposed subjects in Beijing, China: a repeated-measure study. Environ. Int. 48, 71–77. https://doi.org/10.1016/J.ENVINT.2012.06.020.

Hoxha, M., Dioni, L., Bonzini, M., Pesatori, A.C., Fustinoni, S., Cavallo, D., Carugno, M., Albetti, B., Marinelli, B., Schwartz, J., Bertazzi, P.A., Baccarelli, A., 2009. Association between leukocyte telomere shortening and exposure to traffic pollution: a cross-sectional study on traffic officers and indoor office workers. Environ. Health 8, 41. https://doi.org/10.1186/1476-069X-8-41.

Katoto, P.D.M.C., Byamungu, L., Brand, A.S., Mokaya, J., Strijdom, H., Goswami, N., De Boever, P., Nawrot, T.S., Nemery, B., 2019. Ambient air pollution and health in Sub-Saharan Africa: current evidence, perspectives and a call to action. Environ. Res. 173, 174–188. https://doi.org/10.1016/J.ENVRES.2019.03.029.

Klausbruckner, C., Annegarn, H., Henneman, L.R.F., Rafaj, P., 2016. A policy review of synergies and trade-offs in South African climate change mitigation and air pollution control strategies. Environ. Sci. Policy 57, 70–78. https://doi.org/10.1016/J.ENVSCI.2015.12.001.

Koehler, K.A., Peters, T.M., 2015. New methods for personal exposure monitoring for airborne particles. Curr. Environ. Heal. Reports 2, 399–411. https://doi.org/10.1007/s40572-015-0070-z.

Kuehn, B.M., 2014. WHO: more than 7 million air pollution deaths each year. J. Am. Med. Assoc. 311, 1486. https://doi.org/10.1001/jama.2014.4031.

Ling, X., Zhang, G., Chen, Q., Yang, H., Sun, L., Zhou, N., Wang, Z., Zou, P., Wang, X., Cui, Z., Liu, J., Ao, L., Cao, J., 2016. Shorter sperm telomere length in association with exposure to polycyclic aromatic hydrocarbons: results from the MARHCS cohort

study in Chongqing, China and in vivo animal experiments. Environ. Int. 95, 79–85. https://doi.org/10.1016/J.ENVINT.2016.08.001.

Martens, D.S., Nawrot, T.S., 2016. Air pollution stress and the aging phenotype: the telomere connection. Curr. Environ. Heal. Reports 3, 258–269. https://doi.org/10.1007/s40572-016-0098-8.

Martens, D.S., Nawrot, T.S., 2018. Ageing at the level of telomeres in association to residential landscape and air pollution at home and work: a review of the current evidence. Toxicol. Lett. 298, 42–52. https://doi.org/10.1016/J.TOXLET.2018.06.1213.

Martens, D.S., Plusquin, M., Gyselaers, W., De Vivo, I., Nawrot, T.S., 2016. Maternal pre-pregnancy body mass index and newborn telomere length. BMC Med. 14, 148. https://doi.org/10.1186/s12916-016-0689-0.

Martens, D.S., Cox, B., Janssen, B.G., Clemente, D.B.P., Gasparrini, A., Vanpoucke, C., Lefebvre, W., Roels, H.A., Plusquin, M., Nawrot, T.S., 2017. Prenatal air pollution and newborns' predisposition to accelerated biological aging. JAMA Pediatr 171, 1160–1167. https://doi.org/10.1001/jamapediatrics.2017.3024.

Matsha, T.E., Hassan, M.S., Kidd, M., Erasmus, R.T., 2012. The 30-year cardiovascular risk profile of South Africans with diagnosed diabetes, undiagnosed diabetes, pre-diabetes or normoglycaemia: the Bellville, South Africa pilot study. Cardiovasc. J. Afr. 23, 5–11. https://doi.org/10.5830/CVJA-2010-087.

Mazidi, M., Penson, P., Banach, M., 2017. Association between telomere length and complete blood count in US adults. Arch. Med. Sci. 13, 601–605. https://doi.org/10.5114/aoms.2017.67281.

McAlary, T., Groenevelt, H., Disher, S., Arnold, J., Seethapathy, S., Sacco, P., Crump, D., Schumacher, B., Hayes, H., Johnson, P., Górecki, T., 2015. Passive sampling for volatile organic compounds in indoor air-controlled laboratory comparison of four sampler types. Environ. Sci. Process. Impacts 17, 896–905. https://doi.org/10.1039/C4EM00560K.

Miri, M., Rostami Aghdam Shendi, M., Ghaffari, H.R., Ebrahimi Aval, H., Ahmadi, E., Taban, E., Gholizadeh, A., Yazdani Aval, M., Mohammadi, A., Azari, A., 2016. Investigation of outdoor BTEX: concentration, variations, sources, spatial distribution, and risk assessment. Chemosphere 163, 601–609. https://doi.org/10.1016/j.chemosphere.2016.07.088.

Miri, M., Nazarzadeh, M., Alahabadi, A., Ehrampoush, M.H., Rad, A., Lotfi, M.H., Sheikhha, M.H., Sakhvidi, M.J.Z., Nawrot, T.S., Dadvand, P., Hassan, M., Rad, A., Hassan, M., Hassan, M., Javad, M., Sakhvidi, Z., Nawrot, T.S., Ehrampoush, M.H., Rad, A., Lotfi, M.H., Sheikhha, M.H., Sakhvidi, M.J.Z., Nawrot, T.S., Dadvand, P., 2019. Air pollution and telomere length in adults: a systematic review and meta-analysis of observational studies. Environ. Pollut. 244, 636–647. https://doi.org/10.1016/j.envpol.2018.09.130.

Montuschi, P., Barnes, P.J., ROBERTS, L.J., Robersts, L.J., 2004. Isoprostanes: markers and mediators of oxidative stress. FASEB J. 18, 1791–1800. https://doi.org/10.1096/fj.04-2330rev.

Müezzinler, A., Zaineddin, A.K., Brenner, H., 2013. A systematic review of leukocyte telomere length and age in adults. Ageing Res. Rev. 12, 509–519. https://doi.org/10.1016/J.ARR.2013.01.003.

Oeseburg, H., De Boer, R.A., Van Gilst, W.H., Van Der Harst, P., 2010. Telomere biology in healthy aging and disease. Pflugers Arch. Eur. J. Physiol. 459, 259–268. https://doi.org/10.1007/s00424-009-0728-1.

O'Neill, M.S., Breton, C.V., Devlin, R.B., Utell, M.J., 2012. Air pollution and health: emerging information on susceptible populations. Air Qual. Atmos. Heal. 5, 189–201. https://doi.org/10.1007/s11869-011-0150-7.

O'Sullivan, R.J., Karlseder, J., 2010. Telomeres: protecting chromosomes against genome instability. Nat. Rev. Mol. Cell Biol. 11, 171–181. https://doi.org/10.1038/nrm2848.

Palmes, E.D., Gunnison, A.F., DiMattio, J., Tomczyk, C., 1976. Personal sampler for nitrogen dioxide. Am. Ind. Hyg. Assoc. J. 37, 570–577. https://doi.org/10.1080/0002889768507522.

Pegas, P.N., Alves, C.A., Evtyugina, M.G., Nunes, T., Cerqueira, M., Franchi, M., Pio, C.A., Almeida, S.M., Freitas, M.C., 2011. Indoor air quality in elementary schools of Lisbon in spring. Environ. Geochem. Health 33, 455–468. https://doi.org/10.1007/s10653-010-9345-3.

Pieters, N., Janssen, B.G., Dewitte, H., Cox, B., Cuypers, A., Lefebvre, W., Smeets, K., Vanpoucke, C., Plusquin, M., Nawrot, T.S., 2016. Biomolecular markers within the core axis of aging and particulate air pollution exposure in the elderly: a cross-sectional study. Environ. Health Perspect. 124, 943–950. https://doi.org/10.1289/ehp.1509728.

Ridker, P.M., 2016. From C-reactive protein to interleukin-6 to interleukin-1: moving upstream to identify novel targets for atheroprotection. Circ. Res. 118, 145–156. https://doi.org/10.1161/CIRCRESAHA.115.306656.

Sanders, J.L., Newman, A.B., 2013. Telomere length in epidemiology: a biomarker of aging, age-related disease, both, or neither? Epidemiol. Rev. 35, 112–131. https://doi.org/10.1093/epirev/mxs008.

Seedat, Y.K., Rayner, B.L., 2013. The abridged South African hypertension guideline

2011. S. Afr. Fam. Pract. 55, 111–116. https://doi.org/10.1080/20786204.2013.10874319.

Sitas, F., Egger, S., Bradshaw, D., Groenewald, P., Laubscher, R., Kielkowski, D., Peto, R., 2013. Differences among the coloured, white, black, and other South African populations in smoking-attributed mortality at ages 35-74 years: a case-control study of 481,640 deaths. Lancet (London, England) 382, 685–693. https://doi.org/10.1016/S0140-6736(13)61610-4.

South African Department of Environmental Affairs, 2007. Long Term Mitigation Scenarios Strategic Options for South Africa. [WWW Document]. Dep. Environ. Aff. Tour. Report (accessed 3.8.2019). https://open.uct.ac.za/bitstream/handle/11427/16804/Scenario_Building_Team_Long_Term_Mitigation_2007.pdf?sequence=1&isAllowed=y.

South African Western Cape Government, 2014. Western Cape State of Air Quality Management Report : 2013. [WWW Document]. (accessed 7.1.2019). https://www.westerncape.gov.za/eadp/files/atoms/files/SoAR_2014.pdf.

Strijdom, H., De Boever, P., Walzl, G., Essop, M.F., Nawrot, T.S., Webster, I., Westcott, C., Mashele, N., Everson, F., Malherbe, S.T., Stanley, K., Kessler, H.H., Stelzl, E., Goswami, N., 2017. Cardiovascular risk and endothelial function in people living with HIV/AIDS: design of the multi-site, longitudinal EndoAfrica study in the Western Cape Province of South Africa. BMC Infect. Dis. 17, 1–9. https://doi.org/10.1186/s12879-016-2158-y.

Targa, J., Loader, A., 2008. Diffusion Tubes for Ambient NO2 Monitoring: Practical Guidance for Laboratories and Users. [WWW Document]. Rep. to Defra Devolved Adm. Harwell (accessed 3.11.2019). https://uk-air.defra.gov.uk/assets/documents/reports/cat05/0802141004_NO2_WG_PracticalGuidance_Issue1a.pdf.

Valdes, A., Andrew, T., Gardner, J., Kimura, M., Oelsner, E., Cherkas, L., Aviv, A., Spector, T., 2005. Obesity, cigarette smoking, and telomere length in women. Lancet 366, 662–664. https://doi.org/10.1016/S0140-6736(05)66630-5.

Wang, L., Liu, C., Meng, X., Niu, Y., Lin, Z., Liu, Y., Liu, J., Qi, J., You, J., Tse, L.A., Chen, J., Zhou, M., Chen, R., Yin, P., Kan, H., 2018. Associations between short-term exposure to ambient sulfur dioxide and increased cause-specific mortality in 272 Chinese cities. Environ. Int. 117, 33–39. https://doi.org/10.1016/j.envint.2018.04.019.

Ward-Caviness, C.K., Nwanaji-Enwerem, J.C., Wolf, K., Wahl, S., Colicino, E., Trevisi, L., Kloog, I., Just, A.C., Vokonas, P., Cyrys, J., Gieger, C., Schwartz, J., Baccarelli, A.A., Schneider, A., Peters, A., 2016. Long-term exposure to air pollution is associated with biological aging. Oncotarget 7, 74510–74525. https://doi.org/10.18632/oncotarget.12903.

Weng, N., 2002. Regulation of telomerase expression in human lymphocytes. Springer Semin. Immunopathol. 24, 23–33. https://doi.org/10.1007/s00281-001-0093-4.

Weng, N.P., Granger, L., Hodes, R.J., 1997. Telomere lengthening and telomerase activation during human B cell differentiation. Proc. Natl. Acad. Sci. U.S.A. 94, 10827–10832. https://doi.org/10.1073/PNAS.94.20.10827.

Wentzensen, I.M., Mirabello, L., Pfeiffer, R.M., Savage, S.A., 2011. The association of telomere length and cancer: a meta-analysis. Cancer Epidemiol. Biomark. Prev. 20, 1238–1250. https://doi.org/10.1158/1055-9965.EPI-11-0005.

World Health Organization: Regional Office for Europe, 2010. WHO Guidelines for Indoor Air Quality: Selected Pollutants. World Heal. Organ. https://doi.org/10.1186/2041-1480-2-S2-I1. [WWW Document].

World Health Organization, 2016. World Health Statistics - Monitoring Health for the Sustainable Development Goals. [WWW Document]. World Heal. Organ (accessed 5.8.2019). https://www.who.int/gho/publications/world_health_statistics/2019/en/.

World Health Organization, 2018. World Health Organization releases new global air pollution data. [WWW Document]. World Heal. Organ (accessed 3.8.2019). http://ccacoalition.org/en/news/world-health-organization-releases-new-global-air-pollution-data.

World Health Organization Expert Committee on Physical Status, 1995. Physical Status: the Use and Interpretation of Anthropometry. [WWW Document]. (accessed 4.9.2019). http://www.who.int/childgrowth/publications/physical_status/en/.

Xu, Y., Lindh, C.H., Jönsson, B.A.G., Broberg, K., Albin, M., 2018. Occupational exposure to asphalt mixture during road paving is related to increased mitochondria DNA copy number: a cross-sectional study. Environ. Health 17, 29–39. https://doi.org/10.1186/s12940-018-0375-0.

Zglinicki, T. Von, Saretzki, G., Ladhoff, J., Fagagna, F.D.A.D., d'Adda di, Jackson, S.P.P., 2005. Human cell senescence as a DNA damage response. Mech. Ageing Dev. 126, 111–117. https://doi.org/10.1016/j.mad.2004.09.034.

Zhao, B., Vo, H.Q., Johnston, F.H., Negishi, K., 2018. Air pollution and telomere length: a systematic review of 12,058 subjects. Cardiovasc. Diagn. Ther. 8, 480–492. https://doi.org/10.21037/cdt.2018.06.05.

Łatka, P., Nowakowska, D., Nowomiejska, K., Rejdak, R., 2018. How air pollution affects the eyes — a review. Ophthalmol. Times J. 3, 58–62. https://doi.org/10.5603/oj.2018.0032.

International Journal of
Environmental Research and Public Health

MDPI

Article

Personal NO$_2$ and Volatile Organic Compounds Exposure Levels are Associated with Markers of Cardiovascular Risk in Women in the Cape Town Region of South Africa

Frans Everson [1], **Patrick De Boever** [2,3,*], **Tim S. Nawrot** [3], **Nandu Goswami** [4], **Mashudu Mthethwa** [1], **Ingrid Webster** [1], **Dries S. Martens** [3], **Nyiko Mashele** [1], **Sana Charania** [1], **Festus Kamau** [1] **and Hans Strijdom** [1]

[1] Division of Medical Physiology, Faculty of Medicine and Health Sciences, Stellenbosch University, P.O. Box 241, Cape Town 8000, South Africa
[2] Health Unit, Flemish Institute for Technological Research (VITO), 2400 Mol, Belgium
[3] Centre for Environmental Sciences, Hasselt University, 3590 Diepenbeek, Belgium
[4] Division of Physiology, Otto Loewi Research Center of Vascular Biology, Immunity and Inflammation, Medical University of Graz, 8036 Graz, Austria
[*] Correspondence: patrick.deboever@vito.be; Tel.: +32-14-335145

check for updates

Abstract: Exposure to ambient NO$_2$ and benzene, toluene ethyl-benzene and m+p- and o-xylenes (BTEX) is associated with adverse cardiovascular effects, but limited information is available on the effects of personal exposure to these compounds in South African populations. This 6-month follow-up study aims to determine 7-day personal ambient NO$_2$ and BTEX exposure levels via compact passive diffusion samplers in female participants from Cape Town, and investigate whether exposure levels are associated with cardiovascular risk markers. Overall, the measured air pollutant exposure levels were lower compared to international standards. NO$_2$ was positively associated with systolic and diastolic blood pressure (SBP and DBP), and inversely associated with the central retinal venular equivalent (CRVE) and mean baseline brachial artery diameter. o-xylene was associated with DBP and benzene was strongly associated with carotid intima media thickness (cIMT). Our findings showed that personal air pollution exposure, even at relatively low levels, was associated with several markers of cardiovascular risk in women residing in the Cape Town region.

Keywords: air pollution; nitrogen dioxide; BTEX; cardiovascular risk; South Africa

1. Introduction

Ambient air pollution is a global health concern and is associated with numerous adverse health effects including cardiovascular disease (CVD) [1–3]. The health effects of ambient air pollution are mostly attributable to small particles and chemically reactive compounds with pro-oxidative potential [4–7]. Previous reports have suggested that the adverse cardiovascular effects associated with air pollution exposure may be due to autonomic nervous system dysregulation of vascular tone and heart rates [8,9], and pro-atherosclerotic processes such as oxidative stress, inflammation, and endothelial dysfunction [9–11]. Although several chemical components present in ambient air have been implicated in adverse cardiovascular outcomes (e.g., nitrogen and carbon oxides, and particulate matter (PM)), the specific contributions and underlying mechanisms of exposure to individual components are not well understood [1,12,13].

The World Health Organization (WHO) has identified gaseous pollutants such as NO_2 and PM with a diameter of ≤ 2.5 μm ($PM_{2.5}$) as the air pollutants that are most dangerous to public health [14]. Other gaseous pollutants in ambient air include polycyclic aromatic hydrocarbons (PAHs) such as benzene, toluene ethyl-benzene and m+p- and o-xylenes (BTEX) [15–18]. These gaseous pollutions are mostly produced as a result of the incomplete combustion of fossil fuels during industrial, vehicle, and household activities and are therefore considered a good proxy for general air quality and combustion-related emissions [15–18]. Due to their small molecular size (molecular diameter: <0.1 nm), these ambient air pollutants are able to passively enter the blood circulation during respiration (predominant route of exposure) and disseminate throughout the body, even at the cellular and nuclear levels where they can exert their harmful effects [1,7,19].

Reports on air pollution levels and related health effects are mostly based on data from the developed world, while the situation in developing countries remains under-reported [20–23]. A recently published systematic review by Katoto et al. (2019) highlighted the lack of air pollution data from the sub-Saharan Africa (SSA) region [23]. The authors identified only 23 published research articles from SSA (of which 14 were from South Africa) that reported on the health effects associated with ambient air pollution. It is evident, however, that data from personal quantitative exposure measurements are under-reported, and none of these studies investigated the effects of air pollution on vascular health and function. The review furthermore reported on studies demonstrating urban air pollution levels of up to 10–20 times greater than recommended WHO standards in some SSA locations [23]. In light of these findings and knowledge gaps, the overarching aims of the current study were to: (1) determine current levels of personal NO_2 and BTEX exposure during two 1-week time periods in a repeated-measurements study (6-month follow-up) of apparently healthy women residing in the Cape Town region of South Africa, and (2) determine whether current levels of personal NO_2 and BTEX exposure are associated with markers of cardiovascular risk, including blood pressure (systolic blood pressure (SBP) and diastolic blood pressure (DBP), respectively), flow-mediated vasodilatation (FMD), retinal blood vessel widths, and carotid intima media thickness (cIMT).

2. Materials and Methods

2.1. Study Ethics, Design, and Population

The current study formed part of a larger parent study called EndoAfrica and participants for the current study were recruited from the healthy control study group of the parent study [24]. Ethical clearance for the current study was obtained from the Health Research Ethics Committee of Stellenbosch University (ethics reference number: S16/07/114), which subscribes to the principles of the Helsinki Declaration (1975). The study followed a non-interventional, longitudinal (6-month follow-up) cohort design. Healthy volunteering female participants of mixed ancestry were randomLy recruited for the first assessment visit (baseline) from September 2016 to August 2017 at primary health care clinics in the Cape Town region. All participants were from the residential areas of Elsies River, Bishop Lavis, and Ravensmead. All 6-month assessment visits (follow-up) were completed by February 2018. Qualified research nurses recruited, screened, and obtained informed consent from all participants. Participants who were <18 years of age, with human immunodeficiency virus/acquired immunodeficiency syndrome (HIV/AIDS; confirmed with a rapid HIV test; SD Bioline HIV 1/2 3.0 immunochromatographic test kit; Standard Diagnostics, Republic of Korea), with current tuberculosis (confirmed from participant clinic files), pregnant (confirmed with a pregnancy test), <3 months post-partum, of poor health, or with a current or previous history of heart disease were excluded.

2.2. Air Quality and Temperature Monitoring

Each participant was equipped with a Gradko rapid NO_2 device (Gradko International Ltd., Winchester, UK), a Radiello[TM] BTEX passive diffusion sampler (Sigma-Aldrich Inc., MO, USA), and an ACR SmartButton® temperature logger (ACR Systems Inc., Surrey, B.C., Canada) placed in the

Int. J. Environ. Res. Public Health **2019**, 16, 2284

3 of 18

external mesh pocket of a backpack (Figure A1a–d). The mesh pocket allowed for unrestricted continuous contact with ambient indoor and outdoor temperature and air (Figure A1e). Although previous studies have measured personal sampling within a 30 cm hemisphere from the face [25,26], personal exposure for the current study was measured within a hemisphere of 50 to 60 cm from the face (Figure A1f). Participants carried the backpack at all times (except during periods of sleep and bathroom use when the backpack was placed next to their beds) for a 7-day period. Temperature was recorded continuously at 30-minute intervals while the NO_2 and BTEX samplers allowed for continuous passive diffusion and accumulation of NO_2 and BTEX. Following continuous 7-day measurements, participants returned for the first assessment visit, during which the backpacks were collected, data were extracted from the temperature loggers via ACR TrendReader® software (ACR Systems Inc., Surrey, B.C., Canada), and the average temperature (°C) for the 7-day period was recorded. Once collected, the NO_2 and BTEX samplers were sealed, stored at 4 °C and sent for quantification according to the manufacturer's protocol.

NO_2 samplers were sent to Gradko International Ltd. laboratories (United Kingdom Accreditation Services (UKAS) accredited)) for quantification according to UKAS method GLM 7 [27]. A calibration curve (blank with only deionized water, 15, 30, 60, 90 120 μg/mL) was prepared from a standard nitrate solution (1 g/L nitrite ion (NO_2^-)). The color reagent was prepared as previously described [28] and used in a sample:sulphanilamide solution:N-1 (naphthyl-1) ethylene diamine dihydrochloride solution (NEDD) ratio of 1:2:2 (0.003 g NEDD per 1 g sulphanilamide). After sample elution (preparation: 20 % triethanolamine (TEA) solution/80% deionized water), NO_2 concentrations were determined via chemiluminescence ultraviolet (UV) spectrophotometry (UVS04 Camspec M550; Spectronic Camspec Ltd., Leeds, UK). Calibration standards and linearity checks were used to calibrate the spectrophotometer, and mid-range and zero standards were analyzed at intervals throughout the sequence for quality assurance. The calibration curve was used to calculate the NO_2^- concentration for each sample. The ambient NO_2 concentration was calculated from NO_2^- concentrations and expressed as $\mu g/m^3$ [29].

BTEX samplers were sent to the Flemish Institute for Technology and Research (VITO; Mol, Belgium) for quantification as previously described [30,31]. BTEX samples were extracted from exposed samplers by means of elution in the Radiello™ glass tube containing the cartridge (2 mL carbon disulphide (CS_2; Sigma-Aldrich, MO, USA) and 12.5 μL 2-fluorotoluene internal standard (Sigma-Aldrich, MO, USA)). The tube was stirred for 30 minutes on a rotational shaker. BTEX quantification was performed by means of gas chromatography (Thermo Trace) and a mass spectrometer (Thermo DSQ II with helium as carries gas (a constant flow of 1 mL/min)). A cross-bond diphenyl/dimethylpolysiloxane column (RTX 502.2; 0.25 mm by 30 m) with a 1.4 μm-thick film was used for sample separation (temperature program: 35 °C for 5 minutes, 14 °C/minute increment until 245 °C). Equipment calibration was performed by injecting the standard solution (benzene, ethyl-benzene, toluene, m-xylene, p-xylene, and o-xylene in CS_2 (Sigma-Aldrich, MO, USA)) at 0.03 to 30 μg/g before analysis. Sample concentrations were calculated from chromatograms using a standard curve. The limit of detection (LOD) was calculated as 3.3 (standard deviation (SD) of areas/slope). Samples with conc. <LOD were not presented. Results were expressed as average NO_2 and BTEX exposure concentration ($\mu g/m^3$) for the 7-day measuring period. The same procedure was followed for the 6-month follow-up visits.

2.3. Study Endpoints

2.3.1. Health Questionnaire and Anthropometric Measurements

At each visit, participants completed a comprehensive questionnaire to collect data on age, smoking status (defined as smoking or non-smoking), socioeconomic information (including employment status defined as either unemployed, part-time employed, or full-time employed), and lifestyle (hours of sleep at night defined as 1 to 3 hours, between 3 and 6 hours, 6 to 9 hours, and >9 hours). Qualified research

nurses measured fasting blood glucose levels (mmol/L) by finger prick (Gluco Plus[TM], Cipla DIBCARE, Bellville, South Africa) and collected fasting blood and mid-stream urine samples. Cardiovascular measurements included SBP and DBP (calculated as an average of 3 measurements at 5-minute intervals on the left arm and expressed in mmHg) via an Omron M6 automatic digital blood pressure monitor (Omron Healthcare, Kyoto, Japan). Hypertension was defined as either SBP of ≥140 mmHg or DBP of ≥90 mmHg, based on the South African Hypertension Society guidelines [32]. Body mass (kg) was determined on an electronic scale, and height (cm) was decided by means of a stadiometer. Finally, body-mass index (BMI) was expressed as kg body weight/m^2 height.

2.3.2. Biochemical Analysis

Fasting whole blood was collected in blood collection tubes (SGVac, The Scientific Group (Pty) Ltd.; Milnerton, Western Cape, SA). Serum was extracted from whole blood samples and stored at −80 °C. Serum samples were analyzed by the South African National Health Laboratory Service (NHLS; Tygerberg Hospital, Cape Town, South Africa), a South African National Accreditation System (SANAS)-accredited laboratory, for high-sensitivity C-reactive protein (hsCRP) levels by means of an IMMAGE® Immunochemistry Systems and Calibrator 5 Plus assay kit (Beckman Coulter, Inc., CA, USA). This specific chemiluminescence analysis was based on the highly sensitive Near Infrared Particle Immunoassay rate methodology where anti-CRP antibody-coated particles bind to the CRP in the serum sample resulting in an insoluble aggregate formation and turbidity. Samples were prepared for analysis by adding 4.5 µL serum sample, 42 µL antibody-coated particles (particle-bound goat and mouse anti-CRP antibody), 125 µL buffer 4 and 42 µL diluent (sodium azide: <0.1% (*w/w*)). The hsCRP concentration was determined automatically as the rate of aggregate formation (directly proportional). For the purposes of this study, increased hsCRP was defined as hsCRP levels of >3 mg/L based on previous reports suggesting that hsCRP levels above this cut-off value are associated with increased cardiovascular risk [33].

Mid-stream urine samples were obtained at each visit, placed on ice and immediately delivered to the NHLS for the quantification of urinary creatinine levels by means of chemiluminescence (cobas®-c analyzer and CREP2 kit; Roche Diagnostics, Basel, Switzerland). The principal of the method was based on the enzymatic formation of hydrogen peroxide (catalyzed by peroxidase) that reacted with 2,4,6-triiodo-3-hydroxybenzoic acid for quinone imine chromogen. Creatinine levels were determined by the color intensity of the quinone imine chromogen (directly proportional).

2.3.3. Urinary Analysis of Metabolites of Volatile Organic Compounds

Additional mid-stream urine samples were stored at −80 °C and sent to VITO (Mol, Belgium) for level determinations of the following urinary metabolites: N-acetyl-S-(3-hydroxypropyl)-L-cysteine (HPMA; a marker of acrolein exposure [34]), N-acetyl-s-(phenyl)-L-cysteine (PMA; a marker of benzene exposure [35]), N-acetyl-s-(benzyl)-L-cysteine (BMA; a marker of toluene exposure [36]), trans,trans-muconic acid (MU; a marker of benzene exposure [35]), and 3+4-methylhippuric acid (3+4MHA; a marker of o-, m-, and p-xylene exposure [37]). Samples were prepared using 10 µL urine, 25 µL mixed internal standard (2000 ng/mL in methanol:water(1:1, *v:v*)) MU-d4 and 3 (Santa Cruz Biotechnology, TX, USA), and 4 MHA-d7 (Toronto research chemicals Inc., ON, Canada) with 465 µL 1% acetic acid (HAc; Merck, NJ, USA). A matrix-matched calibration curve was applied for the quantification of HPMA, BMA, and PMA to compensate for the matrix effect. To achieve this, spiked urine samples were used containing 10 µL urine, 25 µL mixed internal standard (MU-d4 and 2,3 and 4 MHA-d7: 2000 ng/mL, 20 µL low and high spiked standards (low spike: HPMA, 37.5 ng/mL; PMA, 0.25 ng/mL; MU 5.0 ng/mL, BMA, 1.25 ng/mL; 3+4MHA, 20.0 ng/mL; and high spike: HPMA, 75.0 ng/mL PMA, 0.5 ng/mL; MU, 10.0 ng/mL; BMA, 2.5 ng/mL; 3+4MHA, 40.0 ng/mL (Toronto research chemicals Inc., ON, Canada)) and 445 µL 1% HAc in ultra-pure water.

Twenty microliters of each sample was injected in an ultra-performance liquid chromatography (UPLS; Waters I-class Acquity UPLC system, Milford, MA, USA)/mass spectrometry (MS; Waters Xevo

TQ-S tandem in the negative electrospray ionization mode (ESI$^-$)). An Acquity UPLC$^\circledR$ high-strength silica T3 column (50 mm × 2.1 mm; 1.8 μm; at a constant temperature of 40 °C) with UV detection (Photodiode array (PDA) detector set at 259 nm) was used for the simultaneous quantification of the urinary metabolites [38]. Retained compounds were eluted with 4 mL HAc solution (10%, *v:v*). Levels of metabolites were calculated based on the corresponding matrix-matched calibration curve.

2.3.4. Assessment of Endothelial Function, Carotid Intima Media Thickness, and Retinal Microvascular Caliber

Vascular endothelial function was assessed via FMD of the right brachial artery, 3–4 cm proximal to the elbow. FMD was measured in the supine position with a mobile Esaote MyLab^{TM} Five portable ultrasound device (Genoa, Italy) with an Esaote Doppler probe (LA523, 12 MHz) connected to computerized software with edge detection technology (Quipu Cardiovascular Suite™; Pisa, Italy) as previously described [24,39]. Briefly, the computerized software determined the mean baseline brachial artery lumen diameter (mm) over a 60-second period, followed by a 5-minute ischaemic occlusion (inflation of a manual blood pressure cuff on the forearm to 50 mmHg supra-systolic pressure). Following the 5-minute ischaemic occlusion, deflating the blood pressure cuff triggered reactive hyperaemia and the maximum brachial artery lumen diameter (μm) was recorded during this period. The maximum lumen diameter displacement during reactive hyperaemia from the mean baseline measurements was expressed as the percentage of the mean baseline brachial lumen diameter (% FMD).

The cIMTs of the left and right carotid arteries were determined by B-mode ultrasonography as previously described [40,41]. cIMT measurements were performed in the supine position with the head tilted in a 45° angle upwards. The diameter of carotid intima was determined using an Esaote MyLab^{TM} Five portable ultrasound device (Genova, Italy) and a B-linear-mode Esaote Doppler probe (LA523, 12 MHz, Genoa, Italy) connected to computerized software (RF-QIMT software, Genova, Italy) specific for the determination of carotid metrics. Measurements were taken 5 mm proximal to the dilation of the carotid bulb. The mean of the left and right carotid diameter and mean of the left and right cIMT were calculated and used for statistical analysis.

Additionally, retinal images were captured with a Canon CR2 digital camera (Canon Europa NV, The Netherlands) and analyzed with semi-automated software (MONA REVA 2.1.1 developed at VITO; https://mona.health) by trained investigators using a standardized protocol as previously described [24]. Briefly, the central retinal arteriolar equivalent (CRAE) of the 6 largest arterioles and the central retinal venular equivalent (CRVE) of the 6 largest venules were determined in the area between 0.5 and 1 disc diameter from the optic disc margin and also expressed as a CRAE/CRVE ratio (AVR). The calculations of the vessel metrics were based on the revised Parr-Hubbard formulas as reported previously [42].

2.4. Statistical Analysis

All statistical analyses were performed with IBM$^\circledR$ SPSS$^\circledR$ software (version 25; New York, NY, USA). Depending on data distribution, a paired sample Student's *t*-test (parametric) or Wilcoxon signed-rank test (non-parametric) was used to identify significant differences between baseline and follow-up visits. A Spearman's Rho correlation (nonparametric data) was used to identify correlations between variables. To determine the association between NO$_2$ or individual BTEX compounds or total BTEX (a summation of all individual BTEX compounds for each participant as a proxy for combined effect of BTEX) and different cardiovascular outcomes, a linear mixed model (LMM) regression analysis was used with participants nested in each visit. Variables with skewed data distribution (BTEX and total BTEX) were log-transformed for regression analysis. To evaluate personal air pollution effects on cardiovascular outcomes independent of potential confounding effects, we selected a priori covariates that are known determinants for cardiovascular outcomes and variables with a potential link with personal air pollution exposure and cardiovascular outcomes. These include age, BMI,

Int. J. Environ. Res. Public Health **2019**, 16, 2284

6 of 18

smoking, socio-economic status (reflected by employment), sleep, and ambient temperature [43–47]. For estimated effects on SBP and DBP, the statistical model included NO_2 or BTEX or total BTEX as an exposure variable, participants at each time point as a random effects factor variable with random intercept to account for possible inter-individual variation while adjusting for age, BMI, date of assessment visit, and average temperature as continuous fixed effects and smoking status, employment status, and hours of sleep at night as fixed categorical variables. For effects on other vascular outcomes, we additionally adjusted LMMs for SBP. To determine estimated effects on % FMD and cIMT, the mean brachial diameter and carotid diameter were additionally adjusted for, respectively. Q-Q plots of the residuals were used to test the assumptions of linearity. The significance threshold was set at $p < 0.05$ for all statistical analysis.

3. Results

3.1. Baseline Population Characteristics

A total number of 77 female participants were recruited for the study. Sixteen participants who completed their baseline visits did not consent to continue with the 6-month follow-up visit and were excluded from the study. A total number of 61 healthy female participants (mean ± SD age at baseline: 42.5 ± 13.4 years) of mixed ancestry completed both assessment visits (Table 1).

The majority of participants were current smokers (69%; smoking frequency, <20 cigarettes/day), but none reported any history of heart or other current serious health problems. Participants were mostly unemployed (49%). Most participants were overweight with a mean ± SD BMI of 27.7 ± 8.4 kg/m². Most participants ($n = 37$; 61%) reported that they sleep 6 to 9 hours per night. The mean ± SD SBP and DBP values (SBP: 122.5 ± 19.9) mmHg, and DBP: 84.2 ± 12.0 mmHg) were within the normal range (Table 2). In total, 11 participants (18%) presented with hypertension (either SBP of ≥140 mmHg or DBP of ≥90 mmHg) at baseline. The median hsCRP level was above the 3 mg/L cut-off value, and the majority of participants ($n = 35$; 61%) exhibited elevated hsCRP levels.

Table 1. Baseline study population characteristics ($n = 61$).

Variable	Baseline
Age (years)	42.5 ± 13.4
Smoking status	
Current smoker (n)	42 (69%)
Employment	
Unemployed (n)	30 (49%)
Part-time (n)	25 (41%)
Full-time (n)	6 (10%)
Hours of sleep per night	
<3 h (n)	1 (2%)
3 to ≤6 h (n)	7 (12%)
6 to ≤9 h (n)	37 (61%)
>9 h (n)	16 (25%)
BMI, kg/m³ (n)	27.7 ± 8.4
High-sensitivity C-reactive protein (mg/L) [a, b]	6.3 (0.2 to 37.1)
Elevated hsCRP (>3 mg/L)	
Yes (n)	35 (61%)
No (n)	22 (39%)
Urine creatinine (mmol/L)	13.5 ± 7.1

Data presented as mean ± SD or n (%); [a] data presented as median (range); [b] sample size: $n = 57$.

Int. J. Environ. Res. Public Health **2019**, *16*, 2284

7 of 18

Table 2. Baseline cardiovascular parameters (*n* = 61).

Variable	Baseline
Blood pressure	
Systolic blood pressure (SBP); mmHg)	122.5 ± 19.9
Diastolic blood pressure (DBP; mmHg)	84.15 ± 12.0
Hypertension	
(Either SBP of >140 mmHg or DBP of >90 mmHg)	
Yes, *n*	15 (25%)
No, *n*	46 (75%)
Flow-mediated vasodilatation [a]	
Brachial diameter (mm)	3.22 ± 0.69
% Flow-mediated Dilatation (% FMD) [b]	5.21 (−7.93 to 23.50)
Retinal caliber [c]	
Central retinal arteriolar equivalent (CRAE; μm)	157.9 ± 16.4
Central retinal venular equivalent (CRVE; μm)	238.4 ± 20.1
CRAE/CRVE ratio (AVR)	0.66 ± 0.06
Carotid artery	
Carotid diameter (mm)	7.16 ± 0.84
Carotid intima media thickness (cIMT; μm)	657.2 ± 159.3

Data presented as mean ± SD or *n* (%); [a] sample size: *n* = 60; [b] data presented as median (range); [c] sample size: *n* = 58.

3.2. Personal Ambient Exposure Variable Outcomes and Urinary Metabolites

The mean NO_2 and median benzene, ethyl-benzene, m+p-xylene, and o-xylene levels were significantly higher at the baseline visit compared to at the follow-up visit (Table 3). Personal toluene exposure accounted for ~50% of the total BTEX exposure level at baseline and follow-up visits, while benzene exposure was the lowest at both baseline and follow-up visits. The mean temperature did not differ between baseline and follow-up (Table 3). Strong positive correlations were observed between all personal exposure concentrations ($p < 0.001$) (Table A1). No significant differences in urinary metabolites were observed between baseline and follow-up visits.

Table 3. Air pollution characteristics at baseline and 6-month follow-up (*n* = 61).

Variable	Baseline	Follow-Up
Temperature [a, b] (°C)	21.6 ± 3.2	21.9 ± 2.7
Personal air pollution measurements		
NO_2 [a, c] (μg/m^3)	13.6 ± 4.8	10.6 ± 4.7 **
Total BTEX [c, d] (μg/m^3)	43.0 (12.0 to 327.7)	34.31 (7.1 to 405.1)
Benzene [c] (μg/m^3)	3.9 (0.7 to 14.2)	2.2 (0.5 to 9.3) *
Toluene [c] (μg/m^3)	22.1 (5.6 to 189.2)	18.0 (3.7 to 284.1)
Ethyl-benzene [c] (μg/m^3)	2.8 (1.1 to 34.4)	2.3 (0.7 to 21.4) *
m+p-xylene [c] (μg/m^3)	9.2 (3.4 to 117.4)	7.5 (2.0 to 74.8) *
o-xylene [c] (μg/m^3)	3.2 (1.2 to 43.8)	2.7 (0.7 to 24.7) *
Urinary metabolites [e]		
HPMA [f] (ng/mL)	1686 (92 to 12,793)	1812 (120 to 12,613)
PMA [g] (ng/mL)	0.05 (0.05 to 0.34)	0.05 (0.05 to 0.34)
MU [h] (ng/mL)	62.5 (62.5 to 498.0)	62.5 (62.5 to 595.0)
BMA [i] (ng/mL)	14.7 (2.5 to 588.0)	14.3 (2.5 to 699.0)
3+4MHA [j] (ng/mL)	1061 (31.8 to 9512.0)	845 (50.0 to 32,078.0)

Data presented as median (range) or [a] mean ± SD; [b] the mean represents the average 7-day recorded temperatures (30-minute interval temperature recordings) for each participant prior to the assessment visit, *n* = 60. [c] Values reflect the mean 7-day average during the 7-day period prior to the assessment visit, *n* = 56 to 61. [d] Values represent the mean values of the sum of individual BTEX measurements for each participant as a proxy for total BTEX exposure. [e] Values of samples below limit of detection (LOD) were replaced by LOD/2. [f] Samples concentrations above LOD (>80 ng/mL; baseline/follow-up: *n* = 61/61). [g] Samples concentrations above LOD (>0.09 ng/mL; baseline/follow-up: *n* = 10/6). [h] Samples concentrations above LOD (>125 ng/mL; baseline/follow-up: *n* = 14/20). [i] Samples concentrations above LOD (>5 ng/mL; baseline/follow-up: *n* = 46/45). [j] samples concentrations above LOD (>100 ng/mL; baseline/follow-up: *n* = 60/58). * $p < 0.05$; ** $p < 0.01$.

Int. J. Environ. Res. Public Health **2019**, *16*, 2284

8 of 18

3.3. Air Pollution Exposure and Cardiovascular Endpoints

NO_2 exposure was positively associated with blood pressure and negatively associated with blood vessel diameters. Each SD increment (4.96 µg/m^3) in NO_2 was associated with 2.42 mmHg (95% CI: 0.03 to 4.80 mmHg; $p = 0.047$) and 1.76 mmHg (95% CI: 0.00 to 3.52 mmHg; $p = 0.050$) increase in SBP and DBP, respectively (Table 4). Each NO_2 SD increment was associated with −2.08 µm (95% CI: −4.13 to −0.02 µm; $p = 0.048$) decrease in CRVE and −0.11 mm (95% CI: −0.19 to −0.03 mm; $p < 0.010$) decrease in mean baseline brachial diameter.

Table 4. Estimated effects of personal NO_2 and total BTEX on vascular outcomes.

Variable	Exposure Variable	Estimate [a,b] (95% CI)	*p*-Values
SBP [c] (mmHg)	NO_2	2.42 (0.03; 4.80)	0.047
	Total BTEX	1.54 (−1.38; 4.46)	0.297
DBP [c] (mmHg)	NO_2	1.76 (0.00; 3.52)	0.050
	Total BTEX	2.07 (0.06; 4.07)	0.043
CRAE [d] (µm)	NO_2	−0.47 (−2.25; 1.31)	0.599
	Total BTEX	−0.70 (−2.88; 1.47)	0.521
CRVE [d] (µm)	NO_2	−2.08 (−4.14; −0.02)	0.048
	Total BTEX	−0.29 (−3.00; 2.39)	0.829
Mean brachial diameter [d] (mm)	NO_2	−0.11 (−0.19; −0.03)	0.005
	Total BTEX	−0.08 (−0.17; 0.01)	0.090
% FMD [e]	NO_2	−0.11 (−1.00; 0.77)	0.801
	Total BTEX	0.30 (−0.56; 1.15)	0.492
Carotid Diameter [d] (mm)	NO_2	−0.06 (−0.19; 0.08)	0.393
	Total BTEX	−0.12 (−0.26; 0.02)	0.082
cIMT [f] (µm)	NO_2	1.23 (−23.63; 26.09)	0.921
	Total BTEX	12.76 (−10.55; 36.06)	0.275

[a] All models adjusted for date of assessment visit, average temperature, age, body-mass index (BMI), smoking, and employment status (random factor: participant). [b] Estimates expressed as a difference in cardiovascular endpoint for each SD increment in exposure. [c] Additionally adjusted for hours of sleep at night. [d] Additionally adjusted for SBP. [e] Additionally adjusted for SBP and mean brachial diameter. [f] Additionally adjusted for the SBP and carotid diameter.

BTEX exposure was positively associated with blood pressure and cIMT measurements. Each SD increments in total BTEX (2.56 µg/m^3) and o-xylene (2.51 µg/m^3) were associated with a 2.07 mmHg (95% CI: 0.06 to 4.07 mmHg; $p = 0.043$) and 2.00 mmHg (95% CI: 0.21 to 3.80 mmHg; $p = 0.029$) increase in DBP, respectively (Table 4; and Table A2). Each SD (2.08 µg/m^3) increment increase in benzene was positively associated with 24.88 µm (95% CI: 2.19 to 47.57 µm); $p = 0.032$) increase in cIMT (Table A5).

The urinary metabolite 3+4MHA was negatively associated with vascular function as indicated by % FMD with an estimated effect of −1.45% (95% CI: −2.38% to −0.51%; $p = 0.003$) for each SD (3.12 ng/mL) increment in 3+4MHA (Table A4). For more detailed results on effects of exposure on vascular outcomes, refer to Tables A2–A5.

4. Discussion

The current study set out to determine personal air pollution exposure levels as measured by NO_2 and BTEX, in a panel study of female adults residing in the Cape Town region of South Africa, and investigated whether these exposure levels are associated with markers of cardiovascular risk. Major findings of the study are: (1) compared to international air quality standards, our participants' personal exposure to NO_2 and BTEX was relatively low, and (2) despite the relatively low exposure levels, we could demonstrate associations between air pollutants and several cardiovascular parameters: SBP and DBP (NO_2 and BTEX), baseline brachial artery diameter (NO_2), CRVE (NO_2), and cIMT (benzene).

The mean 7-day personal NO_2 exposure concentrations (Table 3) observed during the course of the study (range: 2.94 µg/m^3–25.35 µg/m^3) remained below the recommended WHO, European Union (EU) and South African air quality standards for NO_2: annual exposure of <40 µg/m^3 and 1-hour

exposure of <200 µg/m^3 [48–51]. At baseline, 24 (22%) of the individual mean benzene measurements (range: 0.475 µg/m^3–14.17 µg/m^3) were higher than WHO and EU annual recommended standards (<5 µg/m^3), although the median values were below the standards [17,48].

Furthermore, the mean NO$_2$ and median benzene concentrations at baseline in our study population (NO$_2$: 13.6 ± 4.8 µg/m^3 and benzene: 3.22 (0.77–14.17) µg/m^3) were within the lower range of annual mean ambient NO$_2$ and benzene concentrations of major European cities, with NO$_2$ ranging from 8 µg/m^3 in Stockholm to 43 µg/m^3 in Barcelona, and benzene ranging between 2 and 12 µg/m^3 across various cities [3,52–54].

Compared to other studies from the Western Cape Province, the observed mean personal NO$_2$ levels in our study were comparable with recently reported annual mean NO$_2$ levels from air quality monitoring stations in neighboring areas (Goodwood: 21 µg/m^3; Plattekloof: 10 µg/m^3) [49]. The personal NO$_2$ and individual BTEX concentrations in the current study were furthermore similar to those measured previously (2011–2014) in the Drakenstein sub-district, ~60 km from the City of Cape Town [55]. In this study, household NO$_2$ and BTEX levels (reported as 2-week median values) were measured in more than 500 homes of families of African and mixed ancestry (NO$_2$: 7.9 (Interquartile range (IQR): 3.8–13.3) µg/m^3, benzene: 5.6 (IQR: 2.6–17.1) µg/m^3, toluene: 19.8 (IQR: 9.3–53.2) µg/m^3, ethyl-benzene: 2.1 (IQR: 0.9–53.2) µg/m^3, m+p-xylene: 5.8 (2.4–16.2) µg/m^3, and o-xylene 2.4 (IQR: 1.1–7.0) µg/m^3).

Ambient outdoor BTEX levels are infrequently measured in the Western Cape Province of South Africa. The Provincial Government Report (2013) reported on BTEX levels (measured with passive samplers) from only two locations in one rural town (Riversdale) in the province [49]. The reported values from Riversdale (two locations with benzene concentrations of 0.89 and 1.05 µg/m^3, respectively, toluene concentrations of 2.66 and 1.04 µg/m^3, respectively, ethyl-benzene concentrations of 0.43 and 0.27 µg/m^3, respectively, and xylene concentrations of 1.82 and 1.19 µg/m^3, respectively,) were generally lower than the personal BTEX exposure levels measured in our study [49].

Our results showed that personal NO$_2$ and total BTEX (mostly driven by o-xylene) exposure was positively associated with blood pressure outcomes after adjusting for covariates (Table 4). Both long- and short-term exposure to ambient gaseous pollutants has previously been associated with haemodynamic changes including blood pressure, even at low exposure concentrations [18,56–59].

Our findings support those of Chan et al. (2015) who examined the effects of NO$_2$ and fine PM (≤2.5 µm; PM$_{2.5}$) in a female population and showed that a 10 ppb increase in NO$_2$ was associated with a higher pulse pressure (0.4 mmHg) [60]. In the same study, PM$_{2.5}$ was also associated with higher SBP (1.4 mmHg), pulse pressure (1.0 mmHg), and mean arterial pressure (0.8 mmHg) [60]. The authors speculated that exposure-associated autonomic dysregulation of vascular tone may be a possible underlying mechanism of their findings [60,61]. This may indeed be the case, as our results showed negative associations between NO$_2$ and vessel diameters as indicated by the baseline brachial artery diameter and CRVE. The vasoconstrictive effects of both long-term low-concentrations and short-term high-concentration exposure to ambient air pollution have previously been described [62,63]. In the study by Brook et al. (2002), an inverse relationship with brachial artery diameter (ultrasonography) was also demonstrated in 25 healthy adults, although at higher exposure concentrations (150 µg/m^3 fine PM and 120 ppb O$_3$) and a shorter exposure period (2 hour) compared to our exposure concentrations and exposure period [62]. The authors, in a finding similar to ours, failed to demonstrate ambient air pollution exposure-associated effects on FMD [62].

Previous studies have investigated the possible mechanism involved in air pollution exposure-associated vasoconstriction and suggested possible stimulation of the pulmonary vagal afferent neurons and the subsequent increase in sympathetic nervous system reflex activity or an upregulation (directly or via oxidative stress pathways) of vascular endothelin 1 and 3 (vasoconstrictors) [62,64]; however, more studies are required to elucidate the underlying mechanisms.

Int. J. Environ. Res. Public Health **2019**, *16*, 2284

10 of 18

Benzene exposure was associated with sub-clinical atherosclerotic changes as measured by cIMT in our study with a relatively large estimated effect on cIMT. cIMT is considered a marker of pro-atherosclerotic processes such as inflammation, a strong predictor of future cardiovascular events [65], and increased cIMT has previously been implicated in long-term ambient PM exposure [19,66]. It has also been suggested that women are at higher risk of increased PM-induced cIMT than men [19]. Short-term air pollutant exposure levels in our study were not significantly associated with inflammation (as measured by hsCRP), suggesting that other possible mechanisms may explain the pro-atherosclerotic effects of benzene.

3+4MHA appeared to be a prominent urinary metabolite/tracer for exposure in our study as it strongly correlated with all personal exposure levels (Table A1). 3+4MHA is a urinary marker for toluene (80% inhaled toluene metabolized to BMA or MHA) and the primary metabolite for xylene exposure (95% inhaled xylene metabolized to MHA post-exposure) [38,67–70]. Aside from being a diesel exhaust derivative, xylene is also often used as a solvent in industrial and household products (e.g., adhesives, coatings, degreasers, detergents, dyes, ink, paint, pesticides, polishes, and solvents) [18,56–59].

Xylene is a carcinogen and also associated with central nervous system abnormalities such as brain and neurobehavioral morbidities [71,72]. In our study, the positive association between personal total BTEX and DBP was mostly driven by o-xylene, while no adverse associations between BMA (marker of toluene exposure) and vascular endpoints were observed. The significant association between o-xylene and DBP, as well as between its primary urinary metabolite, 3+4MHA (Table A4), and endothelial function suggests that o-xylene may significantly contribute to vascular dysfunction (increased DBP and reduced endothelial function as measured by % FMD) in our study population. More focused investigations on possible underlying mechanisms are required.

5. Strengths and Limitations

The results from the current study are presented with some strengths and limitations. Strengths of current study include the measurement of personal exposure levels, as opposed to levels obtained from centralized air quality monitoring stations in many previous studies from the SSA region. Personal measurements are generally considered a more accurate representation of exposure levels. An additional strength of the study is the fact that we used measurements of different cardiovascular endpoints to investigate physiological effects. To the best of our knowledge, this study is the first to explore the cardiovascular health effects of personal air pollution exposure, in combination with urinary exposure markers, in the South African research setting.

Limitations of the study include a relatively small sample size representing only women, of whom the majority were smokers. The male participant enrolment rate was low, mostly due to employment obligations that resulted in difficulty to attend assessment visits. The high prevalence of smokers in our cohort may be ascribed to the high smoking rates that have previously been reported in the region [73,74]. The robust correction for the effects of smoking on various outcomes, based only on smoking status, may not have been optimal. Using levels of biomarkers of smoking such as cotinine may have been a more accurate adjustment for the smoking effect and would have also included the effects of possible second-hand smoke. Personal exposure measurements with a 30 cm radius extended in front of the face (within the breathing zone) and the inclusion of blank field samples in the study would also have been more desirable. These factors should be considered in future studies. Additionally, as previously shown, the effects of air pollution vary across sex, ethnicity, and health status [75–77]. Our results represent only the exposure effects in an apparently healthy, female population of mixed ancestry and care should be taken to not extrapolate our findings to the general population.

6. Conclusions

Our results show that personal ambient air pollution exposure in women residing in Cape Town, even at relatively low levels, is associated with markers of cardiovascular risk including blood pressure (SBP and DBP), vascular tone/diameter (baseline brachial artery diameter and CRVE), vascular endothelial function (% FMD), and subclinical atherosclerosis (cIMT).

Author Contributions: Conceptualization, P.D.B., T.S.N., N.G., H.S.; methodology, F.E., P.D.B., T.S.N., N.G., M.M., I.W., D.S.M., N.M., S.C., F.K. and H.S.; software, P.D.B.; validation, F.E., P.D.B., T.S.N., N.G., D.S.M. and H.S.; formal analysis, F.E., P.D.B., T.S.N., D.S.M. and H.S.; investigation, F.E., M.M., I.W., D.S.M., N.M., S.C., F.K. and H.S.; resources, P.D.B., T.S.N., I.W. and H.S.; data curation, F.E., M.M., I.W., N.M., S.C., F.K. and H.S.; writing—original draft preparation, F.E.; writing—review and editing, F.E., P.D.B., T.S.N., N.G., M.M., I.W., D.S.M., N.M., S.C., F.K and H.S.; visualization, F.E.; supervision, P.D.B., T.S.N., N.G. I.W., D.S.M. and H.S.; project administration, F.E., P.D.B., T.S.N., N.G., M.M., I.W. and H.S.; funding acquisition, P.D.B., T.S.N., N.G. and H.S.

Conflicts of Interest: The authors declare no conflict of interest.

Appendix A

Figure A1. Photos of samplers used for personal exposure measurements: (**a**) Gradko rapid air NO_2 sampler (product: DIFRAM-100; UKAS method: GLM 7; detection limit: <0.2 μg/m^3 for 1-week exposure); (**b**) activated Gradko rapid air NO_2 sampler; (**c**) Radiello^{TM} diffusive cartridge (right) and diffusive body attached to a triangular support plate (left) (products: Rad130, RAD120, and RAD121; detection limit for BTEX: 0.05, 0.01, 0.01, and 0.01 μg/m^3, respectively; calibration: CS_2); (**d**) ACR Systems Inc. temperature logger (product: SmartButton (01-0187); detection limit: −40 °C to 85 °C); (**e**) air monitoring devices in the mesh pocket of a backpack (product: Barron BB0110 Curve and Arch Design backpacks); (**f**) backpack worn by participants with samplers located 50 to 60 cm from the face.

Table A1. Spearman's Rho correlations coefficients (*r*) for all personal measures of exposure and urinary metabolites.

	NO$_2$	Benzene	Toluene	Ethyl-benzene	m+p-xylene	o-xylene
Personal Exposure [a]						
Benzene	0.616 ***					
Toluene	0.452 ***	0.461 ***				
Ethyl-benzene	0.622 ***	0.585 ***	0.652 ***			
m+p-xylene	0.642 ***	0.595 ***	0.658 ***	0.983 ***		
o-xylene	0.643 ***	0.589 ***	0.667 ***	0.972 ***	0.989 ***	
Total BTEX [b]	0.524 ***	0.474 ***	0.951 ***	0.790 ***	0.798 ***	0.808 ***
Urinary metabolites [c]						
HPMA	0.081	0.186 *	−0.020	−0.002	0.023	0.017
PMA	0.117	0.011	−0.218 *	−0.112	−0.105	−0.123
MU	0.061	0.152	−0.009	−0.749	−0.038	−0.024
BMA	−0.051	−0.070	0.120	−0.023	−0.018	−0.005
3+4MHA	0.273 **	0.341 ***	0.218 *	0.192 *	0.215 *	0.210 *

[a] *n* = 111 to 113; [b] values represent the mean values of the sum of individual BTEX measurements for each participant;
[c] *n* = 111 to 121; * *p* < 0.05; ** *p* < 0.01; *** *p* < 0.001.

Table A2. Estimated effects of personal NO$_2$, total BTEX, BTEX, and 3+4MHA urinary metabolite on SBP and DBP.

Variable	Exposure Variable	Estimate [a,b] (95% CI)	*p*-Values
SBP [c] (mmHg)	NO$_2$	2.42 (0.03; 4.80)	0.047
	Total BTEX	1.54 (−1.38; 4.46)	0.297
	Benzene	2.51 (−0.21; 5.22)	0.070
	Toluene	0.92 (−2.04; 3.88)	0.539
	Ethyl-benzene	1.44 (−1.15; 4.03)	0.272
	m+p-xylene	1.62 (−1.01; 4.25)	0.224
	o-Xylene	2.12 (−0.50; 4.74)	0.112
	Urinary metabolite [d]		
	3+4MHA	−0.52 (−3.10; 2.05)	0.687
DBP [c] (mmHg)	NO$_2$	1.76 (0.00; 3.52)	0.050
	Total BTEX	2.07 (0.06; 4.07)	0.043
	Benzene	1.19 (−0.73; 3.10)	0.220
	Toluene	1.77 (−0.25; 3.80)	0.086
	Ethyl-benzene	1.58 (−0.20; 3.36)	0.080
	m+p-xylene	1.72 (−0.09; 3.53)	0.062
	o-xylene	2.01 (0.21; 3.80)	0.029
	Urinary metabolite [d]		
	3+4MHA	−0.40 (−2.28; 1.48)	0.673

[a] All models adjusted for date of assessment visit, average temperature, age, BMI, smoking, and employment status (random factor: participant). [b] Estimates expressed as a difference in cardiovascular endpoint for each SD increment in exposure. [c] Additionally adjusted for hours of sleep at night. [d] Additionally adjusted for hours of sleep at night and urine creatinine.

Table A3. Estimated effects of personal NO$_2$, total BTEX, BTEX, and 3+4MHA urinary metabolite on CRAE and CRVE.

Variable	Exposure Variable	Estimate [a,b] (95% CI)	*p*-Values
CRAE [c] (μm)	NO$_2$	−0.47 (−2.25; 1.31)	0.599
	Total BTEX	−0.70 (−2.88; 1.47)	0.521
	Benzene	−0.54 (−2.51; 1.42)	0.582
	Toluene	−0.74 (−2.90; 1.43)	0.500
	Ethyl-benzene	−0.49 (−2.24; 1.26)	0.579
	m+p-xylene	−0.60 (−2.40; 1.21)	0.511
	o-xylene	−0.68 (−2.53; 1.16)	0.461
	Urinary metabolite [d]		
	3+4MHA	−0.57 (−2.297; 1.167)	0.517

Table A3. *Cont.*

Variable	Exposure Variable	Estimate [a,b] (95% CI)	*p*-Values
CRVE [c] (μm)	NO$_2$	−2.08 (−4.14; −0.02)	0.048
	Total BTEX	−0.29 (−3.00; 2.39)	0.829
	Benzene	−0.67 (−3.11; 1.78)	0.588
	Toluene	−0.40 (−3.11; 2.31)	0.768
	Ethyl-benzene	−0.53 (−2.64; 1.58)	0.616
	m+p-xylene	−0.50 (−2.62; 1.62)	0.638
	o-xylene	−0.61 (−2.85; 1.63)	0.587
	Urinary metabolite [d]		
	3+4MHA	−0.14 (−2.19; 1.91)	0.890

[a] All models adjusted for date of assessment visit, age, BMI, average temperature, smoking, and employment status (random factor: participant). [b] Estimates expressed as a difference in cardiovascular endpoint for each SD increment in exposure. [c] Additionally adjusted for SBP. [d] Additionally adjusted for SBP and urine creatinine.

Table A4. Estimated effects of personal NO$_2$, total BTEX, BTEX, and 3+4MHA urinary metabolite on FMD measurements.

Variable	Exposure Variable	Estimate [a,b] (95% CI)	*p*-Values
Mean brachial diameter [c] (mm)	NO$_2$	−0.11 (−0.19; −0.03)	0.005
	Total BTEX	−0.08 (−0.17; 0.01)	0.090
	Benzene	−0.01 (−0.10; 0.08)	0.760
	Toluene	−0.09 (−0.17; 0.01)	0.065
	Ethyl-benzene	−0.08 (−0.17; 0.00)	0.057
	m+p-xylene	−0.06 (−0.15; 0.02)	0.144
	o-xylene	−0.06 (−0.15; 0.03)	0.189
	Urinary metabolite [d]		
	3+4MHA	0.02 (−0.07; 0.11)	0.647
% FMD [e]	NO$_2$	−0.11 (−1.00; 0.77)	0.801
	Total BTEX	0.30 (−0.56; 1.15)	0.492
	Benzene	−0.01 (−0.87; 0.85)	0.982
	Toluene	0.36 (−0.50; 1.22)	0.403
	Ethyl-benzene	0.35 (−0.76; 0.90)	0.870
	m+p-xylene	0.07 (−0.77; 0.92)	0.862
	o-xylene	0.16 (−0.68; 1.00)	0.705
	Urinary metabolite [f]		
	3+4MHA	−1.45 (−2.38; −0.51)	0.003

[a] All models adjusted for date of assessment visit, age, BMI, average temperature, smoking, and employment status (random factor: participant). [b] Estimates expressed as a difference in cardiovascular endpoint for each SD increment in exposure. [c] Additionally adjusted for SBP. [d] Additionally adjusted for SBP and urine creatinine. [e] Additionally adjusted for SBP and baseline brachial diameter. [f] Additionally adjusted for the SBP, baseline brachial diameter, and urine creatinine.

Table A5. Estimated effects of personal NO$_2$, total BTEX, BTEX, and 3+4MHA urinary metabolite on carotid artery measurements.

Variable	Exposure Variable	Estimate [a,b] (95% CI)	*p*-Values
Carotid diameter [c] (mm)	NO$_2$	−0.06 (−0.19; 0.08)	0.393
	Total BTEX	−0.12 (−0.26; 0.02)	0.082
	Benzene	−0.07 (−0.20; 0.07)	0.331
	Toluene	−0.11 (−0.25; 0.03)	0.132
	Ethyl-benzene	−0.10 (−0.22; 0.02)	0.097
	m+p-xylene	−0.10 (−0.23; 0.02)	0.109
	o-xylene	−0.09 (−0.22; 0.04)	0.156
	Urinary metabolite [d]		
	3+4MHA	−0.07 (−0.20; 0.07)	0.325

Int. J. Environ. Res. Public Health **2019**, *16*, 2284

14 of 18

Table A5. *Cont.*

Variable	Exposure Variable	Estimate [a,b] (95% CI)	*p*-Values
cIMT [e] (µm)	NO$_2$	1.23 (−23.63; 26.09)	0.921
	Total BTEX	12.76 (−10.55; 36.06)	0.275
	Benzene	24.88 (2.19; 47.57)	0.032
	Toluene	9.37 (−13.24; 31.99)	0.407
	Ethyl-benzene	9.10 (−14.32; 32.52)	0.437
	m+p-xylene	8.64 (−15.36; 32.64)	0.471
	o-xylene	13.06 (−10.74; 36.85)	0.274
	Urinary metabolite [f]		
	3+4MHA	−10.56 (−30.75; 9.63)	0.302

[a] All models adjusted for date of assessment visit, age, BMI, average temperature, smoking, and employment status (random factor: participant). [b] Estimates expressed as a difference in cardiovascular endpoint for each SD increment in exposure. [c] Additionally adjusted for SBP. [d] Additionally adjusted for SBP and urinary creatinine. [e] Additionally adjusted for SBP and mean brachial diameter. [f] Additionally adjusted for the SBP, mean carotid diameter, and urinary creatinine.

References

1. Kampa, M.; Castanas, E. Human health effects of air pollution. *Environ. Pollut.* **2008**, *151*, 362–367. [CrossRef] [PubMed]

2. Zhang, J.; Smith, K.R. Indoor air pollution: A global health concern. *Br. Med. Bull.* **2003**, *68*, 209–225. [CrossRef] [PubMed]

3. World Health Organization: Regional Office for Europe. WHO Guidelines for Indoor Air Quality: Selected Pollutants. Available online: https://afro.who.int/publications/selected-pollutants-who-guideline-indoor-air-quality (accessed on 18 February 2019).

4. Meng, Q.; Richmond-Bryant, J.; Lu, S.E.; Buckley, B.; Welsh, W.J.; Whitsel, E.A.; Hanna, A.; Yeatts, K.B.; Warren, J.; Herring, A.H.; et al. Cardiovascular outcomes and the physical and chemical properties of metal ions found in particulate matter air pollution: A QICAR study. *Environ. Health Perspect.* **2013**, *121*, 558–564. [CrossRef] [PubMed]

5. Bourdrel, T.; Bind, M.-A.; Béjot, Y.; Morel, O.; Argacha, J.-F. Cardiovascular effects of air pollution. *Arch. Cardiovasc. Dis.* **2017**, *110*, 634–642. [CrossRef] [PubMed]

6. Mills, N.L.; Donaldson, K.; Hadoke, P.W.; Boon, N.A.; MacNee, W.; Cassee, F.R.; Sandstrom, T.; Blomberg, A.; Newby, D.E. Adverse cardiovascular effects of air pollution. *Nat. Clin. Pract. Cardiovasc. Med.* **2009**, *6*, 36–44. [CrossRef] [PubMed]

7. Mills, N.L.; Miller, M.R.; Lucking, A.J.; Beveridge, J.; Flint, L.; Boere, A.J.F.; Fokkens, P.H.; Boon, N.A.; Sandstrom, T.; Blomberg, A.; et al. Combustion-derived nanoparticulate induces the adverse vascular effects of diesel exhaust inhalation. *Eur. Heart J.* **2011**, *32*, 2660–2671. [CrossRef] [PubMed]

8. Künzli, N.; Tager, I.B. Air pollution: From lung to heart. *Swiss Med. Wkly.* **2005**, *135*, 697–702. [PubMed]

9. Kelly, F.J.; Fussell, J.C. Role of oxidative stress in cardiovascular disease outcomes following exposure to ambient air pollution. *Free Radic. Biol. Med.* **2017**, *110*, 345–367. [CrossRef]

10. Brook, R.D.; Rajagopalan, S.; Pope, C.A.; Brook, J.R.; Bhatnagar, A.; Diez-Roux, A.V.; Holguin, F.; Hong, Y.; Luepker, R.V.; Mittleman, M.A.; et al. Particulate matter air pollution and cardiovascular disease: An update to the scientific statement from the american heart association. *Circulation* **2010**, *121*, 2331–2378. [CrossRef] [PubMed]

11. Nelin, T.D.; Joseph, A.M.; Gorr, M.W.; Wold, L.E. Direct and indirect effects of particulate matter on the cardiovascular system. *Toxicol. Lett.* **2012**, *208*, 293–299. [CrossRef] [PubMed]

12. Bernstein, J.A.; Alexis, N.; Barnes, C.; Bernstein, I.L.; Bernstein, J.A.; Nel, A.; Peden, D.; Diaz-Sanchez, D.; Tarlo, S.M.; Williams, P.B. Health effects of air pollution. *J. Allergy Clin. Immunol.* **2004**, *114*, 1116–1123. [CrossRef] [PubMed]

13. Mannucci, P.M.; Harari, S.; Martinelli, I.; Franchini, M. Effects on health of air pollution: A narrative review. *Intern. Emerg. Med.* **2015**, *10*, 657–662. [CrossRef] [PubMed]

14. Łatka, P.; Nowakowska, D.; Nowomiejska, K.; Rejdak, R. How air pollution affects the eyes—A review. *Ophthalmol. J.* **2018**, *3*, 58–62. [CrossRef]

15. Collart, P.; Dubourg, D.; Levêque, A.; Sierra, N.B.; Coppieters, Y. Short-term effects of nitrogen dioxide on hospital admissions for cardiovascular disease in Wallonia, Belgium. *Int. J. Cardiol.* **2018**, *255*, 231–236. [CrossRef] [PubMed]

16. Miri, M.; Rostami Aghdam Shendi, M.; Ghaffari, H.R.; Ebrahimi Aval, H.; Ahmadi, E.; Taban, E.; Gholizadeh, A.; Yazdani Aval, M.; Mohammadi, A.; Azari, A. Investigation of outdoor BTEX: Concentration, variations, sources, spatial distribution, and risk assessment. *Chemosphere* **2016**, *163*, 601–609. [CrossRef] [PubMed]

17. World Health Organization. Ambient Air Pollution: A Global Assessment of Exposure and Burden of Disease. Available online: https://www.who.int/phe/publications/air-pollution-global-assessment/en/ (accessed on 15 March 2019).

18. Bolden, A.L.; Kwiatkowski, C.F.; Colborn, T. New look at BTEX: Are ambient levels a problem. *Environ. Sci. Technol.* **2015**, *49*, 5261–5276. [CrossRef]

19. Autrup, H. Ambient air pollution and adverse health effects. *Procedia Soc. Behav. Sci.* **2010**, *2*, 7333–7338. [CrossRef]

20. Smith, K.R.; Mehta, S. The burden of disease from indoor air pollution in developing countries: Comparison of estimates. *Int. J. Hyg. Environ. Health* **2003**, *206*, 279–289. [CrossRef]

21. Cohen, A.J.; Anderson, H.R.; Ostro, B.; Pandey, K.D.; Künzli, N.; Gutschmidt, K.; Pope, A.; Samet, J.M.; Smith, K. The global burden of disease due to outdoor air pollution. *J. Toxicol. Environ. Health* **2006**, *68*, 1301–1307. [CrossRef]

22. Coker, E.; Kizito, S.; Coker, E.; Kizito, S. A narrative review on the human health effects of ambient air pollution in Sub-Saharan Africa: An urgent need for health effects studies. *Int. J. Environ. Res. Public Health* **2018**, *15*, 427. [CrossRef]

23. Katoto, P.D.M.C.; Byamungu, L.; Brand, A.S.; Mokaya, J.; Strijdom, H.; Goswami, N.; De Boever, P.; Nawrot, T.S.; Nemery, B. Ambient air pollution and health in Sub-Saharan Africa: Current evidence, perspectives and a call to action. *Environ. Res.* **2019**, *173*, 174–188. [CrossRef] [PubMed]

24. Strijdom, H.; De Boever, P.; Walzl, G.; Essop, M.F.; Nawrot, T.S.; Webster, I.; Westcott, C.; Mashele, N.; Everson, F.; Malherbe, S.T.; et al. Cardiovascular risk and endothelial function in people living with HIV/AIDS: Design of the multi-site, longitudinal EndoAfrica study in the Western Cape Province of South Africa. *BMC Infect. Dis.* **2017**, *17*, 1–9. [CrossRef] [PubMed]

25. Grammer, L.C.; Harris, K.E.; Yarnold, P.R. Effect of Respiratory Protective Devices on Development of Antibody and Occupational Asthma to an Acid Anhydride. *Chest* **2002**, *121*, 1317–1322. [CrossRef] [PubMed]

26. Rodes, C.E.; Lawless, P.A.; Evans, G.F.; Sheldon, L.S.; Williams, R.W.; Vette, A.F.; Creason, J.P.; Walsh, D. The relationships between personal PM exposures for elderly populations and indoor and outdoor concentrations for three retirement center scenarios. *J. Expo. Anal. Environ. Epidemiol.* **2001**, *11*, 103–115. [CrossRef] [PubMed]

27. Targa, J.; Loader, A. Diffusion Tubes for Ambient NO$_2$ Monitoring: Practical Guidance for Laboratories and Users. Available online: https://uk-air.defra.gov.uk/assets/documents/reports/cat05/0802141004_NO2_WG_PracticalGuidance_Issue1a.pdf (accessed on 6 March 2019).

28. Palmes, E.D.; Gunnison, A.F.; Dimattio, J.; Tomczyk, C. Personal sampler for nitrogen dioxide. *Am. Ind. Hyg. Assoc. J.* **1976**, *37*, 570–577. [CrossRef] [PubMed]

29. Akdemir, A. The creation of pollution mapping and measurement of ambient concentration of sulfur dioxide and nitrogen dioxide with passive sampler. *J. Environ. Heal. Sci. Eng.* **2014**, *12*, 1–9. [CrossRef] [PubMed]

30. McAlary, T.; Groenevelt, H.; Disher, S.; Arnold, J.; Seethapathy, S.; Sacco, P.; Crump, D.; Schumacher, B.; Hayes, H.; Johnson, P.; et al. Passive sampling for volatile organic compounds in indoor air-controlled laboratory comparison of four sampler types. *Environ. Sci. Process. Impacts* **2015**, *17*, 896–905. [CrossRef]

31. Pegas, P.N.; Alves, C.A.; Evtyugina, M.G.; Nunes, T.; Cerqueira, M.; Franchi, M.; Pio, C.A.; Almeida, S.M.; Freitas, M.C. Indoor air quality in elementary schools of Lisbon in spring. *Environ. Geochem. Health* **2011**, *33*, 455–468. [CrossRef]

32. Seedat, Y.K.; Rayner, B.L. The abridged South African hypertension guideline 2011. *S. Afr. Fam. Pract.* **2013**, *55*, 111–116. [CrossRef]

33. Ridker, P.M. From C-reactive protein to interleukin-6 to interleukin-1: Moving upstream to identify novel targets for atheroprotection. *Circ. Res.* **2016**, *118*, 145–156. [CrossRef]

34. Stevens, J.F.; Maier, C.S. Acrolein: Sources, metabolism, and biomolecular interactions relevant to human health and disease. *Mol. Nutr. Food Res.* **2008**, *52*, 7–25. [CrossRef] [PubMed]

35. Qu, Q.; Shore, R.; Li, G.; Su, L.; Jin, X.; Melikian, A.A.; Roy, N.; Chen, L.C.; Wirgin, I.; Cohen, B.; et al. Biomarkers of benzene: Urinary metabolites in relation to individual genotype and personal exposure. *Chem. Biol. Interact.* **2005**, *153–154*, 85–95. [CrossRef] [PubMed]

36. Angerer, J.; Schildbach, M.; Krämer, A. Sp-Toluylmercapturic acid in the urine of workers exposed to toluene: A new biomarker for toluene exposure. *Arch. Toxicol.* **1997**, *72*, 119–123. [CrossRef]

37. Jacobson, G.A.; McLean, S. Biological Monitoring of Low Level Occupational Xylene Exposure and the Role of Recent Exposure. *Ann. Occup. Hyg.* **2003**, *47*, 331–336. [PubMed]

38. Pirkle, J.L.; De Jesus, V. Laboratory Procedure Manual: Volatile Organic Compounds (VOCs): Urine Ultra Performance Liquid Chromatography with Electro Spray Tandem Mass Spectrometry. Available online: https://wwwn.cdc.gov/nchs/data/nhanes/2011-2012/labmethods/UVOC_G_MET_VOC_Metabolites.pdf (accessed on 6 June 2019).

39. Charakida, M.; Masi, S.; Luscher, T.F.; Kastelein, J.J.P.; Deanfield, J.E. Assessment of atherosclerosis: The role of flow-mediated dilatation. *Eur. Heart J.* **2010**, *31*, 2854–2861. [CrossRef] [PubMed]

40. Simova, I. Intima-Media Thickness: Appropriate Evaluation and Proper Measurement, Described. Available online: https://www.escardio.org/Journals/E-Journal-of-Cardiology-Practice/Volume-13/Intima-media-thickness-Appropriate-evaluation-and-proper-measurement-described (accessed on 20 April 2019).

41. Mendonça, J.A.; Bisetto de Andrade, B.; Braga de Aquino, J.L.; Leandro-Merhi, V.A.; Damian, G.B.; De Andrade, B.B.; De Aquino, J.L.B.; Leandro-Merhi, V.A.; Damian, G.B. Spectral Doppler and automated software-guided ultrasound assessment of bilateral common carotid intima-media thickness in spondyloarthritis: Is there a correlation with clinical findings? *Drugs Context* **2018**, *7*, 1–9. [CrossRef] [PubMed]

42. Knudtson, M.D.; Lee, K.E.; Hubbard, L.D.; Wong, T.Y.; Klein, R.; Klein, B.E.K. Revised formulas for summarizing retinal vessel diameters. *Curr. Eye Res.* **2003**, *27*, 143–149. [CrossRef] [PubMed]

43. Langham, M.C.; Zhou, Y.; Chirico, E.N.; Magland, J.F.; Sehgal, C.M.; Englund, E.K.; Mohler, E.R.; Guo, W.; Barhoum, S.; Wehrli, F.W. Effects of age and smoking on endothelial function assessed by quantitative cardiovascular magnetic resonance in the peripheral and central vasculature. *J. Cardiovasc. Magn. Reson.* **2015**, *17*, 19. [CrossRef]

44. Huxley, R.; Mendis, S.; Zheleznyakov, E.; Reddy, S.; Chan, J. Body mass index, waist circumference and waist:hip ratio as predictors of cardiovascular risk—A review of the literature. *Eur. J. Clin. Nutr.* **2009**, *64*, 16–22. [CrossRef]

45. Jerrett, M.; Burnett, R.T.; Brook, J.; Kanaroglou, P.; Giovis, C.; Finkelstein, N.; Hutchison, B. Do socioeconomic characteristics modify the short term association between air pollution and mortality? Evidence from a zonal time series in Hamilton, Canada. *J. Epidemiol. Community Health* **2004**, *58*, 31–40. [CrossRef]

46. Kakkoura, M.; Kouis, P.; Papatheodorou, S.I.; Paschalidou, A.K.; Ziogas, K.; Kakkoura, M.; Ziogas, K.; Paschalidou, A.K.; Papatheodorou, S.I. The effect of ambient air temperature on cardiovascular and respiratory mortality in Thessaloniki, Greece. *Sci. Total Environ.* **2018**, *647*, 1351–1358.

47. Watson, N.F.; Badr, M.S.; Belenky, G.; Bliwise, D.L.; Buxton, O.M.; Buysse, D.; Dinges, D.F.; Gangwisch, J.; Grandner, M.A.; Kushida, C.; et al. Recommended Amount of Sleep for a Healthy Adult: A Joint Consensus Statement of the American Academy of Sleep Medicine and Sleep Research Society. *J. Clin. Sleep Med.* **2015**, *11*, 591–592. [PubMed]

48. European Environment Agency. Air Quality in Europe—2018 Report. Available online: http://www.eea.europa.eu/publications/air-quality-in-europe-2012 (accessed on 25 March 2019).

49. South African Western Cape Government. Western Cape State of air Quality Management Report: 2013. Available online: https://www.westerncape.gov.za/eadp/files/atoms/files/SoAR2014.pdf (accessed on 25 March 2019).

50. World Health Organization. World Health Organization Guidelines for Indoor Air Quality: Household Fuel Combustion. Available online: http://www.who.int/indoorair/guidelines/hhfc/HHFC_guidelines.pdf (accessed on 25 March 2019).

51. Davidson, A.; Naidoo, D. State of Environment Outlook Report for the Western Cape Province—Air Quality. Available online: http://eadp.westerncape.gov.za/sites/default/files/your-resource-library/WCSoEOR_07_ClimateChange.pdf (accessed on 25 March 2019).

52. Degraeuwe, B.; Thunis, P.; Clappier, A.; Weiss, M.; Lefebvre, W.; Janssen, S.; Vranckx, S. Impact of passenger car NOX emissions on urban NO2 pollution—Scenario analysis for 8 European cities. *Atmos. Environ.* **2017**, *171*, 330–337. [CrossRef]

53. Kuklinska, K.; Wolska, L.; Namiesnik, J. Air quality policy in the U.S. and the EU—A review. *Atmos. Pollut. Res.* **2014**, *6*, 129–137. [CrossRef]

54. World Health Organization. *WHO Air Quality Guidelines for Europe*, 2nd ed.; Available online: https://apps.who.int/iris/handle/10665/107335 (accessed on 25 March 2019).

55. Vanker, A.; Barnett, W.; Nduru, P.M.; Gie, R.P.; Sly, P.D.; Zar, H.J. Home environment and indoor air pollution exposure in an African birth cohort study. *Sci. Total Environ.* **2015**, *536*, 362–367. [CrossRef] [PubMed]

56. Franchini, M.; Mannucci, P.M. Air pollution and cardiovascular disease. *Thromb. Res.* **2012**, *129*, 230–234. [CrossRef] [PubMed]

57. Hoffmann, B.; Luttmann-Gibson, H.; Cohen, A.; Zanobetti, A.; de Souza, C.; Foley, C.; Suh, H.H.; Coull, B.A.; Schwartz, J.; Mittleman, M.; et al. Opposing effects of particle pollution, ozone, and ambient temperature on arterial blood pressure. *Environ. Health Perspect.* **2012**, *120*, 241–246. [CrossRef] [PubMed]

58. Weichenthal, S.; Hatzopoulou, M.; Goldberg, M.S. Exposure to traffic-related air pollution during physical activity and acute changes in blood pressure, autonomic and micro-vascular function in women: A cross-over study. *Part. Fibre Toxicol.* **2014**, *11*, 70. [CrossRef]

59. Yang, B.; Qian, Z.; Howard, S.W.; Vaughn, M.G.; Fan, S.; Liu, K.; Dong, G. Global association between ambient air pollution and blood pressure: A systematic review and meta-analysis. *Environ. Pollut.* **2018**, *235*, 576–588. [CrossRef]

60. Chan, S.H.; Van Hee, V.C.; Bergen, S.; Szpiro, A.A.; DeRoo, L.A.; London, S.J.; Marshall, J.D.; Kaufman, J.D.; Sandler, D.P.; Kaufman, J.D.; et al. Long-term air pollution exposure and blood pressure in the sister study. *Environ. Health Perspect.* **2015**, *123*, 951–958. [CrossRef]

61. Chen, J.-C.; Wang, X.; Wellenius, G.A.; Serre, M.L.; Driscoll, I.; Casanova, R.; McArdle, J.J.; Manson, J.E.; Chui, H.C.; Espeland, M.A. Ambient air pollution and neurotoxicity on brain structure: Evidence from women's health initiative memory study. *Ann. Neurol.* **2015**, *78*, 466–476. [CrossRef] [PubMed]

62. Brook, R.D.; Brook, J.R.; Urch, B.; Vincent, R.; Rajagopalan, S.; Silverman, F. Inhalation of fine particulate air pollution and ozone causes acute arterial vasoconstriction in healthy adults. *Circulation* **2002**, *105*, 1534–1536. [CrossRef] [PubMed]

63. Adar, S.D.; Klein, R.; Klein, B.E.K.; Szpiro, A.A.; Cotch, M.F.; Wong, T.Y.; O'Neill, M.S.; Shrager, S.; Barr, R.G.; Siscovick, D.S.; et al. Air pollution and the microvasculature: A cross-sectional assessment of in vivo retinal images in the population-based multi-ethnic study of atherosclerosis (MESA). *PLoS Med.* **2010**, *7*, e1000372. [CrossRef] [PubMed]

64. Langrish, J.P.; Lundbäck, M.; Mills, N.L.; Johnston, N.R.; Webb, D.J.; Sandström, T.; Blomberg, A.; Newby, D.E.; Sandström, T.; Lundbäck, M.; et al. Contribution of endothelin 1 to the vascular effects of diesel exhaust inhalation in humans. *Hypertension* **2009**, *54*, 910–915. [CrossRef] [PubMed]

65. Bots, M.L.; Hoes, A.W.; Koudstaal, P.J.; Hofman, A.; Grobbee, D.E. Common carotid intima-media thickness and risk of stroke and myocardial infarction: The Rotterdam Study. *Circulation* **1997**, *96*, 1432–1437. [CrossRef] [PubMed]

66. Sheppard, L.; Watson, K.; Budoff, M.; Sampson, P.D.; Barr, R.G.; Diez Roux, A.V.; Jacobs, D.R.; Kaufman, J.D.; Vedal, S.; Polak, J.F.; et al. Fine particulate air pollution and the progression of carotid intima-medial thickness: A prospective cohort study from the Multi-Ethnic Study of Atherosclerosis and Air Pollution. *PLoS Med.* **2014**, *10*, e1001430.

67. Corn, M. *Handbook of Hazardous Materials*; Elsevier Science: Amsterdam, The Netherlands, 1993; ISBN 0323139558.

68. Interaction Profile For: Benzene, Toluene, Ethylbenzene, and Xylenes (BTEX). Available online: https://pdfs.semanticscholar.org/3ad5/8812c08fd4d51c7652eff236c5a88be8444a.pdf?_ga=2.123559363.973190570.1527186213-1785467536.1527186213 (accessed on 24 May 2019).

69. Hormozi, M.; Mirzaei, R.; Nakhaee, A.; Payandeh, A.; Izadi, S.; Dehghan Haghighi, J.; Rahimpoor, R. Quantification of urinary metabolites of toluene and xylene isomers as biological indices of occupational exposure in printing industry workers. *Heal. Scope* **2019**, in press. [CrossRef]

70. Langman, J.M. Xylene: Its toxicity, measurement of exposure levels, absorption, metabolism and clearance. *Pathology* **1994**, *26*, 301–309. [CrossRef]

Int. J. Environ. Res. Public Health **2019**, *16*, 2284

18 of 18

71. Bolla, K.I.; Schwartz, B.S.; Stewart, W.; Rignani, J.; Agnew, J.; Ford, D.P. Comparison of neurobehavioral function in workers exposed to a mixture of organic and inorganic lead and in workers exposed to solvents. *Am. J. Ind. Med.* **1995**, *27*, 231–246. [CrossRef]

72. Celik, A.; Aydin, N.; Ozcirpici, B.; Saricicek, E.; Sezen, H.; Okumus, M.; Bozkurt, S.; Kilinc, M. Elevated red blood cell distribution width and inflammation in printing workers. *Med. Sci. Monit.* **2013**, *19*, 1001–1005.

73. Croxford, J.; Viljoen, D. Alcohol consuption by pregnant women in the Western Cape. *SAMJ* **1999**, *89*, 962–965. [PubMed]

74. Reddy, P.; Zuma, K.; Shisana, O.; Kim, J.; Sewpaul, R.; Jonas, K.; Sewpaul, R. Prevalence of tobacco use among adults in South Africa: Results from the first South African national health and Nutrition Examination Survey. *S. Afr. Med. J.* **2015**, *105*, 648–655. [CrossRef] [PubMed]

75. Oliveira, A.R.; Campos Neto, A.A.; de Andrade, M.J.O.; de Medeiros, P.C.B.; dos Santos, N.A. Organic solvent exposure and contrast sensitivity: Comparing men and women. *Braz. J. Med. Biol. Res.* **2018**, *51*, e6568. [CrossRef] [PubMed]

76. O'Neill, M.S.; Breton, C.V.; Devlin, R.B.; Utell, M.J. Air pollution and health: Emerging information on susceptible populations. *Air Qual. Atmos. Heal.* **2012**, *5*, 189–201. [CrossRef] [PubMed]

77. Walton, R.T.; Mudway, I.S.; Dundas, I.; Grigg, J.; Marlin, N.; Koh, L.C.; Aitlhadj, L.; Vulliamy, T.; Jamaludin, J.B.; Wood, H.E.; et al. Air pollution, ethnicity and telomere length in east London schoolchildren: An observational study. *Environ. Int.* **2016**, *96*, 41–47. [CrossRef] [PubMed]